25 August 2006 | $10

Science

Freshwater Resources

AAAS

Volume 313, Issue 5790

COVER

Raindrops are a welcome source of freshwater replenishment. Nonetheless, maintaining a clean and plentiful water supply remains a worldwide concern. A special section beginning on page 1067 highlights some of the scientific and engineering challenges in managing this vital and increasingly scarce resource.

Photo: Getty Images

DEPARTMENTS

EDITORIAL

SPECIAL SECTION

Freshwater Resources

INTRODUCTION

REVIEWS

PERSPECTIVES

NEWS

>> Editorial p. 1019; News story p. 1034; Book Review p. 1046; Review p. 1061

NEWS OF THE WEEK

NEWS FOCUS

CONTENTS continued **>>**

Science

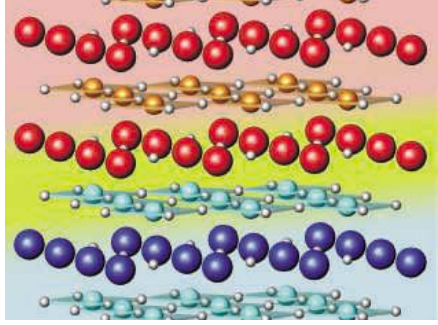

SCIENCE EXPRESS

www.sciencexpress.org

BIOCHEMISTRY

Structure of the Exon Junction Core Complex with a Trapped DEAD-Box ATPase Bound to RNA
C. B. F. Andersen et al.
A structure of a complex that binds to new mRNA reveals how two proteins inhibit the ATPase activity of an RNA helicase to ensure tight binding.
10.1126/science.1131981

GEOCHEMISTRY

Oxygen Isotope Variation in Stony-Iron Meteorites
R. C. Greenwood, I. A. Franchi, A. Jambon, J. A. Barrat, T. H. Burbine
Oxygen isotope measurements show that two similar groups of stony meteorites have different origins and that one likely comes from the asteroid Vesta.
10.1126/science.1128865

PHYSICS

Tunable Quasi–Two-Dimensional Electron Gases in Oxide Heterostructures
S. Thiel, G. Hammerl, A. Schmehl, C. W. Schneider, J. Mannhart
Application of an electric field can tune the conductance of the interface region between layered oxides by orders of magnitude.
10.1126/science.1131091

IMMUNOLOGY

Reversal of the TCR Stop Signal by CTLA-4
H. Schneider et al.
A protein responsible for preventing unwanted immune responses discourages extended liaisons between activated immune cells.
10.1126/science.1131078

LETTERS

BOOKS *ET AL.*

EDUCATION FORUM

PERSPECTIVES

TECHNICAL COMMENT ABSTRACTS

CELL BIOLOGY

REVIEW

OCEAN SCIENCE

BREVIA

PALEONTOLOGY

RESEARCH ARTICLE

NEUROSCIENCE

CONTENTS continued **>>**

REPORTS

AAAS
ADVANCING SCIENCE, SERVING SOCIETY

SCIENCE (ISSN 0036-8075) is published weekly on Friday, except the last week in December, by the American Association for the Advancement of Science, 1200 New York Avenue, NW, Washington, DC 20005. Periodicals Mail postage (publication No. 484460) paid at Washington, DC, and additional mailing offices. Domestic individual membership and subscription (51 issues): $139 ($74 allocated to subscription). Domestic institutional subscription (51 issues): $650; Foreign postage extra: Mexico, Caribbean (surface mail) $55; other countries (air assist delivery) $85. First class, airmail, student, and emeritus rates on request. Canadian rates with GST available upon request, GST #1254 88122. Publications Mail Agreement Number 1069624. **Printed in the U.S.A.**

Change of address: Allow 4 weeks, giving old and new addresses and 8-digit account number. **Postmaster:** Send change of address to AAAS, P.O. Box 96178, Washington, DC 20090–6178. **Single-copy sales:** $10.00 current issue, $15.00 back issue prepaid includes surface postage; bulk rates on request. The identification code for *Science* is 0036-8075. *Science* is indexed in the *Reader's Guide to Periodical Literature* and in several specialized indexes.

CONTENTS continued **>>**

Breakneck biting.

SCIENCE**NOW**

www.sciencenow.org DAILY NEWS COVERAGE

Ant Takes a Bite out of Speed Record
Quick-fire chompers accelerate hunting, hasten retreat.

Premature Births Linked to Gene Variant
Finding may explain higher incidence of preemies in African-American population.

Not a Drop to Drink
Report finds global freshwater supplies dwindling faster than thought.
>> Freshwater Resources section p. 1067

Scientific conference on ice.

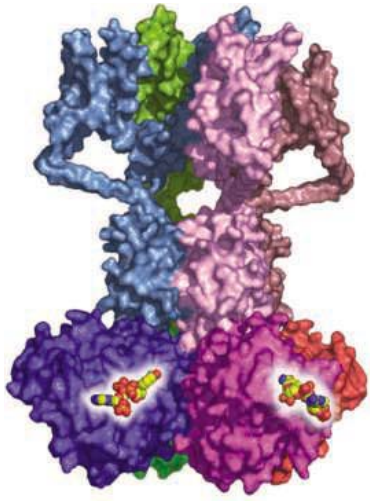

Channel or enzyme?

SCIENCE'S **STKE**

www.stke.org SIGNAL TRANSDUCTION KNOWLEDGE ENVIRONMENT

PERSPECTIVE: Multifunctional Potassium Channels—Electrical Switches and Redox Enzymes, All in One
S. H. Heinemann and T. Hoshi
A potassium channel subunit acts as a redox enzyme that can modulate channel inactivation.

PROTOCOL: Real-Time Measurements of Protein Affinities on Membrane Surfaces by Fluorescence Spectroscopy
F. Philip and S. Scarlata
Find out how to quantify protein interactions using FRET.

SCIENCE **CAREERS**

www.sciencecareers.org CAREER RESOURCES FOR SCIENTISTS

GLOBAL: Special Feature—Seeing the World Through Science
R. Arnette
Scientists describe their most memorable conference experiences.

MISCINET: Educated Woman, Chapter 54—Phoenix Rising
M. P. DeWhyse
Micella takes us through the excitement of dissertation defense day.

UK: Eng.D.—An Applied Doctorate
L. Blackburn
In the United Kingdom, professional doctorate degrees provide an alternative to the Ph.D.

CANADA: A New University Means New Jobs in Ontario
A. Fazekas
Established in 2003, the University of Ontario Institute of Technology is still hiring science faculty.

MISCINET: Is There an M.D./Ph.D. in My Future?
MentorDoctor Team
The team advises an undergraduate interested in practicing medicine and research.

Separate individual or institutional subscriptions to these products may be required for full-text access.

EDITED BY STELLA HURTLEY AND PHIL SZUROMI

Ecology Then and Now

Plants and their insect predators form a complex and evolving ecosystem (see the Perspective by **Kitching**). **Wilf *et al.*** (p. 1112) show that the Cretaceous-Paleogene extinction complicated plant-insect coevolution for perhaps several million years. In one location after the extinction, a limited species of leaves reveal diverse insect predation. In another, many species of leaves show limited types of predation. Thus, in some locations, plants seemed to have evolved without much insect predation, while in others, insects evolved despite limited plant diversity. In contrast, **Novotny *et al.*** (p. 1115) compared present-day insect host specificity and diversity on phylogenetically comparable sets of plants in tropical and temperate forests. Coexistence of numerous herbivore species in tropical forests did not seem to reflect narrower niches; instead, herbivore species richness appeared to be driven by plant diversity.

A Sandwich with Extra Palladium

In the 50 years since Wilkinson's characterized ferrocene, chemists have manipulated nearly every metal in the periodic table into a sandwich between planar cyclic aromatic hydrocarbons. However, despite the available space between the flanking rings, the central compounds have almost never contained more than one metal center. **Murahashi *et al.*** (p. 1104) prepared and characterized a compound with three palladium atoms sandwiched between tropylium rings, and another with five palladium atoms sandwiched between naphthacenes. The structures present an interesting boundary case between discrete molecules and layered solids.

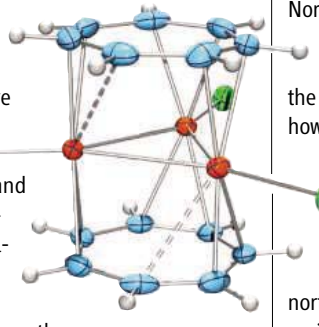

Supersolid Flow in Grain Boundaries?

When two reservoirs of a liquid are brought together, their levels will equilibrate to a common level. Recent experiments have found evidence of "supersolid" behavior in solid ^{4}He, where superfluid-like mass flow through the solid was observed. How a solid can flow like a superfluid has been controversial. **Sasaki *et al.*** (p. 1098, published online 3 August; see the 4 August news story by **Cho**) reexamined mass flow between two reservoirs of superfluid ^{4}He separated by a barrier of solid helium and propose a model in which superflow along grain boundaries in the solid accounts for the observed mass transport.

Freshen This

The Nordic and Atlantic Subpolar Oceans of the Northern Hemisphere became less saline during the past half-century, and **Peterson *et al.*** (p. 1061) address the problem of the origin of the necessary freshwater inputs. They examined how precipitation onto the ocean, river discharge, glacial melt, and sea ice melt have changed recently in comparison to a baseline from 1936 to 1955. This understanding is particularly important in light of projections of a continued increase in precipitation in high northern latitudes and the critical role that this region is thought to play in regulating ocean circulation and global climate.

Neuronal Stimulation and Recording

It would be useful to interrogate or modify the electrophysiology of neurons in detail. One promising approach is to use small field-effect transistors (FETs). **Patolsky *et al.*** (p. 1100) assembled arrays of p- and n-type silicon nanowires and then used polylysine patterning to direct the growth of rat cortical neurons on the wires so that the dendrites and axons of a single neuron could be stimulated or interrogated at up to 50 locations along one axon in physiological media. The action potentials induced with the usual glass microelectrode or with the nanowire transistors were comparable, and the nanowire junctions could be used to inhibit signals as well as measure propagation speeds.

Migrating Moons

Pluto's two recently discovered moons travel in orbits that appear to be influenced by the largest satellite, Charon. The two moons' orbits are circular and coplanar with that of Charon, which suggests that they formed in a common impact as opposed to being captured independently. However, all three moons lie at large distances from Pluto, so if they were formed together in a collision they must have migrated outward. **Ward and Canup** (p. 1107, published online 6 July; see the Perspective by **Lissauer**) propose that the two moons were created in the same impact that produced Charon. To avoid the disruption of the system as it expanded, the two small moons remained in corotation resonances with Charon. Corotation type resonances, similar to those that constrain Neptune's ring arcs, would not have altered the eccentricities of the satellites after capture.

Moderate Methane Changes

The atmospheric concentration of methane, a powerful greenhouse gas that is also a useful tracer of global carbon cycling, varied dramatically between cold and warm periods of Earth history during the past 800,000 years. The causes of these variations are still unclear. **Schaefer *et al.*** (p. 1109) analyzed West Greenland ice to develop a record of the stable isotopic composition of the carbon in atmospheric methane at the end of the last deglaciation, when the concentration of methane in the

CREDITS (TOP TO BOTTOM): M. JANDA (2005); MURAHASHI *ET AL.*

atmosphere increased from 500 to 750 parts per billion in less than 200 years. The carbon-isotopic composition of methane changed remarkably little, implying that the methane was being released from tropical wetlands rather than ocean clathrates.

Linking LTP with Learning and Memory

The phenomenon of synaptic long-term potentiation (LTP) was discovered more than 30 years ago in the hippocampus. Although it is commonly thought that hippocampal LTP is induced by learning, there has not been a direct demonstration (see the Perspective by **Bliss *et al.***). **Whitlock *et al.*** (p. 1093) recorded field potentials from multiple sites in hippocampal area CA1 before and after single-trial inhibitory avoidance learning. Field potentials increased on a subset of the electrodes, and these could be specifically related to the learning event. **Pastalkova *et al.*** (p. 1141) reversed hippocampal LTP in freely moving animals using a cell-permeable inhibitor of a protein kinase. Reversal was accompanied by a complete disruption of previously acquired long-term memory in a place avoidance task, even when the kinase inhibitor was infused only during the consolidation interval. This result suggests that LTP was necessary for storing spatial information.

Dealing with DNA Damage

Cells need to be able to respond to DNA damage to restrict its consequences for the organism as a whole. **Dornan *et al.*** (p. 1122) found a new target for the protein kinase ATM (which when mutated causes ataxia telangiectasia, a disease that renders patients sensitive to ionizing radiation and an increased risk of cancer). ATM is activated in response to DNA damage and phosphorylates COP1, an E3 ubiquitin ligase that controls ubiquitination and degradation of the key tumor suppressor protein p53. This phosphorylation appears to cause COP1 to turn on itself, mediating its own autoubiquitination and consequent degradation, leading to the accumulation of p53. In tissue cultures, this phosphorylation event appears to be necessary for p53-dependent tumor suppressor activity in response to DNA damaging agents.

Getting to Grips with Gut Flora

All mammals rely on a factory of symbiotic microorganisms living in the gut to help process nutrients into usable forms, but if these bacteria escape containment, they can trigger damaging inflammatory responses. Mammals use several adaptive and innate systems to keep the gut flora in check, including microbicidal peptide defensins, lysozymes, and lectins. **Cash *et al.*** (p. 1126; see the Perspective by **Strober**) have discovered that the expression of a carbohydrate-binding protein—a lectin—is induced by the intestinal microbial population from Paneth cells in the crypts. This lectin is among the most highly expressed proteins in the small intestine, recognizes peptidoglycan, and is directly bactericidal. Indeed sufferers of inflammatory bowel disease tend to express elevated levels of C-type lectins.

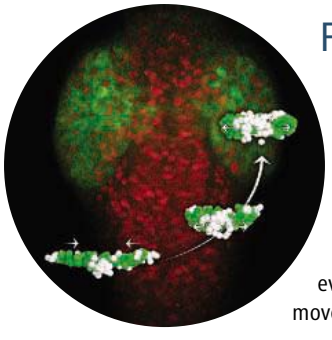

CREDIT: REMBOLD *ET AL.*/PETRA RIEDINGER, EMBL HEIDELBERG

Fish Eyes

Cell movements and molecular factors direct organ development. **Rembold *et al.*** (p. 1130) used high-resolution in vivo imaging to reconstruct eye morphogenesis at the single-cell level in wild-type, mutant, and mosaic fish. Hundreds of cells representing retinal progenitor cells and presumptive forebrain cells are tracked simultaneously. The analyses indicate that retinal progenitor cells actively migrate during optic vesicle evagination and that the optic vesicle forms from individual cell movements, not tissue movements.

Diabetes—An Unfolding Story

Obesity triggers stress in the endoplasmic reticulum (ER), a network of intracellular membranes involved in protein folding and trafficking. That ER stress in turn disrupts insulin signaling. **Ozcan *et al.*** (p. 1137) investigated whether a class of small-molecule drugs that normalize ER function, called "chemical chaperones," might have therapeutic benefits in type 2 diabetes. These drugs were found to correct hyperglycemia and restore insulin sensitivity in genetically obese and diabetic mice, suggesting that they merit further study as a potential therapy for human diabetes.

Call for Entries

Student Poster Competition

PUT YOURSELF IN THE PICTURE.

2007 AAAS Annual Meeting
15-19 February, San Francisco

"Science and Technology for Sustainable Well-Being"

Put yourself in the picture by presenting a poster at the AAAS Student Poster Session. It provides a great opportunity to present your research and offers an excellent venue for extended informal discussion with meeting attendees.

Accepted posters will be listed in the 2007 AAAS Meeting Poster Book. Winners will be published in *Science*. Free registration opportunities are available as are travel assistance grants, please see the Web site for futher details.

Deadline for submission: **Monday, 13 November 2006.**
See the Web site for full details: **www.aaasmeeting.org/student.**

"To raise new questions, new possibilities, to regard old problems from a new angle, requires creative imagination and marks real advance in science." Albert Einstein

www.aaasmeeting.org/student

AAAS
ADVANCING SCIENCE, SERVING SOCIETY

Donald Kennedy is the Editor-in-Chief of *Science*.

Brooks Hanson is Deputy Editor for physical sciences at *Science*.

What's a Wetland, Anyhow?

ANYONE INTERESTED IN WATER AND ENVIRONMENTAL SCIENCE SHOULD STUDY THE U.S. Supreme Court's opinion—or, more precisely, its three rather different opinions—in the recent case called *Rapanos vs. United States*. Don't tune out if you're in Asia, Europe, or elsewhere, because this is NOT merely a domestic issue! Water quality is critical internationally, improvements in water quality have been a major source of global public health benefits (see the special section, p. 1067), and U.S. regulatory approaches are sometimes copied elsewhere.

Here's what the Court was facing. The Clean Water Act mandates that the U.S. Army Corps of Engineers issue regulations defining what fits under the act's umbrella term "waters of the United States." The Court of Appeals for the Sixth Circuit had upheld federal jurisdiction over Michigan wetlands in *Rapanos*, finding that there were hydrologic connections between the site and nearby ditches and drains, and thence to navigable waters. Defendants appealed to the Supreme Court, which issued its opinions on 19 June 2006.

The Court's fundamental split will surprise few. Justice Scalia, representing the views of Roberts, Alito, Thomas, and himself, offered a very restrictive definition of wetlands: They must have surface connections to navigable waters. That view would have stripped regulatory protection from lands historically treated as wetlands by the Corps of Engineers. On the other side, Justice Stevens, for Souter, Ginsberg, and Breyer, favored a definition that includes groundwater with a significant nexus of connection to more distant navigable waters. Justice Kennedy wrote the decisive opinion, in effect bouncing the matter back to the appellate court. His position favored the "significant nexus" view, adding that the determination would essentially be a scientific matter, within the proper scope of the regulatory agency's authority. That leaves the matter approximately where it was, but the tone of the opinions is revealing with respect to the depth and tenor of the disagreement on the Court.

There are jabs and needles everywhere. Stevens said that Scalia's opinion "disregards its own obligation to interpret laws rather than make them." The Chief Justice's separate opinion criticized the Corps for failing to issue regulatory revisions after an earlier Court decision, saying that it had an "essentially boundless view of the scope of its power." Scalia, in what reads like a dissenting opinion, said that the Stevens definition of wetlands was "beyond parody." Ouch.

This case also signals how different justices might apply science as a guide to decision-making. "Beyond parody" might also fit Scalia's effort to define terms used in hydrology. His search for commonplace labels as proxies for scientific definitions must have left his copy of *Webster's Dictionary* dog-eared from overuse; the text cites it over and over again. His opinion shows no awareness of what hydrologic investigations have demonstrated about the interconnectedness of ground and surface waters. Neither is there any suggestion that groundwater moves (it does) or that it regularly feeds surface streams or lakes, often keeping these waters flowing between rainstorms. The essential message is: "If you can't see it, it doesn't matter."

There is a missing precedent here. An earlier Supreme Court case, *Borden Ranch and Tsakopoulos vs. U.S. Army Corps of Engineers and U.S. Environmental Protection Agency*, ended in a 4-4 tie, thereby letting stand a decision that fined Tsakopoulos for a plowing technique that the government said would damage the underlying wetland. Ironically, Kennedy had recused himself because he knew Tsakopoulos. Given his views in *Rapanos*, he would likely have sided with the government, creating a precedent that might have moved the Court not to hear *Rapanos*.

Two take-home lessons seem clear. First, Kennedy is knowledgeable about environmental science; Scalia has little knowledge or perhaps only little interest. Second, despite the meager opportunity for direct scientific input to the Court, concerned scientists could help federal agencies work out realistic scientific standards for defining a "significant nexus" and get those into the Code of Federal Regulations. They might also be useful in the next big case, when the Court will decide whether carbon dioxide is a pollutant under the Clean Air Act. Perhaps they could give the justices something more scientifically helpful than Webster.

– Donald Kennedy and Brooks Hanson

10.1126/science.1132934

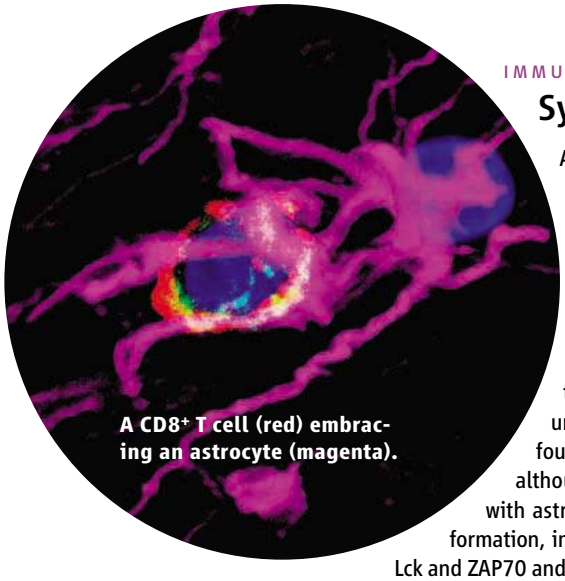

A CD8+ T cell (red) embracing an astrocyte (magenta).

IMMUNOLOGY

Synapse Formation in the Brain

A productive meeting of a T cell and an antigen-presenting cell results in the formation of an immunological synapse between the membranes of the two cells, a crucial step in promoting T cell activation. Concentrated within synapses are the adhesion protein LFA1, T cell receptors, peptide-MHC complexes, and downstream signalling components. Two concentric domains of the synapse have been characterized: peripheral and central supramolecular activation clusters (pSMACs and cSMACs). Although both domains can be observed in vitro, difficulty seeing them in vivo has prompted discussion of their importance in effective immune responses. Using a rat model with a documented immune response to virally infected astrocytes in the brain, Barcia *et al.* found that both $CD4^+$ and $CD8^+$ T cells were required for clearance of infected cells, although only $CD8^+$ cells entered the brain parenchyma to establish close contact with astrocytes. These contacts exhibited features characteristic of immune synapse formation, including recruitment and phosphorylation of the intracellular tyrosine kinases Lck and ZAP70 and a membrane reorganization into intimate three-dimensional apposition. More striking was the detection of cSMAC- and pSMAC-like regions, defined by the central and peripheral distributions of the T cell receptor and LFA1, respectively. Typical synapse structures were seen both before and during the immune-mediated clearance of infected astrocytes, suggesting their direct involvement in the antiviral response. — SJS

J. Exp. Med. **203**, 10.1084/jem.20060420 (2006).

CHEMISTRY

Bounding Biomineralization

Many organisms build skeletons or shells out of calcium carbonate, either by localizing its crystallization or by stabilizing the otherwise short-lived amorphous form. In general, control of this process has been attributed to a mix of proteins, polymers, and magnesium ions on the assumption that each plays roughly the same role in inhibiting the nucleation and growth of crystalline calcite.

DiMasi *et al.* have used in situ synchrotron x-ray reflectivity to distinguish the roles played by these different substances. Specifically, they monitored the formation of amorphous calcium carbonate films on monolayers of arachidic acid placed against a subphase of saturated aqueous calcium bicarbonate, while varying the concentration of additives, including $MgCl_2$ and the sodium salt of poly(acrylic acid)—a model of naturally occurring aspartate in proteins. The magnesium ions were found to introduce an induction period, delaying the onset of film formation, but had little influence on the subsequent growth of the film. Changing the polymer concentration also did not affect the growth rate of the films but did affect the lifetime of the metastable amorphous phase before it crystallized or redissolved into the solution. Finally, by varying the trough depth, the authors could tune the path length for the diffusion of carbon dioxide during film formation; this component of the study revealed an inverse relation between solution depth and growth rates. Overall, these results clarify the means of controlling the growth of amorphous mineral phases, of interest both in natural processes and in materials fabrication. — MSL

Phys. Rev. Lett. **97**, 45503 (2006).

PROTEOMICS

You Are What You Eat

Plant biomass contains a lower percentage of N than animal biomass because plants have relatively more carbohydrate and less protein. To look more deeply at elemental aspects, Elser *et al.* compared the proteomes of nine plants and nine animals. The proteomes of plants were found to have a lower N content than those of animals; on average, animals had 7% more N atoms per amino acid. Furthermore, N content is related to overall gene expression level in such a way that, on average, plants have a lower N content in genes that are more highly expressed, whereas no discernible correlation with expression existed in the animal proteomes. These findings may reflect an eco-physiological selection away from the use of N-rich amino acids in plants, perhaps as a result of a greater sensitivity to limiting N supplies. — LMZ

Mol. Biol. Evol. **23**, 10.1093/molbev/msl068 (2006).

BIOPHYSICS

Sensory Discrimination

An attractive (or noxious) signal might come from any direction, so how can a single cell remain on the lookout in all directions? *Escherichia coli* are known to cope by interspersing periods of directional swimming with tumbling, which reorients them randomly. The single-celled slime mold *Dictyostelium* lives socially and has taken advantage of this lifestyle to apportion the community's detectors to cover all points of the compass.

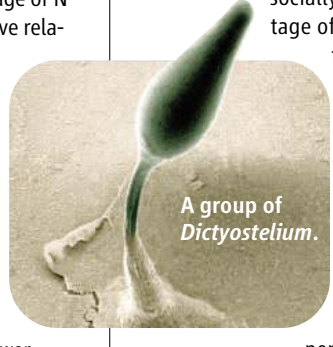

A group of *Dictyostelium*.

Samadani *et al.* show that single *Dictyostelium* cells respond reproducibly (as assessed by the angular location of a cAMP-sensing component) to 10 trials of a fixed pulse of cAMP, yet this angle varies over more than 180° when measured across 40 cells. Nevertheless, the population response, summed over orientation and magnitude, yields a peak unerringly directed at the origin of the pulse. Each cell's innate inclination can be modeled as a function of (i) the overall mobilization of sensor components, (ii) the degree to which the components are distributed

CREDITS (TOP TO BOTTOM): BARCIA *ET AL.*, *J. EXP. MED.* **203**, 10.1084/JEM.20060420 (2006); DR. RICHARD KESSEL & DR. GENE SHIH

asymmetrically, and (iii) the orientation of the peak of asymmetry. Each cell's response can then be calculated as the vector sum of the intrinsic properties and the stimulus, and this captures the observed behaviors of the population, behaviors that are similar to the orientation selectivity of visual cortex neurons. This analogy leads one to wonder how the intrinsic orientations are divvied up and maintained in a *Dictyostelium* community. — GJC

Proc. Natl. Acad. Sci. U.S.A. **103**, 11549 (2006).

CHEMISTRY

Fill in the Blanks

Protease activity can be quantified in fluorescent or colorimetric assays, but such assays can require substrate modification, lengthy incubation times, and extensive workup procedures, along with relatively large sample volumes. Orosco *et al.* have fabricated a silicon-based photonic crystal device that exhibits picomolar sensitivity in analyzing microliter aliquots of pepsin and produces a rapid response visible to the eye. Furthermore, no molecular labeling is necessary.

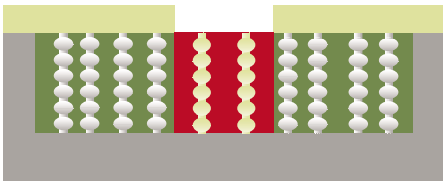

Schematic of the photonic crystal device detecting protein fragments (yellow).

Photonic crystals block transmission of specific wavelengths of light through periodic alternation of high-refractive-index solid regions and low-refractive-index pores. The authors etched p-doped silicon to create the pores and then methylated the pore surfaces to keep out polar buffer solution. The top surface was then coated with a hydrophobic layer of zein protein. Application of pepsin caused the protein to fragment and fall into the pores, which in turn raised the refractive index in the pore region and led to a redshift in the reflected light. — PDS

Adv. Mater. **18**, 1393 (2006).

APPLIED PHYSICS

Muscling in on Optical Gratings

Optical microelectromechanical devices have found many applications as light splitters, modulators, and tunable gratings. Most such applications have relied on micromachined hard materials, which are capable of fast response but only over a limited mechanical range. Aschwanden and Stemmer show that soft materials such as electroactive polymers, or artificial muscles, can be used to extend that mechanical response because of the enormous strains (~380%) they can sustain when a voltage is applied. The authors pattern their elastomeric polymer with an initial grating period of 1 μm and append carbon black electrodes using contact printing. By sweeping the bias across these electrodes up to 4.5 kV, they can continuously vary the grating period over a range of up to 32% (to a 1.3-μm period). This change is sufficient to tune the transmission wavelength across the optical spectrum from blue to red, suggesting the possibility of display technology applications if the driving voltage can be diminished. — ISO

Opt. Lett. **31**, 2610 (2006).

Science stke AAAS

www.stke.org

<< An Up-and Down-Regulator

The liver is a key controller of fuel utilization, and insulin acts to inhibit hepatic gluconeogenesis and activate lipogenesis, thereby preventing excessive glucose release during the fed state. Phosphatidylinositol 3-kinase (PI3K) is a mediator of insulin signaling and is a dimer of a catalytic subunit (p110) and a regulatory subunit (p85). Phosphatidylinositol (3,4,5)-trisphosphate (PIP_3), the product of PI3K, is metabolized by the lipid phosphatase PTEN. Taniguchi *et al*. created a liver-specific knockout of the p85 subunit in mice and found that, contrary to expectations, these mice showed increased liver responsiveness to insulin and had lower circulating glucose, free fatty acids, and triglyceride concentrations than wild-type littermates. Muscle and adipose glucose utilization was also increased in the knockout mice. Although the knockout mice showed decreased hepatic PI3K activity and decreased levels of the p110 subunit (p85 stabilizes p110), insulin produced a prolonged elevation in hepatic PIP_3 and a higher activation of Akt, a kinase regulated by PIP_3, as compared to wild-type mice. The increase in PIP_3 appeared to be due to decreased PTEN activity in the livers of the knockout mice, suggesting that p85 regulates not only the production of PIP_3 but also its metabolism. — NRG

Proc. Natl. Acad. Sci. U.S.A. **103**, 12093 (2006).

CREDIT: ADAPTED FROM *ADV. MATER.* **18**, 1393 (2006)

www.sciencemag.org

Science

1200 New York Avenue, NW
Washington, DC 20005
Editorial: 202-326-6550, FAX 202-289-7562
News: 202-326-6500, FAX 202-371-9227

Bateman House, 82-88 Hills Road
Cambridge, UK CB2 1LQ
+44 (0) 1223 326500, FAX +44 (0) 1223 326501

Subscription Services For change of address, missing issues, new orders and renewals, and payment questions: 866-434-AAAS (2227) or 202-326-6417, FAX 202-842-1065. Mailing addresses: AAAS, P.O. Box 96178, Washington, DC 20090-6178 or AAAS Member Services, 1200 New York Avenue, NW, Washington, DC 20005

Institutional Site Licenses please call 202-326-6755 for any questions or information

Reprints: Author Inquiries 800-635-7181
Commercial Inquiries 803-359-4578
Corrections 202-326-6501

Permissions 202-326-7074, FAX 202-682-0816

Member Benefits Bookstore: AAAS/BarnesandNoble.com bookstore www.aaas.org/bn; Car purchase discount: Subaru VIP Program 202-326-6417; Credit Card: MBNA 800-847-7378; Car Rentals: Hertz 800-654-2200 CDP#343457, Dollar 800-800-4000 #AA1115; AAAS Travels: Betchart Expeditions 800-252-4910; Life Insurance: Seabury & Smith 800-424-9883; Other Benefits: AAAS Member Services 202-326-6417 or www.aaasmember.org.

science_editors@aaas.org	(for general editorial queries)
science_letters@aaas.org	(for queries about letters)
science_reviews@aaas.org	(for returning manuscript reviews)
science_bookrevs@aaas.org	(for book review queries)

Published by the American Association for the Advancement of Science (AAAS), *Science* serves its readers as a forum for the presentation and discussion of important issues related to the advancement of science, including the presentation of minority or conflicting points of view, rather than by publishing only material on which a consensus has been reached. Accordingly, all articles published in *Science*—including editorials, news and comment, and book reviews—are signed and reflect the individual views of the authors and not official points of view adopted by the AAAS or the institutions with which the authors are affiliated.

AAAS was founded in 1848 and incorporated in 1874. Its mission is to advance science and innovation throughout the world for the benefit of all people. The goals of the association are to: foster communication among scientists, engineers and the public; enhance international cooperation in science and its applications; promote the responsible conduct and use of science and technology; foster education in science and technology for everyone; enhance the science and technology workforce and infrastructure; increase public understanding and appreciation of science and technology; and strengthen support for the science and technology enterprise.

Information for Contributors

See pages 102 and 103 of the 6 January 2006 issue or access www.sciencemag.org/feature/contribinfo/home.shtml

TOOLS

Get the Drift

Animations and diagrams can provide a rough guide to continental movements over time. But for a more precise picture, head for the Plate Tectonic Reconstruction Service from the Ocean Drilling Stratigraphic Network, a consortium sponsored by two German universities. The calculator determines continental locations at any time in the last 150 million years. The basic mapper plots plate positions at a specific time, and the advanced mapper lets you enter the coordinates of a modern site and find its location at different points in the past. Forward-thinking users can even project future plate movements. >> www.odsn.de/odsn/services/paleomap/paleomap.html

EDUCATION

News You Can View

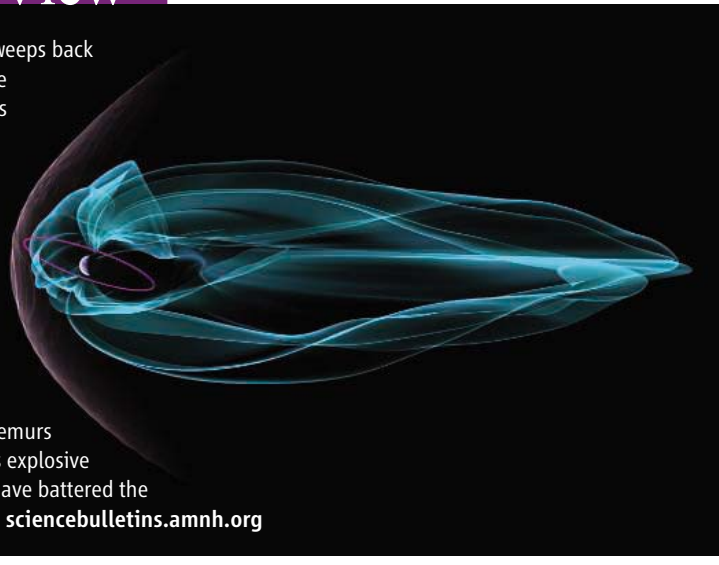

Constant buffeting from the solar wind sweeps back the outer layers of Earth's magnetosphere (shown in blue at right). The image comes from the American Museum of Natural History's Science Bulletins, which uses catchy multimedia to explain discoveries in astrophysics, earth science, and biology. Aimed at students and the general public, the site posts weekly Snapshots that focus on new findings, such as what recent studies of debris from the comet Tempel 1 reveal about its origins. Features let you spend time with researchers trying to save the imperiled lemurs of Madagascar and probing Yellowstone's explosive past—three massive volcanic eruptions have battered the area in about the last 2 million years. >> **sciencebulletins.amnh.org**

LINKS

The Making of Medicine

Curious about what kinds of parasites might have tormented Louis XIV? Want to learn about skull surgery in ancient Mesoamerica or how the PET scanner was invented? A good starting point is the History of Biomedicine, a virtual encyclopedia from the Karolinska Institute in Sweden that corrals links to hundreds of Web pages. The offerings follow the rise of Western medicine and science from the ancient Greeks to the 21st century, and include sections on other cultures such as China. You can connect to writings by figures such as the sanitary reformer Edwin Chadwick, whose 1842 report on the condition of Britain's poor concluded that "the annual loss of life from filth and bad ventilation are greater than the loss from death or wounds in any wars … in modern times." >> www.mic.ki.se/History.html

RESOURCES

Soil Saviors >>

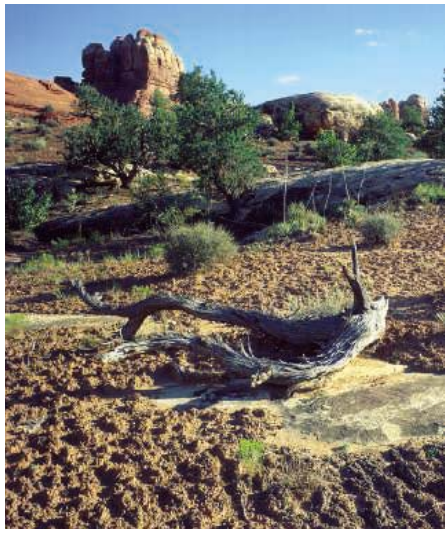

In dry ecosystems where plants are scarce, organisms such as cyanobacteria, mosses, and lichens keep the soil from blowing and washing away. These dirt-dwellers and the chemicals they release harden the surface, forming so-called biological soil crusts. Learn more about the crucial layer at this primer from the U.S. Geological Survey's Canyonlands Research Station in Moab, Utah. Get the basics at Crusts 101, which introduces the cast of organisms and explains the layer's ecological importance. Crusts not only provide stability, for instance, but they can increase the amount of water that percolates into the soil. Readers hungry for more can download a 90-page textbook. The gallery shows landscapes that boast healthy crust (right) and examples of the severe erosion that ensues when livestock or vehicles crush the delicate surface. >> www.soilcrust.org

IMAGES

Lights, Camera, Swim

To add some action to an oceanography lecture or just enjoy vibrant underwater footage, splash over to ReefVid from marine ecologist Peter Mumby of the University of Exeter in the U.K. The site is awash with more than 500 free video clips of reef life around the world. The videos, some of which run for several minutes, allow virtual divers to get the eye from a passing reef shark, plow through a throng of *Mastigias* jellyfish (left), and more. Visitors can watch the videos online or download them for use in PowerPoint presentations. >> www.reefvid.org

Send site suggestions to >> netwatch@aaas.org
Archive: www.sciencemag.org/netwatch

CREDITS (TOP TO BOTTOM): AMERICAN MUSEUM OF NATURAL HISTORY; USGS; PETER J. MUMBY

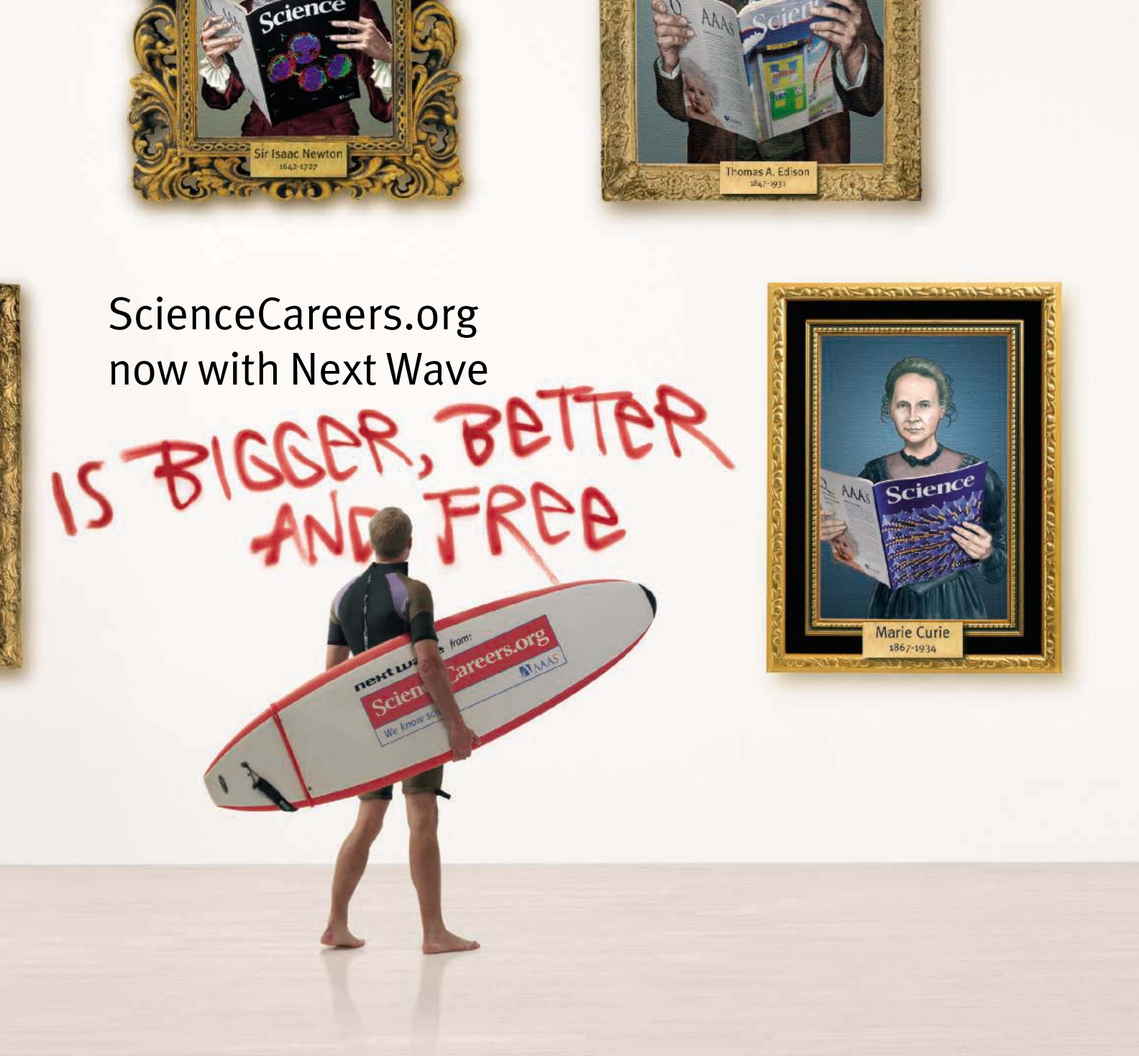

ScienceCareers.org now with Next Wave

ScienceCareers.org is the leading careers resource for scientists. And now it offers even more. In addition to a brand new website with easier navigation, ScienceCareers.org now includes Next Wave, the essential online careers magazine. Next Wave is packed with features and articles to help advance your science career – all for free.

- Hundreds of job postings
- Career tools from Next Wave
- Grant information
- Resume/CV Database
- Career Forum

www.sciencecareers.org

ScienceCareers.org
We know science AAAS

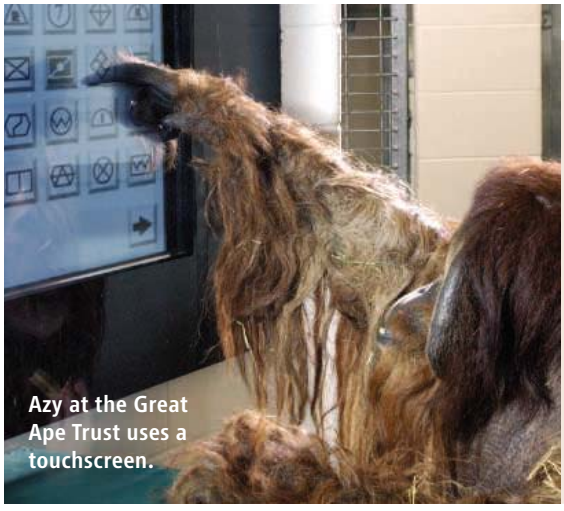
Azy at the Great Ape Trust uses a touchscreen.

can u turn on ur cam pls?

Webcams may be the hottest new thing in great ape culture. Orangutans from three continents could soon be communicating virtually and may even be able to present each other with bananas at the push of a button.

The idea came from Dutch conservationist Willie Smits, who runs an orangutan shelter and rehabilitation center in Borneo, Indonesia. Touchscreens will soon allow its residents to see and hear counterparts in Apenheul Primate Park in Apeldoorn, the Netherlands; later, the three orangutans at the Great Ape Trust of Iowa in Des Moines may go online as well.

The idea of Webcamming apes isn't far-fetched, says Josep Call of the Max Planck Institute for Evolutionary Anthropology in Leipzig, Germany, because the animals can understand video and learn to use computers. The main goal is to catch the public's imagination and make them aware of the grave threats—primarily deforestation—to orangutans' future, says Apenheul spokesperson Anouk Ballot. But getting hooked up will also "be a lot of fun" for the animals. It may offer research opportunities as well, says Rob Shumaker of the Great Ape Trust, who already uses touchscreens in studies of orangutans' ability to use symbols and syntax.

Mussel Power

When it comes to adhering to a surface, wet or dry, nothing beats a mussel. A new study sheds light on the bivalves' sticky secret.

An amino acid called DOPA is believed responsible for the remarkable qualities of mussel glue, which attaches the mollusks to surfaces via tough strings called byssal threads.

To test whether DOPA can bond with metal or body tissue, Phil Messersmith, a biomedical engineer at Northwestern University in Evanston, Illinois, and colleagues tethered a single DOPA molecule to the tip of an atomic force microscope. They then touched the tip to a titanium dioxide surface and measured the force needed to pull the DOPA off the surface. It took 800 piconewtons to do the trick—almost 4 times the force needed to break the strongest known protein link. When bonding to an organic surface, DOPA goes a step further, forming covalent bonds—the sharing of electrons between atoms—the researchers reported online last week in the *Proceedings of the National Academy of Sciences*. But unlike covalent bonds, the DOPA bond can re-form if the attachment is broken.


Mussels stick via hundreds of tough threads.

Herbert Waite, a marine biochemist at the University of California at Santa Barbara, says the study indicates that mussels can stick to virtually any surface. That property should be useful for biomedical devices, says Messersmith, who is testing whether DOPA can affix a nonstick polymer coating onto implants to prevent buildup of materials from blood.

LOOKING FOR UGLY SHEEP >>


Extremely bald sheep.

Australian scientists are hoping to find a few good mutants among the nation's 100 million sheep, mostly highly prized merinos.

In an effort to improve the breed, the South Australian Research and Development Institute has launched a campaign to locate "extreme sheep" throughout the country. "We are trying to encourage wool producers here to retain sheep they would otherwise cull, so that we can study what is going wrong in [their] skin and follicles," explains Simon Bawden, a molecular biologist at the institute.

Advertisments have drawn 10 samples from sheep with various skin and hair problems, such as highly matted wool, straight rather than crimped fibers, or bare patches. The team hopes to find the relevant genes so breeders can eventually produce sheep with finer, stronger, and more plentiful wool.

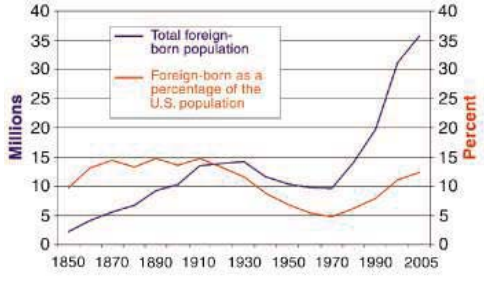

U.S. POPULATION GROWS, DIVERSIFIES

While population growth in poor countries is booming, growth in developed nations has ceased—with the exception of the United States, which is slated to hit the 300 million mark this fall. "The number 3 spot in global population [after China and India] is something that we are likely to hold onto for a very long time," said demographer Carl Haub of the Population Reference Bureau of Washington, D.C., which last week issued its annual World Population Data Sheet.

As the chart above shows, the percentage of non-native born U.S. residents is now approaching late 19th-century levels after hitting a low of 5% in 1970.

CREDITS (TOP TO BOTTOM): GREAT APE TRUST; *THE STOCK JOURNAL*; PHILLIP MESSERSMITH/NORTHWESTERN UNIVERSITY; SOURCE: POPULATION REFERENCE BUREAU

Frozen treasure 1029

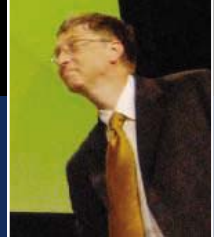

Promises unfulfilled 1031

AVIAN INFLUENZA

Pushed by an Outsider, Scientists Call for Global Plan to Share Flu Data

In an unexpected show of cooperation, scientists from more than 30 countries have announced a plan to start sharing their often closely held data on avian influenza. A group of influenza researchers, experts in intellectual property and bioinformatics, and a sprinkling of Nobel laureates are calling for a global consortium whose members would commit to putting any genetic data from bird flu into the public domain as soon as possible. Their letter is slated to be published online by *Nature* this week.

Peter who? Completely unknown in the influenza world, consultant Peter Bogner (*left*) played an important role in uniting scientists, says CDC's Nancy Cox (*right*).

"I am so happy. I feel that maybe I should quit working and start arranging flowers," says Ilaria Capua, a virologist at Istituto Zooprofilattico Sperimentale delle Venezie in Legnaro, Italy, who kicked off the debate in March when she called for such global openness (*Science*, 3 March, p. 1224). But other flu researchers caution that many key details remain to be fleshed out, including how to get the governments of affected countries to comply with the deal.

In a strange twist, a key figure in the initiative is a strategic consultant and former TV executive from Santa Monica, California, named Peter Bogner. A complete outsider to the flu community, Bogner co-authored the statement and traveled the world on his own dime in the past few months collecting signatures. Bogner has "been extremely important as a catalyst," says Nancy Cox, chief of the influenza division at the U.S. Centers for Disease Control and Prevention (CDC) in Atlanta, Georgia, another key player.

Analyzing the genomes of avian influenza samples allows scientists to understand how the virus is spreading and changing over time. But the sequence of many isolates is not publicly available. Some governments don't want to release raw sequence data because it might disadvantage their own scientists or because the information might be used commercially. Some scientists also withhold sequence data while preparing a paper. At the initiative of the World Health Organization (WHO), however, much of the data are available to about 17 labs in a password-protected compartment of the flu database at Los Alamos National Laboratory in New Mexico. WHO defends that system as a way to allay the concerns of some governments while giving key researchers access. But critics argue that all researchers should be able to study the data.

Participants in the Global Initiative on Sharing Avian Influenza Data, as the new group is called, promise to enter any new sequences into publicly available databases such as GenBank as soon as possible, but no later than 6 months after they are generated. The signatories include the heads of WHO's four Collaborating Centers (CDC and its counterparts in Parkville, Australia, London, and Tokyo), Malik Peiris of the University of Hong Kong, Chen Hualan of the Animal Influenza Laboratory of the Chinese agriculture ministry, and many others. Among the five Nobelists are genome veteran John Sulston of the Wellcome Trust Sanger Institute in Cambridge, U.K., and Harold Varmus, president of the Memorial Sloan-Kettering Cancer Center in New York City.

The letter does not spell out how the consortium would operate or how it would protect the intellectual-property rights of those who contribute data. Cox says an international advisory board will hash out such policies. Bogner plans to enlist experts at Creative Commons, an organization that offers flexible copyright licenses on the Internet, and CAMBIA, an independent research institute in Canberra, Australia, that fosters collaboration in the life sciences.

The roster of more than 50 signatories includes some who remain skeptical. "I am not sure if it will be effective," says Masato Tashiro, who directs the WHO Collaborating Center in Tokyo and thinks researchers should share virus strains as well as genomic data to accelerate vaccine development. Robert Webster of St. Jude Children's Research Hospital in Memphis, Tennessee—who signed on after "Ilaria Capua pulled my chain a bit"—agrees. Still, "it's a very important first step," says David Lipman, director of the National Center for Biotechnology Information in Bethesda, Maryland. A WHO spokesperson said last week that the agency is studying the letter.

Bogner's role is a bit of an enigma even to those who have worked closely with him. Born in Germany in 1964, Bogner came to the United States in the early 1980s and worked in the TV industry there and abroad before starting his own strategic consulting firm. He says he knew "almost nothing" about flu until he heard about Capua's campaign a few months ago and decided to help out. Well-connected and a frequent participant at the annual celebrity-studded World Economic Forum in Davos, Switzerland, Bogner says he used his "talent to make people talk to each other" to broker the letter. "He certainly has a lot of energy," says Lipman.

Capua says Bogner initially suggested that he was working for U.N. Secretary-General Kofi Annan. Bogner says that the U.N. is one of his clients but not on this issue; indeed, he says, he hasn't been paid a cent for his flu efforts. "In fairness, there are some aspects of this whole story I don't quite understand," says Capua. "But we're getting what we want."

–MARTIN ENSERINK

With reporting by Dennis Normile in Tokyo.

CREDIT: CDC

A really big dig
1034

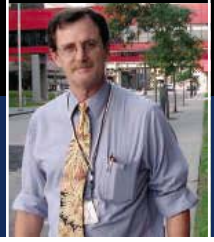

New Orleans bounces back
1038

MATHEMATICS

Perelman Declines Math's Top Prize; Three Others Honored in Madrid

On Tuesday in Madrid, Spain's King Juan Carlos kicked off the International Congress of Mathematicians by awarding the closest equivalent to a Nobel Prize in math to three young stars (see sidebar, below). But the name on everybody's lips was that of the mathematician who had refused his Fields Medal: Grigory Perelman. The 40-year-old Russian recluse was to have been honored for his proof of the legendary Poincaré conjecture. Instead, his refusal added another chapter to the controversial and colorful saga of the problem and its proof.

First posed in 1904, the Poincaré conjecture has become larger than life because of its apparent simplicity and because so many strong mathematicians tried unsuccessfully to solve it. In 1979, William Thurston, then of Princeton University, upped the ante with a more sweeping version called the geometrization conjecture. Finally, in 2000, the newly formed Clay Mathematics Institute (CMI) focused public attention on the problem by placing a $1 million bounty on the Poincaré conjecture, as well as six other problems. In 2002, Perelman posted two preprints on the Internet, totaling 70 pages, which claimed to outline a complete solution of the geometrization conjecture. (That implies a proof of the Poincaré conjecture, which Perelman did not even mention.)

Perelman used a strategy called "Ricci flow," which Richard Hamilton of the State University of New York, Stony Brook, had developed starting in the early 1980s. Perelman met Hamilton and became interested in Ricci flow while visiting the United States in the early 1990s. In 1995, he returned to his native Russia and dropped off the radar screen of Western mathematicians. His 2002 preprints were a bombshell. The following spring, he backed up his claim in a series of invited lectures at Stony Brook and the Massachusetts Institute of Technology (MIT) in Cambridge (*Science*, 18 April 2003, p. 417). And then he disappeared again, leaving others to check his proof and explain it to the world.

Three manuscripts

Three pairs of mathematicians stepped up to the challenge. This April, Huai-Dong Cao of Lehigh University in Bethlehem, Pennsylvania, and Xi-Ping Zhu of Zhongshan University in China published a 300-page refereed article in the *Asian Journal of Mathematics*. Their paper departs from Perelman's proof in certain key places, "due to the difficulties in understanding Perelman's arguments at these points," in the authors' words. The paper ▶

2006 Fields Medal Recipients >>

(*From left to right*) Andrei Okounkov, Wendelin Werner, Terence Tao, and Grigory Perelman (declined award).

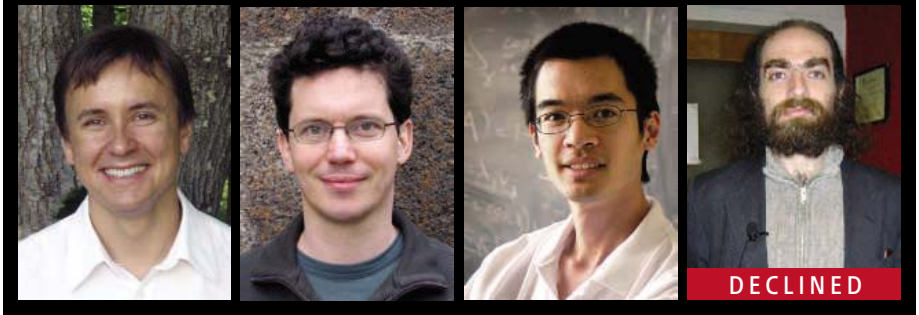

Okounkov, Tao, and Werner Capture Fields Medals, 'Math's Nobels'

The Fields Medal is awarded every 4 years to recipients who by custom are 40 years old or younger. This year's honorees:

• **Andrei Okounkov** of Princeton University, 37, for work that connects the relatively new theories of random matrices and random surfaces to classical ideas of algebraic geometry and combinatorics. His work with Richard Kenyon of the University of British Columbia in Vancouver, Canada, involves a model of random surfaces called the "dimer model," formed by randomly pairing up triangles in a lattice (see figure). Okounkov and Kenyon proved that the boundary between the "melted" region and the "frozen" regions (here shown in yellow) approximates a particular type of curve given by polynomial equations.

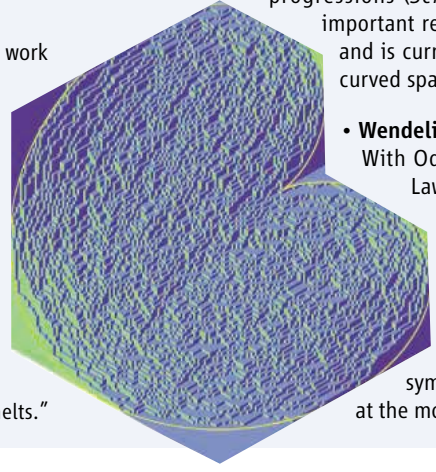

Have a heart. Okounkov's work predicts shape of a mathematical crystal as it "melts."

• **Terence Tao** of the University of California, Los Angeles, 31. His best-publicized work was a proof with Ben Green of the University of Bristol in the U.K. of a long-unsolved conjecture in number theory—namely, that the sequence of prime numbers contains arbitrarily long arithmetic progressions (*Science*, 21 May 2004, p. 1095). He has done important research in geometry and mathematical physics and is currently exploring the vibrations of a surface in a curved space.

• **Wendelin Werner** of Université de Paris-Sud, Orsay, 37, With Oded Schramm of Microsoft Research and Greg Lawler of Cornell University, Werner derived new precise estimates of the amount of irregularity in a Brownian motion trajectory as part of studying phase transitions in two dimensions (*Science*, 8 December 2000, p. 1883). He helped show that various other random processes, such as percolation, have a special symmetry property known as conformal invariance at the moment they undergo a phase transition. **–D.M.**

CREDITS (TOP TO BOTTOM): A. OKOUNKOV/PRINCETON UNIVERSITY

allowed Cao and Zhu to claim "the first written account of a complete proof of the Poincaré conjecture and the geometrization conjecture of Thurston."

In June, Bruce Kleiner and John Lott of the University of Michigan, Ann Arbor, released a manuscript that had evolved publicly online since Perelman's visit. Its gradually increasing detail helped cement the community's acceptance of Perelman's work. "They were the main people who carried the torch forward over the last 3 years," says Michael Anderson of Stony Brook University. Finally, last month, John Morgan of Columbia University and Gang Tian of MIT completed a manuscript that will be published as a book. Their work, like Kleiner and Lott's, sticks closely to Perelman's outline.

Perelman's exegetes have played a crucial role in making his work accessible to other researchers, says James Carlson, president of CMI. "Like a program written in open-source code, many eyes will be looking at it," he says. "Instead of having to work out the arguments by themselves, mathematicians will be left with the much easier task of verifying that the worked-out details are correct."

The wait begins

According to CMI's rules, the $1 million for each Millennium Prize can be presented 2 years after the proof is published in a refereed journal. Even though Perelman's own papers have never been formally published, Carlson confirms that the clock is now ticking toward awarding the first prize. "Close to 2 years from now, we will form a committee to study the issue," Carlson says.

Shing-Tung Yau of Harvard University thinks that Hamilton deserves a share. "For 20 years, he worked on this problem alone, with some help from me. The part he proved is absolutely nontrivial, and it was devised purposely to solve this problem," says Yau. At present, however, Yau's seems to be a minority view. "Perelman broke through the barriers," says Robert Greene of the University of California, Los Angeles. "If Perelman's papers didn't exist, I think we would still be stuck. It's the unsticking that counts."

Some mathematicians who know him, however, think Perelman would simply decline the Millennium Prize as well. "When I talked with him at Stony Brook [in 2003], I had the impression that he's not interested in it at all," Anderson says. If Perelman refuses the award, Carlson says, CMI may consider other uses for the $1 million, such as contributing it to Russian mathematics or to the International Mathematics Olympiad, which Perelman won with a perfect score in 1982. **–DANA MACKENZIE**

Dana Mackenzie is a writer in Santa Cruz, California.

PALEOANTHROPOLOGY

Skeptics Seek to Slay the 'Hobbit,' Calling Flores Skeleton a Modern Human

Strange new hominid or just another modern human? That's still an open question for the "hobbit" bones unearthed in Liang Bua cave on the Indonesian island of Flores. Their discoverers described them 2 years ago as a new species, *Homo floresiensis*, but critics have insisted from the start that the leading specimen, a 1-meter-tall, 18,000-year-old skeleton with a brain the size of a grapefruit, was that of a diseased *Homo sapiens*.

Hobbit critic. Teuku Jacob and Etty Indriati argue that the tiny Flores skull (different skull pictured here) is that of a diseased modern human.

This week, the skeptics laid out their most detailed case yet in the *Proceedings of the National Academy of Sciences* (*PNAS*). The paper argues that living people have some of the traits claimed to be unique to *H. floresiensis*, and that the lone skull is simply deformed. "This is not a new species," says co-author Robert Eckhardt of Pennsylvania State University in State College. "This is a developmentally abnormal individual."

But the hobbit's discoverers and others who have also studied the original specimens are unimpressed. "Complete nonsense," snaps Peter Brown of the University of New England in Armidale, Australia, who did the original anatomical analyses. The paper "cherry-picked features and ignored counterevidence," adds Susan Larson of Stony Brook University in New York, who has linked the hobbit shoulder to an ancient human species, *H. erectus* (*Science*, 19 May, p. 983). "Nothing they say has caused me to question my assessment."

The new paper is the first full-length critique in a high-profile journal, and researchers on both sides have long awaited the data in it. The authors include Teuku Jacob of Gadjah Mada University in Yogyakarta, who in a contentious incident borrowed the Flores bones for study in November 2004 (*Science*, 25 March 2005, p. 1848). In 2005, Jacob and others, including Gadjah Mada colleague Etty Indriati, also studied 76 modern Rampasasa pygmies living only a few kilometers from Liang Bua cave.

The team uses several lines of evidence to challenge the hobbit's novelty. One new argument is that a hominid could not have evolved in isolation on Flores because fossils show that elephants reached the island twice, and so humans probably also arrived more than once; lack of isolation would have prevented the evolution of a new dwarf species, they say.

The team further argues that the skull, part of the specimen labeled LB1, is so asymmetrical that it must have suffered from a developmental deformity. Mirror imaging the left side of LB1's skull and putting those halves together creates a distinctly different face than two right halves put together in the same way.

The paper also reports new data showing that some Rampasasa pygmies lack chins and have odd premolar teeth, features identified as distinctive in *H. floresiensis*. The original work on the Liang Bua bones "largely looked for 'otherness'—finding reasons to believe that this population is entirely different from anything that has been seen before," says Indriati. "That simply isn't true." The Rampasasa results are "relevant and revealing," agrees Robert D. Martin of the Field Museum in Chicago, Illinois, who has argued in print that LB1 suffered from microcephaly, a genetic disorder marked by a puny brain.

But other experts are fiercely critical of the *PNAS* paper. "My first reaction was, 'How did this get published? Was there any peer review?' " says brain evolution expert Ralph Holloway of Columbia University. (Eckhardt reports that there were five ▶

CREDIT: E. INDRIATI

external reviewers, chosen by the team in accordance with *PNAS* guidelines.) Holloway adds that he thinks the brain of LB1 shows "possible pathologies" but not for the reasons cited by Jacob and his co-authors.

Others are ready to rebut each point in the paper. The first elephant colonization was too early to have any bearing on the hobbit debate, says Russell Ciochon of the University of Iowa in Iowa City. And the paper's focus on skull distortion is misplaced, adds Brown, because it happened after death, when the specimen was buried deeply in the cave.

As for the treatment of chins, which relies on a photo of a living Rampasasa, it is "superficial indeed," because one must look at a jaw without its covering of flesh to see whether a chin is present, says Colin Groves of Australian National University in Canberra. (Groves and colleagues compare the hobbit to microcephalics and modern humans, including those from Asia, and conclude in a paper in press in the *Journal of Human Evolution* that it is indeed a new species.) Other details, such as claimed signs of pathology in LB1's leg bones, constitute "a flimsy house of cards," says Bill Jungers of Stony Brook University, who studied the bones last year in Jakarta.

Given these flatly contradictory statements, it's likely to take some time for the field to settle on a coherent view of ancient hobbits. "We have a ways to go before the controversy is resolved," says Indriati. The battle of the shire is far from over.

–ELIZABETH CULOTTA

ARCHAEOLOGY

After 2 Millennia on Ice, a Nomad Resurfaces

BERLIN—Decked in a magnificent fur mantle and gilded wooden headdress, a nomad—probably a fierce warrior—was buried more than 2200 years ago in the icy highlands of Mongolia. This week, a team of archaeologists, led by Hermann Parzinger, director of the German Archaeological Institute in Berlin, announced that they had found his partially mummified remains. The finding will reveal more about the culture and conditions that preserved the body. It is urgent work, observers say, because a warmer environment could destroy specimens like this.

In 2004, the 30-member team from Germany, Russia, and Mongolia surveyed more than a dozen stone-covered burial mounds in northwestern Mongolia. Last year, they returned to the 2600-meter-high plateau in the Altai region, a remote mountain range that borders Russia, China, and Mongolia, with electromagnetic sensors, temperature probes, and other instruments to look for ice layers that might indicate intact burials.

Well preserved. A Scythian buried with fur, felt boots, and horses.

CREDIT: GERMAN ARCHAEOLOGICAL INSTITUTE

Parzinger has made spectacular finds before. In 2001, he pulled nearly 20 kilograms of artfully worked jewelry out of a similar grave mound in the Russian republic of Tuva. Archaeologists say the Altai plateaus are the burial grounds of the Pazyryk, members of a larger Scythian culture that occupied Central Asia as early as the 9th century B.C.E. and struck fear into the hearts of the ancient Greeks and Persians.

Scythians used a distinctive type of embalming, says Esther Jacobson-Tepfer, an archaeologist and art historian at the University of Oregon, Eugene. "They removed the innards and filled the body with sweet-smelling grasses." High-status individuals were dressed, surrounded by goods, and buried under earth and stone mounds, or kurgans.

Shortly after burial, water sometimes seeped through the stones and froze, forming ice lenses insulated by the stone mounds above and permafrost underneath. The body found this summer was surrounded by slain horses and dressed in felt boots. Fantastical animal tattoos were visible on the man's skin. "Instead of archaeology, the material culture is so well preserved it's almost a kind of ethnography," Parzinger says.

Parzinger's success comes as the Altai's permafrost is melting fast. "The warming up of the general climate is a danger for these kurgans," Parzinger says. As rising temperatures threaten to bring the mummies out of deep freeze, the Scythian royalty may face decay and disintegration for the first time in millennia.

–ANDREW CURRY

Andrew Curry is a writer in Berlin.

Controls Sought . . .

AIDS researchers have known for years that a small percentage of people infected with HIV do not show symptoms of the disease, but they have yet to understand why. Now immunologist Bruce Walker of Massachusetts General Hospital in Boston has identified about 100 so-called elite controllers in the Boston area and says that dozens of investigators want to join an international consortium he's organizing to uncover genetic or immunological clues to this group's good health.

Elite controllers—thought to number about 3000 in the United States—by definition show no immune damage and have unusually low levels of the AIDS virus in their blood 1 year after being infected, despite taking no anti-HIV drugs. Walker says a consortium could perform haplotype mapping of the controllers, comparing their genes with those of uninfected people. One key difference encoded within the controllers' DNA, for example, may be high levels of so-called PD-1 receptors; these immune cell surface proteins, Walker's lab reported online 20 August in *Nature*, appear to play a key role in controlling HIV replication.

The proposed effort, for which Walker has received $2.5 million from the Mark and Lisa Schwartz Foundation to launch, "could provide important insights into what's important to intervene with prevention strategies," says virologist Douglas Richman of the University of California, San Diego, who has joined the consortium.

–JON COHEN

. . . Controls Eased

The U.S. Department of Defense (DOD) has abandoned a controversial proposal that would have required universities to keep a watchful eye on foreign nationals involved in defense research. DOD proposed the rules 13 months ago to prevent the transfer of sensitive technologies to countries seen as security threats. Under the proposal, universities not only had to supplement the normal export licenses for the researchers with new "unique badging requirements" but also with "segregated work areas" for foreigners (*Science*, 22 July 2005, p. 544). Academic lobbyists said that a tougher regime would scare off needed foreign expertise and that existing rules were sufficient.

Now the Pentagon has removed the badging and separate work area requirements, bringing its rules in line with those at the Commerce and State departments. "We're pleased," says Toby Smith of the Association of American Universities of the plan, for which comments will be accepted until 13 October.

–YUDHIJIT BHATTACHARJEE

Double Bill. Former U.S. President Bill Clinton and the world's richest man, Bill Gates, packed the hall at the 2006 international AIDS conference.

INFECTIOUS DISEASE

At International AIDS Conference, Big Names Emphasize Big Gaps

TORONTO, CANADA—When Bill and Melinda Gates gave the keynote speech here at the XVI International AIDS Conference, it signaled that this mega, biannual meeting had evolved far from its roots as the premier gathering for researchers to swap their latest scientific findings. "It's a marker that AIDS has made it as one of the landmark issues of our times like global warming and security issues," said Peter Piot, who heads the Joint United Nations Programme on HIV/AIDS.

The Gateses—whose foundation has committed $1.9 billion to battling the epidemic—helped set the tone for the gathering, during which scientists, clinicians, activists, and celebrities repeatedly emphasized that more needs to be done to prevent and treat HIV infection. "We know more, and we have more, and there's a greater will to do more," said Helene Gayle, co-chair of the meeting, which attracted 26,000 attendees and ran from 13 to 18 August. But, she added, "there are still too many areas where we're not doing enough."

According to new figures from the World Health Organization (WHO), at the end of June 2006, 6.8 million infected people in low- and middle-income countries needed anti-HIV drugs, but only 1.65 million were receiving them. "We're still behind the eight ball," said former U.S. President Bill Clinton, whose foundation helps countries negotiate lower prices for antiretroviral drugs. Scaling up access to drugs won't solve all problems, either. "We can't treat ourselves out of this epidemic," said epidemiologist Kevin De Cock, the new head of WHO's HIV/AIDS program. In his keynote speech, Bill Gates did a crude mathematical exercise and concluded that, with 38.6 million infected people in the world, it would soon cost a minimum of $13 billion a year just for the drugs required to treat everyone in need. "Treatment without prevention is simply unsustainable," he said.

A key limitation to both treatment and prevention efforts is that 90% of infected people do not know their status. De Cock and many others stressed the need to move beyond voluntary counseling and testing to "provider-initiated testing," in which health-care workers recommend, without insisting, that people get screened for HIV. Botswana for the past 2 years has increased testing with this "opt-out" policy, and nearby Lesotho recently launched a "know your status" campaign.

With trials ongoing in several countries, one of the most promising prevention strategies is pre-exposure prophylaxis (PrEP)—providing anti-HIV drugs to the uninfected. Leigh Peterson of Family Health International in Research Triangle Park, North Carolina, described the combined results of studies in Nigeria, Ghana, and Cameroon that involved 936 women at high risk of becoming infected. The women took either the anti-HIV drug tenofovir or a placebo each day. Although too few infections occurred to determine whether PrEP worked, the researchers mainly aimed to assess safety, and no one appeared harmed by the drug. Nor was there any indication that PrEP encouraged people to take more risks, as some feared: Women in both arms of the study reported using condoms more frequently than at the trial's start and also reduced their number of sexual partners. "They're very intriguing results," said Kenneth Mayer, who directs the Brown University AIDS Program in Providence, Rhode Island.

Uganda has been widely praised for reducing HIV prevalence in the 1990s, in part through campaigns that led people to limit their number of partners. But results from a large, multiyear study suggest that such gains are hard to sustain. In the Masaka district—chosen as a representative rural area—prevalence increased in both men (5.6% to 6.7%) and women (6.7% to 8.9%) between 2000 and 2005. New infection rates also were strikingly high in men between the ages of 40 and 49. Leigh Anne Shafer, an epidemiologist with the U.K.'s Medical Research Council who conducted the study with the Uganda Ministry of Health, said she does not know what accounts for the rising prevalence but thinks that people may have "prevention fatigue," leading to increased risky sexual behavior.

More disturbing news came from a report suggesting that "extensively" drug-resistant (XDR) tuberculosis—in which people fail all TB drugs—may be a much more widespread problem than appreciated. Worldwide, only 347 cases of XDR were identified between 2000 and 2004. But Neel Ghandi of Albert Einstein College of Medicine in New York City reported here that of 544 tuberculosis patients in KwaZulu-Natal, South Africa, 53 were dually infected with HIV and XDR TB; 52 died quickly. "It's ominous," says Gerald Friedland of Yale University, who headed the study. "XDR TB may be present in other locations, but it has not been looked for because it requires culturing TB, and that's minimally available in Africa. It needs to be looked for more aggressively now."

On a more hopeful note, researchers reported encouraging new data about an anti-HIV drug from Merck that won much attention this winter (*Science*, 17 February, p. 943) for rescuing people who had developed resistance to every other antiretroviral drug. A 24-week study showed that this so-called integrase inhibitor, when given in combination ▶

CREDIT: GETTY IMAGES

with other antiretroviral drugs to previously untreated people, quickly reduced the virus to undetectable levels. "This is a tremendous drug," said Joseph Eron, a clinician at the University of North Carolina, Chapel Hill, who has patients in the study.

The usual roar of AIDS activists assailing governments and researchers was muted this year, as attendees from many quarters blasted South Africa's leaders for still flirting with the idea that HIV doesn't cause AIDS. Canadian Prime Minister Stephen Harper also attracted scathing reprimands from activists, researchers, and even a U.N. official for not attending the meeting. "Your action sends a message that you do not regard HIV/AIDS as a critical priority," charged conference co-chair Mark Wainberg, who heads the McGill University AIDS Centre in Montreal, Canada. "Clearly all of us here tonight disagree with you." Wainberg received a standing ovation. **–JON COHEN**

STEM CELLS

Scientists Derive Line From Single Embryo Cell

In an advance touted as a way around the current political logjam, scientists have developed a method for deriving human embryonic stem (hES) cell lines without destroying an embryo. Although not yet very efficient, the technique, reported online in *Nature* this week, could in theory allow scientists to derive new hES cell lines that might be eligible for federal funding under current rules.

In the past few years, scientists have proposed several alternatives to deriving hES cells that would not require destruction of a human embryo (*Science*, 24 December 2004, p. 2174). One idea is to grow a cell line from a single cell removed from an early embryo, leaving the rest of the embryo intact. Doctors do such biopsies when they perform preimplantation genetic diagnosis (PGD), which allows a couple undergoing in vitro fertilization (IVF) to screen out embryos carrying genetic diseases.

Last year, Robert Lanza of Advanced Cell Technology (ACT) in Worcester, Massachusetts, and his colleagues reported that they had found a way to culture a single cell from an early mouse embryo so that it grew into a line of hES cells (*Science*, 21 October 2005, p. 416). Now they have refined their technique to apply it to human cells.

The ACT scientists thawed 16 frozen embryos donated by couples who had undergone IVF treatments and no longer needed the embryos. The team then allowed the embryos to develop to the morula stage, at which the embryo contains 8 to 16 cells, also called blastomeres. They used a pipette to separate the blastomeres and then cultured each one separately to see whether it would grow into an hES cell line. More than half of the 91 blastomeres divided at least once, and 28 formed clumps that grew in culture.

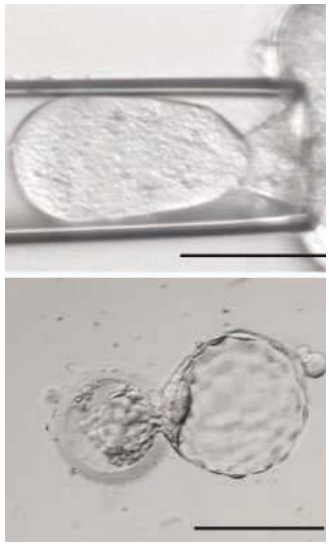

Light touch. A single cell taken from an eight-cell human embryo (*top*) can be coaxed to grow into an hES cell line, while the rest of the embryo can develop to the blastocyst stage (*bottom*) and beyond.

CREDIT: *NATURE*

The scientists transferred the clumps to cultures in which other hES cells, marked with green fluorescent protein, were already growing. In two cases, the transferred cells grew into cultures that behaved like hES cells. (In others, they failed to grow or grew into cells resembling trophectoderm, the cells that go on to form the placenta.)

Lanza says researchers could use the technique to derive hES cells from embryos undergoing PGD. Researchers could allow the removed blastomere to grow overnight, giving it time to divide. One cell could then be used for the genetic diagnosis, and the other could be cultured into an hES cell line. The embryo could be implanted and go on to develop into a full-term pregnancy.

James Battey, chair of the Stem Cell Task Force at the National Institutes of Health (NIH) in Bethesda, Maryland, says the paper is an interesting proof of principle but doesn't resolve all ethical and legal questions. Federal law prohibits funding for work that "endangers" human embryos, he notes. Because the PGD biopsy does carry some risk to the embryo, he says, it's not clear whether cells derived using the new technique would be eligible for NIH funds.

–GRETCHEN VOGEL

Embryo Law Reconsidered

Australia's Parliament is expected next month to debate ending its 4-year-old ban on therapeutic cloning. Prime Minister John Howard had long supported the ban and opposed any such debate, but last week, he said he would allow a "conscience" vote on the issue.

Former health minister Kay Patterson is drafting a bill to allow the work, and Parliament watchers say a vote is likely unless Howard relents. If a vote happens, says backbencher Mal Washer, it has a good chance of passing. "I think we'll have more people vote for this bill than we had for RU-486," he said in a radio interview, referring to a recent vote that eased restrictions on the use of the abortion drug.

–ELIZABETH FINKEL

Pounds for Papers

The American Physical Society (APS), a leading publisher of physics journals, will next month make full-text articles free for all to read online when they're published—for a one-time fee that anyone can pay. Many commercial and nonprofit journals already offer a pay-for-open-access option; some rely entirely on author fees so they can be free to all readers. APS said last week that it will begin by charging a per-article fee of $975 for its *Physical Review* journals and $1300 for the elite *Physical Review Letters*. APS Editor-in-Chief Martin Blume calls the move a step toward "possibly being fully open access someday." At least one institution wants to pay; CERN, the European particle physics lab near Geneva, Switzerland, aims to raise funds to make all particle physics papers freely accessible.

–JOCELYN KAISER

New Vatican Astronomer

George Coyne, the Vatican astronomer who has been a vocal critic of intelligent design, has been fired. Last week, the Vatican announced that Coyne, 73, is being replaced by Argentinian astronomer and Jesuit priest José Gabriel Funes. Last fall, Coyne had a public conflict with Cardinal Christoph Schönborn, a critic of evolution and close adviser to Pope Benedict XVI.

Coyne, Vatican astronomer since 1978, could not be reached for comment but will remain on the staff of the Vatican Observatory Research group at the University of Arizona, Tucson. Lawrence M. Krauss, a physicist at Case Western Reserve University in Cleveland, Ohio, who is involved in the evolution conflict, says the news came as "a shock."

–CONSTANCE HOLDEN

SPACE SCIENCE

NASA Chief Blasts Science Advisers, Widening Split With Researchers

NASA Administrator Michael Griffin this week read the riot act to the outside scientists who advise him, accusing them of thinking more of themselves and their research than of the agency's mission. Griffin's harsh comments come on the heels of the resignation of three distinguished scientists from the NASA Advisory Council (NAC), two of whom have questioned Griffin's plan to dramatically scale back a host of science projects (*Science*, 12 May, p. 824).

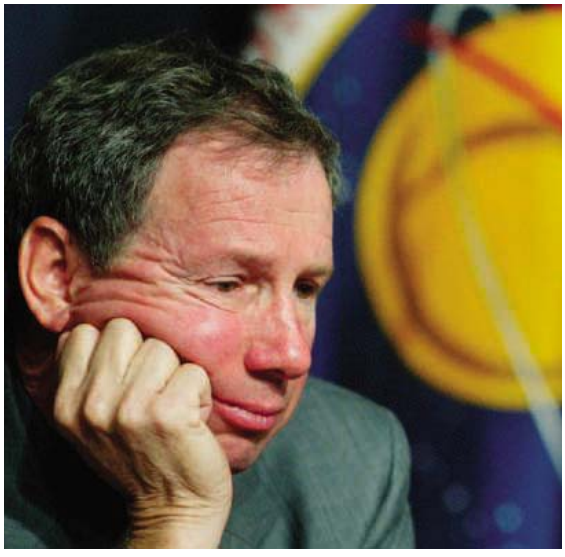

Unhappy family? NASA's Michael Griffin and his science advisers aren't on the same page.

"The scientific community … expects to have far too large a role in prescribing what work NASA should do," Griffin wrote council members in a blistering 21 August message. "By 'effectiveness,' what the scientific community really means is 'the extent to which we are able to get NASA to do what we want to do.' "

The outside engineers, scientists, and educators on the council traditionally offer advice on the agency's policies, budget, and projects. Placed in limbo for nearly a year after Griffin took over as NASA chief in spring 2005, NAC was reorganized this spring under the leadership of geologist Harrison Schmitt, a former U.S. senator and Apollo astronaut who is very enthusiastic about President George W. Bush's plans to send humans back to the moon and to Mars. Schmitt replaced Charles Kennel, director of the Scripps Institution of Oceanography in San Diego, California, who resigned last week from his post as chair of the council's science committee. Two other NAC members—former NASA space science chief Wesley Huntress and Provost Eugene Levy of Rice University in Houston, Texas—resigned last week in response to a direct request from Griffin that they step down.

Schmitt and members of that committee have clashed repeatedly in recent months over the role of science at the space agency. In a pointed 24 July memo to science committee members, Schmitt complained that they lacked "willingness to provide the best advice possible to Mike," refused to back Griffin's decision to cut research funds for astrobiology or recommend an alternative cut, and resisted considering the science component of future human missions to the moon. "Some members of the committee," he concluded, "are not willing to offer positive assistance to Mike."

Both Levy, a physicist, and Huntress, an astrochemist now at the Carnegie Institution of Washington, D.C., say they support human space exploration but fear that science is now taking a back seat after years of a careful balance between human and robotic efforts. NASA spokesperson Dean Acosta acknowledged that the scientists and Schmitt "weren't working well together," and that Griffin telephoned Huntress and Levy last week to ask for their resignations. Griffin's memo points to what he calls "the inherent and long-standing conflict of interest" of giving advice to an agency on which members depend for funding. And he offers them a clear way out. "The most appropriate recourse for NAC members who believe the NASA program should be something other than what it is, is to resign."

Huntress says Griffin told him that his advice exceeded the council's charge. "This is a different NAC. Our advice was simply not required nor desired," Huntress told *Science*. The current council, he adds, "has no understanding or patience for the science community process." Kennel, who had been named chair of NAC's science committee, was unavailable for comment, but Norine Noonan, a former NAC member and dean of math and science at the College of Charleston in South Carolina, called Griffin's action "very distressing" for scientists. "If we can't have a robust debate at the NAC level," she says, "then where in the heck is it supposed to happen?"

–ANDREW LAWLER

CHEMISTRY

New in Nanotech: Self-Folding Delivery Boxes

"Some assembly required." Those words on a box from the store spell agony for a parent. Chemists face similar headaches while designing new drug-delivery agents or trying to control their actions in the body. But researchers in Maryland may have found a pain reliever.

In a paper published online last week in the *Journal of the American Chemical Society*, researchers at Johns Hopkins University in Baltimore, Maryland, reported creating tiny two-dimensional cutouts that fold themselves up into porous cubes and other 3D containers. The containers can then be used to ferry compounds to a site where chemists want them to react. Metal versions can even be steered there using magnetic fields.

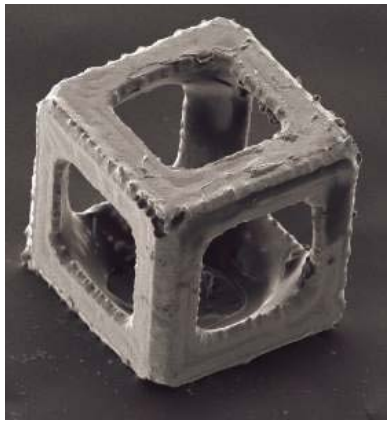

Presto. A series of six flat squares fold themselves into 3D cubes.

Researchers say the new nanocontainers could be useful as novel drug-delivery vehicles and in tiny lab-on-a-chip reactors. "This is very elegant work," says Mauro Ferrari, a nanomedicine expert at the University of Texas Health Science Center in Houston. "It brings an innovative element to the field of controlled release of drugs. [But] it has a long way to go" before it can help patients, he warns.

Team leader David Gracias, a chemical ▶

CREDITS (TOP TO BOTTOM): REUTERS; ZHIYONG GU/JOHNS HOPKINS UNIVERSITY

engineer, says the idea for porous nanocontainers grew out of decades of work in patterning computer chips. The first steps involved producing ultraprecise 2D structures on flat silicon slabs and other surfaces. In recent years, the chip industry's primary patterning technique, called photolithography, has also spawned efforts to craft everything from tiny gears to microscopic channels and reservoirs for tiny chemical reactors. But making 3D porous containers remained a challenge.

Gracias and his lab members—graduate student Timothy Leong, postdoctoral candidate Zhiyong Gu, and undergraduate Travis Koh—made their nanocubes using standard photolithography techniques to etch a series of six squares, 100 to 200 micrometers on a side, each shot through with anywhere from one to hundreds of tiny holes. These squares were attached to one another in a crucifix pattern, with a strip of metal between each square that acted both as hinges and solder. The tiny crucifixes were placed in a liquid bath and heated until the hinges melted. Surface tension along the faces of the crucifixes caused the square faces to collapse into cubes. As the bath cooled, the hinges hardened again, soldering the faces in place.

Gracias's team then filled the cubes with different reagents that would leak out at different rates depending on the size of the pores and used them to carry out a variety of chemical reactions. The researchers also used magnetic fields to redirect cubes made out of nickel and other metals.

Ferrari notes that metallic nanoparticles capable of delivering drugs aren't new. And he warns that it could take years to prove that the cubes are safe and effective in clinical settings. The "great upside" of the Johns Hopkins team's work, he says, is that they can build upon advances in lithography to create very precise structures.

Someday, Ferrari predicts, transistors, sensors, and other information-processing devices may be implanted directly onto their carriers to control exactly when and where chemicals are released. Now, if only parents could get toys to assemble themselves.

–ROBERT F. SERVICE

ASTRONOMY

Satellite's X-ray Vision Clinches the Case for Dark Matter

A fantastically energetic collision between clusters of galaxies has demolished a challenge to the law of gravity, providing the clearest evidence yet for the existence of intergalactic dark matter.

For decades, astronomers have inferred that unseen matter lurks within and between galaxies. Luminous stars alone, they realized, don't exert enough gravitational force to explain how individual galaxies spin and clusters of galaxies clump together. Something invisible must be pulling, too.

Dark evidence. A composite image depicting normal matter (pink) and gravity (blue) shows dark matter's presence in the "bullet cluster" of galaxies.

CREDITS: NASA/CXC/CFA/M. MARKEVITCH *ET AL.*

Some of the extra matter in galactic clusters is just hot gas. But even more mass seems to exist in the form of "nonbaryonic" dark matter, made of something other than ordinary atoms.

A few holdouts have insisted that the observations could be explained by modifying the law of gravity at great distances. But a new result from the Chandra X-ray Observatory satellite offers clear-cut evidence that dark matter really does infuse galactic clusters. "It demonstrates beyond a reasonable doubt that dark matter exists," says Sean Carroll, a cosmologist at the University of Chicago, Illinois, not involved in the study.

Speaking this week at a NASA briefing, astronomers reported on new Chandra images of the "bullet cluster" of galaxies, 1E0657-56, created by an energetic collision of smaller clusters. It is the most explosively violent such merger ever observed, said astrophysicist Maxim Markevitch of the Harvard-Smithsonian Center for Astrophysics in Cambridge, Massachusetts.

The shock wave from the cluster collision dragged the hot gas between galaxies into its unusual shape but would not have affected dark matter, which interacts only via gravity. Consequently, the explosive collision stripped the ordinary gaseous matter away from the nonbaryonic dark matter.

"Because of this collision, for the first time, we're actually able to see dark and ordinary matter separated in space. And this proves in a simple and direct way that dark matter exists," Markevitch said at the briefing.

With no dark matter, the gravity of the cluster would remain concentrated on the gas, which vastly outweighs the galaxies it surrounds. But in fact, the gravitational field of the cluster no longer matches the location of the gas. Astronomers measured the cluster's gravitational influence by tracking its effect on the light from more distant "background" galaxies, a phenomenon known as gravitational lensing. The results show a clear separation between the gas and the gravity.

"In the bullet cluster, we've seen for the first time a large spatial separation in the sky between where the majority of the normal matter is found and where most of the gravity is found," said team leader Douglas Clowe of the University of Arizona, Tucson. "This cannot be explained by altered gravity for normal matter." A paper describing the results will be published in *Astrophysical Journal Letters*.

While the new result specifically demonstrates the existence only of intergalactic dark matter, it strengthens the case for dark matter within galaxies as well. The same dark matter could explain both why clusters of galaxies do not fly apart and why galaxies themselves rotate as rapidly as they do, Carroll says. There is no need to invoke modifications to Newtonian gravity.

Carroll pointed out that it remains possible that the laws of gravity may need to be modified. But those modifications can no longer do away with dark matter. "No matter what you do, you're going to have to believe in dark matter," he said at the briefing. "It is once and for all the case that dark matter does exist."

–TOM SIEGFRIED

Tom Siegfried is a writer in Los Angeles, California.

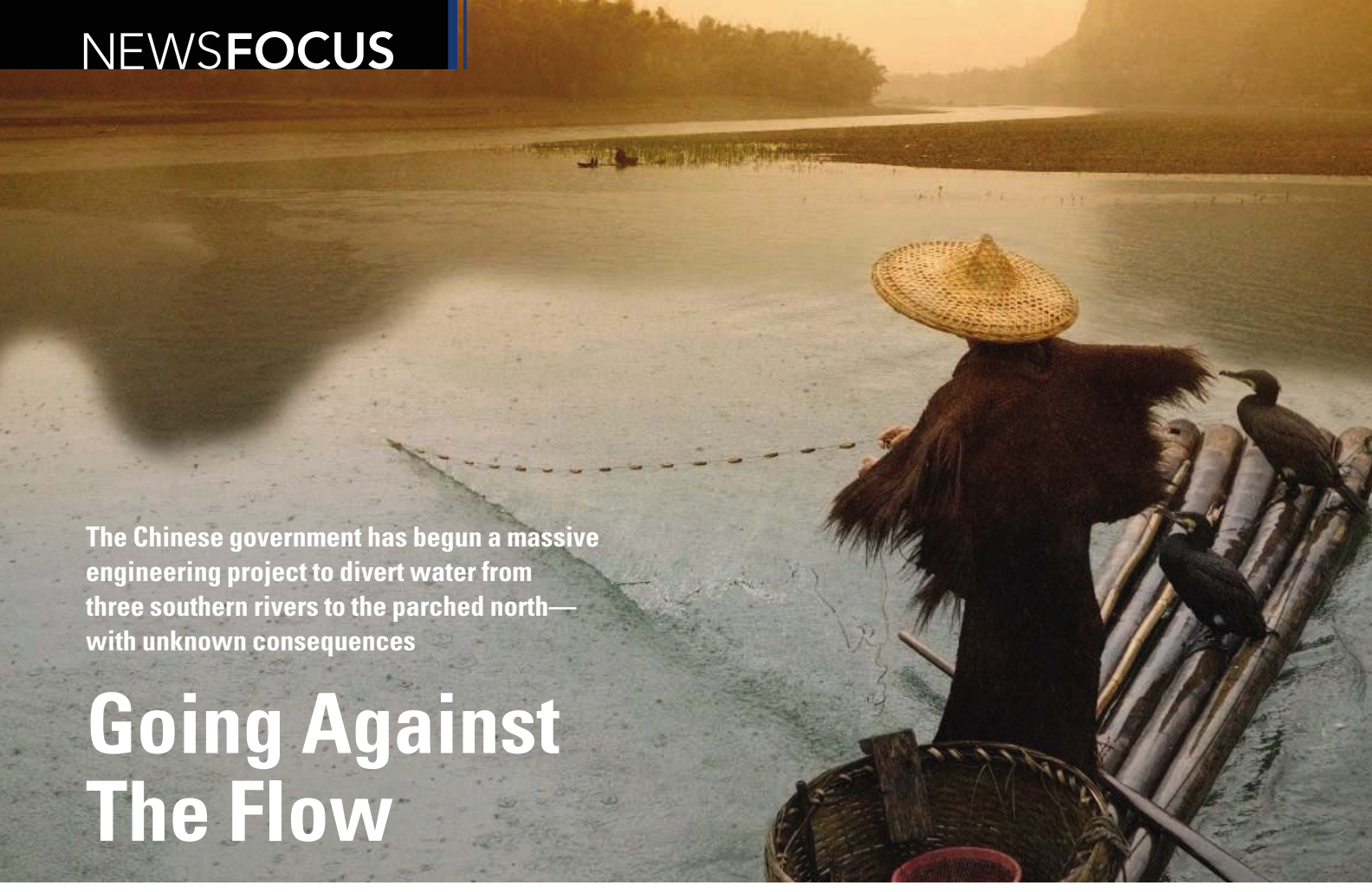

The Chinese government has begun a massive engineering project to divert water from three southern rivers to the parched north—with unknown consequences

Going Against The Flow

BEIJING—A half-century ago, Mao Zedong offered a seemingly simple exhortation to his young Communist nation: "Lend some water from the Yangtze River to the Yellow River." But the massive engineering challenges and costs of funneling a surfeit of water from China's moist south to its parched north kept Mao's grand vision in check—until now. In one of the biggest civil engineering projects ever undertaken, the Chinese government has embarked on a controversial 500 billion yuan ($62.5 billion) effort to shift water from three southern river basins to its populous and thirsty northern provinces.

The South-North Water Transfer Scheme involves a series of canals, pumping stations, reservoirs, and dams that would supply water to the north for drinking and for irrigation. Excavation is under way on the eastern and central routes, each more than 1000 kilometers long, and last month, engineers completed a tunnel beneath the Caohe River that will allow water on the central route to begin flowing to Beijing in 2008. Work on a third, more complex, route that would link watersheds in Tibet and western China is not expected to start for at least another decade (see map on p. 1035). If all goes according to plan, by 2050, some 44.8 billion cubic meters of water—roughly the annual runoff of the Yellow River—will be diverted northward each year to meet the needs of almost half a billion people. By comparison, California's vaunted transfer system conveys one-tenth that volume of water from north to south.

But the attempt to transform the landscape of central China is not without its critics. There are worries that pollution in southern rivers—the Yangtze, the Hanjiang, and the Huai—will contaminate northern climes, and that the shift will endanger southern ecosystems, especially Tibet's fragile watersheds. "It's quite dangerous," warns Ye Qian, a climatologist with the U.S. National Center for Atmospheric Research in Boulder, Colorado, and the International Research Center of Creeping Environmental Problems in Lanzhou, China. The project's economics are hotly debated as well.

Still, many Chinese scientists deem the massive waterworks to be the best fix for a looming crisis. Relentless desertification in the north is eroding biodiversity and concentrating pollutants in smaller bodies of water, curtailing supplies of potable water. China's Ministry of Water Resources predicts that even with stepped-up conservation efforts, the annual shortfall of water for drinking and irrigation in the Yellow and Hai river basins will exceed 21 billion cubic meters by 2010. If the water-transfer project were not implemented, officials say, that deficit would swell to 32 billion cubic meters by 2030. The government estimates that 96 million Chinese, mostly in northern rural areas, now lack sufficient drinking water.

"We're trying to recover a healthy water cycle," says Xia Jun, a hydrologist at the Institute of Geographical Sciences and Natural Resources of the Chinese Academy of Sciences (CAS) in Beijing. Xia believes that the transfer scheme, coupled with water-conservation measures, would do just that over the next few decades. Ye, however, blasts the project as the latest in a string of risky engineering solutions to problems that China could tackle with more benign measures. "If you have the right water management, you can save the same amount that they intend to transfer," he argues. "Why are they doing this now? Because they have the money and people need jobs. But they need to think more about the consequences."

Rearranging nature

One point of universal agreement is that northern China's water resources are growing perilously scarce. Aquifers in the north—an area covering 428,000 square kilometers with a population of 437 million—are being

CREDIT: GETTY IMAGES

sucked dry. In the Beijing region, for instance, the groundwater table has steadily receded from an average of 10 meters below the surface in 1975 to 35 meters in 2005. In the Haihe River Basin, in which 95% of available water is exploited, the 305 cubic meters of water resources per capita is less than 5% of the global average, says Xia. The Yellow River is so heavily siphoned that in dry months it often peters out before reaching the East China Sea. In 1997, the river stopped short a record 226 days, its dry bed extending as far as 700 kilometers inland. The simple fact, Xia says, is that "North China has become more arid."

Aggravating the situation are a burgeoning population, intensive agriculture, and rapid industrialization. Amid the boom, few people are mindful of conservation, an attitude that scientists say needs to change. To prevent the squandering of water diverted north, the central government has ordered northern cities to implement water-conservation measures before the diversion begins, says Liu Changming, a top expert on the south-north project at Beijing Normal University. Xia agrees: "We need to build a water-saving society."

Southern China, on the other hand, is chin deep in water. More than 90% of the Yangtze River's annual flow of 960 billion cubic meters from its headwaters in the Himalayas and tributaries empties into the sea. That statistic also applies to the Hanjiang River, which flows into the Yangtze near Wuhan and will be tapped for the central route.

Scientists have mulled plans for a south-north transfer ever since Mao's famous 1953 proclamation, and Ye says it fits with the government's overall philosophy. "China is driven by engineers," says Ye. "Mao said, 'Man can overcome nature.' " But it wasn't until the early 1990s, as China's economy began to heat up and the desiccation of northern China accelerated, that the first feasibility studies were conducted. The Communist Party leadership gave its blessing in 1995, when then-Premier Li Peng, a hydrological engineer who was also a force behind the Three Gorges dam, predicted that the project would "benefit dozens of Chinese generations."

Work on the 1150-kilometer eastern route kicked off in 2003. Water will be lifted by pumps 65 meters above the Yangtze, the third largest river in the world, to an ancient Grand Canal, segments of which have operated continuously since the 5th century B.C.E. The canal bed, now being widened and deepened, will dive under the Yellow River via a tunnel before reaching its terminus in Tianjin. A branch will conduct water to major cities in eastern Shandong Province. Engineers intend to turn on the taps next year, with plans eventually to divert 14.8 billion cubic meters along this route from the Yangtze, an amount that represents less than 2% of the river's flow.

The 1277-kilometer central route poses a tougher challenge. Its centerpiece is Danjiangkou dam on the Hanjiang River. Engineers are now raising the height of the dam by 15 meters, increasing its holding capacity by two-thirds. The larger reservoir would both supply water for the central route and diminish the threat of periodic flooding in Wuhan, central China's biggest city, and other parts of Hubei Province. As a result, however, some 224,000 people from villages near the reservoir are being relocated; many have already left.

The western route would link the mountainous headwaters of the Yangtze and Yellow Rivers and transfer the most water of the three lines: 17 billion cubic meters per year. It is expected to offset severe desertification and irrigate 2 million hectares across four provinces. Another benefit, proponents say, is that infusing water near the Yellow River's headwaters will reduce sediment buildup along the riverbed and avert or mitigate seasonal floods. However, complicated engineering and unanswered ecological questions are likely to delay construction until at least 2020, says Liu.

A foul flow?

Environmental concerns have dogged the project every step of the way, starting with pollution. Some $1.75 billion is being spent on measures to clean up the Huaihe River, a feeder for the eastern route and one of the most polluted rivers in China. The Hanjiang River is also a major headache. "The middle and lower parts of the Hanjiang have already been seriously polluted by industrial wastes," says Du Yun, a hydrologist at CAS's Institute of Geodesy and Geophysics in Wuhan. Four major algal blooms on the river since the early 1990s have triggered mass fish kills. The central route would draw off approximately 16% of Hanjiang's flow, concentrating pollutants and prompting Du to anticipate "big impacts on the environment and water ecology."

To mitigate that threat, engineers later this year will start excavating a canal from the Yangtze to the middle Hanjiang to boost flow. Ideally, the canal would connect with the Hanjiang as close as possible to the Danjiangkou dam, but due to engineering difficulties, it will enter 300 kilometers downriver, leaving a significant stretch of the Hanjiang heavily polluted, says Du. One planned remedy is to dam and dredge the Hanjiang to boost flow. But in-depth studies on whether this will dilute pollutants, as hoped, are "still lacking," he says. To make matters worse, Li Guoying of the government's Yellow River Water Resources Commission announced earlier this month that the water ministry plans to start ferrying water northward from the Danjiangkou reser-

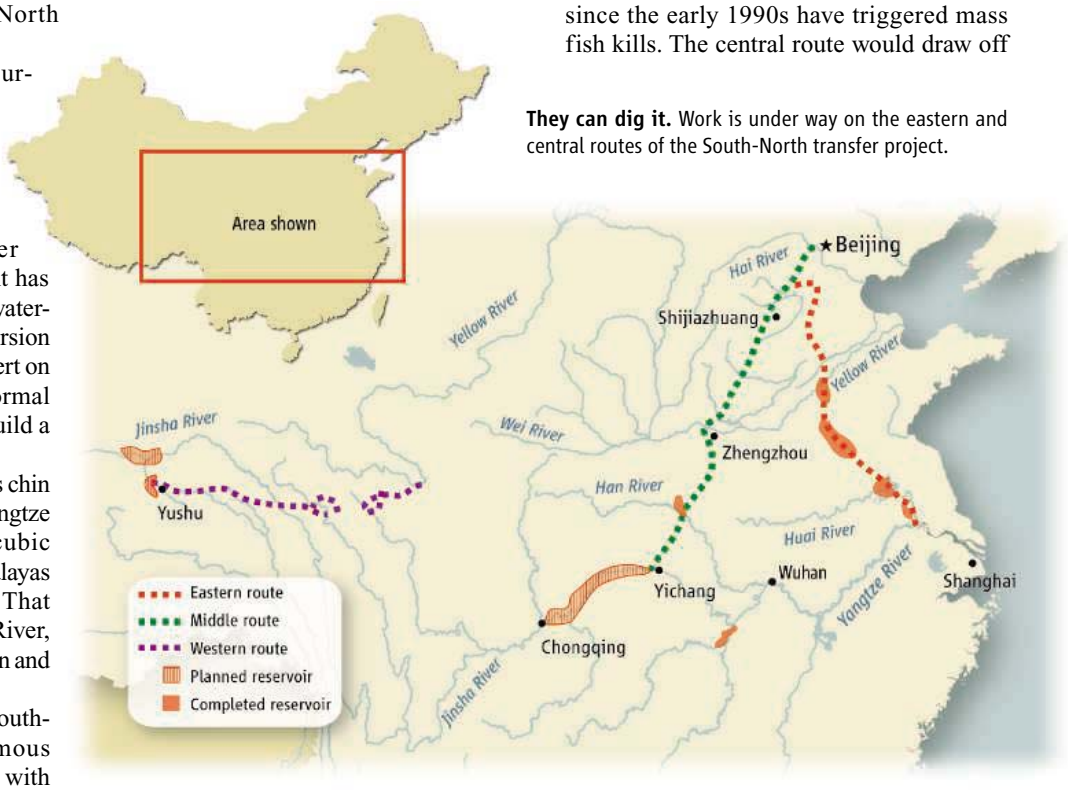

They can dig it. Work is under way on the eastern and central routes of the South-North transfer project.

CREDIT: K. BUCKHEIT KRAUSE/*SCIENCE*; SOURCE: C. LIU AND H. ZHENG, WATER RESOURCES DEVELOPMENT 18 453-471, 2002

Controversial Rivers Project Aims to Turn India's Fierce Monsoon Into a Friend

NEW DELHI—China's gargantuan South-North Water Transfer Scheme (see main text) may not hold the record as the largest civil water project for long. India is planning a similar endeavor that could cost twice as much and eventually shift four times the volume of water.

The $120 billion Interlinking of Rivers Project would primarily divert monsoon runoff from 12 rivers in eastern India to parched western states via canals, tunnels, and reservoirs. The project has support across the political spectrum; India's President A. P. J. Abdul Kalam says it offers "the promise of freeing the country from the endless cycle of floods and droughts." But critics view it as an impending disaster and decry the envisioned resettlement of tens of thousands of people. "It would spell doom for the people who would be affected and uprooted," contends Medha Patkar of the Save the Narmada Campaign in Barwani.

For India, water is feast or famine. During the monsoon season from July to September, when the country receives 80% of its annual rainfall, vast swaths of the east are inundated, while the west suffers crippling shortages. Flood damages have climbed from $13 million in 1953 to an annual average of $335 million, according to the government's Task Force on Interlinking of Rivers. Yet India's billion-plus people—16% of the world population—have access to only 4% of the planet's fresh water, posing a rising threat to India's food security. Although irrigation over the past half-century has quadrupled India's grain harvest to 213 million tons per year, production must double by 2050 to keep pace with India's population growth, experts say, and irrigated land must increase from 95 million to 160 million hectares. India's maximum irrigation potential through conventional methods is assessed at 140 million hectares. The Interlinking Project, backers say, would more than close that gap, providing water to irrigate some 35 million hectares.

More than a century ago, planners fantasized about diverting India's eastern floodwaters into southern and western river basins, but the idea was dismissed as far-fetched. "Gigantism always casts an irresistible spell on our bureaucracy," says an ardent critic of the plan, Ramaswamy R. Iyer, a former secretary of the Ministry of Water Resources who's now with the Center for Policy Research in New Delhi. But India has proved adept at smaller-scale transfers. In the late 19th century, the Periyar River in southern India was dammed and a 1740-meter-long tunnel excavated to carry water eastward to the neighboring Vaigai Basin. The waterworks still functions, irrigating 81,000 hectares and driving a 140-megawatt power station. And in the north, the Rajasthan Canal uses a barrage and canals to divert Himalayan glacial runoff to Rajasthan's deserts. "These projects have been highly beneficial and have not caused any noticeable environmental damage," says Suresh Prabhu, former Interlinking task force chair.

The idea of the grandest waterworks of all was resurrected not by engineers but by a lawyer, Ranjit Kumar, who in 2002 petitioned India's Supreme Court to force the government to take the long-standing scheme off the shelf and implement it. In a 5 May 2005 ruling, the court decreed that the project must start by 2007 and the bulk of it be completed by 2016. In response to concerns from Bangladesh, which gets most of its fresh water from Himalaya-fed rivers, India has pledged to hold off on part of the project that would tie Himalayan rivers into the scheme.

Audacious in scope, the project would link 37 rivers through 12,500 kilometers of canals. Backers recite a litany of benefits. Each year, some 178 cubic kilometers of water would be diverted westward, providing drinking water for at least 10 million households and irrigation water. Run-of-the-river turbines would generate 34 gigawatts of electricity, while storage dams would mitigate flooding, particularly in the Ganga and Brahmaputra basins. The canals, planned to be 50 to 100 meters wide and more than 6 meters deep, would facilitate navigation. Engineering challenges include burrowing through mountains and moving water against gravitational flow, whereas societal issues include the resettlement of people from river valleys converted into reservoirs.

In this first stage of the mammoth project, which won government approval last August, a 230-kilometer canal will be dug to divert water

voir as early as 2008—a full 2 years before the Yangtze-Hanjiang diversion canal and the dredging projects are completed. The gap "could cause irreversible losses to biodiversity in the middle and lower Hanjiang River," Du asserts.

One life form that scientists would rather not see blossom as a result of the project is the schistosome parasite. Oncomelania snails, riddled with the blood flukes that cause schistosomiasis, are endemic in the part of Jiangsu Province where the eastern route originates. Zhou Xiaonong of the Institute of Parasitic Disease in Shanghai has been lobbying authorities to take steps to control schistosomiasis—such as lining riverbanks with cement and setting up more observation stations for the parasite—before the eastern route begins moving water.

Another concern stems from reduced flow in the southern rivers. Experts are not worried about the impact during the peak summer and early autumn months, when regular downpours recharge the Yangtze and other rivers. But even the intended 5% reduction during the dry season or a drought could have serious consequences for the Yangtze Basin, says Chen Jiyu, a hydrologist at East China Normal University in Shanghai. Such a reduction, he says, could lead to seawater backwash into the Yangtze estuary that would reduce freshwater supplies to Shanghai and weaken its capacity to dilute pollutants.

Zhang Jiyao, director of the water-diversion office of the State Council, has vowed that the spigots feeding the eastern route will be shut during dry seasons. Project engineers

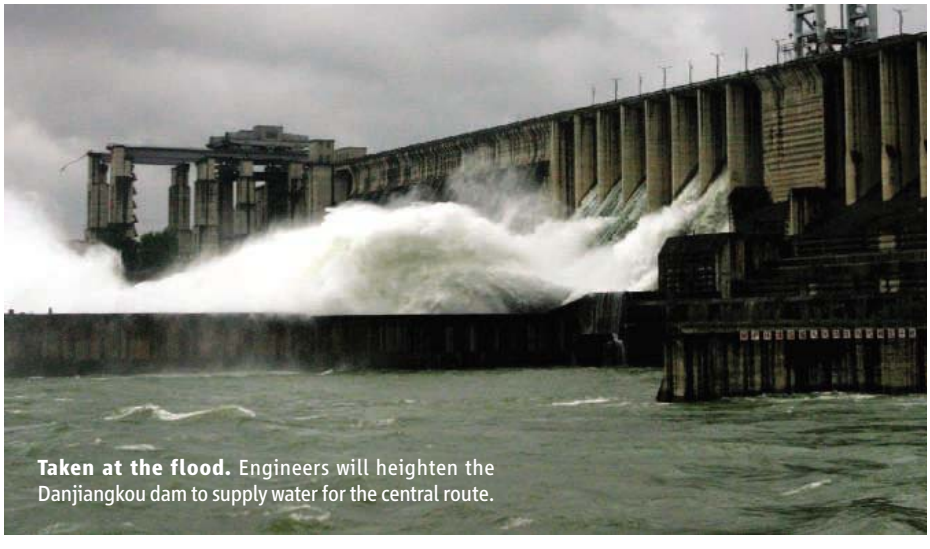

Taken at the flood. Engineers will heighten the Danjiangkou dam to supply water for the central route.

CREDIT: NEWSPHOTO

from the Ken River to the Betwa River in northern Madhya Pradesh province. A dam and small hydroelectric plant will be built in the Panna tiger reserve. Work on the $1.1 billion pilot effort is under way and scheduled to be completed in 8 years.

Critics assail even this relatively modest beginning. The Ken-Betwa link "will cause horrific devastation," says physicist Vandana Shiva, director of the Research Foundation for Science, Technology, and Ecology in New Delhi. According to a foundation analysis, forest clearance to excavate the Ken-Betwa canal will exacerbate runoff and degrade biodiversity. And in Madhya Pradesh, Shiva says, farmers might shift from producing rice and legumes for the domestic market to water-intensive crops such as sugar cane. The result, Shiva predicts, will be "ecological breakdown" and "political instability." Prabhu scoffs at the claims. The project, he says, "is expected to greatly reduce the regional imbalance in the availability of water" and thereby reduce the potential for strife.

Current of discontent. People protest construction of a dam in Madhya Pradesh that would submerge their land.

A dearth of credible data hampers debate, says Tushar Shah of the International Water Management Institute in Colombo, Sri Lanka: "What should have been a national debate based on analysis, reason, and cold calculus is rapidly turning into a cacophony of discordant prejudices, opinions, preferences, and assertions." Shah is leading an analysis of the overall project for the Consultative Group on International Agricultural Research in Washington, D.C., assessing factors such as flow rates and exploring strategies for maximizing use of runoff. A report is expected in April 2008.

A thorough study "is essential for evaluating the long-term consequences of interlinking rivers," says V. Rajamani, a geologist at Jawaharlal Nehru University in New Delhi. Flooding, he notes, is a natural process that enriches basins with silt deposits. Key issues, such as the effects of sedimentation loss and alterations in water and nutrient supply, "are huge unknowns," he says. Those uncertainties could make the Interlinking of Rivers Project a $120 billion gamble.

–PALLAVA BAGLA

have set the cutoff at flows of less than 8000 cubic meters per second at the Datong hydrological station on the lower Yangtze, some 600 kilometers upriver of the estuary. Chen, however, argues that the threshold should be at least 50% higher, considering the heavy demand for water by industry and agriculture along the lower Yangtze. He has urged planners to build a facility to gather runoff and water-quality data in the estuary. However, Chen says, "I have seen no effort to collect these data and integrate them into water-diversion decisions."

At the same time, the canal could revive one long-standing woe. The falling water table, although crippling water supplies, has ameliorated soil salinity in the fertile agricultural plains of Hebei and Henan provinces. A rising water table could carry salts back up to the topsoil, says Liu. One straightforward solution would be a ban on irrigation channels along the water-diversion routes, says Pei Yuansheng, a water-resource expert at the China Institute of Water Resources and Hydropower Research in Beijing. Only wells should be permitted, he says. Pei would like the government to subsidize the sinking of new wells.

A bigger question is how the proposed western route will impact the region's ecology. "Our main target for ecological protection is leaving enough water for fish," says Liu Suxia of the Institute of Geographical Sciences and Natural Resources in Beijing. Her team has been reviewing previous ecological studies and querying local experts. Detailed surveys, she says, will come later.

Fiscal infighting

The economic impact of the scheme, like its ecological consequences, is opaque. The necessity to overcome gravity on the eastern route could make the new water twice as expensive, raising its price in Tianjin to the equivalent of approximately 50 U.S. cents per ton. Much of that increase is expected to be passed on to consumers.

And it's not clear which authorities will manage the resource, both in reservoirs and stored in underground aquifers. "Feuds over water ownership penetrate nearly every step of planning, construction, operation, and even the scientific research process," says Chen Xiqing, a hydrologist at Hohai University in Nanjing. "A key problem," he says, is that China "lacks a legal framework to coordinate conflicts between the central and local governments and between different regions." Shandong and Jiangsu provinces are embroiled in a fight over water rights, sources say.

Ironically, climate change could render parts of the water scheme superfluous. Chinese and U.S. models predict that northern China will become increasingly wet as average temperatures rise. That shift may begin as early as next decade, Ye says. He and others are pressing the government to reconsider plans to forge ahead with the western route, which is not a fait accompli. But "no one can stop" the eastern and central routes, says Ye. The vast experiment is well under way—and both China and the world are awaiting the consequences.

–RICHARD STONE AND HAWK JIA

Hawk Jia is a writer in Beijing.

CREDIT: PALLAVA BAGLA/*SCIENCE*

HURRICANE KATRINA

One Year After, New Orleans Researchers Struggle to Rebuild

Labs are up and running but short-staffed, and the departure of key scientific talent means the city's research institutions have much rebuilding ahead

NEW ORLEANS, LOUISIANA—The Medical Education Building at Louisiana State University (LSU) still has a smudged black line from floodwaters, and the bottom doors are blocked by orange pylons and marked "Contractor Entrance Only." A visitor has to find her way in via the crosswalk from the student dormitory next door. But up on the sixth floor, developmental biologist Oliver Wessely's lab is humming with students doing experiments. Setting aside a petri dish of frog embryos, Wessely reflects on the past year: He's come a long way since Hurricane Katrina, which cost him his frogs and all but one (luckily, pregnant) transgenic mouse. "Right now, I can't complain," he says. "My research is progressing."

Life has changed, however: For one, the hallways are eerily quiet. Five of his department's 12 research faculty members have left or been laid off. "You have much less people around here. Much less interactivity. … The biggest issue for research will be [restoring] a more intellectually stimulating atmosphere," Wessely says.

One year after the 29 August 2005 storm, research in New Orleans is getting back on its feet. Most lab buildings have been open since early 2006, and scientists say they're catching up on experiments. Worries have eased somewhat since the National Institutes of Health (NIH) announced last month that it will allow its grantees to apply for 1-year funded extensions, giving them a chance to make up for the lost year before they must compete for funding again. "I don't want to suggest everything is perfectly back to normal. … We have tremendous challenges. [But] I would say we have beaten the odds," says Paul Whelton, dean of Tulane's medical school and senior vice president for health sciences of the Tulane Health Sciences Center.

But not everyone is so optimistic. Researchers still lack some basic lab services and are hampered by staff shortages. Medical schools have suffered deep cuts in clinical and teaching faculty, which erodes morale. And although the overall number of research faculty members at the city's institutions hasn't dropped that much, some departments and programs have sustained serious losses in numbers of both key senior scientists and young researchers.

Swamped. LSUHSC a few days after Hurricane Katrina.

The future of research in New Orleans, scientists say, will hinge on whether new faculty members—as well as postdocs and graduate students—will want to live and work in the struggling city. That's unclear in a place that still has less than half its pre-Katrina population and remains plagued with scarce and overpriced housing, boarded-up businesses, and power outages—not to mention the threat of another hurricane. Full-scale faculty recruiting, officials say, is on hold until the end of November. "We've got to get past this hurricane season," says Whelton.

Open for business

On the surface, New Orleans's main universities with research programs—LSU's Health Sciences Center (LSUHSC), Tulane, and the University of New Orleans (UNO)—appear relatively unscathed. At Tulane's uptown campus, which suffered little flooding, stately late 19th-century limestone buildings are again surrounded by manicured lawns.

After replacing walls and repairing flooding damage to basement power equipment, Tulane managed to open its downtown medical campus in January. LSUHSC's downtown complex—except for the badly damaged dental school—officially opened in February, although elevators weren't working in some buildings, and amenities such as distilled water were lacking for several months. Many labs at UNO on Lake Pontchartrain have also been open since late January, although some items, such as fume hoods and power outlets, are not completely fixed.

Following the evacuation, most scientists spent the fall of 2005 at far-flung host universities. Once they began trickling back in January, they set about repairing or replacing equipment and replenishing reagents, cell lines, and animals lost during the power outages—this time, taking care to send some samples and transgenic animals to colleagues outside New Orleans. Companies that sell reagents and mice have offered discounts, the state and universities have come up with some money to rebuild labs, and NIH and the National Science Foundation have awarded supplements for replacing equipment and supplies. "I don't think anybody's not able to do the science they want to because of a lack of funding," says Joseph Moerschbaecher, vice chancellor for academic affairs at LSUHSC.

The modest progress can't make up for the loss of critical mass, however. Universities now lack support staff—janitors, secretaries, and the like—as well as lab workers. LSU's transgenic animal facility lost its director and remains closed, Wessely says, and other core facilities, such as a peptide synthesis lab, are unavailable. LSUHSC genetics chair Bronya Keats says, "There's no doubt that it's still taking longer to get things done."

Even more painful, many researchers have lost postdocs and grad students. Tulane biochemist Art Lustig says half his lab staff didn't return. "They were just afraid," he says. The remaining grad student and postdoc, who are catching up on studies of yeast telomeres, "are exhausted."

All three universities suffered a slump in new grad students this fall. LSU attracted only half the usual 50 to 60 new basic science students. New enrollment at Tulane's medical school is down by about one-third, says virologist Robert Garry. Whereas these schools managed to retain most returning grad students, UNO has been hit much harder: Its total graduate enrollment, which includes business and liberal arts programs, has dropped to 2000, about half what it was prestorm, says UNO graduate school dean Robert Cashner.

CREDIT: IRWIN THOMPSON/*DALLAS MORNING NEWS*/CORBIS

The biggest blow to universities' research efforts, however, is the loss of faculty members. Several hundred were temporarily laid off or lost their jobs due to budget pressures at LSU and Tulane last December (*Science*, 16 December 2005, p. 1753), in large part because both medical schools had few patients and no major hospitals for months. Many worry that LSUHSC will have to furlough more staff members if it can't open hospitals quickly and begin generating clinical income.

Although most researchers were shielded from these cuts, many have left town anyway, often taking their grants with them. LSUHSC has lost about 20 of 80 NIH-funded faculty members, both young professors and leaders such as cancer center director Oliver Sartor, now at Harvard, and Stephen Lanier, chair of pharmacology, who's leaving for the Medical University of South Carolina. Tulane's cancer center lost five of 34 basic researchers, says director Roy Weiner, including Tyler Curiel, who left this month to head the San Antonio Cancer Institute in Texas. Tulane's School of Science and Engineering is down 15 of 115 faculty members, including ecologists, psychologists, and biomedical engineers. And UNO's College of Sciences has lost 19 research faculty members, says Cashner. "It's almost like an artery was cut open," says David Mullin, chair of Tulane's cell and molecular biology department, which lost four of 12 faculty members.

Surprisingly, both medical schools say their NIH research funding has held steady, partly because of new grants; half of the $13 million drop in overall research funding at LSU (see graph) was clinical income from halted trials, says Moerschbaecher.

Slow recovery

Many of those who chose to leave either had lost their homes or their spouses were laid off, say officials from all three universities. "Some people just couldn't take it," says Moerschbaecher. Others were discouraged by the gloomy prospects for New Orleans's recovery. "It's the situation in the city more than the school," says LSU neuroscientist Jeffrey Magee, who left for Howard Hughes Medical Institute's Janelia Farm in Virginia after 20 years in New Orleans.

Indeed, those remaining still face tremendous obstacles. The city is only now getting traffic lights working; it still suffers from power outages and water-main breaks. In faculty enclaves such as Lakeview and Gentilly, many houses are up for sale, and some faculty members are living in rented apartments or Federal Emergency Management Agency trailers while battling insurance companies and deciding whether to rebuild. Many businesses remain closed. "It's going to take 10 years" to recover, predicts LSUHSC biochemistry chair Arthur Haas.

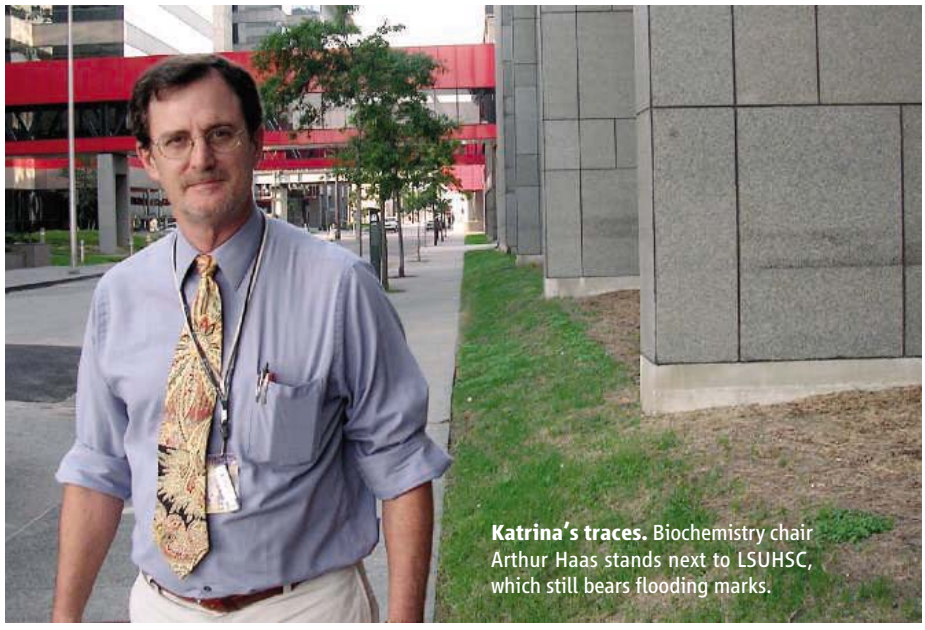

Katrina's traces. Biochemistry chair Arthur Haas stands next to LSUHSC, which still bears flooding marks.

With living conditions so grim, universities are scrambling to keep more faculty members from leaving. LSU hopes that a $25 million pot of money proposed by the state board of regents for new, collaborative research and education projects will persuade some to stay. Tulane last spring set aside $10 million in insurance money for small grants to help researchers rebuild their labs; this fall, they can compete for another $10 million for new projects. "This is a tough town right now. … People need a reason to stay," Whelton says.

One bright spot, say medical school officials, is the 1-year funded extensions that NIH decided to allow after sending a delegation to New Orleans in March. "That's going to be incredibly helpful to us," Moerschbaecher says. NIH is making the awards available only to researchers who stay in New Orleans: "Anything that helps stabilize the institutions will be beneficial," says Joe Ellis of the NIH Office of Extramural Research. Although the announcement was only for single-investigator awards, NIH will consider extending multi-investigator projects on a case-by-case basis, Ellis says.

Even with such enticements, many scientists say they are keeping their eyes open for job offers elsewhere. "If I can't get postdocs soon, in 2 years, I'll lose everything. I know what it takes to get grants," says biochemist Iris Lindberg of LSUHSC.

Despite the obstacles, university officials are optimistic that they will be able to recruit new faculty members. UNO received a couple of hundred applications for two computer science faculty slots, Cashner notes. Nicholas Altiero, dean of Tulane's School of Science and Engineering, says he's had "some very good candidates" for two open positions, one in environmental science, a field that is poised to grow in post-Katrina New Orleans. Even biomedical scientists may see opportunities, suggests cancer researcher Matthew Burow of Tulane. Tulane "is a different institution, but there are positives," he says. "Younger scientists may see a place where they can … begin to build programs. There will be people out there who hopefully see that."

–JOCELYN KAISER

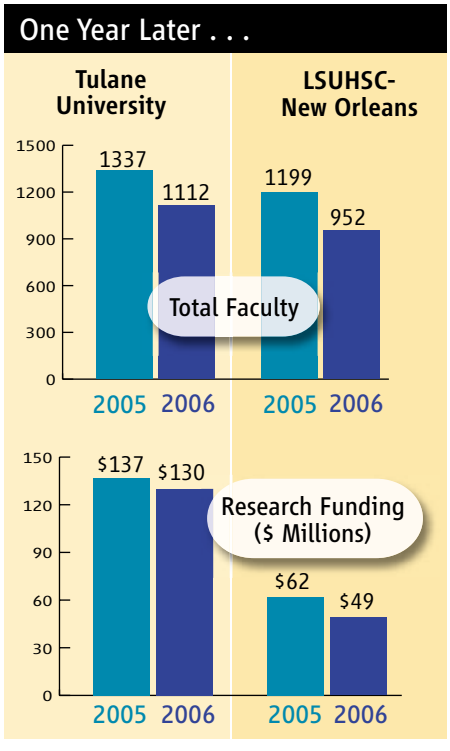

CREDITS (TOP TO BOTTOM): J. KAISER/*SCIENCE*; SOURCE: TULANE, LSUHSC-NO (LSUHSC FUNDING AS OF 1 MARCH 2006)

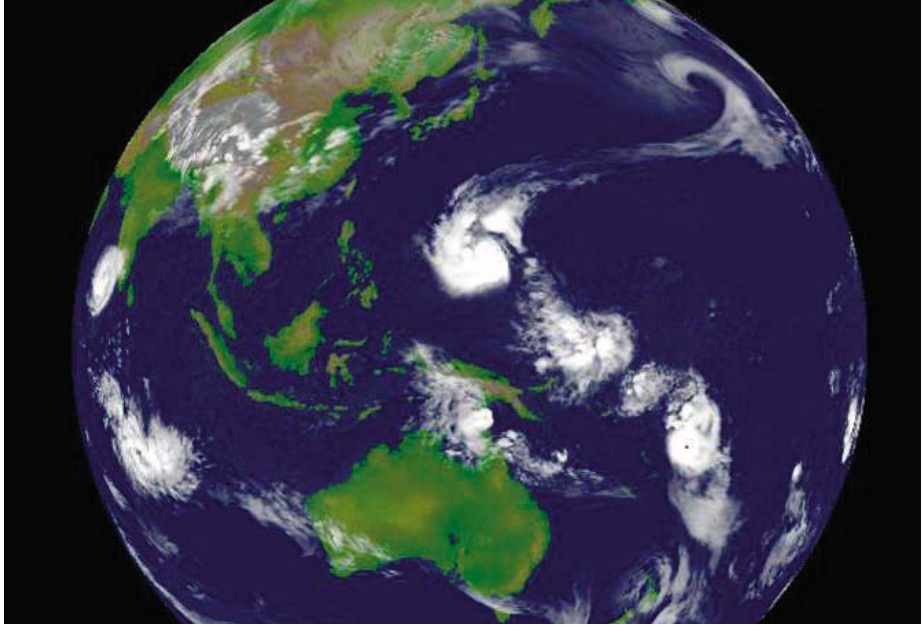

Sharper still. Typhoon Suda (*center*) looks almost real in this 3.5-kilometer simulation.

METEOROLOGY

Sharpening Up Models for a Better View of the Atmosphere

The exponential rise of computing power and the 2002 arrival of the great Earth Simulator computer have driven atmospheric models to extremes

Machines simulating Earth's atmosphere are producing ever-more-detailed pictures of weather and climate, thanks to ever-increasing computer power. And that new detail is now beginning to let researchers shed some of the approximations and downright fabrications they once needed to get anything useful out of their models. The new view of the atmosphere "looks very, very different" from that of less detailed model simulations, says modeler Jerry D. Mahlman of the National Center for Atmospheric Research in Boulder, Colorado. "It's a very important thing to do."

Supercomputers now run at once-undreamed-of speeds—many tens of teraflops (tens of trillions of floating point operations per second). In weather forecasting models, part of this exponentially improving computing power has always gone into increasing model resolution. Modelers do that by moving the isolated points at which atmospheric properties are calculated—the model's grid points—closer together. It's like a pointillist painter going from big splotches of color to smaller and smaller dabs that show greater and greater detail. Global weather-forecasting models are down to grid-point spacing of a few tens of kilometers in the horizontal. Climate modelers, in contrast, have favored a spacing of about 200 kilometers, says modeler Kevin Hamilton of the University of Hawaii, Manoa. That gave them simulations that bore some resemblance to real weather maps but that run for not just a week but centuries.

Then, in 2002, Japanese researchers turned on the 40-teraflops Earth Simulator. "The Japanese had two advantages," says Hamilton. "They were willing to invest an enormous amount of money, on the order of a billion [U.S.] dollars." And they had some very clever engineers figuring out how to build a unique, hybrid supercomputer that efficiently combines the conventional approach of simultaneously running large numbers of cheap processors with processors specially designed to accelerate atmospheric model calculations.

Spurred by the Earth Simulator, climate and meteorology researchers in Japan and around the world are pushing the resolution of their global models to new extremes. In a *Geophysical Research Letters* paper published 14 July, modeler Bo-Wen Shen of NASA's Goddard Space Flight Center in Greenbelt, Maryland, and colleagues report how they simulated 5 days in the life of Hurricane Katrina on NASA's newer, 61-teraflops Columbia supercomputer at the Ames Research Center in Mountain View, California. Global models have generally failed to produce intense tropical storms, but when the resolution was dropped from 20 kilometers to 10 kilometers, the simulated Katrina intensified to about the same extremely low central pressure as the real Katrina. It had winds nearly as strong spiraling around a suitably compact eye.

Shen and his colleagues then turned off the model's convective parameterization, the part of the model that tells it how, where, and when buoyant air will rise in puffy clouds and thunderheads. Even without that guidance, the simulated storm bore the same strong resemblance to the real thing. Apparently, the higher-resolution model was producing realistic convection—which powers tropical cyclones—all by itself from the smaller details of hurricane workings, without being told what to do.

In another high-resolution tropical cyclone study, reported last April, modeler Kazuyoshi Oouchi of the Earth Simulator Center in Yokohama, Japan, and colleagues simulated 10 years of global tropical cyclone activity both under present conditions and under warmer, greenhouse conditions. On the Earth Simulator, they ran a 20-kilometer-resolution model. Under present conditions, the model produced a reasonable rendition of the number, strength, and geographic distribution of storms. Under greenhouse warmth, the number of tropical cyclones around the world actually decreased 30%, but the number of more intense storms increased substantially. That supports upward trends in storm intensity recently reported from analyses of observations (*Science*, 5 May, p. 676).

Global simulations have driven resolution to even smaller scales. Modeler Hiroaki Miura and colleagues at the Frontier Research Center for Global Change in Yokohama, Japan, have been running a model called NICAM—Nonhydrostatic Icosahedral Atmosphere Model—on the Earth Simulator at resolutions of 7 and 3.5 kilometers. That is nearly fine enough to resolve individual clouds. When run without convective parameterization, the 7-kilometer-resolution version of NICAM showed signs of being less sensitive than a lower-resolution model to rising greenhouse gases.

The new high-resolution work is producing intriguing hypotheses, says Mahlman. But he and others still have reservations. "Is new science being produced or just really cool pictures?" he asks. With computing resources growing exponentially and staffing not, he says, computer power might overwhelm the available brainpower. All the more reason to remember that a model—no matter how super—is only a model.

–RICHARD A. KERR

CREDIT: H. MIURA/FRONTIER RESEARCH CENTER FOR GLOBAL CHANGE, JAMSTEC

EDITED BY YUDHIJIT BHATTACHARJEE

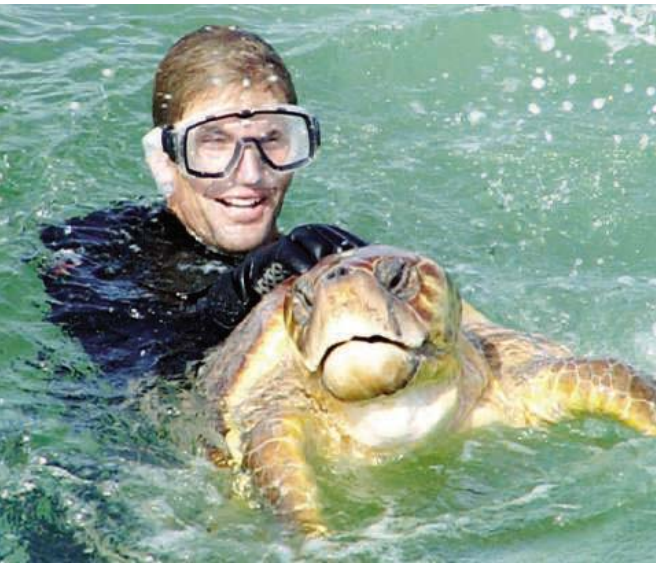

Deaths

TRAGIC DROWNING. When Boyd Lyon and his fellow marine researchers from the University of Central Florida sailed out into the Gulf Coast on 10 August, all they intended was a visual survey of green sea turtles. But Lyon, a 37-year-old graduate student, decided also to try to capture one of the animals and bring it ashore for blood and tissue sampling. The attempt cost him his life.

About three miles north of Sebastian Inlet in Brevard County, Lyon dived into the water to catch a 136-kg adult. To the horror of his graduate adviser Llewellyn Ehrhart and the four other researchers on the boat, he never resurfaced. "There is a pretty good chance he did get his hands on the turtle, but something terrible happened down there that took Boyd down," says Ehrhart. The U.S. Coast guard found Lyon's body 4 days later.

"Boyd was just a passionate, enthusiastic person who loved what he did," says fellow student Kelly Borrowman. "He went at [his research] with 100% effort no matter what time of the day it was or how much sleep he had had."

INSIDE GOVERNMENT

WITH THE CURRENT. Craig McLean says the ocean taught him a valuable lesson while he was captain of a 69-meter research vessel for the National Oceanic & Atmospheric Administration (NOAA). "It's better to understand than to try to redirect," he says. He'll be keeping that in mind as he charts the course for NOAA's $192 million research grants program.

After a few years of professional diving, McLean, 49, joined NOAA to plot nautical charts in 1981 and worked his way up. He has an undergraduate degree in zoology and a law degree, which he used enforcing environmental laws. From 2001 to 2004, he directed NOAA's ocean exploration program, diving in remote submersibles to the wreck of the *Titanic* and to hydrothermal vents at the Galápagos Rift. He starts his new job this week.

NEW NCI CHIEF. John Niederhuber, the incoming director of the National Cancer Institute (NCI), says he will try to preserve the number of new research grants awarded by the institute every year as it attempts to cope with a flat budget. But some programs will have to be trimmed, he says.

Niederhuber, 68, who was named to his new position last week, joined the $4.8 billion institute as a deputy director last fall from the University of Wisconsin in Madison. He has been NCI's acting director since June, after former director Andrew von Eschenbach was nominated to head the Food and Drug Administration (*Science*, 21 April, p. 357). Niederhuber won out over several potential candidates interviewed by the White House.

FOLLOW UP

NO SHOW. Four months after being named head of the Global HIV Vaccine Enterprise (*Science*, 7 April, p. 51), Adel Mahmoud is walking away from the job. Enterprise officials and Mahmoud, 65, say they made a "mutual decision" to part ways. It looked like "a misfit," says Mahmoud, an infectious disease specialist who was to start at the Enterprise next month after retiring as head of Merck's vaccine program.

The Enterprise is an ambitious effort that hopes to better coordinate the search for an HIV vaccine. Mahmoud was supposed to discuss the organization's plans last week at the 16th International AIDS Conference in Toronto, Canada. The talk was instead given by Jose Esparza, acting-head of the Enterprise, who told *Science* that final contract negotiations with Mahmoud fell through.

"This really sets the field back," says Mitchell Warren, of the AIDS Vaccine Advocacy Coalition. The Enterprise will begin a new search for a leader immediately.

In the Courts >>

IN OTHER WORDS. The longtime chair of the mechanical engineering department at Ohio University in Athens, which is embroiled in a plagiarism scandal, has sued the university for damaging his reputation. Jay Gunasekera is seeking $25,000 after a May report from a university panel concluded that Gunasekera "either failed to monitor the writing in [his] advisees (sic) theses or simply ignored academic honesty, integrity and basically supported academic fraudulence." The report found 37 cases of plagiarism among graduate theses, 16 of which were written by Gunasekera's students. In June, Gunasereka stepped down as chair, a position he had held since 1987, but he remains on the faculty.

The plagiarism scandal erupted in 2004, when a graduate student found that many theses contained plagiarized passages. In May, a university committee laid most of the blame on Gunasekera and two other faculty members.

Gunasekera would not comment on the suit, but his attorney John Marshall told the *Columbus Dispatch* that the university "had absolutely no evidence … that Dr. Gunasekera was aware of any of the plagiarism." In a written statement, the university said it would "vigorously defend the lawsuit," adding that it "has a duty to investigate matters of academic integrity."

Got a tip for this page? E-mail people@aaas.org

CREDITS (TOP TO BOTTOM): COURTESY OF UNIVERSITY OF CENTRAL FLORIDA; BERT FOX/*NATIONAL GEOGRAPHIC*; RICK FATICA/OHIO UNIVERSITY

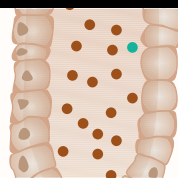

LETTERS

edited by Etta Kavanagh

Preserving the Jarawa's Future

PALLAVA BAGLA'S ARTICLE ON THE TRIBES OF THE ANDAMAN ISLANDS asks whether the Indian government should "isolate" or "integrate" tribal peoples like the Jarawa and the Sentinelese ("Isolate or engage? Indigenous islanders pose challenge for India," News Focus, 7 July, p. 34). In my experience through my work with Survival International (*1*), tribal peoples can only survive if their rights to ownership of their land, and to determine their own future, are respected.

In the case of the Jarawa, the Indian government's failure to uphold their rights may lead to the tribe being wiped out completely. Local poachers are invading the Jarawa's forest, bringing disease and violence, and hunting the animals on which the tribe depends. Earlier this year, the Jarawa suffered an outbreak of measles, a disease that has annihilated thousands of tribes worldwide.

The legal mechanisms to protect the Jarawa are all in place: Poaching and entry into the Jarawa reserve are illegal, the Indian supreme court has ordered the closure of an infamous road that brings settlers into the heart of the Jarawa's land, and the local administration's own policy states that the Jarawa must be allowed to live "according to their own genius." However, these measures are yet to be implemented.

Unless India acts now to save the Jarawa, it is likely that they will meet the same fate as their Great Andamanese cousins: dependent on government handouts, riddled with alcohol problems, and reduced to a fraction of their former number.

STEPHEN CORRY

Director, Survival International, 6 Charterhouse Buildings, London EC1M 7ET, UK.

Reference

1. See www.survival-international.org.

Ice Sheets and Sea Level

IN THE TANDEM PAPERS ON THE STABILITY OF the Antarctic and Greenland Ice Sheets by J. T. Overpeck, B. L. Otto-Bliesner, and co-workers ("Paleoclimatic evidence for future ice-sheet instability and rapid sea-level rise," J. T. Overpeck *et al.*, Reports, 24 Mar., p. 1747; "Simulating Arctic climate warmth and icefield retreat in the last interglaciation," B. L. Otto-Bliesner *et al.*, Reports, 24 Mar., p. 1751), firm statements are made about the possible contributions of these ice sheets to future sea-level change. Several doubtful assumptions are made, and the quality of model results seems to be overvalued.

The estimate of the contribution of the Greenland Ice Sheet (GIS) to the higher sea-level stand in the Eemian interglacial (between 2.2 and 3.4 m) is based on the assumption that there was no ice at the location of the Dye-3 ice core in southern Greenland. However, Eemian ice has been found at the base of this ice core (*1*). The presence of Eemian ice in south and coastal Greenland implies that the GIS was essentially intact in a much warmer climate and could not have contributed more than 1 to 2 m to sea-level rise.

For the Arctic Climate Impact Assessment (ACIA), we have used the output from five different state-of-the-art climate models to calculate possible changes in the volume of Arctic ice masses for the next 100 years (*2*). Among these models is the one used by Otto-Bliesner, Overpeck, and co-workers (the NCAR Community Climate System Model). For the same greenhouse gas scenario (IPPC-B2), the differences in model output are striking, especially concerning precipitation in the Arctic. Some models predict a significant increase in snowfall over the GIS; others do not. Given the additional problems in calculating ablation (because the climate model does not resolve the melt zone of the GIS), we think that the uncertainty in the predicted Eemian mass balance, and consequently the response of the ice-sheet model, is very large.

There is no justification for extrapolating observed changes on a short time scale (a decade or less) to longer term trends. Natural variability is large on virtually all scales and generated by nonlinear processes in the system. During recent years, the weather over Greenland has been warmer, and the effect on run-off and the dynamics of outlet glaciers is now clearly seen. We should follow this closely, but not conclude at this moment that "sea-level rise could be faster than widely thought," as stated by Overpeck *et al.*

The statement by Overpeck *et al.* that "our inference that the Antarctic Ice Sheet likely contributed to sea-level rise during the [last interglaciation period] indicates that it could do the same if the Earth's climate warms sufficiently in the future" requires a comment. This possibility was mentioned decades ago by J. H. Mercer and T. Hughes [see (*3*)]. However, this statement implies that it would not happen without warming. Actually, it is possible that the West Antarctic Ice Sheet will continue to shrink (as it has probably been doing during the entire Holocene) even without warming. Several physical processes give ice sheets a very long memory (e.g., low temperatures of the older, deeper ice layers affecting ice viscosity, slow response of Earth's crust to a changing ice load, ice-age dust layers coming to the surface and affecting melt rates, etc.). In spite of admirable efforts in ice-sheet modeling, measuring from space, and laborious in situ observations, we are uncertain about what the ice sheets

CREDIT: OLIVIER BLAISE

would do without any change in climate.

JOHANNES OERLEMANS,[1] DORTHE DAHL-JENSEN,[2] VALÉRIE MASSON-DELMOTTE[3]

[1]Institute for Marine and Atmospheric Research, Utrecht University, Princetonplein 5, Utrecht 3584 CC, The Netherlands. [2]Niels Bohr Institute, University of Copenhagen, DK-2100 Copenhagen OE, Denmark. [3]Laboratoire des Sciences du Climat et de l'Environnement (IPSL/CEA/CNRS/UVSQ), Bat 701, L'Orme des Merisiers, CEA Saclay, 91 191 Gif-sur-Yvette cédex, France.

References

1. W. Dansgaard, H. B. Clausen, N. Gundestrup, S. Johnsen, C. Rygner, in *Greenland Ice Core: Geophysics, Geochemistry, and the Environment*, C. C. J. Langway, H. Oeschger, W. Dansgaard, Eds. (American Geophysical Union, Washington, DC, 1985), pp. 71–76.
2. J. Oerlemans *et al.*, *Ann. Glaciol.*, in press.
3. M. Oppenheimer, *Nature* **393**, 325 (1998).

Response

WE THANK OERLEMANS *ET AL.* FOR THEIR INTEREST and insights. However, none of the points raised affect our result that future "sea-level rise could be faster than widely thought."

Recent observations indicate shrinkage of both the Greenland Ice Sheet (GIS) [e.g., (*1*)] and the Antarctic Ice Sheet (AIS) [e.g., (*2*)]. Although long-term trends may be contributing, especially for the AIS, much work shows that recent warming has contributed to the mass loss [e.g., (*1*, *3*–*5*)]. Furthermore, some of the "fast" processes by which warming contributes to ice-sheet mass loss are not fully represented in the comprehensive ice-flow models that informed, e.g., the IPCC Third Assessment Report (*6*, *7*).

To these results, we added historical perspective: Whatever the details, the last time the Arctic was significantly warmer than today, global sea level was at least 4 to 6 m above present level, and most of this sea-level rise had to be the result of polar ice sheet melting. With warming projected for the future, and despite the important remaining uncertainties, we believe that this evidence shows that accelerated sea-level rise from the polar ice sheets could occur.

Oerlemans *et al.* do raise issues that warrant clarification. They suggest that there was a larger Eemian (last interglaciation) GIS than we inferred, based on the presence of isotopically enriched, possibly Eemian ice at the base of the Dye 3 ice core. However, this enriched ice does not prove that the GIS southern dome survived the peak interglacial warmth in the period 130,000 to 125,000 years ago. In contrast, the lack of ice from the previous glaciation argues for ice-sheet removal from the site at some point in the Eemian. The enriched ice at Dye 3 can be interpreted as (i) late-Eemian "growth ice," when the ice sheet reestablished itself in southern Greenland (*8*), or (ii) ice that flowed into the region from central Greenland or from a surviving but isolated southern dome (*9*). An improved understanding of the response of the GIS to the last interglacial warmth will come from an ice core that penetrates the full Eemian [e.g., (*10*)]. If Eemian mass loss from the GIS was smaller than our calculations, a correspondingly larger mass loss from the AIS is necessary to explain the reconstructed Eemian sea-level high-stand of +4 to +6 m.

We share Oerlemans *et al.*'s interest in the long-term trend in ice-sheet behavior [e.g., (*11*)] and their respect for the pioneering work of Mercer, Hughes, and others. We agree that Earth-system models exhibit important differences in regional reconstructions, including those in the Arctic. However, the success of the model we used (CCSM2, an improved version of the NCAR model used in ACIA) in simulating peak-Eemian conditions matching available paleoclimatic data increases our confidence in our results.

We look forward to working with Oerlemans *et al.* and other members of the com-

munity to narrow the uncertainties on this critical topic.

JONATHAN T. OVERPECK,[1] BETTE L. OTTO-BLIESNER,[2] GIFFORD H. MILLER,[3] RICHARD B. ALLEY,[4] DANIEL R. MUHS,[5] SHAWN J. MARSHALL[6]

[1]Institute for the Study of Planet Earth, University of Arizona, Tucson, AZ 85721, USA. [2]National Center for Atmospheric Research, Post Office Box 3000, Boulder, CO 80307, USA. [3]Institute of Arctic and Alpine Research, University of Colorado, Campus Box 450, Boulder, CO 80309, USA. [4]Department of Geosciences, Pennsylvania State University, 0517 Deike Building, University Park, PA 16802, USA. [5]U.S. Geological Survey, Mail Stop 980, Box 25046, Federal Center, Denver, CO 80225, USA. [6]Department of Geography, University of Calgary, Calgary, AB T2N 1N4, Canada.

References

1. R. Thomas *et al.*, *Geophys. Res. Lett.* **33**, L10503 10.1029/2006GL026075 (2006).
2. I. Velicogna, J. Wahr, *Science* **311**, 1754 (2006).
3. J. Box *et al.*, *J. Clim.*, in press.
4. A. Shepherd, D. Wingham, T. Payne, P. Skvarca, *Science* **302**, 856 (2003).
5. T. A. Scambos, J. A. Bohlander, C. A. Shuman, P. Skvarca, *Geophys. Res. Lett.* **31**, L18402 10.1029/2004GL020670 (2004).
6. IPCC, *The Science of Climate Change* (Cambridge Univ. Press, Cambridge, 2001).
7. R. B. Alley, P. U. Clark, P. Huybrechts, I. Joughin, *Science* **310**, 456 (2005).
8. R. M. Koerner, D. A. Fisher, *Ann. Glaciol.* **35**, 19 (2002).
9. N. Lhomme, G. K. C. Clarke, S. J. Marshall, *Quat. Sci. Rev.* **24**, 173 (2005).
10. D. J. Dahl-Jensen *et al.*, "The last interglacial and beyond: A northwest Greenland deep ice core drilling project," International Partnerships in Ice Core Sciences, http://www.pages.unibe.ch/science/initiatives/ipics/data/ipics_neem.pdf (2005).
11. R. B. Alley, I. M. Whillans, *J. Geophys. Res.* **89C**, 6487 (1984).

CORRECTIONS AND CLARIFICATIONS

Perspectives: "Dangerously seeking linear carbon" by R. H. Baughman (19 May, p. 1009). The second sentence of the teaser should have read "A solid state polymerization reaction avoids this problem and may allow synthesis of these elusive products."

TECHNICAL COMMENT ABSTRACTS

COMMENT ON "Cell Type Regulates Selective Segregation of Mouse Chromosome 7 DNA Strands in Mitosis"

James E. Haber

Armakolas and Klar (Reports, 24 February 2006, p. 1146) suggested that segregation of mouse chromosome 7, after induction of a site-specific crossover between homologous chromosomes, is driven by a preferential inheritance of the old Watson and the old Crick DNA strands. However, this interpretation only considered half of the possible outcomes. The conjecture fails when all possible outcomes are examined.

Full text at www.sciencemag.org/cgi/content/full/313/5790/1045b

RESPONSE TO COMMENT ON "Cell Type Regulates Selective Segregation of Mouse Chromosome 7 DNA Strands in Mitosis"

Amar J. S. Klar and Athanasios Armakolas

To explain how all chromosome recombinants can become homozygous for a marker located distal to the crossover point, we proposed that mitotic recombination must be restricted to two specific chromatids and that the selective chromatid segregation process follows recombination. We refute Haber's contention that our results can be explained by the conventional X-segregation process if recombination of all possible combinations of chromatids is considered.

Full text at www.sciencemag.org/cgi/content/full/313/5790/1045c

Letters to the Editor

Letters (~300 words) discuss material published in *Science* in the previous 6 months or issues of general interest. They can be submitted through the Web (www.submit2science.org) or by regular mail (1200 New York Ave., NW, Washington, DC 20005, USA). Letters are not acknowledged upon receipt, nor are authors generally consulted before publication. Whether published in full or in part, letters are subject to editing for clarity and space.

WATER RESOURCES

For Our Thirsty World, Efficiency or Else

Sandra L. Postel

When the Rivers Run Dry
Water—The Defining Crisis of the Twenty-First Century

Fred Pearce

Beacon Press, Boston, 2006. 336 pp. $26.95. ISBN 0-8070-8572-3.

By now we've all heard the prediction: Water will be the oil of the 21st century. As competition for water heats up, it will reshape national economies and geopolitical alliances, maybe even cause wars. But the prophetic phrase misses something big and fundamental. Unlike oil, fresh water has no substitutes. Although societies will transition away from oil (and hopefully soon), there is no transitioning away from water. And above all is the obvious: water is essential to life—not just to human life, but to the myriad species that make this world tick and hum to our great benefit.

In *When the Rivers Run Dry: Water—The Defining Crisis of the Twenty-First Century*, Fred Pearce provides a compelling compendium of place-based water stories that reveal just how ground-shifting the world's water predicament will be. A veteran science journalist, the author traveled to more than 30 countries during his research, unearthing dramas that put a human face on sobering facts and figures.

Many rivers around the globe are overtapped and no longer discharge much water to the sea. Make a list—Yellow, Indus, Ganges, Nile, Colorado—and the big question comes into focus: Where will the water needed for future food production come from? Pearce spends a good bit of time on various facets of this question—and for good reason. Irrigation accounts for the lion's share of the world's water consumption, 70 percent globally and 90 percent in many Asian countries, where nature doles out long dry seasons. One-fifth of China's wheat and one-seventh of its corn are produced, in good years, in the coastal province of Shandong, which is last in line to receive the flow of the Yellow River. Farmers have already abandoned millions of acres of cropland in the water-stressed Yellow River basin, and in the summer of 2000 a mini–water war broke out in Shandong as thousands of farmers tried to siphon water slated for cities from a reservoir. Likewise, at the lower end of the Indus River, impoverished Pakistani farmers are fleeing from their dry fields to the slums of Karachi, where unemployment and crime are rampant and al-Qaeda replenishes its ranks.

As major rivers dwindle to a trickle, farmers and cities alike pump more water from underground. Globally as much as one-tenth of the world's food may be produced with water drawn from declining aquifers. In India, at least a quarter of the farmers are overtapping aquifers, withdrawing water faster than those underground sources are recharging, and setting the stage for a " 'colossal anarchy' " as more wells and fields are abandoned.

With demands pressing against finite supplies, it matters how water gets divvied up. Typically rivers, lakes, and other freshwater ecosystems receive an ever-shrinking residual slice of the water pie, often too little to sustain fisheries, biodiversity, wetlands for water purification, and other vital services. The Aral Sea is now a well-known poster child of aquatic ruin—more salty desert than watery lake after decades of excessive river diversions. Although Pearce admits to having "a sneaking love of large dams," he concludes that China's decision to build a cascade of them on the upper Mekong River would be a catastrophe for "the entire ecological infrastructure on which much of Southeast Asian rural life is built."

Pearce devotes limited space to the complexities of hydropolitics. But he pulls no punches in documenting the "hydrological apartheid" that now exists in the Jordan River basin. Today each Palestinian in the occupied West Bank uses less than a quarter as much water as a neighboring Israeli. Palestinian families around Nablus spend between 20 and 40 percent of their incomes to buy water, while Israeli settlers enjoy green lawns and swimming pools. Pearce calls the 1967 Six Day War "the first modern water war," citing none other than Ariel Sharon, an Israeli commander in that war and later prime minister, who wrote: "The Six-Day War really started on the day Israel decided to act against the diversion of the Jordan." Before that war, less than a tenth of the Jordan River watershed was within Israel's borders; by the war's end, Israel controlled the vast majority of it, including Syria's Golan Heights and key aquifers under the West Bank.

Pearce generally is thin on prescriptions for solving the problems he lays out so persuasively, but his stories and numerous interviews offer tempting glimmers of a more productive way forward. In the Jordan basin, for example, a more equitable distribution of water might painlessly be achieved if Israel chose to use its desalinated water to free up West Bank groundwater for the Palestinians. If that were to be combined with a sharp reduction of irrigated agriculture, which accounts for about two-thirds of Israel's water use but contributes two percent to its gross domestic product, hydrologic security for all is not out of reach.

Although *When the Rivers Run Dry* offers little fresh analysis (and, much to my chagrin, no list of references), its collection of anecdotes and examples point away from big

Overtapped flow. Due to the diversion of Colorado River water for agriculture and urban use, in most years the river no longer reaches the Gulf of California.

CREDIT: VISIBLE EARTH/NASA

The reviewer is at the Global Water Policy Project, 107 Larkspur Drive, Amherst, MA 01002–3440, USA. E-mail: spostel@globalwaterpolicy.org

dams, massive diversions, and other large-scale supply solutions and toward more demand-focused, local-level, working-with-nature approaches. In India, a vibrant grassroots movement to capture rainwater is replenishing aquifers. "Water tables have risen so much in Rajasthan," Pearce writes, "that five ancient desert rivers … have returned to the map." Drip irrigation, which delivers water directly to the roots of plants, holds vast potential to increase "crop per drop," but is the technology of choice on only about 1 percent of the world's irrigated land. Overall, eliminating the enormous waste of water, especially in agriculture, could return flows to rivers and replenish aquifers, but the heavy subsidies that discourage efficiency and productivity remain stubbornly in place.

The ideas that Pearce puts forth have in common a deep respect for, and understanding of, the water cycle and the myriad services that nature provides through it. If scientific and technological ingenuity focused more on working productively with that cycle rather than on further manipulating it, perhaps human needs for water can be harmonized with those of the ecosystems that sustain us.

10.1126/science.1132334

BROWSINGS

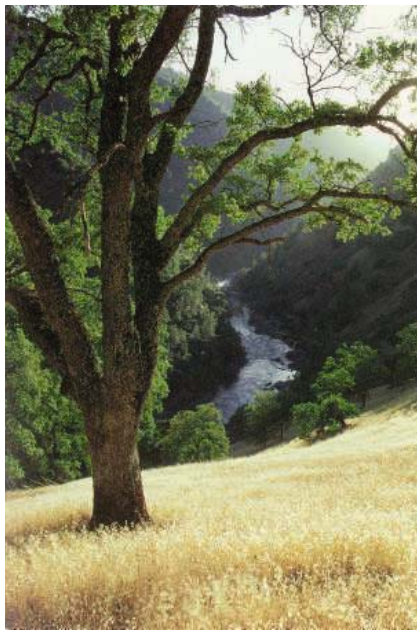

Rivers of America.
Tim Palmer. Abrams, New York, 2006. 224 pp. $40, C$50, £24.95. ISBN 0-8109-5485-0.

Photographers have long been captivated by flowing water. Here Palmer, the author of several previous books on river conservation and specific rivers, offers a selection of scenes of unspoiled waterways from around the United States. Short essays sketch the impact rivers have had on his life, their importance to ecosystems, the threats they face (from dams and pollution to exotic species and riverside development), and steps being taken on their behalf. But the book is primarily a celebration of the visual aesthetics of rivers (right, the Tuolumne in the Sierra Nevada foothills).

Ogallala Blue.
Water and Life on the High Plains. William Ashworth. Norton, New York, 2006. 344 pp. $26.95, C$35.50. ISBN 0-393-05842-5.

To 19th-century explorers and surveyors, the High Plains, west of the 100th meridian, seemed the Great American Desert. Despite sufficient rainfall to make the region semiarid, they believed the shortgrass prairie worthless for farming. Today, the land accounts for over 20% of the U.S. agricultural output. Most of the water that fuels this harvest comes from the Ogallala Aquifer. Ashworth tells the story of this groundwater and the people it sustains. He discusses the origins of the fossil water and the sheet of erosional debris that contains it, extraction technologies (such as centrifugal pumps and center-pivot sprinklers), and the range of approaches to allocating, managing, and conserving the resource. Five trillion gallons are being withdrawn from the aquifer each year. Although draconian predictions of the Ogallala's fate have gone unrealized, Ashworth argues that the reprieve is likely only to be temporary.

Bird Coloration.
Geoffrey E. Hill and Kevin J. McGraw, Eds. Harvard University Press, Cambridge, MA, 2006. Volume 1, Mechanisms and Measurements. 631 pp. $95, £59.95, €87.50. ISBN 0-674-01893-1. Volume 2, Function and Evolution. 519 pp. $95, £59.95, €87.50. ISBN 0-674-02176-2.

These two volumes offer students and researchers a wide-ranging account of how and why birds often display bold and brilliant colors. An initial section covers perception and measurement. Subsequent chapters discuss the pigments (e.g., melanins and carotenoids) and feather structures that produce colors. Next, contributors consider how genes, the environment, and hormones control color expression. In the second volume, the authors examine avian uses of color, including concealment, mate choice, and signaling. Two contributors review the selective pressures driving the evolution of avian colors and patterns. A final chapter describes an approach to reconstructing the coloration of ancestral avian lineages.

PHILOSOPHY OF SCIENCE

Science Undermined by Our Limited Imagination?

Tim Lewens

Kyle Stanford's admirably clear and engaging *Exceeding Our Grasp* addresses the most basic question in the philosophy of science: Should we believe what scientific theories tell us about the world? Stanford is not asking the trivial question of whether our theories are correct in every detail. Everyone will agree that many of the fine-grained claims in molecular genetics, quantum physics, and biological anthropology, for example, are likely to need substantial revision in the future. The question is instead whether we should think our best theories—in chemistry, physics, biology, and elsewhere—are even close to the truth. So-called scientific realists say yes. Stanford says no.

In defense of this striking claim, Stanford's book develops what he calls "the problem of unconceived alternatives." His argument is a close relative of an older philosophical argument known as the "pessimistic induction," which begins by claiming that the history of science is predominantly a history of failure. Time and again, theories that enjoyed impressive predictive and practical successes, and that were regarded as beyond doubt, have later been rejected as fundamentally mistaken. The argument concludes that the theories we now hold to be true will eventually go the same way.

Stanford (a philosopher of science at the University of California, Irvine) diverges from a simple defense of the pessimistic induction by shifting the argumentative focus from scientific theories to scientists. He tries to show that past scientists have typically failed to consider (let alone evaluate) important alternatives to the theories they have ended up espousing. The central chapters of the book consist of a series of case studies in neglect, all in the domain of 19th-century theories of development and inheritance.

The reviewer is in the Department of History and Philosophy of Science, University of Cambridge, Free School Lane, Cambridge CB2 3RH, UK. E-mail: tml1000@cam.ac.uk

Consider Darwin's theory of pangenesis, which he defended in his 1868 work *The Variation of Animals and Plants Under Domestication* (*1*). Darwin argued that the accepted phenomena of inheritance can be explained on the assumption that each adult organ produces tiny particles, which Darwin called "gemmules," of a character specific to that organ. Particles produced by different organs collect together in the sex cells and are passed on to offspring, where they direct the formation of new organs resembling those which produced them. Stanford argues that Darwin failed to consider a whole class of alternative explanations for parent-offspring resemblance that attribute similarities between parents and offspring to the production of each organism by a common cause. Something like the common cause view is endorsed by many theorists today; on this view, the offspring's traits resemble those of its parents not because the character of the parent's traits causally influences the character of the offspring's traits, but because the genetic material that originally produced the parent's traits also produces the offspring's traits.

In cases like this we can use today's theories to expose the theoretical blind spots of earlier thinkers. But Stanford's aim is not to congratulate modern scientists on how much more perceptive they are than their predecessors. He argues that there is no reason to think that we are any less susceptible than Darwin to the pervasive phenomenon of cognitive oversight. According to Stanford, history suggests that modern scientists, too, are currently overlooking alternative theoretical options of a wholly alien sort, which will only be apparent to scientists of the future. This persistent failure of the scientific imagination means that we should expect the truth to lie in the vast space of theories to which we are blind, rather than in the small areas that we are able to survey.

Exceeding Our Grasp
Science, History, and the Problem of Unconceived Alternatives

by P. Kyle Stanford

Oxford University Press, Oxford, 2006. 248 pp. $45. ISBN 0-19-517408-9.

Stanford's book deserves to be widely read. Its central argument is clearly stated, its conclusion is radical, it engages in a productive fashion with detailed case studies, and it lays down several substantial challenges to scientific realism. Lastly, it is consistently thought-provoking.

One of the thoughts it provokes is that Stanford's argument may prove far more than he wants it to. At various points, he implies that his antirealism is built on the belief that cognition in *Homo sapiens* is simply not up to discovering the workings of the world. This belief, in turn, is justified on the basis of the documented history of human scientists' failures to conceive of important alternative theories. But which specific human weaknesses are supposed to make our species' scientific claims vulnerable to Stanford's sceptical argument? Is it a question of our having a maximum IQ that is too low? or imaginative faculties that are somewhat too restrictive?

Path of thoughts. Darwin would ponder problems as he strolled laps around his "thinking path," the Sandwalk at Down House.

Another way of asking this question is to consider how, on Stanford's view, an imaginary species of alien scientist would need to think in order to generate reliable scientific knowledge. Suppose we assume, with Stanford, that the pervasive failure to conceive of important alternative theories truly licenses scepticism about theoretical claims. It seems to follow that the theoretical claims of any imaginable species that acquires concepts by interacting with the world around it are likely to come into the sceptical firing line. For any such species, the formulation of advanced theories is not possible when science begins. Rather, interactions with the world enable the gradual expansion of the repertoire of concepts its members can use to describe the world. For these species, earlier scientists are consequently unable to conceive of theoretical possibilities entertained by later scientists. A species of this kind might be able to shrug off Stanford's argument if its history of science is one of pathological hedging. Its early theories are logically as weak as can be; hence they need never be rejected, for they are never shown false. But it is hard to see why such a way of doing science is more likely to get to the truth than our own.

So far as I can see, the only other kind of species that might be able to elude Stanford's argument is a cognitive superspecies, which finds out about the workings of the world by exhaustively considering, at the very beginning of its own history of science, every relevant theoretical possibility there is, no matter how complex. It might then settle on just one theory, which would not change much for the rest of that species' existence. A species like this, which has the miraculous ability to formulate advanced theories of the world prior to interacting with it, would not be vulnerable to Stanford's induction, for it would have no history of unconceived alternatives.

My worry, then, is that in spite of the detailed case studies of human science Stanford presents in *Exceeding Our Grasp*, the apparent conclusion to draw from his argument is not that our species has an idiosyncratic set of weaknesses that handicap our abilities to find out about the world. Instead his argument points to a far stronger claim, namely that if a scientific community's repertoire of concepts expands over time as it interacts with the world, then that community cannot generate theoretical knowledge effectively. I do not know whether Stanford would embrace such a sweeping conclusion. In any case, perhaps my own failure to conceive of how, on Stanford's view, theoretical scientific knowledge is possible for any nonmiraculous species, is merely another confirming instance of the induction he so tenaciously defends.

Reference

1. C. Darwin, *The Variation of Plants and Animals Under Domestication* (John Murray, London, 1868).

10.1126/science.1131579

CREDIT: P. KYLE STANFORD

INQUIRY LEARNING

Teaching and Assessing Knowledge Integration in Science

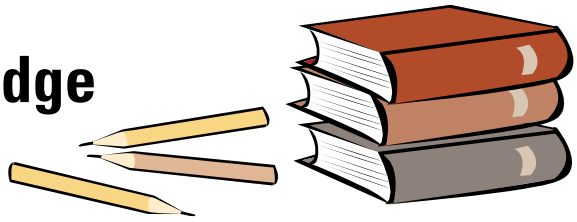

Marcia C. Linn,[1]* Hee-Sun Lee,[2] Robert Tinker,[3] Freda Husic,[1] Jennifer L. Chiu[1]

Interactive visualizations combined with online inquiry and embedded assessments can deepen student understanding of complex ideas in science.

Students grapple with multiple, conflicting, and often confusing ideas while they learn scientific concepts. Research has shown that instruction is both effective and durable when teachers use students' ideas as a starting point and guide the learners as they articulate their repertoire of ideas, add new ideas including visualizations, sort out these ideas in a variety of contexts, make connections among ideas at multiple levels of analysis, develop ever more nuanced criteria for evaluating ideas, and regularly reformulate increasingly interconnected views about the phenomena (*1*, *2*). We refer to this process as knowledge integration.

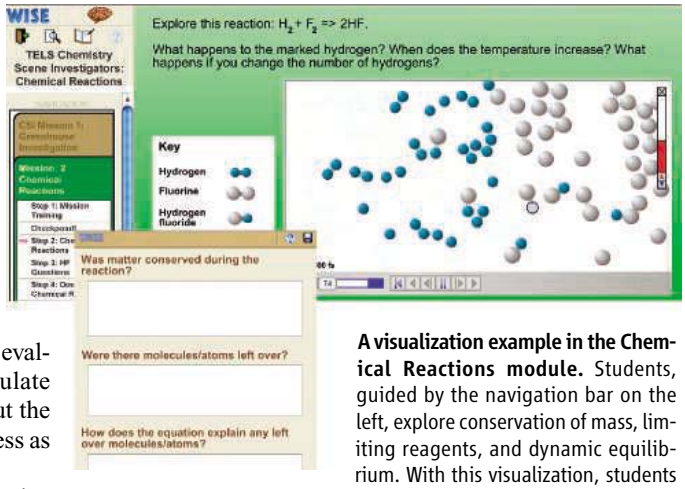

A visualization example in the Chemical Reactions module. Students, guided by the navigation bar on the left, explore conservation of mass, limiting reagents, and dynamic equilibrium. With this visualization, students examine the effects of heat and number of molecules on chemical reactions and explain their ideas in embedded notes shown on the left (*21*).

Common testing procedures emphasize recall of scientific information over deep understanding of science reasoning (*3*), and as a result, teachers focus most of their time on "covering" the many required topics. This approach leaves teachers with little time to help students integrate their ideas (*4*) or engage in scientific inquiry as mandated by national standards (*5*, *6*) and leaves students with isolated ideas, little understanding of science reasoning, and a perception that science is not relevant to everyday life (*7*).

The Technology-Enhanced Learning in Science (TELS) Center has developed interactive lessons that improve inquiry learning by strengthening knowledge integration and taking advantage of visualization technologies in both instruction and assessment. TELS designs visualizations of scientific phenomena (*8*) and embeds them in instructional modules (see figure, above) to help students integrate their ideas (*9*, *10*). The TELS Center created two modules each for the science courses most common in middle school (life, physical, and earth sciences) and high school (biology, chemistry, and physics). Topics selected were those from the science standards that teachers say are most challenging. TELS designed assessments to measure knowledge integration about the module topics.

Participants and Design

TELS studied two time-delayed cohorts of students. We recruited teachers in 16 schools across five states and assessed the performance of their students at the end of one school year after they studied the typical curriculum (3712 Typical Cohort students) using TELS assessments in six courses. The next year, we offered teachers at these schools one or two 5-day TELS modules to use instead of their previous treatment of comparable content. We tested the performance of new students in the same schools who had the opportunity to study TELS (4520 TELS Cohort students) at the end of the second school year, using a subset of the items from the first year that aligned with TELS modules as well as new items that served as a baseline for future modules. We used this assessment sample of 8232 sixth- to twelfth-grade students to analyze item properties of multiple choice and explanation items in both years of TELS assessments. Twenty-six of the 43 teachers participated in both Typical and TELS Cohort assessments and taught one or two TELS modules in the subject area of the assessment. We used this comparison sample of 4328 students to analyze the overall impact of TELS modules and the impact of TELS by science course and teacher.

TELS Modules

Designed by partnerships of discipline experts, learning researchers, classroom teachers, and technology specialists using the Web-based Inquiry Science Environment (WISE), TELS modules guide students in research-based knowledge integration practices using an online map and embedded assessments (*11*, *12*). TELS modules make science visible by representing unseen phenomena such as molecular reactions (*13*). They showcase the relevance of science with current scientific dilemmas such as choosing among treatment options for cancer, interpreting claims about global warming, or selecting an energy-efficient car. One life science module connects the design of a cancer medication to a visualization of the stages of mitosis. A physics module allows students to experiment with variables governing deployment of airbags. Teachers can access student ideas online in real time and use them to tailor instruction.

The TELS high school chemical reactions module uses an interactive visualization (see figure, above) to help students explore factors influencing greenhouse gases. The inquiry map guides students to articulate their ideas, test their predictions, critique each other's views, and distinguish new and elicited ideas. Typical chemistry students have difficulty connecting symbolic and visual representations of reactions and often fail to account for conservation of mass and the effects of heat and temperature. Static representations in textbooks lead some chemistry students to report that molecules are malleable or colored and to argue that molecules stop moving after they react (*14*, *15*). The TELS chemical reactions module helps

[1]Graduate School of Education, University of California, Berkeley, CA 94720, USA. [2]Department of Education, Tufts University, Medford, MA 02155, USA. [3]Concord Consortium, Concord, MA 01742, USA.

*Author for correspondence. E-mail: mclinn@berkeley.edu

students sort out these ideas using an interactive visualization with which students can gather evidence about limiting reagents and study the relationship between molecular behavior and temperature by modifying inputs such as temperature or proportions of reactants (*16*). TELS modules help students act like scientists, comparing viewpoints, generating criteria for selecting fruitful ideas, fitting ideas together in arguments, gathering evidence for their own views, and critiquing the arguments generated by their peers.

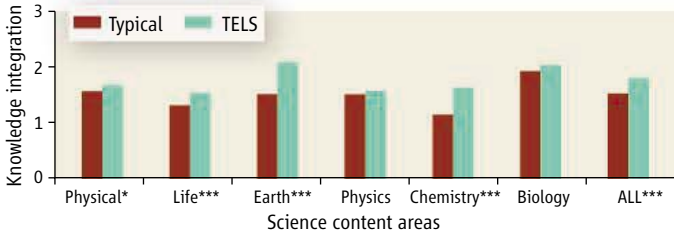

Explanation item performance of Typical and TELS Cohorts. TELS modules led to significant improvement in knowledge integration scores for physical science, life science, earth science, and chemistry. *$P < 0.05$, **$P < 0.01$, and ***$P < 0.001$. Knowledge integration: 0 = no answer/off-task, 1 = no link, 2 = partial link, and 3 = full link. The TELS cohort significantly outperformed the Typical Cohort on the explanation items, with an effect size (ES) = 0.32***, as well as within all middle school course levels (physical, ES = 0.16*; life, ES = 0.35***; earth, ES = 0.64***) and within the high school chemistry course (ES = 0.81***). Students moderately improved on physics (ES = 0.09) and biology (ES = 0.11).

TELS Assessments and Scoring

To measure inquiry skills as defined by the science standards, TELS created assessments composed of multiple-choice and explanation items that asked students to connect ideas in arguments. TELS researchers created tests for each of the six courses that include items from our research as well as items published by national, international, and state assessments. We scored all of the multiple-choice items dichotomously. We used the TELS knowledge integration rubric to capture progressively more sophisticated levels of reasoning on explanation items (*16*).

We analyzed the properties of all 201 items administered to the assessment sample (*16*). We found that the items were highly correlated and that 97.5% measured the same dimension of learning. In addition, higher scores in each explanation item were obtained by students who were estimated to have higher knowledge integration abilities.

Overall, 98% of the 83 explanation items scored with knowledge integration rubrics were highly capable of discriminating respondents with high knowledge integration abilities from those with low knowledge integration abilities. Only 16% of the 118 multiple-choice items showed similar discrimination. Of multiple-choice items, 39% did not have acceptable discrimination indices (*16*).

Student Performance

The 26 teachers in the cohort comparison study spent between 2 and 10 days implementing the TELS modules. A few teachers had to shorten their lessons due to school scheduling, but 31% completed two modules.

To determine the impact of TELS, we used 50 items that were administered to both cohorts and aligned with the modules. Overall, for the multiple-choice items, TELS had no impact (Typical mean = 55.0% correct; TELS mean = 54.8% correct; effect size = 0.007). For the explanation items, TELS resulted in improvement equal to more than a quarter of a standard deviation (Typical mean = 1.52; TELS mean = 1.78, effect size = 0.32, $P < 0.001$). As expected, because the explanation items are better able to discriminate levels of knowledge integration, they showed more sensitivity to instruction. We analyzed TELS, teacher, and science-course effects and found significant effects for TELS and teacher (*16*). Improvement was similar across science courses and individual comparisons were significant for four of the six courses (see figure, above).

Teachers varied in their access to technology, experience with inquiry, prior knowledge of their students, and experience with technology, all of which could contribute to the teacher effect. We expect TELS effects to become more consistent as teachers gain experience and we use embedded assessments along with teacher feedback to improve the modules. These findings also underscore the importance of professional development. Teachers in TELS have asked for additional opportunities to learn the pedagogy of knowledge integration.

Discussion

When students engage in inquiry and learn to integrate their ideas, they are prepared to apply what they learn in science classes to contexts beyond the classroom. For schools to teach inquiry and knowledge integration, both instruction and assessment need to change. Our findings and other similar studies show that typical multiple-choice science assessments are not sensitive to instruction designed to promote coherent (*17*, *18*) or deep understanding of science topics (*19*).

Assessments that require students to link and connect ideas clarify what we mean by inquiry learning and have the potential of stimulating lifelong scientific understanding. TELS students not only gained understanding of the topic they had studied but also learned to construct arguments, critique explanations written by their peers, and respond to feedback from their teachers. Just as students gain some advantage from experience with multiple-choice items (*20*), so might students benefit from experience constructing scientific explanations as encouraged in TELS modules.

TELS technologies enable students to connect scientific visualizations to their understanding of complex scientific ideas. They help guide students to make sense of visualizations rather than viewing them as amusing movies. These connections can benefit students in their future courses, prepare students to deal with scientific dilemmas, and encourage learners to view computer-presented information more critically.

References and Notes

1. M. C. Linn, E. A. Davis, P. Bell, Eds., *Internet Environments for Science Education* (Lawrence Erlbaum Associates, Mahwah, NJ, 2004).
2. M. C. Linn, in *Cambridge Handbook of the Learning Sciences*, R. K. Sawyer, Ed. (Cambridge Univ. Press, New York, 2006), pp. 243–264.
3. L. Stern, A. Ahlgren, *J. Res. Sci. Teach.* **39**, 889 (2002).
4. N. B. Songer, Congressional Testimony; full text available online (edworkforce.house.gov/hearings/109th/21st/mathscience051905/songer.htm).
5. National Research Council, *National Science Education Standards* (NRC, Washington, DC, 1996).
6. S. H. Singer, M. L. Hilton, H. A. Schweingruber, Eds., *America's Lab Report* (National Academic Press, Washington, DC, 2005).
7. M. C. Linn, S. Hsi, *Computers, Teachers, Peers: Science Learning Partners* (Lawrence Erlbaum Associates, Mahwah, NJ, 2000).
8. Q. Xie, R. Tinker, *J. Chem. Edu.* **83**, 77 (2006).
9. Y. Bhattacharjee, *Science* **310**, 224 (2005).
10. TELS Center (telscenter.org).
11. M. C. Linn *et al.*, *Edu. Tech.* **46**, 54 (2006).
12. J. D. Bransford *et al.*, Eds., *How People Learn* (National Academy Press, Washington, DC, 1999).
13. The visualizations were created using Concord Consortium (molo.concord.org) softtware.
14. R. Ben-Zvi *et al.*, *J. Chem. Edu.* **63**, 64 (1986).
15. R. Ben-Zvi *et al.*, *Edu. Chem.* **24**, 117 (1987).
16. Materials and methods are available on *Science* Online.
17. J. A. Shymansky *et al.*, *J. Res. Sci. Teach.* **20**, 387 (1983).
18. D. F. Walker, J. Schaffarzik, *Rev. Edu. Res.* **44**, 83 (1974).
19. D. B. Clark, M. C. Linn, *J. Learn. Sci.* **12**, 451 (2003).
20. L. A. Shepard, *Edu. Res.* **29**, 4 (2000).
21. The animated visualization is available online (http://telscenter.org/Videos/ChemModel.mov).
22. Based on work supported by NSF under grants 0334199 and 0455877. Any opinions, findings, and conclusions or recommendations expressed in this material are those of the authors and do not necessarily reflect the views of the NSF. We thank O. L. Liu for help with the psychometric analysis, anonymous reviewers for helpful comments, and the TELS partners and the TELS schools for their dedication to improving science learning.

Supporting Online Material
www.sciencemag.org/cgi/content/full/313/5790/1049/DC1

10.1126/science.1131408

ECOLOGY

Are Global Conservation Efforts Successful?

Global conservation efforts have prevented the extinction of 31 bird species over the past century, but these and many others may yet be lost as a result of continuing threats to their habitats.

Ana S. L. Rodrigues

Human actions affect ecosystems worldwide, leading to irreversible losses in biodiversity. These changes were faster in the past 50 years than at any time in human history, and this acceleration is projected to continue (*1*), despite diverse efforts to prevent these losses. Do these efforts make any measurable difference in the global state of biodiversity? The combined results of the 2006 World Conservation Union (IUCN) Red List of Threatened Species (*2*) and of a study by Butchart *et al.* (*3*) provide the first opportunity to assess the impact of global conservation investment on biodiversity.

Measuring global conservation impact is not simple. Biodiversity is not easily quantified (*4*), and resources for monitoring it fall woefully short (*5*). Moreover, innumerable conservation activities take place worldwide, with approaches as diverse as single-species management, ecosystem restoration, environmental education, and political lobbying. Their scales range from local to global, with various degrees of coordination, replication, and synergy among them. Overall conservation impact can thus not be measured as the summed impacts of individual actions.

One useful approach is to compare the observed change in global biodiversity with the predicted change in the absence of such efforts. In the best-case scenario, conservation action would maintain biodiversity at a stable level, because global biodiversity does not increase on a time-scale relevant to human enterprise. More realistically, conservation action might be considered successful if it slows down the human-induced rate of global biodiversity decline.

This approach can now be applied to birds, the best-studied vertebrate group. The 2006 IUCN Red List reports 135 bird species that have become extinct since 1500 (*2*). The numbers of extinctions per century increased steadily to 49 in the 19th century, but then appear to decline to 43 in the period from 1901 to 2006 (see the first figure). This could be mistaken as evidence that the human impact on birds has weakened. However, recent extinctions are underestimated because of the time lag between the disappearance of a species from the wild and the confirmation of its extinction.

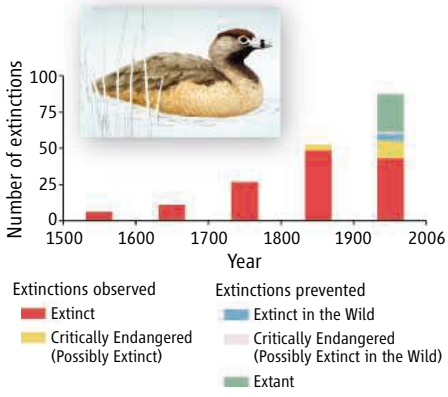

Bird extinction trends. Estimated numbers of bird extinctions in the past five centuries, and of extinctions prevented through conservation action. See the Supporting Online Material for information on the species in each class. **(Inset)** The Atitlán grebe (*Podilymbus gigas*) was driven to extinction in 1986 in its native Lake Atitlán, Guatemala (*9*).

For a species to be listed as "Extinct" on the IUCN Red List, exhaustive surveys must have been undertaken in all known or likely habitat throughout its historic range, at appropriate times, and over a time frame appropriate to its life cycle and life form (*6*). To avoid the "Romeo error" (*7*) of giving up on a species when it is not yet too late, conservationists are reluctant to designate species as "Extinct" if there is any chance that they may still persist (*8*). A framework has been developed to examine relevant evidence and judge as objectively as possible which species may already be extinct (*8*). Fifteen birds are listed as "Critically Endangered (Possibly Extinct)" in the 2006 IUCN Red List (*2, 9*), revealing an uninterrupted upward trend of extinction rates (see the first figure).

Butchart and colleagues (*3*) add the missing piece required to evaluate conservation impact. Using data on population sizes, population trends, threatening processes, and conservation actions, they identify at least 26 bird species surviving in the wild that would have very probably gone extinct if conservation programs for them had not been undertaken. Four additional species are classified as "Extinct in the Wild" and one as "Critically Endangered (Possibly Extinct in the Wild)," only surviving (or possibly only surviving) in captive breeding programs (*2, 8*). These 31 species represent the gain in extant bird species attributable to conservation action, providing a measure of the success of global conservation in preventing bird extinctions (see the second figure). In the absence of conservation, the rates of bird extinctions would thus have increased dramatically into the present (see the first figure).

This is the first time that global conservation impact has been quantified with a direct biodiversity measure, rather than with indicators of conservation effort such as area protected (*10*) or money invested (*11*). Nonetheless, this is a crude appraisal that uses a narrow measure of biodiversity and inevitably underestimates the overall impact of conservation efforts. Conservation efforts aim at much more than avoiding the ultimate extinction of species, including preventing species from becoming threatened in the first place and ensuring the health of the ecosystem processes that support biodiver-

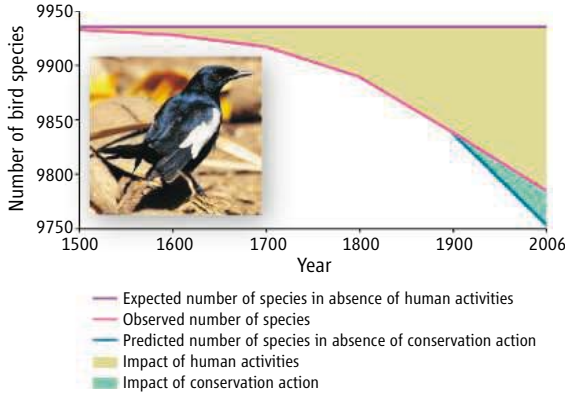

Conservation impact. Estimated impact of global conservation action on preventing extinction, compared to the impact of human activities on overall bird species richness. Total numbers of species are based on the taxonomy followed in (*2, 9*). **(Inset)** Extinction of the Seychelles magpie-robin (*Copsychus sechellarum*) was prevented through a conservation program that included translocations, habitat management, and eradication of invasive species (*9*).

The author is in the Department of Zoology, University of Cambridge, Cambridge CB4 1AD, UK. E-mail: aslr2@cam.ac.uk

sity. Measures of conservation impact with finer temporal and ecological resolution are urgently needed to assess progress toward the United Nations 2010 Biodiversity Target of reducing the rate of biodiversity loss (*5*).

Moreover, there is no room for complacency. None of the 31 bird species can be declared as saved; most still face a very high risk of extinction and depend on continued conservation efforts (*2, 3*). Preventing each of these extinctions has typically required a mix of conservation interventions, including actions that might benefit other threatened species in the same localities (such as habitat protection and predator control; 22 species) and species-specific actions (such as captive breeding and translocations; 21 species).

A major increase in global conservation resources would be required to extend such dedicated efforts into each of the thousands of threatened species (*2*). Just among birds, 1210 species are listed as threatened (*2, 9*). The populations of 217 highly threatened bird species are confined to single sites (*12*) and could be lost very rapidly. The number of bird extinctions is expected to increase rapidly in the near future, unless considerable action is taken.

Nonetheless, it is encouraging that bird conservation actions worldwide are making a noticeable dent in the bleak scenario of global biodiversity loss. In many cases, this may simply amount to buying a little time, but while a species is extant we can still have hope for its recovery in the future. Extinction, on the other hand, is forever.

References and Notes

1. Millennium Ecosystem Assessment, *Ecosystems and Human Well-Being: Biodiversity Synthesis* (World Resources Institute, Washington, DC, 2005).
2. IUCN, *2006 IUCN Red List of Threatened Species* (IUCN, Gland, Switzerland, 2006); available at www.iucnredlist.org.
3. S. H. M. Butchart, A. J. Stattersfield, N. J. Collar, *Oryx* **40**, 266 (2006).
4. K. J. Gaston, Ed., *Biodiversity—A Biology of Numbers and Difference* (Blackwell Science, Oxford, 1996).
5. A. Balmford *et al.*, *Science* **307**, 212 (2005).
6. IUCN, *Red List Categories and Criteria—Version 3.1* (IUCN, Gland, Switzerland, 2001).
7. N. J. Collar, *Oryx* **32**, 239 (1998).
8. S. H. M. Butchart, A. J. Stattersfield, T. M. Brooks, *Bull. Br. Ornithol. Club* **126A**, 7 (2006).
9. BirdLife International, *Data Zone: Species* (BirdLife International, Cambridge, UK, 2006); available at www.birdlife.org/datazone/species.
10. S. Chape, J. Harrison, M. Spalding, I. Lysenko, *Philos. Trans. R. Soc. London Ser*. B **360**, 443 (2005).
11. A. N. James, K. J. Gaston, A. Balmford, *Nature* **401**, 323 (1999).
12. T. H. Ricketts *et al.*, *Proc. Natl. Acad. Sci. U.S.A.* **102**, 18497 (2005).

13. I am grateful to A. Balmford, T. Brooks, S. Butchart, N. Collar, and J. Pilgrim for comments, and to R. Thomas at BirdLife International for providing access to the bird pictures. Funding was provided by a Marie Curie Intra-European Fellowship under the European Community Sixth Framework Programme.

10.126/science.1131302

Supporting Online Material

www.sciencemag.org/cgi/content/full/313/5790/1051/DC1
Tables S1 to S5
References

IMMUNOLOGY

Unraveling Gut Inflammation

The barrier between our gut flora and body depends on immune cell action and secreted antibacterial molecules in the gut wall.

Warren Strober

Our intestinal mucosa, particularly that lining the large bowel and terminal ileum, is in constant contact with a resident microflora that is both luxuriant and complex: It consists of some 100 trillion discrete prokaryotic cells comprising an astonishing variety of Gram-positive and Gram-negative facultative aerobic and anaerobic organisms (*1*). Under normal circumstances, the presence of this vast biotic mass is useful and benign in that it helps prevent colonization of the bowel by pathogens and does not in itself evoke inflammatory immune responses (the normal mucosal immune system is tolerant of its many antigens). Nevertheless, this flora can also cause disease, because there is now good evidence that excessive mucosal immune responses to components of the microflora, either due to abnormal or impaired effector or regulatory (suppressor) cell activity of the host, is the prime cause of inflammatory bowel disease (IBD) (*2*). One way by which cells in the intestinal milieu may prevent this possible outcome is to apply a number of checks on the resident microflora that control its overall size and composition. On page 1126 of this issue, Cash *et al*. (*3*) characterize one such check—the ability of epithelial cells lining parts of the mucosa to produce RegIIIγ (regenerating islet 3 gamma), a C-type lectin with bactericidal properties. This substance may not only regulate the mix of intestinal organisms, but may also eliminate potential pathogens that cannot be controlled by the microflora alone.

Production of RegIIIγ was previously shown to be up-regulated in mouse intestinal cells after induction of mucosal inflammation and in patients with IBD (*4*). Cash *et al.* found that it is the product of Paneth cells, secretory epithelial cells at the base of the intestinal crypts in the terminal part of the small intestine (see the figure). However, these cells may not be the only site of production because RegIIIγ is also produced in the large bowel, which lacks Paneth cells (*4*). In addition, they found that RegIIIγ and its human homolog, HIP/PAP, bind to a carbohydrate component of peptidoglycan, a proteoglycan in the bacterial coat of most bacteria, particularly Gram-positive bacteria. The authors observed that such binding leads to bacterial killing, thus making RegIIIγ one of a number of antibacterial (antimicrobial) substances produced by Paneth cells. This arsenal also includes lysozyme, secretory phospholipase A2, angiogenin 4, and α-defensins (5). That said, it may be that RegIIIγ fills a particular antibacterial niche because it targets intestinal Gram-positive bacteria such as *Enterococcus fecalis* rather than the more predominant intestinal Gram-negative bacteria.

To underscore the possible significance of RegIIIγ, Cash *et al.* indicate the importance of strict sequestration of resident microbial organisms, lest they cross into the host's interior milieu and cause inflammation and/or sepsis. They also point out that deficiencies in the production of antimicrobial peptides, the α-defensins, are associated with Crohn's disease, a form of IBD. Each of these points requires some discussion.

The authors are quite correct to point out that entry of bacteria into mucosa lying beneath the intestinal epithelium—the lamina propria of the gut wall—may lead to inflammation. This was shown in studies of transgenic mice that were genetically engineered to have faulty N-cadherin function, and thus created leaky "tight" junctions between epithelial cells in spatially defined areas of the intestine. This allowed bacteria in the mucosal microflora to breach the

The author is in the Laboratory of Host Defenses, National Institutes of Health. Bethesda, MD 20892-1890. USA. E-mail: wstrober@niaid.nih.gov.

epithelial barrier and cause inflammation in affected areas, but not in areas where tight junctions were intact (*6*).

Despite these findings, it is now well established that resident flora do interact with antigen-presenting cells in the lamina propria and/or actually cross the epithelial barrier without causing inflammation. For instance, antigen-presenting dendritic cells in the lamina propria extend processes between epithelial cells and into the gut lumen. By this periscope-like activity, they take up bacteria or antigens associated with bacteria in the microbial flora (*7, 8*). In addition, it has been demonstrated that a commensal organism introduced into the gut lumen of a germ-free mouse gains rapid entry into the gut-associated tissue of the mouse by some as yet unidentified route (*9*). Whereas most bacteria thus entering the mucosa are killed by macrophages, some survive in dendritic cells for a limited time, where they are processed for stimulation of B lymphocytes. The B cells, in turn, produce noninflammatory immunoglobulin A (IgA) responses that can inhibit binding of microorganisms to ordinary (columnar) epithelial cells. The IgA responses also promote bacterial uptake across specialized cells (M cells) overlying Peyer's patches, the lymphoid follicles embedded in the mucosa. Finally, it has been observed that so-called probiotic organisms (commensal bacteria with anti-inflammatory properties) activate regulatory T lymphocytes when introduced into the lumen of mice that have the ability to inhibit subsequent induction of inflammatory responses (*10*). Evidently, these microorganisms gain access to mucosal lymphoid tissue (dendritic cells) or else the induction and expansion of the regulatory immune cells would not be possible.

The picture that emerges from these and other studies is that the epithelial barrier is actually quite porous and there is a constant interplay between resident microbial flora and mucosal immune elements and perhaps even limited entry of organism into the host mucosal system. However, why such interaction and entry do not provoke inflammation or is in fact anti-inflammatory whereas wholesale entry of organisms causes inflammation is not at all clear. One attractive possibility is that the development of inflammation depends on the degree to which bacterial entry is accompanied by robust cellular signaling via innate immune mechanisms, most notably signaling by bacterial components in the flora that function as ligands for Toll-like receptors (TLRs) expressed on immune cells. In the case of invading pathogens, such signaling leads to vigorous stimulation of antigen-presenting cells that initiate and sustain host-protective inflammatory responses. In contrast, in the case of commensals penetrating the epithelial barrier, such signaling may be weak and unable to incite inflammation, unless the organisms enter in great numbers. This explanation fits well with recent evidence that mutations in *Card15* are a susceptibility factor in Crohn's disease (*11*). The *Card15* gene encodes NOD2, an intracellular protein that recognizes a peptide component of peptidoglycan, the same bacterial component recognized by RegIIIγ. In mice, NOD2 functions mainly as a regulatory element that limits the TLR2 response to peptidoglycan (*11*). This strongly implies that *Card15* mutations and consequent defective NOD2 function lead to overly robust responses to TLR2 ligands associated with commensal organisms that set the stage for the inflammation of Crohn's disease.

This conclusion brings us to the second point—the role of Paneth cell–derived antibacterial factors in the pathogenesis of IBD. Paneth cell production of α-defensin–5 is decreased in patients with Crohn's disease, whereas production of other antibacterial factors by these cells is not changed (*12*). Furthermore, the production of this defensin is particularly decreased in patients bearing a *Card15* mutation, thus tying α-defensin production to a Crohn's disease susceptibility gene. Its relation to α-defensin production is probably due to NOD2 expression in both Paneth and dendritic cells; in the former, it is involved in inducing α-defensin production. Finally, in bacterial killing assays, extracts of intestinal tissue from patients with Crohn's disease and decreased α-defensin production, exhibited a somewhat lower capacity to kill *Staphylococcus aureus* and *Escherichia coli* in vitro. These and other data suggested that the α-defensin defect is not a secondary manifestation of the inflammation, and that abnormally low α-defensin production is a primary defect in Crohn's disease. This concept stands on its head the previously prevailing concept that IBD, including Crohn's disease, is due to a dysregulated and excessive response of mucosal immune cells to the resident micro-

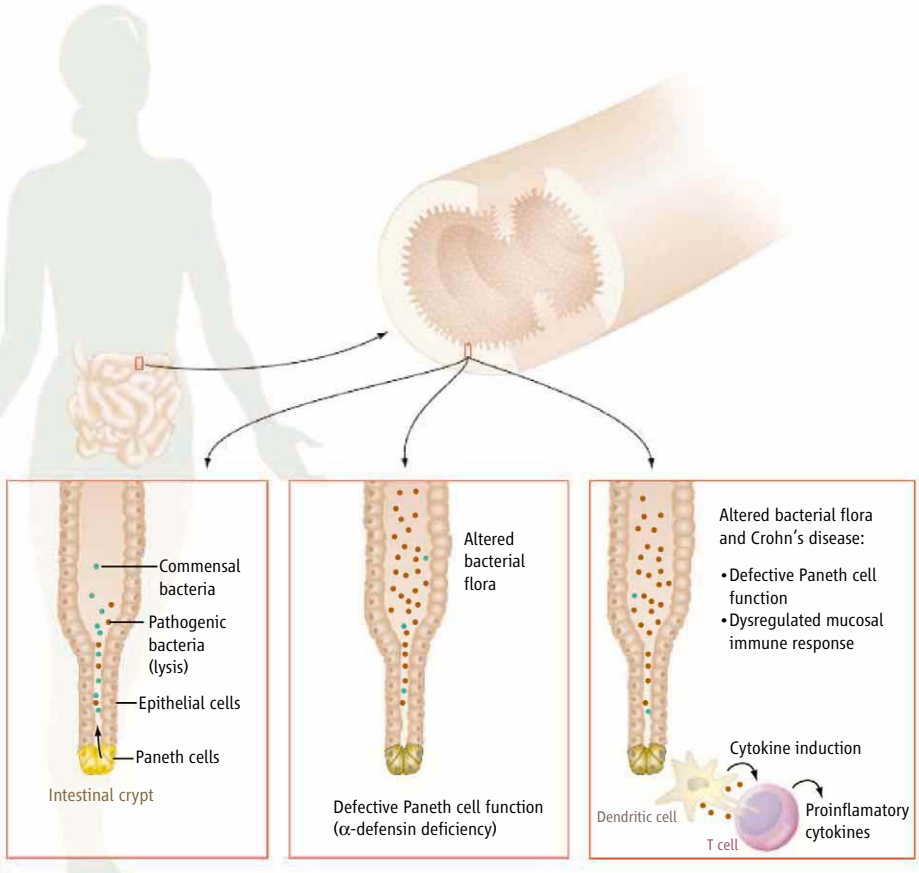

Antibacterial factors in mucosal homeostasis. The secretion of Paneth cell factors (including RegIIIγ) into the intestinal crypts regulates the number and type of bacteria in the crypt space and gut lumen under normal conditions and during the introduction of a potential pathogen. Loss of Paneth cell function (including decreased α-defensin production) results in bacterial overgrowth. Inflammatory bowel disease (Crohn's Disease) involves a dysregulated mucosal immune response.

CREDIT: P. HUEY/*SCIENCE*

flora. Instead, it posits that the excessive response is, rather, a secondary event that follows from the primary alteration in the microflora related to the α-defensin deficiency.

Before we can accept this new theory of Crohn's disease pathogenesis, however, several other experimental and clinical observations have to be considered. The first is that because the mucosal immune system is in constant contact with the bacterial microflora in the normal state, it is not clear that bacterial overgrowth in the gut lumen or intestinal crypts would necessarily lead to mucosal inflammation. Second, whereas Crohn's disease of the ileum is associated with decreased α-defensin production, there is no evidence that a similar defect applies to the large intestine, where the disease occurs in many patients, even in those with NOD2 mutations. Third, and perhaps most important, there are several mouse models in which impaired Paneth cell function leads to abnormal secretion of all antibacterial factors, not only α-defensins. In one such model, mice have a mutation in the cystic fibrosis transmembrane conductance regulator gene and consequently manifest some of the features of cystic fibrosis, namely decreased fluid in secretions and insolubility of secreted mucus (*13*). As a result, such as mice have blocked intestinal crypts, resulting in severe intestinal bacterial overgrowth, a phenomenon also noted in patients with cystic fibrosis. Despite this defect, the mice do not develop chronic inflammation of the bowel wall that characterizes Crohn's disease; nor do patients with cystic fibrosis. Likewise, no bowel wall inflammation develops in other models of Paneth cell deficiency, including mice with matrilysin deficiency that cannot elaborate mature, active defensins (*14*).

The lack of support for the view that an α-defensin secretion abnormality is a primary factor in IBD pathogenesis raises the probability that the primary defect lies in the response of the mucosal immune system to antigens in the microflora rather than in the capacity of these antigens to evoke an inflammatory response. This doesn't mean that defensins and other antibacterial substances such as RegIIIγ play no role in IBD pathogenesis, because these substances can act as gate-keepers that to some extent control the ability of organisms in the microflora to move through the epithelial barrier and, in so doing, incite disease in an already dysregulated mucosal immune system.

References

1. R. E. Ley *et al.*, *Cell* **124**, 837 (2006).
2. G. Bouma, W. Strober, *Nat. Rev. Immunol.* **3**, 521 (2003).
3. H. L. Cash, C. V. Whitham, C. L. Behrendt, L. V. Hooper, *Science* **313**, 1126 (2006).
4. H. Ogawa *et al.*, *Inflamm. Bowel Dis*. **9**, 162 (2003).
5. M. E. Selsted, A. J. Ouellette, *Nat. Immunol*. **6**,551 (2005).
6. M. L. Hermiston, J. I. Gordon, *Science* **270**, 1203 (1995).
7. M. Rescigno *et al.*, *Nat. Immunol*. **2**, 361 (2001).
8. J. H. Niess *et al.*, *Science* **307**, 254 (2005).
9. A. J. Macpherson, T. Uhr, *Science* **303**, 1662 (2004).
10. C. Di Giacinto *et al.*, *J. Immunol*. **174**, 3237 (2005).
11. W. Strober *et al.*, *Nat. Rev. Immunol*. **6**. 9 (2006).
12. J. Wehkamp *et al.*, *Proc. Natl. Acad. Sci*. U.S.A. **102**, 18129 (2005).
13. O. Norkina, T. G. Burnett, R. C. De Lisle, *Infect. Immun.* **72,** 6040 (2004).
14. C. L. Wilson *et al.*, *Science* **286**, 113 (1999).

10.1126/science.1131997

ASTRONOMY

Growing Apart in Lock Step

Like our Moon, Pluto's satellite system was probably produced by a giant impact. The orbits of the smaller Nix and Hydra apparently result from interactions with the larger moon Charon.

Jack J. Lissauer

Two small moons of Pluto, Nix and Hydra, were discovered last year in images taken with the Hubble Space Telescope (*1*). Both travel on nearly circular orbits, in the same plane and direction as Pluto's much larger inner moon, Charon. Nix's orbital period is somewhat less than four times that of Charon, and Hydra orbits in slightly less time than it takes Charon to complete six revolutions. The dynamical aspects of this system are analogous to the regular satellite systems of the giant planets Jupiter, Saturn, and Uranus. However, the giant planets contain considerable amounts of gas, and their moons, none of which exceeds 1/4000th the mass of its planet, grew within disks composed of gas and solid particles that orbited the planets in their youth (*2*). In contrast, Charon's mass is greater than 10% that of Pluto, and the pair is believed to have formed as the result of a partially elastic and disruptive giant impact (*3*). This giant impact model, which is also the preferred scenario for the origin of Earth's Moon, yields a closely bound pair, separated by only a few radii of the larger body. Tidal forces subsequently expanded the separation to its present distance of more than 16 Pluto radii. But analogous tides would barely move the recently found small moons of Pluto, and the impact model cannot account for the formation of moons on nearly circular orbits so far from the planet. On page 1107 of this issue (*4*), Ward and Canup report a mechanism by which Charon could have pushed Nix and Hydra outward from initial orbits much closer to Pluto, thereby providing a unified explanation for the origin and evolution of this intriguing four-body system (see the figure).

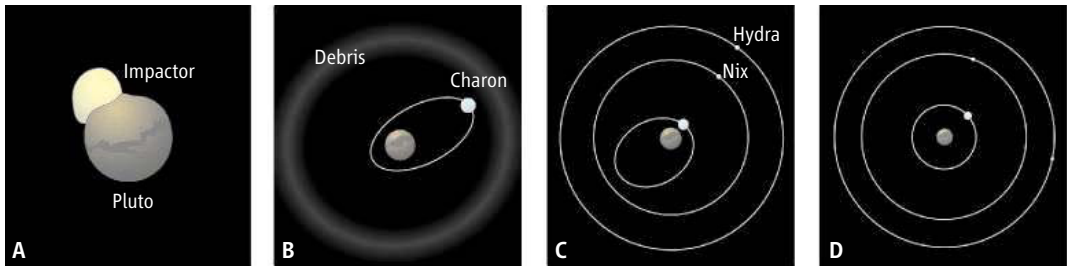

Formation and evolution of Pluto's satellite system. (**A**) A giant impact results in the (almost) intact capture of the large moon Charon. (**B**) This leads to a highly eccentric orbit for Charon and a disk of small debris orbiting the Pluto-Charon pair. (**C**) The tiny moons Nix and Hydra accreted from this disk, which produces nearly circular orbits. As tidal forces caused Charon's orbit to recede from Pluto, the moons Nix and Hydra became trapped in the 4:1 and 6:1 orbital resonances of Charon. (**D**) Charon pushed the moons ahead of itself until tides damped Charon's eccentricity and the resonances were broken, leaving the substantially expanded system of moons on circular orbits that is observed today.

CREDIT: P. HUEY/SCIENCE

The author is at NASA, Ames Research Center Moffett Field, CA 94035, USA. E-mail: jlissauer@mail.arc.nasa.gov

It has been known for more than 40 years that a moon whose orbit is tidally evolving away from a planet can trap a more distant moon in an orbital resonance, pushing the exterior moon outward ahead of itself (*5*). As the inner orbit expands due to tidal forces, the satellites thereby maintain the commensurate mean motions and move outward together (*6*).

The ratio of energy to angular momentum required to expand an orbit without changing its eccentricity is just the orbital frequency. So if energy is transferred outward to a moon with a longer orbital period, not enough angular momentum is available to maintain the circularity of the orbits, and the eccentricity of one or both moons increases (*7*). In the case of Jupiter's large inner moons Io, Europa, and Ganymede, which are locked in a 4:2:1 resonance identified by Pierre-Simon Laplace two centuries ago, tides raised by Jupiter on the satellites damp this eccentricity, producing persistent volcanic activity on Io and a liquid ocean below Europa's thin ice crust. Pluto itself was pushed hundreds of millions of kilometers away from the Sun by Neptune, as this giant planet migrated outward (as a back reaction from throwing solid bodies sunward, however, not solar tides) (*8*). Pluto is still locked in a 3:2 resonance with Neptune, and its high eccentricity is evidence of this migration.

But what of Nix and Hydra, which travel on circular orbits and are too small and distant to have their orbital eccentricities tidally damped? The answer is that the resonances in which Pluto's tiny moons were trapped, both were maintained by and acted to enhance (albeit not by much) the eccentricity of Charon. Charon, being much larger as well as closer to Pluto, has its eccentricity damped in a time that is much less than the age of the solar system. Indeed, for this mechanism to work, Charon must have initially been on a highly eccentric orbit, which would be expected if it was captured nearly intact after an inelastic collision (*3*), rather than having accreted from a giant impact-produced disk (the preferred mechanism for the formation of Earth's Moon).

Ward and Canup have offered a model that explains the origin of the orbital configuration of Pluto's three known satellites via tidal expansion from a compact system that was produced by a giant impact. Their model requires the impact origin of an intact Charon, which previous models (*3*) suggest is likely only if the Pluto impactor was a homogeneous mixture of ice and rock. Hence, the model of Ward and Canup also predicts that Nix and Hydra are made of ice-rock mixtures. Pluto is by far the brightest and best known of the Trans-Neptunian Objects (TNOs). Once believed to be a planet-sized body, it is now viewed as one of the larger members of a populous class of distant solar system bodies. Many other TNOs are known to have moons. Observations of the orbital characteristics of additional, smaller moons of such minor planets could indicate whether their observed large moons were formed by giant impacts or purely gravitational capture (*9*).

References and Notes

1. H. A. Weaver et al., *Nature* **439**, 943 (2006).
2. J. B. Pollack, *Protostars and Planets II* (Univ. Arizona Press, Tucson, 1985).
3. R. M. Canup, *Science* **307**, 546 (2005).
4. W. R. Ward, R. M. Canup, *Science* 313, 1107 (2006); published online 6 July 2006.
5. P. Goldreich, *Mon. Not. Roy. Astron. Soc*. **130**, 159 (1965).
6. Moons trapped in such orbital resonances always have conjunctions (pass one another) near the place where their elliptical orbits are farthest apart. If the outer moon is moving too fast, conjunction occurs where the radial separation of the orbits is decreasing. This means that the outer moon gets pulled forward after conjunction more than it was pulled back before conjunction, resulting in a net transfer of orbital energy and angular momentum from the inner moon to the outer moon, expanding the outer moon's orbit and thereby slowing its orbital motion. Consequently, the next conjunction occurs closer to the longitude where the radial separation is maximized. For further details, see S. J. Peale, *Ann. Rev. Astron. Astrophys*. **14**, 215 (1976), and especially his figure 1.
7. J. J. Lissauer *et al*., *Icarus* **58**, 159 (1984).
8. R. Malhotra, *Nature* **365**, 819 (1993).
9. P. Goldreich *et al*., *Nature* **420**, 643 (2002).

10. This work was funded by NASA's Planetary Geology and Geophysics program, WBS 811073.02.01.01.12.

10.1126/science.1128447

ECOLOGY

Crafting the Pieces of the Diversity Jigsaw Puzzle

Herbivorous insect species are more numerous in tropical than in temperate forests. Studies of present-day forests and fossil leaf patterns show how plant diversity controls insect diversity.

R. L. Kitching

After his encounter with the Atlantic rainforest of Brazil, Charles Darwin observed that "the land is one great, wild, untidy, luxuriant hothouse, made by Nature for herself" (*1*). Increasing knowledge of the forest fauna over the past 30 years has only underscored Darwin's point: 978 species of beetles from six trees in Venezuela, 160 species of grasshoppers in 60 trees in Amazonia, 218 species of ants from 19 trees in Sabah—the list goes on (*2*). Dobzhansky, with characteristic prescience, asked "why?" as early as 1950 (*3*). He suggested that the animals of the Tropics were fundamentally different from those of temperate regions: In general, tropical species were more specialized, with niche limits defined by interactions among species rather than by physical or chemical factors. This has proved very difficult to test; indeed, it moved surreptitiously from hypothesis to dogma without any very critical evaluation. This difficulty is nowhere more acute than in the case of tropical herbivores. Two reports in this issue, one by Novotny *et al*. (*4*) on page 1115 and the other by Wilf *et al*. (*5*) on page 1112 shed light on both old and new aspects of these issues.

The relationships between the diversity of tropical trees and that of the associated arthropods have been central in the exciting if somewhat circular debates on global species richness. It is relatively easy to count the number of tree species in a forest and to extrapolate this count to a region, continent, or even planet. If each tree species supports a certain number of herbivorous insects, then we can extrapolate to a global estimate of herbivore richness. With a few further assumptions, we can obtain an overall number of all arthropod species. That the estimates range from 5 to 100 million (*6*) suggests that this is not an exact science.

The Novotny/Basset group based in Papua New Guinea has been one of only two or three groups that have measured tropical host specificity empirically by field collecting, larval rearing, and choice experiments. Based on

The author is at the Australian School of Environmental Studies, Griffith University, Brisbane, Queensland 4111, Australia. E-mail: r.kitching@griffith.edu.au

thousands of rearing records from almost 60 tree species, they have constructed a database that promises answers to many fundamental questions on herbivory and diversity. They showed previously (*7*) that host plant phylogeny plays a key role in determining levels of specialization in dominant groups of insect herbivores. But how to use this information to say something general about insect herbivory in tropical as opposed to temperate ecosystems?

The problem is the perennial one of just what is a legitimate comparison: how to line up insect responses to ecosystems that, on the one hand, exhibit a tree diversity of perhaps 200 per hectare with one with perhaps 20? This is compounded when host plant records from temperate forests have been accumulated by centuries of anecdotal observation rather than by the intense, controlled observation of the best current tropical studies. In a masterful piece of interdisciplinary work, Novotny and his colleagues have overcome these problems and come up with an utterly unexpected answer. First, they applied their "tropical" methods to a mature forest in central Europe. They then used the power of GenBank to produce a phylogeny for the 14 tree species studied in Moravia. In a stroke of remarkable originality they then extracted from their database from New Guinea the 14 tree species that presented a phylogeny most closely congruent with the central European data set. So they were able to make a legitimate quantitative comparison of herbivore host specificity in temperate and tropical forests. There was no difference in the distribution of host specificities between the two regions. The huge richness of herbivorous insects in tropical rainforests is driven by the phylogenetic diversity of the plant assemblage in those forests and not by any fundamental differences in the nature of the niches of the herbivores.

The Novotny *et al*. result supports the general idea of a post-Pleistocene equilibrium (setting aside the anthropogenic clearing of trees on a vast scale) and an explanation of the herbivore diversity that we observe in nature. Simply stated, the Novotny law becomes: "Herbivore richness in forests is related positively to the phylogenetic breadth of its supporting tree assemblage."

In a fascinating contrast, Wilf *et al*. have used the vast deposits of leaves from Cretaceous and Tertiary beds in North America to demonstrate that an equilibrium world is, geologically speaking, but a temporary end point rather than a constant property of ecosystems. Leaves carry with them species-specific patterns of herbivore activity. They show clearly that after the Cretaceous-Tertiary (K-T) mass extinction about 65 million years ago, recovery of herbivore richness was both slow and, more important, patchy. The rainforest-like faunas of the Castle Rock site in Colorado show a Paleocene herbivore signal more diverse than anything from the Cretaceous. In contrast, most other more temperate floras from the Paleocene show a dramatic reduction in herbivore signal. Bringing the two results together, Cretaceous assemblages should obey the Novotny law, whereas post–K-T ones may deviate from it significantly. With only a modestly richer database than the currently available one, this contention could be tested and so combine paleoecology and its modern counterpart in a productive way.

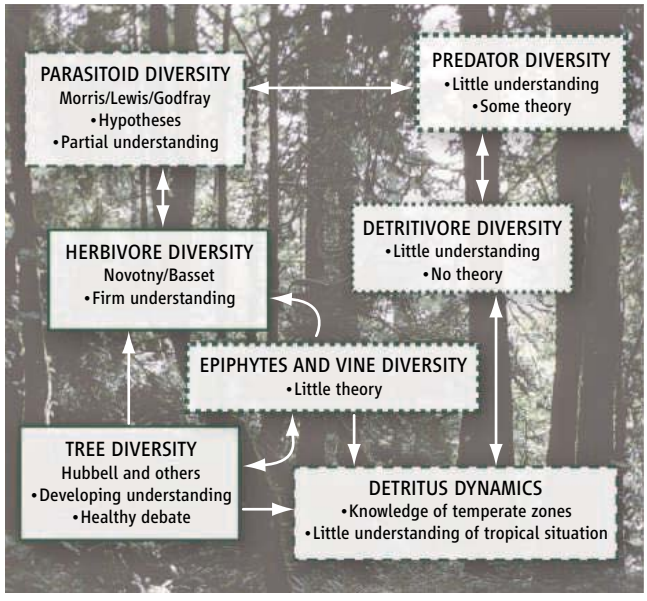

Components of biodiversity in the forest. The diagram depicts a highly simplified rainforest food web. Dashed or dotted boxes indicate areas for which general explanations of diversity are either incomplete (dashed) or lacking (dotted) altogether.

The firm basis of understanding as to just why herbivores are so diverse in tropical forests is part of a recent and welcome transition in tropical ecology. Over the past few decades, we have built up an impressive body of data that identifies biodiversity patterns in tropical rainforests. There remains much to be done, but there is enough information that we can look for general mechanistic explanations of the patterns. A recent flurry of activity followed Hubbell's work (*8*), resulting in an active, firmly based debate on the generation of rainforest tree diversity. The initial proposition of equivalence across all trees of whatever species, melded with essentially random replacement processes (the "neutral" theory), produced results that mimicked well some commonly used species/abundance relationships. That such relationships could be generated with patently unrealistic assumptions has refocused attention on how we look at and interpret diversity data. The heated debate that followed points now to a more deterministic theory focusing on the idea of rare species advantage. The generalizations that emerge from the work of Novotny *et al*. mean that we can extend our understanding of biodiversity-generating processes to the next trophic level—the herbivores. Their results make clear the "bottom-up" effects of plant diversity on the herbivore assemblage. There are undoubtedly "top-down" effects as well. Here the work of Lewis and Godfray (*9*) and Morris *et al*. (*10*) shows that apparent competition among host species is mediated through their assemblage of parasitoids—larval insects that prey on their hosts from the inside, so to speak.

In a simplified, general, rainforest food web (see the figure), the consensus (or at least the basis for a healthy debate) that we may now expect on tree diversity and the associated herbivores leaves several components requiring explanation: the third trophic level comprising the parasitoids and predators, and the externally maintained food chains based on decomposition processes (plus, incidentally, a general understanding of the interaction between herbivores and the epiphytes and vines so characteristic of tropical forests).

Processes determining the diversity of predators await their champions. Parasitoid assemblages are better understood as modifiers of herbivore diversity than as community-level objects in themselves. There has long been work on the top-down role of predators and parasitoids as modifiers of the assemblages of potential prey items, notably the idea that key predators can be the forces that flip whole food webs among different equilibria. We also have some controversial evidence of invariant or at least constrained predator-prey statistics within simple food webs (*11*), but mechanistic explanations are lacking. Finally, there are the chewers of rubbish—the "garbos" (if I may be permitted an Australianism). Arthropods that feed either on fungi or directly on detritus and its associated

PHOTO CREDIT: PHOTO.COM

microorganisms make up as much as 30 to 40% of the rainforest fauna. General patterns for these components are few, and diversity-generating mechanisms are entirely conjectural at this time (*12*). There remains much to do, but this is an exciting time for rainforest ecologists. Encouraging progress toward a general theory has been made, and the field, laboratory, and statistical tools surely exist to maintain this drive.

References and Notes

1. C. Darwin, *Journal of Researches* (James Murray, London, 1845).
2. See references in N. E. Stork *et al.*, *Canopy Arthropods* (Chapman & Hall, London, 1997).
3. T. Dobzhansky, *Am. Sci.* **38**, 209 (1950).
4. V. Novotny *et al.*, *Science* **313**, 1115 (2006); published online 13 July 2006 (10.1126/science.1129237).
5. P. Wilf *et al.*, *Science* **313**, 1112 (2006).
6. N. E. Stork, *Biol. J. Linn. Soc.* **35**, 321 (1988).
7. V. Novotny *et al.*, *Nature* **416**, 841(2002).
8. S. Hubbell, *Unified Neutral Theory of Biodiversity and Biogeography* (Princeton Univ. Press, Princeton, NJ, 2001).
9. R. J. Morris, O. T. Lewis, H. C. J. Godfray, *Nature* **428**, 310 (2004).
10. R. J. Morris *et al.*, *Ann. Zool. Fenn.* **42**, 449 (2005).
11. R. L. Kitching, *Food Webs and Container Habitats* (Cambridge Univ. Press, Cambridge, UK, 2000).
12. S. Hattenschwiler *et al.*, *Annu. Rev. Ecol. Evol. Syst.* **36**, 191 (2005).

13. I thank S. Boulter, C. Godfray, O. Lewis, S. Pimm, and N. Stork for comments on earlier drafts of this article.

10.1126/science.1131117

PHYSICS

Surface Transfer Doping of Semiconductors

The local conductivity of semiconductors can be changed by incorporating various atoms into the semiconductor material. New work shows that manipulation of the surface can produce the same effect.

Jürgen Ristein

"Doping" of semiconductors—that is, the local manipulation of their conductivity—is a key technology for electronic devices. Without doping, for example, a gallium nitride sample larger than the White House would be needed to host a single mobile charge at room temperature; for diamond, not even the volume of the globe would be sufficient. It is only through doping that semiconductors become useful electronic materials. Recent studies have revealed an unconventional way to achieve doping through surface engineering.

Doping of semiconductors is usually achieved by incorporating atoms of appropriate elements into the host lattice of the semiconductor. The dopants either release an excess electron as a free negative charge carrier to the semiconductor (n-type doping) or they consume one more electron for chemical bonding than they brought with them (p-type doping). In the latter case, the "stolen" electron behaves like a positive charge carrier—a hole—in the semiconductor.

The electrons or holes remain weakly bound to the dopants that carry their respective counter charge, and it takes a characteristic activation energy Δ to release them as free charge carriers. For effective dopants, this energy is rather small. At room temperature, it is easily supplied by the vibrations of the semiconductor atoms, and one ends up with free charge carriers of one sign and fixed ionized dopants with opposite charge. This situation is sketched for p-type doping in the figure (left panel).

The author is in the Lehrstuhl für Physik Universität Erlangen-Nürnberg, 91058 Erlangen, Germany. E-mail: juergen.ristein@physik.uni-erlangen.de

If the dopants are distributed homogeneously in the semiconductor lattice, then so will be the mobile charge carriers. Positive and negative charge cancel, and on average, no electric field acts on the mobile charge carriers. For electronic devices to function, the doping must therefore be inhomogeneous. Inhomogeneous doping results in local variations of electron and hole concentrations, which tend to equalize by diffusion. The result is a delicate equilibrium between charge separation and electric field that determines the electrical response of a device to externally applied voltages. The simplest such device is the p-n junction, which consists of a p-type and an n-type doped layer of the same semiconductor.

In all classical devices, the dopants are impurity atoms introduced into the bulk of the semiconductor. But doping can also be achieved by an electron exchange between a semiconductor and dopants situated at its surface. The surface dopants—below, we will use acceptors for illustration—possess unoccupied molecular orbitals for electrons (UMOs). If the energetically lowest of these orbitals (called LUMO) is close to the valence band maximum of the semiconductor, it will steal an electron from the semiconductor, just as classical acceptors do (see the figure, right panel). As a result, holes will form in the semiconductor, and negative charge will be localized on the surface acceptors (*1*). This charge separation will automatically establish an electrostatic potential that confines the holes in a perpendicular direction but leaves them free to move parallel to the surface.

This kind of p-type surface transfer doping has recently been demonstrated for fullerene (*2*) and fluorofullerene molecules (*3*) serving as surface acceptors on hydrogen-terminated diamond. The hydrogen termination leads to an exceptionally low ionization energy for the diamond; the fullerenes were chosen for their high electron affinities. For $C_{60}F_{48}$ (*4*), the activation energy Δ is even negative, and each molecule brought onto the diamond surface creates a hole (*1*).

The electronic states at the surface are not necessarily associated with molecular adsorbates. In fact, the first observation of p-type surface transfer doping of diamond involved a complex electrochemical system, in which hydrated ions acted as surface acceptors (*5*). These ions were usually created unintention-

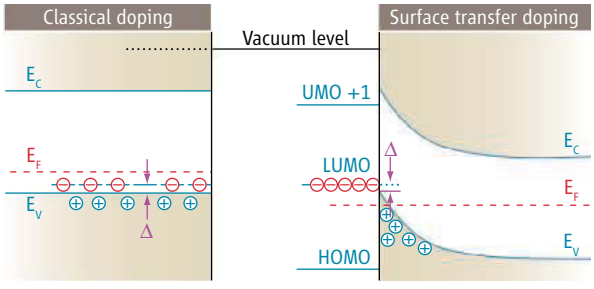

Beyond conventional doping. This band diagram illustrates classical p-type doping (**left**) and p-type surface transfer doping (**right**), using the energy of an electron in free space as a reference (vacuum level). E_c and E_v are the energies of the conduction band minimum and the valence band maximum, respectively. The balance between electrons localized in acceptor states and free holes in the valence band is expressed by the constant Fermi energy E_F. The closer E_F is to E_v, the higher the local density of holes. LUMO and HOMO are the lowest unoccupied and highest occupied molecular orbitals of the surface acceptors, respectively.

ally when hydrogen-terminated diamond was exposed to the atmosphere (*6*, *7*). In this electrochemical variant of surface transfer doping, the redox potential of the hydrated ions effectively determines the effective acceptor level of the electronic system (*8*).

There are several reasons why diamond is particularly susceptible to p-type transfer doping. First, its electron affinity can be tailored to the lowest value of all semiconductors by simple hydrogen termination of the surface bonds. Second, because no solid oxide is present on its surface, intimate contact with surface dopants is possible. Finally, the bulk conductivity is low and will not mask the effect of the transfer doping.

Under similarly favorable conditions, p-type surface transfer doping was very recently observed for silicon (*9*). In these experiments, the sheet conductivity of very thin silicon layers (10 to 40 nm) on top of a SiO substrate was measured. After appropriate preparation, the Si surface atoms rearrange and form rows of asymmetric dimers. With this reconstruction, unoccupied surface states close to the valence band maximum of silicon are formed; these states play the role of the LUMO, with an activation energy of 0.3 eV. [This energy is called "effective band gap" in (*9*).]

In the field of carbon nanotubes, surface transfer doping is in fact the method of choice for manipulating electronic conductivity. Nanotubes essentially consist of one or a few rolled-up sheets of graphene, and donors or acceptors are naturally positioned on the surface of these tubes rather than incorporated into the rigid graphene layers. The electrical conductivity of carbon nanotubes changes markedly upon exposure to different gases (*10*, *11*). In some cases, this behavior has shown striking similarities to electrochemical surface transfer doping of diamond (*12*).

Surface transfer doping thus appears to be the mechanism behind a variety of surface electronic phenomena. When controlled, it may become a valuable tool for engineering micrometer- and nanometer-scale electronic devices.

References

1. J. Ristein, *J. Phys. D: Appl. Phys*. **39**, R71 (2006).
2. P. Strobel *et al.*, *Nature* **430**, 439 (2004).
3. P. Strobel *et al.*, *Diam. Rel. Mat.* **14**, 451 (2005).
4. L. Hedberg *et al.*, *J. Phys. Chem. A* **108**, 4731 (2004).
5. F. Maier *et al.*, *Phys. Rev. Lett*. **85**, 3472 (2000).
6. I. M. Landstrass, K. V. Ravi, *Appl. Phys. Lett*. **55**, 975 (1989).
7. I. M. Landstrass, K. V. Ravi, *Appl. Phys. Lett.* **55**, 1391 (1989).
8. M. Riedel, J. Ristein, L. Ley, *Diam. Rel. Mat*. **13**, 746 (2004).
9. P. Zhang *et al.*, *Nature* **439**, 703 (2006).
10. P.G. Collins *et al.*, *Science* **287**, 1801 (2000).
11. J. Kong *et al.*, *Science* **287**, 622 (2000).
12. J. Foord *et al.*, *Diam. Rel. Mat*. **11**, 856 (2002).

10.1126/science.1127589

NEUROSCIENCE

ZAP and ZIP, a Story to Forget

How are memories stored and retrieved? Long-awaited evidence shows directly that the strength of synaptic connections in hippocampal neurons underlies both processes.

Tim V. P. Bliss, Graham L. Collingridge, Serge Laroche

How do brains store memories? The leading candidate for the role is a form of synaptic plasticity known as long-term potentiation (LTP), a persistent increase in the strength of synapses linking interconnected neurons in cortical networks. LTP can be induced experimentally by the application of a brief train of electrical stimuli, known to practitioners of the art as the tetanus or ZAP (*1*, *2*). On pages 1093 and 1141 of this issue, Whitlock *et al.* and Pastalkova *et al.* substantially advance the case for LTP as a neural mechanism for memory (*3*, *4*). Both studies focus on LTP in the hippocampus, a region of the brain necessary for the formation of episodic memories in humans and for spatial learning and memory in rodents. Pharmacological or genetic manipulations that suppress the induction of LTP generally lead to impairment of spatial learning, as predicted by the LTP and memory hypothesis. But there has been little evidence for two other critical predictions: (i) Hippocampus-dependent learning should lead to observable LTP at hippocampal synapses, and (ii) suppression of LTP after learning a task should abolish the memory of that task. It is these gaps in the evidence for the LTP and memory hypothesis that are addressed in the new studies.

Enhanced online at www.sciencemag.org/cgi/content/full/313/5790/1058

An important advance was made earlier this year when an LTP-like increase in hippocampal synaptic responses was observed in mice that were trained in a hippocampus-dependent procedure known as trace eyeblink conditioning (*5*). Learning and synaptic potentiation both failed to develop in the presence of a drug that blocks the *N*-methyl-D-aspartate (NMDA) receptor, the glutamate receptor subtype that controls the induction of LTP (*6*). This finding strongly suggests that the potentiation is indeed LTP rather than some other facilitatory process.

This conclusion has now been further strengthened by the study of Whitlock *et al*., who recorded from multiple sites in the hippocampus. The authors looked for evidence of LTP in rats that had learned to avoid entering the dark compartment of a two-compartment box where they had previously received a mild electric shock. The findings are illuminating. LTP was indeed observed, but at only a small proportion of recording electrodes. In a critical further experiment, Whitlock *et al*. show that after a ZAP, less LTP is seen at these electrodes than at those where no change was seen after learning. This partial occlusion of LTP establishes that the learning-induced potentiation is itself genuine LTP. The field response seen at each electrode reflects the activity of many neurons in the immediate vicinity and may conceal a combination of LTP at some synapses and its counterpart, long-term depression (LTD), at others. Whitlock *et al*. used a clever biochemical assay to differentiate between LTP and LTD, based on the fact that different phosphorylation sites on the GluR1 subunit of the alpha-amino-3-hydroxy-5-methylisoxazole-4-propionate (AMPA) receptor are phosphorylated in LTP and LTD. After learning, changes in phosphorylation were seen that reflect LTP but not LTD. This is surprising, given the widely held view that LTP at one subset of synapses needs to be balanced by LTD at another subset to maintain stability in the hippocampal network. This finding suggests that other forms of activity-dependent depression are recruited.

But perhaps the biggest puzzle thrown up by this study is why LTP—given that it could be detected at all at the population level—was

T. V. P. Bliss is in the Division of Neurophysiology, MRC National Institute for Medical Research, Mill Hill, London NW7 1AA, UK. G. L. Collingridge is at the MRC Centre for Synaptic Plasticity, University of Bristol, Bristol BS8 1TD, UK. S. Laroche is at Neurobiologie de l'Apprentissage, de la Mémoire et de la Communication (NAMC), CNRS UMR 8620, Universite Paris Sud, 91405 Orsay, France. E-mail: tbliss@nimr.mrc.ac.uk; g.l.collingridge@bristol.ac.uk; serge.laroche@ibaic.u-psud.fr

seen at only some electrodes. The assumption is usually made that memory is sparsely but uniformly distributed across the hippocampal neural network (*7*). The present results suggest instead a "currant-bun" model of memory storage, with clumps or hotspots of synaptic change concentrated in cell subpopulations that are themselves distributed so sparsely that only a small proportion of electrodes placed 0.25 mm apart are close enough to a hotspot to detect an increased response.

The transient nature of the biochemical changes noted by Whitlock *et al*. (*3*) suggests that the particular AMPA receptor phosphorylation states they examined mark only the early cellular events in the life of potentiated synapses. So what could be responsible for encoding longer-lasting changes? In the search for molecules that could be involved in the maintenance of LTP, a prime candidate called protein kinase M zeta (PKMζ) has recently emerged. PKMζ is the constitutively active, catalytic fragment of PKCζ, an atypical form of protein kinase C that does not require Ca^{2+} or diacylglycerol for its activation. PKMζ is transcribed independently of PKCζ under the control of an internal promoter in the PKCζ gene, and its mRNA is then transported to dendrites (*8*). Here, PKMζ maintains the late, protein synthesis–dependent phase of LTP by increasing the number of AMPA receptors that are expressed at synapses (*9*). This area of research has been greatly advanced by the introduction of ZIP, a specific, membrane-permeant peptide that mimics the autoregulatory domain of PKMζ and thus acts as an inhibitor (*10*). ZIP blocks preestablished late-phase LTP when applied to hippocampal slices an hour or two after the induction of LTP, thereby demonstrating the importance of PKMζ in the maintenance of LTP (*11*).

Building on this observation, Pastalkova *et al*. have now used ZIP to eliminate synaptic potentiation in the dentate gyrus of the hippocampus in the awake rat after learning, to assess whether stored memory is lost. The authors first confirmed that ZIP effectively reverses established LTP when injected into the rat hippocampus 22 hours after LTP induction, without affecting baseline synaptic transmission, a prerequisite to their behavioral study. They were then able to reverse any LTP-like effect induced during learning, with the prediction that this would lead to retrograde amnesia. An avoidance task was used in which rats move on a slowly rotating circular platform containing a nonrotating shock zone defined by landmarks. Rats rapidly learn to avoid the shock zone whenever the rotating platform brings them close to it. Bilateral injection of ZIP into the hippocampus 22 hours after learning caused a complete and persistent loss of the acquired spatial memory. Thus, ZIP caused retrograde amnesia in this case. There was, however, no evidence that ZIP caused anterograde amnesia, because rats could relearn the task and form a long-term memory of it. Can ZIP affect a more remote memory? Evidently so, because the same loss of a previously established spatial memory was observed when ZIP was injected 30 days after learning. Hence, this study demonstrates that an agent that reverses synaptic potentiation by inhibiting PKMζ also erases an established memory.

Could ZIP potentially obliterate all established memories? A great deal of evidence suggests that the storage of episodic memories is eventually taken over by neocortical areas (*12*).

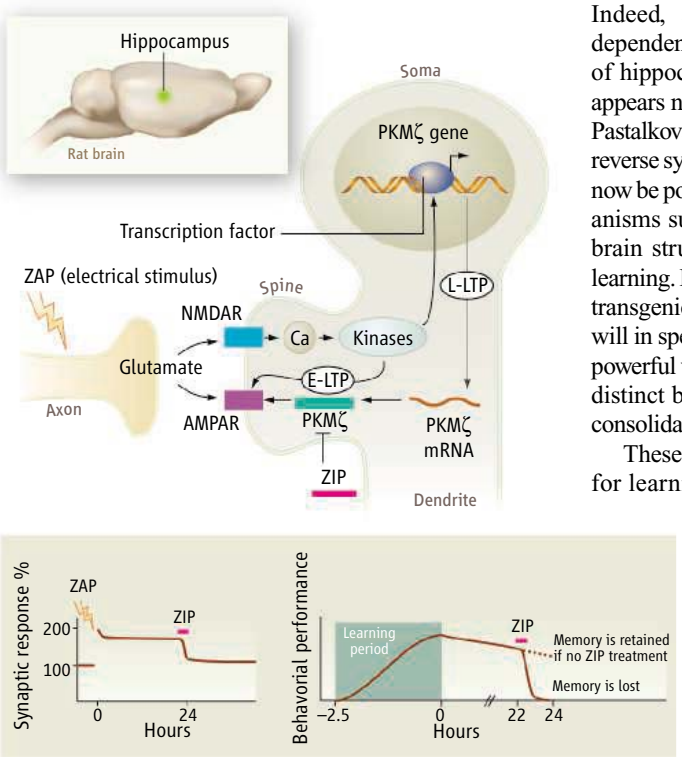

Learning hotspots in the brain. Long-term potentiation (LTP), or enhanced synaptic strength, in the hippocampus underlies memory and learning. ZAP, or a train of electrical stimulation, induces LTP. The peptide ZIP abolishes LTP when infused into the rat hippocampus 22 hours after LTP is induced. Protein kinase M zeta is part of a neuronal signaling pathway that is involved in the maintenance of both late LTP (L-LTP) and memory.

Indeed, at 30 days some hippocampus-dependent memories are immune to blockade of hippocampal function (*13*), although this appears not to be the case for the task used by Pastalkova *et al*. (*4*). Using a similar strategy to reverse synaptic potentiation with ZIP, it should now be possible to test whether LTP-like mechanisms support memory storage in different brain structures and at different times after learning. Future studies could also benefit from transgenic strategies to turn ZIP on and off at will in specific cell types. This could provide a powerful way to address the function of LTP in distinct brain areas in processes of learning, consolidation, recall, and reconsolidation.

These new data support a two-phase model for learning and memory (see the figure). During learning, L-glutamate activates NMDA receptors in hippocampal neurons, and the associated Ca^{2+} influx activates a variety of Ca^{2+}-dependent enzymes (kinases), triggering the early, protein synthesis–independent phase of LTP (E-LTP). This mechanism involves an increase in AMPA receptor function (*2*). In parallel, a signal passes to the nucleus and induces the transcription of PKMζ mRNA. The de novo synthesis of PKMζ maintains an increased number of AMPA receptors at potentiated synapses (L-LTP). The signal that leads to activation of PKMζ transcription during LTP is not known, although putative binding sites for transcription factors are present in the gene's promoter region. Zif268 is a transcription factor required for late-phase LTP (*14*), raising the pleasing prospect of a tale to tell of ZAP, ZIF, and ZIP.

References

1. T. V. P. Bliss, T. Lømo, *J. Physiol.* **232**, 331 (1973).
2. T. V. P. Bliss, G. L. Collingridge, *Nature* **361**, 31 (1993).
3. J. R. Whitlock, A. J. Heynen, M. G. Shuler, M. F. Bear, *Science* **313**, 1093 (2006).
4. E. Pastalkova *et al*., *Science* **313**, 1141 (2006).
5. A. Gruart, M. D. Muñoz, J. M. Delgado-Garcia, *J. Neurosci.* **26**, 1077 (2006).
6. G. L. Collingridge, S. J. Kehl, H. McLennan, *J. Physiol.* **334**, 33 (1983).
7. S. J. Martin, P. D. Grimshaw, R. G. M. Morris, *Annu. Rev. Neurosci.* **23**, 649 (2000).
8. A. I. Hernandez *et al*., *J. Biol. Chem.* **278**, 40305 (2003).
9. D. S. Ling, L. S. Benardo, T. C. Sacktor, *Hippocampus* **16**, 443 (2006).
10. D. S. Ling *et al*., *Nat. Neurosci.* **5**, 295 (2002).
11. P. Serrano, Y. Yao, T. C. Sacktor, *J. Neurosci.* **25**, 1979 (2005).
12. B. J. Wiltgen, R. A. M. Brown, L. E. Talton, A. J. Silva, *Neuron* **44**, 101 (2004).
13. I. Izquierdo, J. H. Medina, *Neurobiol. Learn. Mem.* **68**, 285 (1997).
14. M. W. Jones *et al*., *Nat. Neurosci*. **4**, 289 (2001).

10.1126/science.1132538

INTERNATIONAL

AAAS Aids Thriving Vietnam in S&T Development Campaign

China and India get most of the headlines, but Vietnam is quietly emerging as a powerhouse of Asian economic development. With an economic growth forecast of 7% per year over the next 5 years, it is second only to China, and like China, the nation's leaders are focused on science and technology.

Now AAAS, joined by partners in U.S. government and education, is working with high-ranking Vietnamese leaders to promote S&T cooperation between the two countries and to encourage sustainable urban development and improved science education. Last May, a high-level delegation from the National Assembly of Vietnam visited AAAS in Washington, D.C., to discuss development of a legal framework that would encourage S&T growth in their country. In July, AAAS helped organize a high-level development conference in Hanoi.

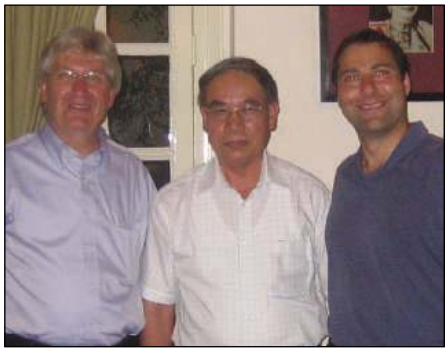

Anthony "Bud" Rock, who oversees global engagement for Arizona State University (left); Bui Hai, Vietnam's vice minister of science and technology; and Vaughan Turekian, AAAS chief international officer.

"The leaders of Vietnam have a very clear understanding of the importance of S&T investment," said Vaughan Turekian, chief international officer at AAAS. "They see China, they see Korea and Japan, and they see that these countries are all investing heavily in science and technology."

Thirty-one years have passed since the bitter end of the Vietnam War, but the United States and Vietnam recently have built closer relations. The two nations restored diplomatic ties in 1995, and this spring, they agreed in principle on terms for Vietnam to join the World Trade Organization. In November, leaders of 21 Pacific Rim countries—including U.S. President George W. Bush—are scheduled to meet in the capital city of Hanoi for the Asia-Pacific Economic Cooperation (APEC) summit.

"The United States engages Vietnam on a broad spectrum of science and technology issues, a dialogue that has improved as the overall bilateral relationship has broadened," said U.S. Ambassador to Vietnam Michael W. Marine. "I believe that as Vietnam continues to develop, our cooperation on science and technology will continue to deepen."

Turekian and high-ranking officials from Arizona State University worked with the Vietnamese Ministry of Science and Technology and the U.S. embassy to organize the Vietnam-U.S. Scientific Forum on 24 July, which explored issues of sustainability and science education. During the 5-day visit, the U.S. delegation was hosted by Bui Hai, Vietnam's vice minister of science and technology, and also met with Minister of Agriculture and Rural Development Cao Duc Phat, among others.

Anthony "Bud" Rock, a career U.S. State Department diplomat who joined Arizona State this year with responsibility for the university's global engagement portfolio, said that the university has a strong program in sustainable urban growth, while AAAS has an international network of scientists who can provide guidance as Vietnam works to strengthen university-based science education.

"Our goal is to work with the Vietnamese toward a science-based approach to policy development and a science-based approach to sustainable urban development," Rock said, "and to make science a cornerstone of education reform in the country."

Turekian said that the next step for AAAS may be to organize Vietnamese-U.S. scientific exchanges and workshops.

SCIENCE POLICY

A Week Among S&T Leaders

A cadre of top U.S. policy experts is scheduled to speak at this year's AAAS Leadership Seminar in Science and Technology Policy, including John H. Marburger III, head of the president's Office of Science and Technology Policy; David Kay, former U.N. chief nuclear weapons inspector in Iraq; and former U.S. Rep. John Porter (R-Ill.).

The third annual seminar runs from 13 to 17 November in Washington, D.C. Enrollment is limited to 30; the deadline is 13 October. For more information, see www.aaas.org/spp/leadership.

SCIENCE COMMUNICATION

AAAS Has High Profile at Euroscience 2006

Hundreds of scientists, policy experts, and educators attended the second Euroscience Open Forum last month in Munich, and AAAS was prominent with a strong presentation on science communication, appearances by some of its top officials, and exhibition booths.

The AAAS delegation featured Chief International Officer Vaughan Turekian, *Science* International Managing Editor Andrew Sugden, and Ginger Pinholster, director of the Office of Public Programs. *Science* had a booth at the conference, as did EurekAlert!, the premier science-news service for reporters.

Pinholster headed a panel of U.S. and European communication experts before a packed room at the Forum am Deutschen Museum on 16 July. She detailed the results of a new survey that provided insight into the challenges confronting science journalists worldwide.

For scientists and their institutions, the survey of 614 reporters and 445 public information officers offered a compelling message: Reporters need experts who can articulate science and technology in a clear, compelling way. They need to know that researchers are trustworthy. And they need strong visual images to illustrate their stories.

Also featured on the panel were Gerd Gigerenzer of the Center for Adaptive Behavior and Cognition at the Max Planck Institute for Human Development in Berlin; Julia Fischer of the German Primate Center in Göttingen, Germany; Clive Cookson, an editor for the *Financial Times* in London; Patrick Illinger, an editor for the *Süddeutsche Zeitung* in Munich; and Rick Weiss, a reporter for the *Washington Post.*

The panel was sponsored by the Max Planck Society and EurekAlert!.

Trajectory Shifts in the Arctic and Subarctic Freshwater Cycle

Bruce J. Peterson,[1]* James McClelland,[2] Ruth Curry,[3] Robert M. Holmes,[4] John E. Walsh,[5] Knut Aagaard[6]

Manifold changes in the freshwater cycle of high-latitude lands and oceans have been reported in the past few years. A synthesis of these changes in freshwater sources and in ocean freshwater storage illustrates the complementary and synoptic temporal pattern and magnitude of these changes over the past 50 years. Increasing river discharge anomalies and excess net precipitation on the ocean contributed ~20,000 cubic kilometers of fresh water to the Arctic and high-latitude North Atlantic oceans from lows in the 1960s to highs in the 1990s. Sea ice attrition provided another ~15,000 cubic kilometers, and glacial melt added ~2000 cubic kilometers. The sum of anomalous inputs from these freshwater sources matched the amount and rate at which fresh water accumulated in the North Atlantic during much of the period from 1965 through 1995. The changes in freshwater inputs and ocean storage occurred in conjunction with the amplifying North Atlantic Oscillation and rising air temperatures. Fresh water may now be accumulating in the Arctic Ocean and will likely be exported southward if and when the North Atlantic Oscillation enters into a new high phase.

The hydrologic system, including precipitation minus evaporation (P-E), terrestrial ice, sea ice, and ocean circulation, is a major component of ongoing changes in land and ocean ecosystems of the Arctic (*1*). Precipitation at high latitudes is increasing (*2*, *3*), river discharge is rising (*4*), glaciers (*5*) and the Greenland Ice Sheet (*6*) are shrinking, and the sea ice cover of the Arctic Ocean is decreasing in both thickness and extent (*7*). In recent decades, the Nordic Seas and Subpolar Basins experienced a remarkable freshening (*8*–*10*). Half of the total freshening occurred rapidly during the early 1970s, a period called the Great Salinity Anomaly (GSA) (*11*), but the freshening continued at a lesser rate until the late 1990s (*10*). These manifold changes in the freshwater (FW) system were largely synchronous and correlated with the amplifying North Atlantic Oscillation (NAO) index and rising air temperatures that characterized the period 1950–2000 (*2*–*4*, *12*). Here, we synthesize these observations in order to mechanistically link the Arctic FW system to the North Atlantic, including its subtropical basins.

To focus our synthesis, we pose a simple question: Can the increases in FW inputs from both atmospheric moisture convergence and from melting Arctic ice account for the recently documented freshening of the North Atlantic? Our approach is to calculate annual and cumulative FW input anomalies from net precipitation (P-E) on the ocean surface, river discharge (P-E on land), net attrition of glaciers, and Arctic Ocean sea ice melt and export for the latter half of the 20th century and compare these fluxes to measured rates of FW accumulation in the Atlantic's Nordic-Subpolar-Subtropical basins (hereafter NSSB) during the same period. These are estimates and budgets of FW anomalies (changes in fluxes and stocks relative to defined baselines during the years 1936–1955) and not budgets of total FW fluxes and stocks (*13*). A recent review of the Arctic Ocean FW budget (*14*) complements this review of changes in the FW cycle.

The domain for this synthesis (Fig. 1) includes the Arctic Ocean and its watershed, the Canadian Archipelago, Baffin Bay, Hudson Bay and its watershed, the Nordic Seas, Subpolar Basins, and the deep (>1500 m) subtropical basins of the North Atlantic. Anomalies of FW inputs were estimated by using the sources in Table 1 and compared to estimates of FW storage that were previously reported for the Nordic and Subpolar Seas (*10*) but here expanded to incorporate the deep Subtropical Basins (*13*). The present analysis of river discharge supplements previous reports of sustained Eurasian river runoff increases since the late 1960s (*4*, *15*) by incorporating the entire Arctic Ocean watershed and updating the records through 2003. Bering Strait plays a substantial role in the Arctic FW budget but is excluded here because long-term (1955–2000) changes in FW transport are unknown (*16*, *17*). A lack of adequate salinity data precludes assessing changes in the total FW content of the Arctic Ocean, although some information is available on changes in upper ocean

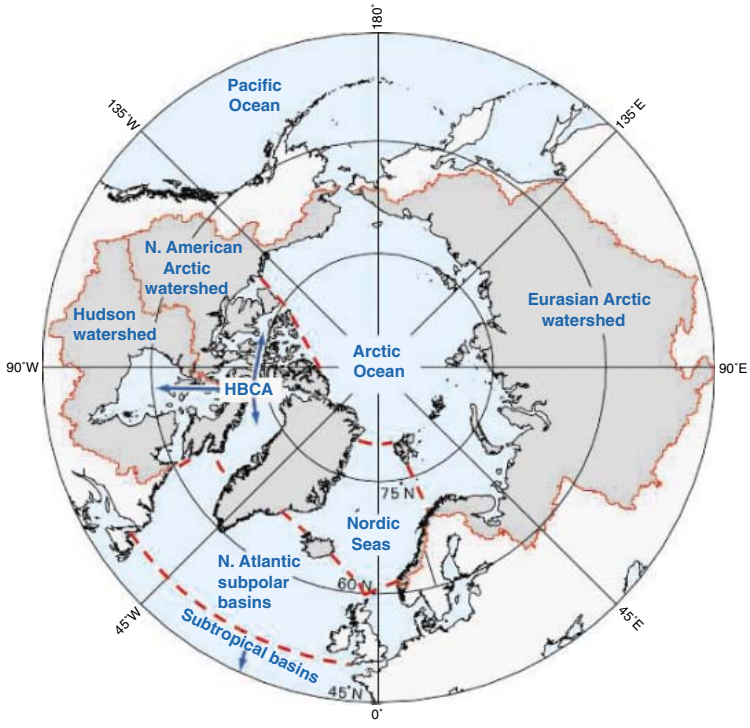

Fig. 1. Polar projection map showing the watershed and ocean domains used for estimates of freshwater anomalies. Solid red lines delineate watershed boundaries used for calculations of river discharge anomalies. Dashed lines separate regions of the ocean surface used for calculations of P-E anomalies and define the boundaries used for freshwater storage analysis in the Nordic Seas and the North Atlantic Subpolar Basins (*10*).

[1]Ecosystems Center, Marine Biological Laboratory, Woods Hole, MA 02543, USA. [2]Marine Science Institute, University of Texas at Austin, Port Aransas, TX 78373, USA. [3]Woods Hole Oceanographic Institution, MS 21, Woods Hole, MA 02543, USA. [4]Woods Hole Research Center, 149 Woods Hole Road, Falmouth, MA 02540, USA. [5]International Arctic Research Center, 930 Koyukuk Drive, Post Office Box 75340, Fairbanks, AK 99775, USA. [6]Applied Physics Laboratory, University of Washington, 1013 NE 40th Street, Seattle, WA 98105, USA.

*To whom correspondence should be addressed. E-mail: peterson@mbl.edu

Table 1. Contemporary anomalies for major FW sources to the Arctic Ocean, HBCA, Nordic Seas, and Atlantic Subpolar Basins. Anomalies for river discharge and P-E are relative to a 1936–1955 baseline. Anomalies for small glaciers and ice caps include melt from the pan-Arctic watershed, Arctic and subarctic islands, and ice caps around but not connected to the Greenland Ice Sheet. Anomalies for sea ice focus specifically on melting of stocks in the Arctic Ocean. Anomalies for small glaciers and ice caps, the Greenland Ice Sheet, and sea ice are relative to a water balance of zero (no net change in volume). In all cases, positive values indicate excess FW inputs to the ocean. Dashed entries indicate no estimates. R-ArcticNET v3.0 is a river discharge archive, and ERA-40 is a reanalysis of atmospheric observations.

Freshwater sources	References	Years covered in references	Avg. anomaly ± SE for 1990s (km^3 $year^{-1}$)	% relative to 1936–1955 baseline
Rivers flowing into the Arctic Ocean	Peterson *et al.* (*4*) R-ArcticNET v3.0 (*55*) Wu *et al.* (*14*)	1936–1999 2000–2003 1900–2050	163 ± 34	+5.3
Rivers flowing into Hudson Bay	Déry *et al.* (*56*)	1964–2000	−59 ± 16	−8.0
Small glaciers, ice caps	Dyurgerov and Carter (*5*)	1961–2001	38 ± 13	—
Greenland Ice Sheet	Box *et al.* (*6*)	1991–2000	81 ± 38	—
P-E, Arctic Ocean	ERA-40 (*57*)	1958–2001	124 ± 72	+7.6
P-E, HBCA	ERA-40 (*57*)	1958–2001	81 ± 33	+15.6
P-E, Nordic Seas	ERA-40 (*57*)	1958–2001	67 ± 28	+17.8
P-E, Subpolar Basin	ERA-40 (*57*)	1958–2001	336 ± 73	+16.8
Sea ice	Rothrock *et al.* (*7*)*	1987–1997	817 ± 339	—
TOTAL			1649	

*Rothrock *et al.* (*7*) reported observed changes in sea ice thickness annually from 1987–1997 and also modeled changes over a wider time frame (1951–1999). Thickness has been converted to freshwater volume following Wadhams and Munk (*58*).

salinities (*18*). Complete mass balance estimates for the Greenland Ice Sheet are not available for the entire 1955–2000 period; thus, only its recent (1990s) and potential future FW contributions are discussed (*2*, *3*, *6*, *19*, *20*).

Freshwater Anomalies

Estimates of flux and cumulative volumetric anomalies are given for eight different FW sources (Fig. 2 and Table 1) (*13*): river discharge to the Arctic Ocean and to Hudson Bay, P-E over the Arctic Ocean and over the Hudson Bay–Baffin Bay–Canadian Archipelago open water region (hereafter HBCA), Arctic glacier melt (excluding the Greenland Ice Sheet), Arctic sea ice attrition (*21*), and P-E over the Nordic Seas and Subpolar Basins. Of the individual records, sea ice exhibited the greatest interannual variability in flux anomalies (±1200 km^3 $year^{-1}$ for 5-year averages) and the largest amplitude of cumulative change over the record (15,000 km^3, expressed as net FW melt equivalent). Summed over the entire spatial domain, however, the change in combined cumulative P-E anomalies (ocean P-E plus runoff from land) from their lowest values in 1965–1970 to peak values in the year 2000 was ~20,000 km^3, somewhat larger than sea ice input. Arctic glacier melt (excluding Greenland) played a relatively small but growing role in the total anomaly history (*5*). Greenland's massive ice sheet has also exhibited net shrinkage in recent years (*6*, *19*). Its average net melt during the 1990s was estimated at ~80 km^3 $year^{-1}$ (*6*) (Table 1) but appears to have recently increased to ~220 km^3 $year^{-1}$ (*20*).

Despite increasing FW contributions to the Arctic Ocean during the latter half of the 20th century, the near-surface layers of the Arctic Ocean became saltier (*18*). This increase in salinity suggests that the anomalous FW contributions were exported along with an additional quantity of FW drawn from Arctic Ocean storage [Supporting Online Material (SOM) text]. Swift *et al.* (*18*) described salinity increases in the upper 175 m of the Arctic Ocean between the periods 1949–1975 and 1976–1993. These salinity increases were evident in all areas of the Arctic Ocean except parts of the Makarov and the northeasternmost Canada basins [boxes 9 and 13, figure 1 in (*18*)]. By using the data of Swift *et al.* (*18*), we calculate that depth-weighted mean salinity increased in the 0- to 50-m layer by 0.39 practical salinity units (psu), in the 50- to 100-m layer by 0.11, and in the 100- to 175-m layer by 0.05, with little change at greater depths. The salinity increase between the midpoints of the 1945–1975 and the 1976–1993 periods was equivalent to a withdrawal of ~4000 km^3 of FW at a rate of ~180 km^3 $year^{-1}$. However, the sparsity of available data precludes further assessment of Arctic Ocean volumetric changes with any confidence.

FW storage in the NSSB over the years 1953–2003 experienced a net gain of ~17,000 km^3, which included an initial loss of ~8000 km^3 in the 1950s and early 1960s followed by a sustained period of FW accumulation of ~25,000 km^3 from 1965 to 1995 (Fig. 3C). The greatest rate of accumulation, ~10,000 km^3 in a 5-year period, occurred in the 1970s, the time of the GSA.

Of the three NSSB regions, the largest and most rapid changes occurred in the Subpolar Basins (Fig. 3C). Although the bulk of Arctic sea ice and other FW exports flow southward through Fram Strait, only a small part spreads from the East Greenland Current into the interior of the Nordic Seas, with most being transported directly through Denmark Strait into the Subpolar Basins (*22*). Almost no excess FW entered the deep Subtropical Basins until after 1987 (Fig. 3C), when deep convection in the Subpolar Basins produced extremely cold but fresh, dense waters. All of the FW anomalies exported to the subtropics (total ~9000 km^3) were stored at depths > 1500 m. Of this total, about half accumulated below 2200 m and is linked to upstream changes in the products of Nordic Seas overflows and entrainment that ventilate these deep subtropical basins. The other half, which accumulated at depths between 1500 to 2200 m, is linked to changes in Labrador Sea water properties (*23*).

Collectively comparing the FW source and ocean FW sink records, two features of the histories emerge: (i) the overall synchrony of changes and (ii) their timing relative to changes in global surface air temperature (SAT), the NAO index, and the associated Northern Annular Mode (NAM) index (*24*) (Figs. 2 and 3). Although year-to-year comparisons of FW sources and sinks are largely impractical (*25*), the synchrony of trajectories and shifts across the individual records suggests dividing the timeline (T) into four periods: T1, the years before the GSA period (through 1965), characterized by a persistent negative NAO phase and relatively cool global SAT; T2, the GSA period itself (1966–1980), with multiyear oscillations of the NAO and a transition to increasing SAT; T3, the subsequent years (1981–1995), when the NAO was in a positive phase and the global SAT was rising; and T4, the years after the 1995–96 retreat of the NAO to a neutral phase, during which SAT continued to increase.

Concomitant changes in all of the major FW input anomalies near the T1-T2 boundary (Fig. 2) indicate an abrupt trajectory shift in the Arctic and Subarctic FW cycle during the late 1960s to early 1970s. This trajectory shift was associated with sharply increased P-E over the Subpolar Basins, Nordic Seas, Arctic Ocean, and HBCA region (Fig. 2). Simultaneously, Eurasian river discharge began to exhibit positive anomalies, while Hudson Bay river discharge began to diminish. Sea ice, which had been accumulating in the Arctic Ocean from 1950 to 1965, reversed direction in 1965 to a variable but sustained decline over subsequent decades (*7*).

Over the next 30 years, T2 and T3, the NAO index and global air temperatures trended upward with decadal bumps, the individual FW sources fluctuated in harmony, and cumulative FW inputs largely paralleled ocean storage. This synchrony in FW sources and NSSB storage, however, did not hold completely after 1995, period T4, when the NAO and the NAM retreated to more neutral values while global and arctic SAT continued to rise (*26*). Near-surface waters in the Subpolar Basins and Nordic Seas became more saline (*27*) as P-E over the ocean domains declined, but anomalies of river discharge to the Arctic Ocean (primarily Eurasian discharge) remained strongly positive and river discharge anomalies to Hudson Bay became positive. Glacial and Greenland Ice Sheet melting continued at an accelerated pace (*5*, *19*), and sea ice reached record area minima in summer and winter (*28*). Increasing river discharge and melting rates of sea ice and glaciers during recent years appear to be coupled with increasing temperature, whereas the ocean P-E anomalies remain closely tied to the dynamics governing the NAO and the NAM.

Atmospheric Moisture Flux Convergence

The cumulative contributions of (i) local P-E (Subpolar and Nordic Seas), (ii) remote P-E (Arctic Ocean–HBCA P-E plus Arctic Ocean–Hudson Bay river discharge), (iii) sea ice, and (iv) glacier melt were summed and compared to the cumulative NSSB FW storage anomalies by normalizing all records to 1965, when the entire system shifted and ocean FW storage was lowest (Fig. 4 and Table 2). The sum of all P-E anomalies (local plus remote) (Fig. 4) constituted half (~16,000 km^3) of the total FW collectively added since 1965, and with the exception of the years 1986–1988 the annual flux anomalies were uniformly positive in sign between 1970–2000, in contrast to negative anomalies that prevailed before 1970. This trajectory shift in atmospheric moisture flux convergence onto the high northern latitudes complemented FW losses from the low-latitude Atlantic, Pacific, and Indian oceans that were diagnosed through salinity changes over the same time period (*9*, *29*, *30*) and the large-scale mid-latitude drying since 1998 documented for the Northern Hemisphere (*31*). The preponderance of evidence indicates that a global redistribution of FW has taken place. Whether or not this involved increased global rates of total evaporation, precipitation, and atmospheric moisture transport, i.e., an acceleration of the entire global hydrologic cycle, remains undetermined.

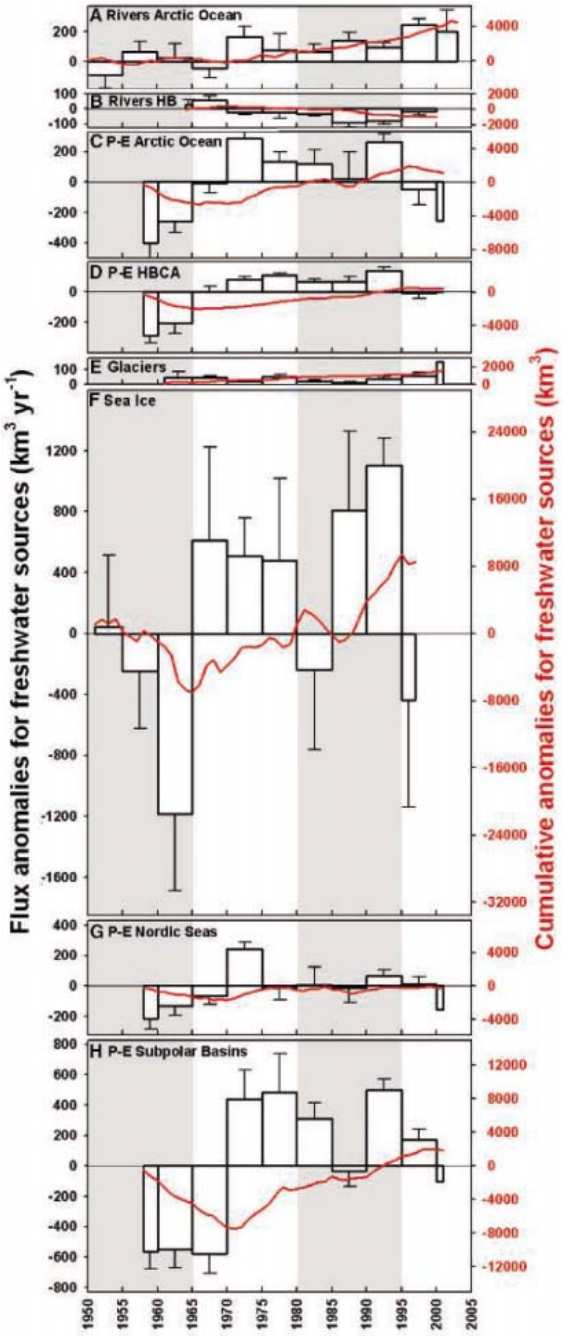

Fig. 2. Time course of FW source anomalies. (**A**) River discharge into Arctic Ocean, (**B**) river discharge to Hudson Bay, (**C**) P-E over Arctic Ocean, (**D**) P-E over HBCA, (**E**) glacier melt (excluding Greenland), (**F**) Arctic Ocean sea ice attrition, (**G**) P-E over Nordic Seas, and (**H**) P-E over Subpolar Basins. Bars show average anomalies and standard errors for 5-year increments, except when data are not available for the full period. In these cases, the narrower width of the bars reflects the number of years in the average. The continuous red lines represent cumulative freshwater anomalies (scale on right-hand axis). Positive anomalies represent excess FW inputs to the ocean. The alternating white and gray areas delineate time intervals that are discussed in the text (T1 to T4) when comparing source anomaly patterns to changes in ocean storage.

Annual P-E fluxes within the individual Arctic and subarctic domains and within the overall domain (remote plus local) exhibit decadal variability that tracks the NAO index. This relationship was previously noted for Eurasian and Hudson Bay river discharges (*4*, *32*), P-E onto the Nordic and Subpolar Seas (*33*), and atmospheric moisture flux convergence into the polar cap north of 70°N (*34*). Although specific details of the dynamics governing the NAO and the NAM remain elusive, their amplification in recent decades may reflect a nonlinear response to rising greenhouse gas concentrations and ozone depletion through a variety of mechanisms. These include stratospheric cooling and intensification of the polar vortex (*35*, *36*), Arctic sea ice loss (*37*), and atmospheric teleconnections to elevated Indian Ocean sea surface temperatures (*38*, *39*) and are part of a growing body of evidence suggesting that factors are aligning to favor continued amplification of the NAO and the NAM, and thus elevated amounts of P-E at the high latitudes, in the 21st century (*26*).

Arctic Ocean FW Exports

The Arctic FW budget includes an average oceanic FW influx from the Pacific of ~2500 km^3 year^{-1} (*17*) and FW and sea ice exports to the North Atlantic of ~8000 km^3 year^{-1} (*40*–*42*), with the balance (~5500 km^3 year^{-1}) supplied by atmospheric moisture flux convergence over the Arctic Ocean and its watershed (*14*). Direct measurement of these fluxes is difficult, and their interannual variability remains uncertain. However, the consequences of variability in Arctic Ocean export are visible as interannual changes in Arctic sea ice volume and as North Atlantic FW pulses such as the GSA. Several studies have suggested that these changes are choreographed by a broad-scale dynamical system that alternately accumulates FW and sea ice in the Arctic and exports them to the North Atlantic (*43*–*46*). The mechanism involves changes in strength of the Arctic high sea level pressure (SLP) cell leading to Arctic Ocean circulation regimes, which alternately favor retention and release of sea ice and FW. To the extent that Arctic SLP is governed by the same processes that control the NAO and the NAM, one should expect Arctic FW exports and the NAO and the NAM to be linked.

The sparse Arctic Ocean observational record precludes direct verification of this dynamical framework, but the timing and the magnitude of Arctic FW release episodes can be diagnosed by comparing the NSSB storage history to local and remote FW sources. The NSSB FW budget is maintained by three essential components: (i) local P-E on the Nordic and Subpolar Seas, (ii) horizontal FW fluxes from the Arctic and the HBCA, and (iii) saline ocean inflows from the subtropics. After removing the local P-E contribution, the residual FW storage anomaly represents the net sum of oceanic fresh and saline inflows. A positive FW residual implies a dominance of Arctic inflow, a negative FW residual implies a dominance of subtropical inflow, and a zero residual implies a net balance between them.

The cumulative FW storage and local P-E diverge after 1965, with local P-E inputs accounting for less than 30% of the changes in NSSB FW storage from 1965 to 2000 (Fig. 4). Net changes in FW sources, storage, and residuals (NSSB storage minus local P-E) were computed for each period (Table 2). The residuals indicate periods of enhanced (T2 and T3) and diminished (T4) Arctic FW influences on the NSSB storage anomaly history. Cumulative FW input and storage were about equal during T2 and T3, whereas cumulative input exceeded storage during T1 and T4, implying that excess FW was accumulating in the Arctic during those periods [although no estimates of FW melt equivalent are available for the continued sea ice attrition reported after 1997 (*28*)].

During T1, the NAO and the NAM were in a negative phase and trending downward, NSSB FW storage declined at a rate of ~400 km^3 year^{-1}, and sea ice and FW were both accumulating in the Arctic. Over the next 30 years (T2 and T3), the NAO and the NAM were trending upward to a persistently high phase, and NSSB FW storage increased dramatically (average rate of +800 km^3 year^{-1} but episodic), accounting for nearly the entire sum of anomalous FW source inputs. The NAO and the NAM switched to extreme low values in 1995–1996 but did not settle into a persistent high or low phase thereafter (T4), and the sum of available FW source inputs increased slightly. This excess of Arctic FW had little net influence on the NSSB FW storage, which declined at a rate of ~400 km^3 year^{-1}, implying that Arctic FW exports also retreated with the NAO index. Marked changes did occur in the Subpolar Basins as saline subtropical surface waters flowed into the subpolar and Nordic circulations (*27*), but about half of the subpolar FW losses were matched by FW gains in the subtropical deep basins. The relatively small net FW decrease (residual ~ –2700 km^3) over the entire NSSB system during T4 implies that subtropical saline inflows slightly exceeded Arctic FW inflows from 1995 onward. The larger implication is that the FW presently accumulating in the Arctic will find its way into NSSB storage if and when the atmospheric circulation patterns re-establish a weakened Arctic high SLP and positive NAO and NAM phase.

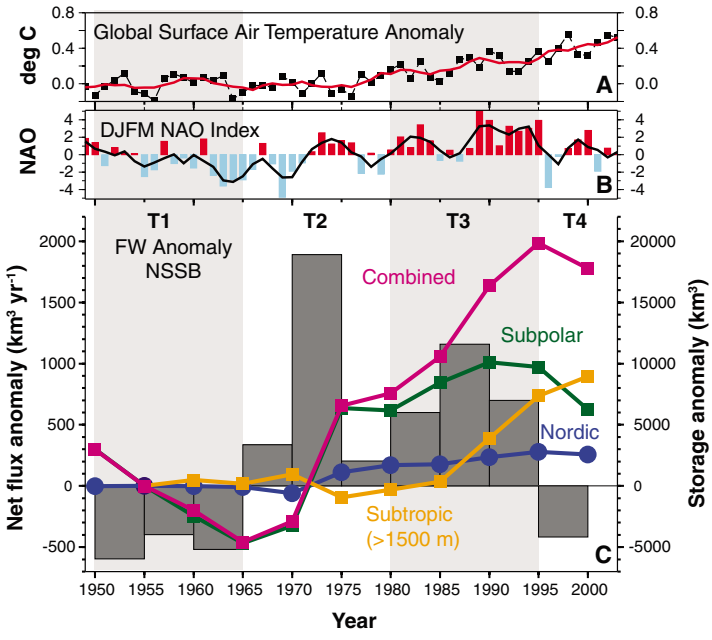

Fig. 3. North Atlantic Ocean FW storage anomalies, NAO index, and global surface temperature anomaly, 1950–2005. Gray shading delineates four time periods (T1 to T4) described in text. (**A**) Global SAT anomalies (*53*). Black dashed curve and symbols are annual anomalies; red curve is 5-year running mean. (**B**) Winter [December through March (DJFM)] NAO index (*54*). Blue and red bars are annual index values; black curve is 5-year running mean. (**C**) FW storage anomalies (km^3) relative to 1955 for Nordic Seas (blue), Subpolar Basins (green), deep (>1500 m) Subtropical Basins (orange), and all regions combined (purple). Ocean anomalies represent 5-year averages and center on years marked with symbols. Bars denote net flux anomalies (km^3 year^{-1}), computed as difference in storage between consecutive time periods.

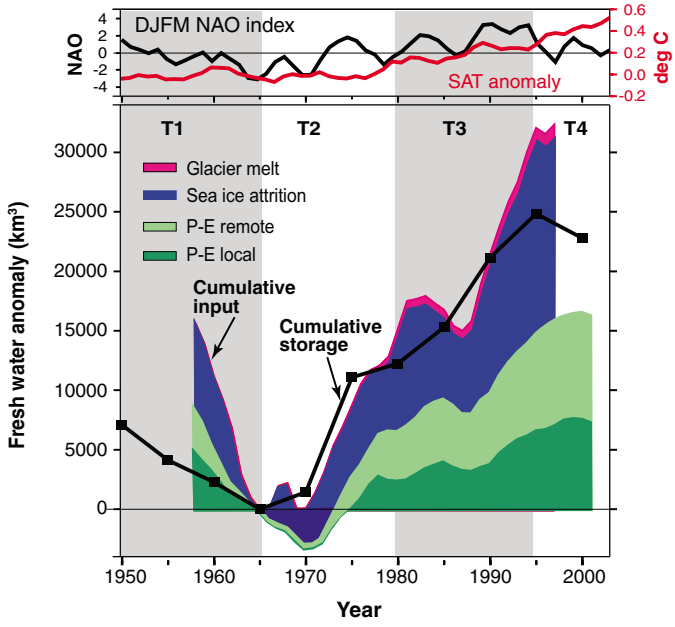

Fig. 4. Comparison of FW source anomalies and FW storage anomalies relative to 1965 (units are km^3). Black curve is cumulative NSSB ocean FW storage. Colored areas represent cumulative FW contributions from P-E local (Subpolar plus Nordic Seas, dark green), P-E remote (Arctic Ocean, HBCA, and river discharge, light green), sea ice attrition (blue), and glacier melt (red). Source contributions are stacked to show total FW source input.

Meridional Overturning Circulation

Numerous modeling studies have identified mechanisms linking North Atlantic salinity distributions to changes in strength of the meridional overturning circulation (MOC). An abundant literature exists on this topic, and the interested reader is referred to (*47*–*49*) as a starting place. If changes in the MOC's northward transport of subtropical saline surface waters were governing the NSSB FW storage variability, we might infer a weakening of the MOC between 1965–1995, when residual FW storage (after removing the local P-E contributions) and therefore the net oceanic FW influx increased. However, the subtropical surface waters themselves were characterized by increased salinities in this time period (*9*), ruling them out as a likely source of the FW anomaly. Indeed, simulations of 20th century climate using HadCM3 reproduced the high-latitude freshening, traced its source to Arctic sea ice and in-

Table 2. Approximate volumetric FW gains or losses (in km^3) for each time period and various FW source or sink components. T1, T2, and T3 span 15 years each, T1a is the subset of T1 for which P-E estimates are available, and T4 encompasses the post-1995 period for which measurements are available. P-Eremote is the sum of Arctic Ocean P-E, HBCA P-E, Arctic rivers, and Hudson rivers. P-Elocal is the sum of Nordic Seas and Subpolar Basins P-E. Storage – P-Elocal is referred to in text as residual NSSB FW gain or loss. Question marks identify time periods where data coverage was not sufficient for calculations.

	1951–1965 T1	1958–1965 T1a	1966–1980 T2	1981–1995 T3	1996–2001 T4
Sea ice attrition	–7000	–6000	+8000	+8400	?
Glacier melt	?	?	+600	+300	+400
Arctic Ocean P-E	?	–2500	+2100	+2000	–500
HBCA P-E	?	–1900	+1000	+1400	0
Arctic rivers	0	+500	+1000	+1500	+1500
Hudson rivers	?	?	+100	–1000	–100
P-Eremote	?	–3800	+4100	+3900	+800
P-Elocal	?	–5700	+2500	+4200	+700
NSSB storage	–7100	–4100	+12,200	+12,600	–2000
Storage – P-Elocal	?	+1600	+9700	+8400	–2700

creased river runoff, and diagnosed a slightly enhanced MOC over this same time period (*49*).

In more than 2 decades of direct measurements, the MOC's principal source currents, the northward flow of warm surface waters through Florida Strait (*50*) and the southward flows of cold, dense waters from the Nordic Seas across Denmark Strait and through the Faroe Bank Channel, have not exhibited sustained changes in flow strength. The eastern overflow did appear to slow for a few years between 1999 and 2001 but recovered its usual strength in subsequent years (*10*). Although Bryden *et al.* (*51*) reported evidence for a recent (post-1998) MOC weakening across 25°N, the transport changes estimated in that study are very near the error limits of the calculation. Moreover, the reported MOC slackening was accompanied by salinity increases in the near-surface layers of the eastern Subpolar and Nordic Seas (Fig. 3 and fig. S1) (*27*), opposite in sign to expectations. Rather, the overall balance between anomalous FW inputs and ocean FW storage suggests that Arctic exports, governed by atmospheric circulation modes and warming, dominated the observed NSSB freshening from 1965–1995 without need to invoke changes in the MOC. Those exports declined after 1995, and subtropical saline influences began to dominate the net storage changes in the NSSB at about the same rate (–400 km^3 year^{-1}) as was the case between 1950–1965.

Thus, although we cannot exclude a role for changes in the MOC in the observed freshening of the North Atlantic, the overall agreement between anomalous FW inputs and changes in ocean FW storage suggests that increased high-latitude FW inputs were primarily responsible for the observed freshening during 1965–2000.

Present and Future Implications

Variability observed in the high-latitude hydrologic system reflects interplay of SAT and atmospheric circulation patterns. The Arctic, HBCA, Nordic, and Subpolar regions are all affected by global SAT, because SAT influences high-latitude moisture flux convergence, and by regional SAT, because SAT influences cryosphere melt. Atmospheric modes, such as the NAO and the NAM, modulate the pathways that redistribute atmospheric moisture, affect regional temperature regimes, and orchestrate the circulation of sea ice and surface waters in the Arctic Ocean. These modes play an important role in the timing and magnitude of North Atlantic freshening through their impacts on local P-E and on the alternate accumulation and release of sea ice and FW from the Arctic Ocean and HBCA into the NSSB.

In the 2000s, pervasive changes have continued to modify the Arctic hydrologic system in ways that reflect both the neutral state of the NAO and the NAM and the influence of rising temperatures. Sea ice continued to decline (*28*) despite the post-1995 retreat of the NAO and the NAM and probable reduced Arctic exports to the NSSB, the surface waters of the Beaufort Gyre exhibited widespread freshening (*52*), and melting of the Greenland Ice Sheet accelerated (*19*). Although meltwater contributions from Arctic glaciers and the Greenland Ice Sheet have thus far played a relatively minor role in the FW anomaly record, rising temperatures will undoubtedly amplify that contribution in potentially dramatic ways (*20*). As we look to future decades, the interplay between the NAO and the NAM and the continuation of global greenhouse warming will determine whether the Arctic–North Atlantic FW cycle continues its upward trend of increasing high-latitude FW inputs and ocean FW storage or shifts once again to a new trajectory.

References and Notes

1. J. T. Overpeck *et al.*, *Eos* **86**, 309 (2005).
2. J. T. Houghton *et al.*, Eds., *Climate Change 2001: The Scientific Basis. Contribution of Working Group I to the Third Assessment Report of the IPCC* (Cambridge Univ. Press, Cambridge, 2001).
3. ACIA 2005, *Arctic Climate Impact Assessment: Scientific Report* (Cambridge Univ. Press, Cambridge, in press).
4. B. J. Peterson *et al.*, *Science* **298**, 2171 (2002).
5. M. B. Dyurgerov, C. L. Carter, *Arct. Antarct. Alp. Res.* **36**, 117 (2004).
6. J. E. Box, D. H. Bromwich, L. S. Bai, *J. Geophys. Res.* **109**, 10.1029/2003JD004451 (2004).
7. D. A. Rothrock, J. Zhang, Y. Yu, *J. Geophys. Res.* **108**, 10.1029/2001JC001208 (2003).
8. R. R. Dickson *et al.*, *Nature* **416**, 832 (2002).
9. R. Curry, B. Dickson, I. Yashayaev, *Nature* **416**, 826 (2003).
10. R. Curry, C. Mauritzen, *Science* **308**, 1772 (2005).
11. R. R. Dickson, J. Meincke, S.-A. Malmberg, A. J. Lee, *Prog. Oceanogr.* **20**, 103 (1988).
12. M. C. Serreze *et al.*, *Clim. Change* **46**, 159 (2000).
13. Materials and methods are available as supporting material on *Science* Online.
14. M. C. Serreze *et al.*, *J. Geophys. Res.*, in press.
15. P. Wu, R. Wood, P. Stott, *Geophys. Res. Lett.* **32**, 10.1029/2004GL021570 (2005).
16. R. A. Woodgate, K. Aagaard, T. J. Weingartner, *Geophys. Res. Lett.* **32**, 10.1029/2004GL021880 (2005).
17. R. A. Woodgate, K. Aagaard, *Geophys. Res. Lett.* **32**, L02602 (2005).
18. J. H. Swift, K. Aagaard, L. Timokhov, E. G. Nikiforov, *J. Geophys. Res.* **110**, 10.1029/2004JC002312 (2005).
19. R. B. Alley, P. U. Clark, P. Huybrechts, I. Joughin, *Science* **310**, 456 (2005).
20. E. Rignot, P. Kanagaratnam, *Science* **311**, 986 (2006).
21. Sea ice attrition is defined as melt plus export, whereas negative attrition equals accumulation plus import.
22. K. Aagaard, E. C. Carmack, *J. Geophys. Res.* **94**, 14485 (1989).
23. R. G. Curry, M. S. McCartney, T. M. Joyce, *Nature* **391**, 575 (1998).
24. D. W. J. Thompson, J. M. Wallace, *Science* **293**, 85 (2001).
25. Comparisons between FW inputs and ocean accumulation for short intervals (5 years) in Fig. 4 must be made with care. The FW source anomaly calculations are based on annual fluxes, and cumulative points represent net contributions through the year at which they are plotted. Points for FW storage in the NSSB are estimated from 5-year average ocean salinity fields and are centered on the middle year of each pentad (for example, the average of storage estimates for 1958–1962 is plotted at 1960). Thus, the timing of input and storage events in Fig. 4 are an indication of events happening in roughly, but not exactly, the same time frame. The FW source and storage estimates do not permit tracking FW dynamically as it moves through the system. Comparing cumulative volumes in general circumvents this deficiency and issues of time lags between FW input and downstream ocean storage.
26. M. Serreze, J. A. Francis, *Clim. Change* **76**, 241 (2006).
27. H. Hátún, A. B. Sandø, H. Drange, B. Hansen, H. Valdimarsson, *Science* **309**, 1841 (2005).
28. W. Meier, J. Stroeve, F. Fetterer, K. Knowles, *Eos* **86**, 326 (2005).
29. A. P. S. Wong, N. L. Bindoff, J. A. Church, *Nature* **400**, 440 (1999).
30. H. L. Bryden, E. L. McDonagh, B. A. King, *Science* **300**, 2086 (2003).
31. M. Hoerling, A. Kumar, *Science* **299**, 691 (2003).
32. S. J. Déry, E. F. Wood, *Geophys. Res. Lett.* **32**, 10.1029/2005GL022845 (2005).
33. S. A. Josey, R. Marsh, *J. Geophys. Res.* **110**, 10.1029/2004JC002521 (2005).
34. A. N. Rogers, D. H. Bromwich, E. N. Sinclair, *J. Clim.* **14**, 2414 (2001).
35. D. Shindell, D. Rind, N. Balachandran, J. Lean, P. Lonergan, *Science* **284**, 305 (1999).
36. D. W. J. Thompson, J. M. Wallace, G. Hegerl, *J. Clim.* **13**, 1018 (2000).
37. V. Semenov, L. Bengtsson, *Geophys. Res. Lett.* **30**, 1781 (2003).
38. J. W. Hurrell, M. P. Hoerling, A. S. Phillips, T. Xu, *Clim. Dyn.* **23**, 371 (2004).
39. M. P. Hoerling, J. W. Hurrell, T. Xu, *Science* **292**, 90 (2001).

40. M. P. Meredith *et al.*, *Geophys. Res. Lett.* **28**, 1615 (2001).
41. S. J. Prinsenberg, J. Hamilton, *Atmos. Ocean* **43**, 430101 (2001).
42. T. Vinje, N. Nordlund, A. Kværnbekk, *J. Geophys. Res.* **103**, 10437 (1998).
43. A. Y. Proshutinsky, M. A. Johnson, *J. Geophys. Res.* **102**, 12493 (1997).
44. A. Y. Proshutinsky, R. H. Bourke, R. A. McLaughlin, *Geophys. Res. Lett.* **29**, 2100 (2002).
45. I. G. Rigor, J. M. Wallace, R. L. Colony, *J. Clim.* **15**, 2648 (2002).
46. L. Mysak, S. Venegas, *Geophys. Res. Lett.* **25**, 3607 (1998).
47. J. Marotzke, *Proc. Natl. Acad. Sci. U.S.A.* **97**, 1347 (2000).
48. S. Rahmstorf, *Clim. Dyn.* **12**, 799 (1996).
49. P. Wu, R. Wood, P. Stott, *Geophys. Res. Lett.* **31**, L02301 (2004).
50. M. O. Baringer, J. C. Larsen, *Geophys. Res. Lett.* **28**, 3179 (2001).
51. H. L. Bryden *et al.*, *Nature* **438**, 655 (2005).
52. A. Proshutinsky *et al.*, *Eos* **86**, 368 (2005).
53. Global SAT values were taken from the National Climatic Data Center (www.ncdc.noaa.gov/oa/climate/research/anomalies/anomalies.html).
54. NAO index values were taken from the National Center for Atmospheric Research (www.cgd.ucar.edu/cas/jhurrell/indices.info.html).
55. Combined discharge from the six largest Eurasian rivers reached a record high of 2060 km^3 $year^{-1}$ in 2002. Data was compiled from R-ArcticNET (www.r-arcticnet.sr.unh.edu/v3.0).
56. S. J. Déry, M. Stieglitz, E. C. McKenna, E. F. Wood, *J. Clim.* **18**, 2540 (2005).
57. S. M. Uppala *et al.*, *Q. J. R. Meteorol. Soc.* **131**, 2961 (2005).
58. P. Wadhams, W. Munk, *Geophys. Res. Lett.* **31**, L11311 10.1029/2004GL020039 (2004).

59. This paper is dedicated to J. E. Hobbie, who introduced the senior author to the study of Arctic fresh waters. We thank B. Chapman for calculations of P-E. Funding was provided by NSF (grants OPP-0229302, OPP-0436118, OPP-0327664, OPP-0352754, OPP-0519840, and OCE-0326778), Office of Naval Research (grant N00014-02-1-0305), and NASA (grant IDS-03-0000-0145).

Supporting Online Material

www.sciencemag.org/cgi/content/full/313/5790/1061/DC1
Materials and Methods
SOM Text
Fig. S1
Table S1

10.1126/science.1122593

page 1088

INTRODUCTION

A Thirsty World

THE SEARCH FOR FRESH WATER—TO DRINK, TO BATHE IN, TO IRRIGATE CROPS—is a problem as old as civilization. Across the ages, cities have thrived where the supply is abundant and collapsed in the face of drought. Remarkably, despite the technological progress characterizing the modern era and the fact that most of Earth's surface is covered by oceans, the availability of fresh water remains a pressing concern throughout the world. In this special section, we highlight some of the diverse contemporary scientific and engineering projects dedicated to obtaining and maintaining freshwater resources.

We begin with a Review by Oki and Kanae (p. 1068) on current understanding of the natural water cycle, and in particular the role of climate change in determining freshwater abundance. A related Review in this week's issue by Peterson *et al.* (p. 1061) focuses more specifically on the Arctic region. Even in regions of abundant fresh water, contamination and disease can disable local communities. Schwarzenbach *et al.* (p. 1072) present a Review of chemical contamination problems. They note that although effective strategies have been implemented to remediate large-scale pollutants, a substantial amount of work looms ahead to cope with the numerous different compounds that are present at lower concentrations. In particular, collaborative efforts among chemists, geologists, and toxicologists are increasingly important to characterize the complex interactions of these compounds in the environment. Fenwick's Perspective (p. 1077) follows with an optimistic view of the ongoing effort to combat waterborne diseases accompanying development programs in Africa, highlighting the role of drug donations from the pharmaceutical industry.

It may seem strange to many people that modern societies cannot fulfill their water needs simply by purifying ocean water. Tal offers a Perspective (p. 1081) about the multipronged strategy—of which desalination is an increasing component—that Israel has adopted to procure fresh water in an arid environment. Bohannon highlights the resource issues specific to the Gaza region in an accompanying News story (p. 1085). Another News story by Service (p. 1088) focuses more broadly on current developments in desalination technology. Additionally, two related stories by Stone and Jia (p. 1034) and Bagla (p. 1036) in the magazine's News Focus section describe large-scale engineering efforts in China and India to supply fresh water across extensive geographical areas.

Inevitably, water resource management is a political problem as well as a scientific one (see the related Editorial by Kennedy and Hanson on p. 1019). It is clear that ensuring adequate supply will necessitate continuing collaborations across a great range of disciplines. The approaches described here offer a measure of hope for the future.

– JAKE YESTON, ROBERT COONTZ, JESSE SMITH, CAROLINE ASH

Freshwater Resources

CONTENTS

See also related Editorial page 1019; News stories pages 1034 and 1036; Review page 1061

CREDIT: REED SAXON/AP

Science

REVIEW

Global Hydrological Cycles and World Water Resources

Taikan Oki[1,2,3]*† and Shinjiro Kanae[1,4]*

Water is a naturally circulating resource that is constantly recharged. Therefore, even though the stocks of water in natural and artificial reservoirs are helpful to increase the available water resources for human society, the flow of water should be the main focus in water resources assessments. The climate system puts an upper limit on the circulation rate of available renewable freshwater resources (RFWR). Although current global withdrawals are well below the upper limit, more than two billion people live in highly water-stressed areas because of the uneven distribution of RFWR in time and space. Climate change is expected to accelerate water cycles and thereby increase the available RFWR. This would slow down the increase of people living under water stress; however, changes in seasonal patterns and increasing probability of extreme events may offset this effect. Reducing current vulnerability will be the first step to prepare for such anticipated changes.

All organisms, including humans, require water for their survival. Therefore, ensuring that adequate supplies of water are available is essential for human well-being. Although our planet is often called the "Blue Planet," warnings of increasing water scarcity in the world are common. However, unlike oil, water circulates, forming closed hydrologic cycles. The amount of water will not diminish on shorter than geological time scales (*1*). Given this background, how could water scarcity become a widespread reality within a few decades (*2*)?

A common explanation is that even though there is a lot of water on Earth, only about 2.5% is fresh water, and because most of that water is stored as glaciers or deep groundwater, only a small amount of water is easily accessible. This answer is only partly correct: Rather than looking only at the stocks of water resources, assessments should concentrate mainly on the flows (Fig. 1) (*1*, *3*–*5*). The amount of water stored in all the rivers in the world is only 2000 km^3, much less than the annual water withdrawal of 3800 km^3/year (Fig. 1). Clearly, a more adequate measure of water availability is the 45,500 km^3/year of annual discharge, which flows mainly through the rivers from continents to the sea.

What Is the Meaning of a Circulating Resource?

Unlike most other natural resources, water circulates naturally. When it evaporates, it changes from liquid to gas and eventually recondenses as a liquid. Water assimilated during photosynthesis becomes part of carbohydrates stored in plants, but ultimately reverts to water again by decomposition.

When used, water loses properties such as purity, heat content, and potential gravitational energy, but eventually, most degraded water resources are refreshed by natural processes in the hydrological cycle, which is mostly driven by solar energy. When considering water flux as the most relevant measure of water resources, the speed of water circulation becomes crucial. Mean residence times of water molecules—i.e., how long they stay in a given reservoir—can be estimated by dividing the volume of the reservoir by the mean flux into and out of it. For rivers unaffected by human interventions, the mean residential time of water is about two and a half weeks (*1*). In contrast, the recharge rate of some groundwater aquifers is very slow, and the mean residential time is considered to be hundreds or even thousands of years. When water is extracted from such an aquifer, it will take a very long time, measured on a human time scale, to return to the original volume stored; in practice, that water is exhausted once it has been used. Because it took so long to accumulate, the groundwater in such aquifers is sometimes called fossil water.

How Much Renewable Fresh Water Is Available?

Can human demand for water be fully met by using only circulating renewable freshwater resources (RFWR)? The answer is both yes and no. Even though RFWR is naturally recycled, the circulation rate is determined by the climate system, and there is an upper limit to the amount of RFWR available to human society. On the global scale, current withdrawals are well below this limit, and if the water cycle is managed wisely, RFWR can cover human demand far into the future. Appropriate water management is a crucial point.

Conventional engineers of water resources consider the water withdrawn from surface and groundwater as water resources and evapotranspiration as a loss of water from the precipitated water. In that sense, precipitation minus evapotranspiration over land is a measure of the maximum available RFWR. The major part of this available RFWR is surface water, particularly river discharge. However, some part of the water, approximately 10% of total river discharge (*6*), infiltrates to deep underground and will never appear as surface water but discharge into the ocean directly from groundwater.

In contrast to the conventional view, it has been noted that evapotranspiration from nonirrigated cropland also is a water resource that is beneficial to society (*7*). To distinguish between this kind of resource and conventional resources, evapotranspiration flow has been named green water, and conventional withdrawal from rivers and groundwater has been named blue water (*7*).

About 3800 km^3/year of RFWR (blue water) is currently withdrawn by human beings, and that accounts for less than 10% of the maximum available RFWR in the world (Fig. 1). Evapotranspiration is estimated to be 7600 km^3/year from cropland and 14,400 km^3/year from permanent grazing land. Cropland and grazing land account for about one-third of the total terrestrial evapotranspiration.

Can We Use All the RFWR?

Why should we be concerned about water scarcity when presently only 10% of maximum available blue water and 30% of green water resources are used? The reason is the high variability of water resource availability in time and space (*8*). For example, the monthly mean discharge at the Obidos station in the Amazon River differs by a factor of 2 between the highest and the lowest months, even for climatologically averaged values. River discharge is more variable in smaller river basins in general, and daily river discharge is, of course, more variable than monthly river discharge. Because of this temporal variability, it is impractical to use 100% of the available RFWR for human society. Flow during floods and wet seasons cannot be used during the low flow seasons unless storage systems are in place. That is why there are millions of artificial reservoirs, lakes, and ponds in the world and why most of the major rivers are regulated (*9*). Total capacity of this artificial storage is estimated to 7200 km^3 (*10*), about twice the annual water withdrawal.

Another reason that RFWR can be insufficient is its uneven spatial distribution. Annual runoff (Fig. 2A) can be considered as the maximum available RFWR if water from upstream cannot be reused downstream because of consumptive

[1]Institute of Industrial Science, The University of Tokyo, 4-6-1 Komaba, Meguro-ku, Tokyo 153-8505, Japan. [2]Japan Science and Technology Agency, 4-1-8 Honcho, Kawaguchi-shi, Saitama 332-0012, Japan. [3]Frontier Research Center for Global Change, Japan Agency for Marine-Earth Science and Technology, 3173-25 Showa, Kanazawa-ku, Yokohama 236-0001, Japan. [4]Research Institute for Humanity and Nature, 457-7 Motoyama, Kamigamo, Kita-ku, Kyoto 603-8047, Japan.

*These authors contributed equally to this work.
†To whom correspondence should be addressed. E-mail: taikan@iis.u-tokyo.ac.jp

use or water pollution (*11*). Runoff is accumulated through river channels and forms river discharge (Fig. 2B). River discharge can be considered as the potentially maximum available RFWR if all the water from upstream can be used. Both runoff and river discharge are concentrated in limited areas, and the amounts range from nearly zero in desert areas through more than 2000 mm/year of runoff in the tropics and more than 200,000 m^3/s of discharge on average near the river mouth of the Amazon. Furthermore, the water demands for ecosystems and navigation should also be met, and all the RFWR cannot be used only for human beings.

How Are the World Water Resources Assessed?

In the late 1960s, the International Hydrological Decade promoted studies on world water balances, and pioneering estimates were published in the 1970s (*5*, *12*, *13*). Shiklomanov (*4*) assembled country statistics on water withdrawals in the past and present and made future projections. Recent advances in information technologies have enabled global water-balance estimations at finer spatial resolution (*11*, *14*, *15*). Water withdrawals now can be distributed into grid boxes, using the distributions of population and the irrigation area as proxies, and compared with the available RFWR in each grid box (*11*, *14*, *15*).

The water scarcity index is defined as $Rws = (W - S)/Q$, where W, S, and Q are the annual water withdrawal by all the sectors, the water use from desalinated water, and the annual RFWR, respectively. A region is usually considered highly water stressed if Rws is higher than 0.4 (*7*, *11*, *14*, *15*). It is considered to be a reasonable, although not definitive, threshold value because not all the RFWR can be used by human society. Data with shorter time scales will enable more detailed assessments considering the effects of temporal variability in the hydrological cycles.

In the era of the "Anthropocene" (*16*), where human impacts on natural processes are large and widespread, it no longer makes sense to study only natural hydrological cycles. For this reason, some studies have started to consider the impact of human interventions on the hydrological cycles, thereby simulating more realistically the hydrological cycles on a global scale. In such studies, human withdrawals are subtracted from the river flow (*15*), and the regulation of flow regime by major reservoirs is incorporated (*17*).

The distribution of the water scarcity index Rws (*11*), recalculated with the latest multimodel ensemble estimates (*3*), is shown in Fig. 2C. Rws is high in Northern China, in the area on the border between India and Pakistan, in the Middle East, and in the middle and western areas of the United States. Based on this assessment, approximately 2.4 billion people are currently living in highly water-stressed areas (*18*).

Can the "Virtual Water Trade" Alone Save the Water-Stressed Regions?

Transporting water over long distances, from regions where water is abundant to dry regions under water stress, is only feasible when gravity can be used. The demand for high-quality drinking water is limited to a few liters per person per day and can be met through international trade or by desalination. However, other demands for water for households, industry, and agriculture require up to one metric ton of water per day per

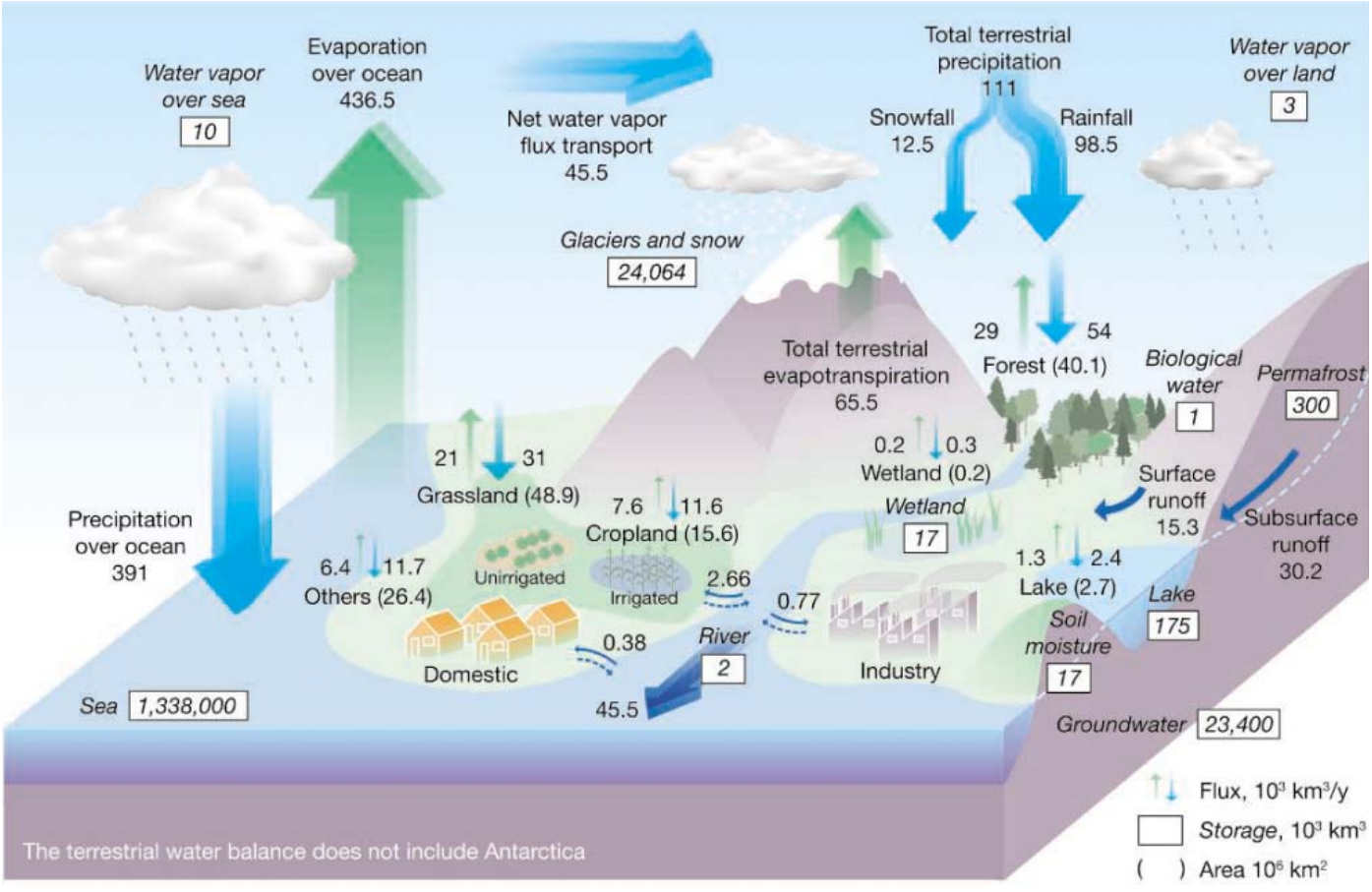

Fig. 1. Global hydrological fluxes (1000 km^3/year) and storages (1000 km^3) with natural and anthropogenic cycles are synthesized from various sources (*1*, *3*–*5*). Big vertical arrows show total annual precipitation and evapotranspiration over land and ocean (1000 km^3/year), which include annual precipitation and evapotranspiration in major landscapes (1000 km^3/year) presented by small vertical arrows; parentheses indicate area (million km^2). The direct groundwater discharge, which is estimated to be about 10% of total river discharge globally (*6*), is included in river discharge.

person in developing countries and considerably more in developed countries. Therefore, the supply for these sectors must be inexpensive, which means that transporting water by tanker or other high energy–consuming means is generally not realistic (*8*).

On the other hand, water demand for food and industrial production in dry regions can be offset by importing food or industrial goods. Such trade is called "virtual water trade" (*19*–*21*). The weight of traded goods is normally just a small fraction, such as $\frac{1}{100}$ to $\frac{1}{1000}$, of the weight of the water required to produce that goods, so transporting goods is considerably easier than transporting the water itself. Total international "virtual water trade" is estimated to be about 1000 km^3/year (*20*, *21*), although only a part of that "virtual water trade" is done to compensate for water shortage (*22*).

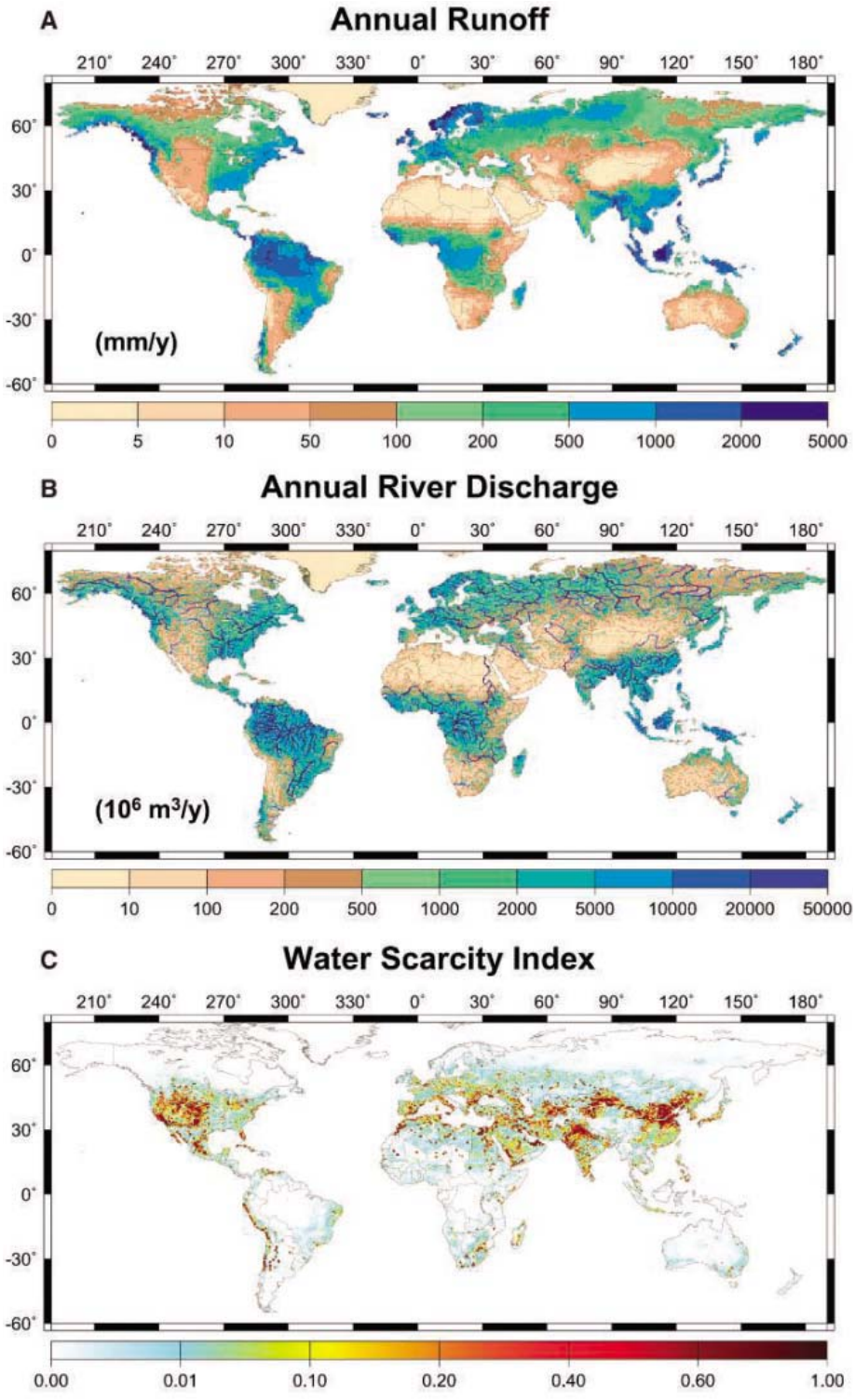

Fig. 2. Global distribution of (**A**) mean annual runoff (mm/year), (**B**) mean annual discharge (million m^3/year), and (**C**) water scarcity index *Rws* (*3*, *11*). Water stress is higher for regions with larger *Rws*.

Problems of water, food, health, and poverty are interlinked in many developing countries, particularly in the regions where freshwater resources are scarce, the local economy is too weak to allow import of food from outside on a large scale, and desalination plants are impractical to implement.

On the contrary, once water supply is secured by appropriate infrastructure investments and improved management, public health conditions improve, food supply stabilizes, the potential for industrial development increases, and the time that was earlier devoted to acquiring water can be used for more productive work or educational opportunities. This is the reason that the target "Reduce by half the proportion of people without sustainable access to safe drinking water" (*23*) is one of the Millennium Development Goals of the United Nations.

How Will Water Use Change in the Future?

The global population will certainly grow, at least for several decades, and water demand will increase as a result. Water demand per person will most likely also increase due to economic growth. For example, an expected growth of meat consumption will increase the water demand for fodder production.

The ultimate objectives of future-oriented world water resource assessments are to show the international community what will happen if we continue to manage our water resources as we do today and to indicate what actions may be needed to prevent undesirable outcomes. In that sense, studies of future world water resources are successful if their predictions based on business-as-usual are proven wrong. In line with this, plausible scenarios informed by past experiences and current trends are built for future projections of the demand side.

In the agricultural sector, which is estimated to withdraw two-thirds of world water withdrawals and which accounts for 90% of total water consumption in the world (*4*), in the period from 1961 to 2004, crop yield per area increased by a factor of 2.3, more than the rate of population growth (2.0), and the total crop yield increased by a factor of 2.4, even though the area of cropland increased by only 10% and harvested area increased less than that (*24*). This phenomenal growth was to a large extent due to a doubling of the irrigation area and the

corresponding increase of water withdrawal for irrigation in addition to the increased usage of fertilizer. Domestic per capita water use has increased with gross domestic product (GDP) growth, but in many developed countries this increase seems to have come to an end; in some countries, domestic per capita water use is now decreasing. Such trend shifts should be considered in predictions of future water use. Industrial water use has also increased along with GDP, but recycling technology has reduced the net intake of water for factories. For example, nearly 80% of water used in the industrial sectors in Japan is currently recycled (*25*).

There are concerns that in the decades ahead, water withdrawals for irrigation cannot be increased as required and that the lack of water will impede necessary growth of food production. However, *Rws* in developing countries is generally low, which means that they should have a potential to increase their water withdrawals. A key challenge for these countries should be how to implement soft measures (such as legislation, policies, and market mechanisms) in addition to technical ones to simultaneously increase the supply and manage the demand wisely (*26*).

What Effects Will Climate Change Have on RFWR?

The effect of global climate change on hydrological cycles is still uncertain, but higher temperatures will turn some part of snowfall into rainfall, the snowmelt season will be earlier, and, as a result, the timing and volume of spring flood will change substantially (*27*). Nearly half of the world's population depends on groundwater sources for drinking water supply and for other uses (*28*). Sea level rise will cause saline water intrusion into groundwater aquifers near the coasts and will decrease the available groundwater resources. On the water demand side, changes in the seasonal pattern have not been estimated globally, and a comprehensive description of groundwater withdrawal in the world is largely lacking.

Lack of seasonal details in existing assessments is the reason that crude annual average measures such as the water scarcity index *Rws* and the Falkenmark's indicator or the "water crowding indicator" $Aw = Q/C$ (*4*), where C is population size, are still being used. Of course, there have been advances in world water resource assessments; projections on the demand side now are based on the Intergovernmental Panel on Climate Change's Special Report on Emissions Scenarios, making them consistent with future climate projections (*18*, *29*, *30*), and uncertainties in the projections of future hydrological cycles are reduced by the use of multimodel ensemble technique (*18*, *31*, *32*).

Figure 3 compares three assessments of the number of people who will live in regions with high water stress until the end of the 21st century (*11*, *18*, *29*, *30*). Even though the projections vary by scenario, their estimates correspond fairly well. Notably, climate change is expected to accelerate the global hydrological cycles, and precipitation will increase on average. Evapotranspiration will not increase as much as precipitation globally because elevated CO_2 concentration induces stomata closure and reduces transpiration (*33*), and river discharge will increase on global scale because of the increased precipitation and the reduced transpiration (*31*, *32*). As a result, the available RFWR is expected to increase at a higher rate than water demand, calculated from population and economic growth. Because of this, the water scarcity index *Rws* and the water crowding indicator *Aw*, both based on annual RFWR, show that water stress will be reduced on a macro scale, except for the A2 scenario, which represents a very heterogeneous world with high population growth. However, the decrease in the number of people under water stress is only marginal and the results should not be viewed too optimistically because they are based on estimates of annual RFWR. Other anticipated impacts of climate change on water resources, such as modification of seasonal variation of available RFWR, degradation of water quality, and associated changes in water resource management, are not taken into account. Furthermore, precipitation will become more intense and intermittent, and the risks of floods and droughts will increase, sometimes in the same region of the world (*34*). These changes in risks are not well considered in current global assessments on future water resource management.

Nevertheless, it is certain that there are people who are already suffering from water shortage today and that any change in the hydrological cycle will demand changes in water resource management, whether the change is caused by global warming or cooling, or by anthropogenic or natural factors. If society is not well prepared for such changes and fails to monitor variations in the hydrological cycle, large numbers of people run the risk of living under water stress or seeing their livelihoods devastated by water-related hazards such as floods.

How Can Hydrological Science Help Solve World Water Issues?

Detailed knowledge of global water resources certainly has been enriched over the 40 years that have passed since the International Hydrological Decade. Water cycles on Earth can now be measured and simulated on finer temporal and spatial scales with detailed models of each hydrological process, and the current and future status of the global water system can be illustrated (Figs. 1 to 3). In contrast to these achievements in studies of the natural hydrological cycles, data about the social aspects of water use are not easily available.

Finally, the future development of hydrology requires improved communication between scientists and policy-makers to ensure that hydrological expertise is translated into actions

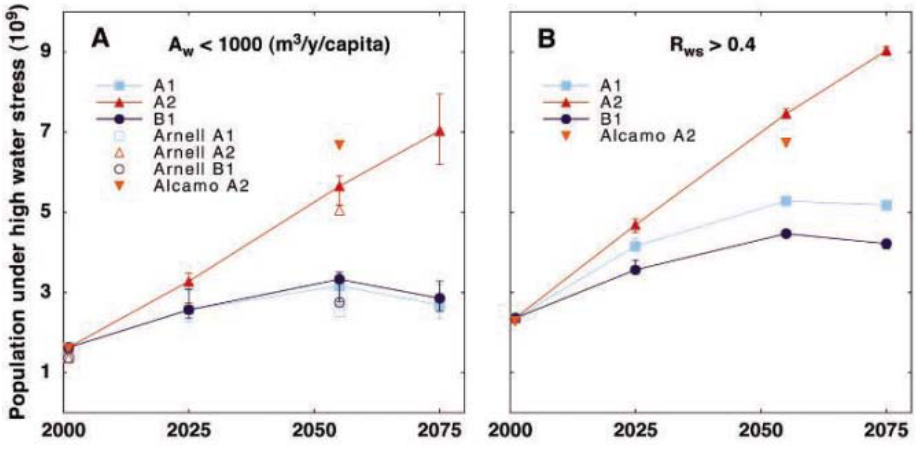

Fig. 3. Current and future projections of population under high water stress under three business-as-usual scenarios of the Intergovernmental Panel on Climate Change's Special Report on Emissions Scenarios. Threshold values are set to be **(A)** the water-crowding indicator $Aw = Q/C < 1000$ m³/year per capita and **(B)** the water scarcity index $Rws = (W - S)/Q > 0.4$, where Q, C, W, and S are renewable freshwater resources (RFWR), population, water withdrawal, and water generated by desalination, respectively. Error bars indicate the maximum and minimum population under high water stress corresponding to the RFWR projected by six climate models. Climatic conditions averaged for 30 years are used for the plots at 2025 (averaged for 2010 to 2039), 2055 (averaged for 2040 to 2069), and 2075 (averaged for 2060 to 2089).

that address water challenges (*35*) and to make sure that scientists understand what kinds of knowledge are required by policy-makers and by society at large.

References and Notes

1. T. Oki, in *Encyclopedia of Hydrological Sciences*, M.G. Anderson, J. McDonnell, Eds. (Wiley, New York, 2005), vol. 1, pp. 13–22.
2. M. W. Rosegrant, C. Ximing, S. A. Cline, *Environment* **45**, 24 (2003).
3. P. A. Dirmeyer *et al.*, *Bull. Am. Meteorol. Soc.*, in press.
4. I. A. Shiklomanov, Ed., *Assessment of Water Resources and Water Availability in the World* (World Meteorological Organization/Stockholm Environment Institute, Geneva, Switzerland, 1997).
5. V. I. Korzun, *World Water Balance and Water Resources of the Earth*, vol. 25 of *Studies and Reports in Hydrology* (UNESCO, Paris, 1978).
6. T. M. Church, *Nature* **380**, 579 (1996).
7. M. Falkenmark, J. Rockstrom, *Balancing Water for Humans and Nature* (Earthscan, London, 2004).
8. S. L. Postel, G. C. Daily, P. R. Ehrlich, *Science* **271**, 785 (1996).
9. C. Nilsson, C. A. Reidy, M. Dynesius, C. Revenga, *Science* **308**, 405 (2005).
10. *World Register of Dams* (International Commission on Large Dams, Paris, 1998).
11. T. Oki *et al.*, *Hydrol. Sci. J.* **46**, 983 (2001).
12. M. I. Lvovitch, *Trans. Am. Geophys. Union* **54**, 28 (1973).
13. F. Baumgartner, E. Reichel, *The World Water Balance: Mean Annual Global, Continental and Maritime Precipitation, Evaporation and Runoff* (Ordenbourg, München, Germany, 1975).
14. C. J. Vörösmarty, P. Green, J. Salisbury, R. B. Lammers, *Science* **289**, 284 (2000).
15. J. Alcamo *et al.*, *Hydrol. Sci. J.* **48**, 339 (2003).
16. P. J. Crutzen, *Nature* **415**, 23 (2002).
17. N. Hanasaki, S. Kanae, T. Oki, *J. Hydrol.* **327**, 22 (2006).
18. N. Utsumi, thesis, The University of Tokyo (2006).
19. J. A. Allan, *Yale Univ. For. Environ. Studies Bull.* **103**, 141 (1998).
20. T. Oki *et al.*, in *Value of Water Research Report Series No. 12*, A. Y. Hoekstra, Ed. (UNESCO-IHE, Delft, Netherlands, 2003), pp. 221–235.
21. A. K. Chapagain, A. Y. Hoekstra, *Value of Water Research Report Series No. 13* (UNESCO-IHE, Delft, Netherlands, 2003).
22. H. Yang, P. Eichert, K. C. Abbaspour, A. B. Zehnder, *Environ. Sci. Technol.* **37**, 3048 (2003).
23. UN Millennium Development Goals (www.un.org/millenniumgoals/index.html).
24. FAOSTAT (http://faostat.fao.org/).
25. *Water Resources in Japan* (Ministry of Land, Infrastructure, and Transport, Tokyo, 2005).
26. P. Gleick, *Science* **302**, 1524 (2003).
27. Intergovermental Panel on Climate Change, *Climate Change, 2001: The Science Basis* (Cambridge Univ. Press, Cambridge, UK, 2001).
28. World Water Day (www.worldwaterday.org/wwday/1998/).
29. J. Alcamo *et al.*, personal communication.
30. N. W. Arnell, *Glob. Environ. Change* **14**, 31 (2004).
31. D. Nohara, A. Kitoh, M. Hosaka, T. Oki, *J. Hydromet.*, in press.
32. P. C. D. Milly, K. A. Dunne, A. V. Vecchia, *Nature* **438**, 347 (2005).
33. N. Gedney *et al.*, *Nature* **439**, 835 (2006).
34. Y. Hirabayashi *et al.*, in preparation.
35. T. Oki, C. Valeo, K. Heal, Eds., *Hydrology 2020: An Integrating Science to Meet World Water Challenges, IAHS Publication 300* (IAHS, Wallingford, UK, 2005).

36. We thank our research group members at Institute of Industrial Science, The University of Tokyo for comments and support, particularly Y. Shen, M. Bengtsson, Y. Agata, H. Kim, and N. Utsumi. We also thank the anonymous reviewers for comments. For financial support, we thank Core Research for Evolutional Science and Technology (CREST), the Japan Science and Technology Agency (JST), the Research Institute for Humanity and Nature (RIHN), the special coordination funds for promoting science and technology by the Japan Cabinet Office, and Global Environment Research Fund (GERF) of the Ministry of the Environment of Japan.

10.1126/science.1128845

REVIEW

The Challenge of Micropollutants in Aquatic Systems

René P. Schwarzenbach,* Beate I. Escher, Kathrin Fenner, Thomas B. Hofstetter, C. Annette Johnson, Urs von Gunten, Bernhard Wehrli

The increasing worldwide contamination of freshwater systems with thousands of industrial and natural chemical compounds is one of the key environmental problems facing humanity. Although most of these compounds are present at low concentrations, many of them raise considerable toxicological concerns, particularly when present as components of complex mixtures. Here we review three scientific challenges in addressing water-quality problems caused by such micropollutants. First, tools to assess the impact of these pollutants on aquatic life and human health must be further developed and refined. Second, cost-effective and appropriate remediation and water-treatment technologies must be explored and implemented. Third, usage and disposal strategies, coupled with the search for environmentally more benign products and processes, should aim to minimize introduction of critical pollutants into the aquatic environment.

About one-fifth of the world's population does not have access to safe water, and two-fifths suffer the consequences of unacceptable sanitary conditions (*1*). Pathogens in water cause more than 2 million deaths annually; most are children under the age of 5. The increasing chemical pollution of surface and groundwaters, with largely unknown long-term effects on aquatic life and on human health, could easily lead to a problem of similar or even greater magnitude. More than one-third of the Earth's accessible renewable freshwater is used for agricultural, industrial, and domestic purposes, and most of these activities lead to water contamination with numerous synthetic and geogenic compounds (Table 1). It therefore comes as no surprise that chemical pollution of natural waters has already become a major public concern in almost all parts of the world.

Industry and municipalities use about 10% of the globally accessible runoff and generate a stream of wastewater, which flows or seeps into rivers, lakes, groundwater, or the coastal seas (*1*). These wastewaters contain numerous chemical compounds in varying concentrations. About 300 million tons of synthetic compounds annually used in industrial and consumer products partially find their way into natural waters (Table 1). Additional pollution comes from diffuse sources from agriculture, where 140 million tons of fertilizers and several million tons of pesticides are applied each year (*2*). In the European Union, for instance, there are more than 100,000 registered chemicals, of which 30,000 to 70,000 are in daily use (EINECS, European Inventory of Existing Chemical Substances). The input of 0.4 million tons of oil and gasoline components through accidental spills represents yet another important source of water pollution. Other notable sources of contamination are the intrusion of salty water into groundwater due to overexploitation of aquifers; the human-driven mobilization of naturally occurring geogenic toxic chemicals, including heavy metals and metalloids (Table 1); and the biological production of toxins and malodorous compounds.

To date, an effective and sustainable global strategy against this insidious and mostly unseen contamination of aquatic environments barely exists. Source controls and technical systems, such as wastewater treatment plants, function as partial barriers, particularly in highly industrialized countries, but major challenges remain. The source, behavior, and treatment of the relatively small number of macropollutants (*3*) such as acids, salts, nutrients, and natural organic matter, occurring at μg/liter to mg/liter concentrations, are relatively well understood: High nutrient loads can lead to increased primary production,

Eawag, Swiss Federal Institute of Aquatic Science and Technology, 8600 Dubendorf, Switzerland, and Institute of Biogeochemistry and Pollutant Dynamics, ETH Zurich, 8092 Zurich, Switzerland.

*To whom correspondence should be addressed. E-mail: rene.schwarzenbach@env.ethz.ch

oxygen depletion, and toxic algal blooms. In such cases, the challenges are to predict ecosystem responses, to optimize treatment technologies, and to develop integrated policies at the scale of river basins (*4*).

It is far more difficult to assess the effect on the aquatic environment of the thousands of synthetic and natural trace contaminants that may be present in water at low to very low concentrations (pg/liter to ng/liter) (*5*, *6*). Table 2 illustrates a range of micropollutants of possible toxicological concern. These chemicals have been found ubiquitously in natural waters in the past 25 years, not only in industrialized areas but also in more remote environments. Some chemicals are not degraded at all (e.g., heavy metals) or only very slowly (e.g., persistent organic pollutants such as DDT, lindane, or polychlorinated biphenyls). They can therefore be transported via water or air to locations hundreds or even thousands of miles away from their source (*7*, *8*). Those compounds that are less persistent and not prone to long-range transport may still be of concern if they are continuously emitted or form problematic (bio)transformation products (*9*, *10*). Examples of this category include hormones and drugs, or persistent degradation products of surfactants such as nonylphenol.

Assessing the impact of micropollutants in aquatic systems is a formidable task requiring improved analytical and modeling tools to probe the distribution, bioavailability, and biological effects of single compounds and of chemical mixtures. Methods to classify existing and new chemicals on the basis of their potential to harm humans and the environment must also be refined. Mitigation technologies to reduce the impact of micropollutants, as well as strategies to minimize their introduction into the environment, require further development. A complementary approach is the advancement of "green" chemistry, which entails design of more environmentally friendly industrial processes and more benign products.

Here we review the scientific challenges in addressing these issues. We frame the concerns primarily from an environmental-protection perspective with a focus on aquatic ecosystems, but without neglecting the human health issues. Protecting natural waters against chemical pollution safeguards aquatic life and thus, directly

Table 1. Dimensions of water problems: water use and macro- and micropollutant fluxes.

Human appropriation of freshwater supply (km^3/year) (4)	
Total global runoff	40,700
Accessible global runoff	12,500
Water withdrawals (total)	4,430
Agriculture	2,880
Industry	975
Municipalities	300
Reservoir losses	275
Fluxes of macropollutants with world rivers (10^6 tons/year) (46)	
Total inorganic nitrogen (~75% anthropogenic)	21
Total phosphorus (60% anthropogenic)	5.6
Anthropogenic inputs of heavy metals to aquatic systems (10^6 tons/year) (47)	
Zn, Cr, Ni, Pb, Cu, Cd, Hg	0.3–1
Anthropogenic fluxes affecting water quality (10^6 tons/year) (2, 48)	
Global fertilizer production (2000)	140
Global pesticide production	5
Synthetic organic chemicals production	300
Oil spills (average 1980–2000)	0.4

Table 2. Examples of ubiquitous water pollutants.

Origin/usage	Class	Selected examples	Related problems	References
Industrial chemicals	Solvents	Tetrachloromethane	Drinking-water contamination	(*49*)
	Intermediates	Methyl-*t*-butylether		
	Petrochemicals	BTEX (benzene, toluene, xylene)		
Industrial products	Additives	Phthalates		(*7*)
	Lubricants	PCBs (polychlorinated biphenyls)	Biomagnification, long-range transport	
	Flame retardants	Polybrominated diphenylethers		(*50*)
Consumer products	Detergents	Nonylphenol ethoxylates	Endocrine active transformation product (nonylphenol)	(*51*)
	Pharmaceuticals	Antibiotics	Bacterial resistance, nontarget effects	(*52*)
	Hormones	Ethinyl estradiol	Feminization of fish	(*12*)
	Personal-care products	Ultraviolet filters	Multitude of (partially unknown) effects	(*53*)
Biocides	Pesticides	DDT	Toxic effects and persistent metabolites	(*11*, *54*)
		Atrazine	Effects on primary producers	(*55*)
	Nonagricultural biocides	Tributyltin	Endocrine effects	(*56*)
		Triclosan	Nontarget effects, persistent degradation product (methyl-triclosan)	(*57*)
Geogenic/ natural chemicals	Heavy metals	Lead, cadmium, mercury		(*47*)
	Inorganics	Arsenic, selenium, fluoride, uranium	Risks for human health	(*37*)
	Taste and odor	Geosmin, methylisoborneol	Drinking-water–quality problems	
	Cyanotoxines	Microcystins		(*58*)
	Human hormones	Estradiol	Feminization of fish	(*59*)
Disinfection/oxidation	Disinfection by-products	Trihalomethanes, haloacetic acids, bromate	Drinking-water–quality, human health problems	(*60*)
Transformation products	Metabolites from all above	Metabolites of perfluorinated compounds	Bioaccumulation despite low hydrophobicity	(*61*)
		Chloroacetanilide herbicide metabolites	Drinking-water–quality problems	(*62*)

or indirectly, human health. Production of drinking water from highly polluted raw water may be technically feasible and even necessary in regions of extreme water scarcity. In general, however, purification is much easier and much more cost-effective if the raw water already meets high quality standards. Additional exposure routes to waterborne pollutants may cause health risks, e.g., direct skin contact or contamination of aquatic food sources (e.g., fish) and agricultural products. Hence, any measures taken to prevent the chemical pollution of surface and groundwater resources will not only improve ecosystem health, but will also benefit both the production of clean water and safe food for human consumption.

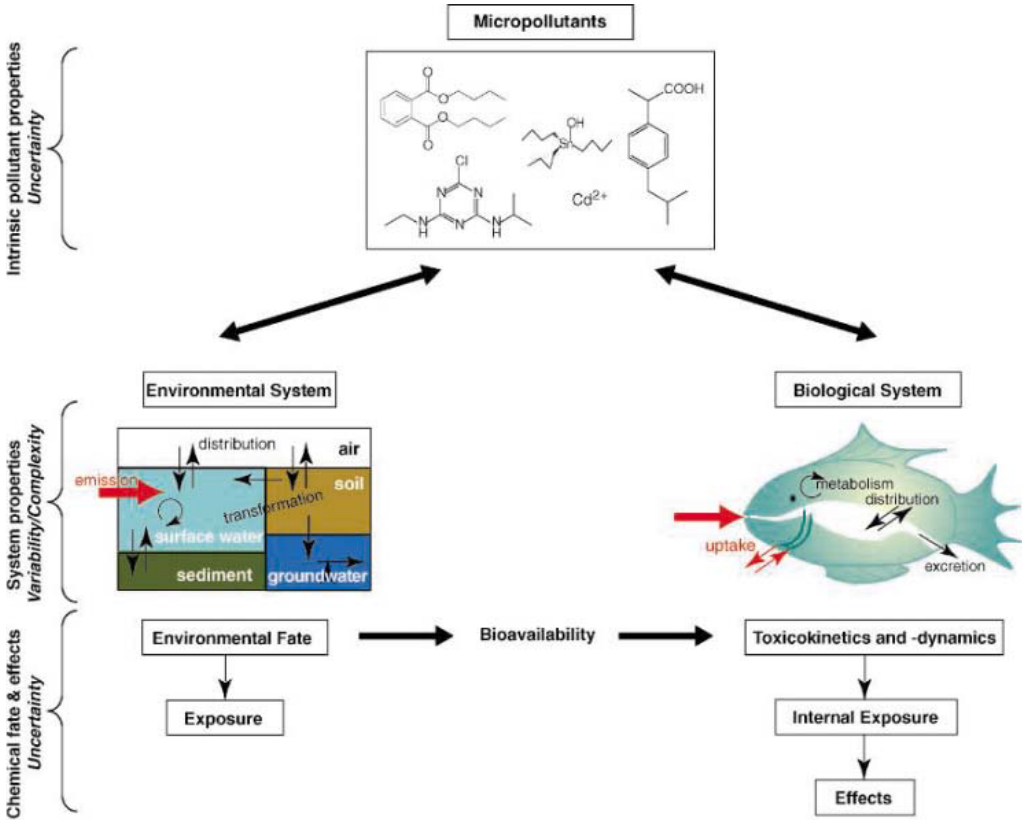

Fig. 1. Consistent exposure and effect assessment is possible if processes in the environmental system and in the organisms (biological system) are treated with the same modeling structure and tools. Within this concept, pollutants interact with environmental and biological systems according to their intrinsic physicochemical properties and reactivities, yielding a characteristic pattern of environmental and internal exposure concentrations for each pollutant. Final exposure and effect assessment according to this concept will always be subject to uncertainty due to inherent variability and complexity of both environmental and biological systems. Quantification and explicit communication of irreducible uncertainties therefore need to be an integral part of exposure and effect assessment.

Assessment of Micropollutants in Aquatic Systems

The assessment of whether or not a particular compound is a pollutant is based upon an understanding of its exposure, i.e., its input, distribution and fate in a defined system, and of the effect(s) that the compound has on organisms, including humans, due to its presence in the system. Figure 1 illustrates the key features and commonalities between exposure and effect assessment. Quantification of the pertinent processes that determine a compound's transport, fate, and effect in aquatic systems is a prerequisite for modeling the risks of new and existing chemicals, for designing mitigation strategies, and for adapting manufacturing practices accordingly.

To date, it has been common practice, in particular in European legislation, to divide the risk assessment of chemicals rather strictly into exposure and effect assessment, even though, particularly on a molecular level, there is considerable overlap. Therefore, a lot of synergy can be realized as research groups specialized in exposure assessment increase their cooperation with colleagues in the field of effect evaluation. Given the enormous complexity of ecosystems, it is not possible to capture in detail every process related to the behavior of micropollutants. Relevant processes must be described at an appropriate level of complexity to provide appropriate answers to the questions asked. The level of complexity may vary from case to case, but the goal is to make a model as simple as possible and as comprehensive as necessary for the problem in hand.

Exposure assessment in the (aquatic) environment has hinged primarily on analytical measurements of single chemical compounds or of bulk parameters (e.g., total organic halogens) in samples from various environmental compartments—water, sediments, soils, air (*11*)—as well as from organisms of different trophic levels within a food chain (*12*). Such measurements provide important information on the temporal and spatial extent of pollution by known chemicals and can also uncover unexpected contamination (see examples and references in Table 2). However, such phenomenological inventories are of limited value, because they usually do not allow one to draw any generalizable conclusions on the compound's behavior in the environment. Pertinent compound- and system-specific properties and reactivities such as adsorption to solid phases, partitioning between solid and aqueous phases, or the formation of complexes in solution, as well as of abiotic and biological transformations, need to be understood and quantified. Such molecular insights are a prerequisite for reliable exposure assessments of chemical compounds in complex macroscopic systems.

In recent years, much progress has been made in the description of complexation and phase-transfer processes of inorganic and organic micropollutants at the molecular level (*13*, *14*). These new approaches place the great variability of compound and system properties in a much more unified and thus generalizable context. However, there are still many gaps to fill, for example, regarding the compound properties of polar as well as ionizable organic chemicals and of those with a high number of functional groups. Previous research focused mainly on apolar and monopolar compounds like PCBs (polychlorinated biphenyls), PAHs (polycyclic aromatic hydrocarbons), chlorinated solvents, or chlorinated pesticides like DDT or lindane. The modern polyfunctional and often ionizable pesticides, biocides, drugs, and personal-care products, to which attention has more recently turned, require more sophisticated models that additionally account for specific complexation or ionic interactions with other reactants. In addition, the physical form of pollutant (dissolved, colloidal, or particulate) will influence

fate and effect. Manufactured nanomaterials are well-known chemicals in a new dress, i.e., in a physical state that completely changes their fate and behavior. They were initially only considered to be relevant air pollutants, but more recently their potential hazard in aquatic systems has resulted in manifold research initiatives (*15*).

The current primary challenge in assessing and predicting transformation of micropollutants is presented by the biologically mediated class of reactions. In part, this situation stems from the intrinsic difficulty of classifying and quantifying biological activity in complex macroscopic systems. Moreover, in contrast to the models for describing homogeneous chemical and photochemical processes in aquatic systems (*13*), the treatment of enzymatic and surface-mediated reactions is still in its infancy. Hence, future research should be directed more intensively toward developing tools for assessing (bio)transformation processes in environmental settings and toward improving predictive models for biodegradability on the basis of structural information (*16*).

With respect to effect assessment, there is an even greater need for more fundamental approaches that are based on explanatory principles, obtained by investigating the underlying responsible molecular mechanisms instead of comparing empirical data from descriptive studies (*17*). Traditionally, the (eco)toxicity of a given pollutant is determined by standardized tests, with the use of selected model organisms and toxicity endpoints, such as acute toxicity or lethality in algae, daphnia, and fish (*18*). In such standard tests, the effect is related to exposure concentrations in the surrounding medium (water, sediment, or food) and bioavailability. The uptake and the internal concentrations in the organism are often not known, although the concentration at the target site corresponds to the biologically effective dose. The toxicokinetic processes of uptake, internal distribution, metabolism, and excretion (Fig. 1) relate the concentrations at the target site to external exposure. Often it is too tedious or not possible to quantify this cascade of processes. Total internal concentrations can be used in many cases as a surrogate parameter to better assess the observed effects (*19*, *20*).

There are three main modes of toxic action: baseline toxicity, receptor-mediated, and reactive mechanisms (*21*). Baseline toxicity is caused by a nonspecific disturbance of the structure and functioning of biological membranes. Internal effective membrane concentrations of baseline toxicants are constant and independent of the biological species and the type of molecule (*19*, *20*). Thus, much of the apparent biological variability can be resolved if toxicity studies are approached on a mechanistic level. Even for receptor-mediated and reactive mechanisms, a differentiation between the internal concentrations and the intrinsic potency at the target site can help to derive general principles and understand differences in species sensitivity (*21*).

In the environment, organisms (including humans) are exposed not only to isolated micropollutants but to complex chemical mixtures, the individual components of which might be present at concentrations too low to raise concern. However, additive or even synergistic effects can render such mixtures dangerously potent. For example, a recent study has shown that when five estrogenic compounds are mixed in concentrations all below levels at which their individual effects can be detected, their cumulative impact on fish was detrimental (*22*). It was long assumed that only compounds with the same mode of toxic action are concentration-additive in mixtures, but recent research has shown that even mixtures of compounds with different modes of action may cause nonnegligible effects (*23*). These and related findings have shifted the research focus from searches for synergistic effects, which are spectacular but less common, to systematic investigations of mixture effects of noninteracting compounds. Various mixture toxicity concepts have evolved for mixtures of compounds with the same mode of toxic action and for those that act at different target sites (*21*, *23*). These mixture concepts are increasingly being applied in risk assessment of chemical mixtures. For example, Switzerland is currently developing water-quality criteria that include additive effects for mixtures of pesticides in surface waters (*24*).

The mutual interaction of thousands of chemicals in the environment with millions of biological species will ultimately determine whether a given pollutant (mixture) leads to marginal or catastrophic ecological consequences. Nonchemical stressors, such as temperature or ultraviolet light, may further modulate observed ecotoxicological effects (*25*). Clearly, classification rules are necessary to reduce such complexity. Categorizing pollutants according to their primary interactions with biomolecules provides a basis for assigning primary mechanisms of toxicity and resulting modes of toxic action (*21*). The mechanistic bases for toxicity are also steadily emerging from genomics, proteomics, and metabonomics studies (*26*). The genome of a number of classical ecotoxicological model organisms has been sequenced, and some gene chips are already commercially available, facilitating the application of the genomic techniques in environmental applications (*27*). Changes in gene expression profiles, modified protein levels, and alterations in the metabolome upon the exposure to a micropollutant yield valuable information on the mode(s) of toxic action. The challenge is to interpret the wealth of data obtained with the omics techniques and to link the molecular and biochemical effects to in vivo effects and exposure conditions. At present, there is belief that these techniques are a great tool for research and for prioritizing further testing but that they cannot be applied as stand-alone tools in environmental risk assessment. Further limits are that they cannot describe complex interactions in ecosystems, a field that is addressed by stress ecology (*28*).

Mitigation of Aqueous Micropollutants

There is an increasing need for more powerful strategies to mitigate water contamination because industrial chemical use and demand for clean water is steadily rising. On the one hand, these strategies have to aim at reducing the use of critical chemicals and thus their introduction into the environment. On the other hand, they have to focus on the treatment of existing contamination by more efficient and cost-effective methods. The latter case includes both the containment and the remediation of contaminated sites, as well as the treatment of wastewaters and raw waters for human consumption.

Most contaminated sites are rather complex, heterogeneous systems. Consequently, often too little system knowledge is available to apply any remediation technique in an optimal way. It therefore comes as no surprise that more than two decades of research and application of remediation approaches have not shown the expected success. Traditional approaches such as pump-and-treat have turned out to be rather inefficient in that they require active treatment times of several years. Thus, they are economically unfeasible, particularly when considering the vast number of sites with a potential to cause substantial water contamination. Hence, strategies focusing on microbial or abiotic degradation in situ, or natural attenuation, have to be considered as long-term treatment options. This means that processes determining the transport and the transformation behavior of a given micropollutant and of its transformation products must be understood and quantified in detail. Such knowledge forms the basis for sound decisions on whether to leave a contaminated site without any measures or whether additional engineering actions are necessary. Such actions include, for example, enhancing microbial activity by adding appropriate electron donors or acceptors to the system (*29*), or introducing abiotic reactants into contaminated groundwaters such as zero-valent metals in permeable reactive barriers (*30*).

Mitigation of organic micropollutants should be based on knowledge of the mineralization pathways to stable and nontoxic products and their reaction rates. For inorganic micropollutants such as heavy metals, processes that lead to immobilization as insoluble or matrix-bound species need to be identified and quantified. Many of these processes have been studied extensively in laboratory model systems mimicking natural attenuation, and information on rates and products of degradation pathways is available. However, the major challenge is to transfer this

knowledge for the assessment of long-term treatment options to contaminated soils or groundwaters. Because degradation of persistent micropollutants requires the presence of relevant microbial communities and the expression of appropriate enzymes, prediction of in situ rates of microbial attenuation pathways is extremely difficult. To this end, new strategies for monitoring, manipulating, and predicting microbial processes are being developed on the basis of molecular biological methods to identify active microbial communities (*31*) or with stable-isotope techniques, which can be applied to identify and quantify in situ micropollutant transformations (*32*).

In contrast to remediation of contaminated sites, end-of-pipe pollutant mitigation by wastewater and drinking-water treatment has to occur at much shorter time scales of minutes to days. Furthermore, micropollutants are commonly present in much lower concentrations. Therefore, highly selective and rapid reactions have been designed to remove micropollutants in the presence of organic and inorganic matrices that are a thousand- to a million-fold more abundant than the target chemicals. To date, there are a number of fairly standardized unit processes (e.g., chemical and biological oxidation, adsorption, sedimentation, filtration) available to mitigate micropollutants in water treatment by transformation or removal by physical methods, including adsorption and filtration. To allow treatment of large quantities of water per unit time (thousands of m^3/hour), these processes use very reactive oxidants including ozone, OH radicals, chlorine, chlorine dioxide, or permanganate (*33*); high-capacity adsorbents such as activated carbon; or efficient filters such as synthetic membranes.

A major future challenge in wastewater and drinking-water treatment is to improve existing unit processes and to design new ones to remove a large number of chemically very different micropollutants in a broad range of water matrices. For wastewater treatment, this implies optimization of conventional processes for removal of compounds like pharmaceuticals through adsorption and biodegradation in activated sludge treatment (*34*) or using ozone to eliminate, for example, estrogenic compounds (*35*).

For drinking-water treatment, complete mineralization is often not feasible. Therefore, the assessment of reaction products and oxidation by-products, which result from the oxidation of matrix components, e.g., bromate from bromide (*33*), is an important additional challenge. The kinetics and mechanisms of by-product formation need to be investigated in more detail because their toxicity, biological activity, and degradability relative to their precursor are usually not known. Persistent micropollutants can be removed by membrane filtration (nanofiltration and reverse osmosis) or activated carbon (*36*). However, depending on operation time, the adsorption or retention capacity of both approaches decreases due to interference with natural organic matter; in addition, biofouling can lead to clogging of filters. For their successful application, both approaches need improved regeneration strategies, which avoid decreasing their performance and redischarging micropollutants into the environment.

A fundamentally different problem is encountered when there is a widespread occurrence of micropollutants of geogenic origin—for example, selenium, arsenic, or fluoride—in groundwater aquifers of rural areas of developing countries. In this situation, small-scale, household-based removal techniques are often the only possible mitigation strategy due to the lack of a centralized infrastructure. Geogenic micropollutants are found in increased concentrations because their content in some geological formations is elevated and because they are negatively charged and therefore bind weakly to aquifer material under neutral and slightly alkaline pH conditions. In the case of arsenic, it is the anoxic conditions that release reduced arsenic species into groundwaters (*31*). More than 100 million people worldwide drink water with fluoride concentrations exceeding the World Health Organization (WHO) guideline value of 1.5 mg/liter, above which dental or crippling skeletal fluorosis (*37*) can occur; a similar number of people in Southeast Asia (notably Bangladesh) and Southern and Central America drink water with arsenic concentrations above the WHO limit (10 μg/liter), putting them at risk of dermal lesions, cardiovascular damage, or skin cancer (*38*). Meeting the WHO guideline of 10 μg of arsenic per liter is a major drinking-water challenge worldwide for both geochemists and process engineers (*39*). Photochemical oxidation (*40*) or co-oxidation with either Fe(II) or zerovalent-iron (*41*) and subsequent coprecipitation with Fe oxides (or hydroxides) removes arsenic. To date, however, neither approach is reliable, inexpensive, or simple to use. Therefore, none is yet suited for use in developing countries. Currently, the only solution is the monitoring of water resources to identify safe sources of drinking water. In this situation, the challenge is to develop reliable, affordable, and simple field equipment that local inhabitants with little training could use for monitoring. Because many countries are not in the position to monitor their water, it is imperative that scientists further their understanding of the geochemical, geological, climatologic, and land-use factors underlying geogenic contamination of groundwater. Progress will likely come from combining process knowledge with geographic information from remote sensing and other sources to provide better spatial predictions of areas at risk.

Preventive Management of Water Quality

Despite advances in water treatment, a precautionary approach toward water and chemical management—one that reduces introduction of problematic chemicals into the environment in the first place—should be given a high priority for reducing risks to human health and ecosystem integrity.

For this purpose, the tools of "green" or sustainable chemistry are essential. Efficiency engineering of chemical production processes aim to reduce material flows and replace hazardous auxiliary materials (*42*). Prospective chemical risk assessment is mostly used in the context of market authorization, but it also allows for proactive approaches in designing new, more environmentally benign chemical compounds (*43*). The assessment must typically rely on limited, basic information about a compound such as its molecular structure and a few physicochemical properties. The development of sound, mechanistically based quantitative structure-activity relationships is therefore an important task, albeit a challenging one given the multitude of chemical structures. One elegant approach is to design new compounds that contain only natural building blocks, connected by linkages known to be readily cleaved enzymatically. This "benign by design" strategy has, for example, been realized by industry to replace persistent textile auxiliaries used as dispersing agents (*43*).

Once a chemical is in use, contamination of water resources should be avoided to the largest extent possible. Intensive agriculture in the developed world, for instance, is a major cause of diffuse water pollution leading to eutrophication and contamination of surface and groundwater resources with pesticides and veterinary medicines. Field studies have shown that various, spatially highly heterogeneous factors such as soil type, presence or absence of drainage systems, and local topography strongly influence the tendency of a given agricultural area to release pesticides into surface waters through fast-flow processes such as runoff or drainage (*44*). Knowledge of these governing factors is a prerequisite for optimizing management practices at a field or regional level; the next scientific challenge lies in developing the capacity to identify problematic areas by using available geo-referenced information, and in using this information to adapt agrochemical use.

In developing countries, in contrast, the nature of pesticide use and the mitigation options for related problems are quite different. Surveys carried out in Central America, Brazil, and Nigeria reveal acute dangers of direct pesticide poisoning of humans, due to mishandling of equipment and overuse of pesticides through ignorance of the relevant hazards (*45*). Consequently, pesticide concentrations in surface and groundwaters are estimated to be high, but virtually no monitoring data are available. Beyond implementing training and information programs for the farmers, alleviation of this problem also requires identification of those pesticides least likely to be problematic under local conditions. Scientifically, this task requires defining environmental risk-assessment protocols appropriate

for the specific social and ecological conditions encountered in tropical regions (e.g., history and conditions of tropical soils influencing chemical reactivity and partitioning behavior). There is also a need on the part of regulatory authorities to enforce substance bans more strictly. Currently, large quantities of the pesticides used in such poorer regions may not even be authorized for use but can be bought on the black market (*45*).

Outlook

Scientific progress in aquatic micropollutant management clearly depends on interdisciplinary collaboration. Chemists and biologists must work together to harness the potential of new screening techniques for assessing the environmental impact of micropollutants; environmental chemists and engineers must strive to develop synergies between pathogen removal and the oxidation of micropollutants in water-treatment technologies. Furthermore, given the importance of chemicals in modern societies, sustainable solutions can only be found through active involvement of all stakeholders, including consumers, chemical manufacturers, politicians, and public authorities. This cooperation requires that pertinent topics in environmental chemistry, toxicology, and engineering be accorded a more prominent status in future curricula in chemistry, engineering, and the life sciences. With this article we hope to increase awareness of the urgency and global scale of the water-quality problems arising from micropollutants.

References and Notes

1. United Nations Educational, Scientific, and Cultural Organization, World Water Assessment Programme, *Water for People, Water for Life—the United Nations World Water Development Report* (Berghahn Books, Barcelona, 2003).
2. FAO, Statistical Database, http://faostat.fao.org/ (Food and Agriculture Organization of the United Nations, Rome, 2006).
3. M. Mengis, R. Gachter, B. Wehrli, S. Bernasconi, *Limnol. Oceanogr.* **42**, 1530 (1997).
4. R. B. Jackson *et al.*, *Ecol. Appl.* **11**, 1027 (2001).
5. S. Jobling, M. Nolan, C. R. Tyler, G. Brighty, J. P. Sumpter, *Environ. Sci. Technol.* **32**, 2498 (1998).
6. T. Ohe, T. Watanabe, K. Wakabayashi, *Mutat. Res. Rev. Mutat. Res.* **567**, 109 (2004).
7. R. W. Macdonald *et al.*, *Sci. Total Environ.* **254**, 93 (2000).
8. K. Fenner *et al.*, *Environ. Sci. Technol.* **39**, 1932 (2005).
9. M. H. A. Kester *et al.*, *Endocrinology* **141**, 1897 (2000).
10. A. B. A. Boxall, C. J. Sinclair, K. Fenner, D. Kolpin, S. J. Maud, *Environ. Sci. Technol.* **38**, 368A (2004).
11. H. Iwata, S. Tanabe, N. Sakai, A. Nishimura, R. Tatsukawa, *Environ. Pollut.* **85**, 15 (1994).
12. H. Geyer *et al.*, in *The Handbook of Environmental Chemistry*, B. Beek, Ed. (Springer, Berlin, 2000), vol. 2J, pp. 1–166.
13. R. P. Schwarzenbach, P. M. Gschwend, D. M. Imboden, *Environmental Organic Chemistry* (Wiley, New York, ed. 2, 2003).
14. K. U. Goss, *Crit. Rev. Environ. Sci. Technol.* **34**, 339 (2004).
15. M. R. Wiesner, G. V. Lowry, P. Alvarez, D. Dionysiou, P. Biswas, *Environ. Sci. Technol.* **40**, 4336 (2006).
16. D. Aronson, R. S. Boethling, P. H. Howard, W. Stiteler, *Chemosphere* **63**, 1953 (2006).
17. J. L. M. Hermens, G. T. Ankley, J. P. Sumpter, *Environ. Sci. Technol.* **38**, 446A (2004).
18. G. Rand, *Fundamentals of Aquatic Toxicology: Effects, Environmental Fate and Risk Assessment* (Taylor & Francis, Washington, DC, ed. 2, 1995), pp. 3–67.
19. L. S. McCarty, D. Mackay, *Environ. Sci. Technol.* **27**, 1719 (1993).
20. B. I. Escher, J. L. M. Hermens, *Environ. Sci. Technol.* **38**, 455A (2004).
21. B. I. Escher, J. L. M. Hermens, *Environ. Sci. Technol.* **36**, 4201 (2002).
22. J. V. Brian *et al.*, *Environ. Health Perspect.* **113**, 721 (2005).
23. R. Altenburger, H. Walter, M. Grote, *Environ. Sci. Technol.* **38**, 6353 (2004).
24. N. Chevre *et al.*, *Environ. Sci. Technol.* **40**, 426 (2006).
25. E. H. W. Heugens, A. J. Hendriks, T. Dekker, N. M. van Straalen, W. Admiraal, *Crit. Rev. Toxicol.* **31**, 247 (2001).
26. A. L. Miracle, G. T. Ankley, *Reprod. Toxicol.* **19**, 321 (2005).
27. T. Lettieri, *Environ. Health Perspect.* **114**, 4 (2006).
28. N. Van Straalen, *Environ. Sci. Technol.* **37**, 324A (2003).
29. D. W. Major *et al.*, *Environ. Sci. Technol.* **36**, 5106 (2002).
30. S. F. O'Hannesin, R. W. Gillham, *Ground Water* **36**, 164 (1998).
31. S. A. Pombo, J. Kleikemper, M. H. Schroth, J. Zeyer, *FEMS Microbiol. Ecol.* **51**, 197 (2005).
32. M. Elsner, L. Zwank, D. Hunkeler, R. P. Schwarzenbach, *Environ. Sci. Technol.* **39**, 6896 (2005).
33. U. von Gunten, *Water Res.* **37**, 1443 (2003).
34. A. Joss, *Water Res.* **39**, 4585 (2005).
35. M. M. Huber *et al.*, *Environ. Sci. Technol.* **39**, 4290 (2005).
36. L. D. Nghiem, A. I. Schafer, M. Elimelech, *Environ. Sci. Technol.* **39**, 7698 (2005).
37. WHO, *Guidelines for Drinking-Water Quality* (World Health Organization, Geneva, 2004).
38. P. L. Smedley, D. G. Kinniburgh, *Appl. Geochem.* **17**, 517 (2002).
39. M. Berg *et al.*, *Environ. Sci. Technol.* **35**, 2621 (2001).
40. S. J. Hug, L. Canonica, M. Wegelin, D. Gechter, U. von Gunten, *Environ. Sci. Technol.* **35**, 2114 (2001).
41. C. Su, R. W. Puls, *Environ. Sci. Technol.* **35**, 1487 (2001).
42. W. McDonough, M. Braungart, P. T. Anastas, J. B. Zimmerman, *Environ. Sci. Technol.* **37**, 434A (2003).
43. P. G. Rieger *et al.*, *J. Biotechnol.* **94**, 101 (2002).
44. C. Leu, H. Singer, C. Stamm, S. R. Muller, R. P. Schwarzenbach, *Environ. Sci. Technol.* **38**, 3835 (2004).
45. A. V. Waichman, J. Römbke, M. O. A. Ribeiro, N. C. S. Nina, *Environ. Sci. Pollut. Res.* **9**, 423 (2002).
46. R. E. Turner, N. N. Rabalais, D. Justic, Q. Dortch, *Biogeochemistry* **64**, 297 (2003).
47. J. O. Nriagu, J. M. Pacyna, *Nature* **333**, 134 (1988).
48. A. P. McGinn, in *State of the World 2002* (Worldwatch Institute, Norton, New York, 2002).
49. ECETOC, "Monitoring and modelling of industrial organic chemicals, with particular reference to aquatic risk assessment," *Tech. Report No. 990317* (European Centre for Ecotoxicology and Toxicology of Chemicals, Brussels, Belgium, 1999).
50. P. Eriksson, E. Jakobsson, A. Fredriksson, *Environ. Health Perspect.* **109**, 903 (2001).
51. M. Ahel, W. Giger, M. Koch, *Water Res.* **28**, 1131 (1994).
52. D. W. Kolpin, E. T. Furlong, M. T. Meyer, E. M. Thurman, S. D. Zaugg, *Environ. Sci. Technol.* **36**, 1202 (2002).
53. C. Daughton, T. Ternes, *Environ. Health Perspect.* **107** (suppl. 6), 907 (1999).
54. A. Bignert *et al.*, *Environ. Pollut.* **99**, 177 (1998).
55. K. R. Solomon *et al.*, *Environ. Toxicol. Chem.* **15**, 31 (1996).
56. S. Tanabe, *Mar. Pollut. Bull.* **39**, 62 (1999).
57. A. Lindstrom *et al.*, *Environ. Sci. Technol.* **36**, 2322 (2002).
58. C. Svrcek, D. W. Smith, *J. Environ. Eng. Sci.* **3**, 155 (2004).
59. R. I. L. Eggen *et al.*, *Pure Appl. Chem.* **75**, 2445 (2003).
60. S. D. Richardson, J. E. Simmons, G. Rice, *Environ. Sci. Technol.* **36**, 198A (2002).
61. J. W. Martin, D. M. Whittle, D. C. G. Muir, S. A. Mabury, *Environ. Sci. Technol.* **38**, 5379 (2004).
62. M. L. Hladik, J. J. Hsiao, A. L. Roberts, *Environ. Sci. Technol.* **39**, 6561 (2005).

63. We thank Eawag, ETH Zurich, and the Swiss National Science Foundation for continuous support of our work.

10.1126/science.1127291

PERSPECTIVE

Waterborne Infectious Diseases—Could They Be Consigned to History?

Alan Fenwick

The development of water resources, particularly in Africa, has changed the face of the continent, opening up land for agriculture, providing electric power, encouraging settlements adjacent to water bodies, and bringing prosperity to poor people. Unfortunately, the created or altered water bodies provide ideal conditions for the transmission of waterborne diseases and a favorable habitat for intermediate hosts of tropical parasitic infections that cause disease and suffering. The recent progress in control of these waterborne and vector-borne diseases, such as guinea worm, schistosomiasis, lymphatic filariasis, and onchocerciasis, suggests that many of them could be controlled effectively by 2015, which is the target for reaching the Millennium Development Goals. Donations of safe and effective drugs by several pharmaceutical companies, funds for delivering these donated drugs from foundations and bilateral donors, and effective global health partnerships should make these diseases history.

About 15% of the world's population lives in areas of water stress. Many people struggle to obtain access to enough water to drink, keep clean, and meet their other needs to live. Two and a half billion people (more than a third of the world's population) have no access to improved sanitation, and more than 1.5 million children die each year from diarrheal disease (*1*). In rural areas, particularly in Africa, the same water that is

essential to life may be the cause of infections that lead to suffering, chronic disability, and death. A clean, treated water supply to each house may be the norm in the West, but in developing countries, especially in rural Africa, access to both clean water and sanitation are rare, and waterborne infections are commonplace. Ironically, in developing countries, plentiful permanent surface water—including rivers, streams, lakes, dams, and irrigation schemes—exacerbates the risk of waterborne diseases (*2*, *3*), which infect millions (Table 1). One of the earliest water schemes in Africa provides a case study showing how a network of damaging health consequences can develop alongside water resource development.

The Sennar Dam and the Gezira Scheme in Sudan

The first major dam across one of Africa's great rivers (the Blue Nile) was proposed in 1911 to provide electricity and gravity-fed irrigation to 1 million feddans (1 feddan = 1.04 acres) of flat land between the Blue and White Niles to the south of Khartoum in Sudan. The ''Gezira Scheme'' was completed in 1924 and was so commercially successful that it was doubled in size in the 1940s and 1950s with construction of the Managil Extension. The main crops were cotton (on 25% of the land), wheat, groundnuts, and vegetables. In 1914, when construction started, Egyptian labor was imported to hand-dig the canals. The schistosome life cycle (through a snail intermediate host; Fig. 1) had only recently been fully determined, but "bilharzia" was recognized as a scourge of agricultural workers in Egypt (*4*). Steps were therefore taken to screen the Egyptian workers imported to build the Gezira Scheme canals, and individuals diagnosed as infected were treated with tartar-emetic (potassium antimony tartrate) before they were allowed to enter Sudan for employment (*5*). For 80 years, the Gezira scheme has produced fine cotton and cash crops and has been responsible for the prosperity of farmers and agricultural laborers, but also, despite the attempts at public health, for widespread infection with malaria and schistosomiasis. Although there were intermittent attempts to confront both diseases with vector control and treatment, they only increased in severity as the canals matured, became infested with weeds, and supported more and more mosquitoes and snails (*6*, *7*). The Gezira scheme was the subject of the first integrated disease-control program, which ran from 1978 to 1990 as the Blue Nile Health Project (BNHP), combining provisions of clean water and latrines with annual house spraying against mosquitoes, snail control using molluscicides, and (when it became available) praziquantel for treatment against schistosomiasis (*8*, *9*). The high cost of praziquantel meant that regular retreatment was not sustainable and treatment stopped when BNHP closed in 1990. Nevertheless, the positive effect of treatment was still apparent several years later when Homeida *et al.* (1988) found less liver disease than would have been expected (*10*). The infection history of the residents of the Gezira scheme shows how water development and disease are closely linked, and throughout the 20th century, several similar examples have emerged of disease outbreaks linked to water resource management (*11*). The High Dam on the Nile at Aswan (1960), later dams on the Senegal and Volta rivers, and a multitude of small dams and irrigation projects have all caused spectacular increases in schistosomiasis, malaria, and other waterborne diseases (Fig. 1) in upstream lakes and downstream irrigated areas (*12*, *13*). In 2006, the three gorges dam in China is about to produce a similar environmental change that may lead to the return of schistosomiasis as a major public health problem in areas served by the dam (*14*).

Waterborne Diseases

During the second half of the 20th century, increased prevalence of water-related diseases became an inevitable consequence of development projects that promoted transmission of several classes of disease. First, fecal contamination of water and subsequent ingestion of pathogens resulted in cholera, diarrhea, and guinea worm infestation. Second, infections by snail-borne trematodes, primarily schistosomiasis (blood fluke), were acquired passively during water contact. Third, some parasites were transmitted by vectors that breed in water, such as malaria, onchocerciasis, and lymphatic filariasis. A related problem exists in Asia, where foodborne trematodes (e.g., *Paragonimus* and *Clonorchis*) are acquired from eating uncooked fish. Unfortunately, during the 20th century, when many water development projects were initiated, prevention and treatment for most of these diseases were not readily available and were in any case too expensive for those in need of treatment; for many of these diseases, this still remains the case.

In all, diarrheal diseases caused by over 20 viral, bacterial, and parasitic infections are responsible for 2 to 2.5 million deaths annually. Transmission commonly results from fecal contamination of drinking water but can be reduced by clean (filtered) water supplies and sanitation; better advocacy, particularly to mothers; and availability of oral rehydration salt therapy (*15*).

Table 1. Prevalence of seven water-related diseases in Africa.

Condition	Cases in Africa (ref.)
Hookworm	198 million (*37*)
Ascariasis	173 million (*37*)
Schistosomiasis	166 million (*38*)
Trichuriasis	162 million (*37*)
Lymphatic filariasis	46 million (*39*)
Onchocerciasis	18 million (*30*)
Dracunculiasis	<0.1 million (*16*)

Guinea Worm—Close to Eradication

Guinea worm, which has caused untold misery in infected people and has had major socioeconomic consequences because of the suffering and incapacity, could at last be close to eradication (*16*). Infection is acquired when water fleas (*Cyclops* sp.), the intermediate host harboring the encysted larval stages of the guinea worm (*Dracunculus hominis*), are ingested by people drinking unfiltered water from canals, pools, and wells (Fig. 1). In time, adult worms develop, usually under the skin of the legs, and can grow to 1 m in length. When mature and gravid, the worm ulcerates the skin and protrudes to release larvae into water, in a painful and disabling process. The cycle is completed when *Cyclops* ingest the larvae. The only way to remove the adult worm from inside the host is to extract it slowly from the body by winding it around a stick. If the worm is broken or dies, the resulting inflammation and secondary infection can be further disabling. There is no treatment for the worm, but eradication attempts are close to success because of effective advocacy, concerted improvements to clean water supplies, and the use of larvicides, resulting in fewer people ingesting *Cyclops*, and with time fewer infected people contaminating the environment. Fortunately, there is no animal reservoir. In 1995, more than 125,000 cases of guinea worm (50% of which were from Sudan) were reported to the World Health Organization (WHO) from 20 countries, but in 2004, fewer than 16,000 cases (45% from Sudan and 45% from Ghana) remained. If the peace declared in Southern Sudan holds, eradication could be imminent, thanks to the joint efforts of the Carter Center and WHO in providing health education and filters for water. Nigeria, which was a long-time member of the ''big three'' disease-endemic countries, along with Sudan and Ghana, has continued to expand the areas of the country that are free of guinea worm. In 1995, Nigeria reported 16,374 cases, but by 2004, Nigeria was third in the world with just 495 reported cases from 85 villages (*17*).

Department of Infectious Disease Epidemiology, Imperial College, London WC2 1PG, UK. E-mail: a.fenwick@imperial.ac.uk

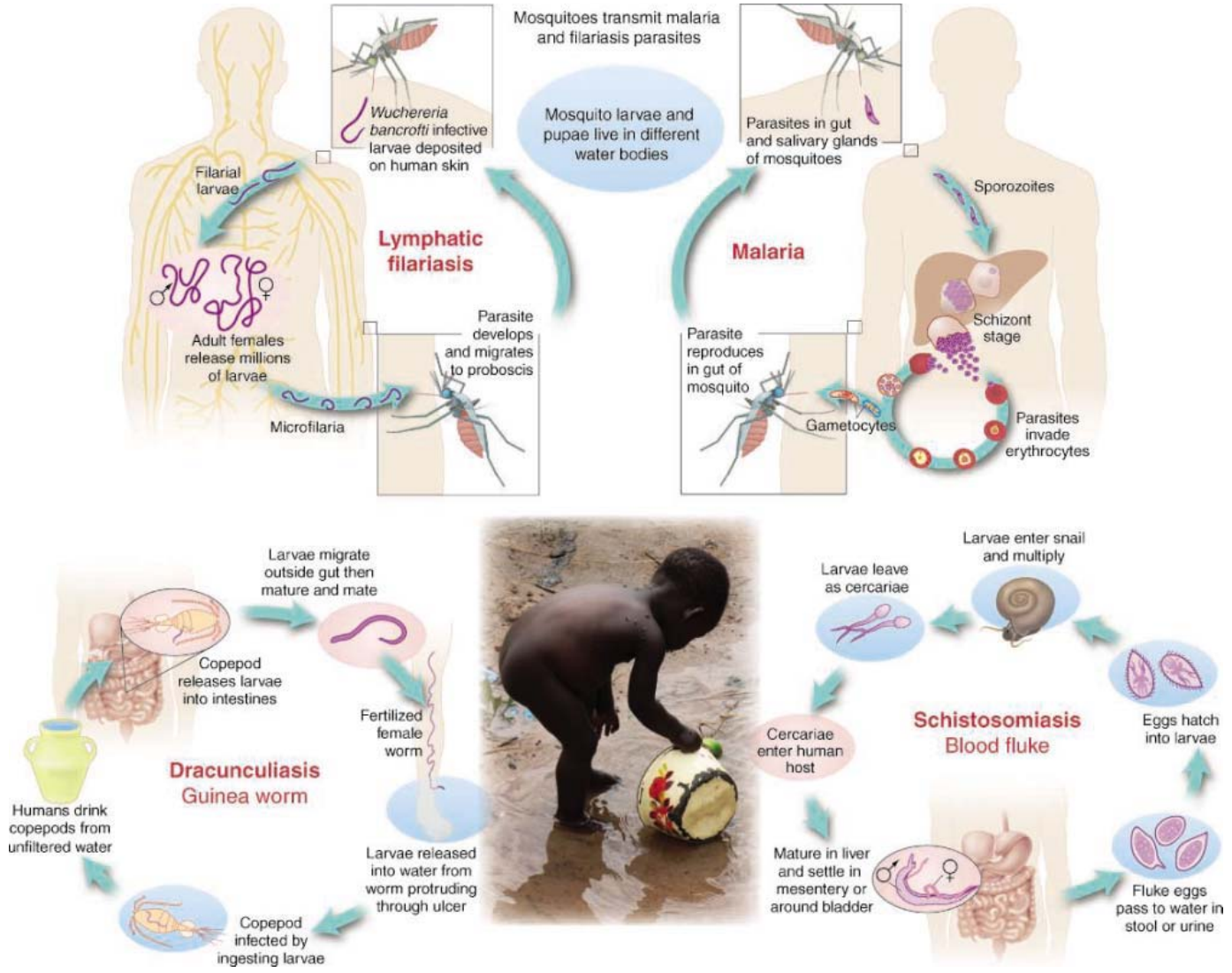

Fig. 1. Simplified life cycles for representative waterborne parasitic diseases commonly affecting humans in association with water development schemes.

Schistosomiasis (Bilharzia)

The life cycle of schistosomiasis requires a human host to harbor the adult worm and a freshwater snail to serve as intermediate host (Fig. 1). In fresh water, schistosome larvae hatch from eggs passed out in the stool or urine and invade the intermediate snail hosts, in which they develop asexually over about 6 weeks into stages infective to humans. These cercariae are then released into the water, where they can infect children playing in the water; women collecting water or engaging in domestic chores; and men swimming, fishing, and irrigating crops. Water development projects, and the consequent concentrations of human settlements and increased water contact, lead to heavy worm infections in people, more eggs reaching the water, and greater human pathology: a man-made vicious cycle. The consequences of *Schistosoma mansoni* are severe; the disease manifests as anemia, malnourishment, and stunted growth in children, and in later life it affects the liver and causes fibrosis, portal hypertension, ascites, and hematemesis (esophageal bleeding that is usually fatal). Those infected with *Schistosoma haematobium* present with blood in urine, and in the longer term they suffer from bladder calcification, kidney damage, and bladder cancer. Women may suffer acutely from genital schistosomiasis (*18*). Infection with schistosomiasis also brings with it increased vulnerability to malaria episodes and HIV infection (*19*).

Schistosomiasis has recently spread alarmingly in Africa. WHO estimated in 1971 that, globally, 600 million people were at risk of contacting schistosomiasis, and 200 million were infected (*20*). The geographical distribution of the at-risk areas is now different (*21*), and revised estimates suggest that in Africa alone, 700 million may be at risk and almost 200 million infected (*3*). Schistosomiasis prevalence in Central and South America, Egypt, and China has been reduced markedly as a result of improved socioeconomic development and chemotherapy, and schistosomiasis has been eliminated from Japan and Puerto Rico (*22*). Of all the parasitic diseases, schistosomiasis is the one that has benefited most from man-made water resource development in Africa. Lakes and irrigation schemes resulting from construction of dams have created ideal habitats for snails to colonize and breed explosively (*23*). For example, a barrage at Diama, Senegal, was constructed in 1986 on the Senegal River to prevent the intrusion of sea water into the river, and a dam was built at Manantali, Mali, in 1987 on the Bafing River to control the

flow of water and to generate electricity. Together, these developments have been responsible for the introduction of *S. mansoni* into the Lower and Middle Valleys of the Senegal River Basin and subsequent spread of the parasite in the human population, accompanied by new foci of *S. haematobium*. The reduction in salinity and change from an acidic to an alkaline environment in the water benefited both the fecundity and growth of freshwater snails and the transmission of the parasite, while the creation of new irrigation canals and expansion of the rice fields provided new habitats for intermediate snail hosts to colonize. Meanwhile, the concentration of human settlements close to water bodies often means that people have to use the same water for domestic, religious washing, and hygiene purposes. The water's edge may provide the only privacy, allowing human excreta infected with schistosome eggs to reach the water.

Since 1988, praziquantel has been available for the effective treatment of schistosomiasis. Its original cost was $1 per 600 mg tablet, but the drug cost had fallen to just $0.08 by 2002. Since that date, praziquantel has been used in six countries in sub-Saharan Africa to treat millions of people, and it has had marked success. Just one round of treatment reduced the prevalence of *S. haematobium* infection in Burkina Faso from 90% to less than 5% and reduced the intensity of infection in Mali by 90% (*24*). In Uganda, three rounds of treatment reduced the prevalence of the *S. mansoni* infection by more than 50% and the intensity by 90%, as well as reducing the intensity of hookworm by 95% (*25*).

Malaria and Other Vector-Borne Diseases

The risk of vector-borne diseases also increases as open water sources increase (Fig. 1). Malaria is still the infection which rightly attracts the most attention; a child in Africa dies from malaria every 30 s in 2006. Control of mosquitoes is difficult because the malaria parasite is capable of developing resistance to treatment after treatment, and each new treatment is more expensive than the last (*26*). The latest treatment hope for malaria is artemesinin-combination therapy, and the most effective method for controlling malaria and other mosquito-borne infections is impregnated bednets, provided their use is widespread; unfortunately, the supply of nets in endemic areas remains woefully low. The Global Fund for control of HIV/AIDS, tuberculosis, and malaria and the WHO Roll Back Malaria program have not reached their targets. However, with increased bednet coverage and increased political will from politicians and senior Ministry of Health officials, the situation should improve.

Different water bodies support different vectors of human parasites. Mosquitoes carrying malaria and lymphatic filariasis (Fig. 1) usually prefer smaller and stagnant water bodies, whereas faster moving water is needed for larval stages of *Simulium* spp. black flies, the vectors of onchocerciasis (river blindness) (*27*). Lymphatic filariasis (elephantiasis) and onchocerciasis cause terrible disfigurement and blindness, respectively, in millions of people near to appropriate water bodies (*28*, *29*). Over the past 25 years, areas in West Africa have been made free of onchocerciasis transmission through the Onchocerciasis Control Program (OCP), and in the remaining hyper- and meso-endemic foci in Africa, continued annual distribution of ivermectin will keep onchocerciasis controlled to a point where it is no longer a public health problem or constraint to economic development (*30*). The reduction achieved in lymphatic filariasis after five rounds of mass drug administration, as demonstrated in Egypt, is also encouraging (*31*).

Intestinal Helminths

Intestinal worms (hookworm, *Ascaris*, and *Trichuris* spp.) affect many millions of people in rural developing countries, and each ecological area supports its own population of intestinal worms. Thus, damp and grassy conditions maximize the survival of hookworm eggs and larvae, whereas eggs of ascaris are transferred from person to person by way of contaminated soil. These worms add to the parasitic burden of the rural Africans attracted to water development projects. Polyparasitism is common and has been grossly underestimated for many years. The probability is that, in total, worm parasites account for 500,000 deaths annually and 57 million Disability Adjusted Life Years, equivalent to the disease burden of HIV, malaria, or tuberculosis (*32*).

Integrated Control of These Diseases

Since 2000, there has been a positive change in attitude toward the control of schistosomiasis, lymphatic filariasis, and onchocerciasis, accompanied by an improvement in the availability of drugs (*26*). Praziquantel, the drug of choice for schistosomiasis since 1980, has recently dropped in price by more than 90%, and through the Schistosomiasis Control Initiative, more than 20 million treatments were carried out in 2005 to 2006 (*27*, *28*). By contrast, the cost of molluscicides has increased, and the toxicological danger posed to the environment has rendered the idea of using chemicals for snail control almost obsolete.

Three drug companies—Merck, GlaxoSmithKline (GSK), and Johnson & Johnson—have embarked on drug donation programs. Merck committed to donate ivermectin (Mectizan) (Mectizan Donation Program) to prevent river blindness in 1986 [supporting the Onchocerciasis Control Program, subsequently called the African Program for Onchocerciasis Control (APOC)]. This donation was extended after the discovery that Mectizan combined with albendazole was capable of preventing transmission of lymphatic filariasis. Supporting Merck's continued donation, GSK made a commitment in 1997 to offer free albendazole until lymphatic filariasis is eliminated, and now the combination is available to endemic countries with a national control plan through the Global Alliance for Elimination of Lymphatic Filariasis. However, the drugs kill only juvenile stages of this parasite; thus, annual mass treatment in endemic areas will be needed for another 6 to 8 years—the life span of the adult worms—to completely eliminate infection without vector control (*33*). Unfortunately, Mectizan cannot be given to very young children or pregnant women, which may prohibit elimination, but the benefits of these programs could be immense; the treatment substantially reduces suffering, disfigurement, and resulting stigma and increases productivity. The Johnson & Johnson donation of mebendazole for intestinal helminth treatment will start in 2006. This donation, combined with the reduction in the price of praziquantel, will allow cost-effective treatment for the hitherto neglected helminth infections. The coverage in Africa of these donated and cheap drugs has increased from virtually zero in 1986, to the APOC countries by 2000, to between 20 and 80 million individuals annually in 2006 (*34*).

The Hope for the Future

By 2015, the target date for achievement of the Millennium Development Goals, the integration of control of several disease control programs will likely lead to the control of morbidity or even the elimination of infections of up to seven Neglected Tropical Diseases. The current generation of children in many countries could soon be free of parasitic worm infections, better nourished, and better able to attend school and perform in class. The partnership members must now increase the coverage 10-fold to all those in need of treatment (which may be up to 500 million) by cooperating and integrating the programs in order to maximize their delivery of drugs and optimize safety, costs, and cost benefits over a 5-year period (*35*). With funding likely to emerge from donors during the years 2006 to 2015, national control programs are expected to reduce the prevalence, intensity of infection, and resulting morbidity to levels that no longer constitute a public health problem.

Despite the accompanying dangers of water development, the current situation in Africa is such that most people living close to major rivers and lakes in Africa need not be subjected to the waterborne diseases that previously plagued them. The vertical control programs with the tools to prevent death, blindness, and disfigurement have proved that they can work, and by 2006 they are reaching ever more people with donated or inexpensive drugs. The health of children in areas that have been reached is improving, and they are gaining a better start in life. The tools are available, and political will has been activated. WHO has grasped the challenge of integrating the control of neglected waterborne diseases and is now in a position to lead the world's global health partnerships into the next final control of morbidity due to waterborne diseases (*36*), which may indeed mean that they can be consigned to history.

References and Notes

1. Y. Schirnding, W. Onzivu, A. O. Adede, *Bull. World Health Org.* **80**, 970 (2002).
2. J. Keiser *et al.*, *Am. J. Trop. Med. Hyg.* **72**, 392 (2005).
3. P. Steinmann, J. Keiser, R. Bos, M. Tanner, J. Utzinger, *Lancet Infect. Dis.* **6**, 411 (2006).
4. R. T. Leiper, *J. RAMC* **25**, 1 (1915).
5. A. Crichton-Harris, *J. Med. Biogr.* **14**, 8 (2006).
6. W. H. Greany, *Ann. Trop. Med. Parasitol.* **46**, 298 (1952).
7. W. H. Greany, *Ann. Trop. Med. Parasitol.* **46**, 250 (1952).
8. A. A. el Gaddal, *J. Trop. Med. Hyg.* **88**, 47 (1985).
9. A. A. el Gaddal, *Mem. Inst. Oswaldo Cruz* **84**, (Suppl 1), 117 (1989).
10. M. A. Homeida *et al.*, *Lancet* **2**, 437 (1988).
11. M. Homeida *et al.*, *Am. J. Trop. Med. Hyg.* **39**, 196 (1988).
12. I. Talla *et al.*, *Ann. Soc. Belg. Med. Trop.* **70**, 173 (1990).
13. I. Paperna, *Z. Tropenmed. Parasitol.* **21**, 411 (1970).
14. P. J. Hotez *et al.*, *Emerg. Infect. Dis.* **3**, 303 (1997).
15. M. O'Ryan, V. Prado, L. K. Pickering, *Semin. Pediatr. Infect. Dis.* **16**, 125 (2005).
16. M. Barry, *Am. J. Trop. Med. Hyg.* **75**, 1 (2006).
17. D. R. Hopkins, E. Ruiz-Tiben, P. Downs, P. C. Withers Jr., J. H. Maguire, *Am. J. Trop. Med. Hyg.* **73**, 669 (2005).
18. E. F. Kjetland *et al.*, *Am. J. Trop. Med. Hyg.* **72**, 311 (2005).
19. P. Druilhe, A. Tall, C. Sokhna, *Trends Parasitol.* **21**, 359 (2005).
20. "Schistosomiasis control," *WHO Tech. Rep. Ser.* 515 (1973).
21. "Prevention and control of schistosomiasis and soil transmitted helminths," *WHO Tech. Rep. Ser. 912* (2002).
22. D. Engels, L. Chitsulo, A. Montresor, L. Savioli, *Acta Trop.* **82**, 139 (2002).
23. V. R. Southgate, *J. Helminthol.* **71**, 125 (1997).
24. A. Garba, S. Toure, R. Dembele, E. Bosque-Oliva, A. Fenwick, *Trends Parasitol.* **22**, 322 (2006).
25. B. S. Kabatereine *et al.*, *Bull. World Health Org.*, in press.
26. G. Edwards, G. A. Biagini, *Br. J. Clin. Pharmacol.* **61**, 690 (2006).
27. T. L. Lakwo, R. Ndyomugyenyi, A. W. Onapa, C. Twebaze, *Med. Vet. Entomol.* **20**, 93 (2006).
28. D. Molyneux, *Filaria J.* **2**, 13 (2003).
29. K. Y. Dadzie, *Afr. Health* **19**, 13 (1997).
30. Y. Dadzie, M. Neira, D. Hopkins, *Filaria J.* **2**, 2 (2003).
31. R. M. Ramzy *et al.*, *Lancet* **367**, 992 (2006).
32. P. Hotez, J. Bethony, S. Brooker, M. Albonico, *Lancet* **365**, 2089 (2005).
33. J. O. Gyapong, V. Kumaraswami, G. Biswas, E. A. Ottesen, *Expert Opin. Pharmacother.* **6**, 179 (2005).
34. A. Fenwick, *Trans. R. Soc. Trop. Med. Hyg.* **100**, 200 (2006).
35. P. J. Hotez *et al.*, *PLoS Med.* **3**, e102 (2006).
36. L. Savioli, D. Engels, H. Endo, *Lancet* **365**, 1520 (2005).
37. N. R. de Silva *et al.*, *Trends Parasitol.* **19**, 547 (2003).
38. M. J. van der Werf *et al.*, *Acta Trop.* **86**, 125 (2003).
39. N. Zagaria, L. Savioli, *Ann. Trop. Med. Parasitol.* **96** (suppl. 2), S3 (2002).

40. I thank P. Hotez, A. Koukounari, D. Molyneux, and J. Webster for assistance in the preparation of this article. The Schistosomiasis Control Initiative is funded by a grant from the Bill and Melinda Gates Foundation.

10.1126/science.1127184

PERSPECTIVE

Seeking Sustainability: Israel's Evolving Water Management Strategy

Alon Tal

The water management policies adopted to address Israel's chronic scarcity have not been without environmental consequences. Yet, through a trial-and-error process, a combined strategy of water transport, rainwater harvesting, and wastewater reuse and desalination, along with a variety of water conservation measures, have put the country on a more sustainable path for the future.

At a time when many dry-land nations face water resource crises (*1*, *2*), Israel's water management experience offers a substantial basis for optimism. Some 60 years of developing water sources and delivery systems, along with technological innovation and regulatory programs, have strengthened national efforts to provide water to a growing population and agricultural sector. At the same time, this growth has led to a number of adverse environmental consequences that future policies will need to address. These include seawater intrusion into overpumped aquifers, groundwater nitrification from fertilizers and sewage, and contamination from industrial pollutants, garbage dumps, gas stations, and myriad nonpoint sources (*3*, *4*). Here, I focus on the relative successes and ramifications of what, in retrospect, has been a trial-and-error process.

The major focus in Israeli water policy is and has always been expanding supply. Israel's sole natural freshwater lake, Kinneret (also called the Sea of Galilee or Lake Tiberias), holds roughly one-third of the country's replenishable water supply. Along with the mountain aquifer system, which provides an additional 20%, it lies in a transboundary watershed that is still the subject of international dispute. Nonetheless, even before a final allocation deal is brokered, annual water availability is less than 250 m^3 per person (250,000 liters). The internationally recognized Falkenmark indicator sets 1000 m^3 per person as a minimum annual level below which countries experience water stress; hence, present supplies place Israel at 50% of the annual per capita "absolute scarcity" level of 500 m^3 (*5*).

The principal national investments in increasing water supply have involved four initiatives: (i) integrated management of Lake Kinneret and groundwater aquifers, which feed into an integrated national water grid; (ii) water harvesting via a network of rain-fed reservoirs; (iii) wastewater treatment and reuse for irrigation; and (iv) desalination of seawater and brackish groundwater.

Water Transport

Massive water transport projects have greatly expanded irrigation and domestic supply in arid regions from California to Libya (*6*–*8*). However, the associated water quality problems and mining of nonrenewable aquifers can lead to a steady decline in available water resources. Israel's adaptive experience in this context is instructive.

Beginning in 1964, water has been conveyed from Israel's relatively wet northern Galilee (precipitation up to 700 mm/year) to depleted central aquifers and to the arid southlands (precipitation 20 to 200 mm/year) via a "National Water Carrier" (Fig. 1). Although this undertaking led to a large increase in cultivated land and harvests in the country's semiarid regions, it also exacerbated salinity problems and, to a lesser extent, raised turbidity levels in water.

Mitrani Department of Desert Ecology, Blaustein Institutes for Desert Research, Ben-Gurion University of the Negev, Sede Boqer 84990, Israel. E-mail: alontal@bgu.ac.il

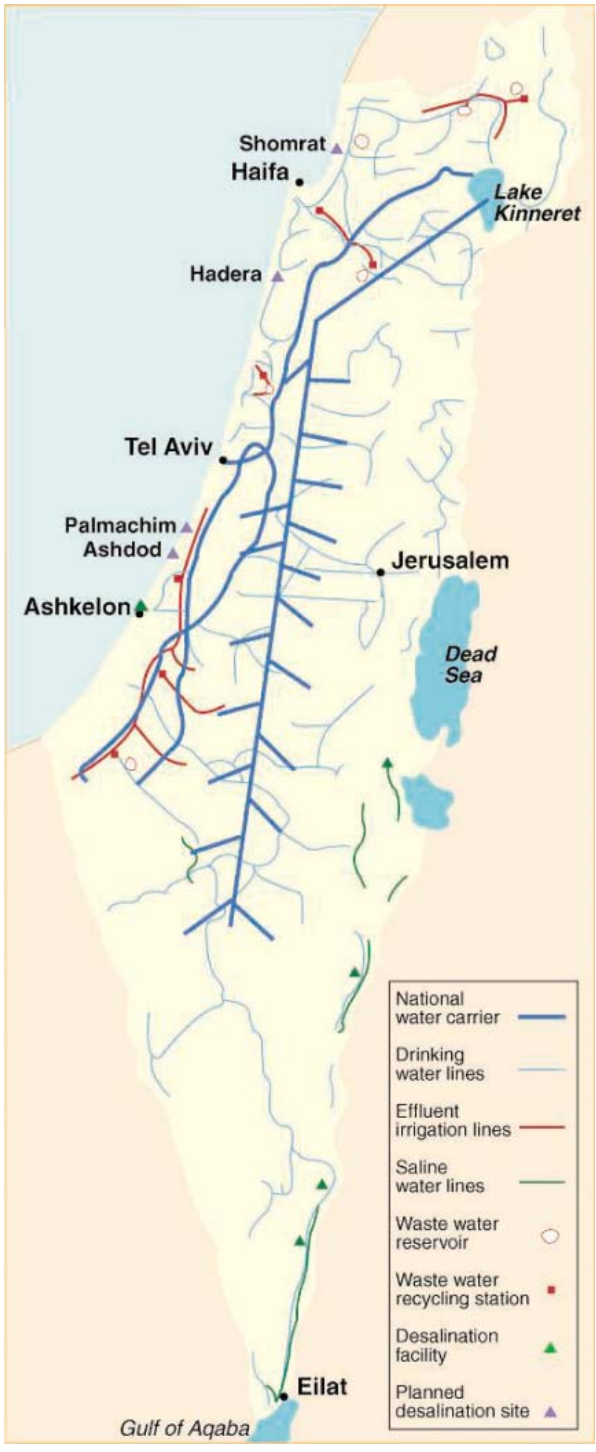

Fig. 1. The National Water Carrier and other major water resources.

The water originating in Lake Kinneret was relatively salty, with average chloride concentrations reaching 390 mg/liter (*9*). Diversion of saline streams that fed Lake Kinneret to the lower Jordan River during the 1970s reduced concentrations to between 220 and 270 mg/liter. Nonetheless, water transport still contributes an estimated 170,000 metric tons of chlorides to the soils and groundwater in the center of the country (*10*). Present efforts focus on conscientious management of the surrounding watershed, further reduction of Kinneret salinity levels, and dilution of National Water Carrier flow with low-salt, desalinized waters. Some experts and environmentalists argue that the long-term salinization damage—along with the steady desiccation of the Dead Sea, deprived of the Jordan River water—justifies the decommissioning of the National Water Carrier (*11*).

At the same time, the suspended solid levels in the water supply, arising from natural turbidity in Lake Kinneret, have raised aesthetic and health concerns. A new system of sand filtration and treatment for the reservoirs of the National Water Carrier will begin operating in autumn 2006 to control turbidity and also to increase pH levels, thereby reducing the corrosivity of the water and minimizing chemical reactions with other water sources. Although this upgrade was delayed for some time because of its expense, an internal cost-benefit analysis showed that the investment was easily justified.

Water Harvesting and Reservoirs

Water supplies in Israel have been augmented by an aggressive program of collecting rainwater, spearheaded by the Jewish National Fund (JNF), a public-interest corporation. Starting in the 1980s, a network of 178 reservoirs was established across the country's rain gradient, with most located in semiarid and hyperarid regions. The system currently collects 125 million m^3/year, which constitutes 7% of the total water in Israel's system, collectively capable of irrigating 300 million m^2 of farmland (*12*).

The first wave of reservoirs relied on damming and impounding floodwaters, with the primary objective of replenishing groundwater. Beyond the reduced evaporation, the filtration associated with percolation through underlying soils enhances water quality. (However, pressure from farmers to control this stored water has often resulted in direct connection of the reservoirs to irrigation systems, so that these water quality improvements frequently are not realized.) Reservoirs can also bring the added benefits of fish farming, recreation, and swimming. Most of the recently constructed reservoirs hold treated wastewater, stored before agricultural use during the summer and autumn dry seasons. With the anticipated increase in overall water supply due to desalination technologies (see below), the need for reservoirs to store the resulting effluents will grow, especially during the rainy winter season when irrigation demand is low.

Although reservoirs can expand water supplies in arid regions, the creation of this harvesting infrastructure requires capital that is often unavailable at the local level. Depending on size and underlying soil composition, reservoirs with a capacity of 0.5 to 2 million m^3 take between 1 and 2 years to build and cost $1 million to $5 million. Once built, however, reservoirs serve to empower the local agricultural communities that operate them and would otherwise remain highly reliant on the country's centralized water bureaucracy. Communities can determine irrigation rates and storage regimes during the dry seasons. Water quality monitoring is a critical operational component in efforts to mitigate the risk of high concentrations of phosphates, phenols, nitrates, boron, and pesticides found in agricultural discharges and to control salinity in wastewater reservoirs.

Wastewater Reuse

In 1953 Israel drafted the world's first set of standards for wastewater reuse, and effluent recycling emerged as a central element of Israeli domestic water policy (*13*). At present, 91% of all municipal sewage in Israel is treated, 73% of which is recycled [versus 2.5% in the United States (*14*)], contributing roughly one-fifth of Israel's total supply. Typically, the effluents reaching farm operations come from nearby cities, with the exception of Tel Aviv's metropolitan plant, which transports roughly one-quarter of the country's sewage (130 million m^3/year) 100 km southward to the Negev desert. Treatment is based on an activated sludge process that incorporates additional nitrogen removal. After treatment, the water is piped to spreading bases where it is injected into the ground for recharge of a regional aquifer. Here the water undergoes additional filtering and seasonal storage before it is pumped for irrigation (*15*).

Concerns about the effect of sewage recycling initially focused on public health

and led to the authorization of the Ministry of Health as the oversight agency for matters concerning effluent treatment and reuse. During the 1970s, a major epidemiological study in 81 agricultural communities compared health effects among farmers who used sewage effluents with those who did not, but found no significant difference in morbidity and mortality trends (*16*). Starting in 1992, a new standard for secondary treatment facilities required a maximum concentration of 20 mg/liter BOD (biological oxygen demand, a measure of organic pollution in wastewater) and 30 mg/liter for TSS (total suspended solids). However, this "20/30" secondary sewage treatment level proved inadequate for a variety of reasons.

The range of crops that can be grown at this treatment level is relatively narrow because of the presence of pathogens in the effluents. Directly consumed vegetables, for example, are excluded from allowable crops at this treatment level, as are many fruit trees. The salinity in the wastewater posed risks to soils and fresh water sources. Boron compounds, common in detergents, were not efficiently removed and accumulated in recycled wastewater, contributing to soil structure problems. Moreover, during the 1980s, industrial solvents such as toluene and benzene began to appear in Israeli rural well samples (*17*). Their presence was attributed to inadequate sewage treatment and widespread irrigation with effluents.

It became clear that effluent standards at 20/30 levels—which make sense in regions such as Europe, where the river dilution factor is considerable—are insufficient in arid environments, where wastewater is recycled or supplies most of the baseline flow in naturally ephemeral streams. Ultimately, ecosystem recovery in Israeli rivers will have to be based on higher quality effluents (*18*). In April 2005, the Israeli government approved the recommendations of an expert committee that increased the stringency of sewage treatment requirements. Maximum BOD and TSS were reduced to 10 mg/liter. The standard contains a long list of new criteria for salinity as well as concentrations of boron, heavy metals, and nutrients. The criteria are dichotomous, with limits set for agricultural irrigation often differing from those set for wastewater discharged into streams. For example, an ammonia standard of 20 mg/liter is set for agricultural reuse, whereas concerns about eutrophication led to a stringent 1.5 mg/liter requirement for discharge into streams. The banning of boron in detergents has already resulted in reduced wastewater concentrations.

The estimated cost of the 10-year phase-in of advanced tertiary sewage treatment is $220 million (*19*). The economic burden for meeting the new standards will be much easier in the large municipal facilities than in the nonmechanized smaller plants that produce a quarter of the country's effluents.

Desalination

Desalination constitutes the most recently adopted component of Israel's water management strategy. In the past, prohibitively high costs limited the scope of desalination to reverse-osmosis facilities in remote southern agricultural communities and at the Red Sea resort town of Eilat, where no viable alternative water source existed. Today the combination of modern membrane technologies, reduced energy consumption, and the economies of scale associated with mass production yields very-high-quality drinking water on Israel's Mediterranean coast at a cost of less than $0.60 per 1000 liters (1 m^3).

Inland desalination facilities, designed to treat large local supplies of brackish groundwater with lower salt concentrations, are expected to produce water at roughly $0.30/$m^3$. Figure 2 shows the general cost reduction trends associated with desalination worldwide. These rates belie the logic of the much-discussed Israeli acquisition of Turkish water (*20*) to be shipped by tankers, which at present prices would cost more than twice as much as the desalinized alternative.

The new economic dynamics led to a 2002 government decision to build five new reverse-osmosis desalination plants over the coming years. The facilities are expected to produce more than 300 million m^3/year, adding some 15% to present drinking water supplies (*21*). Table 1 shows the Israel Water Commission's anticipated growth in water production.

In 2005 the VID Desalination Company consortium opened the first of these desalination plants in the Mediterranean city of Ashkelon, having received rights to build and operate the $250 million facility for 25 years (*22*). With production of 100 million m^3/year, it is currently the largest reverse-osmosis seawater desalination plant in the world. The average energy demand is 3.85 kWh per m^3 of water. Mounting oil costs have not raised water prices much beyond the original target of $0.52/$m^3$. Seawater is pumped via three submerged high-density plastic pipelines that stretch 1 km into the sea. Water is collected at a depth of 7 m, the approximate midpoint between the surface and the seafloor. The seawater undergoes a pretreatment process in two parallel production lines to ensure reliability in the event of blockages. A two-stage gravel, sand, and anthracite filtration process precedes the water's entry into the facility's 32 reverse-osmosis treatment trains, filling four stories and containing 40,000 membrane elements. Fouling of the membrane stacks is avoided by adding phosphonate antiscalant chemicals before the water reaches the stacks.

Although there was little active opposition to Israel's new desalination initiative, several environmental concerns have been articulated. These concerns include the loss of public coastal open spaces, the cumulative impact of brine discharges into a concentrated area of the sea, and the additional greenhouse gases associated with the attendant electricity generation (*23*). The quality of the water itself, however, is excellent.

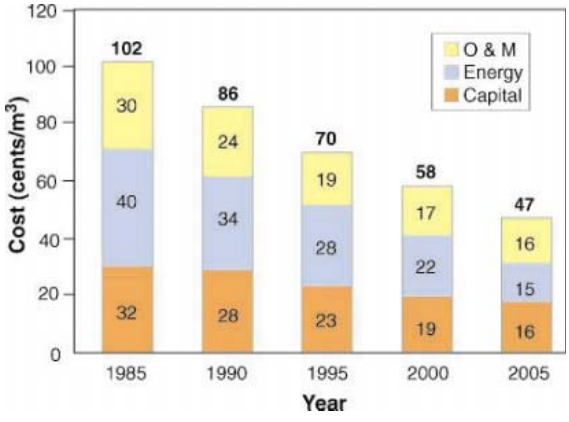

Fig. 2. Trends in cost breakdown: Reverse-osmosis seawater desalination. Source: Israel Water Commission, 2005.

Table 1. Planned expansion of the Israeli water supply. Source: Israel Water Commission, 2005.

	Established or projected water supply (million m^3)								
	2002	2003	2004	2005	2006	2007	2008	2009	2010
Seawater desalination	—	—	—	40	110	130	140	270	315
Recycling system	—	—	—	—	—	15	35	35	35
Brackish water desalination	1	8	15	20	30	55	55	55	55
Water imports	—	—	—	—	—	—	—	—	50
Total additional potable water	1	8	15	60	140	200	230	360	455
Treated effluents (for agriculture)	295	332	359	390	441	461	471	491	509

The new Ashkelon plant, for example, incorporates a treatment process to address the natural boron concentration in seawater; with a removal efficiency of 92%, the process reduces boron concentrations down to a mere 0.4 mg/liter. Chloride levels after treatment are so low (20 mg/liter) that the desalinated water is actually mixed into the national water grid to dilute the high salinity in the "fresh" water. When the city of Be'er Sheva began using the desalinated water in early 2006, chlorides in the sewage effluents it sent to agriculture plummeted to 100 to 150 mg/liter, concentrations that even critics of widespread sewage reuse find sustainable.

Conservation and Demand Management

Despite the primary policy focus on increasing supply, Israel's Water Commission has also strengthened conservation and demand management programs as part of an overall national strategy. In the urban sector, most economic analyses suggest that demand for water is highly inelastic and thus not responsive to price regulation (*24*). Rather, a combination of technology diffusion (upgrading of inefficient plumbing infrastructure, along with car wash and toilet regulations) and seasonal usage restrictions for spray irrigation has kept industrial and domestic per capita water consumption steady despite the rise in living standards during the past 40 years (*25*).

The most striking increase in water use efficiency has occurred in the agricultural sector. During Israel's first half-century, the country's population grew by a factor of 7 while agricultural production expanded by a factor of 16 (*26*). At the same time, the proportion of high-quality fresh water allocated to farmers steadily declined. The invention and introduction of drip irrigation in Israel during the 1960s was the most important innovation behind this increase in "crop per drop."

Drip irrigation solves several vexing problems for farmers. The paramount challenge in irrigation has always been to control the salinity that accumulates in soils as plants absorb water but leave the salts behind. By decreasing overall water delivery, drip irrigation reduces residual salts. Nonetheless, drainage systems that collect and dispose of saline leachate remain important components of a sustainable system in soil with low permeability (*27*). In addition, drip technology facilitates cultivation on steep terrains and in shallow soils, with computerized systems delivering nutrients and oxygen to the root zones at optimal intervals for their use by growing plants.

A new generation of subsurface drip irrigation systems provides additional improvements by maintaining a dry soil surface. Drippers are typically buried at 7 to 30 cm under the soil surface (*28*). The subsurface positioning of drip emitters conserves water, controls weeds, minimizes runoff and evaporation, increases longevity of the system, eases the use of heavy equipment in the field, and prevents human contact with low-quality water (*29*). Moreover, subsurface irrigation reduces labor, obviating seasonal installation and collection of surface drip system laterals. Installing a system constitutes a relatively expensive capital investment and is hardly trouble-free. Clogging and root infiltration have been mitigated by a variety of filtration and chemical approaches.

Outlook

Israel still faces considerable water management challenges. The Dead Sea, the lowest and saltiest lake on the planet, is literally disappearing, with an average annual drop in water level of 1.2 m/year. This is a predictable result of the 1 billion m^3/year diversion of the natural flow from Lake Kinneret and the Jordan and Yarmoukh rivers (*30*). Compliance with industrial discharge standards remains spotty. Urbanization and proliferation of paved surfaces threaten to undermine aquifer recharge (*31*). Streams, whose natural base flow has largely been replaced by effluents, cannot support ecological systems. A renewed peace process would undoubtedly lead to greater water allocation demands from Palestinians and perhaps Jordanians and Syrians (*32*). Finally, the existing pollution in aquifers is severe enough (or the taste from chlorination unpleasant enough) to motivate more than 70% of the public to buy bottled water (*33*).

Given the anticipated water concessions to Israel's neighbors associated with future peace agreements, expansion of the water supply will be necessary to maintain present levels of agricultural, domestic, and industrial activities. In addition, a new statutory commitment to stream restoration will further increase demand as water managers begin returning a "fair share" to the ecosystem. Present indicators suggest that continued technological development, coupled with ongoing water conservation and pollution prevention policies, should enable the country to meet these future hydrological challenges. At the same time, experience teaches us that new technologies have environmental ramifications that must be anticipated and addressed if water management is to be sustainable.

References and Notes

1. D. Ward, *Water Wars: Drought, Flood, Folly and the Politics of Thirst* (Riverhead, New York, 2002).
2. F. Pearce, *When the Rivers Run Dry: Water, the Defining Crisis of the Twenty-First Century* (Beacon, Boston, 2006).
3. C. Gvirtsman, *Water Resources of Israel* (Yad Ben Tsvi, Jerusalem, 2002).
4. "Sources of Water Pollution" (Israel Ministry of Environmental Protection, 2 March 2006; available at www.sviva.gov.il).
5. M. Falkenmark *et al.*, *Nat. Resour. Forum* **13**, 258 (1989).
6. M. Reisner, *Cadillac Desert: The American West and Its Disappearing Water* (Penguin, New York, 1993).
7. M. de Villiers, *Water* (Stoddart, Toronto, 1999).
8. R. Glennon, *Water Follies: Groundwater Pumping and the Fate of America's Fresh Waters* (Island, Washington, DC, 2002).
9. A. Tal, *Pollution in a Promised Land: An Environmental History of Israel* (Univ. of California Press, Berkeley, CA, 2002).
10. D. Zaslavsky, *Below the Red Line: Regarding the Water Crisis in Israel* (Technion, Haifa, 2002).
11. *Let the Jordan River Flow* (Friends of the Earth Middle East, Tel Aviv, 2005).
12. Water for Life, *KKL Policy for Establishing a Water Network to Serve the Israeli Public and Water Industry* (Jewish National Fund, Jerusalem, 2004).
13. H. Shuval, *Water Quality Management Under Conditions of Scarcity: Israel as a Case Study* (Academic Press, New York, 1980).
14. National Academy of Science, *Use of Reclaimed Water and Sludge in Food Crop Production* (National Academies Press, Washington, DC, 1996).
15. S. Gabbay, *The Environment in Israel* (Ministry of Environment, Jerusalem, 2002).
16. B. Fattal *et al.*, *Developments in Arid Zone Ecology and Environmental Quality* (Balaban, Philadelphia, 1981).
17. L. Muszkot *et al.*, *Adv. Mass Spectrom.* **11**, 1728 (1990).
18. M. Juanico, E. Friedler, *Water Sci. Tech.* **40**, 43 (1999).
19. "Ministerial Committee Unanimously Votes to Adopt the Recommendations of the Inbar Commission" (Israel Ministry of Environmental Protection, 19 April 2005; available at www.sviva.gov.il/Enviroment).
20. P. Gleick, *The World's Water: Biennial Report on Freshwater Resources* (Island, Washington, DC, 2002).
21. Y. Dreizin, presentation at the Water for Life in the Middle East Conference, Anatolia, Turkey, 12 October 2004 (Israel/Palestine Center for Research and Information; available at www.ipcri.org/watconf/dreizin2.pdf).
22. G. Kronenberg, *Desalination* **166**, 457 (2004).
23. N. Becker, *Initial Assessment Quantifying Externalities of Desalination Facilities in Israel and Comparison of Alternatives' Costs* (Friends of the Earth Middle East, Tel Aviv, 2004).
24. J. Dalhuisen *et al.*, *Land Econ.* **79**, 292 (2003).
25. *Agamit* **176**, 4 (2006).
26. J. Fedler, *Israel's Agriculture in the 21st Century* (Ministry of Foreign Affairs, Jerusalem, 2002).
27. D. Hillel, *Salinity Management for Sustainable Irrigation* (World Bank, Washington, DC, 2000).
28. A. Tal, A. Ben Gal, P. Lawhon, D. Rassas, *Sustainable Water Management in the Drylands: Recent Israeli Experience* (Ministry of Foreign Affairs, Jerusalem, 2005).
29. A. Ben-Gal, N. Lazorovitch, U. Shani, *Vadose Zone J.* **3**, 1407 (2004).
30. N. Hasson, *Ha'aretz*, 12 April 2006, p. 1.
31. U. Shamir, N. Carmon, in *Impacts of Urban Growth on Surface and Groundwater Quality*, B. Ellis, Ed. (International Association of Hydrological Sciences Publication 259, Wallingford, UK, 1999).
32. E. Feitelson, *Polit. Geogr.* **21**, 293 (2002).
33. *Environmental Poverty Report* (Israel Union for Environmental Defense, Tel Aviv, 2005).

34. I thank U. Shamir, Y. Rosenthal, and H. Shuval for their insightful comments and suggestions.

10.1126/science.1126011

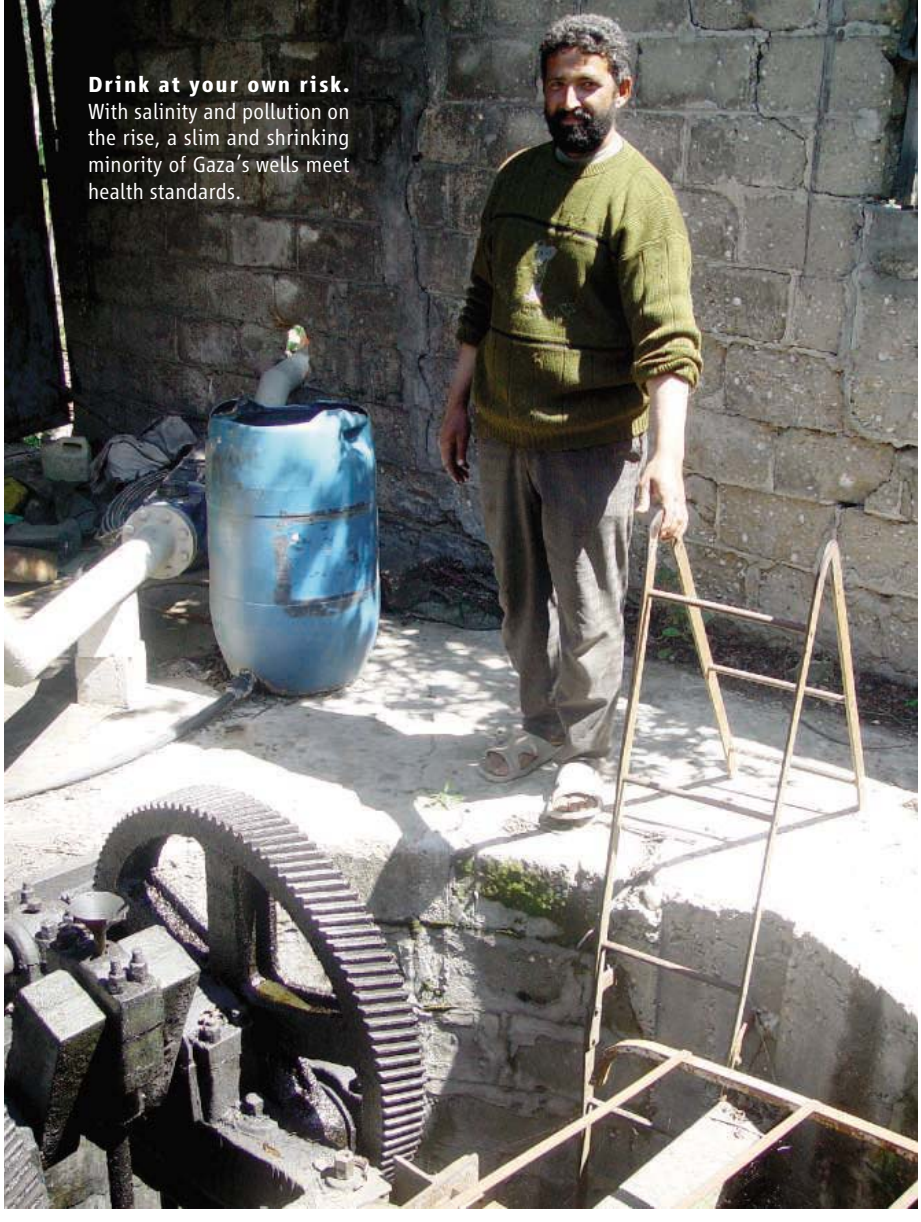

Drink at your own risk. With salinity and pollution on the rise, a slim and shrinking minority of Gaza's wells meet health standards.

CREDIT: J. BOHANNON/*SCIENCE*

NEWS

Running Out of Water—and Time

Geography, politics, and war combine to make the Gaza Strip a worst-case scenario for water-resource planners

RAFAH—You can almost hear the collective sigh of relief as the angry sun sets over this dusty city on Gaza's Egyptian border. This is when five of Ali Abu Taha's sons arrive, unwinding their kaffiyehs and gathering around the charcoal fire where a pot of tea is already boiling. The unprecedented visit of a foreign guest calls for a demonstration of the hospitality for which the Bedouins are famous. The seat of honor is offered, and some of the family's most valuable possessions are laid out on the carpet for display: a battered old AK-47 rifle and several bottles of home-filtered water. The gun is a family heirloom that rarely sees light, but the water is indispensable. "The filter cartridges are very expensive and hard to get into Gaza," says one of the sons, Mohammed, "but this one should hold up for another month, *insha'Allah*." Not only does it provide the drinking water for Abu Taha's clan—about 100 people, a third of them his grandchildren—but by enabling them to bottle and sell water to neighbors, it provides one of their few sources of income.

"I don't recommend drinking too much of this," says Mohammed as he fills a glass with unfiltered water from the tap. One sip of the pongy brine is enough to understand why. As a general rule, the farther south one goes in Gaza, the worse the water becomes, and Rafah is the end of the line. The Palestinian Authority issues warnings from time to time urging the public to buy bottled water, especially for the very young or elderly. But for the average Gazan—with an annual income of $600—a $1 gallon of water is a luxury.

For Abu Taha, who grew up as a Bedouin in the nearby Negev desert, making efficient use of scarce water resources is nothing new. The problem is that the 1.4 million people crammed into the Gaza Strip—most of them the children of refugees who fled their homes in the 1948 and 1967 Arab-Israeli wars—depend on a shallow aquifer for water. But year by year, that source is becoming more contaminated by salt and pollution. Most wells already produce water that is nonpotable by standards set by the World Health Organization.

Water scarcity is a perennial problem in the region, but nowhere is it worse than in Gaza. "It is a microcosm of the entire Middle East," says Eric Pallant, an environmental scientist at Allegheny College in Meadville, Pennsylvania, who has collaborated with both Israelis and Palestinians on water problems. "If you can figure out how to make water sustainable there, then you can do it anywhere." Several Gaza water projects have been planned by donor countries in recent years, including state-of-the-art wastewater treatment and desalination plants, but all have fizzled due to security concerns and sanctions slapped onto the new Hamas-led Palestinian government. Israel's withdrawal of settlers and troops from Gaza last year is a bittersweet victory for the Palestinians. Although they are fully in control of Gaza's water for the first time, they must now scramble to save it before it becomes irreversibly contaminated.

Water woes

It is a tense first day on the job for Mohammad Al-Agha, the Hamas minister of agriculture. Like a thunderstorm that never quite arrives, Israeli artillery pounds the landscape to the north where Palestinian militants have been launching rockets over the border. After a brief welcome party in his new Gaza City office, Al-Agha, a geologist from nearby Islamic University, and the small group of experts responsible for managing Gaza's water resources meet with *Science* to discuss their plans. The conversation is interrupted twice when fighter jets scream overhead and strike nearby targets with missiles, causing the building to shudder.

At a glance, the Gazans' water woes seem insurmountable. The only natural fresh source available is the coastal aquifer, a soggy sponge of sediment layers that slopes down to the sea a few dozen meters beneath their feet (see figure). Its most important input is the meager 20 to 40 centimeters of annual rainfall that sprinkles over Gaza's 360-square-kilometer surface—about twice the area of Washington, D.C.—giving between 70 and 140 million cubic meters (MCM) of water per year. Most of that water evaporates, but between 20 and 40 MCM penetrates the sandy sediment to feed the aquifer. Another 15 to 35 MCM, depending on whom you ask, flows in under the border from Israel, while irrigation and leaky pipes are estimated to return 40 to 50 MCM, for a total annual recharge of 75 to 125 MCM.

Tight spot. Urban pollution, agricultural contamination, and saltwater intrusion from the Mediterranean Sea give Gaza's aquifer a dicey future.

The aquifer's only natural output is the 8 MCM per year that should exit into the Mediterranean, providing a crucial barrier against the intrusion of seawater. So if no more than about 100 MCM were tapped from the aquifer per year, it could last forever. But Gaza's 4000 wells suck out as much as 160 MCM yearly, says Ahmad Al-Yaqoubi, a hydrologist who directs the Palestinian Water Authority. This estimated 60-MCM annual water deficit is why the water table is dropping rapidly and already reaches 13 meters below sea level in some places. Saltwater from the Mediterranean as well as deeper pockets of brine get sucked in to fill the gap. "The saltwater intrusion is well under way," says Al-Yaqoubi, "especially in the coastal areas and to the south." About 90% of wells already have salinity exceeding the WHO-recommended maximum of 250 parts per million (ppm). The accelerating rate of saltwater intrusion alone could make the Gaza aquifer unusable within 2 or 3 decades, according to a 2003 report by the United Nations Environment Programme.

But there may be far less time on the clock. The aquifer is also mixing with a cocktail of pollutants from Gaza's sewage and agriculture. "Besides salt, our number-one contaminant is nitrate from solid waste and fertilizers," says Yousef Abu Safieh, an environmental scientist based in Gaza City who heads the Palestinian Environmental Quality Authority. The maximum safe concentration of nitrate according to WHO is 45 ppm. "In our sampling, we find that most wells have about 200 ppm, and wells close to agricultural runoff can even hit 400," says Abu Safieh. Two Palestinian governmental studies led by Abu Safieh point to patterns of disease matching the distribution of water contamination. The higher the salinity of local water, the higher the incidence of kidney disease, he says, and nitrate concentration correlates with Gaza's high incidence of blue baby syndrome: a loss of available oxygen in the blood that can cause mental retardation or be fatal.

It is the job of a water utility to clean up such contamination and make sure that safe water comes out of the tap, but there is no such unified utility in Gaza. Instead, the strip is covered by a patchwork of fragmented water infrastructure. Gaza's three wastewater treatment plants are far from adequate. The largest, south of Gaza City, was designed to treat 42,000 cubic meters per day—the amount produced by 300,000 people—but now faces a daily inflow of more than 60,000 cubic meters, says Al-Yaqoubi: "This has overwhelmed the biological step of the treatment process." As an emergency measure to prevent sewage from overflowing, barely treated wastewater is now piped to the coast, where the dark gray liquid can be seen, and smelled, flowing along the beach. Meanwhile, the 40% of Gazans without access to a centralized sewage-disposal system contribute to the burgeoning cesspits. A 40-hectare lake of sewage that has formed in northern Gaza is a menace to people at the surface and the aquifer beneath.

These threats to the water supply are serious, says Al-Yaqoubi, but "water scarcity is of course the problem that will never go away." Considering that crop irrigation gobbles up 70% of Gaza's water and fertilizers contribute most of the nitrate contamination, firmer control of agriculture by Al-Agha's ministry seems like a necessary first step in saving the aquifer from ruin. "The problems continue to spiral," says Mac McKee, a hydrologist at Utah State University in Logan, who has collaborated with Gazans for the past 10 years, because "the Palestinian Authority has not succeeded in applying effective controls on well-drilling and pumping." About half of Gaza's wells have been dug illegally, mostly by farmers to irrigate small plots of cropland.

"If you try to tell farmers to stop using their wells, they come out with guns," says Ehab Ashour, a water engineer who works for international development agencies in Gaza. And with the struggle for power intensifying between the Hamas and Fatah leaderships, the prospect of better enforcement seems dimmer than ever. For his part, Al-Agha says a crackdown on well-digging isn't even on the table. "We can't do this from an economic standpoint," he says. "Over 60% of people here are farming. We are all locked into this jail, so we have to grow our own food and at the same time try to produce something we can export."

Asking families in Gaza to use less water is also "out of the question," says David Brooks, an environmental scientist who was an adviser during the Israeli-Palestinian water negotiations—a mandate of the Oslo Peace Accords—until they collapsed in 2003 and is now at Friends of the Earth in Ottawa, Canada. Average daily domestic water consumption in Gaza is about 70 liters per person—used not only in homes but also hospitals, schools, businesses, and

SOURCES: UNIVERSITY OF TEXAS; UNEP-GRID, GENEVA

public institutions—whereas 100 liters per capita per day is the generally agreed minimum for public health and hygiene. (By comparison, average consumption in Israel is 280 liters per day.) So the only way forward is to secure new sources of fresh water and make existing sources stretch farther, says Abu Safieh. There are several strategies for doing this, he says, "and we are pursuing all of them."

Making more with less

If you stand on any hill in Gaza and look west, a tantalizing source of water shimmers into view. If only the salts could be efficiently removed, the Mediterranean is a virtually limitless supply for desalination plants. Indeed, this very water is feeding some of the world's most advanced facilities less than an hour's drive up the coast in Israel (see Tal, p. 1081).

For any long-term solution in Gaza, "desalination will be absolutely necessary," says McKee. A desalination plant capable of providing Gaza with 60 MCM of drinking water per year was part of a plan drawn up by the United States Agency for International Development (USAID) in 2000. Money to build the $70 million plant, along with $60 million to lay down a carrier system to pipe the water across Gaza, was ready to go from USAID when the second intifada broke out just months later, stalling the project. It was officially frozen in 2003 after a bombing killed three members of a U.S. diplomatic convoy in Gaza.

Besides producing more drinking water, the priority is to deal with Gaza's sewage, says Al-Yaqoubi, not only to prevent a public health disaster but also to recycle some of the precious water back into the system. A trio of wastewater treatment plants that could handle Gaza's entire load has been promised by USAID, the World Bank, Germany, Finland, and Japan, but "nothing has happened," he says, because of the Hamas election victory.

In relation to stretching the current water supply farther, there is one positive legacy of Israeli occupation in Gaza. By working on Israeli farms, "we have become very comfortable with new technologies," says Al-Yaqoubi. In spite of the official freeze on international aid to the Palestinian government, projects aiming to improve farming in Gaza "are ongoing by many donors," he says. The most important is drip irrigation, delivering water directly to roots through a network of tubes. Coupling this with a computerized system that automatically pumps just enough water from a well to meet the plants' daily needs can make irrigation up to 70% more efficient over the long run.

But for the immediate crisis, the country best placed to help Gaza may be Israel. Before the taps were shut this year after Hamas was elected, 5 MCM per year of drinking water was being piped into Gaza by Mekorot, the Israeli national water company, and an additional 5 MCM had been agreed. That water does not come free, but it is nevertheless a freshwater source separate from the ailing aquifer.

"We know how serious the situation is in Gaza," says Saul Arlosoroff, a member of Mekorot's board of directors and a former Israeli deputy water commissioner. "The first priority is to get these people enough clean drinking water, and the second is to prevent salinity from irreversibly destroying their soil." Arlosoroff says Israelis and Palestinians working in the water sector have a special relationship. "We understand each other, and we know that these problems require cooperation," he says, "but the atmosphere between Gaza and Israel is worse now than at any time in our history."

Across the border, Abu Safieh is similarly disappointed. "There was a time when I could talk with my Israeli counterpart constructively about our environmental problems," he says, but he has not had any contact in years. Al-Agha says he plans to turn to Egypt for help. For importing and exporting, as well as perhaps for obtaining the abundant electricity needed to desalinate water, he says, "our hope is to the south."

The present turmoil also prevents what Brooks calls "the easiest and best solution" to Gaza's environmental problems: reducing the number of people living there. "Gaza can't sustain that population, and any real solution will require people to leave," he says. Most Gazans "will never give up hope of returning to their homes," says Abu Safieh, but for now, "we will work to make the best of the bad situation."

–JOHN BOHANNON

Danger signs. Sewage gushes out onto Gaza's beaches from a failing wastewater treatment plant. Plans to upgrade the infrastructure remain frozen.

CREDIT: J. BOHANNON/*SCIENCE*

NEWS

Desalination Freshens Up

Cheaper materials, more efficient equipment, and some promising new approaches could make large-scale extraction of clean water a major force in the battle against global thirst

Efforts to provide clean, fresh water for the world's inhabitants seem to be moving in the wrong direction. According to the World Health Organization, 1 billion people do not have access to clean, piped water. A World Resources Institute analysis adds that 2.3 billion people—41% of Earth's population—live in water-stressed areas, a number expected to climb to 3.5 billion by 2025. To make matters worse, global population is rising by 80 million a year, and with it the demand for new sources of fresh water.

Wealthy countries are by no means immune. In arid parts of the United States and many other countries, groundwater resources are already dwindling, and supplies that remain are becoming increasingly brackish. Environmental concerns have drastically limited the building of new dams in recent decades. In many areas, "we are already wringing all the water out of the systems that they have," says Thomas Hinkebein, a geochemist at Sandia National Laboratories in Albuquerque, New Mexico. "[We] have to start developing new sources of water."

Such concerns have made desalination—the process of removing salts and suspended solids from brackish water and seawater—a fast-growing alternative. According to a 2004 report by the U.S. National Research Council, more than 15,000 desalination plants now operate in more than 125 countries, with a total capacity of turning out 32.4 million cubic meters (m^3) of water a day, about one-quarter of the amount consumed by U.S. communities each year. With numerous areas around the globe facing long-term severe water shortages, "I don't see [the demand for desalination] slowing down any," says Michelle Chapman, a physical scientist at the U.S. Bureau of Reclamation in Denver, Colorado, and co-chair of a desalination research program funded by the U.S. Office of Naval Research.

But desalination faces its own problems. The two technologies at the heart of conventional desalination plants—evaporation and reverse osmosis (RO), which involves pushing water through a semipermeable membrane that blocks dissolved salts—both require huge amounts of energy. A typical seawater RO plant, for example, requires 1.5 to 2.5 kilowatt-hours (kWh) of electricity to produce 1 m^3 of water; a thermal distillation plant sucks up to 10 times that amount. Countries such as Saudi Arabia may be able to afford to run such facilities, but for most other countries, the cost was already too high even before oil prices went through the roof.

Yet despite those worrisome trends, the prospects for desalination have brightened considerably in the past few years. New engineering designs have slashed the cost of desalination plants, particularly membrane-based RO systems, and new technologies as

CREDIT: IDE TECHNOLOGIES

High flow. This reverse-osmosis plant in Ashkelon, Israel, will eventually turn out 100 million cubic meters of fresh water a year.

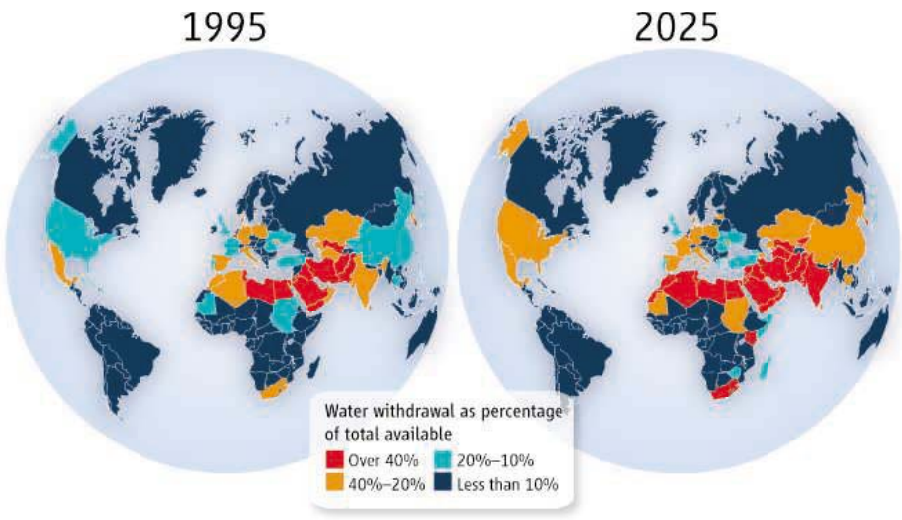

Stressed out. Spreading water shortages underscore the need for new solutions.

diverse as nanotechnology and novel polymers are expected to drive down operating costs in the years ahead. "There is a huge body of research going on," says Hinkebein, who also oversees a broad collaboration on charting a future road map for desalination technology. "Progress has been a bit incremental for a number of years," adds Anne Mayes, a materials scientist and membrane specialist at the Massachusetts Institute of Technology (MIT) in Cambridge. "But now new opportunities are starting to open up. We're going to see some very different technologies being developed in the near future."

Faster, cheaper, better

Desalination has ancient roots. Aristotle and Hippocrates described the process of evaporating salt water to make fresh water in the 4th century B.C.E. In modern times, desalination kicked into gear in the early 20th century. By the mid-1950s, hundreds of desalination plants were on line. Most were based on evaporation, a technique that continues to turn out about half of the globe's desalinated water. Although typically more expensive, the technique remains popular in the Middle East, largely because it is well-suited for dealing with the high levels of salts and suspended solids in the water of the Persian Gulf.

Elsewhere, most new plants being built today use RO because the process requires far less energy. As its name implies, the technology reverses the process of osmosis: the natural tendency of water molecules to flow through a semipermeable membrane to dilute a chemical solution on the other side, in this case seawater. To force water molecules to travel the other way requires pressure—at least 3 megapascals (MPa), but more typically 6 MPa—which in turn requires electricity. Historically, an RO plant has used 10 to 15 kWh of electricity to produce 1 m^3 of fresh water.

Between 1980 and 2000, improvements in pumps and other equipment in RO plants dropped the amount of energy needed to produce fresh water by about half, says John MacHarg, CEO of the Affordable Desalination Coalition (ADC), a San Leandro, California–based group of 22 municipalities, state agencies, and desalination companies looking to improve seawater desalination technology. Since 2000, energy requirements have again dropped by about half, thanks to new energy-recovery devices called isobaric chambers that redirect pressure from the waste brine to low-pressure incoming water. These devices recover up to 97% of the energy. Their resounding success has already made them an integral part of the newly designed desalination plants. In one such plant, which started up last fall in Ashkelon, Israel, for example, isobaric chambers have helped lower the cost of desalinated water to $0.527 cents per m^3, among the cheapest ever by a desalination facility.

Such price drops are now widely expected to continue. By combining energy-recovery devices with new low-pressure membranes and other commercially available advances, this spring ADC members set a new world record for low-cost desalination, dropping the energy needed to 1.58 kWh per m^3 of water produced. At that rate, a seawater desalination plant could supply a typical U.S. household with fresh water for the amount of power needed to light an 80-watt light bulb, MacHarg says. That figure, he adds, could change the equation of how to supply places such as southern California with water, because it takes the same amount of energy to pump freshwater from northern California to Los Angeles.

Juggling act

Still, MacHarg and others say there is plenty of room for improvement, particularly with the membranes at the heart of RO systems. "Basically, [membrane] technology hasn't changed much in the last 40 years," says Thomas Mayer, a desalination expert at Sandia. "The polymer films are fairly standard nylon-type materials that work reasonably well."

These membranes need to accomplish two somewhat contradictory goals at the same time: They must allow water to flow through at a high rate while blocking nearly all dissolved salts. Conventional membranes are made of plastics called aromatic polyamides, which prevent 99.9% of salt ions from passing through but still allow a reasonable flux of water. The plastics can strike the balance because they contain charged chemical groups that repel salt ions, while under high pressure the neutral water molecules actually dissolve into the continuous membrane sheet and pass through to the other side.

The aromatic polyamides were initially so much better than their predecessors that researchers have only recently begun to look for ways to improve them, says Benny Freeman, a polymer chemist at the University of Texas (UT), Austin. They do have big drawbacks: They require high pressure, and therefore energy, to push the water through, and they are also prone to biofouling, in which thin films of organic material coat the surface of the membrane and block water from going through.

One simple way to stop fouling is to add chlorine, much as municipal water treatment plants do to fight pathogens. Unfortunately, chlorine attacks the nitrogen-hydrogen bonds that hold polyamide polymers together, opening holes that allow salts to wiggle through the membranes. So Freeman's group, in conjunction with chemist James McGrath of Virginia Polytechnic Institute and State University (VT) in Blacksburg, has recently begun developing new chlorine-resistant polymers. The researchers have designed membranes made of sulfonated polysulfones, which lack the vulnerable N-H bonds that chlorine attacks. Other researchers had previously tried to add sulfonated groups to membrane polymers after the polymers were already made, McGrath says, an approach that made them difficult to reproduce, and they often degraded quickly. Instead, the UT-VT team created sulfonated polymer building blocks that they then linked together in a more tightly controlled manner.

SOURCE: WORLD METEOROLOGICAL ORGANIZATION; GLOBAL ENVIRONMENT OUTLOOK, UNEP

The strategy seems to be working. In May at a meeting of the North American Membrane Society in Chicago, Illinois, Freeman reported that the UT-VT group's new membranes transmit more water than traditional aromatic polyamides do while screening 99% of the salt ions. Whereas conventional membranes begin to break down after 8000 hours of exposure to chlorinated water, the new membranes show no signs of decay—meaning it may be possible to make membranes that don't have to be replaced. Freeman and his team are now tweaking the formula for the plastic in hopes of improving the 99% salt-rejection figure.

Mayes is taking a different tack to improve desalination membranes. Her group at MIT creates membranes from polymer molecules reminiscent of tiny combs. In this case, the combs' "backbone" is made up of water-fleeing molecules such as polyvinylidene fluoride (PVF), a common membrane component. Attached to this backbone are myriad "teeth" composed of short water-attracting polyethylene oxide (PEO) segments. As the polymer forms, these two different segments try to separate from one another, just as the water-fleeing and water-loving properties of oil and water cause them to separate. The result is that the PEO segments circle around one another, creating an array of tiny 2-nanometer-diameter pores in the PVF membrane.

The resulting membranes pass water with a very high flux. They also resist fouling, because the PEO units bind with water molecules so strongly that they give biomolecules few handholds to attach themselves to.

For now, however, the pores are still big enough that salt ions readily flow through. The membranes could still be useful as pretreatment filters to remove larger suspended solids before the water is sent to the RO filter, Mayes says. But she hopes to improve their salt-trapping ability, either by adding charged groups to the backbone portion of the molecules to repel charged ions or by shortening the PEO side chains to make the pores smaller.

Olgica Bakajin, a physicist at Lawrence Livermore National Laboratory in California, is also looking to tiny pores to improve her team's membranes. Bakajin and her colleagues have spent years studying how fluid moves through nano-sized devices. Their calculations showed that water would likely whisk quickly through the smooth, hollow centers of carbon nanotubes, each of which is only 1 or 2 nanometers across. So they decided to make a filter from an array of 89 tiny membranes, each 50 micrometers on a side and consisting of a silicon nitride film

Double duty. A pilot project at a California power plant purifies seawater used for cooling.

perforated by thousands of carbon nanotubes. In a paper published in the 19 May issue of *Science* (p. 1034), Bakajin and her team reported that it took only a single atmosphere of pressure (or 100 kPa) to get water to cross their membranes, although in this case they were tested with fresh water rather than salt water. "We thought our membrane had ruptured," Bakajin says. But it hadn't, and when they studied their pores in detail, they found that they were transporting 1000 times more water than expected.

Sandia's Mayer says he is "very excited" about the new result: "We're sorry we didn't do it first." Bakajin acknowledges that she and her colleagues still don't know why nanotubes are such good water transporters. But if carbon nanotube–based membranes can be scaled up and made to exclude salts—both of which are big unknowns at this point—it could enable desalination facilities to sharply reduce the amount of energy required to purify water.

Other low-energy desalination techniques are also on the horizon. In one, called forward osmosis, researchers try to harness normal osmotic pressure for making freshwater. They start with freshwater and seawater separated by a membrane and spike the freshwater side with a high concentration of sugar. Freshwater flows through the membrane as it works to dilute the high sugar concentration. "The problem is that you end up with sweetened water," says Menachem Elimelech, an environmental engineer at Yale University. In place of sugar, Elimelech and colleagues have been experimenting with dissolved ammonium salts, such as ammonium bicarbonate. The salts draw fresh water through the membrane without the need for added pressure. Then, by heating the solution to 58°C, Elimelech's team causes the dissolved salts to form ammonia and carbon dioxide gases, which are easily separated from the water. "If we can use waste heat, the process can be very economical," Elimelech says.

Two other technologies are also looking to waste heat and very cheap starting materials to make easily affordable desalination systems. One, dubbed "dewvaporation," is the brainchild of James Beckman, a chemical engineer at Arizona State University, Tempe. The other, called membrane distillation, has been pioneered by Kamalesh Sirkar, a chemical engineer at the New Jersey Institute of Technology in Newark. Beckman's dewvaporation apparatus vaporizes water in one compartment, sending it over a barrier to another where it condenses; Sirkar's membrane distillation passes the water vapor through pores in a membrane that liquid water or larger ions cannot traverse. Both processes are well on their way to proving themselves in the real world. Sirkar's membrane-distillation system is now being put through its paces by United Technologies in East Hartford, Connecticut, and dewvaporation is being evaluated as an option to create freshwater by the city of Phoenix, Arizona.

Beckman and Sirkar say the advantage of their systems is that they can work with a variety of waste-heat sources, such as steam from industrial plants or even solar energy. That versatility could make them especially advantageous for developing countries. Chapman notes that such systems can be particularly useful as add-ons to conventional RO systems. RO plants typically convert only about 50% to 70% of salt water to fresh water and must treat and dispose of the waste brine—a costly process. Because these novel systems can potentially evaporate all the water and leave only solid salts behind, they promise to save governments a lot of money, Chapman says.

It's unclear whether such novel systems will be able to compete with industrial-scale RO and thermal desalination plants. But Chapman points out that the needs of different communities vary widely when it comes to water, depending on the quality of the water source among other factors. "All water sources are different," Chapman says. "So there will probably be a place for all of these technologies"—and no doubt plenty of thirsty users as well.

–ROBERT F. SERVICE

CREDIT: REED SAXON/AP

For news and research with impact, turn to *Science*

There's only one source for news and research with the greatest impact – *Science*. With over 700,000 weekly print readers, and millions more online, *Science* ranks as one of the most highly read multidisciplinary journals in the world. And for impact, *Science* can't be beat. According to the recently released Thomson ISI Journal Citation Report 2005, *Science* ranked as the No. 1 most-cited multidisciplinary journal with a citation factor of 31. Founded in 1880 by inventor Thomas Edison, and published by the nonprofit AAAS, *Science*'s reputation as the leading source for news, research, and leading edge presentation of content continues to grow. Looking for news and research that will impact the world tomorrow? Then look in *Science*.

www.sciencemag.org

To join AAAS and receive your own personal copy of *Science* every week go to **www.aaas.org/join**

Science
AAAS

An Aegialodontid Upper Molar and the Evolution of Mammal Dentition

Alexey V. Lopatin[1] and Alexander O. Averianov[2]

The most obvious key synapomorphy of the therian mammals is their tribosphenic dental pattern: having the lingual cusp of an upper molar (protocone) that fits into the talonid basin of its lower counterpart. The contact of protocone to talonid basin, during the final stage of tooth occlusion, acts like the pestle in a mortar, thus adding grinding function to the dentition. This feature substantially increases effectiveness of food processing and permitted evolution of a wide range of dietary specializations. Functional tribospheny developed repeatedly during mammalian evolution (*1*) but was successful only in the Boreosphenida (Theria plus proximal relatives). The earliest stage in the development of boreosphenidan tribospheny has remained poorly understood, being documented only by lower molars of Early Cretaceous Aegialodontidae (*2*–*4*), which have a distinct, albeit small talonid basin and two or three talonid cusps. Notably, not a single upper molar of aegialodontid or related mammal has been known, and the critical stage of development of tribospheny, namely the appearance of the protocone, has remained undocumented by fossils. In a hypothetical reconstruction of an aegialodontid upper molar (*5*), the presence of the protocone was inferred from presence of an additional wear facet 5 in the talonid basin of *Aegialodon*. Here, we describe the aegialodontid upper molar (possibly M2), which confirms the presence of a distinct protocone in this group.

The specimen (Fig. 1, A to C) was collected from the Aptian-Albian locality Hövöör (also called Khoboor) in Mongolia by the Soviet-Mongolian Paleontological Expedition in the early 1970s. The outline of the molar forms an isosceles triangle. The labial cusps are fused at the bases, with very short and shallow centrocrista. The parastylar groove is well pronounced; the preparastyle is distinct. The postmetacrista is more transverse than the preparacrista and bears a well-developed postmetacrista cusp (cusp c). The protocone is distinct but small and very low; it is less that one-third of the paracone height. The preprotocrista and the preparacrista provide for double-rank prevallum-postvallid shearing, a distinctive synapomorphy of Boreosphenida (*1*). See Fig. 1A for the localization of wear facets; note a distinct facet 5. By crown size and relative development of the protocone, the upper molar structurally agrees with lower molars of *Kielantherium gobiense* Dashzeveg, 1975 from the same locality (*3*, *4*) and thus may be confidently referred to the same aegialodontid species.

The upper molar of *Kielantherium* is generally similar to the hypothetical upper molar of *Aegialodon* (*5*), differing mostly in having a less pronounced height differential between the paracone and metacone, more transverse postmetacrista, and lack of paraconule (Fig. 1D). Compared with *Peramus* and *Deltatheridium*, the closest relatives of *Kielantherium* with known upper dentition, the tooth is likely a M2. The upper molar of *Kielantherium* is very similar to that of *Peramus* in the labial part, but lingually it is strikingly dissimilar in having a distinct protocone. Morphologically, *Kielantherium* is truly intermediate between pretribosphenic *Peramus* and basal tribosphenic mammals like *Pappotherium*. It was proposed (*6*) that Aegialodontia are structurally ancestral to Metatheria but not Eutheria on the basis of similarity between aegialodontids and stem metatherians (Deltatheroida) in having four lower molars with similar structure. The upper molar of *Kielantherium* does not confirm this hypothesis. By having the preparastyle, it is reminiscent of early eutherians, like *Prokennalestes*, but not metatherians. Analysis of the *Kielantherium* upper molar suggests that divergence of metatherian and eutherian lineages took place on a more derived morphological stage than exemplified by *Kielantherium*.

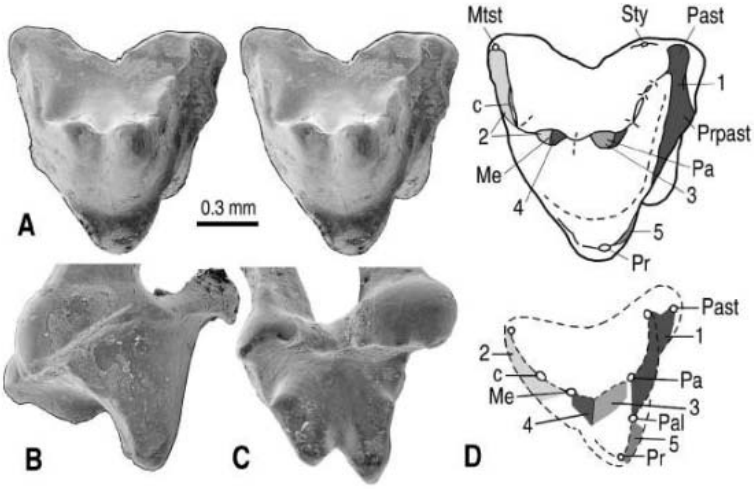

Fig. 1. (**A** to **C**) *Kielantherium gobiense* Dashzeveg, 1975, specimen PIN (Paleontological Institute, Russian Academy of Sciences, Moscow) 3101/110, right upper molar in occlusal [(A) stereopair, with explanatory drawing], anterior (B), and labial (C) views. (**D**) *Aegialodon dawsoni* Kermack *et al*., 1965, hypothetically reconstructed right upper molar [after (*5*), reversed and modified]. Abbreviations: 1 to 5 indicate wear facets 1 to 5 [after (*5*)]; c, cusp c; Me, metacone, Mtst, metastyle; Pa, paracone; Pal, paraconule; Past, parastyle; Pr, protocone; Prpast, preparastyle; Sty, stylocone.

References and Notes

1. Z.-X. Luo, R. L. Cifelli, Z. Kielan-Jaworowska, *Nature* **409**, 53 (2001).
2. K. A. Kermack, P. M. Lees, F. Mussett, *Proc. R. Soc. London Ser. B* **162**, 535 (1965).
3. D. Dashzeveg, *Nature* **256**, 402 (1975).
4. D. Dashzeveg, Z. Kielan-Jaworowska, *Zool. J. Linn. Soc.* **82**, 217 (1984).
5. A. W. Crompton, in *Early Mammals*, D. M. Kermack, K. A. Kermack, Eds. (Academic Press, London, 1971), pp. 65–87.
6. L. G. Marshall, Z. Kielan-Jaworowska, *Lethaia* **25**, 361 (1992).
7. We thank Z. Kielan-Jaworowska and R. Cifelli for reading of the manuscript and comments. Supported by the Russian Fund of Basic Research grants 04-04-49637, 04-04-49113, 04-05-64805, and 05-04-48493; President of Russia grants MD-255.2003.04 and NSH-6228.2006.4; and the Russian Science Support Foundation.

Supporting Online Material

www.sciencemag.org/cgi/content/full/313/5790/1092/DC1
Fig. S1

10 April 2006; accepted 12 June 2006
10.1126/science.1128530

[1]Paleontological Institute, Russian Academy of Sciences, Profsojuznaya ul. 123, Moscow 117997, Russia. E-mail: alopat@paleo.ru. [2]Zoological Institute, Russian Academy of Sciences, Universitetskaya nab. 1, St. Petersburg 199034, Russia. E-mail: lepus@zin.ru

Learning Induces Long-Term Potentiation in the Hippocampus

Jonathan R. Whitlock,[1,2]* Arnold J. Heynen,[1]* Marshall G. Shuler,[1] Mark F. Bear[1]†

Years of intensive investigation have yielded a sophisticated understanding of long-term potentiation (LTP) induced in hippocampal area CA1 by high-frequency stimulation (HFS). These efforts have been motivated by the belief that similar synaptic modifications occur during memory formation, but it has never been shown that learning actually induces LTP in CA1. We found that one-trial inhibitory avoidance learning in rats produced the same changes in hippocampal glutamate receptors as induction of LTP with HFS and caused a spatially restricted increase in the amplitude of evoked synaptic transmission in CA1 in vivo. Because the learning-induced synaptic potentiation occluded HFS-induced LTP, we conclude that inhibitory avoidance training induces LTP in CA1.

The phenomenon of LTP, discovered over 30 years ago in the hippocampus (*1*, *2*), has attracted enormous attention. Literally thousands of papers have been published on hippocampal LTP, all predicated on the assumption that LTP reveals an important mechanism for memory in the brain. Remarkably, however, there still has not been a direct demonstration that hippocampal LTP is actually induced by learning.

There may be several reasons why learning-induced LTP has been difficult to demonstrate in hippocampus (*3*). First, many hippocampally dependent learning tasks are iterative and so require many training trials to form a memory. Slight differences in the rate of learning across animals could smear and, therefore, obscure time-sensitive markers of LTP when averaged together. Second, the synaptic changes that underlie hippocampally dependent learning may be sparse and widely distributed, which would make potentiated synapses difficult to detect in a vast sea of unmodified connections. Third, it is now appreciated that information can be stored effectively by long-term depression (LTD), as well as by LTP (*4*). Simultaneous induction of LTP and LTD at different synapses may cancel one another when studied at a population level.

The first two problems were overcome by use of the inhibitory avoidance (IA) paradigm. IA training creates a stable memory trace in a single trial and causes substantial changes in gene expression in area CA1 of dorsal hippocampus, which suggests that this is a site of robust synaptic plasticity (*5*–*7*). The problem of simultaneous bidirectional modifications was overcome by the use of new biomarkers that can detect LTP and LTD occurring at different synapses (*8*–*10*).

Hippocampal glutamate receptors are phosphorylated after IA training. IA memory is rapidly acquired, very stable, and dependent on the hippocampus (*11*–*13*). Training consisted of allowing rats to cross from an illuminated chamber into a dark chamber where a foot shock was delivered (*14*). Memory of this experience was measured as the tendency for the animals to avoid the dark side in subsequent trials (fig. S1A). Acquisition of the avoidance response, like the phenomena of LTP and LTD, required *N*-methyl-D-aspartate (NMDA) receptor activation (fig. S1B). Control cohorts either entered the dark side without receiving a shock (i.e., "walk-through" controls) or were given a foot shock in the dark side and immediately removed from the apparatus before they could form the context-shock association (*15*, *16*) (i.e., "shock-only" controls).

The C terminus of the α-amino-3-hydroxy-5-methyl-4-isoxazolepropionic acid receptor (AMPAR) GluR1 subunit undergoes distinct phosphorylation and dephosphorylation events following LTP and LTD (*8*). Specifically, serine 831 (Ser^{831}) is phosphorylated after LTP, and Ser^{845} is dephosphorylated after LTD. These changes in phosphorylation alter the function of the AMPAR and contribute to expression of LTP and LTD. More importantly for our purposes, they "mark" synapses as having recently undergone modification and can be used to detect the occurrence of LTP and LTD, even if they occur simultaneously at different synapses.

Therefore, we dissected out the dorsal hippocampus of trained and control animals and assayed the phosphorylation state of GluR1 at Ser^{831} and Ser^{845}. Important features of our experimental design for this and subsequent biochemical experiments included the use of yoked controls (trained versus walk-through, and shocked versus naïve); particular care to be in the linear range of the immunoblot assays to detect small changes; and quantitative analysis of the immunoblots without experimenter knowledge of the experimental condition (*14*).

Although phosphorylation at Ser^{845} did not differ in trained versus walk-through animals [98.3 ± 7.7% of controls; *t* test, $P > 0.05$ (Fig. 1A)], we found an increase in phosphorylation at Ser^{831} 30 min following IA training [126.7 ± 9.4% of controls; *t* test, $P = 0.005$ (Fig. 1B)]. In contrast, no changes in phosphorylation of either site were observed in the shock-only group relative to nonshocked controls. In addition, neither Ser^{831} nor Ser^{845} phosphorylation differed between trained and control animals in samples prepared from the cerebellum.

To see if training-induced phosphorylation of Ser^{831}, like LTP and memory, requires NMDA receptor activation, additional groups of animals were injected intraperitoneally (i.p.) with (*RS*)-3-(2-carboxypiperazin-4-yl)-propyl-1-phosphonic acid (CPP; 10 mg/kg, i.p.) or saline before training. No increase in Ser^{831} phosphorylation was observed in the CPP group (92.5 ± 9.9% of controls; *t* test, $P > 0.05$), but the increase was replicated in animals given pretraining injections of saline [120.7 ± 5.7% of controls; *t* test, $P < 0.025$ (Fig. 1C)]. A time-course analysis determined that the enhancement in Ser^{831} phosphorylation peaked 30 min posttraining, but was indistinguishable from controls by 2 hours posttraining (Fig. 1G).

IA training causes delivery of AMPARs to hippocampal synaptoneurosomes. LTP is associated with the delivery of AMPARs to synapses, and LTD is associated with the removal of AMPARs from synapses (*10*). Because we saw an enhancement in phosphorylation at Ser^{831} and no decrease in phosphorylation at Ser^{845}, we hypothesized that IA training was associated with a net increase in AMPARs at synapses. Therefore, we performed immunoblot analysis of the synaptoneurosome (SNS) biochemical fraction. The SNS preparation provides a modest enrichment for synaptic proteins that is sufficient to detect trafficking of AMPARs after LTP in area CA1 of adult rats in vivo (*10*, *14*).

We found that IA-trained animals showed significantly elevated GluR1 and GluR2 protein levels in the SNS fraction relative to walk-through cohorts 30 min after conditioning [GluR1, 129.9 ± 4.9% of controls; *t* test, $P < 0.002$; GluR2, 128.1 ± 8.2% of controls; *t* test, $P < 0.04$ (Fig. 1, D and E)]. This effect was specific to AMPAR-type glutamate receptors, as we did not detect an increase in the protein levels for the NR1 subunit of NMDA receptors [102.7 ± 9.1% of controls; *t* test, $P > 0.05$ (Fig. 1F)]. Similar to the enhancement in phosphorylation at Ser^{831}, these effects were rapid and transient (Fig. 1, H and I). It is noteworthy that the increases in AMPAR protein levels were specific to associative learning (shock-only samples were 96.7 ± 10.4% of nonshocked controls; for GluR1; 93.5 ± 17.8% of controls for GluR2; *t* test, $P > 0.05$, in both cases). We did not detect

[1]Howard Hughes Medical Institute, The Picower Institute for Learning and Memory, Department of Brain and Cognitive Sciences, Massachusetts Institute of Technology, Cambridge, MA 02139, USA. [2]Department of Neuroscience, Brown University, Providence, RI 02912, USA.

*These authors contributed equally to this work.
†To whom correspondence should be addressed: mbear@mit.edu

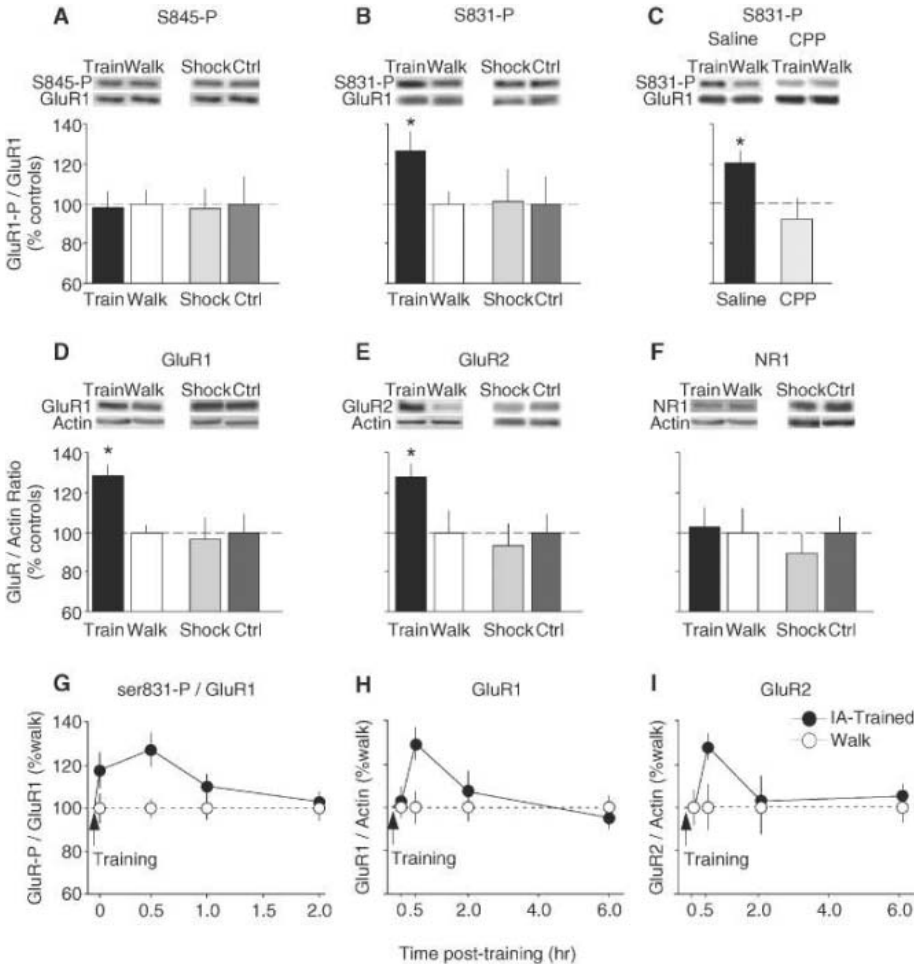

Fig. 1. IA training alters AMPAR phosphorylation and trafficking in the hippocampus. (**A**) Phosphorylation of Ser^{845} in trained animals (black bars, n = 18) and shock-only animals (light gray bars, n = 13) did not differ from yoked controls (white and dark gray bars, respectively) 30 min after conditioning, whereas (**B**) phosphorylation at Ser^{831} was elevated significantly in trained animals (n = 14), but not in shock-only controls (n = 13). Error bars indicate SEM in this and all subsequent figures. (**C**) The enhancement in Ser^{831} phosphorylation persisted in animals given pretraining injections of saline (black bar, n = 18), but was blocked by pretraining injections of CPP (light gray bar, n = 19). (**D** and **E**) Additionally, an increase in GluR1 and GluR2 protein levels in SNS was observed 30 min after IA training (n = 11 for GluR1; n = 12 for GluR2), but not in shock-only controls (n = 8). (**F**) No change was observed for NR1 in IA-trained (n = 12) or shock-only control animals (n = 8). (**G** to **I**) Time-course analyses demonstrated that training-related changes in Ser^{831} phosphorylation, GluR1 and GluR2 protein levels were rapid and transient, reaching peak values 30 min after training.

training-related changes in AMPAR protein levels in SNS prepared from the cerebellum of trained animals, nor did we detect any changes in the protein levels of GluR1, GluR2, or NR1 in crude hippocampal homogenates.

IA training produces an enhancement of field excitatory postsynaptic potential (fEPSP) slope in area CA1 in vivo. The biochemical changes in AMPARs after IA training are similar to those reported after LTP, not only in direction, but also in magnitude (*10*). This comparison suggested the possibility that we might be able to observe a change in synaptic transmission following IA training using electrophysiology.

We monitored synaptic transmission in CA1 by stimulating the Schaffer collateral axons before and after IA training, as is routinely done in LTP experiments in vivo (*14*). However, unlike an LTP experiment—which has the advantage that the affected synapses are specifically those activated by the stimulating electrode—we did not know a priori where to record changes after IA. We therefore implanted a multielectrode recording array in the apical dendritic layer of CA1 to monitor the strength of synaptic transmission evoked in different locations by stimulation of the Schaffer collateral axons (Fig. 2A).

Baseline fEPSP measurements were first obtained in freely moving animals that were well habituated to the recording box. Data collection was then temporarily suspended while the rats were given IA training, allowed to walk through the apparatus without a shock, or given the shock only. After this experience, the animals were returned to the recording box, and measurements of synaptic transmission resumed. A fourth group of animals ("naïve") remained in the recording box without being handled.

An example of the effect of IA training in one rat is shown in Fig. 2B. Note that although the fEPSP slope in the majority of channels shows a slight decrease after behavioral conditioning, two channels exhibit a substantial increase which is apparent immediately and persists for the duration of the recording session. Consequently, the average response across all channels (seven in this example) is about the same after training as before, but the between-channel variance is greatly increased.

Data from all channels in all animals in all groups are displayed in Fig. 2, C to F. In six trained animals, 12 of 44 electrodes showed increases >10% above baseline. In contrast, of the 140 electrodes comprising all of the recordings from control animals, not one showed an average fEPSP slope enhancement >10% above baseline. Comparison of the cumulative probability distributions of fEPSP slope changes from the 4 behavioral conditions confirmed a significant difference between the IA trained group and all control groups at 30 min, 1 hour, and 2 hours postconditioning [Kolmogorov-Smirnov (K-S) test, $P < 0.05$ at all time points (Fig. 2, G to I)]. Additional animals, receiving different types of experience on successive days (e.g., walk-through on day 1 followed by training on day 2), provided a within-animal comparison of the effects of different types of experience, and yielded comparable results (fig. S2).

We consistently observed a gradual decrease in the fEPSP slope in the postconditioning time period in the majority of electrodes that failed to potentiate after IA training (see Fig. 2, B and C). Thus, when data from all electrodes in all trained animals are averaged, little posttraining change is apparent relative to baseline (Fig. 3A). The postconditioning decreases in fEPSP slope over time do not appear to be a specific consequence of training, however, because they are apparent in the walk-through (Fig. 3B) and shock-only (Fig. 3C) groups. This difference between trained and control groups is particularly clear when the percentage of all channels with responses greater or less than one standard deviation (SD) from the baseline distribution is plotted against time (Fig. 3, E to G). Only in the trained group do we observe an abrupt and persistent increase in the fraction of channels with responses >1 SD above the baseline (Fig. 3E). However, gradual increases in the fraction of channels with responses >1 SD below baseline are seen in trained, walk-through, and shock-only groups (see also fig S3).

Decreases in fEPSP slope tended to occur coherently across electrodes within a given animal and correlated significantly with changes in the electroencephalogram (EEG) [theta/delta

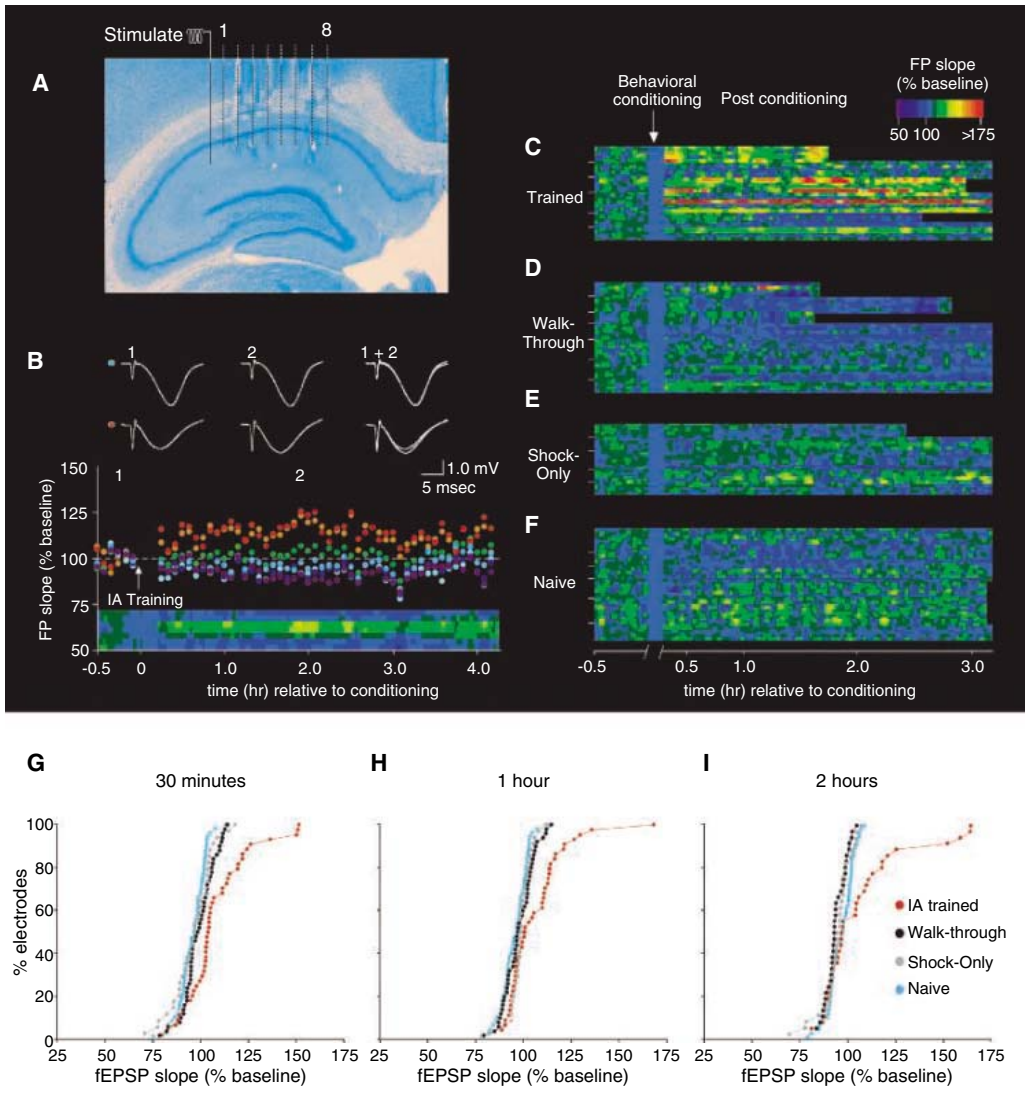

Fig. 2. IA training results in an enhancement of fEPSPs in area CA1 of the hippocampus in vivo. (**A**) Multielectrode recording arrays consisting of eight electrodes were implanted into CA1 of dorsal hippocampus. The Nissl-stained coronal section demonstrates electrode placement in the apical dendritic layer of CA1 (exact recording depths for five of eight electrodes are marked by lesions at electrode tips). (**B**) fEPSP slope measures collected every 30 s (displayed as averages of 5-min bins) from a single animal showing learning-related fEPSP enhancements after IA training. Two electrodes showed fEPSP enhancements ~15% above baseline (red and orange circles). fEPSP slope is represented by color on the inset beneath, where each row on the plot corresponds to individual electrodes. fEPSP waveforms (above) were obtained (top) from an electrode that did not show a training-related enhancement in slope, and (bottom) from an electrode where a 14% enhancement was observed. (**C** to **F**) Color plots representing fEPSP slope measures taken from six trained animals, seven walk-through controls, five shock-only controls, and six naïve controls; white tick-marks indicate individual animals in each group. Each animal was naïve at the time of behavioral conditioning (inclusion of additional animals receiving more than one type of experience appears in fig. S2). Of 44 recording electrodes, 12 showed average fEPSP slope measures >10% above baseline after IA training, although none of the 140 electrodes from control conditions showed such enhancements. Warmer colors indicate fEPSP slope enhancements; cooler colors represent decreases. (**G** to **I**) Cumulative probability distributions of fEPSP slope for IA-trained (red circles, $n = 44$ electrodes), walk-through (black circles, $n = 50$ electrodes), shock-only (light gray, $n = 35$ electrodes), and naïve animals (blue, $n = 55$ electrodes) demonstrate that fEPSP slope measures were enhanced in trained animals relative to controls (K-S test, $P < 0.05$) at 30 min, 60 min, and 120 min.

ratio (*17*); see fig. S4]. We also noted that of the four groups studied, naïve animals—which are not handled during the recording session—showed the least tendency for gradual reductions in fEPSP slope (Fig. 3, D and H). Thus, we interpret the coherent decreases in fEPSP slope as reflecting changes in the behavioral state of the animals over the duration of the recording experiments. However, we cannot rule out the possibility that LTD-like changes also contribute.

Although changes in fEPSP slope that happen coherently across multiple electrodes within an animal may result from changes in brain state, changes recorded at some electrodes but not others must be accounted for by local modifications. Therefore, we calculated the standard deviation of fEPSP slope measures across electrodes within individual animals before and after conditioning. In the naïve group, which remained unhandled in the recording box for 4 hours, the average within-animal variance increased by 43% over the duration of the recording session (Fig. 3L). Comparable values were seen in the walk-through (58% increase) and shock-only (35% increase) conditions (Fig. 3, J and K). However, the average within-animal variance increased to 256% of the baseline interval in IA-trained animals [significantly greater than controls; one-way ANOVA, $F(3,124) = 14.98$, $P < 0.0001$ (Fig. 3I)]. Because increased variability in evoked responses did not correlate with increased across-channel variability in the spontaneous EEG (see fig. S5), we conclude that a specific consequence of IA training is a spatially heterogeneous potentiation of synaptic transmission in some, but not all recording locations in dorsal CA1. Such changes are consistent with theoretical proposals for the structure of distributed associative memories (*18*).

Learning-related enhancements of fEPSP slope occlude subsequent LTP in vivo. The spatially restricted increases in fEPSP slope after IA training were not associated with local changes in the power spectrum of the spontaneous EEG (fig. S6), and were not accompanied by changes in paired-pulse ratio (fig. S7)—changes that might be expected if highly localized changes in temperature were responsible (*19*), rather than LTP. However, the most incisive approach to address the question of whether the modification we observe reflects LTP is to see if the learning-induced change occludes tetanus-induced potentiation.

Therefore, we trained an additional group of animals and compared changes in fEPSP slopes after training with the subsequent enhancements induced by repeated application of high-frequency stimulation (HFS) to saturate LTP. We found a significant inverse correlation

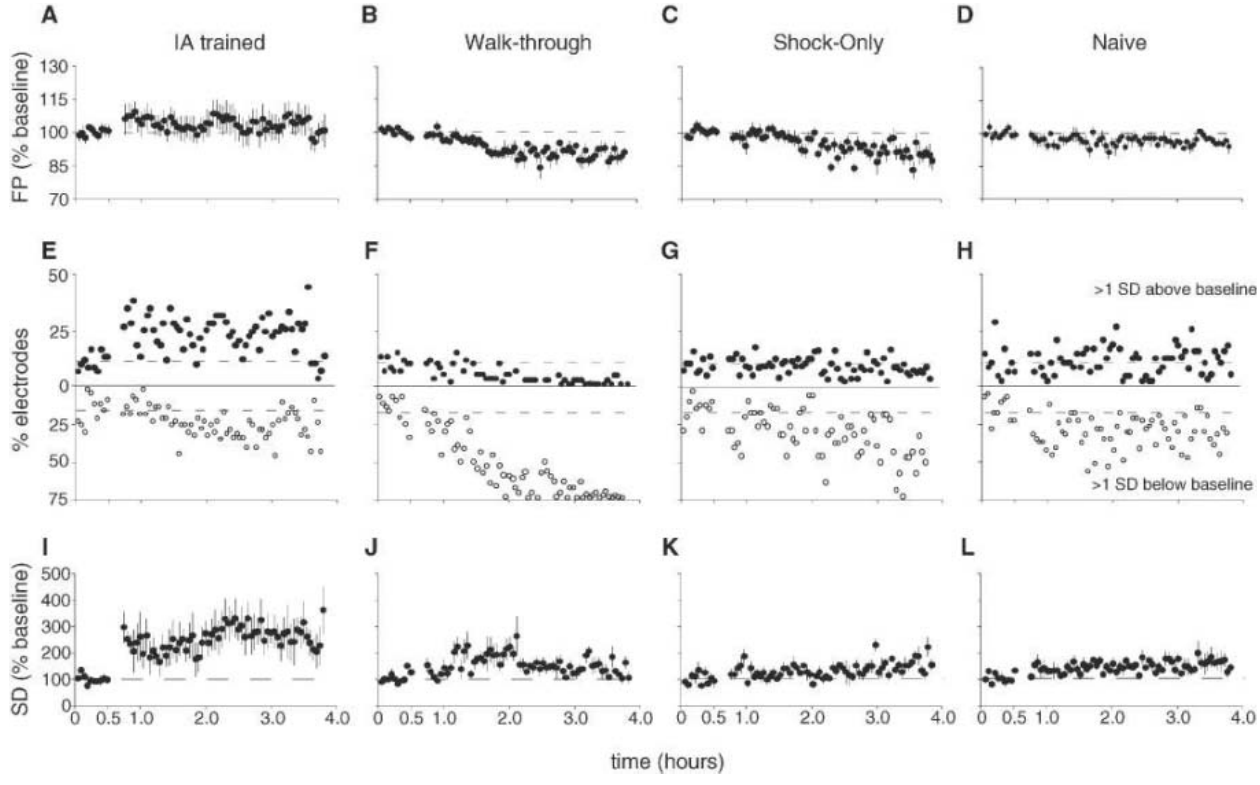

Fig. 3. Learning-related enhancements in IA-trained animals are obscured in group fEPSP averages, but are revealed by analyses of the distribution of responses. (**A** to **D**) Effect of experience on means ± SEM of all electrodes in all animals normalized to baseline. Because IA training affected a subpopulation of electrodes, the group average for fEPSP slope remained within 5% of the preconditioning baseline after IA training (A), whereas average fEPSP slope measures declined over time postconditioning in the walk-through, shock-only, and "naïve" conditions (B to D). (**E** to **H**) Effect of experience on the fraction of electrodes with responses greater or less than 1 SD of the baseline distribution. About 16% of electrodes show responses >1 SD during baseline. However, after training 33.2% of 44 electrodes had fEPSP slope values >1 SD above the baseline distribution [(E), filled circles], whereas fEPSP slope in electrodes from control groups did not increase. The percentage of channels >1 SD below baseline (open symbols) increased over time in all groups (F to H). (**I** to **L**) Within-animal variation in responses across electrodes. Plotted are the mean across-electrode standard deviations (±SEM), normalized to the baseline values. Variability in fEPSP slope measures across electrodes increased to more than 250% of the baseline mean after IA training (I), whereas variability remained within ~60% of the baseline mean for controls (J to L). Each animal included in this analysis was naïve at the time of behavioral conditioning (inclusion of additional animals receiving more than one type of experience appears in fig. S3).

between the amount of behaviorally induced potentiation and the amount of LTP induced by HFS—that is, electrodes where fEPSPs were enhanced after IA showed less subsequent LTP in response to HFS, whereas electrodes that did not exhibit enhancements of fEPSPs after IA training showed a greater magnitude of subsequent LTP [$R = 0.41$, $P < 0.01$ (Fig. 4A)]. This finding contrasts with the expected correlation of initial fEPSP size and LTP magnitude [which reflects cooperativity; see fig. S8 and (*20*)].

The occlusion of LTP by learning can also be illustrated by comparing the time course of average LTP in those electrodes that expressed a >10% training-induced increase in fEPSP slope with those electrodes (in the same animals) that did not (Fig. 4B). Electrodes showing fEPSP enhancements after training had significantly less subsequent LTP (121.1% of renormalized, pre-HFS baseline) than "control" electrodes [136.1%; repeated measures ANOVA, group × time interaction, $F(3,42) = 3.61$, $P < 0.025$; Fisher's protected least significant difference (PLSD) for final HFS epoch, $P < 0.02$]. Furthermore, LTP in IA-enhanced electrodes saturated after the first series of HFS, whereas LTP in "control" electrodes did not saturate until after the second series of HFS (Fig. 4B), which indicated that electrodes showing learning-related fEPSP enhancements were closer to their ceiling for LTP expression before HFS delivery. Importantly, the two groups of electrodes did not differ in their total capacity for LTP expression when the data were expressed as a percentage of the pre-IA training baseline [ANOVA, $F(3,42) = 0.36$, $P > 0.55$].

Discussion. LTP induced in hippocampal area CA1 by HFS of the Schaffer collaterals has properties that have made it the premiere model to study possible memory mechanisms (*21*, *22*). It is induced rapidly by stimulation that appears physiological; it has properties that enable association of temporally contiguous events; and it can be very stable over time (*23*, *24*). Strictly speaking, however, LTP is a "memory" only of having one's brain electrically stimulated. Proving that hippocampal LTP actually reveals the mechanisms of memory therefore remains an important goal (*3*).

Two criteria must be fulfilled to conclude that two events induce a change by a common mechanism: mimicry and occlusion. Here we have shown that IA training mimics the effects of HFS by causing (i) an immediate, NMDA receptor–dependent increase in phosphorylation of GluR1 at Ser^{831} without affecting phosphorylation of GluR1 at Ser^{845}; (ii) delivery of GluR1 and GluR2, but not NR1, to the synaptoneurosome biochemical fraction; and (iii) an increase in the slope of the evoked fEPSP without affecting paired-pulse facilitation. We have also shown that IA-induced increases in the evoked fEPSP partially occlude subsequent LTP by HFS in vivo. We therefore conclude that IA training induces LTP in CA1.

Biochemical changes after IA reported here and in several previous studies (*6*, *25*–*28*) are of the same type and magnitude as those seen after HFS in dorsal hippocampus. However, unlike memory (fig. S1), the changes in AMPARs observed in our study were no longer detectable hours after training (Fig. 1). Perhaps the LTP-like change in synaptic transmission in CA1 is

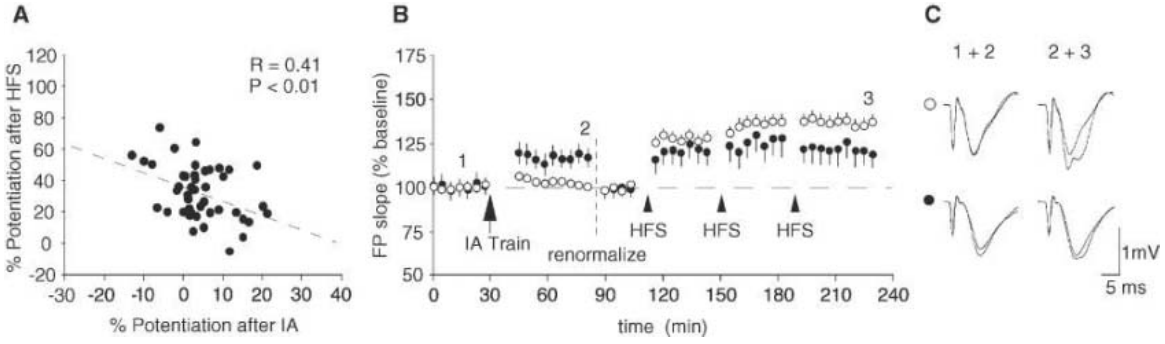

Fig. 4. Learning-associated fEPSP slope enhancements occlude subsequent LTP in the hippocampus of freely behaving animals. (**A**) An inverse correlation was observed between the magnitude of fEPSP slope enhancements after IA training and the magnitude of subsequent LTP in vivo (R = 0.41, $P < 0.01$). (**B**) Of 44 recording electrodes, nine from seven animals were enhanced by >10% above pretraining baseline; the average enhancement was 16.5% above baseline (black circles). Electrodes not showing a training-related enhancement of fEPSP slope ("control" electrodes) averaged 2.4% above pretraining baseline (open circles). LTP was saturated after the first HFS series in electrodes showing learning-related fEPSP enhancements (Fisher's PLSD for HFS 1 versus HFS 2, $P > 0.50$), whereas "control" electrodes showed additional potentiation after the second HFS series (Fisher's PLSD for HFS 1 versus HFS 2, $P = 0.012$). Furthermore, electrodes showing fEPSP enhancements after IA training showed less LTP than control electrodes after the final series of HFS (121.1 versus 136.1%, respectively; Fisher's PLSD, $P < 0.02$). Data from the last 30 min of each epoch was used for statistical comparisons. (**C**) Representative fEPSP traces taken from two electrodes in the same animal before IA training (1), after training (2), and after LTP saturation (3).

only transient. Arguing against this possibility, however, is the direct observation that fEPSPs on some electrodes remained potentiated for ≥3 hours after IA. Another possibility is that the expression mechanism for LTP shifts to the presynaptic side of the synapse over time. Arguing against this hypothesis, however, is the finding that paired-pulse facilitation in potentiated channels remains unaffected >75 min after training (see fig. S7). A third possibility suggested by inspection of the cumulative probability distributions in Fig. 2 and fig. S2 is that the fraction of synapses enhanced relative to the control conditions is winnowed over time. Although some electrodes continue to show a substantial and stable enhancement after 2 hours, this residual, spatially restricted change may be below our biochemical detection threshold.

Experience-dependent changes in evoked responses have been reported previously in the hippocampus (*19*, *29*–*33*). A potential complication in interpreting all such findings, including ours, is that experience can also alter temperature in the hippocampus (via changes in blood flow) which, in turn, alters the properties of synaptic transmission (*34*–*36*). However, there are several reasons that this is an unlikely explanation for our results. First, the potentiation observed after IA is highly local, restricted to a subset of recording electrodes. Second, another physiological measure that is sensitive to temperature, the paired-pulse ratio (*36*), was unchanged at electrodes showing potentiation (fig. S7). Third, and perhaps most definitively, electrodes showing learning-induced increases in fEPSP slope displayed less HFS-induced LTP, which would not be expected if brain temperature were raised.

Less LTP has also been reported in hippocampal slices ex vivo after contextual fear conditioning (*37*). Although this finding is consistent with the hypothesis that learning induces LTP in vivo, an equally plausible explanation is that conditioning causes a generalized inhibition of plasticity in the hippocampus. Our experiments discriminate between these possibilities by showing in the same animal in vivo that the effect of learning on LTP is restricted to those regions that display synaptic potentiation after learning. Such a localized occlusion of LTP by learning is strong evidence that IA and HFS increase synaptic transmission in CA1 by a common mechanism.

A recent report of contemporaneous experiments in mice indicates that another type of aversive associative memory—trace eye-blink conditioning—also causes a detectable (apparently more global) increase in synaptic transmission in CA1 and that induction of LTP by HFS of the Schaffer collaterals during conditioning disrupts memory formation (*33*). Although it has not yet been formally established that trace conditioning induces LTP per se, it is noteworthy that this type of learning is also sufficient to produce increases in hippocampal synaptic transmission large enough to be detected. Perhaps LTP is so robust in CA1 because it plays a special role in formation of memories used to avoid or anticipate danger. More subtle bidirectional modifications might be reserved for memories less basic to survival.

References and Notes

1. T. Lomo, *Philos. Trans. R. Soc. London Ser. B* **358**, 617 (2003).
2. T. V. Bliss, T. Lomo, *J. Physiol.* **232**, 331 (1973).
3. S. J. Martin, P. D. Grimwood, R. G. Morris, *Annu. Rev. Neurosci.* **23**, 649 (2000).
4. M. F. Bear, *Proc. Natl. Acad. Sci. U.S.A.* **93**, 13453 (1996).
5. S. Impey *et al.*, *Nat. Neurosci.* **1**, 595 (1998).
6. S. M. Taubenfeld, K. A. Wiig, M. F. Bear, C. M. Alberini, *Nat. Neurosci.* **2**, 309 (1999).
7. S. M. Taubenfeld *et al.*, *J. Neurosci.* **21**, 84 (2001).
8. H. K. Lee, M. Barbarosie, K. Kameyama, M. F. Bear, R. L. Huganir, *Nature* **405**, 955 (2000).
9. H. K. Lee, K. Kameyama, R. L. Huganir, M. F. Bear, *Neuron* **21**, 1151 (1998).
10. A. J. Heynen, E. M. Quinlan, D. C. Bae, M. F. Bear, *Neuron* **28**, 527 (2000).
11. R. L. Isaacson, W. O. Wickelgren, *Science* **138**, 1104 (1962).
12. I. Izquierdo *et al.*, *Behav. Neural Biol.* **58**, 16 (1992).
13. C. A. Lorenzini, E. Baldi, C. Bucherelli, B. Sacchetti, G. Tassoni, *Brain Res.* **730**, 32 (1996).
14. Materials and methods available as supporting online material.
15. M. S. Fanselow, *Learn. Motiv.* **17**, 16 (1986).
16. M. S. Fanselow, *Anim. Learn. Behav.* **18**, 264 (1990).
17. K. Louie, M. A. Wilson, *Neuron* **29**, 145 (2001).
18. D. Marr, *Philos. Trans. R. Soc. London Ser. B* **262**, 23 (1971).
19. E. I. Moser, *Behav. Brain Res.* **71**, 11 (1995).
20. B. L. McNaughton, R. M. Douglas, G. V. Goddard, *Brain Res.* **157**, 277 (1978).
21. T. V. Bliss, G. L. Collingridge, *Nature* **361**, 31 (1993).
22. T. V. Bliss, G. L. Collingridge, R. G. Morris, *Philos. Trans. R. Soc. London Ser. B* **358**, 607 (2003).
23. R. G. Morris *et al.*, *Philos. Trans. R. Soc. London Ser. B* **358**, 773 (2003).
24. W. C. Abraham, J. M. Williams, *Neuroscientist* **9**, 463 (2003).
25. M. Cammarota *et al.*, *Neurobiol. Learn. Mem.* **64**, 257 (1995).
26. M. Cammarota, R. Bernabeu, I. Izquierdo, J. H. Medina, *Neurobiol. Learn. Mem.* **66**, 85 (1996).
27. M. Cammarota, R. Bernabeu, M. Levi De Stein, I. Izquierdo, J. H. Medina, *Eur. J. Neurosci.* **10**, 2669 (1998).
28. L. R. Bevilaqua, J. H. Medina, I. Izquierdo, M. Cammarota, *Neuroscience* **136**, 397 (2005).
29. D. J. Weisz, G. A. Clark, R. F. Thompson, *Behav. Brain Res.* **12**, 145 (1984).
30. P. E. Sharp, B. L. McNaughton, C. A. Barnes, *Brain Res.* **339**, 361 (1985).
31. B. L. McNaughton, C. A. Barnes, G. Rao, J. Baldwin, M. Rasmussen, *J. Neurosci.* **6**, 563 (1986).
32. E. J. Green, B. L. McNaughton, C. A. Barnes, *J. Neurosci.* **10**, 1455 (1990).
33. A. Gruart, M. D. Munoz, J. M. Delgado-Garcia, *J. Neurosci.* **26**, 1077 (2006).
34. E. Moser, I. Mathiesen, P. Andersen, *Science* **259**, 1324 (1993).
35. C. A. Erickson, B. L. McNaughton, C. A. Barnes, *Brain Res.* **615**, 275 (1993).
36. P. Andersen, E. I. Moser, *Hippocampus* **5**, 491 (1995).
37. B. Sacchetti *et al.*, *Eur. J. Neurosci.* **15**, 143 (2002).

38. This project was supported by the Howard Hughes Medical Institute and the National Institute of Mental Health. We thank E. Sklar, K. Clayton, K. Miller, M. Linden, and S. Meagher for assistance and M. Wilson for helpful discussion.

Supporting Online Material

www.sciencemag.org/cgi/content/full/313/5790/1093/DC1
Materials and Methods
Figs. S1 to S8
References

30 March 2006; accepted 30 June 2006
10.1126/science.1128134

Superfluidity of Grain Boundaries and Supersolid Behavior

S. Sasaki,[1]* R. Ishiguro,[1]† F. Caupin,[1] H. J. Maris,[1,2] S. Balibar[1]*

When two communicating vessels are filled to a different height with liquid, the two levels equilibrate because the liquid can flow. We have looked for such equilibration with solid ^{4}He. For crystals with no grain boundaries, we see no flow of mass, whereas for crystals containing several grain boundaries, we detect a mass flow. Our results suggest that the transport of mass is due to the superfluidity of grain boundaries.

The principle of communicating vessels states that if a vertical open tube is half-immersed in a liquid bath, the liquid levels inside and outside the tube equilibrate to a common height. If the top of the tube is closed, the pressure (P) above the liquid can be different inside and outside the tube, causing the levels to stay at different heights. This observation was used by Evangelista Torricelli to devise the first barometer in 1643. Furthermore, if all of the air surrounding the setup is removed, then the liquid is in equilibrium with its vapor at a well-defined P (the saturated vapor pressure), and the difference in height (h) vanishes. We have performed a similar experiment with ^{4}He at its liquid/solid equilibrium. We found that hydrostatic equilibrium can be achieved via frictionless mass flow through the solid. These results provide further evidence for the "supersolid" behavior reported by Kim and Chan (KC) (*1*, *2*) and now confirmed by three other experimental groups (*3*–*5*). However, we have shown that mass transport probably takes place within superfluid grain boundaries (GBs) (*6*) and is quite different from the scenario of Bose-Einstein condensation of vacancies proposed by others (*7*–*10*).

KC studied a torsional oscillator filled with solid ^{4}He and determined that 1% of their sample mass was superfluid below 50 mK because it decoupled from the oscillations of its container (*1*, *2*, *11*). They called this phenomenon supersolidity, but its interpretation remains controversial (*3*, *6*, *12*–*16*). In particular, other work (*3*) has found that supersolid behavior was no longer observed when their crystals were annealed for 10 hours between 1.4 and 1.5 K. In (*3*), it was concluded that crystal defects are essential for the existence of supersolidity, although KC did not observe any effect of annealing. After KC's observations, another study looked for mass flow inside porous Vycor glass filled with solid ^{4}He (*17*) but found no mass flow at low temperature. This experiment was perhaps sensitive to the pinning of the lattice to the side walls. Although lattice pinning was probably not as important in a follow-up experiment in which the geometry of the setup was more open (*18*), we decided to look for mass flow in a large tube and in a situation where no lattice deformation was necessary.

In our experiment, we partially filled a glass test tube (inner diameter D = 1 cm) with solid ^{4}He grown from liquid ^{4}He (Fig. 1) and observed it with a charge-coupled device camera through the windows of a cryostat (Fig. 2). We started with a configuration where the liquid/solid interface inside the tube was higher than outside. If mass can flow through the solid, gravity drives the system to the equilibrium state where both interfaces are at the same level. This is because thermal effects are negligible (*19*–*21*). Furthermore, the crystal cannot slip against the wall tube because it is blocked by the geometry of the setup (*22*, *23*). The levels can move only by local crystallization and melting, with the lattice being immobile. However, because the solid density (ρ_C) is 10% higher than the liquid density (ρ_L) (*24*), relaxation requires mass flow from the liquid inside the tube to the liquid outside. If the top of the tube were open, mass transport through the bulk liquid would be very efficient and, because the liquid/solid interface is very mobile at low temperature, the levels would relax with a very short time constant (0.2 μs at 50 mK) (*25*). But the top of the tube is closed, and the relaxation is limited by the resistance to mass flow through the solid. As we shall see, there is no substantial mass flow along the glass/helium interface in our experiment.

Although a similar experiment provided a negative result (*26*), the crystal relaxation in that experiment required crystal growth into a narrow space. During growth, crystals are usually faceted, and facets are easily pinned by surface defects (*25*). In our case, the crystal has to melt inside the tube, so that facets disappear.

To prepare solid ^{4}He inside the tube, the pressure outside the tube needs to be much higher than inside. To satisfy this condition, for 4 to 10 s the melting pressure (P_m) was 25.7 bars at 1.3 K inside the tube and 26 bars at 1.4 K outside the tube (*24*). This could be achieved during growth by temporarily increasing the flow rate into the cell through its fill line. This procedure was repeated several times in order to solidify most of the helium inside the tube. Each time, the crystal grew at a speed in the

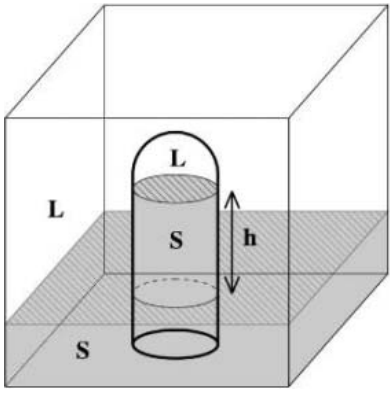

Fig. 1. A schematic of a 1-cm-diameter test tube partly filled with solid helium (S) in contact with liquid helium (L) above. After preparing the liquid/solid interface (hatched area) at a higher level inside the tube than outside (distance represented by h), we observed a relaxation to the same level on both sides of the tube if a continuous path along GBs connected these two regions.

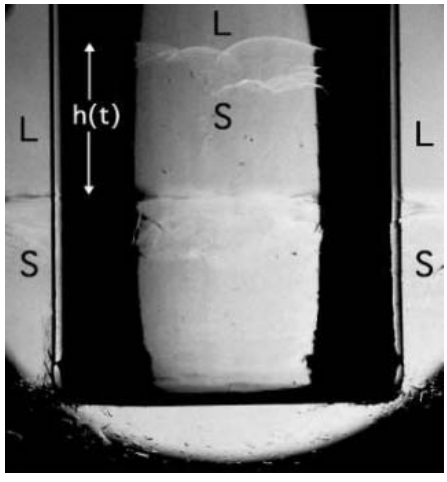

Fig. 2. Photograph of solid helium prepared at 1.3 K. The interface between the liquid (L) and the solid (S) shows cusps where GBs emerge. Outside the tube, which appears black because of refraction effects, the interface is lower than inside by $h(t)$. Seen on either side and in front, the interface completely surrounds the tube.

[1]Laboratoire de Physique Statistique de l'Ecole Normale Supérieure, Associé aux Universités Paris 6 et Paris 7 et au CNRS, 24 Rue Lhomond, 75231 Paris Cedex 05, France. [2]Department of Physics, Brown University, Providence, RI 02912, USA.

*To whom correspondence should be addressed. E-mail: ssasaki@lps.ens.fr (S.S.); balibar@lps.ens.fr (S.B.)
†Present address: Graduate School of Science, Osaka City University, Osaka 558–8585, Japan.

range from 0.1 to 1 mm/s and several GBs formed, as shown by the presence of cusps at the liquid/solid interface. GBs have a surface tension comparable to that of the liquid/solid interface, so mechanical equilibrium induces macroscopic cusps where GBs meet the liquid/solid interface (Fig. 2). We often observed that cusps disappeared spontaneously, with a typical time constant of 1 hour. It seems that some GBs were able to move transversely before vanishing either on side walls or at the liquid/solid interface, whereas other GBs were pinned, probably to walls, and stayed immobile. The GB motion can be driven by residual stresses in the polycrystalline samples.

After using the above method to prepare crystals, closing the fill line, cooling to 50 mK, melting the outside part of the solid by opening the fill line, and finally bringing its level to 1 cm below the level inside, we watched for a possible relaxation of the interface levels.

We studied 13 crystals, 10 of which showed no or very few cusps inside the tube 2 hours after preparation. For these crystals of good quality, we observed no relaxation. The 1-cm $h(t)$ stayed constant within 50 μm over a time (t) of 4 hours; the interface velocity (V) was less than 3.5×10^{-3} μm s^{-1}. This velocity is at least 300 times less than that expected from KC's picture, where the supersolid density (ρ_s) is 1% and the supersolid mass flows through the bulk crystal at a critical velocity $v_c = 10$ μm s^{-1}. In a tube of cross section $S = \pi D^2/4$, this would give a mass current $J = S\rho_s v_c$. J and V are related through $J = S(\rho_C - \rho_L)V$, so that the corresponding interface velocity would be $V = \rho_s v_c/(\rho_C - \rho_L) = 1$ μm s^{-1}. Our results are not consistent with simple interpretations of KC's experiment in terms of a 1% equilibrium density of vacancies forming a Bose-Einstein condensate in single crystals (*10*).

For three crystals of medium quality, we observed a definite mass transport through the solid. The relaxation of two crystals studied at 50 mK is shown (Fig. 3, crystals 1 and 2). Inside the tube, crystal 1 showed one cusp, which vanished after 1000 s. As long as this cusp was visible, the $h(t)$ between the interface level inside and outside the tube relaxed at a constant velocity (0.6 μm/s) (Fig. 3). When the cusp disappeared, the relaxation stopped. Crystal 2 showed many cusps and relaxed much faster than crystal 1. The interface moved first at 6 μm/s and reached an even more disordered region of the crystal after 500 s, where more cusps were visible and the velocity changed to 11 μm/s. Finally, $h(t)$ reached 0 and stopped. Because a viscous fluid would relax exponentially, a relaxation at constant velocity, on the contrary, is characteristic of superfluid flow at its critical velocity. At the end of the relaxation, several cusps were still visible inside the tube. The equilibrium position at $h = 0$ confirmed that the temperature difference between the two sides of the tube was negligible (*19*). We also tried to regrow the crystal inside by slowly injecting more ^{4}He through the fill line at a constant temperature, but facets developed, which blocked the growth inside.

If the interface with the glass wall is the same as for crystals of good quality, the relaxation in these two crystals should be due to superfluid flow along a thin continuous path that follows GBs across the whole solid. For crystal 1, a single path was cut after a partial relaxation. The mass flow is limited by v_c

$$v_c^{GB} = \frac{\pi D^2}{4ew}\frac{\rho_C - \rho_L}{\rho_s}V = 1.5\frac{a}{e}\frac{D}{w}\frac{\rho_C}{\rho_s}\ \text{m/s} \quad (1)$$

inside a GB that has a width w, a thickness e, and a superfluid density ρ_s; a is equal to 3 Å, which is the thickness of one atomic layer. The above result is consistent with the study of liquid films of atomic thickness adsorbed on a wall (*27*). Although these films had a free surface, similar critical velocities were found (up to 2 m/s).

Having found evidence for a direct current of mass through solid ^{4}He samples at 50 mK, the temperature at which KC first observed supersolidity, we looked for a possible temperature dependence. It is difficult to keep a single GB fixed and to study its properties as a function of temperature, but we have observed similar superflow at 1.13 K in a third crystal that had many defects. This crystal changed relaxation speed several times, and its $h(t)$ finally relaxed to zero at 0.9 μm/s after 4500 s. This observation suggests that GBs are thick enough at P_m for their superfluid transition temperature (T_c) to be close to that of bulk liquid ^{4}He. However, the properties of the GBs might depend on the misorientation between the adjacent crystals.

Let us now consider the possibility that there is a superfluid film between the glass wall and solid helium (*14*, *15*). Because solid ^{4}He partially wets walls (*25*), a superfluid film at the glass/helium interface necessarily has a microscopic thickness e on the order of a. Because crystals of good quality do not relax, we found an upper bound for v_c^W near the glass wall

$$v_c^W = \frac{D}{4e}\frac{\rho_C - \rho_L}{\rho_s}V < 0.28\frac{a}{e}\frac{\rho_C}{\rho_s}\ \text{cm/s} \quad (2)$$

If e were equal to 4 to 8 a as proposed in (*14*), the superfluid film near the wall should be similar to the free liquid films in which the v_c is much larger (*27*). On the contrary, if we assume $e = a$ and $\rho_s/\rho_C \approx 0.04$ as proposed in (*15*), we find $v_c^W < 7$ cm/s. This is possible if the superfluid film near the glass wall is much thinner and denser than inside a GB (*28*) but, in this case, it is probably not thick enough to explain KC's results. It therefore appears difficult to explain the results of both KC's experiments and ours in terms of a superfluid film at the glass/helium interface.

Our results suggest that GBs are superfluid, so that ^{4}He crystals of medium quality are supersolid at the liquid/solid equilibrium pressure P_m; that is, mass transport through them without dissipation is possible. But they are not "supercrystalline" because transport does not occur through their crystalline part. However, the connection of our results with other observations of supersolidity (*1*–*5*) is not straightforward, because our measurements were taken at P_m, whereas others were taken at higher pressures. We now need to study the superfluidity inside GBs more carefully. We expect e and v_c^{GB} to have a sharp variation near P_m,

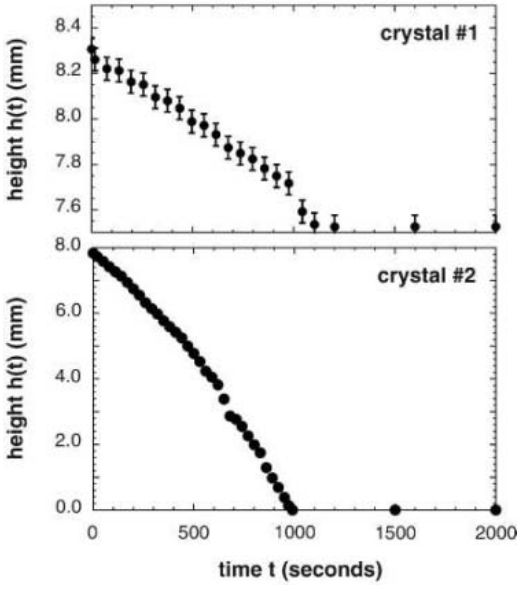

Fig. 3. The $h(t)$ between the liquid/solid interface inside and outside the tube as a function of time for two different crystals. Error bars indicate the accuracy at which heights are measured (+/−50 μm); for crystal 2, they are smaller than the symbol size.

where these quantities should be larger than at $P > P_m$, away from the stability region of the liquid. It is also possible that the superfluid transition temperature T_c^{GB} is considerably lower than 1 K at high P, where superfluidity may concern only a fraction of a monolayer. Unfortunately, to work with a single GB while varying the temperature and P is not easy. One should also study the effect of ^{3}He impurities because these should adsorb on GBs and modify their superfluid properties.

Let us finally consider the values of ρ_s and v_c found in torsional oscillator experiments (*1*–*5*). If the superflow occurs along the GBs in these experiments as well, v_c needs to decrease sharply from meters per second at P_m to micrometers per second above P_m. This is possible if the thickness of GBs also decreases as a function of P. A 1% superfluid density can be achieved with one GB every 100 *e*. We have found that, when growing crystals above 1.8 K from normal liquid helium, as is usually the case when using the blocked capillary method of KC and others, the growth is dendritic and the solid sample is snowball-like, in which the density of defects is so large that it strongly scatters light [see photograph in (*5*)]. It is also possible that KC's experiment is insensitive to annealing because GBs are more strongly pinned in their cell. If GBs are close to each other, elastic interactions might couple them and mimic phase coherence. As a final note, we mention that KC observed that $\rho_s(P)$ increases up to 55 bars before decreasing at higher P. The increase could be due to an increasing number of GBs and the decrease to the vanishing of superfluidity around 200 bars (*29*).

References and Notes

1. E. Kim, M. H. W. Chan, *Nature* **427**, 225 (2004).
2. E. Kim, M. H. W. Chan, *Science* **305**, 1941 (2004).
3. A. S. C. Rittner, J. D. Reppy, published online 22 April 2006 (http://arxiv.org/PS_cache/cond-mat/pdf/0604/0604528.pdf).
4. K. Shirahama, M. Kondo, S. Takada, Y. Shibayama, American Physical Society, Baltimore, MD, 14 March 2006 (abstract G41.00007).
5. A. Cho, *Science* **311**, 1693 (2006).
6. E. Burovski, E. Kozik, A. Kuklov, N. Prokof'ev, B. Svistunov, *Phys. Rev. Lett.* **94**, 165301 (2005).
7. A. F. Andreev, I. M. Lifshitz, *Sov. Phys. JETP* **29**, 1107 (1969).
8. G. V. Chester, *Phys. Rev. A.* **2**, 256 (1970).
9. A. J. Leggett, *Phys. Rev. Lett.* **25**, 1543 (1970).
10. D. E. Galli, L. Reatto, *Phys. Rev. Lett.* **96**, 165301 (2006).
11. This is when KC used natural ^{4}He containing ≈0.1 parts per million of ^{3}He impurities. We used the same natural ^{4}He.
12. B. K. Clark, D. M. Ceperley, *Phys. Rev. Lett.* **96**, 105302 (2006).
13. M. Boninsegni, N. Prokof'ev, B. Svistunov, *Phys. Rev. Lett.* **96**, 105301 (2006).
14. G. Dash, J. S. Wettlaufer, *Phys. Rev. Lett.* **94**, 235301 (2005).
15. S. A. Khairallah, D. M. Ceperley, *Phys. Rev. Lett.* **95**, 185301 (2005).
16. P. W. Anderson, W. F. Brinkman, D. A. Huse, *Science* **310**, 1164 (2005).
17. J. Day, T. Herman, J. Beamish, *Phys. Rev. Lett.* **95**, 035301 (2005).
18. J. Day, J. Beamish, *Phys. Rev. Lett.* **96**, 105304 (2006).
19. Because of radiation through the windows, there is a small heat input inside the tube, but it is less than 1 μW. In principle, P_m inside the tube could thus be different from that outside and maintain an $h(t)$ between the two levels. However, given the heat conductivity of the solid (*20*) and the melting curve $P_m(T)$ (*21*), where T is temperature, one finds that the level difference is less than 3 μm below 0.5 K. We thus expect thermal effects to be unimportant and gravity to be the only relevant parameter governing the shape evolution.
20. B. Bertman, H. A. Fairbank, C. W. White, M. J. Crooks, *Phys. Rev.* **142**, 74 (1966).
21. H. N. Hanson, J. E. Berthold, G. M. Seidel, H. J. Maris, *Phys. Rev. B* **14**, 1911 (1976).
22. In liquid ^{4}He, a 1-cm difference in height induces a difference in P of 2×10^{-4} bars, which is very small compared to the Young modulus $E = 300$ bars of ^{4}He crystals (*23*). As a consequence, it cannot induce the large plastic deformation that would be necessary for the crystal to flow around the tube edge.
23. H. J. Maris, T. E. Huber, *J. Low Temp. Phys.* **48**, 99 (1982).
24. E. R. Grilly, *J. Low Temp. Phys.* **11**, 33 (1973).
25. S. Balibar, H. Alles, A. Y. Parshin, *Rev. Mod. Phys.* **77**, 317 (2005).
26. G. Bonfait, H. Godfrin, B. Castaing, *J. Phys. (Paris)* **50**, 1997 (1989).
27. K. Telschow, I. Rudnick, T. G. Wang, *Phys. Rev. Lett.* **32**, 1292 (1974).
28. K. A. Gillis, S. M. Volz, J. M. Mochel, *Phys. Rev. B* **40**, 6684 (1989).
29. R. Ishiguro, F. Caupin, S. Balibar, *Europhys. Lett.* **75**, 91 (2006).

30. We acknowledge support from Agence Nationale de la Recherche grant 05-BLAN-0084–01 and NSF grant DMR-0305115. R.I. acknowledges support from the Japan Society for the Promotion of Science for a Postdoctoral Fellowship for Research Abroad (April 2004 to March 2006).

5 June 2006; accepted 19 July 2006
Published online 27 July 2006;
10.1126/science.1130879
Include this information when citing this paper.

Detection, Stimulation, and Inhibition of Neuronal Signals with High-Density Nanowire Transistor Arrays

Fernando Patolsky,[1]* Brian P. Timko,[1]* Guihua Yu,[1] Ying Fang,[1] Andrew B. Greytak,[1] Gengfeng Zheng,[1] Charles M. Lieber[1,2]†

We report electrical properties of hybrid structures consisting of arrays of nanowire field-effect transistors integrated with the individual axons and dendrites of live mammalian neurons, where each nanoscale junction can be used for spatially resolved, highly sensitive detection, stimulation, and/or inhibition of neuronal signal propagation. Arrays of nanowire-neuron junctions enable simultaneous measurement of the rate, amplitude, and shape of signals propagating along individual axons and dendrites. The configuration of nanowire-axon junctions in arrays, as both inputs and outputs, makes possible controlled studies of partial to complete inhibition of signal propagation by both local electrical and chemical stimuli. In addition, nanowire-axon junction arrays were integrated and tested at a level of at least 50 "artificial synapses" per neuron.

Electrophysiological measurements made with micropipette electrodes and microfabricated electrode arrays play an important role in understanding signal propagation through individual neurons and neuronal networks (*1*–*5*). Micropipette electrodes can stimulate and record intracellular and extracellular potentials in vitro and in vivo with relatively good spatial resolution of ~100 nm per pipette and ≥10 μm between two pipettes (*2*, *6*–*8*), yet they are difficult to multiplex. Microfabricated structures, such as electrode and field-effect transistor (FET) arrays, have potential for large-scale multiplexing and have enabled recording from both individual neurons and networks (*3*–*5*, *9*–*14*). However, these structures have relatively large sizes (~10 μm and larger on edge), and their interelectrode spacing (>10 μm) has precluded detection and stimulation of neuronal activity at the level of individual axons and/or dendrites.

For a FET array to be used to stimulate, inhibit, and record neuronal signals from numerous locations along the neuronal projections and cell body, the gate dimensions should ideally be on the nanometer scale, and appropriate contact between the neuron and the array must be made. Silicon nanowire (SiNW) FETs (*15*) have been used to detect chemical and biological species (even single virus particles) in solution (*16*–*19*). We show that we can pattern arrays of SiNW FETs on a substrate and passivate the arrays such that they will function in cell-culture media. Polylysine patterning allowed us to direct the growth of rat neurons to ensure that numerous SiNW FET contacts were made to the same neuron, rather than rely on fortuitous overlap. Because the contact length along an

[1]Department of Chemistry and Chemical Biology, [2]Division of Engineering and Applied Sciences, Harvard University, Cambridge, MA 02138, USA.

*These authors contributed equally to this work.
†To whom correspondence should be addressed. E-mail: cml@cmliris.harvard.edu

axon or dendrite projection crossing a NW is only on the order of 20 nm, these devices are highly local and noninvasive probes of neuronal projections. Notably, the typical active junction area for devices, about 0.01 to 0.02 μm^2, is three orders of magnitude smaller than microfabricated electrodes and planar FETs. The small hybrid junction sizes, which are similar to natural synapses, offer important advantages compared with other electrophysiological methods, including spatially resolved detection of signals without complications of averaging extracellular potential changes over a large percentage of a given neuron and integration of multiple elements on the axon and dendrite projections from a single neuron.

Our strategy for preparing SiNW-neuron devices involves assembly of oriented p- and/or n-type SiNWs (*18*, *20*, *21*), interconnection into FET device array structures (*18*, *22*), patterning polylysine as an adhesion and growth factor to define neuron cell growth (*23*, *24*) with respect to the device elements, and growing neurons under standard conditions (*25*). There are several features of the fabrication that are critical to the success of our approach. First, the metal-SiNW contacts must be passivated, because these readily corrode and fail during the relatively harsh conditions of cell culture and subsequent measurement. We developed a simple yet reliable single-step lithography process using an undercut multilayer resist and sequential line-of-sight metal and isotropic silicon nitride passivation layer depositions. Devices prepared in this manner survived continuous cell-culture conditions at 37°C for at least 10 days with >90% yield.

Second, we achieved a high yield of specific SiNW-neuron structures by using a second lithography step to pattern polylysine to define square regions 30 to 60 μm on edge that promote cell body adhesion and projected ~2-μm-wide lines that help to define subsequent neurite growth (Fig. 1A). Under growth conditions, cell suspensions were transferred to patterned chips for ~1 hour of incubation, washed to remove excess cells from regions other than polylysine pattern, and then incubated for an additional 4 to 8 days to allow for neuronal growth (*25*). This overall approach allowed us to vary the addressable NW interdevice separations down to at least 100 nm (*24*) and create a range of device array geometries that varied the number and spatial location of the SiNW junctions with respect to the cell body and neurite projections. We could also incorporate electronically distinct p- and n-type elements in well-defined positions.

Optical images of a representative one-neuron/one-NW device from an array (Fig. 1, B and C, and fig. S1) showed the expected 1:1 hybrid live-cell NW device with selective growth of the axon, verified by marker-specific fluorescence labeling and multicolor confocal microscopy (*25*). Analysis of this and additional chips indicates yields in excess of 90%, where clean patterning of polylysine and attachment of isolated live cells were critical factors.

We elicited action potential spikes using either a conventional glass microelectrode impaled at the soma or the SiNW-axon contact. In either case, we recorded the intracellular potential (IC) and conductance at the microelectrode and NW FET, respectively. All of the electrical experiments reported in this work were carried out at 37°C with chips submerged in electrophysiology bath solution (*26*), and stable NW measurements can be made for at least 24 hours. Figure 1D shows the direct temporal correlation between the potential spikes initiated in the soma and the corresponding conductance peaks measured by the SiNW at the NW-axon junction. Expanded plots of single peaks exhibit shapes characteristic of neuronal action potentials. The direct correlation of the NW conductance peak with intracellular (IC) potential peak is expected for a p-type NW (these devices), because the relative potential at the outer membrane becomes more negative and then more positive (opposite to the measured IC potential) and causes an accumulation of carriers (enhanced conductance) followed by a depletion of carriers (reduced conductance), respectively (*16*, *26*). Devices with n-type SiNWs [fig. S2 and supporting online material (SOM) text] showed signals that were negatively correlated. Moreover, the magnitude of the conductance change is consistent with estimates based on SiNW FET device properties and the range of axon diameters that form the NW-axon junctions (*25*).

Control experiments showed that IC stimulation with higher frequency action potential spikes resulted in correspondence between the potential spikes initiated in the soma and the conductance peaks measured by the NW (fig. S3). Also, no conductance spikes were detected after blocking voltage-dependent sodium channels with tetrodotoxin (TTX) (fig. S4A) (*8*, *27*), after severing the axon anterior to the NW-axon junction (fig. S4B), or when the SiNW element was absent in the same axon-electrode geometry (fig. S4C). In addition, NW-soma hybrid structures allow detection of signals at the soma (fig. S5).

NW devices were used to apply biphasic excitatory pulse sequences (Fig. 1E) to create detectable somatic action potential spikes in 86% of the trials, which is similar to the yield achieved with microelectrodes interfaced with entire cells (*14*). The stimulation process was carried out at least 30 times over a 4-hour period without loss of potential spikes or cell viability (fig. S6A) and thus shows that the excitation, which could involve reversible electroporation or capacitive coupling (*5*, *11*, *28*), does not damage the neurons. The excitation shows a threshold of about 0.4 V and no potential spikes in the presence of TTX or the absence of the SiNW (fig. S6B). In addition, single SiNWs can be used for simultaneous stimulation and detection (fig. S6C).

We next assembled hybrid structures that consisted of a central cell body and four peripheral SiNWs arranged at the corners of a rectangle; polylysine patterning promoted neu-

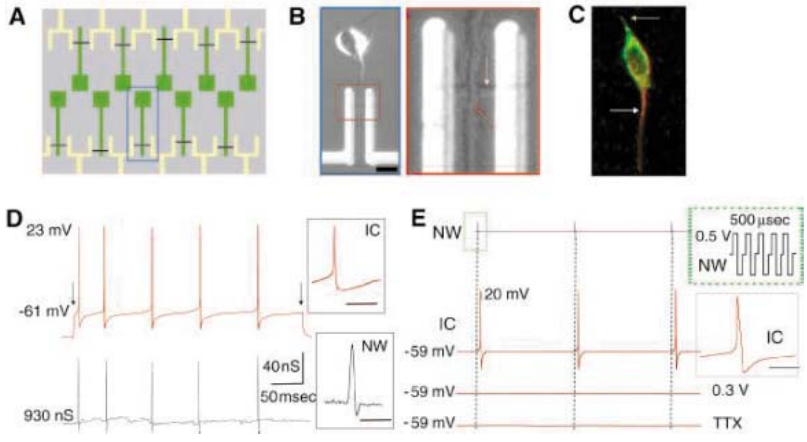

Fig. 1. NW recording and stimulation of neuronal axon signals. (**A**) General schematic of aligned NW-neuron device array. The open blue rectangle highlights a single NW-neuron device. (**B**) Optical image of a single cortex neuron aligned across a single NW device and (red box) a magnified image of the area where the axon crosses the NW. White arrow denotes the nanowire element; red arrow denotes the neuronal axon. (**C**) Confocal fluorescence image for a dual color–labeled cortex neuron after 4 days in culture. The red section (highlighted by the white arrow) highlights the growing axon, and the green short section (highlighted by the gray arrow) represents a dendrite. (**D**) (Top left) IC potential of an aligned cortex neuron (after 6 days in culture) during stimulation with a 500-ms-long current injection step of 0.1 nA. (Bottom left) Time-correlated signal from axon measured with a p-type silicon NW device. (**E**) Local NW-axon stimulation and correlated IC electrical recording of a cortex neuron. IC plots were recorded following a rectangular biphasic train of stimuli with amplitudes of (top) 0.5 V, (middle) 0.3 V, and (bottom) 0.5 V after bath application of 0.5 μM TTX. Green box highlights the train of rectangular biphasic voltage pulses.

rite growth across these elements. A representative optical image (Fig. 2A) shows one NW-axon and two NW-dendrite elements at positions 1, 2, and 3, respectively. Stimulation of action potential spikes in the soma yields correlated conductance peaks in the NW-axon (NW1) and NW-dendrite (NW2 and NW3) devices (Fig. 2B), but no signal was observed in a good detector (NW4) that had no visible neurite overlap.

This multi-NW–neurite array was then used to study spike propagation in the absence of the IC microelectrode with NW1 as a local input to elicit action potential spikes from the axon rather than the cell body. After stimulation with a biphasic pulse sequence (Fig. 2C), we detected back-propagation of the elicited action potential in the two dendrites crossing elements NW2 and NW3. The lack of observed signal from NW4 demonstrates the absence of cross-talk in the hybrid device array.

A linear array of four-NW FETs, a gap, and five-NW FETs was used to investigate simultaneous and temporally resolved propagation and back-propagation of action potential spikes in axons and dendrites, respectively. Optical images (Fig. 2D) revealed that the specific polarity of growth (e.g., axon across the four- or five-FET array) is not controlled but is readily identified by the faster growing projection (the axon) during culture and subsequently by electrical response and postmeasurement fluorescent imaging. On a given "chip," we fabricated ~20 of the repeating NW array structures, and after low-density neuron adsorption and growth, we obtained a yield of ~80% hybrid structures per chip. We then simultaneously detected the conductance output from NWs after IC stimulation at the soma and found that stimulation of action potential spikes in the soma yielded correlated conductance peaks in NW elements that form the NW-axon and NW-dendrite junctions (Fig. 2E).

These data demonstrate several key points. First, seven of the nine independently addressable NW-neurite junctions yield reproducible conductance spikes correlated with IC stimulation. Higher yields of functioning elements have also been achieved, although this ~80% yield still leaves three and four spatially defined local detectors on the dendrite and axon, respectively. While previous studies using glass microelectrodes have recorded spike propagation in axons and dendrites (*6*, *7*, *27*, *29*), axon and dendrite propagation has not been measured simultaneously, nor has the same level or recording points been achieved [although it has been demonstrated that measurements can be taken at multiple points by moving a single-pipette probe (*27*, *29*)].

Second, a comparison of high-resolution conductance-time data (Fig. 2F) demonstrates that the propagation delay of spikes in the dendrite and axon after initiation in the soma can be resolved, and moreover, shows a clear peak reduction and temporal spreading in the

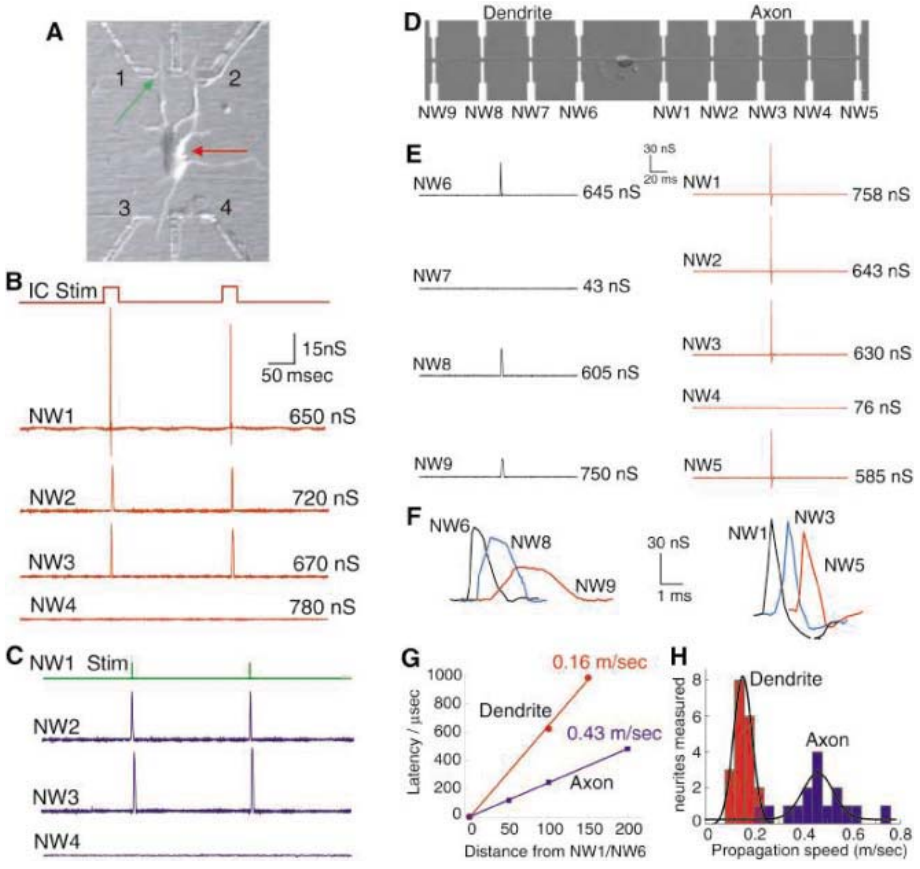

Fig. 2. Multi-NW–neurite structures. (**A**) Optical image of a cortex neuron connected to three of the four functional NW devices in the array. Two possible stimulation approaches are indicated: intracellular stimulation (red arrow in soma) and extracellular NW-based stimulation (green arrow on NW1). (**B**) Trace of intracellular current stimulation (15-ms current injection pulses of 0.5 nA) and resulting NW (NW1, NW2, NW3, and NW4) electrical responses. NW4 is not electrically connected to any section of the neuron and thus functions as an internal control for all the experiments. (**C**) Trace of pulses (trains of five rectangular biphasic-type stimuli, train width of 500 μs) applied to NW1 for antidromic stimulation of the neuron. The response was measured by the NW-dendrite junctions at NW2 and NW3. (**D**) Optical image of a cortex neuron with axon and dendrite aligned in opposite directions. (**E**) Electrical responses measured from NW-dendrite devices (left, NW6 to NW9) and NW-axon devices (right, NW1 to NW5) after intracellular stimulation with a 15-ms, 0.5-nA current pulse. (**F**) Expansion of peaks from (E) elucidating the evolution of peak shape as it propagates along each process. (**G**) Plot showing latency time as a function of distance from NW1 and NW6 for axons (blue) and dendrites (red), respectively. (**H**) Histogram of propagation speed through axons (blue) and dendrites (red).

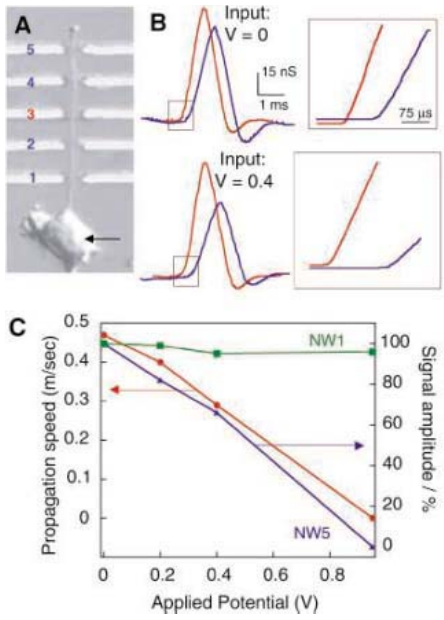

Fig. 3. Electrical modulation of signal propagation. (**A**) Optical image showing the structure of the five-NW–axon structure, where NW3 serves as input. (**B**) Electrical signals recorded at NW1 (red) and NW5 (blue) before (top) and after (bottom) IC stimulation; a bias (hyperpolarizing) of 0.4 V was applied to NW3. (**C**) Plot of spike propagation speed (red) and amplitude (green and blue) as a function of input potential applied to NW3, where signals were recorded at NW1 and NW5.

dendrite, measured by elements 6 to 9, and little change in the axon, recorded by elements 1 to 5. These latter observations are consistent with passive and active propagation mechanisms, respectively (*30*, *31*). By using the first NW (i.e., NW1 and NW6) in each neurite as references, we calculated (Fig. 2G) signal propagation rates of 0.16 m/s for dendrites and 0.43 m/s for axons. In trials with different neurons, we found these rates to have Gaussian distributions of 0.15 ± 0.04 (±SD) and 0.46 ± 0.06 m/s for dendrites and axons, respectively (Fig. 2H); these data are comparable to reported propagation rates measured by conventional electrophysiological (*32*) and optical (*33*–*35*) methods.

Hybrid structures consisting of five independent NW-axon elements (Fig. 3A) were fabricated and used to study the effects of local electrical and chemical inputs on signal propagation. We initially configured the middle NW-axon junction, NW3, as a variable potential input and used the other four NWs elements to record temporally resolved spike propagation after IC stimulation. A comparison of the time-resolved spikes recorded from NW1 and NW5 for input voltages of 0 and 0.4 V (Fig. 3B) shows that there is well-defined slowing of the propagation speed and reduction of the peak amplitude when V(NW3) = 0.4 V. Systematic inhibition and ultimately complete blocking of propagation was observed as the input voltage on NW3 is increased to 0.9 V (Fig. 3C). Indeed, if any one of the first four NW inputs is set at or above the blocking threshold of 0.9 V, no signal propagation is detected at NW5 (fig. S7). The spike amplitude recorded at NW5 was monotonically reduced with increasing input voltage, although no change is observed in the amplitude at NW1, which is equidistant from the input, NW3 (Fig. 3C). These results suggest that mode of action is localized at a given NW-axon input and is consistent with local anodic hyperpolarization of the membrane at NW-axon synapses. This polarization inhibits and ultimately blocks the propagation of action potential spikes (*36*, *37*). In a similar manner, the effects of local chemical inputs, such as TTX, on signal propagation were characterized (SOM text and fig. S8).

Our approach can be readily extended to highly integrated systems. We designed and fabricated a repeating structure that consists of 50 addressable NW-axon elements. This structure was chosen to show the capability of single-cell hybrid structures at much higher density of nanoelectronics devices but could be readily reconfigured, for example, into structures with different geometries, NW-device spacing, and/or multiple cells. An optical image (Fig. 4A) shows that well-aligned neuron growth was achieved. Electrical transport measurements made after neuron growth demonstrate a high yield of good NW FET devices: 43 out of 50 devices had conductance values from 550 to 870 nS. Notably, IC stimulation of action potentials in the soma yields a mapping of the spike propagation by the 43 working devices over the ~500-μm-long axon (Fig. 4B). These data exhibit little decay in peak amplitude from NW1 to NW49 (inset, Fig. 4B), which is consistent with the active propagation process. We fabricated structures containing 150 devices with an inter-device distance of only 400 nm and also successfully used this as a platform for directed neuronal growth (fig. S9).

We believe that the demonstration of large-scale integration of reproducible functional hybrid NW-neuron junctions has a variety of applications. These local NW-neurite junctions enable diverse and controllable multisite inputs while simultaneously mapping signal flow with high spatial and temporal resolution. These capabilities could be used to investigate multiple NW inputs and outputs to a single soma and to study synaptic processing in neural networks (*38*, *39*) with NW-neurite junctions used to reversibly inhibit or stop signal propagation along specific pathways while simultaneously mapping signal flow in dendrites and axons in the network. Second, the demonstrated reproducibility of the NW-cell devices and ability to integrate these hybrid structures on chips in a multicell array format has implications for developing flexible real-time cellular assays, for example, for drug discovery and testing. Last, the NW-neurite junctions can be applied to hybrid circuits where one might integrate different signals with a neuron and subsequently explore nanoelectronic circuit responses, as well as interfaces to implanted devices.

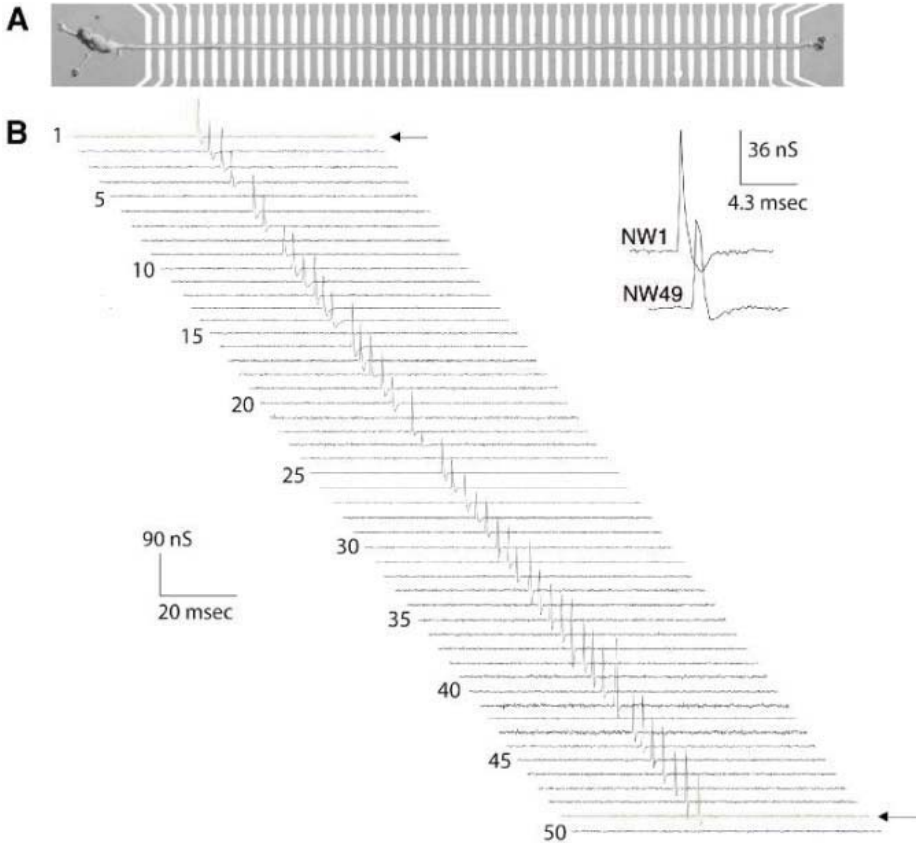

Fig. 4. Highly integrated NW-neuron devices. (**A**) Optical image of aligned axon crossing an array of 50 NW devices with a 10-μm interdevice spacing. (**B**) Electrical data from the 50-device array shown above. The yield of functional devices is 86%. The peak latency from NW1 (top arrow) to NW49 (bottom arrow) was 1060 μs.

References and Notes

1. A. R. Martin, B. G. Wallace, P. A. Fuchs, J. G. Nicholls, *From Neuron to Brain: A Cellular and Molecular Approach to the Function of the Nervous System* (Sinauer Associates Inc., Sunderland, MA, 2001).
2. U. Windhorst, H. Johansson, *Modern Techniques in Neuroscience Research: Electrical Activity of Individual Neurons in Situ: Extra- and Intracellular* (Springer, New York, 1999).
3. S. Marom, G. Shahaf, *Q. Rev. Biophys.* **35**, 63 (2002).
4. W. L. C. Rutten, *Annu. Rev. Biomed. Eng.* **4**, 407 (2002).
5. P. Fromherz, *ChemPhysChem* **3**, 276 (2002).
6. H. Oviedo, A. D. Reyes, *J. Neurosci.* **25**, 4985 (2005).
7. R. C. Froemke, M. M. Poo, Y. Dan, *Nature* **434**, 221 (2005).
8. G. J. Stuart, M. Hausser, *Nat. Neurosci.* **4**, 63 (2001).
9. A. Lambacher *et al.*, *Appl. Phys. A* **79**, 1607 (2004).
10. A. Offenhausser, C. Sprossler, M. Matsuzawa, W. Knoll, *Biosens. Bioelectron.* **12**, 819 (1997).
11. M. Merz, P. Fromherz, *Adv. Funct. Mater.* **15**, 739 (2005).
12. M. Voelker, P. Fromherz, *Small* **1**, 206 (2005).
13. C. D. James *et al.*, *IEEE Trans. Biomed. Eng.* **51**, 1640 (2004).

14. Y. Jimbo, N. Kasai, K. Torimitsu, T. Tateno, H. P. C. Robinson, *IEEE Trans. Biomed. Eng.* **50**, 241 (2003).
15. Y. Huang, C. M. Lieber, *Pure Appl. Chem.* **76**, 2051 (2004).
16. F. Patolsky, G. Zheng, C. M. Lieber, *Anal. Chem.* **78**, 4261 (2006).
17. Y. Cui, Q. Q. Wei, H. Park, C. M. Lieber, *Science* **293**, 1289 (2001).
18. G. F. Zheng, F. Patolsky, Y. Cui, W. U. Wang, C. M. Lieber, *Nat. Biotechnol.* **23**, 1294 (2005).
19. F. Patolsky *et al.*, *Proc. Natl. Acad. Sci. U.S.A.* **101**, 14017 (2004).
20. Y. Cui, Z. Zhong, D. Wang, W. U. Wang, C. M. Lieber, *Nano Lett.* **3**, 149 (2003).
21. G. F. Zheng, W. Lu, S. Jin, C. M. Lieber, *Adv. Mater.* **16**, 1890 (2004).
22. S. Jin *et al.*, *Nano Lett.* **4**, 915 (2004).
23. C. Wyart *et al.*, *J. Neurosci. Methods* **117**, 123 (2002).
24. C. D. James *et al.*, *IEEE Trans. Biomed. Eng.* **47**, 17 (2000).
25. Materials and methods are available as supporting material on *Science* Online.
26. S. M. Sze, in *Physics of Semiconductor Devices* (Wiley, New York, 1981), pp. 431–456.
27. A. T. Gulledge, G. J. Stuart, *J. Neurosci.* **23**, 11363 (2003).
28. M. Tarek, *Biophys. J.* **88**, 4045 (2005).
29. M. E. Larkum, J. J. Zhu, *J. Neurosci.* **22**, 6991 (2002).
30. R. Larry *et al.*, in *Fundamental Neuroscience* (Elseiver Science, San Diego, CA, 2003), pp. 115–136.
31. A. L. Hodgkin, A. F. Huxley, *J. Physiol.* **117**, 500 (1952).
32. L. G. Nowak, J. Bullier, *Exp. Brain Res.* **118**, 477 (1998).
33. R. Yuste, D. W. Tank, D. Kleinfeld, *Cereb. Cortex* **7**, 546 (1997).
34. S. Antic, G. Major, D. Zecevic, *J. Neurophysiol.* **82**, 1615 (1999).
35. H. Kawaguchi, K. Fukunishi, *Exp. Brain Res.* **122**, 378 (1998).
36. N. J. M. Rijkhoff, E. L. Koldewijn, P. E. V. van Kerrebroeck, F. M. J. Debruyne, H. Wijkstra, *IEEE Trans. Biomed. Eng.* **41**, 413 (1994).
37. A. Vuckovic, J. J. Struijk, N. J. M. Rijkhoff, *Med. Biol. Eng. Comput.* **43**, 365 (2005).
38. G. Q. Bi, M. M. Poo, *Nature* **401**, 792 (1999).
39. A. Frick, J. Magee, D. Johnston, *Nat. Neurosci.* **7**, 126 (2004).
40. B.P.T. thanks the NSF for graduate fellowship support. C.M.L. acknowledges support of this work by Defense Advanced Research Projects Agency and Applied Biosystems.

Supporting Online Material
www.sciencemag.org/cgi/content/full/313/5790/1100/DC1
Materials and Methods
SOM Text
Figs. S1 to S10
References

12 April 2006; accepted 18 July 2006
10.1126/science.1128640

Discrete Sandwich Compounds of Monolayer Palladium Sheets

Tetsuro Murahashi,[1]* Mayu Fujimoto,[1] Masa-aki Oka,[1] Yasuhiro Hashimoto,[1] Tomohito Uemura,[1] Yasuki Tatsumi,[1] Yoshihide Nakao,[2] Atsushi Ikeda,[2] Shigeyoshi Sakaki,[2] Hideo Kurosawa[1]*

Despite the abundance of "sandwich" complexes, in which two cyclic aromatic hydrocarbon ligands flank a metal center, this motif has not been extended to sheets of multiple metal atoms. We prepared and isolated two such compounds. In the first, three palladium centers form a planar triangular array, capped by chlorides, between two cycloheptatrienyl ligands. In the second, a pentapalladium sheet adopts an edge-sharing triangle-trapezoid skeleton between two naphthacene rings. The compounds were characterized by x-ray crystallography and nuclear magnetic resonance spectroscopy. The nature of bonding in the clusters was analyzed by quantum calculations.

The chemistry of metal sandwich complexes has developed intensively since the structure of ferrocene $(C_5H_5)_2Fe$ was elucidated in 1952 (*1*, *2*). The motif now plays an important role in catalysis and materials sciences (*3*, *4*). Most of the discrete sandwich complexes possess a mononuclear metal center between two small aromatic carbocyclic ligands, such as cyclopentadienyl or benzene (Fig. 1A). In contrast, compounds in which the carbon rings flank a monolayer of multiple metal atoms have not been isolated as discrete molecules, despite the fascinating implications of such layered sheet structure (Fig. 1B). The potential existence of these compounds was implicated by early observation of facial coordination of cyclopentadienyl or benzene ligands to triangular trimetal cores in a half-sandwich manner (*5*, *6*). More recently, a $Ni_3(benzene)_2$ species was detected through mass spectroscopy in a mixture of $Ni_n(benzene)_m$ clusters generated in the gas phase by laser vaporization (*7*). Stable structures of discrete metal monolayer sandwich compounds have also been discussed in theoretical studies (*8*). Moreover, formation of metal nanosheets between graphene layers has been observed through transmission electron microscopy (TEM) (*9*, *10*), which further stimulates the search for this (carbon sheet)−(metal sheet)−(carbon sheet) interaction in discrete molecules.

We sought to prepare palladium compounds that adopt this layered motif. Palladium is one of the most versatile transition metal catalysts for transformation of organic and inorganic substrates (*11*). Although mononuclear biscyclopentadienyl- and bisbenzene palladium complexes are unknown, polyatomic palladium frameworks seemed likely to form stably between extended unsaturated hydrocarbon ligands, in view of the isolation of bisbenzene dipalladium complexes (*12*, *13*) as well as the efficient formation of Pd sandwich chain compounds (*14*, *15*). Here, we report the successful isolation and structural characterization of two discrete metal monolayer sandwich compounds: $[Pd_3(C_7H_7)_2Cl_3][PPh_4]$ (**1**) and $[Pd_5(naphthacene)_2(toluene)][B(Ar_f)_4]_2$ (**4-toluene**), where $B(Ar_f)_4 = B[3,5\text{-}(CF_3)_2C_6H_3]_4$.

The cycloheptatrienyl (Tr) cation $[C_7H_7]^+$ has been widely studied as a transition metal ligand (*16*–*18*) but has rarely been used in palladium chemistry (*19*, *20*). Surprisingly, the reaction of $[Pd_2(dba)_3]$ (dba = 1,5-diphenyl-1,4-pentadien-3-one) and $[C_7H_7][BF_4]$ in the presence of $[PPh_4]Cl$ in CD_2Cl_2 afforded the biscycloheptatrienyl tripalladium complex $[Pd_3Tr_2Cl_3][PPh_4]$ (**1**) almost quantitatively after 10 min (Fig. 2A). The product **1** was isolated as wine-red microcrystals in 72% yield after recrystallization from hot acetonitrile. The structure of **1** was determined by x-ray diffraction analysis (Fig. 2B). The triangular tripalladium core is sandwiched between two planar cycloheptatrienyl ligands. The Pd−Pd bonds (2.745 to 2.789 Å) are within the range of normal Pd−Pd bond length (*21*). The two cycloheptatrienyl rings are slightly deviated from the mutually eclipsed position. Of the seven carbons in each ring, two pairs, C1-C2 and C3-C4 or C10-C11 and C12-C13, are located within the bonding distance (2.15 to 2.28 Å) from Pd1 and Pd2 or Pd2 and Pd3, respectively. The remaining carbon sets, [C5, C6, C7] or [C8, C9, C14], are bound rather irregularly to Pd3 or Pd1, respectively, with the shorter Pd3−C6 and Pd1−C8 lengths and the longer Pd3−C5, Pd3−C7, Pd1−C9, and Pd1−C14 lengths. The C−C bond lengths of

[1]Department of Applied Chemistry, Graduate School of Engineering, Osaka University, and PRESTO, Japan Science and Technology Agency (JST), Suita, Osaka 565-0871, Japan. [2]Department of Molecular Engineering, Graduate School of Engineering, Kyoto University, Nishikyo-ku, Kyoto 615-8510, Japan.

*To whom correspondence should be addressed. E-mail: tetsu@chem.eng.osaka-u.ac.jp (T.M.); kurosawa@chem.eng.osaka-u.ac.jp (H.K.)

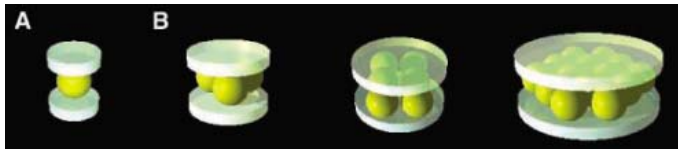

Fig. 1. Illustrated models of (**A**) metallocene and (**B**) hypothetical metal monolayer sandwich compounds.

the cycloheptatrienyl ligands (1.39 to 1.43 Å) indicate electronic delocalization over the seven-membered carbocyclic rings bound to the Pd_3 core. ^{1}H- and $^{13}C\{^1H\}$ nuclear magnetic resonance (NMR) spectra of **1** in CD_2Cl_2 showed sharp singlet resonances for cycloheptatrienyl protons [δ = 4.60 parts per million (ppm)] and carbons (δ = 75.9 ppm), indicating fast dynamic rotation of the cycloheptatrienyl ligands on the tripalladium core in solution (*17*, *22*, *23*).

$[Pd_3Tr_2Cl_3]^-$ was theoretically analyzed by density functional theory (DFT) with B3LYP functional, where the geometry of this complex was optimized with the DFT method (fig. S1 and table S1). We carried out molecular orbital (MO)–based fragment overlap population analysis, where MOs of fragments $[Pd_3Cl_3]^{3-}$ and $[C_7H_7]_2^{2+}$ were used to construct MOs of $[Pd_3(C_7H_7)_2Cl_3]^-$. This analysis (table S5) indicates that the dσ-dσ antibonding orbitals of the $[Pd_3Cl_3]^{3-}$ fragment mainly participate in back-donation to the $[C_7H_7]^+$ ligands (fig. S3). The back-donation from those MOs of $[Pd_3Cl_3]^{3-}$ is also supported by Mulliken and natural atomic orbital (NAO) population analyses (table S4). Although dπ-dπ bonding orbitals also participate in the back-donation (fig. S3), this contribution is smaller than that of dσ-dσ antibonding orbitals. In addition, donation from the π orbital of $[C_7H_7]^+$ to the acceptor orbital of $[Pd_3Cl_3]^{3-}$, where the latter involves Pd−Pd bonding overlap, participates in the interaction between $[Pd_3Cl_3]^{3-}$ and $[C_7H_7]^+$ (fig. S4), although to a smaller extent than the back donation. These results suggest that the donating and back-donating interactions contribute to the Pd−Pd bonding interaction (see supporting online material). Consistent with the above discussion, Wiberg bond order is evaluated to be 0.282, 0.282, and 0.258 for each Pd−Pd pair (scheme S2) (*24*, *25*).

The Pd_3-Tr_2 sandwich framework is robust: No decomposition was observed when a 1,2-dichloroethane solution of **1** was left for 1 week at 60°C under air. Treatment of **1** with $AgBF_4$ in acetonitrile gave the dicationic trisacetonitrile complex $[Pd_3Tr_2(CH_3CN)_3][BF_4]_2$ (**2-CH_3CN**) in 85% isolated yield. The complex **2-CH_3CN** was formed in very low yield (3% after 1 day) by the reaction of $Pd_2(dba)_3$ and $TrBF_4$ in CD_2Cl_2 in the presence of excess acetonitrile. Addition of PPh_3 (5 equiv.) to the dichloromethane solution of **2-CH_3CN** gave the tristriphenylphosphine complex $[Pd_3Tr_2(PPh_3)_3][BF_4]_2$ (**2-PPh_3**) in 87% isolated yield. Preliminary tests of the catalytic activity of the cycloheptatrienyl tripalladium sandwich complexes were promising. For example, Suzuki-Miyaura cross-coupling (*26*–*28*) between 4-bromoacetophenone and phenylboronic acid at 60°C with Cs_2CO_3 proceeded with a catalytic amount (3 mol %) of **1** or **2-CH_3CN**.

We also examined the synthesis of Pd sheet sandwich compounds with the use of polycyclic aromatic hydrocarbons. Although it is known that polycyclic aromatic hydrocarbons are capable of binding more than two metal atoms (*15*, *29*–*35*), no sandwich complex of monolayer metal sheet has been reported. The reaction of $[Pd_2(CH_3CN)_6][BF_4]_2$ (**3**) (*36*) with excess naphthacene in the presence of 2 equivalents of $NaB(Ar_f)_4$ in refluxing 1,2-dichloroethane afforded dark-brown product. Repeated recrystallization from CH_2Cl_2/toluene gave crystalline material of **4-toluene**•3(C_7H_8) in 14% yield (Fig. 3). The surprising sandwich structure of **4-toluene** was determined by x-ray diffraction analysis (Fig. 4, A to C). Two naphthacene ligands coordinate to the penta-palladium sheet through the 12 carbons via μ_5-η^2:η^2:η^2:η^3:η^3-coordination mode. The Pd_5 sheet may be regarded as the edge-sharing triangle-trapezoid metal skeleton, where the Pd4−Pd5 distance (2.916 Å) is relatively long (*21*). One of the four toluene molecules in the unit cell was located near the apex Pd1 atom; the closest distance between the apex Pd1 atom and toluene carbon was 2.52 Å. However, this toluene was disordered and its coordination mode (either η^2 or η^1) could not be definitively assigned. The other three toluene molecules in the unit cell were not coordinated to the metals.

The ^{1}H, $^{13}C\{^1H\}$ NMR, H−H correlation spectroscopy (COSY), heteronuclear multiple-quantum correlation (HMQC), and heteronuclear

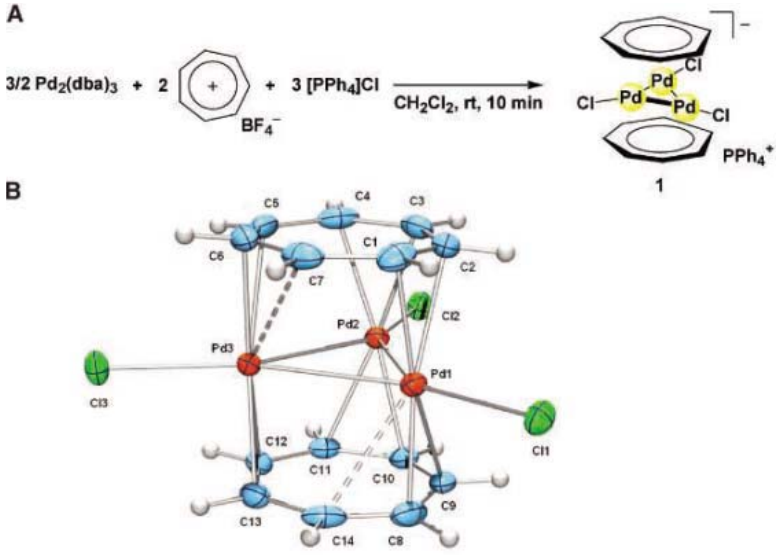

Fig. 2. (**A**) Synthesis of the cycloheptatrienyl tripalladium sandwich complex **1**. (**B**) Thermal ellipsoid (50%) drawing of **1** (PPh_4 cation and water were omitted for clarity). Selected bond lengths (Å) and angles (degrees) are as follows (the number in parentheses is the standard deviation of the last significant digit): Pd1−Pd2, 2.7550(5); Pd2−Pd3, 2.7446(5); Pd3−Pd1, 2.7889(5); Pd1−Cl1, 2.471(1); Pd2−Cl2, 2.471(1); Pd3−Cl3, 2.442(1); Pd1−C1, 2.155(5); Pd1−C2, 2.279(5); Pd2−C3, 2.194(5); Pd2−C4, 2.195(5); Pd3−C5, 2.342(6); Pd3−C6, 2.149(5); Pd3−C7, 2.610(6); Pd1−C7, 2.760(6); Pd1−C8, 2.145(6); Pd1−C9, 2.465(6); Pd2−C10, 2.176(5); Pd2−C11, 2.229(5); Pd3−C12, 2.246(5); Pd3−C13, 2.150(5); Pd3−C14, 2.794(6); Pd1−C14, 2.530(6); Pd1−Pd2−Pd3, 60.94(1); Pd2−Pd3−Pd1, 59.71(1); and Pd3−Pd1−Pd2, 59.34(1).

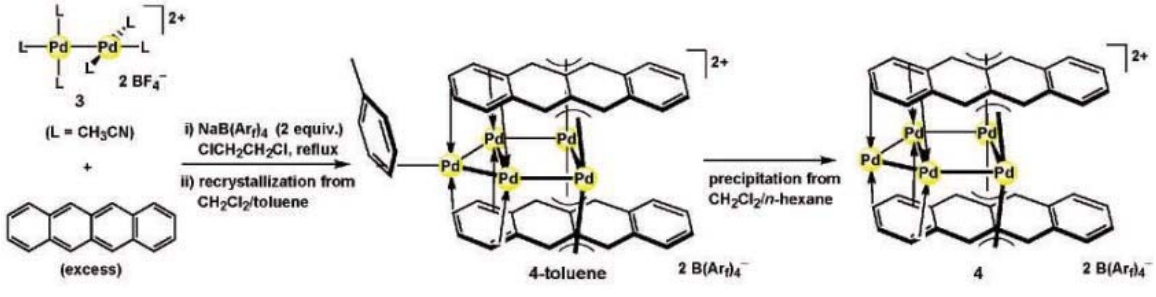

Fig. 3. Synthesis of compounds **4-toluene** and **4**.

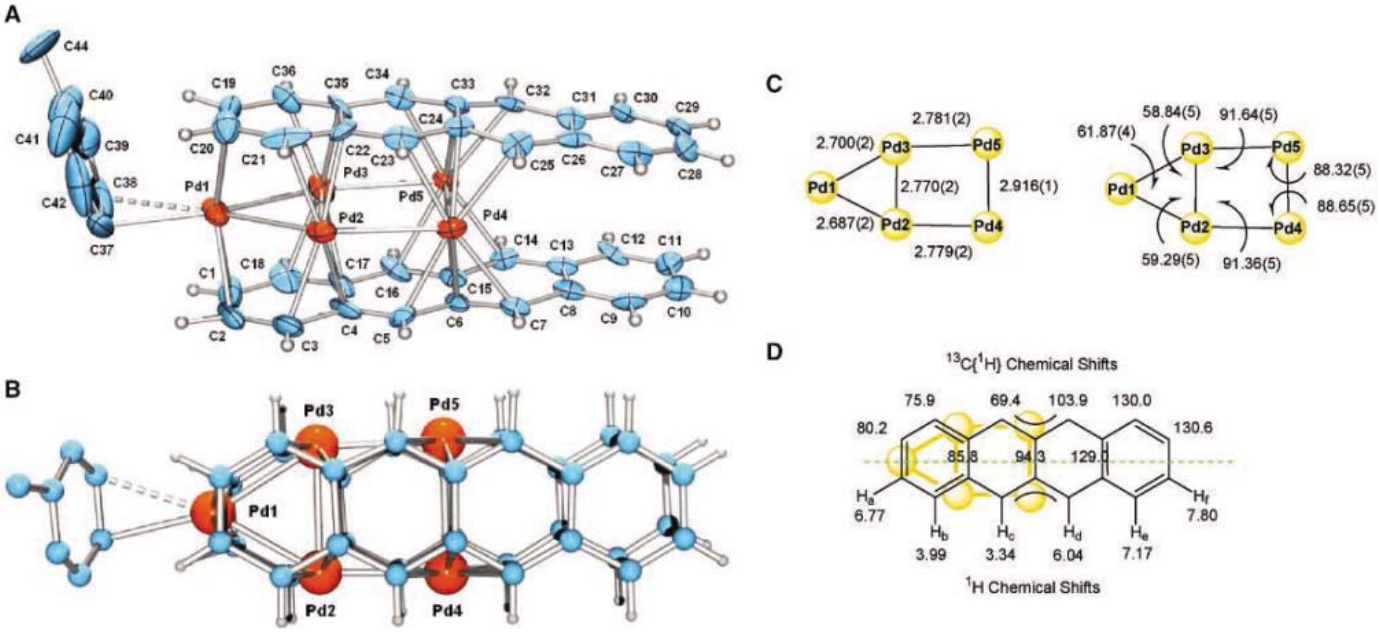

Fig. 4. Molecular structure of the compound **4-toluene**: (**A**) 50% thermal ellipsoids diagram, (**B**) top view with ball-stick drawing. $B(Ar_f)_4$ anions and noncoordinating toluene molecules were omitted for clarity. Selected bond lengths (Å) are as follows: Pd1−C1, 2.29(2); Pd1−C2, 2.30(2); Pd2−C3, 2.26(2), Pd2−C4, 2.19(1); Pd3−C17, 2.19(2); Pd3−C18, 2.29(2); Pd4−C5, 2.30(2); Pd4−C6, 2.16(1); Pd4−C7, 2.34(1); Pd5−C14, 2.33(1); Pd5−C15, 2.18(1); Pd5−C16, 2.38(1); Pd1−C37, 2.52(2); Pd1−C38, 2.68(2). (**C**) bond distances (Å) and angles (degrees) of the Pd_5 sheet in **4-toluene**. (**D**) ^1H and $^{13}C\{^1H\}$ NMR chemical shifts (parts per million) of the unsaturated hydrocarbon ligands of **4-toluene**•$3(C_7H_8)$ in CD_2Cl_2 at 25°C.

multiple-bond correlation (HMBC) analyses in CD_2Cl_2 showed that the resonances for the 12 coordinating carbons were shifted upfield (δ = 69 to 104 ppm) relative to those of free naphthacene (δ = 125 to 132 ppm) (Fig. 4D). No apparent evidence was obtained for coordination of toluene to **4** in solution; toluene resonances appeared at the same chemical shifts as those of free toluene, and no apparent nuclear Overhauser effect (NOE) was observed between any of the naphthacene protons and toluene protons. Addition of *n*-hexane to the dichloromethane solution of **4-toluene**•$3(C_7H_8)$ gave the toluene-free compound **4**, the composition of which was confirmed by the elemental analysis. Complex **4** was stable in CD_2Cl_2. ^1H NMR spectra of **4** in CD_2Cl_2 at 25°C showed naphthacene proton resonances at almost identical chemical shifts to those exhibited by **4-toluene**•$3(C_7H_8)$.

$[Pd_5(naphthacene)_2]^{2+}$ was also theoretically investigated with the DFT method, where the geometry was optimized (fig. S1 and table S1). The MO-based fragment overlap population analysis by the use of MOs of fragments $[Pd_5]^{2+}$ and $[C_{18}H_{12}]_2$ (table S7) and Mulliken and NAO population analyses (table S6) indicate that donation from the naphthacene ligands and back-donation from the $[Pd_5]^{2+}$ moiety contribute to the interaction between the $[Pd_5]^{2+}$ fragment and naphthacene ligands (see supporting online material). The presence of weak Pd−Pd bonding is supported by Wiberg bond order (0.178, 0.198, 0.146, and 0.149 for Pd1−Pd2, Pd1−Pd3, Pd2−Pd4, and Pd3−Pd5 pairs, respectively; nearly zero for Pd2−Pd3 and Pd4−Pd5 pairs) (scheme S2).

We propose that metal monolayer sandwich compounds containing different sizes and shapes of metal sheet can be synthesized using different extended pπ-conjugated carbon frameworks, with the aid of their template effect. We also expect that other metal elements can be used in the monolayer metal sandwich chemistry, in light of the applicability of metallocenes (i.e., sandwich dots, Fig. 1A) to various metal elements. These molecular metal monolayer compounds are potential models of bulk systems such as unsaturated hydrocarbons adsorbed on metal surfaces and the graphite intercalated compounds (GICs) (*37*).

References and Notes

1. G. Wilkinson, M. Rosenblum, M. C. Whiting, R. B. Woodward, *J. Am. Chem. Soc.* **74**, 2125 (1952).
2. E. O. Fischer, W. Pfab, *Z. Naturforsch. B* **7**, 377 (1952).
3. A. Togni, R. L. Halterman, Eds., *Metallocenes: Synthesis-Reactivity-Applications* (Wiley-VCH, New York, 2000).
4. N. J. Long, *Metallocenes* (Blackwell Science, Oxford, 1998).
5. E. O. Fischer, O. S. Mills, E. F. Paulus, H. Wawersik, *Chem. Commun.* **1967**, 643 (1967).
6. M. P. Gomez-Sal, B. F. G. Johnson, J. Lewis, P. R. Raithby, A. H. Wright, *Chem. Commun.* **1985**, 1682 (1985).
7. T. Kurikawa *et al.*, *Organometallics* **18**, 1430 (1999).
8. J. K. Burdett, E. Canadell, *Organometallics* **4**, 805 (1985).
9. M. Shirai, K. Igeta, M. Arai, *Chem. Commun.* **2000**, 623 (2000).
10. J. Walter, *Adv. Mater.* **12**, 31 (2000).
11. J. Tsuji, *Palladium Reagents and Catalysts* (Wiley, Chichester, UK, 2004).
12. G. Allegra, A. Immirzi, L. Porri, *J. Am. Chem. Soc.* **87**, 1394 (1965).
13. M. Gorlov, A. Fischer, L. Kloo, *J. Organomet. Chem.* **689**, 489 (2004).
14. T. Murahashi, E. Mochizuki, Y. Kai, H. Kurosawa, *J. Am. Chem. Soc.* **121**, 10660 (1999).
15. T. Murahashi, T. Uemura, H. Kurosawa, *J. Am. Chem. Soc.* **125**, 8436 (2003).
16. M. L. H. Green, D. K. P. Ng, *Chem. Rev.* **95**, 439 (1995).
17. H. Wadepohl, *Coord. Chem. Rev.* **185–186**, 551 (1999).
18. We abbreviate the cycloheptatrienyl ligand as "Tr" after the conventional name of $[C_7H_7]^+$, tropylium.
19. M. Airoldi, G. Deganello, G. Gennaro, M. Moret, A. Sironi, *Organometallics* **12**, 3964 (1993).
20. W. Fu, R. McDonald, J. Takats, A. H. Bond, R. D. Rogers, *Inorg. Chim. Acta* **229**, 307 (1995).
21. The longest and the shortest Pd−Pd bonds reported are 3.185 Å and 2.391 Å, respectively (*38*).
22. F. A. Cotton, in *Dynamic Nuclear Magnetic Resonance Spectroscopy*, L. M. Jackman, F. A. Cotton, Eds. (Academic Press, New York, 1975), chap. 10.
23. J. W. Faller, *Adv. Organomet. Chem.* **16**, 211 (1977).
24. K. B. Wiberg, *Tetrahedron* **24**, 1083 (1968).
25. For the typical Pd−Pd single bonded complex, $Pd_2Cl_2(PH_3)_4$, Wiberg bond order was calculated to be 0.534.
26. N. Miyaura, K. Yamada, A. Suzuki, *Tetrahedron Lett.* **20**, 3437 (1979).
27. N. Miyaura, A. Suzuki, *Chem. Rev.* **95**, 2457 (1995).
28. F. Diederich, P. J. Stang, *Metal-Catalyzed Cross-Coupling Reactions* (Wiley-VCH, New York, 1998).
29. H. Nagashima, T. Fukabori, K. Aoki, K. Itoh, *J. Am. Chem. Soc.* **115**, 10430 (1993).
30. A. Ayalon *et al.*, *Science* **265**, 1065 (1994).
31. K.-H. Thiele, S. Bambirra, J. Sieler, S. Yelonek, *Angew. Chem. Int. Ed. Engl.* **37**, 2886 (1998).
32. M. Munakata, L. P. Wu, G. L. Ning, *Coord. Chem. Rev.* **198**, 171 (2000).
33. M. R. Haneline, M. Tsunoda, F. P. Gabbai, *J. Am. Chem. Soc.* **124**, 3737 (2002).

34. J. J. Schneider, D. Wolf, C. W. Lehmann, *Inorg. Chim. Acta* **350**, 625 (2003).
35. M. A. Petrukhina, K. W. Andreini, L. Peng, L. T. Scott, *Angew. Chem. Int. Ed. Engl.* **43**, 5477 (2004).
36. T. Murahashi, T. Nagai, T. Okuno, T. Matsutani, H. Kurosawa, *Chem. Commun.* **2000**, 1689 (2000).
37. E. L. Muetterties, T. N. Rhodin, E. Band, C. F. Brucker, W. R. Pretzer, *Chem. Rev.* **79**, 91 (1979).
38. T. Murahashi, H. Kurosawa, *Coord. Chem. Rev.* **231**, 207 (2002).

39. Supported by the Japan Science and Technology Agency (JST) through PRESTO (Structure Control and Function) program; grants-in-aid for Scientific Research from the Ministry of Education, Culture, Sports, Science and Technology of Japan; and Frontier Research Center (FRC), Osaka University. Metrical parameters for the crystal structures of **1** and **4-toluene** are available from the Cambridge Crystallographic Data Centre under reference numbers CCDC-602060 and CCDC-602061, respectively.

Supporting Online Material
www.sciencemag.org/cgi/content/full/313/5790/1104/DC1
Materials and Methods
Figs. S1 to S7
Schemes S1 and S2
Tables S1 to S9
References

23 January 2006; accepted 20 July 2006
10.1126/science.1125245

Forced Resonant Migration of Pluto's Outer Satellites by Charon

William R. Ward* and Robin M. Canup

Two small moons of Pluto have been discovered in low-eccentricity orbits exterior to Pluto's large satellite, Charon. All three satellite orbits are nearly coplanar, implying a common origin. It has been argued that Charon formed as a result of a giant impact with primordial Pluto. The orbital periods of the two new moons are nearly integer multiples of Charon's period, suggesting that they were driven outward by resonant interactions with Charon during its tidal orbital expansion. This could have been accomplished if Charon's orbit was eccentric during most of this orbital evolution, with the small moons originating as debris from the collision that produced Charon.

Hubble Space Telescope observations in May 2005 revealed two previously undetected satellites of Pluto, S/2005 P1 and S/2005 P2 (P1 and P2) (*1*–*3*). The diameters of P1 and P2 are respectively ~160 km and ~120 km if they are as dark as cometary nuclei, but only ~35 km and ~30 km for a Charon-like reflectivity, with each object containing ≤0.2% of Charon's mass. The orbital period, P, of P1 is 38.2065 ± 0.0014 days, whereas that of P2 is 24.8562 ± 0.00013 days. This implies that P1 and P2 have periods of about six and four times the 6.38723-day orbital period of Charon (*1*–*3*), and a nearly 3:2 mutual ratio. Such orbital period ratios are referred to as mean motion commensurabilities, where the mean motion is $n = 2\pi/P$. The moons orbit in the same sense and plane as Charon (*1*), consistent with all three having formed by a common process rather than, for example, through sequential capture events (*4*, *5*).

The favored explanation for Charon's origin is a large impact (*6*, *7*) similar to that believed to have produced Earth's Moon. Charon appears most likely to have formed intact, on an eccentric orbit (*7*). It seems plausible that the impact generated some accompanying orbiting debris as source material for the outer small satellites. However, the present orbital distances of P2 at 41.9 R_P and P1 at 54.8 R_P, where R_P = 1180 ± 15 km is Pluto's radius, are far outside where debris from the type of collision favored for Charon's origin would be expected [e.g., typically within 15 R_P (*7*, *8*)].

Charon occupies a tidal end-state with an orbital period synchronous with Pluto's day and has likely undergone considerable outward tidal migration, perhaps by a factor of ~4, to arrive at its current distance of 16.6 R_P (*9*). The near 6:1 and 4:1 commensurabilities of P1 and P2 naturally lead to the supposition that they were driven outward by resonant torques from Charon (*2*). However, the required degree of expansion is large, and most observed solar system resonant configurations (e.g., that between Neptune and Pluto itself) act to excite the eccentricity of the resonantly perturbed object as the orbital radius of the perturbing object approaches it. This would have led to large, destabilizing eccentricities for P2 and P1. We propose instead that Pluto's small moons were captured into exterior corotation resonances with an eccentrically orbiting Charon. This is the same general type of resonance thought to confine the Neptune ring arcs (*10*, *11*) and does not excite eccentricities, thus providing an explanation for how Pluto's distant new moons could have originated from the same impact event as Charon.

When the period ratio of two satellites is nearly that of two integers, resonant forcing of their orbits acts to maintain the locations of their orbital conjunctions relative to the pericenter of one or both of their orbits. Their mutual gravitational potential can be expanded as a Fourier series (*12*), but near a commensurability, the motion will be dominated by only a few resonant terms. An exterior moon with a period relative to Charon's of $P/P_C \sim (m + 1)$, with $m = 3$ for P2 or $m = 5$ for P1, will be subject to multiple resonant terms of the form $\Phi_{ml}(a, a_c, e, e_c)\cos\phi_{ml}$, with

$$\phi_{ml} = (m + 1)\lambda - \lambda_C - (m - l)\tilde{\omega} - l\tilde{\omega}_C \quad (1)$$

and $0 \le l \le m$ (*13*). Here, λ and $\tilde{\omega}$ are the longitudes of the satellite and its orbital pericenter. Subscripts C refer to Charon, whereas unsubscripted quantities refer to a moon. Resonance capture causes the argument, ϕ_{ml}, of the resonance to librate about some fixed value. The amplitude of a resonant term has the form

$$\Phi_{ml} = -f_{ml}(\alpha)e^{m-l}e_C^l GM_C/a\ ;\ \alpha \equiv a_C/a \quad (2)$$

where a and e are semi-major axis and eccentricity, the quantity $f_{ml}(\alpha)$ is a combination of Laplace coefficients and their derivatives (*12*), and M_C is Charon's mass. For any single resonance, the equations of motion admit two constants (*14*–*16*): the Brouwer integral

$$B = a^2 n[(m + 1)(1 - e^2)^{1/2} - (l + 1)] \quad (3)$$

and the Jacobi integral

$$C = -\tfrac{1}{2}a^2n^2 - \frac{1}{m+1}a^2nn_c + \Phi_{ml}\cos\phi \quad (4)$$

If an exterior moon were forced to migrate as Charon tidally evolved, Eq. 3 gives the moon's eccentricity, $e(t)$, as a function of $a(t)$. For resonances with $l \neq m$, the resonant argument in Eq. 1 contains the moon's longitude of pericenter, $\tilde{\omega}$, and evolution in resonance increases the moon's eccentricity as a increases. Even for an initially zero eccentricity, a fourfold expansion of semi-major axis excites an eccentricity

$$e_{ml} \rightarrow [1 - (2 + l + m)^2/4(m + 1)^2]^{1/2} \quad (5)$$

For $m = 3$ (i.e., the 4:1), the $l \neq m$ resonances would produce $e_{30} = 0.781$, $e_{31} = 0.661$, and $e_{32} = 0.484$. Eccentricities for $m = 5$ (the 6:1) are also substantial ($e \ge 0.4$) for all $l \neq m$ terms. Because objects in the 6:1 and 4:1 resonances are separated in semi-major axis by

Department of Space Studies, Southwest Research Institute, Boulder, CO 80302, USA.

*To whom correspondence should be addressed. E-mail: ward@boulder.swri.edu

only $a_1 - a_2 \approx 0.31a_2 \approx 0.24a_1$, crossing orbits and instability between such objects would be expected for $e \geq 0.3$. However, for the special case of $l = m$, the resonance argument becomes $\phi_{mm} = (m + 1)\lambda - \lambda_C - m\tilde{\omega}_C$, which does not contain the outer moon's pericenter longitude nor excite its eccentricity. Because the resonant amplitude, Φ_{mm}, is proportional to $e_C{}^m$ (Eq. 2), corotation resonances with $m \geq 1$ require an eccentric perturber.

To describe the character of libration in a corotation resonance, we define the corotation distance as where $n(a_{cr}) = \Omega_{ps}$ with $\Omega_{ps} = n_C/(m + 1) + m(d\tilde{\omega}_C/dt)/(m + 1)$ being the so-called pattern speed, and consider a perturbation in a, i.e., $a = a_{cr} + \Delta a$, $\Delta a \ll a_{cr}$. The trajectory is found from the Jacobi integral, which can be recast as (*16*)

$$C + \tfrac{3}{2}a_{cr}^2 n_{cr}^2 - \Phi_{mm} = -\tfrac{3}{8}n_{cr}^2\Delta a^2 - \tfrac{1}{2}\Phi_{mm}\phi^2 = -\tfrac{1}{2}\Phi_{mm}\phi_{\max}^2 \quad (6)$$

and describes an ellipse with major axis $a\phi_{\max}/m$ and minor axis $\Delta a_{\max} = (4\Phi_{mm}/3n_{cr}^2)^{1/2}\phi_{\max}$, as shown in Fig. 1. The maximum radial width of the librating region is $w = 4(\Phi_{mm}/3n_{cr}^2)^{1/2} = 4(e_C^m|f_{mm}|\mu_C/3)^{1/2}a_{cr}$, where $\mu_C \equiv M_C/M_P = 0.116$ and M_P is Pluto's mass (*3*, *17*). Thus, for example, with a Charon eccentricity of $e_C \sim 0.2$, moons librating in the 4:1 and 6:1 corotation resonances would have a $\Delta a/a_{cr} \leq w/a_{cr} \sim 0.03$ and 0.002, respectively. The libration period $2\pi/\omega_{lib}$, with $\omega_{lib} = (m + 1)(3\Phi_{mm}/a_{cr}^2)^{1/2}$ (*16*), is much longer than the orbital period, so that over multiple orbits in inertial space a moon completes a single libration, as seen in the frame rotating with the resonant term (Fig. 2) (*18*).

Now consider the response of a trapped moon to a slow tidal expansion of Charon's orbit according to (*9*)

$$\frac{da_C}{dt} = 3\frac{k_p}{Q_p}\frac{M_C}{M_P}\left(\frac{R_P}{a_C}\right)^5 a_C n_C \; ; \quad \frac{dn_C}{dt} = -\tfrac{3}{2}n_C\frac{\dot{a}_C}{a_C} \quad (7)$$

where $Q_P \sim 10^2$ is Pluto's tidal dissipation parameter, and $k_P \sim 0.055$ is its tidal Love number (*9*). Objects remain trapped in a moving resonance so long as the time, $w/\dot{a}_{cr} = w/\dot{a}_C(m + 1)^{2/3}$, that it takes for Charon to migrate a distance comparable to the libration zone half-width w, is much longer than the libration period (*13*, *16*). This yields an adiabatic condition, $e_C^m f(\alpha) \gg (3\pi)(k_P/Q_P)(R_P/a_C)^5$. Adopting $a_C(0) \approx 4R_P$ leads to a threshold value for Charon's initial eccentricity $e_{crit} \approx (5 \times 10^{-6}/f_{mm})^{1/m}$ (*19*). This requires $e_C \approx 0.2$ for capture of P1, the more difficult to capture moon. Simulations of Charon's intact formation by impact (*7*) find cases with initial eccentricities and semi-major axes comparable to these values. Early resonant trapping of P1 and P2 would allow for them to have originated from impact debris extending only to ~13 R_P, which is reasonable given results of impact simulations (*7*, *8*).

We are interested in the evolution of e_c as Charon's orbit tidally expands, which is given by (*20*)

$$\frac{1}{e_C}\frac{de_C}{dt} \approx \tfrac{19}{8}[sgn\sigma - \tfrac{28}{19}A]\frac{\dot{a_C}}{a_C} \quad (8)$$

where $\dot{a}_C$ is the expansion rate due only to Pluto tides, $\sigma \equiv 2\omega_P - 3n_C$, with ω_P being the spin frequency of Pluto, and $A \approx (k_C/k_P)(Q_P/Q_C)(R_P/R_C)$ where similar densities have been assumed for Pluto and Charon. The first term on the right side of Eq. 8 is due to tides raised on Pluto, whereas the second term is due to tidal dissipation in Charon. Assuming that the k's are dominated by similar rigidities, then $k_C/k_P \sim (R_C/R_P)^2$, $A \sim R_C Q_P/R_P Q_C$, and e_c increases if $Q_P/Q_C \leq \tfrac{19}{28}R_P/R_C \approx 1.3$. Given the uncertainties, Charon's eccentricity could have either grown or decayed during most of its orbital expansion. However, once $\omega_P \leq 3n/2$ toward the end of its expansion, σ reversed sign and e_C decayed.

Because the current eccentricity of Charon is very low as a result of tidal damping, P1 and P2 are probably not now in corotation resonances. On the other hand, it is unlikely they escaped simultaneously. At present $4n_2 - n_C = 3.14 \times 10^{-7}s^{-1}$ (*3*), so that P2 lies slightly inside the nominal positions of the $m = 3$ terms given by $n_2 \approx n_C/4 + (3 - l)\omega_2^C/4$, where $\omega_2^C = \approx 3.87 \times 10^{-8}s^{-1}$ is Charon's contribution to P2's apse precession (*16*). This suggests that P2 escaped from corotation first (perhaps because of a larger libration amplitude), just before Charon's orbital migration halted. Continued occupancy of the 3:2 resonance could have protected P2 from the remaining $m = 3$ resonances by controlling the rate of apse precession, $d\tilde{\omega}_2/dt \approx 3n_1 - 2n_2$. This would have caused the resonance variable ϕ_{33} to circulate, and as Charon continued to migrate outward, the other ϕ_{ml} resonances variables would circulate as well (*16*). Finding P2 in 3:2 libration currently (*21*) would be strong support for this notion, although it is also possible that a small free eccentricity could have caused a transition from libration to circulation as P1 and P2 separated somewhat.

Because most resonances excite large eccentricities, much of the original impact-produced debris may have been destabilized

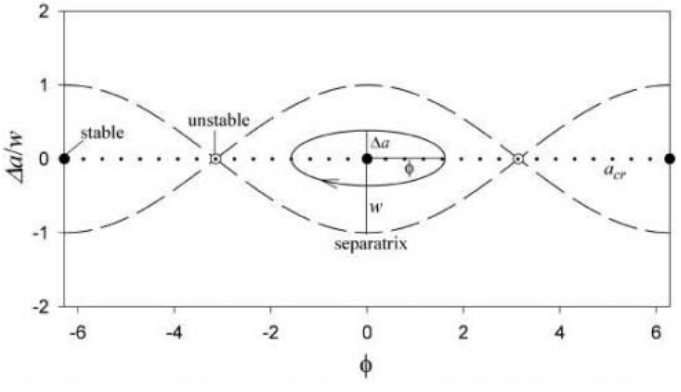

Fig. 1. Schematic of a corotation resonance island, shown in a frame rotating with the resonant pattern speed, Ω_{ps}. Dashed curve indicates the separatrix, dotted line is the corotation distance, and the primary is in the negative y-axis direction. The separatrix separates resonantly librating orbits from nonresonant circulating orbits. Particle trajectories displaced from a stable equilibrium point (filled circles) librate about the point, with each island of libration separated by unstable equilibrium points (open circles).

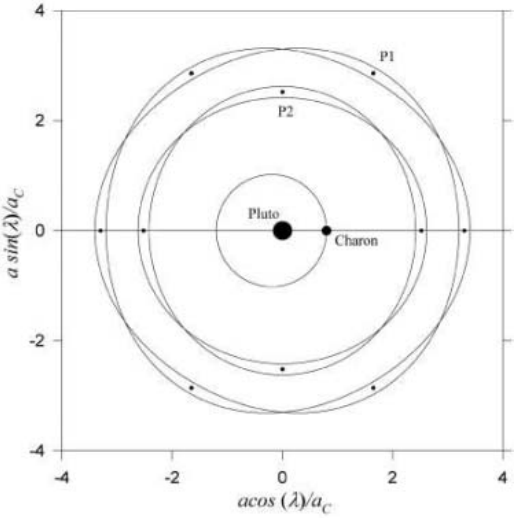

Fig. 2. The $m + 1 = 4$ and $m + 1 = 6$ stability islands for the corotation resonances near P2 and P1, shown when Charon is at pericenter. For each resonance, the $(m + 1)$ islands are confined by a separatrix. The island widths are arbitrarily set to 0.1 for clarity; the actual widths are a function of Charon's eccentricity. The solid point contained in each island is a stable equilibrium about which trajectories librate. Each pattern rotates counter-clockwise at the pattern speed $\Omega_{ps} \approx n_C/(m + 1)$, so for each Charon orbit, a new stable equilibrium point is brought to conjunction at pericenter.

by mutual collisions or scattering into Charon or Pluto. Debris captured into some corotation islands could also have been dislodged through encounters with other high-eccentricity material. Nevertheless, it seems plausible that a fraction comparable to the tiny masses of P1 and P2 might have survived such stochastic removal processes.

What about corotation resonances other than the 4:1 and 6:1? For an eccentric Charon, the 3:1 corotation resonance is nearly overlapped by its Hill sphere at apocenter and was likely not a stable niche. Corotation resonances also occur when $(m + p)n \approx pn_C$ for $p > 1$, but these fall at distances $a_{cr} = (m/p + 1)^{2/3}$ and are shifted inward. Thus, those that fall in the vicinity of P1 and P2 have amplitudes that are dependent on a higher power of Charon's eccentricity (i.e., $\sim e_C^{3p}$, e_C^{5p}) and are weaker. Although transient forced eccentricities may interfere with the stability of adjacent $p = 1$ resonances, it remains an intriguing possibility that smaller, yet undetected moons may orbit Pluto near the 5:1.

Because the corotation resonances we invoke no longer exist, direct diagnostic evidence of this mechanism is elusive. However, a circumstantial case can be made by considering the alternatives. Although there are capture mechanisms (*4*, *5*) to create well-separated secondaries such as some Kuiper belt binaries, they do not select a common orbital plane or direction. In addition, the subsequent hardening of these configurations tends to produce large eccentricities that could not be damped by tidal forces given the small masses of P1 and P2 (*2*). Alternatively, if a protosatellite disk were to extend to sufficient distance to allow the accretion of P1 and P2 in situ, there is no obvious reason why they should be found in near-resonant orbits, because tidal torques are also too weak to migrate them into such configurations. A final unanswered question is how the moons were initially trapped in corotation resonances. One possibility is that a small amount of vapor and/or small particles extended past the location of the 6:1 resonance ($\sim 3.3\ a_C$) and their free eccentricities damped by collisional viscosity. This could have initially populated many resonance sites, but most would be later cleared as eccentricities were excited by resonant migration. Indeed, material comprising P1 and P2 may have begun as ring arcs, except that by lying external to Pluto's Roche limit, single moons were able to accumulate.

References and Notes

1. H. A. Weaver *et al.*, *Nature* **439**, 943 (2006).
2. S. A. Stern *et al.*, *Nature* **439**, 946 (2006).
3. M. W. Buie, W. M. Grundy, E. F. Young, L. A. Young, S. A. Stern, *Astron. J.* **132**, 290 (2006).
4. P. Goldreich, Y. Lithwick, R. Sari, *Nature* **420**, 643 (2002).
5. S. J. Weidenschilling, *Icarus* **160**, 212 (2002).
6. W. B. McKinnon, *Astrophys. J.* **344**, L41 (1989).
7. R. M. Canup, *Science* **307**, 546 (2005).
8. R. M. Canup, *Ann. Rev. Astron. Astrophys.* **42**, 441 (2004).
9. A. R. Dobrovolskis, S. J. Peale, A. W. Harris, in *Pluto and Charon*, S. A. Stern, D. J. Tholen, Eds. (Univ. Arizona Press, Tucson, AZ, 1997), pp. 193–219.
10. P. Goldreich, S. Tremaine, N. Borderies, *Astron. J.* **92**, 490 (1986).
11. F. Namouni, C. Porco, *Nature* **417**, 45 (2002).
12. C. D. Murray, S. F. Dermott, *Solar System Dynamics* (Cambridge Univ. Press, Cambridge, 2001).
13. S. Dermott, R. Malhotra, C. D. Murray, *Icarus* **76**, 295 (1988).
14. D. Brouwer, *Astron. J.* **68**, 152 (1963).
15. P. Goldreich, S. Tremaine, *Astrophys. J.* **243**, 1062 (1981).
16. Methods are available as supporting material on *Science* Online.
17. C. B. Olkin, L. H. Wasserman, O. G. Franz, *Icarus* **164**, 254 (2003).
18. The libration period is $2\pi/\omega_{lib} = T_{orb}(3e_C^{m}f_m(\alpha)\mu_C)^{-1/2}/(m + 1)$. With $e_C = 0.2$, the libration periods for the 4:1 and 6:1 are $\sim$11 and $\sim$112 times the local orbit periods, T_{orb}, respectively.
19. Because the tidal expansion rate (Eq. 7) decreases strongly as $a_C^{-11/2}$, the critical e_C value decreases with orbital radius as well, i.e., $e_{crit} \propto (R_p/a_{cr})^{5/m}$, so that the adiabatic constraint on e_C eases as Charon's orbit expands.
20. P. Goldreich, S. Soter, *Icarus* **5**, 375 (1966).
21. M. H. Lee, S. J. Peale, 2006. Preprint available at http://arxiv.org/abs/astro-ph/0603214.

22. This work was supported by NASA's Planetary Geology and Geophysics Program (W.R.W.) and NSF's Planetary Astronomy Program (R.M.C.). We thank S. A. Stern for communicating discovery results of Pluto's new moons just before publication and the referees for thoughtful comments.

Supporting Online Material

www.sciencemag.org/cgi/content/full/1127293/DC1
SOM Text

13 January 2006; accepted 23 June 2006
Published online 6 July 2006;
10.1126/science.1127293
Include this information when citing this paper.

Ice Record of $\delta^{13}C$ for Atmospheric CH_4 Across the Younger Dryas–Preboreal Transition

Hinrich Schaefer,[1,2*] Michael J. Whiticar,[1] Edward J. Brook,[2] Vasilii V. Petrenko,[3] Dominic F. Ferretti,[4,5] Jeffrey P. Severinghaus[3]

We report atmospheric methane carbon isotope ratios ($\delta^{13}CH_4$) from the Western Greenland ice margin spanning the Younger Dryas–to–Preboreal (YD-PB) transition. Over the recorded ~800 years, $\delta^{13}CH_4$ was around –46 per mil (‰); that is, ~1‰ higher than in the modern atmosphere and ~5.5‰ higher than would be expected from budgets without ^{13}C-rich anthropogenic emissions. This requires higher natural ^{13}C-rich emissions or stronger sink fractionation than conventionally assumed. Constant $\delta^{13}CH_4$ during the rise in methane concentration at the YD-PB transition is consistent with additional emissions from tropical wetlands, or aerobic plant CH_4 production, or with a multisource scenario. A marine clathrate source is unlikely.

Ice core records reveal prominent changes in atmospheric methane concentration [CH_4] associated with abrupt climate change (*1*) but the causes, including source and sink changes, remain controversial (*1*, *2*). Modern contributions from individual sources or sinks have been constrained by the $^{13}C/^{12}C$ ratio of atmospheric methane ($\delta^{13}CH_4$) (*3*, *4*). New analytical techniques extend this approach to air samples from gas occlusions in polar ice. Using ice samples from the Pakitsoq outcrop (Western Greenland) (*5*), we measured $\delta^{13}CH_4$ in air dating between 11,360 and 12,220 years before the present (yr B.P.) (*6*). The record covers the transition between the Younger Dryas (YD) and Preboreal Holocene (PB), when temperature (*7*) and [CH_4] (*1*) increased rapidly at the termination of the last ice age (Fig. 1).

The suitability of Pakitsoq ice for paleostudies has been demonstrated by the agreement of [CH_4] and other geochemical tracers with records from the Greenland Ice Sheet Project 2 (GISP2) ice core (*5*). Samples were collected during three field campaigns (2001 to 2003) by means of oil-free chainsaws and shipped frozen to the University of Victoria. The main data set was measured after wet extraction by gas chromatography–isotope ratio mass spectrometry (GC-IRMS) (*8*). [CH_4] measurements were duplicated at Washington State University. Six samples from three time periods were analyzed for $\delta^{13}CH_4$ at the National Institute of Water and Atmospheric Research (NIWA) using ~100-liter air samples extracted in the field (*8*) (Fig. 1). All samples were dated with a gas age scale derived by comparison of geochemical records from Pakitsoq and GISP2 (*8*). Results are consistent throughout the three field seasons and form a composite data set (Fig. 1).

[1]School of Earth and Ocean Sciences, University of Victoria, Post Office Box 3055, V8W 3P6, Canada. [2]Department of Geosciences, Oregon State University, 104 Wilkinson Hall, Corvallis, OR 97331, USA. [3]Scripps Institution of Oceanography, University of California, San Diego, Mail Code 0244, La Jolla, CA 92093, USA. [4]Institute of Arctic and Alpine Research, University of Colorado, Boulder, CO 80309, USA. [5]National Institute of Water and Atmospheric Research Limited, Post Office Box 14901, Wellington, New Zealand.

*To whom correspondence should be addressed. E-mail: schaefeh@geo.oregonstate.edu

Our $\delta^{13}CH_4$ data reveal several interesting features, two of which we discuss here. First, the YD-PB methane is ^{13}C-enriched by ~1 per mil (‰) relative to modern atmospheric $\delta^{13}CH_4$ (–47.1‰) (*9*) and ~5.5‰ higher than expected from previously proposed natural CH_4 budget scenarios (table S1) (*3*, *10*). Second, there is no significant change in $\delta^{13}CH_4$ across the YD-PB transition. In the Pakitsoq record, $[CH_4]$ rises from 490 to 750 parts per billion by volume (ppbv) at the transition, which is consistent with GISP2 data (*1*, *5*) (Fig. 1A). During the YD, $\delta^{13}CH_4$ has a mean of –46.0 ± 0.5‰ (1σ) (Fig. 1C). Slight variations fall within the envelope of uncertainty. The PB mean $\delta^{13}CH_4$ is –45.7 ± 1.2‰. Surprisingly, there is no significant difference in $\delta^{13}CH_4$ between the two climatic intervals, nor is there an isotope shift during the ~250-ppbv $[CH_4]$ increase.

Pre-anthropogenic $\delta^{13}CH_4$ was expected to be depleted in ^{13}C (relative to modern atmospheric CH_4) because of the absence of fossil fuel combustion, slash-and-burn agriculture, and landfills, all of which emit ^{13}C-enriched CH_4 (*3*). Such ^{13}C depletions are observed in ice from 100 to 300 yr B.P. (*11*–*13*), whereas 400 to 2000 yr B.P. values from the late preindustrial Holocene (LPIH) are unexpectedly ^{13}C-enriched, similar to our YD-PB $\delta^{13}CH_4$ (*12*).

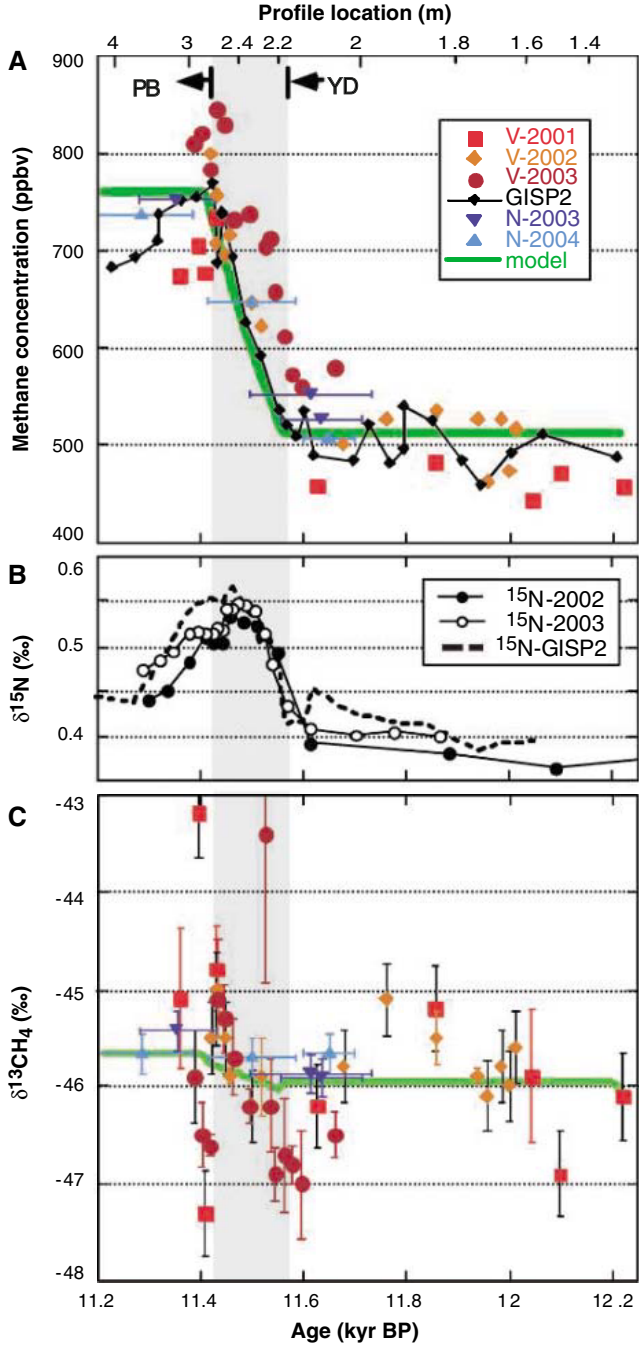

Fig. 1. Methane concentration and $\delta^{13}CH_4$ in Pakitsoq ice samples. **(A)** $[CH_4]$ measured at the University of Victoria (V-2001 to V-2003), at NIWA (N-2003 and N-2004), and from the GISP2 core, together with $[CH_4]$ model results used to constrain the transition source (*8*). The age spread of the samples is indicated by symbol size (V samples, 25 to 35 years) or horizontal bars (N samples, 100 to 240 years). The bottom axis shows sample age according to the Pakitsoq gas age scale (*8*); the top axis shows sample location within the profile (nonlinearity between the axes is due to differential thinning of ice layers). In (A) to (C), vertical shading marks the transition period. **(B)** Pakitsoq and GISP2 $\delta^{15}N$ data (*5*, *7*) show the onset of atmospheric warming (11,570 yr B.P.). **(C)** $\delta^{13}CH_4$ versus sample age. The slight depression of modeled $\delta^{13}CH_4$ (*8*) during the transition (~0.1‰) is due to a temporary imbalance between ^{13}C-depleted emissions and ^{13}C-enriching sinks (*22*). Data have been corrected for gravitational, thermal, and diffusion fractionation (*8*). Colored error bars show the standard error of multiple samples. Black error bars on single measurements show analytical precision (±1σ) derived from standard ice [0.44‰ (n = 11 replicates) in 2001, 0.37‰ (n = 33) in 2002, and 0.48‰ (n = 12) in 2003].

An initial explanation for our high $\delta^{13}CH_4$ was enrichment during postocclusion microbial oxidation of CH_4; that is, a storage artifact. However, this is ruled out because the amount of oxidation required for the observed isotopic shift would be between 15 and 48% (*8*). This would be readily detected as discrepancies between the Pakitsoq and GISP2 $[CH_4]$ records (Fig. 1A).

The difference between $\delta^{13}CH_4$ measured at the YD-PB and LPIH is not an artifact and must result from changes in CH_4 sources or sinks. The multitude of variables affecting atmospheric $\delta^{13}CH_4$ and uncertainties in paleoenvironmental data make it difficult to reconstruct a definitive CH_4 budget for the YD-PB. However, we discuss five possible explanations for the ^{13}C enrichment.

First, biomass burning is the most ^{13}C-enriched ($\delta^{13}CH_4$ ~ –25‰) of all sources (*3*). For the LPIH, elevated pyrogenic emissions of 25 Tg/year have been inferred from ice core $\delta^{13}CH_4$ (*12*). Even with fire emissions of this magnitude, the YD isotope scenario would still be too ^{13}C-depleted (table S1), whereas charcoal records indicate less burning before the LPIH (*14*). Nevertheless, literature estimates (*10*) of late glacial fire emissions (5 Tg/year) may be too low, and pyrogenic CH_4 could possibly contribute to ^{13}C enrichment. In the LPIH, high $\delta^{13}CH_4$ values have been partly attributed to human-made fires (*12*). Interestingly, we observe even higher $^{13}CH_4$ values in the YD-PB, when anthropogenic burning is expected to have been negligible.

Second, geologic (natural thermogenic) sources are usually not included in CH_4 budgets, even though they emit enough ^{13}C-enriched methane today to significantly affect atmospheric $\delta^{13}CH_4$ (*15*). Because of lower overall emissions during the YD, geologic sources probably constituted a larger fraction of the budget than today, leading to higher atmospheric $\delta^{13}CH_4$. Additionally, lower YD sea levels may have increased this source (*16*).

Third, previous CH_4 budget calculations have grouped tropical wetlands with other wetlands, resulting in integrated wetland $\delta^{13}CH_4$ of –58 to –59‰ (*3*, *4*). However, for tropical wetlands alone, flux-weighted mean $\delta^{13}CH_4$ as high as –53 to –55‰ has been reported (*17*). We suggest that tropical wetlands must be treated separately from boreal and temperate wetlands because of differences in climatic response and $\delta^{13}CH_4$. Tropical wetlands could partly account for the measured ^{13}C enrichment (table S1).

Fourth, the recent discovery of aerobic methane production (AMP) from plant material (*18*) has revealed a previously unknown source with high $\delta^{13}CH_4$ (~ –50‰). At estimated emission rates of 150 ± 90 Tg/year (*18*), it may be as important for the natural CH_4 cycle as wetlands (~140 Tg/year) (*19*) and could contribute to higher atmospheric $\delta^{13}CH_4$.

Fifth, there is evidence that Cl in the marine boundary layer (MBL) acts as a CH_4 sink, with a large isotope effect that increases atmospheric $\delta^{13}CH_4$ (*20*).

The potential impact of these five processes on $\delta^{13}CH_4$ can be estimated with isotope mass balance calculations. Although we recognize the considerable uncertainty introduced by the range of reported values and incomplete knowledge of YD conditions, we estimate that none of these processes alone can explain the ^{13}C enrichment. Conversely, the cumulative effect of all five would be too large (table S1). Several processes together could balance the YD isotope budget, but the exact combination cannot be determined without further evidence.

For completeness, one must also consider changes in the ratio of C_3 to C_4 vegetation, temperature-dependent fractionation coefficients, the relative amounts of CH_4 oxidation and production in wetland soils, and weighted total fractionation (α_{WT}) of the overall sink (*21*). These all influence atmospheric $\delta^{13}CH_4$, depending on climatic and anthropogenic factors that were probably different during the YD than today. Preliminary studies lead us to assume that neither the individual (±1‰), nor the combined impact of such changes (^{13}C depletion of 0.7‰), accounts for the $\delta^{13}CH_4$ enrichment.

A primary objective of our study is to understand why $[CH_4]$ increased abruptly during the YD termination. This rise was not associated with a sustained shift between steady states or with an episodic $\delta^{13}CH_4$ excursion (within measurement error) (Fig. 1). The latter observation suggests that the $[CH_4]$ increase was not caused by a short-lived perturbation, such as a release of stored CH_4.

Several lines of evidence suggest that increased emissions triggered by climate change caused the $[CH_4]$ rise (*1*, *2*). We used an atmospheric box model (*22*) to find the $\delta^{13}CH_4$ of these additional emissions or "transition source" required to explain our measured $[CH_4]$ and $\delta^{13}CH_4$ histories (*8*) (Fig. 1). Results depend on whether a MBL sink is considered and other uncertainties in α_{WT}. The model predicts a transition source $\delta^{13}CH_4$ between –53.6 ± 1.5‰ (including a MBL sink) and –50.7 ± 0.7‰ (without a MBL sink) (*23*).

The transition source could have been a combination of two or more sources. If those had different $\delta^{13}CH_4$ values, then their relative emissions would have to fortuitously match in order not to affect atmospheric $\delta^{13}CH_4$. For example, a ^{13}C-enriching component such as wildfire CH_4 or the marine Cl sink could be balanced by a ^{13}C-depleted microbial source. In the absence of unequivocal geologic evidence, these scenarios remain unresolved.

A sink decrease caused by higher volatile organic carbon emissions from forests (*24*) could have increased $[CH_4]$ without significant impact on α_{WT} and $\delta^{13}CH_4$. This scenario requires a large expansion of forests on the short time scale of the $[CH_4]$ increase. This may be compatible with paleobotanical data (*25*, *26*), but seems less likely when rates of ecosystem reorganization are considered. However, a slight sink decrease caused by feedbacks in atmospheric chemistry due to higher $[CH_4]$ is probable (*27*).

Most microbial CH_4 sources, such as boreal and temperate wetlands, animals, and clathrates, have $\delta^{13}CH_4$ of –60‰ or lower (*3*). The calculated impact of each of these sources on the transition mass balance would be –1.3 to –2.2‰ (depending on the assumed sink configuration). This exceeds the least significant difference of 1.1‰ between the YD and PB that would be discernible from our data at the 90% confidence level (based on a two-sided *t* test result of ±0.54‰). Therefore, microbial CH_4 can be ruled out as a sole transition source. However, CH_4 from marine clathrates can become ^{13}C enriched by microbial oxidation as it migrates through sediment and water columns (*28*). Isotopic fractionation associated with the oxidation progressively enriches the remaining CH_4 in ^{13}C relative to the clathrate. In order to match the transition source $\delta^{13}CH_4$, only 30 to 40% of the gas initially released from clathrates could have reached the atmosphere, according to the Rayleigh equation (*8*).

It has been proposed that marine clathrates drove the YD-PB $[CH_4]$ rise and maintained high $[CH_4]$ until mature wetlands developed (~8000 yr B.P.) (*2*). The total amount of clathrate dissociation required by this scenario can be calculated from (i) the magnitude of additional emissions (62×10^{12} g/year) (*1*), (ii) the fact that the latter represent only 30 to 40% of the destabilized clathrate gas, and (iii) the postulated time scale (~3000 years) (*2*), giving a result of 410×10^{15} to 540×10^{15} g of dissociated clathrate carbon. For comparison, only 175×10^{15} g potentially became unstable within the last 100,000-year glacial cycle (*29*), a period with more than 20 abrupt $[CH_4]$ rises (*1*). If clathrate release had driven all 20, then the potentially unstable reservoir for each event would have been exhausted within only ~50 years. In conclusion, our $\delta^{13}CH_4$ record supports neither catastrophic nor gradual clathrate emissions at the YD-PB transition, as is also indicated by CH_4 deuterium ($\delta D\text{-}CH_4$) records (*30*).

Hydrological proxies point to tropical wetlands as a driver of the YD-PB $[CH_4]$ increase (*31*, *32*). The higher of the $\delta^{13}CH_4$ values (–53 to –55‰) reported for tropical wetlands (*17*) closely matches the modeled transition source (especially if the MBL sink is included). The impact of tropical wetlands (0.1 to 0.7‰) on the mass balance during the transition would not be detectable. However, controversy remains about whether wetlands were a source of sufficient magnitude (*19*) and responded quickly enough to climate change (*2*).

In contrast, vegetation-derived AMP (*18*) could have changed quickly and strongly as indicated by paleoreconstructions of net primary productivity (NPP) (*33*). Scaling emission estimates (*18*) to NPP results in a potential increase of AMP by 50% between glacial and interglacial conditions. Terrestrial carbon stocks of vegetation, a possible proxy for AMP, reach equilibrium after climatic change within 250 years (*25*), and a first vegetation response occurs within decades (*26*). These time scales compare well with the observed lag time and duration of the YD-PB $[CH_4]$ increase (*7*). Also, the match between transition-source $\delta^{13}CH_4$ in the non-MBL sink scenario and that of AMP is good. In that case, the mass balance impact would be 0.7‰, which is within the uncertainty of our data. Whether the vegetation response was sufficient to sustain the $[CH_4]$ increase at the YD-PB should be investigated with vegetation models, once estimates of emission rates are confirmed. Our $\delta^{13}CH_4$ data are therefore consistent with a fast-responding AMP source and with the hypothesis that low-latitude wetlands caused $[CH_4]$ rises during the last glacial cycle (*1*).

Further insights into the atmospheric CH_4 budget require a reduction in the uncertainties of methane source and sink strengths and signals, and the combination of higher-precision $\delta^{13}CH_4$ and $\delta D\text{-}CH_4$ data.

References and Notes

1. E. J. Brook, S. Harder, J. Severinghaus, E. J. Steig, C. M. Sucher, *Global Biogeochem. Cycles* **14**, 559 (2000).
2. J. P. Kennett, K. G. Cannariato, I. L. Hendy, R. J. Behl, *Methane Hydrates in Quaternary Climate Change* (American Geophysical Union, Washington, DC, 2003).
3. M. J. Whiticar, in *Atmospheric Methane: Sources, Sinks and Role in Global Change*, M. A. K. Khalil, Ed. (NATO ASI Series, Springer, Berlin, 1993), vol. 113, pp. 138–167.
4. R. Hein, P. J. Crutzen, M. Heimann, *Global Biogeochem. Cycles* **11**, 43 (1997).
5. V. V. Petrenko, J. P. Severinghaus, E. J. Brook, N. Reeh, H. Schaefer, *Quat. Sci. Rev.* **25**, 865 (2006).
6. Years before the present are reported relative to 1950 A.D.
7. J. P. Severinghaus, T. Sowers, E. J. Brook, R. B. Alley, M. L. Bender, *Nature* **391**, 141 (1998).
8. Additional information on materials and methods is available on *Science* Online.
9. J. B. Miller *et al.*, *J. Geophys. Res*. **107**, 10.1029/2001JD000630 (2002).
10. J. A. Chappellaz, I. Y. Fung, A. M. Thompson, *Tellus* **45B**, 228 (1993).
11. H. Craig, C. C. Chou, J. A. Welhan, C. M. Stevens, A. Engelkemeir, *Science* **242**, 1535 (1988).
12. D. F. Ferretti *et al.*, *Science* **309**, 1714 (2005).
13. T. Sowers *et al.*, *Global Biogeochem. Cycles* **19**, 10.1029/2004GB002408 (2005).
14. C. Carcaillet *et al.*, *Chemosphere* **49**, 845 (2002).
15. G. Etiope, A. V. Milkov, *Environ. Geol.* **46**, 997 (2004).
16. B. Luyendyk, J. P. Kennett, J. F. Clark, *Marine Petrol. Geol.* **22**, 591 (2005).
17. P. D. Quay *et al.*, *Global Biogeochem. Cycles* **5**, 25 (1991).
18. F. Keppler, J. T. G. Hamilton, M. Braß, T. Röckmann, *Nature* **439**, 187 (2006).
19. J. O. Kaplan, *Geophys. Res. Lett*. **29**, 10.1029/2001GL013366 (2002).
20. W. Allan, D. C. Lowe, A. J. Gomez, H. Struthers, G. W. Brailsford, *J. Geophys. Res*. **110**, 10.1029/2004JD005650 (2005).

21. The MBL sink strongly affects α_{WT}. Accordingly, all reported sensitivity tests, including the ones on past changes in α_{WT} and transition isotope budgets, have been carried out with and without a MBL sink.
22. P. P. Tans, *Global Biogeochem. Cycles* **11**, 77 (1997).
23. α_{WT} without a MBL sink is taken as 6.4 ± 0.7‰, which is smaller than at present because of decreases in [Cl] (*34*) and soil uptake (*19*); including the MBL sink increases α_{WT} to 9.3 ± 0.7‰. All YD sinks were scaled proportionally to $[CH_4]$ from current estimates (*13*, *20*) to account for decreased loss rates at lower concentrations.
24. J. O. Kaplan, G. Folberth, D. A. Hauglustaine, *Global Biogeochem. Cycles* **20**, 10.1029/2005GB002590 (2006).
25. M. Scholze, W. Knorr, M. Heimann, *Holocene* **13**, 327 (2003).
26. D. Peteet, *Proc. Natl. Acad. Sci. U.S.A.* **97**, 1359 (2000).
27. A. M. Thompson, J. A. Chappellaz, I. Y. Fung, T. L. Kucsera, *Tellus* **45B**, 242 (1993).
28. N. J. Grant, M. J. Whiticar, *Global Biogeochem. Cycles* **16**, 10.1029/2001GB001851 (2002).
29. D. Archer, B. A. Buffett, *Geochem. Geophys. Geosyst.* **6**, Q03002 (2005).
30. T. A. Sowers, *Science* **311**, 838 (2006).
31. Y. J. Wang *et al.*, *Science* **294**, 2345 (2001).
32. K. A. Hughen, T. I. Eglinton, L. Xu, M. Makou, *Science* **304**, 1955 (2004).
33. L. M. Francois, C. Delire, P. Warnant, G. Munhoven, *Global Planet. Change* **16-17**, 37 (1998).
34. A. L. Rice, S. C. Tyler, M. C. McCarthy, K. A. Boering, E. Atlas, *J. Geophys. Res.* **108**, 10.1029/2002JD003042 (2003).
35. We thank N. Reeh and his team from the Technical University of Denmark for field collaboration and helpful discussions; P. Rose for field support; and P. Eby, L. Bjerkelund, P. Franz, K. Riedel, G. Brailsford, and R. Martin for laboratory assistance. Suggestions by two anonymous reviewers greatly improved this manuscript. The project was supported by a German Academic Exchange Service (DAAD) fellowship (H.S.), a Canadian Centre for Climate Modeling and Analysis Environment Canada grant (M.J.W.), a Natural Sciences and Engineering Research Council Discovery Grant (M.J.W.), Canadian Foundation for Climate and Atmospheric Sciences Project Grant GR-417 (M.J.W.), and NSF grants OPP-0221410 (E.J.B.) and OPP-0221470 (J.P.S.).

Supporting Online Material

www.sciencemag.org/cgi/content/full/313/5790/1109/DC1
Materials and Methods
Table S1
References

22 February 2006; accepted 14 July 2006
10.1126/science.1126562

Decoupled Plant and Insect Diversity After the End-Cretaceous Extinction

Peter Wilf,[1]* Conrad C. Labandeira,[2,3] Kirk R. Johnson,[4] Beth Ellis[4]

Food web recovery from mass extinction is poorly understood. We analyzed insect-feeding damage on 14,999 angiosperm leaves from 14 latest Cretaceous, Paleocene, and early Eocene sites in the western interior United States. Most Paleocene floras have low richness of plants and of insect damage. However, a low-diversity 64.4-million-year-old flora from southeastern Montana shows extremely high insect damage richness, especially of leaf mining, whereas an anomalously diverse 63.8-million-year-old flora from the Denver Basin shows little damage and virtually no specialized feeding. These findings reveal severely unbalanced food webs 1 to 2 million years after the end-Cretaceous extinction 65.5 million years ago.

There is little direct evidence from the fossil record about food web recovery after mass extinction. One theoretical model describes the rebuilding of diversity, after a lag period, first for primary producers and then for successively higher trophic levels after additional time lags (*1*). Consistent with this pattern is a 3- to 4-million-year recovery period for pelagic food webs after the Cretaceous-Paleogene boundary (K-T), inferred from isotopic depth gradients (*2*–*4*).

Insect damage on compressed fossil leaves provides abundant information about terrestrial food webs, because the diversity of plants and their insect feeding associations can be directly compared using the same fossils, at high sample sizes and in fine stratigraphic context (*5*–*7*). Modern ecological observations generally show positive correlations between insect herbivore diversity and plant diversity (*8*–*10*), and the evaluation of fossil insect damage can test whether past extinctions disrupted this linkage. In southwestern North Dakota, for example, the K-T event caused a significant floral extinction (*11*) accompanied by a major extirpation of insect feeding morphotypes (*6*). These included diverse and abundant leaf mines and galls, whose extant analogs are typically made by host-specialized insects (*12*, *13*). No significant recovery of specialized feeding was found in 80 m of local section representing the first ~0.8 million years of the 10-million-year Paleocene (*6*), prompting us to examine the geographic and temporal extent of the Paleocene ecological dead zone.

We investigated the recovery of plant-insect associations in the western interior United States, with emphasis on the Paleocene. We focused on insect mines (hereafter "mines") because they are a specialized feeding category commonly preserved in fine morphological detail (Fig. 1) (*14*, *15*). We compared four latest Cretaceous, nine early and late Paleocene, and one early Eocene megafloral sites (Table 1, table S1, and fig. S1) from warm temperate and subtropical fluvial paleoenvironments, selected to optimize preservation and diversity, sample size, stratigraphic control, and temporal and geographic coverage. The sites are located in several basins, forming a composite regional data set. Nearly all the Paleocene samples have similar taxonomic composition and the low floral diversity that is typical of the time period and region (Fig. 2 and tables S2 and S3). The major exception is the Castle Rock flora from the Denver Basin: a highly diverse and compositionally distinct early Paleocene assemblage with tropical rainforest characteristics, located in a warm and humid, apparently geographically restricted, belt on the eastern margin of the Laramide Front Range (*16*–*20*).

For taphonomic consistency, we analyzed only identifiable specimens of angiosperm leaves (excluding monocots) and avoided fragmentary leaves when possible. Samples came from single stratigraphic horizons whenever feasible, and biases were greatly reduced by either making quantitative census collections in the field (*7*) or using museum collections that had at least 400 identifiable specimens (Table 1). We also considered, where indicated below, more than 15,000 additional specimens that did not meet these criteria (table S4). These come from the North Dakota K-T study, Castle Rock, the late Paleocene and early Eocene of southwestern Wyoming, and one Late Cretaceous and two additional early Paleocene sites in the Denver Basin.

We scored each specimen for the presence or absence of 63 distinct insect damage morphotypes (DTs) found in the total data set, allocated to the four functional feeding groups of external foliage feeding, galling, mining, and piercing-and-sucking as described elsewhere (*5*, *14*, *15*) (table S2). Plant richness and DT diversity on bulk samples were standardized to 400 leaf specimens by means of rarefaction and randomized resampling, respectively (Fig. 2). Separately, we evaluated mining morphotype diversity for each of 89 species-site pairs with at least 25 leaf specimens (Fig. 3 and table S2).

The Cretaceous floras are rich, whereas all Paleocene assemblages are depauperate except Castle Rock (Fig. 2A), where plant diversity exceeds that of the Cretaceous samples. Insect damage diversity on bulk samples approximately tracks plant diversity, dropping across the K-T and remaining low until the latest Paleocene (Fig. 2 and table S4). However, insect damage shows a striking inversion with respect to plant richness at Castle Rock and Mexican Hat (Fig. 2). The diverse Castle Rock flora has some of the lowest feeding diversity in our data set. This result holds for all damage

[1]Department of Geosciences and Institutes of the Environment, Pennsylvania State University, University Park, PA 16802, USA. [2]Department of Paleobiology, Smithsonian Institution, Washington, DC 20560, USA. [3]Department of Entomology, University of Maryland, College Park, MD 20742, USA. [4]Department of Earth Sciences, Denver Museum of Nature and Science, Denver, CO 80205, USA.

*To whom correspondence should be addressed. E-mail: pwilf@psu.edu

morphotypes, for specialized damage only, and for mines alone (Fig. 2). Only two mines occur in the Castle Rock sample: two morphotypes on two hosts (Fig. 1, I and J) (*21*).

In contrast, feeding diversity on the depauperate Mexican Hat flora is comparable to that of considerably more diverse Cretaceous floras (Fig. 2). Mining at Mexican Hat is unlike that of any other Paleocene flora we have observed, in its abundance and in its prevalence, diversity, and taxonomic breadth among host plants. Mining occurs on 2.6% of leaves, which is more than double

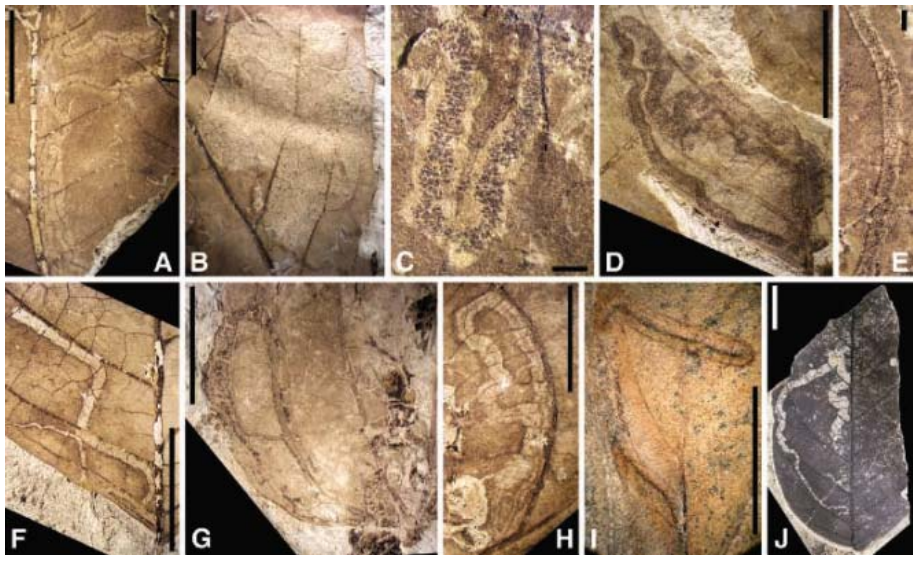

Fig. 1. Representative leaf mines on the botanically depauperate Mexican Hat [(A) to (H)] flora and the diverse Castle Rock [(I) and (J)] flora, both early Paleocene (Table 1). Scale bars, 1 mm in (C) and (E), 1 cm in the other panels. (**A**) Elongate, serpentine, agromyzid dipteran mine (DT104) characterized by a hairline trail of fluidized frass and occurring only on *Platanus raynoldsi* (Platanaceae) [USNM specimen 498154 (National Museum of Natural History)]. (**B**) Blotch mine on *P. raynoldsi* with small ellipsoidal frass pellets (DT36), probably made by a tenthredinid hymenopteran, USNM 498155. A similar mine also occurs on a rare unidentified host at Mexican Hat (not shown in the figure). (**C**) Moderately sinusoidal to linear lepidopteran mine on *P. raynoldsi* with pelleted frass trail of variable width and undulate mine margins (DT91, USNM 498156). (**D**) Sinusoidal mine, probably lepidopteran, on *Juglandiphyllites glabra* (Juglandaceae; fragment, not included in analyses) with frass trail of dispersed rounded pellets oscillating across the full mine width (DT92, USNM 498157). (**E**) Mine on "*Populus*" *nebrascensis* (Trochodendrales) with distinct pelleted frass trail occupying the median 80% of the mine width (DT91, USNM 498158). (**F**) Curvilinear aborted mine lacking frass (DT105) on *J. glabra*, USNM 498159. (**G**) Serpentine lepidopteran mine with thick, initially intestiniform but subsequently looser frass trail (DT41), common throughout the Paleocene in the western interior United States and shown here on *Zizyphoides flabella* (Trochodendraceae), USNM 498160. (**H**) Serpentine lepidopteran mine (DT91) displaying frass detail of early instar stages at bottom, on *Cercidiphyllum genetrix* (Cercidiphyllaceae), USNM 498161. (**I**) Aborted mine on host morphotype CR9, showing confined, linear, median frass trail with lateral reaction rim [DT43, DMNH specimen 26060 (Denver Museum of Nature and Science)]. (**J**) Complete, serpentine, straight-margined mine lacking frass (DT45) on host morphotype CR59, DMNH 26039.

Table 1. Sampling summary. All insect-damage data are new between Mexican Hat and Lur'd Leaves, inclusive. The Cretaceous and Pyramid Butte samples were reanalyzed from our K-T data set (*6*), with the addition of >700 newly analyzed leaf specimens. Data are not adjusted for sample size as in Fig. 2 (see also fig. S1 and table S1).

Sample and time interval	Location	Age (Ma)	Leaf specimens	Leaf species
Early Eocene				
Sourdough* (*5*)	Great Divide Basin, SW WY	53.5	792	22
Latest Paleocene				
Clarkforkian† (*5*)	Washakie Basin, SW WY	56.5	749	10
Late Paleocene				
Lur'd Leaves‡§	Polecat Bench, Bighorn Basin WY	57.5	1360	15
Skeleton Coast‡§	Polecat Bench, Bighorn Basin WY	59.0	835	7
Persites Paradise‡§	Great Divide Basin, SW WY	59.0	963	10
Kevin's Jerky‡§	Washakie Basin, SW WY	59.0	1319	7
Haz-Mat‡§	Washakie Basin, SW WY	59.0	749	4
Early Paleocene				
Castle Rock lower layer* (*19*)	Denver Basin, CO	63.8	2309	130
Mexican Hat‡§ (*30*)	Powder River Basin, SE MT	64.4	2219	16
Pyramid Butte‖ (*11*)	Williston Basin, SW ND	65.5	549	23
Latest Cretaceous				
Battleship‖ (*11*)	Williston Basin, SW ND	65.6	459	40
Dean Street‖ (*11*)	Williston Basin, SW ND	65.7	743	74
Somebody's Garden level‖ (*11*)	Williston Basin, SW ND	66.3	1525	46
Luten's 4H Hadrosaur level‖ (*11*)	Williston Basin, SW ND	66.5	428	26

*Field census, two or more quarries from the same level. †Field census, two quarries from approximately the same level. ‡New collection. §Field census, single quarry. ‖Museum collection from single quarry or multiple quarries at same level, >400 specimens total.

the frequency of any other Paleocene sample (table S1). Most distinctively, the four most abundant host species, which together account for 91% of specimens and are also abundant in our other Paleocene samples (table S2), each have either two or three mine morphotypes (Figs. 1 and 3); mining also occurs on two other locally rare hosts [Fig. 1, B (caption) and E]. The sycamore *Platanus raynoldsi* has mines attributable to three insect orders, namely Hymenoptera (Fig. 1B) and Lepidoptera (Fig. 1C) and numerous mines (on 32 leaves, with up to six mines per leaf) assignable to Agromyzidae within the Diptera (Fig. 1A); the association of agromyzid leaf-miners and Platanaceae does not occur today (*22*).

The only other examples of more than one mine morphotype per species in our data set occur on two Cretaceous hosts from two different sites and on two latest Paleocene and early Eocene Betulaceae (*Corylites* and *Alnus*, respectively) (Fig. 3). Only one of the Mexican Hat mine morphotypes (DT41, Fig. 1G) has been found in the latest Cretaceous of North Dakota, on host plants unrelated to the Mexican Hat dominants (*6*), and three (DT91, DT92, and DT104; Fig. 1) have not been observed in any other North American fossil floras to date. This suggests that the Mexican Hat miners included more newly and regionally evolved taxa, or alternatively long-distance migrants, than regional K-T survivors.

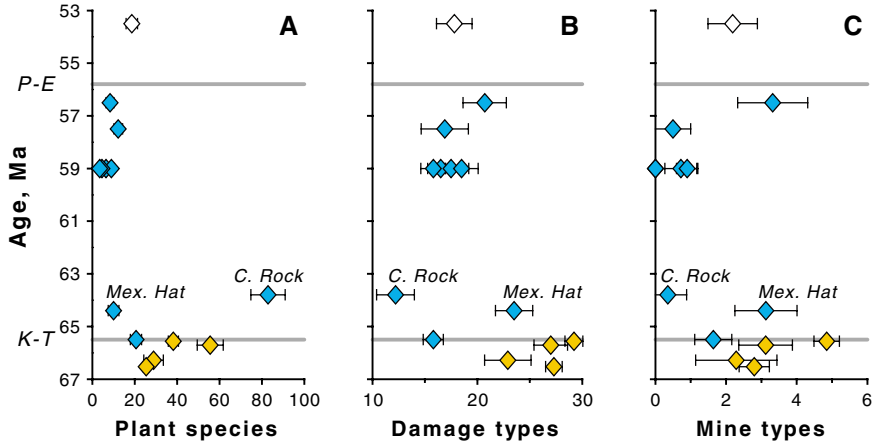

Fig. 2. Plant and insect-feeding diversity for bulk floras (Table 1 and table S1), standardized to sample sizes of 400 leaf specimens each. Orange-yellow data points are Cretaceous floras; blue data points are Paleocene floras. Ma, million years ago. Plant richness (**A**) was standardized by means of rarefaction (*31*), with error bars indicating 95% confidence intervals. Insect damage was standardized by means of random resampling without replacement (*5*, *32*), with ±1σ error bars around the mean of 5000 iterations, both for (**B**) all damage morphotypes and (**C**) mine morphotypes only. There is a strong negative correlation of plant and insect-damage richness for Mexican Hat (Mex. Hat) and Castle Rock (C. Rock). A separate analysis (not shown in the figure) excluded most external feeding and other "generalized" damage morphotypes as in (*6*) but yielded results nearly identical to (B). P-E, Paleocene-Eocene boundary.

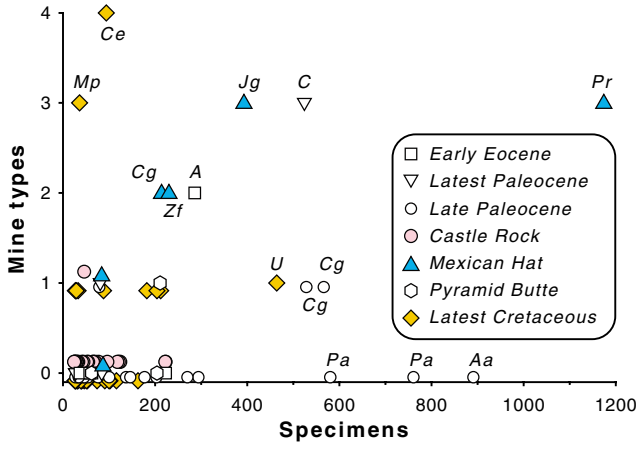

Fig. 3. Leaf-mine morphotype diversity plotted against number of leaf specimens for the 89 species-site pairs in our full data set (Table 1) that had a minimum of 25 leaf specimens at a site. There is high mining diversity on all four common host plants and one relatively rare host in the early Paleocene Mexican Hat flora. A sixth mined host represented by only 11 leaf specimens is not shown, and *Z. flabella* at Mexican Hat was previously found to have an additional morphotype, a blotch mine equivalent to our DT36 (*30*). Labeled outliers are as follows: *A*, *Alnus* sp. (Betulaceae); *Aa*, *"Ampelopsis" acerifolia* (?Cercidiphyllaceae); *Ce*, *Cercidiphyllum ellipticum* (Cercidiphyllaceae); *Cg*, *C. genetrix*; *C*, *Corylites* sp. (Betulaceae); *Jg*, *Juglandiphyllites glabra* (Juglandaceae); *Mp*, *Marmarthia pearsonii* (Lauraceae); *Pa*, *Persites argutus* (Lauraceae); *Pr*, *Platanus raynoldsi* (Platanaceae); *U*, Urticales sp. HC81; *Zf*, *Zizyphoides flabella* (Trochodendraceae). (See references in Table 1 for additional nomenclature.)

Excepting Mexican Hat and the latest Paleocene, our Paleocene floras have few mines by comparison to the Cretaceous (Figs. 2C and 3), a finding corroborated by abundant supplemental data from the Denver Basin and North Dakota (table S4). The five late Paleocene sites from Wyoming (Table 1) contain significant numbers of all four dominant host plants found at Mexican Hat (tables S2 and S3) but yielded only seven mines on 5226 specimens, all of the DT41 type. Five of these occur on *Cercidiphyllum genetrix*, the only regional continuation of a mining association found at Mexican Hat (Fig. 1H).

Sustained recovery of both plant and insect-herbivore diversity began during the warm latest Paleocene (*5*, *23*), wherein herbivory apparently led ahead of plant diversity (Fig. 2). In contrast to Mexican Hat, however, latest Paleocene mining mostly occurred on a single host lineage, the Betulaceae (Fig. 3), which first appeared regionally in the late Paleocene and supported diverse and abundant herbivory through the early Eocene (*5*, *24*, *25*).

The Castle Rock flora is one of the oldest reliable examples of tropical rainforest vegetation (*16*, *17*, *26*), typified today by tough thick leaves with low nutritional value and high tannin content (*27*). The extraordinary but temporary diversification recorded at Castle Rock appears to be related to favorable climatic conditions, the establishment of unpalatable vegetation, and low herbivore pressure in a post-extinction setting. This scenario contrasts with living rainforests, where herbivores are implicated in maintaining and possibly promoting plant diversity (*28*, *29*). Unlike Castle Rock, our other Paleocene samples are dominated by thin-leaved deciduous hosts (table S2) that we infer to have had relatively low defenses and thus to have been vulnerable to opportunistic colonization when herbivore pressure was present, as observed at Mexican Hat.

The Mexican Hat and Castle Rock floras show marked, apparently localized and transient, deviations from theoretical patterns of staged food web recovery (*1*), indicating much greater variance than has previously been considered in the relative numbers of producer and consumer species. Temporally and geographically isolated occurrences of severely unbalanced food webs may be a widespread feature of ecological recovery from mass extinction, resulting from instability, incumbency, and opportunism in drastically simplified ecological landscapes.

References and Notes

1. R. V. Solé, J. M. Montoya, D. H. Erwin, *Philos. Trans. R. Soc. London Ser. B* **357**, 697 (2002).
2. J. C. Zachos, M. A. Arthur, W. E. Dean, *Nature* **337**, 61 (1989).
3. S. D'Hondt, P. Donaghay, J. C. Zachos, D. Luttenberg, M. Lindinger, *Science* **282**, 276 (1998).
4. H. K. Coxall, S. D'Hondt, J. C. Zachos, *Geology* **34**, 297 (2006).
5. P. Wilf, C. C. Labandeira, *Science* **284**, 2153 (1999).
6. C. C. Labandeira, K. R. Johnson, P. Wilf, *Proc. Natl. Acad. Sci. U.S.A.* **99**, 2061 (2002).
7. P. Wilf, C. C. Labandeira, K. R. Johnson, N. R. Cúneo, *Proc. Natl. Acad. Sci. U.S.A.* **102**, 8944 (2005).

8. E. Siemann, D. Tilman, J. Haarstad, M. Ritchie, *Am. Nat.* **152**, 738 (1998).
9. M. G. Wright, M. J. Samways, *Oecologia* **115**, 427 (1998).
10. B. A. Hawkins, E. E. Porter, *Am. Nat.* **161**, 40 (2003).
11. K. R. Johnson, *Geol. Soc. Am. Spec. Pap.* **361**, 329 (2002).
12. J. A. Powell, C. Mitter, B. D. Farrell, in *Handbook of Zoology*, N. P. Kristensen, Ed. (de Gruyter, New York, 1998), pp. 403–422.
13. A. Raman, C. W. Schaefer, T. M. Withers, in *Biology, Ecology, and Evolution of Gall-Inducing Arthropods*, A. Raman, C. W. Schaefer, T. M. Withers, Eds. (Science Publishers, Enfield, NH, 2005), pp. 1–33.
14. C. C. Labandeira, *Rocky Mount. Geol.* **37**, 31 (2002).
15. C. C. Labandeira, K. R. Johnson, P. Lang, *Geol. Soc. Am. Spec. Pap.* **361**, 297 (2002).
16. K. R. Johnson, B. Ellis, *Science* **296**, 2379 (2002).
17. B. Ellis, K. R. Johnson, R. E. Dunn, *Rocky Mount. Geol.* **38**, 73 (2003).
18. K. R. Johnson, M. L. Reynolds, K. W. Werth, J. R. Thomasson, *Rocky Mount. Geol.* **38**, 101 (2003).
19. B. Ellis, K. R. Johnson, R. E. Dunn, M. R. Reynolds, *Denver Mus. Nat. Sci. Tech. Rep.* **2004-2**, 1 (2004).
20. J. O. Sewall, L. C. Sloan, *Geology* **34**, 81 (2006).
21. No mines were present in supplemental, qualitative Castle Rock collections selected for preservation and floral diversity (table S4), a procedure that in our experience increases mine recovery.
22. K. A. Spencer, *Host Specialization in the World Agromyzidae (Diptera)* (Kluwer, Dordrecht, Netherlands, 1990).
23. The increase in feeding diversity from latest Paleocene to early Eocene is significant when comparing total damage morphotypes per species (*5*), whereas bulk feeding diversity and mining diversity are not significantly different between these samples (Fig. 2).
24. One recent molecular and paleobiological study indicated the diversification of a clade of gracillariid moths that colonized the Betulaceae beginning ~62.3 million years ago (*25*).
25. C. Lopez-Vaamonde *et al.*, *J. Evol. Biol.* **19**, 1314 (2006).
26. R. J. Burnham, K. R. Johnson, *Philos. Trans. R. Soc. London Ser. B* **359**, 1595 (2004).
27. P. D. Coley, J. A. Barone, *Annu. Rev. Ecol. Syst.* **27**, 305 (1996).
28. D. H. Janzen, *Am. Nat.* **104**, 501 (1970).
29. C. Wills *et al.*, *Science* **311**, 527 (2006).
30. P. J. Lang, *Fossil Evidence for Patterns of Leaf-Feeding from the Late Cretaceous and Early Tertiary* (thesis, University of London, 1996).
31. J. C. Tipper, *Paleobiology* **5**, 423 (1979).
32. We randomly resampled all leaves, rather than only damaged leaves as in (*7*). The latter approach is effective for floras with high damage diversity, but in Paleocene floras insect damage is generally rare, and many specimens and species would be lost from analysis.

33. We thank Harding Land and Cattle Company for land access; P. Anderson, R. Barclay, C. Brown, E. Currano, D. Danehy, R. Dunn, R. Horwitt, F. Marsh, T. Menotti, M. Nowak, M. Reynolds, J. Thomasson, K. Werth, S. Wing, and Western Wyoming Community College for field and technical assistance; three anonymous reviewers; K.C. Beard, E. Currano, D. Erwin, R. Horwitt, M. Patzkowsky, and J. Zachos for discussion; P. Lang, who noted insect mines at Mexican Hat; and I. Winkler for assistance in identifying Agromyzidae mines. Support was provided by the American Philosophical Society; the Colorado Department of Transportation; the Petroleum Research Fund (grant 35229-G2); the National Geographic Society; the Ryan Family Foundation; the Walcott Fund of the Department of Paleobiology, National Museum of Natural History (NMNH); NSF (grants EAR-0345910, EAR-9805474, DEB-0345750, and EAR-0236489); and the David and Lucile Packard Foundation. This is contribution 120 of the Evolution of Terrestrial Ecosystems Consortium at the NMNH.

Supporting Online Material

www.sciencemag.org/cgi/content/full/313/5790/1112/DC1
Fig. S1
Tables S1 to S4
References

4 May 2006; accepted 18 July 2006
10.1126/science.1129569

Why Are There So Many Species of Herbivorous Insects in Tropical Rainforests?

Vojtech Novotny,[1]* Pavel Drozd,[2] Scott E. Miller,[3] Miroslav Kulfan,[4] Milan Janda,[1] Yves Basset,[5] George D. Weiblen[6]

Despite recent progress in understanding mechanisms of tree species coexistence in tropical forests, a simple explanation for the even more extensive diversity of insects feeding on these plants has been missing. We compared folivorous insects from temperate and tropical trees to test the hypothesis that herbivore species coexistence in more diverse communities could reflect narrow host specificity relative to less diverse communities. Temperate and tropical tree species of comparable phylogenetic distribution supported similar numbers of folivorous insect species, 29.0 ± 2.2 and 23.5 ± 1.8 per 100 square meters of foliage, respectively. Host specificity did not differ significantly between community samples, indicating that food resources are not more finely partitioned among folivorous insects in tropical than in temperate forests. These findings suggest that the latitudinal gradient in insect species richness could be a direct function of plant diversity, which increased sevenfold from our temperate to tropical study sites.

Large numbers of herbivore species in the Tropics relative to temperate communities might reflect differences in (i) host plant species diversity, (ii) numbers of herbivore species per host, and/or (iii) host specificity, the number of plant species hosting each insect species. The tropical maximum in plant species richness is well documented. For instance, there are 5 to 10 times as many plant species per 10,000 km^2 in tropical than in temperate areas (*1*), and woody plant species richness per hectare in the Tropics is on average six times as high as that in temperate forests (156.8 ± 63.6 and 25.2 ± 19.7 species with diameter at breast height ≥10 cm; fig. S1). However, latitudinal differences in host specificity and numbers of insect species per host plant species are more difficult to assess (*2*, *3*).

A recent proliferation of quantitative studies on tropical insect herbivores that include feeding and rearing experiments (*4*–*9*) have not been matched by comparable activity in temperate forests (*10*, *11*), perhaps because patterns of host use are believed to be well documented for temperate herbivores. Much qualitative data on host associations of herbivores accumulated during the past two centuries, particularly in Great Britain and Central Europe, are not directly comparable to recent, quantitative studies in the Tropics (*12*). A temperate-tropical comparison of herbivore communities is further complicated by differences in the phylogenetic diversity of the vegetation. Temperate forests are dominated by a relatively small number of woody plant lineages as compared to tropical forests (*13*).

We compared temperate and tropical communities of folivorous insects using identical sampling protocols and phylogenetically comparable sets of local tree species (*14*). All externally feeding folivorous insects were hand collected from the foliage of 14 woody plant species in a lowland floodplain forest in Moravia, Central Europe, and 14 species in a lowland hill forest in Madang, Papua New Guinea. Caterpillars (Lepidoptera) were also collected from eight woody species in an oak-hornbeam forest in Slovakia, Central Europe, and compared with caterpillars from eight tree species in Papua New Guinea (Madang). Samples of tree species from the local vegetation included both close relatives (i.e., congeneric species) and distantly related plant lineages (i.e., multiple familes and orders) at each site (table S1). Molecular phylogenetic relationships among species sampled at each locality were compiled from the recent literature, and branch lengths were estimated from the large subunit of ribulose-1,5-bisphosphate carboxylase-oxygenase (rbcL) gene sequences. The diverse vegetation of lowland New Guinea provided an opportunity to select subsets of tree species with phylogenetic patterns closely matching those of temperate forest tree

[1]Institute of Entomology, Czech Academy of Sciences and Department of Zoology, University of South Bohemia, Branisovska 31, 370 05 Ceske Budejovice, Czech Republic. [2]Department of Biology, University of Ostrava, Chittussiho 10, 710 00 Ostrava, Czech Republic. [3]National Museum of Natural History and National Zoological Park, Smithsonian Institution, Washington, DC 20013–7012, USA. [4]Department of Zoology, Comenius University, Mlynska dolina B-1, 842 15 Bratislava, Slovakia. [5]Smithsonian Tropical Research Institute, Apartado 0843-03092, Balboa, Ancon, Panama. [6]Department of Plant Biology and Bell Museum of Natural History, University of Minnesota, 220 Biological Sciences Center, 1445 Gortner Avenue, St. Paul, MN 55108–1095, USA.

*To whom correspondence should be addressed. E-mail: novotny@entu.cas.cz

communities (Fig. 1). Highly concordant and correlated branch lengths permitted the comparison of host specificity and herbivore community structure given a nearly identical phylogenetic distribution of food plants. Controlling for the effect of vegetation on phylogenetic diversity enabled a direct comparison of herbivore specificity between these different tropical and temperate communities.

Adult herbivores were experimentally tested for feeding, and larvae were reared to adults. Our analysis included 26,970 feeding records of herbivorous insects representing 850 species (appendices S1 and S2). Folivorous communities included larval and adult feeders of Lepidoptera, Coleoptera, Hymenoptera, and orthopteroids (Orthoptera and Phasmatodea). Larval Lepidoptera dominated both temperate and tropical communities, followed by adult Coleoptera, whereas larval Coleoptera were of marginal importance (Fig. 2).

Although Hymenoptera were limited to temperate samples and orthopteroids were only encountered in the Tropics, tree species in both regions supported similar overall species diversity of leaf-chewing insect species per unit area of foliage (Table 1). The occurrence of more speciose assemblages of insect herbivores in tropical forests as compared to temperate forests therefore cannot be attributed to finer partitioning of foliar resources among herbivore species feeding on the same plant species. Comparable overall species diversity of herbivores resulted from opposing trends in species diversity of larval and adult folivores, being maximally diverse in Central Europe and New Guinea, respectively. Despite considerable differences in the taxonomic composition of

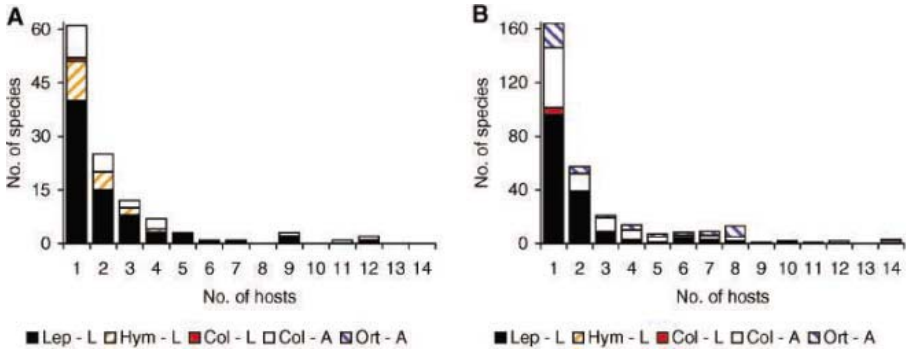

Fig. 2. Host specificity of folivorous insects on (**A**) temperate and (**B**) tropical trees. The number of hosts among the 14 studied tree species (Fig. 1A) is shown for larvae (L) and adults (A) from Lepidoptera, Hymenoptera, Coleoptera, and Orthopteroids. The number of hosts was not significantly different between temperate and tropical folivores, Lepidoptera larvae, and Coleoptera adults (Mann-Whitney test, $P > 0.05$).

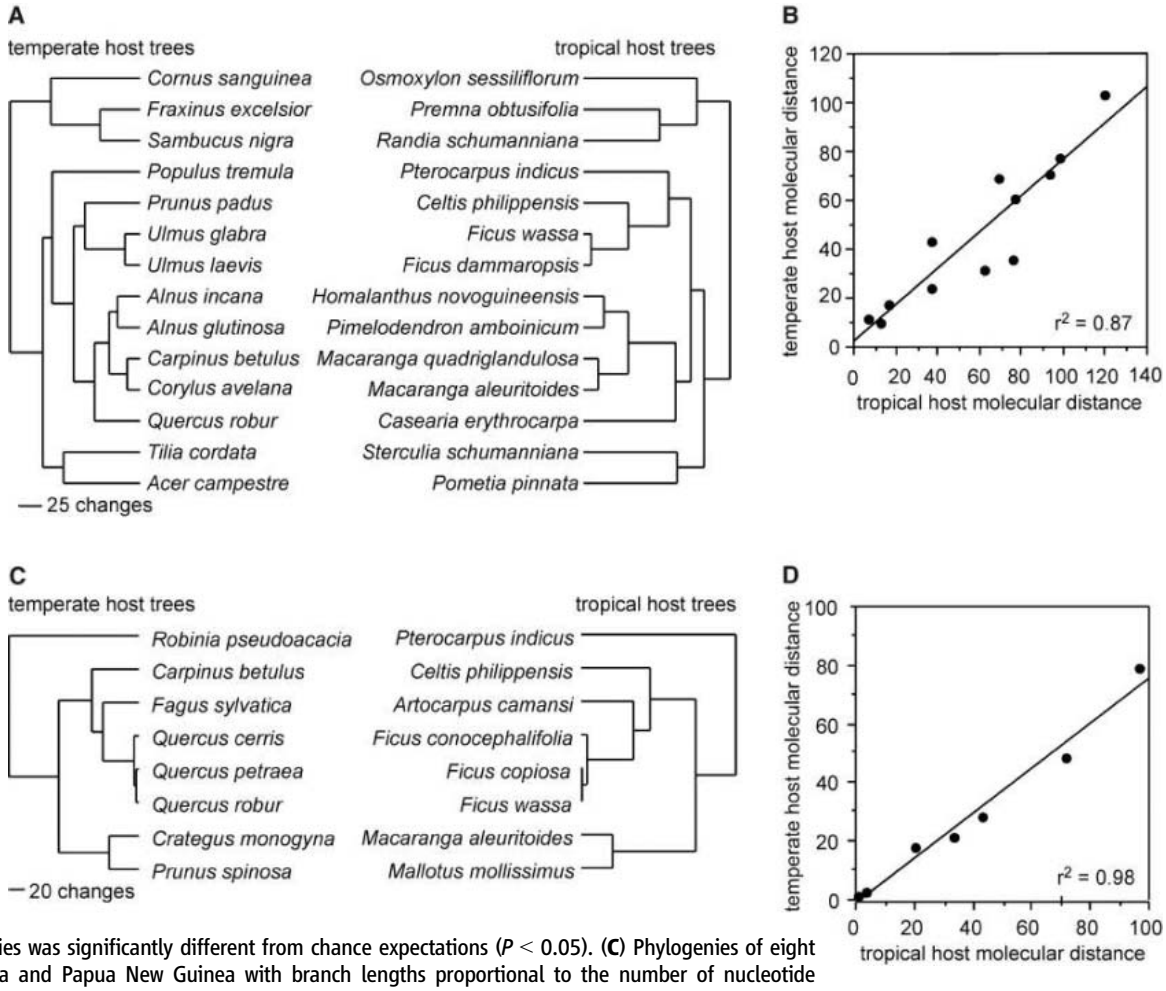

Fig. 1. Phylogenetic relationships and molecular divergence of temperate and tropical trees selected for the comparison of insect herbivore communities. Temperate and tropical plant species spanning the continuum between close relatives and distantly related lineages were paired to control for differences between communities in the phylogenetic distribution of plant resources. Branching order and branch lengths were matched as closely as possible between the temperate and tropical sets of tree species from different clades. (**A**) Phylogenies of 14 tree species from Moravia and Papua New Guinea with branch lengths proportional to the number of nucleotide substitutions in rbcL sequences. (**B**) The correlation of molecular phylogenetic distances between ancestral and descendant nodes for 14 pairs of temperate and tropical tree species was significantly different from chance expectations ($P < 0.05$). (**C**) Phylogenies of eight tree species from Slovakia and Papua New Guinea with branch lengths proportional to the number of nucleotide substitutions in rbcL. (**D**) The correlation of molecular phylogenetic distances between ancestral and descendant nodes for eight pairs of temperate and tropical tree species ($P < 0.001$).

Table 1. Numbers of insect species and individuals per unit area of foliage in larval and adult taxon guilds of folivorous insects reared from temperate and tropical trees. The mean (±SE) values for the density of species and individuals were calculated for insect herbivores from *N* species of study trees. Rows 1 to 8 refer to the Moravia–New Guinea comparison, row 9 to the Slovakia–New Guinea comparison. The temperate-tropical differences were evaluated by *t* test (*$P < 0.05$). Comparative analyses accounting for the statistical nonindependence of tree species yielded results identical to those obtained with *t* tests (supporting online text). N.S., not significant.

No.	Taxon	Guild	Species/100m² foliage		*t* test	Individuals/100m² foliage		*t* test	*N*
			Temperate	Tropical		Temperate	Tropical		
1	Lepidoptera	Larvae	19.9 (1.9)	9.1 (1.3)	*	66.6 (13.5)	36.7 (5.9)	N.S.	14
2	Hymenoptera	Larvae	1.8 (0.4)	0 (0)	*	3.8 (1.1)	0.0 (0.0)	*	14
3	Coleoptera	Larvae	0.1 (0.1)	0.3 (0.1)	N.S.	6.4 (6.3)	2.7 (2.7)	N.S.	14
4	Coleoptera	Adults	5.5 (0.7)	9.5 (0.7)	*	42.9 (12.7)	24.4 (2.6)	N.S.	14
5	Orthopteroids	Adults	0.0 (0.0)	4.2 (0.4)	*	0.0 (0.0)	7.5 (1.3)	*	14
6	All	Larvae	23.5 (2.1)	9.4 (1.3)	*	84.4 (13.4)	40.4 (6.1)	*	14
7	All	Adults	5.5 (0.7)	13.7 (0.9)	*	42.9 (12.7)	31.9 (3.1)	N.S.	14
8	All	All	29.0 (2.2)	23.5 (1.8)	N.S.	127.2 (15.6)	75.2 (5.8)	*	14
9	Lepidoptera	Larvae	19.3 (3.6)	9.2 (2.0)	*	82.5 (18.0)	45.5 (5.9)	N.S.	8

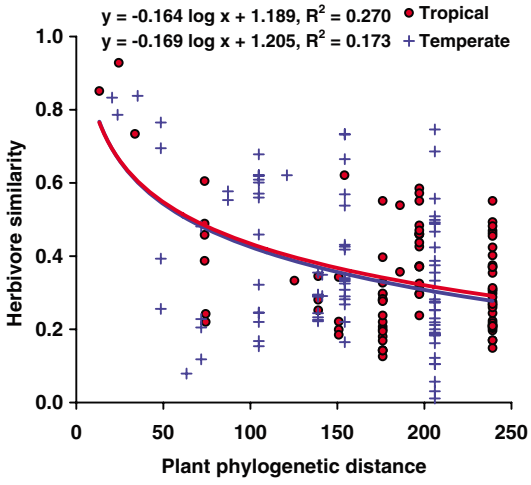

Fig. 3. Similarity of folivorous communities between pairs of host species versus the phylogenetic distance between the hosts in a temperate (crosses) and a tropical (circles) forest. Herbivore similarity was estimated as the proportion of shared species according to the Chao-Sorensen index (*27*); phylogenetic distance was estimated from Fig. 1A as the absolute number of pairwise differences in rbcL sequences from trees listed in table S1. The negative correlation between community similarity and phylogenetic distance was significant in both data sets ($P < 0.05$, Mantel test).

tropical and temperate communities, overall estimates of herbivore species diversity per host plant are of similar magnitude in tropical forests (*4*–*7*, *15*) and temperate forests (*10*, *16*). The absence of a latitudinal trend in the ratio of butterfly to plant species is also consistent with this observation (*17*).

Temperate trees supported a higher overall density of folivores than did tropical trees (Table 1). Lepidoptera and Coleoptera larval densities tended to be higher on temperate trees, but only the density of Hymenoptera larvae was significantly different. The relatively low abundance of larvae on tropical foliage is attributed to high predation, particularly by ants, in the Tropics (*18*, *19*). Predation pressure on tropical trees at our study sites was 18 times as high as that on temperate trees, as measured by the proportion of live insect baits attacked by predators (mostly ants) during 30 min of exposure on the foliage (28 ± 27% in the Tropics and 1.6 ± 0.1% on temperate vegetation; table S2).

The two most important taxon guilds in terms of species numbers and abundance, namely Lepidoptera larvae and Coleoptera adults, as well as the entire folivorous community, showed no difference in host specificity between temperate and tropical trees (Fig. 2). Lepidoptera larvae on temperate trees in Slovakia were less host-specific than were those on the tropical trees, but the mean difference in host range was small (fig. S2), averaging a single host per herbivore in tropical samples versus two hosts per herbivore in temperate samples. The similarity of folivorous communities on any pair of hosts decreased as the phylogenetic distance of hosts increased. The slope of the relation was not significantly different between temperate and tropical tree species, also suggesting a common pattern of host specificity (Fig. 3).

Our findings reject the hypothesis that greater host specificity of tropical herbivores accounts for the greater insect species diversity. Other studies also suggest that there is no difference in host specificity between temperate and tropical communities of insect herbivores. Fiedler (*20*) found no such difference in butterflies, although particular lineages may be more (e.g., Lycaenidae: Polyommatini) or less (e.g., Papilionidae) (*21*) specialized in temperate than in tropical regions. Bark beetles (Coleoptera: Curculionidae) (*22*) and treehoppers (Hemiptera: Membracidae) (*23*) were more specialized in temperate than in tropical regions, whereas a community of temperate caterpillars (*10*) exhibited lower host specificity than was reported from the Tropics (*6*, *8*). However, none of these studies has controlled for the phylogenetic diversity of the vegetation.

There are a few caveats to our conclusions. In particular, our species diversity estimates per 100 m² of foliage may not be representative of those for larger areas of foliage, because tropical communities are known to include numerous rare species that can be detected only with large sample sizes (*24*). The upper-canopy foliage, which was undersampled in this study, can provide additional microhabitats for specialized herbivores, particularly in the Tropics (*25*). Tropical vegetation can also include additional resources that are rare or absent in temperate forests, such as woody climbing plants (*7*).

Despite these caveats, our analysis suggests that the latitudinal gradient in species diversity of herbivorous insects is to a large extent driven by the parallel increase in plant diversity (fig. S1). There was a sevenfold increase in plant diversity from our temperate to tropical study sites, with 21 tree species per hectare with diameter at breast height ≥5 cm in Moravia, as compared to 152 species in Madang (*26*). Our sample of 14 tree species represented 85% of the standing timber in a temperate forest, whereas a phylogenetically comparable subset of tropical forest represented less than 20% of the local vegetation. Greater phylogenetic diversity of tropical vegetation compared to temperate forests rather than greater host specificity of tropical herbivores is the more probable explanation for the extraordinary diversity of tropical insect communities.

References and Notes

1. W. Barthlott, W. Lauer, A. Placke, *Erdkunde. Arch. Wiss. Geogr.* **50**, 317 (1996).
2. T. M. Lewinsohn, V. Novotny, Y. Basset, *Annu. Rev. Ecol. Evol. Syst.* **36**, 597 (2005).

3. V. Novotny, Y. Basset, *Proc. R. Soc. London B* **272**, 1083 (2005).
4. R. J. Marquis, in *Plant-Animal Interactions: Evolutionary Ecology in Tropical and Temperate Regions*, P. W. Price, T. M. Lewinsohn, G. W. Fernandes, W. W. Benson, Eds. (Wiley, New York, 1991), pp. 179–208.
5. Y. Basset, *Ecology* **77**, 1906 (1996).
6. J. A. Barone, *J. Anim. Ecol.* **67**, 400 (1998).
7. F. Ødegaard, *J. Biogeogr.* **27**, 283 (2000).
8. V. Novotny *et al.*, *Nature* **416**, 841 (2002).
9. D. H. Janzen, W. Hallwachs, *Caterpillar rearing voucher databases for the Area de Conservacion Guanacaste in northwestern Costa Rica*, http://janzen.sas.upenn.edu/caterpillars/database.htm (2005).
10. D. J. Futuyma, F. Gould, *Ecol. Monogr.* **49**, 33 (1979).
11. J. O. Stireman *et al.*, *Proc. Natl. Acad. Sci. U.S.A.* **102**, 17384 (2005).
12. L. K. Ward, *Br. J. Entomol. Nat. Hist.* **1**, 153 (1988).
13. I. M. Turner, *The Ecology of Trees in the Tropical Rain Forest* (Cambridge Univ. Press, Cambridge, 2001).
14. Materials and methods are available as supporting material on *Science* Online.
15. D. H. Janzen, *Biotropica* **20**, 120 (1988).
16. R. Karban, R. E. Ricklefs, *Ecology* **64**, 636 (1983).
17. K. J. Gaston, *Funct. Ecol.* **6**, 243 (1992).
18. R. L. Jeanne, *Ecology* **60**, 1211 (1979).
19. L. A. Dyer, *Ecology* **76**, 1483 (1995).
20. K. Fiedler, *Ecotropica* **1**, 51 (1995).
21. J. M. Scriber, in *Chemical Mediation of Coevolution*, K. C. Spencer, Ed. (Academic Press, New York, 1988), pp. 241–301.
22. R. A. Beaver, *Nature* **281**, 139 (1979).
23. T. K. Wood, *Sociobiology* **8**, 299 (1984).
24. P. W. Price, I. R. Diniz, H. C. Morais, E. S. A. Marques, *Biotropica* **27**, 468 (1995).
25. Y. Basset, V. Novotny, S. E. Miller, R. L. Kitching, Eds., *Arthropods of Tropical Forests: Spatio-Temporal Dynamics and Resource Use in the Canopy* (Cambridge Univ. Press, Cambridge, 2003).
26. V. Novotny *et al.*, *Conserv. Biol.* **18**, 227 (2004).
27. A. Chao, R. L. Chazdon, R. K. Colwell, T. J. Shen, *Ecol. Lett.* **8**, 148 (2005).
28. We thank V. Becker, J. Bezdek, J. Brown, K. Darrow, A. Galsworthy, H. van Herwaarden, J. D. Holloway, R. Hoare, M. Horak, S. Lingafelter, K. Maes, J. Miller, E. G. Munroe, P. Naskrecki, J. Patocka, D. Perez, R. Poole, G. A. Samuelson, K. Sattler, G. Setliff, M. Shaffer, M. A. Solis, K. Tuck, and J. Macek for assistance with insect taxonomy; W. Takeuchi for plant taxonomy and M. Andreas, J. Auga, D. Bito, W. Boen, L. Cizek, C. Dal, G. Damag, M. Damag, M. Drozdova, J. Fajcik, S. Hiuk, J. Hulcr, B. Isua, M. Kasbal, T. Kocurek, J. Krajci, R. Kutil, R. Lilip, M. Lubojacka, M. Manaono, M. Mogia, K. Molem, P. Rac, S. Sau, L. Septak, J. Stuglikova, E. Tamtiai, B. Tydlackova, and P. Volkl for field and laboratory assistance; P. Bellingham and the New Zealand National Vegetation Survey databank for forest plot data; and H. Mueller-Landau, J. Leps, and S. Mihulka for helpful comments. The Papua New Guinea government permitted the study; the NSF, NIH, Czech Grant Agency, Czech Academy of Sciences, Czech Ministry of Education, National Geographic Society, Darwin Initiative, and Slovak Grant Agency provided funding.

Supporting Online Material

www.sciencemag.org/cgi/content/full/1129237/DC1
Materials and Methods
Figs. S1 and S2
Tables S1 and S2
References
Appendices S1 and S2

27 April 2006; accepted 13 June 2006
Published online 13 July 2006;
10.1126/science.1129237
Include this information when citing this paper.

Brassinosteroids Regulate Dissociation of BKI1, a Negative Regulator of BRI1 Signaling, from the Plasma Membrane

Xuelu Wang and Joanne Chory*

Brassinosteroids, the steroid hormones of plants, are perceived at the plasma membrane by a leucine-rich repeat receptor serine/threonine kinase called BRI1. We report a BRI1-interacting protein, BKI1, which is a negative regulator of brassinosteroid signaling. Brassinosteroids cause the rapid dissociation of BKI1–yellow fluorescent protein from the plasma membrane in a process that is dependent on BRI1-kinase. BKI1 is a substrate of BRI1 kinase and limits the interaction of BRI1 with its proposed coreceptor, BAK1, suggesting that BKI1 prevents the activation of BRI1.

There are more than 400 serine/threonine receptor–like kinases predicted in the *Arabidopsis* genome (*1*). BRI1, the major brassinosteroid receptor of *Arabidopsis* (*2*–*4*), has been studied using loss-of-function mutants, overexpression, and biochemical analyses to identify the activation and specificity of plant receptor–like kinases (*5*). Brassinosteroids control physiological and developmental processes such as stem elongation, vascular differentiation, seed size, fertility, flowering time, senescence, and resistance to biotic and abiotic stresses (*2*, *6*, *7*). Direct binding of brassinolide (BL), the most active brassinosteroid, to the extracellular domain of BRI1 activates a preformed homo-oligomer. Auto- or trans-phosphorylation of the C terminus of BRI1 then enhances kinase activity and the affinity of BRI1 for BAK1, its proposed coreceptor (*8*–*11*). A version of BRI1 lacking the 41 C-terminal amino acids is a more active receptor but cannot be fully activated, suggesting that other factors are also required to regulate BRI1 activity.

Downstream from BRI1 and BAK1, BIN2, a glycogen synthase kinase-3 family member (*12*), negatively regulates brassinosteroid signaling by phosphorylating members of a plant-specific family of transcriptional regulators, defined by the *BES1* and *BZR1* genes (*13*–*16*). In the presence of brassinosteroids, BIN2 is inhibited by an unknown mechanism, leading to the dephosphorylation of BES1 and BZR1. Dephosphorylated BES1 and BZR1 then homodimerize or cooperate with other transcription factors, which allows DNA binding and regulation of hundreds of brassinosteroid-responsive genes (*15*–*17*).

To investigate the signaling events between the plasma membrane and transcriptional responses, we searched for proteins that interact with BRI1 using yeast two-hybrid screens with a cDNA library from *Arabidopsis* shoot apical meristems. We repeatedly identified two proteins that interacted with the intracellular domains of wild-type or kinase-inactive BRI1: a transthyretin-like protein (TTL), which is a negative regulator of brassinosteroid-related plant growth (*18*), and an expressed protein of unknown function, At5g42750. We designated At5g42750 as *BKI1* for *BRI1 Kinase Inhibitor 1*. A simple modular architecture research tool [(SMART), http://smart.embl-heidelberg.de] predicts *BKI1* to encode a protein of 337 amino acids with two separate Ser-rich domains and an Asn-rich region (Fig. 1A). BLAST searches of the predicted BKI1 amino acid sequence identified a similar gene in rice, as well as multiple expressed sequence tags (ESTs) from other angiosperms, which in several cases appear to contain the entire predicted coding region (Fig. 1B and table S1). The rice protein was previously reported to interact with the kinase domain of rice BRI1, although its function is unknown (*19*). No other similar sequences similarities were identified in other species, which suggests that *BKI1* may be angiosperm-specific.

Sequence alignments indicated that the C-terminal domain of BKI1 is the most conserved region [about 32% identity in the C-terminal region (residues 253 to 337)]. The C terminus was both necessary and sufficient to bind the kinase domain of BRI1 (BRI1-KD) (Fig. 1C). BKI1 associated specifically with the kinase domain of BRI1 and not with TTL, BIN2, or kinase domains of other receptor-like kinases tested, including BAK1 and NIK1, another member of the BAK1 subfamily (Fig. 1D). BKI1 did not interact with CLV1, a leucine-rich repeat receptor-like kinase (LRR-RLK) involved in shoot apical meristem development (*1*), nor did it interact with BRI1's closest relatives, BRL1 and BRL3 (*20*) (fig. S1), indicating that the interaction of BKI1 with BRI1 is highly specific. Glutathione *S*-transferase (GST) pull-down experiments using GST-BRI1-KD and ^{35}S-Met–labeled BKI1-6XHIS further indicated that BKI1 interacts with the kinase domain of BRI1 (Fig. 1E). Immunoprecipitation experiments confirmed that endogenous BRI1 interacted with a BKI1-FLAG fusion protein in vivo (Fig. 1F).

Howard Hughes Medical Institute and Plant Biology Laboratory, The Salk Institute for Biological Studies, 10010 North Torrey Pines Road, La Jolla, CA 92037, USA.

*To whom correspondence should be addressed. E-mail: chory@salk.edu

BKI1's function in brassinosteroid signaling was explored in several ways. First, we made transgenic plants harboring a β-*glucuronidase* (*GUS*) reporter gene expressed from the promoter of *BKI1* to observe the expression pattern of *BKI1* (Fig. 1, G to J) during development. *BKI1* was expressed in leaves, petioles, shoot apices, hypocotyls, roots, and flowers, indicating that *BKI1* and *BRI1* are coexpressed in a number of tissues (*21*). To explore the function of BKI1 in BRI1 signaling, we created RNA interference (RNAi) lines to inhibit *BKI1* RNA levels. Real-time quantitative reverse transcription polymerase chain reaction (qRT-PCR) analysis indicated that the transcript level of *BKI1* was significantly reduced (50% to 76%) in many *RNAi* lines, compared with a control line (Fig. 2A). The *RNAi* lines had longer hypocotyls than the control line grown in short days (control, 2.20 ± 0.09 mm; *RNAi-2*, 2.74 ± 0.08 mm; and *RNAi*-7, 3.09 ± 0.12 mm), and the levels of *BKI1* transcripts were negatively correlated with hypocotyl length, suggesting that BKI1 represses brassinosteroid-related growth (Fig. 2B). In contrast, overexpression of *BKI1* with either a FLAG or a yellow fluorescent protein (YFP) tag resulted in dwarf plants resembling plants harboring weak alleles of *bri1*. These plants had a smaller rosette (under both short-day and long-day conditions), reduced stature and petiole length, rounder rosette leaves, and delayed flowering compared with wild type (Fig. 2, C to F).

To determine whether the dwarf phenotype was the result of altered brassinosteroid sensitivity, we measured the response of a line overexpressing a *BKI1-YFP* fusion protein to BL. In the absence of applied BL, overexpression of *BKI1-YFP* led to about a 40% reduction of hypocotyl length in the light (Fig. 2E), and plants were less sensitive to BL applications by a factor of at least 100 compared with wild type, whereas *det2-1*, a brassinosteroid biosynthetic mutant, was highly responsive to BL treatment (Fig. 2G). Conversely, the *BKI1-YFP* line and *det2-1* were more sensitive to a brassinosteroid biosynthesis inhibitor, BRZ220 (*22*), as indicated by the lower concentration of BRZ 220 needed for the *BKI1-YFP* line (~0.5 μM) to achieve 50% inhibition of hypocotyl length than for Columbia (Col-0) (~2.0 μM) (Fig. 2H).

To determine whether the growth inhibitory effect caused by the overexpression of *BKI1-YFP* was due to an inhibition of BRI1 signaling, we tested the phosphorylation status of a downstream biochemical marker, BES1 (*10*), by immunoblot analysis. Without applied exogenous BL, a considerable amount of dephosphorylated BES1 was present in the wild type, whereas the amount of dephosphorylated BES1 in a *BKI1* overexpression line was almost undetectable, which was similar to *det2-1*. Treatment with 0.1 μM BL for 1 hour strongly stimulated the accumulation of dephosphorylated BES1 in wild type and *det2-1*, but to a lesser extent in the *BKI1-YFP* line (Fig. 2I), suggesting that BRI1 signaling was suppressed by *BKI1* overexpression.

To determine whether overexpression of *BKI1* alters the expression of brassinosteroid-responsive genes, we measured the RNA levels of three brassinosteroid-regulated genes by qRT-PCR, including two down-regulated genes, *CPD* and *DWF4*, and an up-regulated gene,

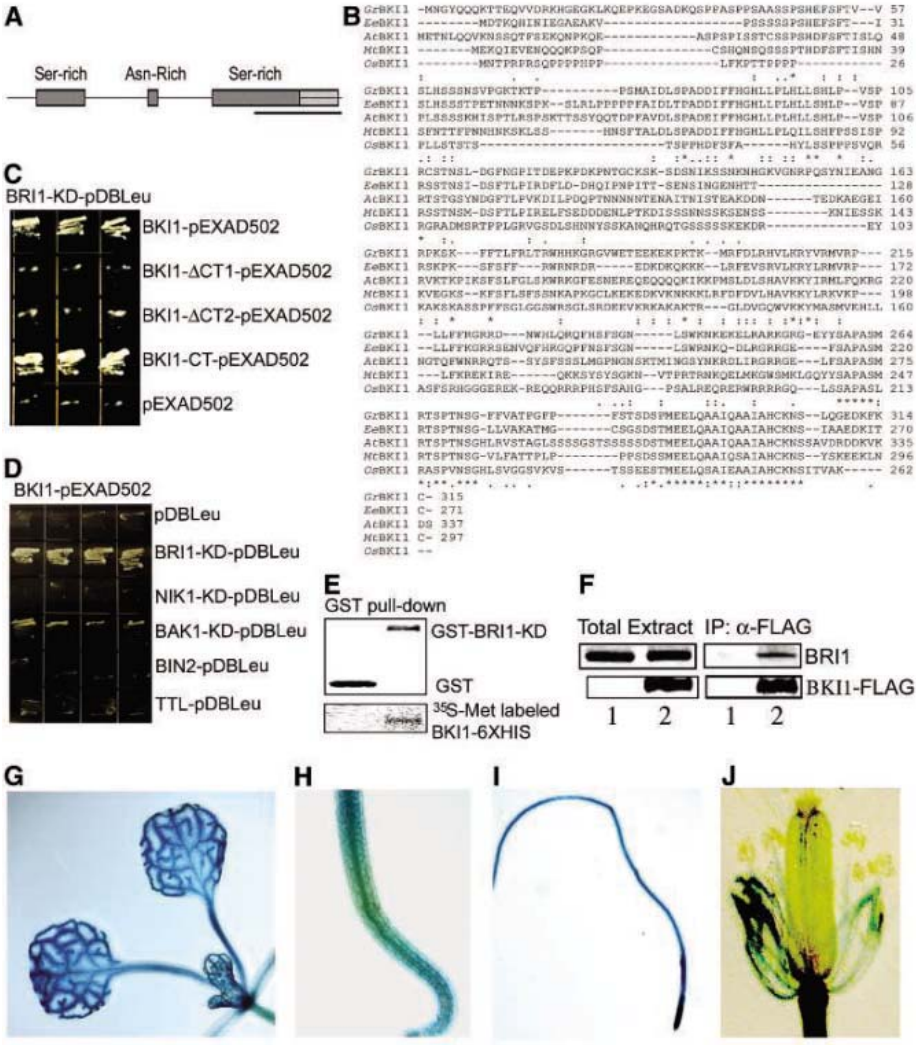

Fig. 1. In vivo and in vitro interaction of BKI1 with BRI1's intracellular domain. (**A**) The predicted domain structure of *At*BKI1. The sequences underlined indicate the region that interacts with BRI1's kinase domain. (**B**) Alignment of the deduced amino acid sequence of *AtBKI1* with *BKI1*-like proteins from *Oryza sativa* (*OsBKI1*; AP005891.3), *Medicago truncatula* (*Mt*BKI1; AC157645_3.1, identified in the database of the Institute for Genome Research), *Gossypium raimondii* (*Gr*BKI1, a putative full-length gene assembled from ESTs CO071302.1, CO081346.1, CO074191.1, and CO081345.1), and *Euphorbia esula* (*Ee*BKI1, a putative full-length gene assembled from ESTs DV136456.1, DV156616.1, DV139943.1, DV131013.1, and DV131013.1). (**C**) The carboxyl domain of BKI1 is necessary and sufficient to interact with BRI1's kinase domain in yeast. Residues of *BKI1* present in the constructs were 1 to 252 (*BKI1-ΔCT1*), 1 to 299 (*BKI1-ΔCT2*), and 253 to 337 (*BKI1-CT*). (**D**) BKI1 specifically interacts with BRI1. BKI1 fused with GAL4-AD (*BKI1-pEXAD502*) specifically interacts with the intracellular domain of BRI1 (BRI1-KD) fused with GAL4-DB in yeast. (**E**) BKI1-6XHIS interacts with GST-BRI1-KD in vitro. In the pull-down product, the GST (left) or GST-BRI1-KD (right) was detected by antibody to GST, and the ^{35}S-Met–labeled BKI1-6XHIS was detected by autoradiography. (**F**) BKI1-FLAG interacts with endogenous BRI1 in planta. 1, Col-0; and 2, BKI1-FLAG overexpression line. BRI1 and BKI1-FLAG were detected by immunoblot with antibody to BRI1 and antibody to FLAG, respectively. (**G** to **J**) *pBKI1::GUS* is ubiquitously expressed. *GUS* reporter gene expression was monitored in 2-week-old seedlings' leaves and shoot apices (G), hypocotyls (H), and roots (I), and in flowers of adult plants (J).

Saur-AC1. As shown in Fig. 2J, compared with wild type, overexpression of *BKI1-YFP* led to a significant increase of the expression of *CPD* and *DWF4* in the absence of BL (*CPD*, 1.63 ± 0.07 versus 1.00; *DWF4*, 2.76 ± 0.08 versus 1.00) or with a treatment of 100 nM of BL for 2.5 hours (*CPD*, 0.83 ± 0.05 versus 0.47 ± 0.03; *DWF*, 0.80 ± 0.06 versus 0.27 ± 0.01). In contrast, the expression of *Saur-AC1* was significantly lower in the *BKI1-YFP* line than wild type in both conditions (no BL, 0.24 ± 0.03 versus 1.00; plus BL, 1.65 ± 0.11 versus 4.68 ± 0.31). Together with the hypocotyl growth results, these results support the interpretation that BKI1 is a negative regulator of brassinosteroid signaling.

To investigate where in the pathway BKI1 acts, we examined the subcellular localization of BKI1-YFP fusion protein in plants. BKI1-YFP was localized to both the plasma membrane and the cytosol in root-tip cells (Fig. 3A). When the *BKI1-YFP* line was grown on medium containing 1 μM BRZ220, which reduces the levels of endogenous brassinosteroids (*22*), the fluorescent signal on the cell surface was enhanced (Fig. 3B). In contrast, when grown on medium containing 1 μM BL, the plasma membrane association of BKI1-YFP was reduced, as indicated by the diminished discrete fluorescent signal on the cell surface (Fig. 3C), suggesting that brassinosteroids might alter the subcellular localization of BKI1-YFP. After BL treatment, we observed that the plasma membrane association of BKI1-YFP was almost completely gone after 5 min and undetectable 10 min later (Fig. 3, G to I, and movie S2); in contrast, the BKI1-YFP signal was unchanged in the control (Fig. 3, D to F, and movie S1).

To assess whether the plasma membrane association of BKI1-YFP was dependent on BRI1, we introduced the *BKI1-YFP* construct into a *bri1-116* background, a null allele of *bri1* that generates a stop codon within the BL binding domain (*21*). In *bri1-116* homozygous seedlings, we observed that a substantial amount of BKI1-YFP was localized to the cell surface. Unlike wild-type plants, BL treatment failed to induce the dissociation of BRI1 (Fig. 3, J to O), indicating that BRI1 is not required for the plasma membrane association of BKI1-YFP but is crucial for the release of BKI1 from the plasma membrane. Likewise, in *bri1-104*, a kinase-inactive allele of *bri1* (*21*) that accumulates normal levels of protein, no BL-induced dissociation of BKI1-YFP from the plasma membrane was observed, suggesting that the kinase activity of BRI1 is required for the dissociation of BKI1-YFP from the plasma membrane (Fig. 3, P to R). These results imply that BL-induced phosphorylation of BKI1 by activated BRI1 is essential for regulating the subcellular localization and association of BKI1 with BRI1. In corroboration, we found that the yeast two-hybrid interaction of BKI1 with a kinase-inactive BRI1 was stronger than with the kinase-active BRI1, although the kinase-active version could still interact with BKI1 (fig. S2). In addition, BKI1 is a substrate of BRI1 kinase in vitro with a Michaelis constant (K_m) of about 1.55 μM (fig. S3A) and is a phosphoprotein in vivo as indicated by

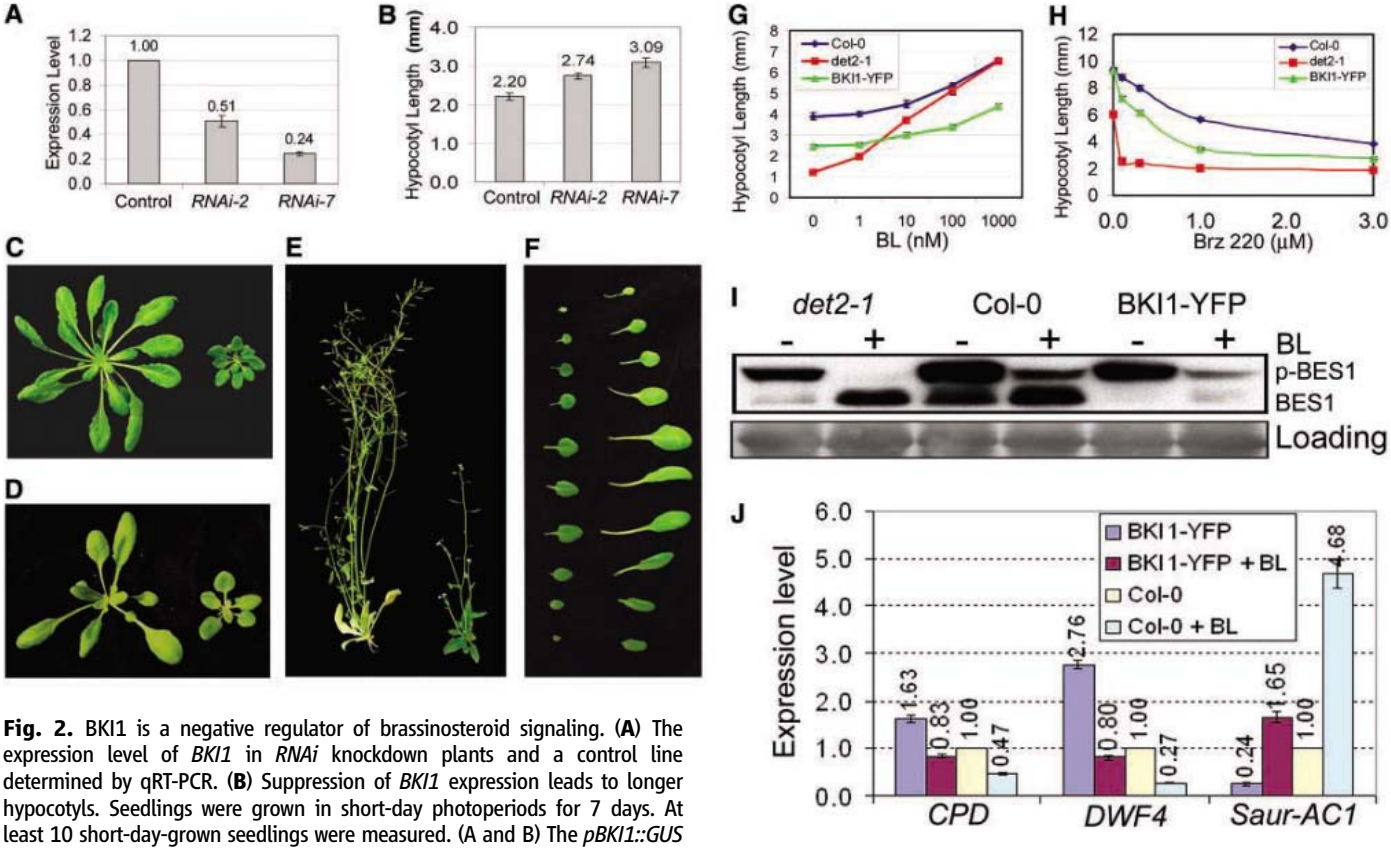

Fig. 2. BKI1 is a negative regulator of brassinosteroid signaling. (**A**) The expression level of *BKI1* in *RNAi* knockdown plants and a control line determined by qRT-PCR. (**B**) Suppression of *BKI1* expression leads to longer hypocotyls. Seedlings were grown in short-day photoperiods for 7 days. At least 10 short-day-grown seedlings were measured. (A and B) The *pBKI1::GUS* line was used as a control. *RNAi-2* and *RNAi-7* were two independent *RNAi* knockdown lines for *BKI1*. (**C** to **E**) Phenotype of plants overexpressing *BKI1-FLAG*, with Col-0 (left) and a *BKI1-FLAG* line (right). (C) Short-day-grown seedlings. (D) Long-day-grown seedlings. (E) Long-day-grown adult plants. (**F**) Leaf morphology of seedlings grown in short days. Col-0 (right) and a *BKI1-FLAG* line (left). (**G**) Overexpression of *BKI1-YFP* leads to a reduced response (hypocotyl length) to BL. At least 20 short-day-grown seedlings were measured. (**H**) Overexpression of *BKI1-YFP* leads to an enhanced response to BRZ220. At least 20 dark-grown seedlings were measured. (**I**) Overexpression of *BKI1-YFP* results in reduced accumulation of dephosphorylated BES1. Immunoblots with antibody to BES1 show levels of phosphorylated BES1 (p-BES1) and dephosphorylated BES1. Bottom band, loading control. (**J**) Overexpression of *BKI1-YFP* alters the expression of BR-regulated genes. *CPD* and *DWF4* are BR down-regulated genes, and *Saur-AC1* is a BR up-regulated gene. In (A), (B), (G), (H), and (J), error bars indicate standard error.

a shift following λ-phosphatase treatment (fig. S3B).

To confirm whether the plasma membrane association of BKI1 is required for it to inhibit BRI1 signaling, we made transgenic plants harboring a BKI1-YFP fusion protein that was tethered to the plasma membrane by adding an N-terminal myristoylation site (*myriBKI1-YFP*). As shown in Fig. 4A, the myriBKI1-YFP was constitutively associated with the plasma membrane even after BL treatment. As expected for a regulator whose inhibitory function is predicted to require an interaction with BRI1 at the plasma membrane, the *myriBKI1-YFP* line had an enhanced dwarf phenotype when compared with plants expressing BKI1-YFP to a similar level (Fig. 4B).

Our results suggest that BKI1 may function early in the brassinosteroid signaling pathway, either as an early signaling component or as a regulator that inactivates or desensitizes the receptor. We looked at the interaction of BKI1 with BIN2, the earliest known signaling component downstream of the brassinosteroid receptor complex, but were unable to detect any interaction using genetic assays in yeast (Fig. 1D). Because BAK1 interactions with BRI1 are more stable after application of brassinosteroids (*11*), we speculated that BKI1 may inhibit the association of BRI1 with positive regulators, e.g., BAK1. To test this prediction, we conducted GST pull-down experiments in vitro and observed that the addition of a BKI1-maltose binding protein fusion (MBP-BKI1) significantly inhibited (by ~62%, $P = 0.000013$) the interaction between the kinase domains of BRI1 and BAK1, whereas the addition of MBP alone did not significantly affect their interaction ($P = 0.219$) (Fig. 4C).

The simplest interpretation of our observations is that plasma membrane–associated BKI1 interacts directly with BRI1 and represses its signaling (Fig. 4D). This model predicts that, in the absence of steroid, BKI1 is localized to the plasma membrane, where it binds to the intracellular domain of a BRI1 homodimer, thus keeping BRI1 from associating with BAK1. Brassinosteroid binding to the extracellular domain of BRI1 induces receptor phosphorylation and activation, as well as its dissociation from BKI1, leaving open binding sites for BAK1 and perhaps other BRI1 substrates. BKI1 binding to BRI1 maintains a low basal activity of BRI1. This low activity allows expression of brassinosteroid biosynthetic genes, which are repressed by BRI1 signaling (*16*, *23*) (Fig. 2J). BKI1's role in BRI1 signaling thus appears to be distinct from that of TTL, a negative regulator of the brassinosteroid signal transduction pathway, which associates with a kinase-active rather than an inactive BRI1 kinase (*18*).

In metazoans, adaptor proteins associate with receptor tyrosine kinases and recruit signaling components to activated receptors (*24*–*26*). BKI1 does not appear to be a typical adaptor, because it must dissociate from the plasma membrane for BRI1 to signal. Rather, BKI1's association with BRI1's kinase domain prevents it from becoming fully activated and may ensure the specificity of BRI1 signaling.

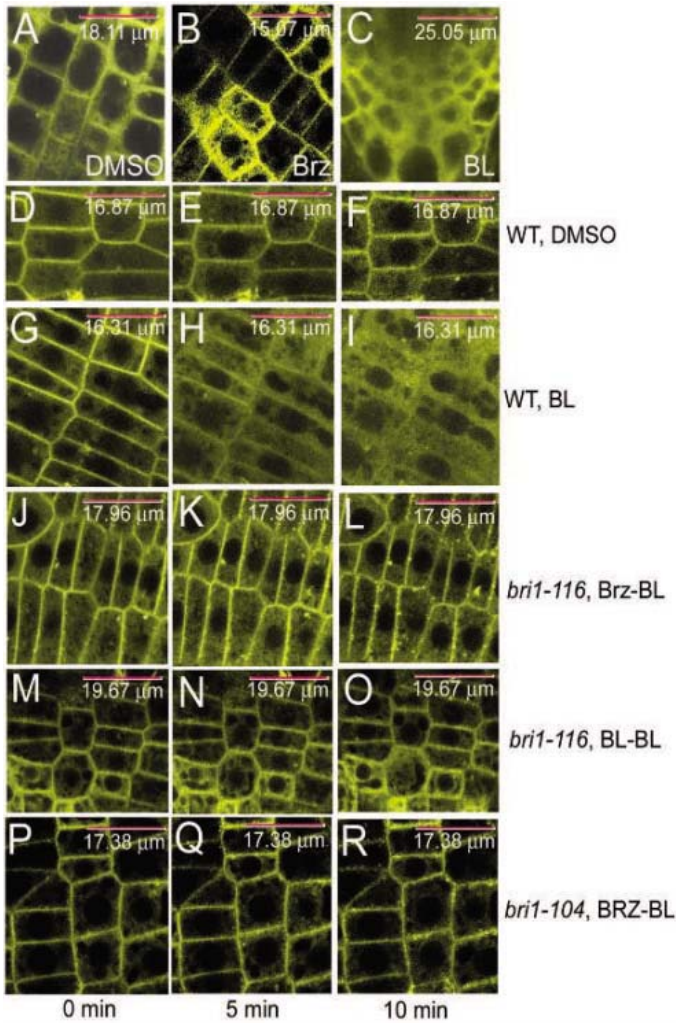

Fig. 3. Brassinosteroid treatment triggers the dissociation of BKI1-YFP from the plasma membrane in a BRI1-dependent manner. (**A**) BKI1-YFP is localized to the plasma membrane and cytosol on Murashige and Skoog (MS) medium. (**B**) BRZ220 enhances the association of BKI1-YFP to the plasma membrane. Seedlings were grown on MS medium containing 1 μM BRZ220. (**C**) BL enhances BKI1-YFP dissociation from the plasma membrane. Seedlings were grown on MS medium containing 1 μM BL. (**D** to **F**) Dimethyl sulfoxide (DMSO) at 0.001% (v/v) does not alter the plasma membrane localization of BKI1-YFP. (**G** to **I**) BL-induced dissociation of BKI1-YFP from the plasma membrane. Seedlings were grown on MS medium containing 1 μM of BRZ220 and treated with 1 μM BL. (**J** to **L**) BKI1-YFP is associated with the plasma membrane in *bri1-116*. Seedlings were grown on MS medium containing 1 μM of BRZ220. *bri1-116* is a null allele of *BRI1* (*21*). (**M** to **O**) BL does not cause dissociation of BKI1-YFP from the plasma membrane in *bri1-116*. Seedlings were grown on MS medium containing 1 μM BL. (**P** to **R**) An active kinase is required for BL-induced dissociation of BKI1 from the plasma membrane. *bri1-104* is a loss-of-function mutation in the kinase domain of *BRI1* (*21*). Seedlings were grown on MS medium containing 1μM BRZ220. (D), (G), (J), (M), and (P) were untreated; (E), (H), (K), (N), and (Q) were treated with BL for 5 min; and (F), (I), (L), (O), and (R) were treated with BL for 10 min.

References and Notes

1. S. H. Shiu, A. B. Bleecker, *Proc. Natl. Acad. Sci. U.S.A.* **98**, 10763 (2001).
2. J. Li, J. Chory, *Cell* **90**, 929 (1997).
3. Z. Y. Wang, H. Seto, S. Fujioka, S. Yoshida, J. Chory, *Nature* **410**, 380 (2001).
4. T. Kinoshita *et al.*, *Nature* **433**, 167 (2005).
5. G. Vert, J. L. Nemhauser, N. Geldner, F. Hong, J. Chory, *Annu. Rev. Cell Dev. Biol.* **21**, 177 (2005).
6. S. D. Clouse, M. Langford, T. C. McMorris, *Plant Physiol.* **111**, 671 (1996).
7. T. Altmann, *Curr. Opin. Plant Biol.* **1**, 378 (1998).
8. K. H. Nam, J. Li, *Cell* **110**, 203 (2002).
9. J. Li *et al.*, *Cell* **110**, 213 (2002).
10. X. Wang *et al.*, *Dev. Cell* **8**, 855 (2005).
11. X. Wang *et al.*, *Plant Cell* **17**, 1685 (2005).
12. J. Li, K. H. Nam, *Science* **295**, 1299 (2002).
13. Z. Y. Wang *et al.*, *Dev. Cell* **2**, 505 (2002).
14. Y. Yin *et al.*, *Cell* **109**, 181 (2002).
15. Y. Yin *et al.*, *Cell* **120**, 249 (2005).
16. J. He *et al.*, *Science* **307**, 1634 (2005).
17. G. Vert, J. Chory, *Nature* **441**, 96 (2006).
18. K. H. Nam, J. Li, *Plant Cell* **16**, 2406 (2004).
19. S. Hirabayashi *et al.*, *Plant Biotechnol.* **21**, 35 (2004).
20. A. Caño-Delgado *et al.*, *Development* **131**, 5341 (2004).
21. D. M. Friedrichsen, C. A. Joazeiro, J. Li, T. Hunter, J. Chory, *Plant Physiol.* **123**, 1247 (2000).
22. K. Sekimata *et al.*, *Tetrahedron Asymm.* **13**, 1875 (2002).
23. K. Tanaka *et al.*, *Plant Physiol.* **138**, 1117 (2005).
24. H. Kouhara *et al.*, *Cell* **89**, 693 (1997).
25. G. R. Guy, P. Yusoff, D. Bangarusamy, C. W. Fong, E. S. Wong, *Cell. Signal.* **14**, 11 (2002).
26. L. J. Holt, K. Siddle, *Biochem. J.* **388**, 393 (2005).
27. S. Mora-Garcia *et al.*, *Genes Dev.* **18**, 448 (2004).
28. Materials and methods are available as supporting material on *Science* Online.

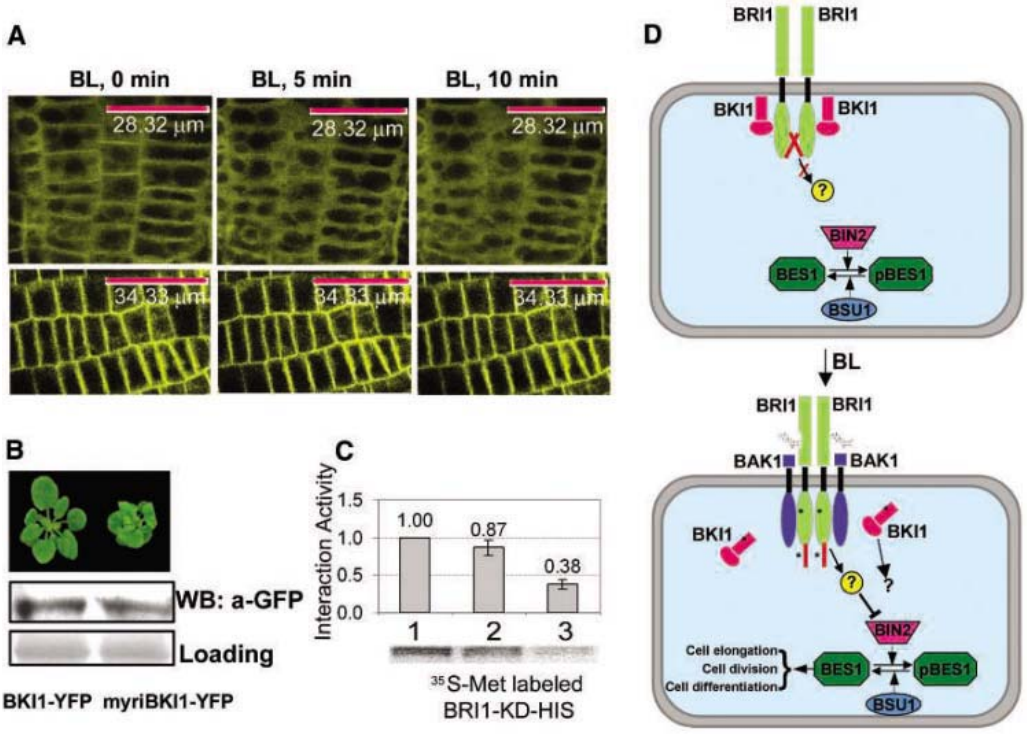

Fig. 4. A model for BKI1 in BRI1 activation. (**A**) A myristoylated BKI1-YFP is constitutively associated with the plasma membrane following BL treatment. Seedlings were grown on MS medium containing 1 μM of BRZ220. The time of BL treatment is indicated. Upper panels, *BKI1-YFP*; lower panels, *myriBKI1-YFP*. (**B**) Overexpression of *myriBKI1-YFP* leads to an enhanced dwarf phenotype. Immunoblots with antibody to green fluorescent protein (GFP) show levels of myriBKI1-YFP and BKI1-YFP. Bottom band, loading control. (**C**) BKI1 inhibits the interaction between the kinase domains of BRI1 and BAK1 in vitro. The total ^{35}S-Met–labeled BRI1-KD-HIS coprecipitated by GST-BAK1-KD was defined as "1." Five replicates were conducted. Error bars indicate standard error. 1, GST-BAK1-KD + ^{35}S-Met-labeled BRI1-KD-HIS; 2, GST-BAK1-KD + ^{35}S-Met-labeled BRI1-KD-HIS + 10 μM MBP; 3, GST-BAK1-KD + ^{35}S-Met-labeled BRI1-KD-HIS + 10 μM MBP-BKI1. The bottom panel shows a representative gel by autoradiography, indicating the pull-down ^{35}S-Met labeled BRI1-KD-HIS. (**D**) A model to illustrate the role of BKI1 in BRI1 signaling. Without BL, BRI1 kinase is kept in a basal state by both its own carboxyl terminal domain and by an interaction with BKI1. Brassinosteroid binding to the extracellular domain of BRI1 induces a conformational change of the kinase domain, leading to the phosphorylation of the C-terminal domain of BRI1 and BKI1, the dissociation of BKI1 from the plasma membrane, and the release of autoinhibition of BRI1. These events lead to the full activation of BRI1 and its association with BAK1 or other substrates. Plasma membrane–dissociated BKI1 may also regulate other unknown components in the brassinosteroid signaling cascade. BSU1 is a nuclear serine/threonine phosphatase involved in the dephosphorylation of BES1 (*27*).

29. This work was supported by a grant from the National Research Initiative of USDA, Cooperative State Research, Education and Extension Service to J.C. and the Howard Hughes Medical Institute (HHMI). We thank T. Asami (RIKEN) for providing BRZ220, Y. Yin for providing BES1 antibody, T. Mockler and J. Meisenhelder for comments on the manuscript, and P. Wigge and D. Weigel for originally providing the yeast two-hybrid library. J.C. is an investigator of HHMI.

Supporting Online Material

www.sciencemag.org/cgi/content/full/1127593/DC1
Materials and Methods
Figs. S1 to S3
Table S1
Movies S1 and S2
References

20 March 2006; accepted 21 June 2006
Published online 20 July 2006;
10.1126/science.1127593
Include this information when citing this paper.

ATM Engages Autodegradation of the E3 Ubiquitin Ligase COP1 After DNA Damage

David Dornan,[1] Harumi Shimizu,[1] Angie Mah,[1] Tanay Dudhela,[1] Michael Eby,[2] Karen O'Rourke,[1] Somasekar Seshagiri,[2] Vishva M. Dixit[1]*

The ataxia telangiectasia mutated (ATM) protein kinase is a critical component of a DNA-damage response network configured to maintain genomic integrity. The abundance of an essential downstream effecter of this pathway, the tumor suppressor protein p53, is tightly regulated by controlled degradation through COP1 and other E3 ubiquitin ligases, such as MDM2 and Pirh2; however, the signal transduction pathway that regulates the COP1-p53 axis following DNA damage remains enigmatic. We observed that in response to DNA damage, ATM phosphorylated COP1 on Ser^{387} and stimulated a rapid autodegradation mechanism. Ionizing radiation triggered an ATM-dependent movement of COP1 from the nucleus to the cytoplasm, and ATM-dependent phosphorylation of COP1 on Ser^{387} was both necessary and sufficient to disrupt the COP1-p53 complex and subsequently to abrogate the ubiquitination and degradation of p53. Furthermore, phosphorylation of COP1 on Ser^{387} was required to permit p53 to become stabilized and to exert its tumor suppressor properties in response to DNA damage.

Genomic integrity is a prerequisite in mammals to maintaining cellular and tissue homeostasis. Given that the majority of tumors display genetic instability (*1*), the malfunction of the DNA-damage sensor system contributes to the selection of transformed somatic cells. ATM acts as a sentinel for DNA damage and phosphorylates key effecter substrates including the tumor suppressor p53, breast cancer–associated gene–1 (BRCA1), and Checkpoint kinase 2 (Chk2) (*2*).

The p53 protein is a critical component of the DNA damage response that induces the expression of a plethora of genes whose products are implicated in cell cycle arrest, senescence, apoptosis, and DNA repair (*3*). Furthermore, mice null for p53 typically develop lymphomas and sarcomas displaying aneuploidy (*4*). In response to DNA damage, p53 is stabilized (*5*, *6*), and ATM directly phosphorylates p53 at the N terminus (*7*) on Ser^{15} and resultantly increases recruitment of the transcriptional coactivator p300 (*8*). ATM also phosphorylates the E3 ubiquitin ligase MDM2 and the related MDMX protein and dampens their ability to

[1]Department of Physiological Chemistry, [2]Department of Molecular Biology, Genentech, Inc., 1 DNA Way, South San Francisco, CA 94080, USA.

*To whom correspondence should be addressed. E-mail: dixit@gene.com

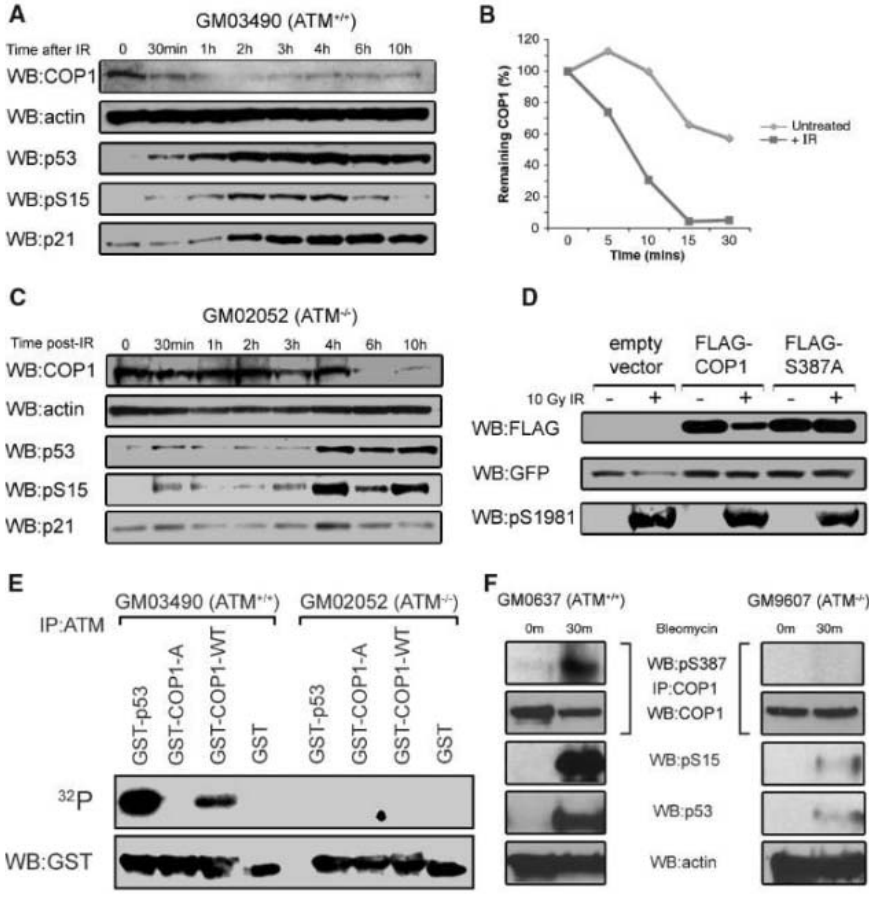

Fig. 1. Dependence of COP1 abundance after DNA damage on phosphorylation at Ser^{387} by ATM. (**A**) Steady-state amounts of COP1 are reduced after IR. GM03490 fibroblasts were irradiated with 10 Gy IR, harvested, and immunoblotted as indicated. (**B**) COP1 abundance after treatment of cells with IR and cycloheximide (CHX). GM0637 (ATM$^{+/+}$) fibroblasts were exposed to 10 Gy IR and, after 2 hours, treated with CHX and sampled at the indicated time points. Bands were quantified by densitometry and represented as a line graph. (**C**) Delayed loss of COP1 in A-T cells. GM02052 fibroblasts were irradiated with 10 Gy IR, harvested, and immunoblotted as indicated. (**D**) Resistance of COP1-S387A to degradation on exposure to IR. U2-OS cells were transfected with COP1-WT or COP1-S387A for 24 hours and subsequently treated with 10 Gy IR for 2 hours before harvesting and immunoblotting. GFP- and pS1981-specific antibodies were used as a transfection control and DNA damage marker, respectively. (**E**) Phosphorylation of COP1 GST peptides containing Ser^{387} in vitro with immunoprecipitated ATM. ATM antibodies were used to immunoprecipitate proteins from lysates of GM03490 and GM02052 fibroblasts exposed to 10 Gy IR for 30 min. Resultant immunoprecipitates were incubated with GST peptides derived from COP1 or p53 for an in vitro kinase assay. (**F**) Phosphorylation of COP1 on Ser^{387} after DNA damage in an ATM-dependent manner. GM0637 and GM9607 fibroblasts were treated with 5 μg/ml bleomycin for the indicated times, and lysates were prepared for immunoprecipitation with antibodies to COP1 or direct immunoblotting.

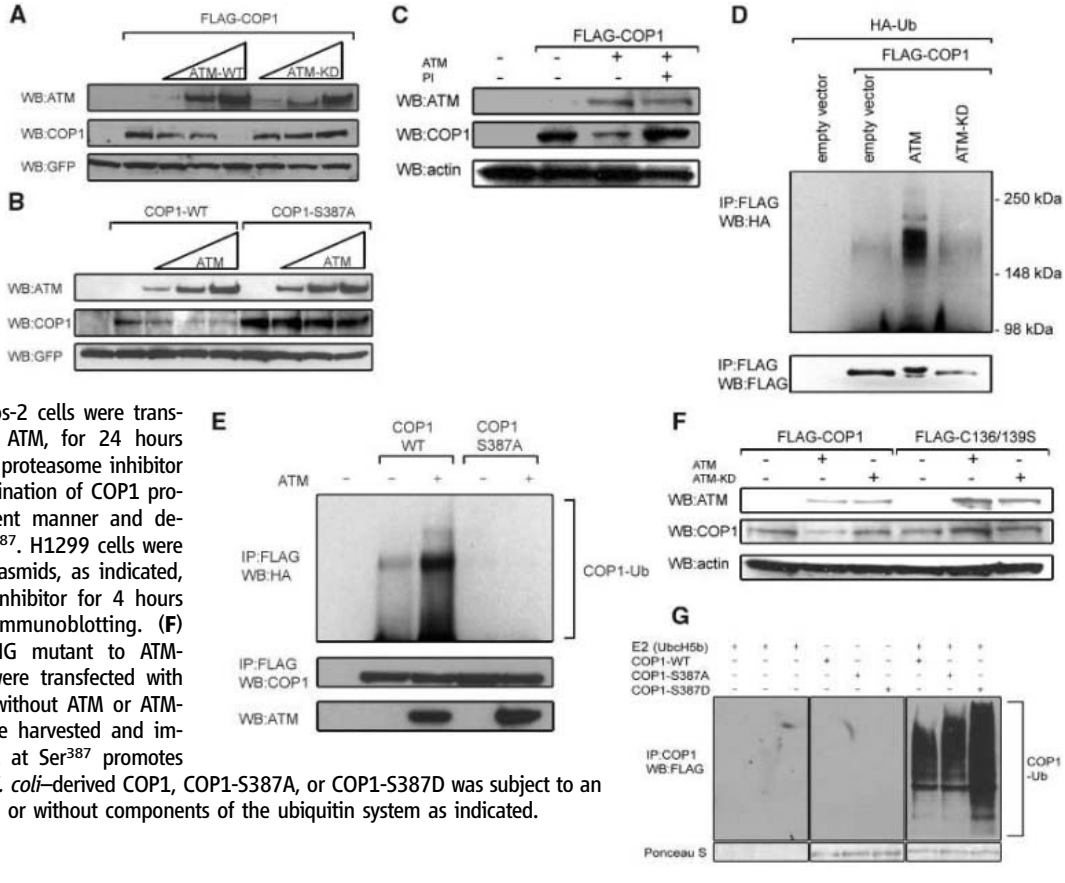

Fig. 2. Auto-E3 degradation of COP1 initiated by ATM. (**A**) Exogenous ATM promotes a reduction in COP1 steady-state levels. Saos-2 cells were transiently transfected with COP1, with or without a titration of ATM or ATM-KD, for 24 hours. (**B**) Resistance of the COP1-S387A mutant to an ATM-mediated reduction in steady-state abundance. Saos-2 cells were transiently transfected with COP1 or COP1-S387A, with or without a titration of ATM, for 24 hours. (**C**) Requirement of the 26*S* proteasome for ATM-induced reduction of COP1. Saos-2 cells were transfected with COP1, with or without ATM, for 24 hours followed by 6 hours' incubation with proteasome inhibitor or vehicle control. (**D** and **E**) Ubiquitination of COP1 promoted by ATM in a kinase-dependent manner and dependence on phosphorylation at Ser^{387}. H1299 cells were transfected for 24 hours with the plasmids, as indicated, and were treated with proteasome inhibitor for 4 hours before immunoprecipitation and immunoblotting. (**F**) Resistance of COP1-C136/139S RING mutant to ATM-induced degradation. Saos-2 cells were transfected with COP1 or COP1-C136/139S, with or without ATM or ATM-KD, for 24 hours before lysates were harvested and immunoblotted. (**G**) Phosphate-mimetic at Ser^{387} promotes autoubiquitination of COP1 in vitro. *E. coli*–derived COP1, COP1-S387A, or COP1-S387D was subject to an autoubiquitination in vitro assay, with or without components of the ubiquitin system as indicated.

negatively regulate p53 (*9*–*11*). The E3 ubiquitin ligase COP1 is also a critical negative regulator of p53 that is overexpressed in breast and ovarian cancers (*12*, *13*); however, the signal transduction pathway that regulates the COP1-p53 axis following DNA damage remains elusive. We therefore examined the steady-state levels of COP1 in fibroblasts after DNA damage induced by 10 Gy of ionizing radiation (IR). Steady-state levels of COP1 started to decline within 30 min and decreased to an almost undetectable level by 1 hour after exposure to IR (Fig. 1A). This correlated closely with an increase in steady-state levels of p53 and activation of the downstream target gene p21 (Fig. 1A and fig. S1). The decreased abundance of COP1 protein was not attributed to a decrease in *COP1* mRNA levels (fig. S1) and occurred with as low as 2 Gy of IR (fig. S2). In addition, the half-life of COP1 was less than 10 min after exposure of cells to 10 Gy IR compared with 30 min for untreated cells (Fig. 1B).

Because ATM is the primary responder in the DNA damage–signaling pathway (*14*), we next determined whether the reduced abundance of COP1 after exposure of cells to IR was dependent on the presence of ATM. We exposed human fibroblasts derived from a patient with ataxia telangiectasia (A-T), which lack functional ATM, to 10 Gy IR. The reduction in steady-state levels of COP1 protein was absent in A-T fibroblasts (Fig. 1C) at early time points. However, COP1 decrease in abundance was evident at later time points, suggesting an alternative pathway may be at play. These observations also occurred after as low as 2 Gy of IR (fig. S3). Thinking that ATM might be directly phosphorylating COP1, we searched for potential phosphorylation sites that conformed to the ATM consensus on COP1 (*15*). Five serine-glutamine (SQ) motifs (fig. S4) are present within COP1; however, the third one, SQ3 (Ser^{387}) was of primary interest, because it is highly conserved between COP1 orthologs (fig. S5) and because mutation of this serine residue to alanine prevented the reduction in steady-state abundance (Fig. 1D), as well as the reduction in the half-life of COP1 in cells exposed to IR (fig. S6).

We used glutathione *S*-transferase (GST) fusion peptides to test whether Ser^{387} was a bona fide target for ATM-mediated phosphorylation in vitro. ATM-specific immunoprecipitates from wild-type cells, but not those from ATM null fibroblasts (Fig. 1E), catalyzed phosphorylation of a peptide harboring Ser^{387} (GST-COP1-WT) and a peptide from p53 having Ser^{15} (GST-p53) (a classical ATM substrate) (*16*). The peptide GST-COP1-A containing S387A, the mutation in which Ser^{387} is replaced by alanine (A), was not phosphorylated. Similar results were obtained with incubation of full-length COP1 with recombinant ATM, but not ATM-kinase dead (ATM-KD) mutant (fig. S7). We used a polyclonal phospho-specific antibody to phosphorylated Ser^{387} (figs. S8, S9, and S10) to determine whether Ser^{387} is indeed phosphorylated in vivo following DNA damage. COP1 phosphorylated at Ser^{387} was readily detected in ATM-WT fibroblasts, whereas this was absent in A-T cells (Fig. 1F).

Together, these data suggested that ATM could be directly responsible for phosphorylation and degradation of COP1 levels. Overexpression of ATM caused a decrease in the abundance of COP1 protein, whereas ATM-KD had no effect (Fig. 2A), and the COP1-S387A mutant expressed in place of COP1-WT was resistant to such ATM-mediated degradation (Fig. 2B).

To find out whether COP1 turnover required the 26*S* proteasome, we treated cells with a proteasome inhibitor after transfection with hemagglutinin-tagged COP1 (HA-COP1) and FLAG-tagged ATM (FLAG-ATM) (Fig. 2C). ATM-induced loss of COP1 was completely abrogated when cells were treated with a proteasome inhibitor. Because recognition of substrates by the 19*S* cap of the proteasome is facilitated by addition of a polyubiquitin chain (*17*), we investigated COP1 to find out if it was ubiquitinated in response to activation of ATM. H1299 cells transfected with HA-tagged ubiquitin, ATM or ATM-KD, and COP1 were treated with proteasome inhibitor to allow accumulation of ubiquitinated substrates. Transfection of COP1 alone revealed a low abundance of ubiquitin products (Fig. 2D). When ATM was transfected with COP1, however, there was an increase in the signal representing ubiquitinated COP1. ATM-KD did not show these effects. This ubiquitination event appeared to be entirely dependent on phosphorylation at Ser^{387}, because no ubiquitination of the COP1-S387A mutant was detected (Fig. 2E). Furthermore, exposure of cells to 10 Gy IR resulted in the enhanced ubiquitination of COP1-WT, whereas this was diminished with the COP1-S387A mutant (fig. S11). If COP1 were autoubiquitinating, then ATM would be unable to promote degradation of a COP1-RING mutant in which both cysteine residues in the RING domain were converted to serine (C136S/C139S). Therefore, we transfected cells with either FLAG-COP1 or FLAG-C136S/C139S and ATM or ATM-KD and assessed steady-state amounts of COP1 protein by immunoblotting (Fig. 2F). The RING mutant was refractory to ATM-induced degradation compared with COP1-WT. To explore the possibility that ATM phosphorylation promotes autoubiquitination of COP1, we generated a COP1-S387D mutant (in which Ser^{387} is replaced by aspartic acid) that was expressed in and purified from *Escherichia coli*, to mimic phosphorylation on this serine residue, for an in vitro autoubiquitination assay (Fig. 2G). The COP1-WT and COP1-S387A proteins had detectable auto-E3 degradation activity, whereas the S387D COP1 mutant showed a substantial increase in auto-E3 ligase activity. Similar results were also obtained from COP1-S387D derived from mammalian cells (figs. S12 and S13).

When we examined the localization of exogenous COP1 in cells by immunofluorescence, COP1 was primarily nuclear; however, after exposure of cells to 10 Gy IR for 2 hours, COP1 was predominantly cytosolic (fig. S14). Endogenous COP1 detected by biochemical fractionation within primary fibroblasts was also exclusively localized to the nuclear fraction in wild-type and A-T fibroblasts (Fig. 3A). Treatment of the wild-type fibroblasts with etoposide resulted in a substantial portion of COP1 redistributed to the cytosolic fraction, but not within the A-T fibroblasts. In addition, within cells expressing the COP1-S387D mutant, COP1 was exclusively cytoplasmic, whereas the COP1-S387A mutant was confined entirely to the nucleus in the presence or absence of DNA damage (Fig. 3B). Biochemical fractionation of wild-type fibroblasts confirmed that the pS387 COP1 species was predominantly localized to the cytosolic compartment (fig. S15).

We wondered whether ATM-mediated regulation of COP1 abundance might contribute to the increase in p53 stability following DNA damage (*5*, *6*). We therefore transfected H1299 cells ($p53^{-/-}$) with constructs encoding FLAG-COP1 with or without HA-p53, treated the cells with bleomycin, and monitored the interaction between COP1 and p53 by immunoprecipitation (Fig. 4A). Interaction between COP1 and p53 was attenuated after DNA damage. In cells expressing the COP1-S387A mutant, DNA dam-

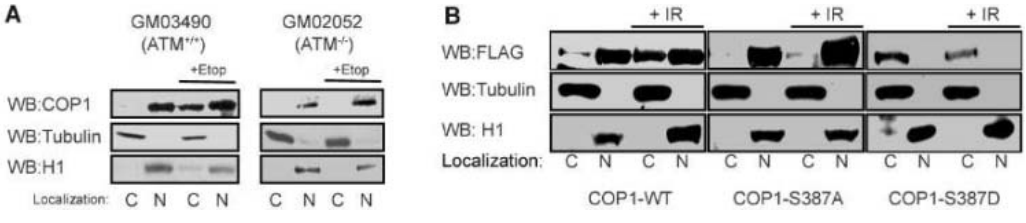

Fig. 3. COP1 localization to the cytoplasm promoted by ATM. (**A**) Cellular fractionation following DNA damage. GM03490 and GM02052 fibroblasts were treated with or without 10 μM etoposide for 30 min; cytoplasmic and nuclear extracts were prepared. (**B**) Requirement of phosphorylation at Ser^{387} for localization to the cytoplasm following DNA damage. H1299 cells were transfected with COP1-WT, COP1-S387A, or COP1-S387D for 24 hours and then irradiated with 10 Gy IR. Cytoplasmic and nuclear extracts were prepared 2 hours after irradiation.

age had no effect on the p53/COP1-S387A complex, which implies that phosphorylation of Ser^{387} is required to disrupt the COP1-p53 complex (Fig. 4B). In addition, modification of Ser^{387} appeared to be sufficient to disrupt the p53-COP1 because binding was reduced between p53 and COP1-S387D mutant (Fig. 4C). Similar results were observed in vitro with purified COP1-S387D and *E. coli*–derived and purified GST-p53 (fig. S16). COP1-S387D derived from *E. coli* also showed a decrease in ability to ubiquitinate p53 in vitro (Fig. 4D). These data suggest that phosphorylation of COP1 on Ser^{387} by ATM might compromise COP1's ability to degrade p53 and to inhibit its tumor suppressor function. Therefore, we transfected Saos-2 cells with p53 and various amounts of COP1-S387D, COP1-S387A, or COP1-WT (Fig. 4E). Proteins from lysates were Western blotted with p53-specific antibody, and a decrease in abundance of p53 was observed after transfection with COP1-S387A or COP1-WT, whereas only a small decrease occurred after cotransfection of COP1-S387D. Furthermore, the COP1-S387D mutant was inefficient at ubiquitinating p53 in vivo (fig. S17).

We used a colony-formation assay to monitor the long-term effects of COP1-WT and COP1-S387D in inhibiting p53-dependent function (fig. S18). In H1299 cells, transfection of p53 resulted in very few surviving colonies (6×10^3 CFU), whereas cotransfection of COP1 with p53 resulted in formation of a greater number of colonies (25×10^3 CFU). However, the COP1-S387D mutant failed to support colony formation (6×10^3 CFU) when p53 was transfected.

To determine whether phosphorylation of COP1 on Ser^{387} was required for p53 stabilization after DNA damage, we transfected H1299 cells with p53 with or without COP1-WT or COP1-S387A, and treated them with or without etoposide for 6 hours (Fig. 4F). Cotransfection of COP1-S387A or COP1-WT with p53 resulted in a reduction in steady-state amounts of p53. However, this reduction in abundance of p53 diminished in cells treated with etoposide. In contrast, the p53 was still reduced in cells expressing the COP1-S387A mutant after addition of etoposide. Cellular viability was also assessed 24 hours after etoposide treatment (Fig. 4G). Expression of COP1-WT diminished the effect of transfected p53 to reduce cell viability; however, this effect of COP1-WT was diminished in cells that had been treated with etoposide. On the contrary, the COP1-S387A mutant retained the ability to inhibit a p53-dependent reduction in cellular viability in cells that had been treated with etoposide. In addition, COP1 ablation by small interfering RNA (siRNA) in A549 cells blunted the fold activation of p53 after DNA damage, which indicated that degradation of COP1 is required for full p53 activation (Fig. 4H). Collectively, these data indicate that phosphorylation at Ser^{387} is required for COP1

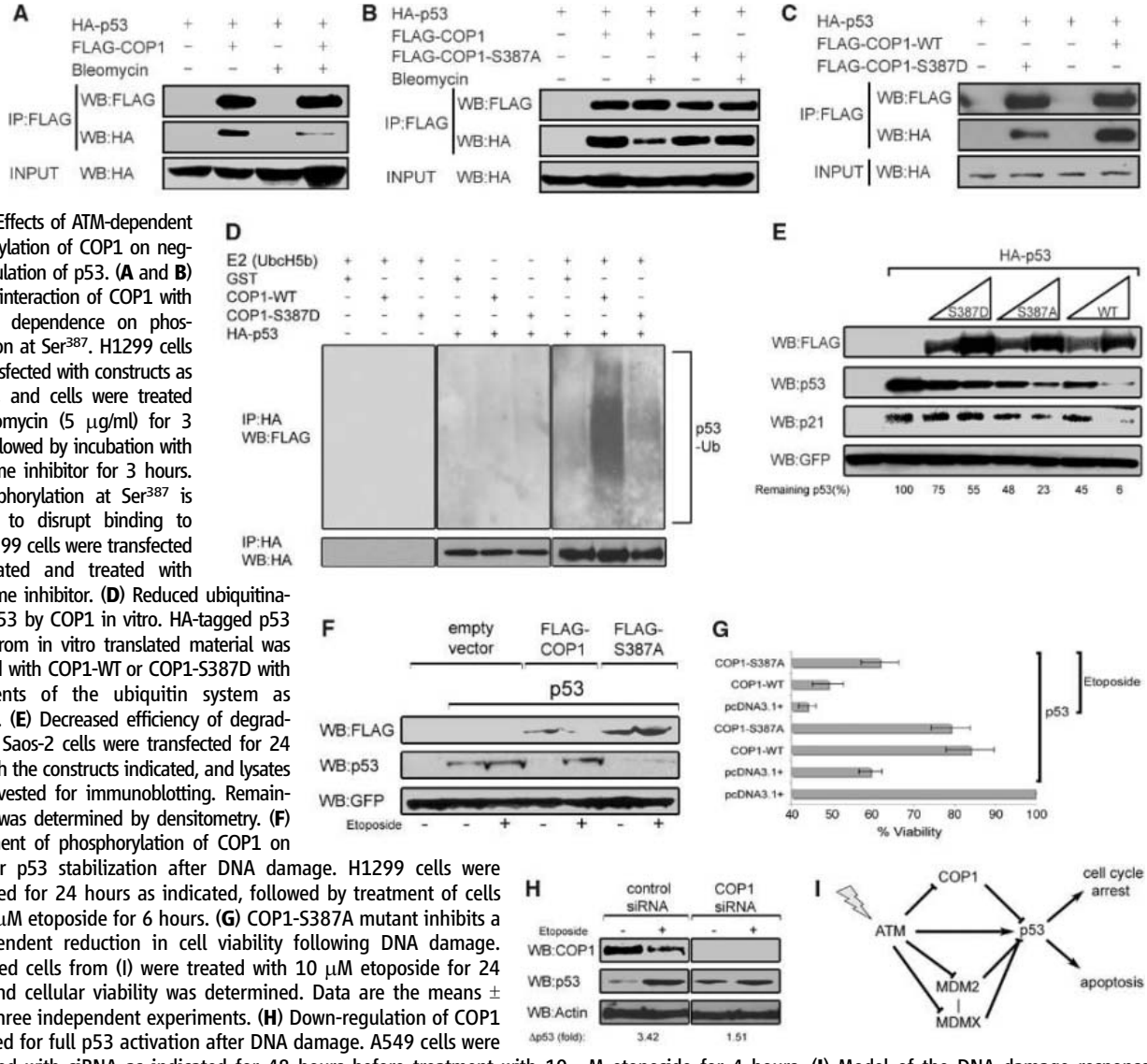

Fig. 4. Effects of ATM-dependent phosphorylation of COP1 on negative regulation of p53. (**A** and **B**) Reduced interaction of COP1 with p53 and dependence on phosphorylation at Ser^{387}. H1299 cells were transfected with constructs as indicated, and cells were treated with bleomycin (5 μg/ml) for 3 hours, followed by incubation with proteasome inhibitor for 3 hours. (**C**) Phosphorylation at Ser^{387} is sufficient to disrupt binding to p53. H1299 cells were transfected as indicated and treated with proteasome inhibitor. (**D**) Reduced ubiquitination of p53 by COP1 in vitro. HA-tagged p53 derived from in vitro translated material was incubated with COP1-WT or COP1-S387D with components of the ubiquitin system as indicated. (**E**) Decreased efficiency of degrading p53. Saos-2 cells were transfected for 24 hours with the constructs indicated, and lysates were harvested for immunoblotting. Remaining p53 was determined by densitometry. (**F**) Requirement of phosphorylation of COP1 on Ser^{387} for p53 stabilization after DNA damage. H1299 cells were transfected for 24 hours as indicated, followed by treatment of cells with 10 μM etoposide for 6 hours. (**G**) COP1-S387A mutant inhibits a p53-dependent reduction in cell viability following DNA damage. Transfected cells from (I) were treated with 10 μM etoposide for 24 hours, and cellular viability was determined. Data are the means ± SEM of three independent experiments. (**H**) Down-regulation of COP1 is required for full p53 activation after DNA damage. A549 cells were transfected with siRNA as indicated for 48 hours before treatment with 10 μM etoposide for 4 hours. (**I**) Model of the DNA damage response pathway between ATM and p53. (**I**) Model of the DNA damage response pathway between ATM and p53.

degradation and to permit p53 stabilization after genotoxic stress, and these observations may help explain the delayed response to genomic abnormalities in A-T patients (Fig. 4I).

References and Notes

1. C. Lengauer, K. W. Kinzler, B. Vogelstein, *Nature* **396**, 643 (1998).
2. Y. Shiloh, *Nat. Rev. Cancer* **3**, 155 (2003).
3. A. J. Levine, W. Hu, Z. Feng, *Cell Death Differ.* **13**, 1027 (2006).
4. L. A. Donehower *et al.*, *Genes Dev.* **9**, 882 (1995).
5. M. B. Kastan, O. Onyekwere, D. Sidransky, B. Vogelstein, R. W. Craig, *Cancer Res.* **51**, 6304 (1991).
6. M. B. Kastan *et al.*, *Cancer Res.* **51**, 4279 (1991).
7. S. Banin *et al.*, *Science* **281**, 1674 (1998).
8. N. Dumaz, D. W. Meek, *EMBO J.* **18**, 7002 (1999).
9. R. Khosravi *et al.*, *Proc. Natl. Acad. Sci. U.S.A.* **96**, 14973 (1999).
10. R. Maya *et al.*, *Genes Dev.* **15**, 1067 (2001).
11. Y. Pereg *et al.*, *Proc. Natl. Acad. Sci. U.S.A.* **102**, 5056 (2005).
12. D. Dornan *et al.*, *Cancer Res.* **64**, 7226 (2004).
13. D. Dornan *et al.*, *Nature* **429**, 86 (2004).
14. C. J. Bakkenist, M. B. Kastan, *Nature* **421**, 499 (2003).
15. S. T. Kim, D. S. Lim, C. E. Canman, M. B. Kastan, *J. Biol. Chem.* **274**, 37538 (1999).
16. J. D. Siliciano *et al.*, *Genes Dev.* **11**, 3471 (1997).
17. J. S. Thrower, L. Hoffman, M. Rechsteiner, C. M. Pickart, *EMBO J.* **19**, 94 (2000).

18. We thank M. Kastan for ATM constructs; Genentech Protein Engineering, Antibody Technology, and core DNA sequencing facility for support services; and L. Corson and W. Mallet for immunofluorescence technical advice.

Supporting Online Material

www.sciencemag.org/cgi/content/full/313/5790/1122/DC1
Materials and Methods
Figs. S1 to S19
References

13 March 2006; accepted 19 June 2006
10.1126/science.1127335

Symbiotic Bacteria Direct Expression of an Intestinal Bactericidal Lectin

Heather L. Cash,[1]* Cecilia V. Whitham,[1]* Cassie L. Behrendt,[1] Lora V. Hooper[1,2]†

The mammalian intestine harbors complex societies of beneficial bacteria that are maintained in the lumen with minimal penetration of mucosal surfaces. Microbial colonization of germ-free mice triggers epithelial expression of RegIIIγ, a secreted C-type lectin. RegIIIγ binds intestinal bacteria but lacks the complement recruitment domains present in other microbe-binding mammalian C-type lectins. We show that RegIIIγ and its human counterpart, HIP/PAP, are directly antimicrobial proteins that bind their bacterial targets via interactions with peptidoglycan carbohydrate. We propose that these proteins represent an evolutionarily primitive form of lectin-mediated innate immunity, and that they reveal intestinal strategies for maintaining symbiotic host-microbial relationships.

The human gut is home to a vast consortium of symbiotic bacteria. Members of this complex microflora metabolize dietary substances, such as plant polysaccharides, that are otherwise indigestible by their human hosts (*1*). Indigenous gut microbes thus make essential contributions to human nutrient metabolism and, in return, inhabit a protected, nutrient-rich environment. Maintaining the mutually beneficial nature of this relationship requires strict sequestration of resident bacteria in the intestinal lumen, as microbial incursions across epithelia can elicit inflammation and sepsis.

Epithelial antimicrobial proteins are evolutionarily ancient innate immune effectors. As key elements of intestinal mucosal defense, they likely play an important role in maintaining mutually beneficial host-microbial relationships by restricting contact between resident microbes and mucosal surfaces. This idea is underscored by the fact that deficiencies in antimicrobial peptide expression are associated with inflammatory bowel disease (IBD) (*2*, *3*), a chronic inflammatory disorder thought to be triggered by resident gut microbes. However, although cationic antimicrobial peptides such as defensins are well-characterized, the full repertoire of gut antimicrobial mechanisms remains undefined. Here we show that resident gut bacteria drive intestinal epithelial expression of a C-type lectin that binds peptidoglycan and has direct antimicrobial activity, revealing a primitive mechanism of lectin-mediated innate immunity.

Paneth cells are key effectors of small intestinal antimicrobial defense. These specialized epithelial cells are located at the crypt base and harbor abundant cytoplasmic secretory granules containing antimicrobial proteins, including α-defensins. To gain new insights into how intestinal surfaces cope with microbial challenges, we used DNA microarrays to identify Paneth cell antimicrobial factors whose expression is altered by bacteria. Paneth cells were harvested by laser capture microdissection from "germ-free" (microbiologically sterile) mice and "conventionalized" mice (germ-free mice reconstituted for 10 days with an intestinal microflora from conventionally raised mice). Paneth cell mRNAs from both groups were amplified to generate complementary RNAs (cRNAs) in sufficient quantity to hybridize to Affymetrix mouse genome 430 2.0 GeneChip arrays. The results of our screen revealed 149 transcripts whose expression was changed 2- to 45-fold by microbial colonization (table S1).

One of the most prominent responses uncovered by our analysis was a 31-fold increase in the abundance of *RegIIIγ* transcripts in Paneth cells from conventionalized as compared with germ-free mice (table S1). Increased expression of *RegIIIγ* mRNA was confirmed by quantitative real-time polymerase chain reaction (Q-PCR) (Fig. 1A) and correlated with increased protein expression (Fig. 1B).

The *Reg* gene family encodes a diverse group of secreted proteins that contain conserved sequence motifs found in C-type lectin carbohydrate recognition domains (CRDs). The Reg family constitutes a distinct group of mammalian C-type lectins, with each member consisting solely of a ~16-kD CRD and N-terminal secretion signal. The family is further classified into subgroups (I, II, III, and IV) on the basis of primary sequence. Several RegIII family members are expressed predominantly in small intestine, including mouse *RegIIIγ* (fig. S1) and human HIP/PAP (*4*, *5*). Inflammatory stimuli, such as bacteria (*5*, *6*) or mucosal damage (*7*), increase gastrointestinal expression of mouse *RegIIIγ*. Furthermore, HIP/PAP expression increases in the mucosa of patients with IBD (*5*, *8*), a disorder characterized by increased mucosal adherence of resident bacteria and chronic intestinal inflammation (*9*). Although mitogenic functions have been suggested for Reg proteins in other tissues (*10*), the biological functions of intestinal RegIII proteins and their role in IBD have remained poorly defined. We show here that RegIIIγ and human HIP/PAP are peptidoglycan-binding proteins with direct antibacterial activity.

Immunogold electron microscopy revealed that RegIIIγ is present in Paneth cell secretory granules (fig. S2). Granule contents are released apically (*11*); their release indicates that RegIIIγ is targeted to the gut lumen, which harbors large resident bacterial populations. Other members of the C-type lectin family, such as the mannose-binding lectin (MBL), bind to microbial surface carbohydrates and trigger innate immune responses (*12*). Therefore, we hypothesized that RegIIIγ might similarly bind intestinal bacteria. Previously, we established a procedure for purification of recombinant mouse RegIIIγ and human HIP/PAP (*13*). We used fluorochrome-conjugated recombinant RegIIIγ to look for binding to a mixed microbial population harvested from the small intestines of conventionally raised mice. Flow cytometry revealed that RegIIIγ bound to a subpopulation of intestinal bacteria (Fig. 1C).

Given that intestinal microbial communities consist of both Gram-positive and Gram-negative species (*14*), we asked whether RegIIIγ bound preferentially to one of these groups. Wheat

[1]Center for Immunology, [2]Department of Microbiology, The University of Texas Southwestern Medical Center at Dallas, 5323 Harry Hines Boulevard, Dallas, TX 75390, USA.

*These authors contributed equally to this work.
†To whom correspondence should be addressed. E-mail: Lora.Hooper@UTSouthwestern.edu

germ agglutinin (WGA) binds to surface peptidoglycan on Gram-positive bacteria, thus distinguishing between Gram-positive and Gram-negative populations (*15*). Dual staining with fluorochrome-conjugated RegIIIγ and WGA revealed that RegIIIγ preferentially bound to the WGA-positive bacterial population (Fig. 1D). Furthermore, we found that RegIIIγ bound to pure preparations of cultured Gram-positive bacteria, including *Listeria innocua* and *Enterococcus faecalis*, with comparatively little binding to preparations of cultured Gram-negative bacteria, including *Salmonella typhimurium* and *Pseudomonas aeruginosa* (Fig. 1E).

These findings suggested that RegIIIγ binds peptidoglycan, a molecule that is exposed on the Gram-positive bacterial surface, but is buried in the periplasmic space of Gram-negative bacteria. To test this idea, we performed pull-down assays using insoluble cell wall peptidoglycan (*16*). Purified RegIIIγ was completely removed from solution by incubation with peptidoglycan and was retained in the peptidoglycan-bound fraction after extensive washing (Fig. 2A). Human HIP/PAP is 65% identical to RegIIIγ and exhibited a similar peptidoglycan binding activity (Fig. 2A). The specificity of both interactions was confirmed by using soluble peptidoglycan (sPGN) to compete for binding to insoluble peptidoglycan (iPGN) (Fig. 2B). Furthermore, we calculated a dissociation constant (K_d) of 11 nM for RegIIIγ and 26 nM for HIP/PAP (fig. S4). These results indicate high-affinity binding to peptidoglycan and are in good agreement with the dissociation constants determined for other known peptidoglycan-binding proteins, including CD14 (*17*) and members of the peptidoglycan-recognition protein (PGRP) family (*18*).

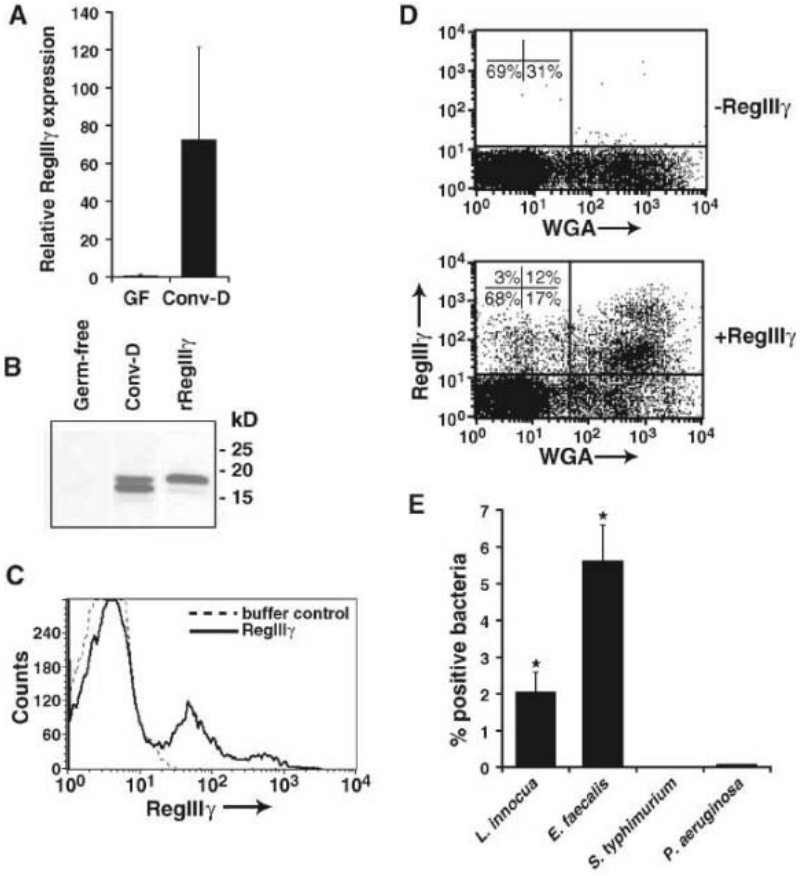

Fig. 1. RegIIIγ is induced by resident intestinal microbes and binds to Gram-positive bacteria. (**A**) *RegIIIγ* mRNA expression in Paneth cells. Paneth cells were harvested by laser-capture microdissection from germ-free and conventionalized small intestines. Q-PCR analysis was performed on RNAs from microdissected Paneth cells from three mice per group. Values were normalized to glyceraldehyde-3-phosphate dehydrogenase (GAPDH) expression, and mean ± SD is plotted (range for conventionalized samples is 42 to 309). Results are expressed relative to one of the germ-free samples. GF, germ-free; Conv-D, conventionalized. (**B**) RegIIIγ protein expression in small intestine. RegIIIγ was detected in mid–small intestinal protein by immunoblot with RegIIIγ-specific antiserum (*13*). The lower band in the protein sample from conventionalized mice likely results from proteolytic cleavage at a trypsin-like site near the N-terminus (*13*), similar to that described for Reglα (*8*). Results are representative of two independent experiments. rRegIIIγ, recombinant RegIIIγ. (**C**) RegIIIγ binds to intestinal bacteria. Flow cytometry reveals binding of AlexaFluor555–conjugated RegIIIγ to intestinal bacteria recovered from conventional mouse small intestine. BSA-AlexaFluor555 showed no binding (not shown). Results are representative of independent experiments with three mice. (**D**) RegIIIγ binds preferentially to Gram-positive intestinal bacteria. Dual-color flow cytometry analysis with WGA-AlexaFluor488 and RegIIIγ-AlexaFluor555 shows preferential binding to the WGA-positive bacterial population. Results are representative of three independent experiments. (**E**) RegIIIγ binds preferentially to cultured Gram-positive bacteria. Formaldehyde-fixed preparations of Gram-positive (*L. innocua* and *E. faecalis*) and Gram-negative bacteria (*S. typhimurium* and *P. aeruginosa*) were incubated with RegIIIγ, followed by detection with RegIIIγ-specific antiserum and Cy3-labeled goat secondary antibody against rabbit IgG, and analyzed by flow cytometry. Results are representative of three experiments. Asterisks indicate statistically significant differences between Gram-positive species and *S. typhimurium* ($P < 0.05$). Preimmune serum controls are shown in fig. S3.

Peptidoglycan consists of extended glycan chains composed of alternating *N*-acetylglucosamine (GlcNAc) and *N*-acetylmuramic acid (MurNAc) residues cross-linked by short peptides (Fig. 2C). Because RegIIIγ and HIP/PAP contain predicted CRDs, we determined whether they recognize the carbohydrate moiety of peptidoglycan. Chitin is composed of β1,4-linked GlcNAc chains that are virtually identical to the peptidoglycan carbohydrate backbone (Fig. 2C). As shown in Fig. 2D, purified recombinant RegIIIγ and HIP/PAP bound to chitin immobilized on Sepharose beads. Both lectins also bound to mannan, a polymer of mannose residues (Fig. 2D). This is consistent with the fact that C-type lectins that bind GlcNAc-containing saccharides frequently also bind mannose-containing saccharides (*19*), owing to the similar arrangements of the 3- and 4-hydroxyls of these sugars. In contrast, neither lectin bound dextran-Sepharose or uncoupled Sepharose (Fig. 2D). No binding was detected to monomeric GlcNAc-Sepharose or mannose-Sepharose, which indicated that both lectins show specificity for polymeric carbohydrates (*13*). Although the C-type lectin family includes members that bind their ligands in a calcium-dependent manner, we found that RegIIIγ and HIP/PAP do not require calcium for binding to peptidoglycan and chitin. Taken together, these results suggest that RegIIIγ and HIP/PAP are pattern-recognition proteins that recognize the microbe-associated molecular pattern represented by the extended glycan chains of peptidoglycan.

Chitin binding activity was also detected in pull-down assays in which we assessed RegIIIγ and HIP/PAP binding to equivalent masses of peptidoglycan and chitin (Fig. 2E). Peptidoglycan bound more RegIIIγ and HIP/PAP than chitin did, which suggested that both lectins bind more avidly to peptidoglycan than to chitin. Neither lectin bound to cellulose, a β1,4-linked glucose polymer.

Our results reveal a carbohydrate ligand preference similar to that of mannose-binding lectin (MBL), a C-type lectin with an established

role in innate immunity. As a serum protein, MBL recognizes invading microbes by binding to surface mannose residues (*12*) or to peptidoglycan (*20*). This binding triggers the lectin-activated complement pathway, which is initiated by recruitment of the serine proteases MASP1 and 2 via interactions with the MBL collagenous domain. In contrast to MBL, RegIIIγ and HIP/PAP consist of secreted CRDs that lack collagenous domains required for complement recruitment. We therefore postulated that RegIIIγ and HIP/PAP might be directly antimicrobial, without requiring additional factors to kill targeted microbes. We tested this idea by adding purified RegIIIγ and HIP/PAP to Gram-positive enteric microbes including *Listeria monocytogenes*, *L. innocua*, and *E. faecalis*, and observed a dose-dependent reduction in the viability of each organism (Fig. 3A). The number of colony-forming units (CFUs) of each microbe declined by 99% after a 2-hour exposure to 5 μM HIP/PAP (Fig. 3A). A similar decline in the viability of *L. monocytogenes* and *L. innocua* was observed after a 2-hour exposure to 5 μM RegIIIγ (Fig. 3A). The viability of *E. faecalis* declined by ~80% after a 2-hour exposure to 10 μM RegIIIγ (Fig. 3A). Thus, the effective antibacterial concentrations of both lectins are similar to those of other intestinal antimicrobial proteins (*21*, *22*). Furthermore, we found that infusion of RegIIIγ into isolated small intestinal segments from *L. innocua* monocolonized mice resulted in a decline in bacterial numbers relative to a buffer infusion (fig. S5), indicating that RegIIIγ is active under native intestinal conditions.

As expected, neither RegIIIγ nor HIP/PAP was bactericidal toward the Gram-negative enteric organisms *Escherichia coli* or *Bacteroides thetaiotaomicron* (Fig. 3A). This is consistent with our observation of preferential binding to Gram-positive bacteria and the fact that peptidoglycan is buried in the periplasmic space of Gram-negative bacteria. Additionally, neither lectin reduced the viability of fungal microorganisms, including *Saccharomyces cerevisiae* and *Candida albicans*.

We used transmission electron microscopy to visualize morphological changes in *L. monocytogenes* cells after exposure to RegIIIγ and HIP/PAP. Our images revealed evidence of cell wall damage and cytoplasmic leakage (Fig. 3B). These results are remarkably similar to those obtained with cationic antimicrobial peptides, such as human β-defensin-3 (*21*), which kill bacteria by cell wall permeabilization. Our findings indicate that lectin-mediated bacterial killing also involves cell wall damage.

RegIIIγ and HIP/PAP bactericidal activities were inhibited with sPGN and chitin fragments, linking peptidoglycan binding to antibacterial function. Addition of 35 μM sPGN to antibacterial assays inhibited the bactericidal activity of both lectins (Fig. 3C). At 10 mM, chitotetraose, a 4-sugar acid hydrolysis fragment of chitin, also fully inhibited the antibacterial activity of both RegIIIγ and HIP/PAP (Fig. 3C). Consistent with the preference of RegIIIγ and HIP/PAP for polymeric sugars, 10 mM monomeric GlcNAc or chitobiose ($GlcNAc_2$) were less inhibitory. These results demonstrate that a soluble oligosaccharide that mimics the peptidoglycan saccharide backbone is sufficient to inhibit lectin antimicrobial activity. These findings are consistent with a model in which lectin binding to surface peptidoglycan carbohydrate precedes microbial killing.

Given RegIIIγ's bactericidal activity, we predicted that its expression patterns would reflect microbial colonization levels in the mouse small intestine. Q-PCR analysis of *RegIIIγ* mRNA levels along the cephalocaudal axis of conventionalized small intestines revealed increasing expression toward the distal region (ileum) (Fig. 4A), concomitant with increasing microbial densities. In contrast, germ-free mice showed minimal *RegIIIγ* expression throughout the small intestine (Fig. 4A). We also assayed for changes in *RegIIIγ* mRNA expression during postnatal intestinal development. *RegIIIγ* mRNA levels rose dramatically during the weaning period [postnatal days (P) 17 to 22] and remained high into adulthood (≥P28) in conventionally raised but not germ-free mice (Fig. 4B). Weaning is associated with dramatic changes in gut microflora composition, as well as withdrawal of maternal immuno-

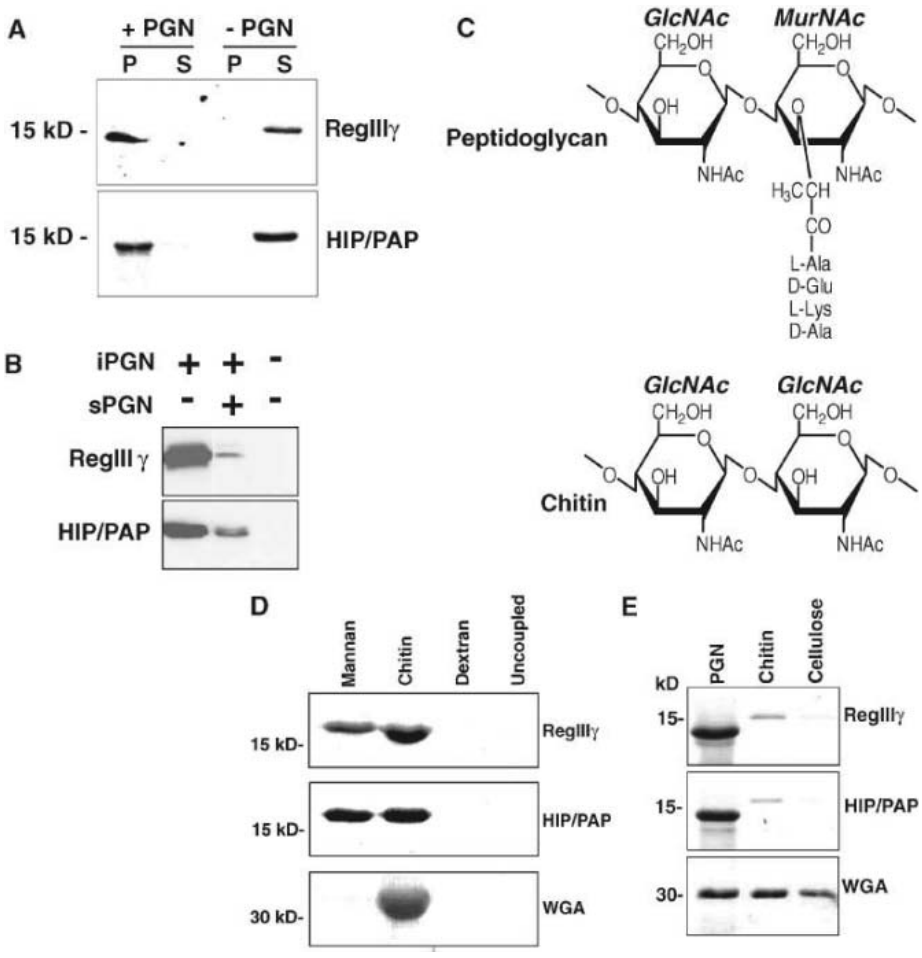

Fig. 2. Mouse RegIIIγ and human HIP/PAP bind peptidoglycan. (**A**) Peptidoglycan pull-down assays. RegIIIγ or HIP/PAP (10 μg of either) was added to 50 μg insoluble *Bacillus subtilis* peptidoglycan and pelleted. Pellet (P) and supernatant (S) fractions were analyzed by SDS–polyacrylamide gel electrophoresis (SDS-PAGE) and Coomassie blue staining. (**B**) sPGN competes with iPGN for lectin binding. Pull-down assays were performed with or without 100 μM soluble *B. subtilis* peptidoglycan. (**C**) Comparison of peptidoglycan and chitin structures. The structure of a typical Gram-positive peptidoglycan is depicted. (**D**) Lectin binding to immobilized polysaccharides. Lectins were bound to immobilized polysaccharide for 2 hours at 4°C. After washing, bound proteins were released by boiling in SDS-PAGE sample buffer and analyzed by SDS-PAGE and Coomassie blue staining. (**E**) Pull-down assays comparing binding to peptidoglycan, chitin, and cellulose. Purified recombinant RegIIIγ or HIP/PAP (10 μg of either) was added to 50 μg of peptidoglycan, chitin, or cellulose and analyzed as in (A). The lower molecular weight forms of RegIIIγ and HIP/PAP in (A) and (E) result from cleavage at an N-terminal trypsinlike site by a peptidoglycan-associated proteolytic activity.

globulin A (IgA) antibodies. The antibacterial activity of RegIIIγ suggests that its expression is elicited as part of a compensatory response to maintain mucosal homeostasis in the face of changing microbial ecology and withdrawal of passive immunity.

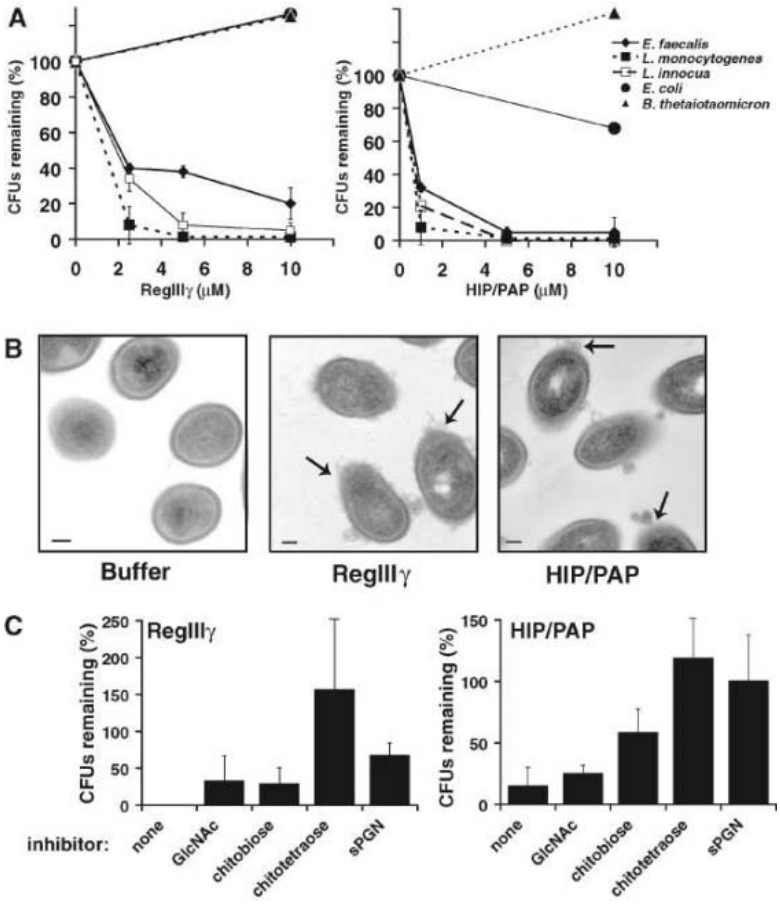

Fig. 3. Mouse RegIIIγ and human HIP/PAP have antibacterial activity against Gram-positive bacteria. (**A**) Percentage of CFUs remaining after exposure to purified RegIIIγ and HIP/PAP. *L. innocua*, *L. monocytogenes*, *E. faecalis*, *Escherichia coli* K12, and *B. thetaiotaomicron* were grown to mid–log phase and incubated with purified lectins. Initial bacterial concentrations ranged from 10^5 to 10^6 CFU/ml. After incubation for 2 hours at 37°C, viable bacteria were quantified by dilution plating. Assays were done in triplicate. Mean ± SD is plotted. (**B**) Transmission electron microscopy of *L. monocytogenes* following a 2-hour exposure to 10 μM purified recombinant RegIIIγ and HIP/PAP. Arrows indicate examples of damaged cell surfaces and cytoplasmic leakage. Scale bar, 100 nm. (**C**) Lectin bactericidal activity is inhibited by chitooligosaccharides and sPGN. GlcNAc, chitobiose ($GlcNAc_2$), or chitotetraose ($GlcNAc_4$) at 10 mM or 35 μM sPGN was added to antibacterial assays performed on *L. innocua* as in (A). Each percentage CFU was calculated relative to a no-lectin control assay containing an identical amount of chitooligosaccharide or sPGN.

Because conventional microflora are composed of diverse microbial societies, we asked whether single enteric bacterial species are sufficient to drive small intestinal *RegIIIγ* expression. As expected, a mixed microbial community recovered from a conventional mouse elicited a ~20-fold increase in *RegIIIγ* expression when introduced into germ-free wild-type C57/b6 mice. In contrast, colonization with the Gram-negative symbiont *Bacteroides thetaiotaomicron* elicited only a 2.5-fold increase in expression, whereas the noninvasive Gram-positive *L. innocua* had no effect on *RegIIIγ* mRNA levels (Fig. 4C). These results indicate that neither organism alone was sufficient to stimulate *RegIIIγ* expression to conventional levels in wild-type mice. However, bacteria that are normally strictly compartmentalized in the intestinal lumen show increased mucosal adherence and invasion in mice that lack mucosal IgA (*23*). We therefore postulated that mucosal defenses such as secretory IgA might be sufficient to sequester *B. thetaiotaomicron* and *L. innocua* in the gut lumen and so could account for the inability of these single species to stimulate *RegIIIγ* expression. Indeed, we found that *B. thetaiotaomicron* and *L. innocua* trigger a 52- and 41-fold increase, respectively, in *RegIIIγ* mRNA expression after colonization of germ-free RAG1-deficient mice, which lack mature lymphocytes and are therefore IgA-deficient (*24*). Wild-type and RAG1-deficient mice were colonized to virtually identical levels (~10^8 CFU/ml ileal contents), which indicated that differences in *RegIIIγ* mRNA expression did not result from differences in total microbial numbers. Our findings thus support a model in which increased bacterial-epithelial contact drives *RegIIIγ* expression as a mechanism to limit potential microbial penetration and maintain mucosal surface integrity.

Together, RegIIIγ and HIP/PAP represent a new family of inducible antibacterial proteins that seek out their microbial targets via interactions with bacterial peptidoglycan. Because they lack domains necessary for complement recruitment and are directly bactericidal, these

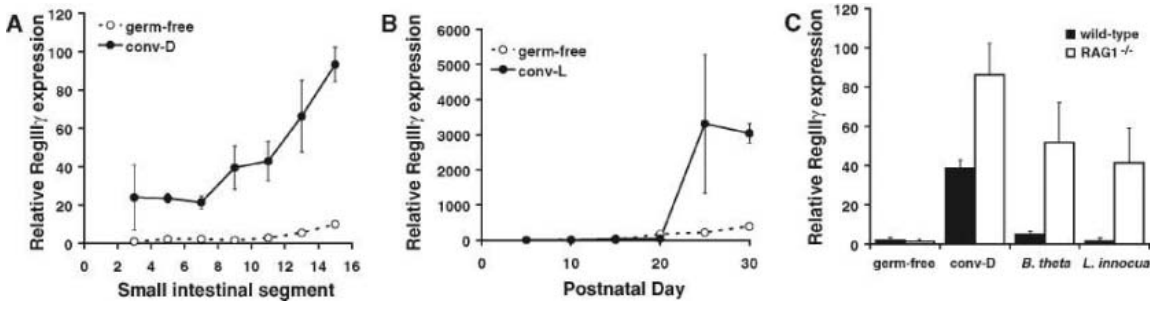

Fig. 4. RegIIIγ expression is triggered by intestinal bacteria. (**A**) RegIIIγ expression along the cephalocaudal axis of the small intestine. Small intestines from adult germ-free or conventionalized (conv-D) NMRI mice were divided into 16 equal segments (numbered proximal to distal) and *RegIIIγ* mRNA expression was determined in specific segments using Q-PCR. Results are representative of experiments in two sets of mice. (**B**) *RegIIIγ* mRNA increases during the weaning period (P17 to 22) in developing conventionally raised NMRI mice. Assays were performed on pooled mid–small intestinal RNAs (for three mice per time point). (**C**) *RegIIIγ* expression is triggered by single Gram-positive or Gram-negative bacterial species in immunodeficient mice. Q-PCR determinations were done on cDNAs from mid–small intestine. Each point represents the average value from three or more different mice. All Q-PCR determinations were performed in triplicate (mean ± SD plotted) and were normalized to 18*S* ribosomal RNA.

proteins reveal a new function for mammalian C-type lectins. We propose that these antibacterial lectins represent an evolutionarily primitive form of lectin-mediated innate immunity, and that the lectin-mediated complement pathway may have evolved from a directly antimicrobial precursor. In support of this idea, simple model organisms such as *Drosophila* and *Caenorhabditis elegans* harbor a number of genes encoding putative C-type lectins that consist solely of a simple CRD with an N-terminal secretion signal (*25*, *26*). The data presented here suggest that these proteins could function in innate antimicrobial defense. Furthermore, the human and mouse Reg families encompass multiple members, many of which are expressed in the gut (*27*). It seems likely that other members of this protein family are also antimicrobial, but may exhibit preferences for different microbial targets.

The discovery of directly antibacterial C-type lectins points to a previously uncharacterized mucosal defense mechanism that helps to sequester the gut microflora and preserve intestinal homeostasis. Our results suggest that RegIIIγ expression is triggered by increased microbial-epithelial contact at mucosal surfaces. Enhanced expression of Reg proteins such as HIP/PAP in IBD patients may therefore be a compensatory response that limits mucosal penetration by gut microbes. Because Reg proteins exhibit increased expression in IBD mucosa (*5*, *8*), whereas α-defensin expression decreases (*2*, *3*), these two groups of antimicrobial proteins are probably regulated by distinct mechanisms. It is not yet known whether Reg expression is triggered by direct bacterial interactions with gut epithelia, or whether other intestinal cells (e.g., macrophages) direct epithelial Reg expression. Further investigation will therefore be required to decipher the host and microbial factors that regulate antimicrobial lectin expression. These studies will contribute to a better understanding of IBD pathogenesis and will provide new insights into how symbiotic host-microbial relationships are maintained.

References and Notes

1. L. V. Hooper, T. Midtvedt, J. I. Gordon, *Annu. Rev. Nutr.* **22**, 283 (2002).
2. J. Wehkamp *et al.*, *Gut* **53**, 1658 (2004).
3. J. Wehkamp *et al.*, *Proc. Natl. Acad. Sci. U.S.A.* **102**, 18129 (2005).
4. L. Christa *et al.*, *Am. J. Physiol.* **271**, G993 (1996).
5. H. Ogawa *et al.*, *Inflamm. Bowel Dis.* **9**, 162 (2003).
6. A. J. Syder *et al.*, *Proc. Natl. Acad. Sci. U.S.A.* **100**, 3467 (2003).
7. S. L. Pull, J. M. Doherty, J. C. Mills, J. I. Gordon, T. S. Stappenbeck, *Proc. Natl. Acad. Sci. U.S.A.* **102**, 99 (2005).
8. B. K. Dieckgraefe *et al.*, *J. Investig. Med.* **50**, 421 (2002).
9. A. Swidsinski *et al.*, *Gastroenterology* **122**, 44 (2002).
10. F. J. Livesey *et al.*, *Nature* **390**, 614 (1997).
11. T. Ayabe *et al.*, *Nat. Immunol.* **1**, 113 (2000).
12. R. A. Ezekowitz, *J. Infect. Dis.* **187** (suppl. 2), S335 (2003).
13. H. L. Cash, C. V. Whitham, L. V. Hooper, *Protein Expr. Purif.* **48**, 151 (2006).
14. P. B. Eckburg *et al.*, *Science* **308**, 1635 (2005).
15. C. Holm, L. Jespersen, *Appl. Environ. Microbiol.* **69**, 2857 (2003).
16. T. Werner *et al.*, *Proc. Natl. Acad. Sci. U.S.A.* **97**, 13772 (2000).
17. R. Dziarski, R. I. Tapping, P. S. Tobias, *J. Biol. Chem.* **273**, 8680 (1998).
18. C. Liu, E. Gelius, G. Liu, H. Steiner, R. Dziarski, *J. Biol. Chem.* **275**, 24490 (2000).
19. K. Drickamer, *Nature* **360**, 183 (1992).
20. J. Nadesalingam, A. W. Dodds, K. B. Reid, N. Palaniyar, *J. Immunol.* **175**, 1785 (2005).
21. J. Harder, J. Bartels, E. Christophers, J. M. Schroder, *J. Biol. Chem.* **276**, 5707 (2001).
22. E. M. Porter, E. van Dam, E. V. Valore, T. Ganz, *Infect. Immun.* **65**, 2396 (1997).
23. A. J. Macpherson *et al.*, *Science* **288**, 2222 (2000).
24. P. Mombaerts *et al.*, *Cell* **68**, 869 (1992).
25. K. Drickamer, R. B. Dodd, *Glycobiology* **9**, 1357 (1999).
26. R. B. Dodd, K. Drickamer, *Glycobiology* **11**, 71R (2001).
27. H. Miyashita *et al.*, *FEBS Lett.* **377**, 429 (1995).

28. The authors wish to thank T. Januszewski for help with electron microscopy and D. Farrar for help with flow cytometry. This work was supported by grants from the NIH (R01 DK070855), the Crohn's and Colitis Foundation of America, and a Burroughs Wellcome Career Award in the Biomedical Sciences (to L.V.H.). H.L.C. was supported by NIH training grant T32-AI007520. L.V.H. is on the scientific advisory board of The Dannon Company. The microarray data are held in U.S. National Center for Biotechnology Information's Gene Expression Omnibus (GEO) and the accession number is GSE5156.

Supporting Online Material

www.sciencemag.org/cgi/content/full/313/5790/1126/DC1
Materials and Methods
Figs. S1 to S5
Table S1
References

7 March 2006; accepted 28 June 2006
10.1126/science.1127119

Individual Cell Migration Serves as the Driving Force for Optic Vesicle Evagination

Martina Rembold,[1] Felix Loosli,[1] Richard J. Adams,[2] Joachim Wittbrodt[1]*

The cellular mechanisms underlying organ formation are largely unknown. We visualized early vertebrate eye morphogenesis at single-cell resolution by in vivo imaging in medaka (*Oryzias latipes*). Before optic vesicle evagination, retinal progenitor cells (RPCs) modulate their convergence in a fate-specific manner. Presumptive forebrain cells converge toward the midline, whereas medial RPCs remain stationary, predetermining the site of evagination. Subsequent optic vesicle evagination is driven by the active migration of individual RPCs. The analysis of mutants demonstrated that the retina-specific transcription factor *rx3* determines the convergence and migration behaviors of RPCs. Hence, the migration of individual cells mediates essential steps of organ morphogenesis.

For over a century, the vertebrate eye has served as a paradigm to study vertebrate organogenesis (*1*). Fate mapping has revealed the origin of retinal progenitor cells (RPCs) and forebrain cells in teleosts (*2*–*4*); however, the cellular mechanisms underlying eye morphogenesis remain unclear. Eye development starts at late gastrula stages with the specification of RPCs within the eye field of the anterior neural plate (*5*). Evagination of the optic vesicles, the first step of eye morphogenesis, is visible after neurulation. We applied in vivo imaging techniques in medaka to reconstruct eye morphogenesis at single-cell resolution. RPCs were specifically marked by fluorescent tagging of the homeobox transcription factor *rx3*, a protein that is expressed in the RPCs from the gastrula to optic vesicle stages (stages 16 to 20) (*6*, *7*). We generated *rx3*::green fluorescent protein (GFP)–transgenic embryos to visualize RPCs during optic vesicle morphogenesis. To follow the movement of all individual cells during optic vesicle evagination, we counterstained all nuclei of the embryo with histone H2B-monomeric red fluorescent protein (H2B-mRFP) (*8*, *9*). These embryos were imaged at high spatial and temporal resolution by confocal in vivo time-lapse microscopy (Fig. 1, A and B, and movie S1) (*10*). At gastrula stages, RPCs (which are GFP-positive cells) are located within the eye field in the anterior neural plate (Fig. 1B at time 0:00). The eye field is surrounded at its anterior-lateral and posterior borders by tel- and diencephalic progenitor cells, respectively (*2*). In the course of neurulation, the eye field converges to the midline and remains as a single domain within the forebrain (Fig. 1B at 03:28). Three hours later, the optic vesicles have evaginated from the neural keel (Fig. 1B at 06:16). It has previously been assumed that the optic vesicles evaginate after the neural keel [the precursor of the central nervous system (Fig. 1A)] has formed. However, at the level of gross morphology, we find that the eye field remains wide and distinct from the neural keel during neurulation as the posterior neural axis narrows, indicating an earlier onset of eye morphogenesis (dashed white

[1]Developmental Biology Unit, European Molecular Biology Laboratory, Meyerhofstrasse 1, 69117 Heidelberg, Germany. [2]Department of Physiology, Development, and Neuroscience, University of Cambridge, Downing Street, Cambridge CB2 3DY, UK.

*To whom correspondence should be addressed. E-mail: jochen.wittbrodt@embl.de

line in Fig. 1B at 03:28). Similar observations have been made in mouse and rat models, in which the optic pit appears during the elevation of the neural plate, thus before neural tube formation (*11*, *12*).

To follow individual cell movements during optic vesicle evagination, we tracked more than 300 individual cells of the eye field and the surrounding forebrain in the acquired four-dimensional (4D) sequences by recording the approximate geometric center of the H2B-mRFP–labeled nuclei. The recorded data were visualized with the use of 3D rendering routines to reconstruct the movements that individual cells underwent during evagination (Fig. 1, D and E, and fig. S1, A to F) (*10*). This analysis revealed that, within the eye field, ventromedial RPCs do not converge and show no net movement toward the midline (red arrows in Fig. 1, D and E). These stationary RPCs keep the eye field wide during neurulation at the site of evagination [Fig. 1, D at 2:36 and E at 2:36 and 4:12 (red arrows); and movies S3 and S4). In contrast, RPCs of the lateral eye field and prospective prosencephalic cells migrate to the midline (yellow and white arrows, respectively, in Fig. 1, D and E). On approaching the midline, the RPCs of the lateral eye field show a biphasic behavior; first they dive ventrally and then migrate laterally into the evaginating optic vesicle [Fig. 1D from 2:36 to 4:12 (yellow arrows) and fig. S1, A to F, (cell 9)]. Therefore, optic vesicle evagination starts during neural keel formation, whereas the neural plate converges at this stage (Fig. 1, D and E). Ventromedial RPCs thus never pass through the neural keel before they evaginate. This precludes a simple evagination of RPCs from the preformed neural keel, as was previously assumed (*13*, *14*).

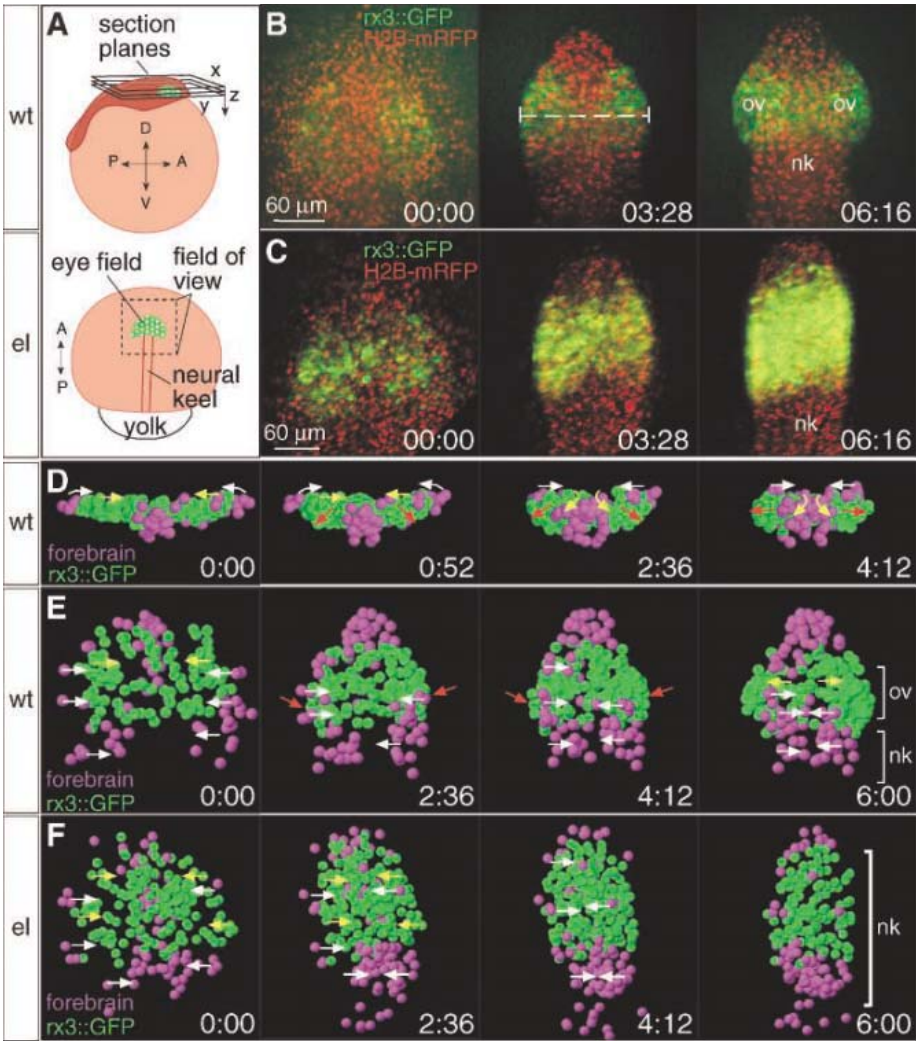

Fig. 1. Fate-specific modulation of convergence. (**A**) Schematics of the imaging setup. D, dorsal; V, ventral; A, anterior; P, posterior. (**B** and **C**) Confocal sections during optic vesicle morphogenesis in wild-type (wt) (B) and *eyeless* (*el*) (C). RPCs, green (*rx3*::GFP); nuclei, red (H2B-mRFP); anterior is at top. (B) Gastrula-stage eye field (time 00:00) condenses to a single domain in the forebrain (03:28), which is wider than the neural keel (dashed white line). Optic vesicles (ov) have evaginated from the neural keel (nk) (06:16). (C) The eye field in *eyeless* does not differ from the wild type [00:00, compare to (B)]. Subsequently, mutant RPCs converge, forming the neural keel (03:28 to 6:16). (**D** to **F**) 4D visualization of tracked cells. Forebrain cells, magenta spheres; RPCs, green spheres. (D) Anterior view, with dorsal at top. (E and F) Dorsal view, with anterior at top. In (D) and (E), stationary wild-type RPCs keep the eye field wide (red arrows, 0:52 to 4:12). Diencephalic cells of the lateral neural plate converge to the midline and form the neural keel (white arrows). Lateral RPCs (yellow arrows) move to the midline, change direction, and contribute to the optic vesicles (2:36 to 6:00). (F) *eyeless* mutant RPCs (yellow arrows) converge as forebrain cells (0:00 to 4:12, white arrows), forming the neural keel (6:00). Time is reported in hh:mm (h, hours; m, minutes).

To further study the mechanism of optic vesicle evagination, we analyzed the medaka *rx3* mutant *eyeless* (*15*). The *rx* homeobox transcription factors are indispensable for vertebrate eye development, and the loss of *rx* function results in the absence of eyes (*15*–*20*). Medaka and zebrafish (*Danio rerio*) *rx3* mutants lack eyes because of a failure of optic vesicle formation despite the presence of RPCs (*15*, *18*, *19*). We performed confocal time-lapse analysis and single-cell tracking in the *rx3* mutant background (Fig. 1, C and F; fig. S1, G to K; movies S2 and S5) (*10*). At late gastrula stages, the mutant eye field is indistinguishable from that of the wild type (Fig. 1, C and F at 0:00). However, at the onset of convergence, all RPCs move toward the midline as do the other forebrain cells (Fig. 1F from 0:00 to 4:12) to form a neural keel (Fig. 1F at 6:00). Initiation of optic vesicle evagination by stationary RPCs of the ventromedial eye field does not occur (Fig. 1, C at 3:28 and F at 2:36). Thus, a crucial first step in vertebrate eye morphogenesis is omitted in the *rx3* mutant, resulting in the localization of RPCs within the neural tube (Fig. 1F at 6:00; Fig. 2, B and D) (*21*).

In the absence of *rx3* function, mutant RPCs adopt a migratory behavior typical of forebrain cells, in that they converge to the midline to form a neural keel. To visualize the changes in cell shape during optic vesicle morphogenesis, we used a *rx3*::membrane yellow fluorescent protein (*rx3*::mYFP) transgenic line to address the correlation of the morphogenetic behavior of RPCs and their morphology (Fig. 2, A and B, and movie S6) and corroborated these findings by immunostaining for α-tubulin (Fig. 2, C and D) (*10*). Wild-type RPCs are highly motile and adopt various shapes during evagination, reflecting their dynamic movement (Fig. 2, A and C, and movie S6). In contrast, mutant lateral RPCs are columnar and form part of the epithelialized wall of the forebrain, surrounding medial rounded mutant RPCs that also fail to evaginate (Fig. 2, B and D, and movie S6). Thus, in the absence of *rx3*, lateral mutant RPCs adopt both the shape and morphogenetic behavior of neuroepithelial cells, resulting in the formation of a neural tube containing nonevaginated RPCs (*15*). This indicates that neuroepithelial morphology and migratory be-

havior are a default state and that *rx3* sets apart a domain that moves and adopts a shape different from that of the forebrain.

The observed epithelialization of mutant RPCs could be the cause for the failure of evagination. However, single-cell tracking revealed that optic vesicle morphogenesis starts before neural tube formation. An alternative explanation is that an altered migratory potential or behavior of mutant RPCs induces the phenotype. We performed mosaic 4D analysis, allowing the simultaneous monitoring and comparison of wild-type and mutant cell behavior during evagination at high resolution. Wild-type cells from embryos ubiquitously expressing a membrane-tethered mRFP (*8*, *9*) were transplanted at the blastula stage to the animal pole of an *eyeless* intercross expressing *rx3*::mYFP (*10*). Wild-type cells transplanted into a wild-type eye field contribute normally to the developing optic vesicles (Fig. 2, E and F). Individual cells located medially before evagination (Fig. 2E) migrate into the optic vesicles to integrate into the vesicular epithelia (Fig. 2F), contributing to their growth (movie S7).

In the mutant background, individual wild-type cells rescue optic vesicle evagination in a cell-autonomous fashion (Fig. 2, G and H, and movie S8). Small but otherwise normal optic vesicles are formed by wild-type cells, whereas mutant cells of the host are found exclusively in the forebrain keel (Fig. 2H, asterisk). 4D volume rendering shows the migratory behavior of wild-type cells in the mutant context (Fig. 3, A to C). At early neurula stages, wild-type RPCs within the mutant eye field are found either at the lateral border, because of the reduced convergence of ventromedial wild-type RPCs, or within the medial eye field (Figs. 2G and 3A). 4D rendering shows that, subsequently, wild-type cells from the medial part of the eye field actively penetrate the surrounding mutant tissue to move laterally, where they merge with the wild-type RPCs in the rescued optic vesicle (Fig. 3, A and B, asterisk, and movie S9). These clusters gradually merge into a single vesicle by posterior movements (Fig. 3C). In contrast, mutant cells form a neural keel and never contribute to the optic vesicles (Figs. 3C and 2H). Movements of wild-type cells in the mutant background can occur either as small groups of cells (Fig. 3, D to F, arrow, and movie S10) or as individual cells that migrate through the mutant tissue of the medial forebrain into the rescued optic vesicles (Fig. 3, G to I, asterisk, and movie S11). Previous transplantation experiments have shown that mutant cells in a wild-type background do not contribute to the forming optic vesicles (*21*). Thus, the observed phenotype in *eyeless* mutant embryos is due to the altered migratory behavior of mutant cells. Optic vesicle formation can be efficiently rescued by wild-type cells. This indicates that the cues directing this migration are not affected in the mutant background.

To further address the migratory properties of wild-type RPCs, we transplanted wild-type cells labeled by *rx3*::mYFP to an unlabeled wild-type background (Fig. 4, A to F) (*10*). Individual RPCs are highly motile and extend lamellipodia (Fig. 4F, arrowhead) and filopodia (Fig. 4F, arrow) as they converge toward the midline (movie S14). Both lamellipodia and filopodia are characteristic features of actively migrating cells. Also, at the beginning of optic vesicle evagination, RPCs extend filopodia (Fig. 4B, solid arrowhead) as well as lamellipodia (Fig. 4B, open arrowhead) (movie S12) in the direction of their movement. Furthermore, migrating RPCs elongate and actively migrate into the forming optic vesicle (Fig. 4C). Finally, cells actively exchange neighbors during their migration. This demonstrates individual cell migration. A representative example is shown in Fig. 4 (D and E). Cell 1 first lies lateral to cell 2 (Fig. 4D, 0:00). Within 40 min, it has moved over cell 2 (Fig. 4E at 0:38, and movie S13). Thus, active single-cell migration of RPCs is a crucial feature of vertebrate eye morphogenesis, both during convergence of the eye field and subsequently during optic vesicle evagination.

Previous studies of optic vesicle formation used fate mapping and gross morphological analysis (*2*–*4*, *13*, *22*). Consequently, models were not available to describe the behavior of cells during the transition from the eye field to optic vesicles. Our time-lapse analysis using fate-labeled RPCs allowed us to resolve the behavior of individual cells in this complex process. We show that the migratory properties of RPCs differ from those of forebrain cells in an *rx3*-dependent manner. Single wild-type cells migrate through the surrounding tissue in *eyeless* mutants, thereby rescuing optic vesicle evagination. We propose a two-step process of optic vesicle formation (Fig. 4G). First, during the gastrula and early neurula stages, ventromedial RPCs show a modulated, slower convergence when compared to the neural plate (Fig. 4G, steps 1 and 2, blocked green arrow), resulting in a wide domain where lateral evagination of the optic vesicle is initiated (Fig. 4G, step 3). In addition, RPCs are prevented from forming the epithelialized neural keel structure of more posterior forebrain cells. Second, RPCs in the forebrain elongate mediolaterally and migrate actively from medial positions laterally, enlarging the volume of the growing optic vesicles (Fig. 4G, step 4). Our 4D analysis indicates that, in both steps, the coordinated migration of individual RPCs is a driving force.

The migration of RPCs could be driven by a neuroectodermal midline signal as proposed for

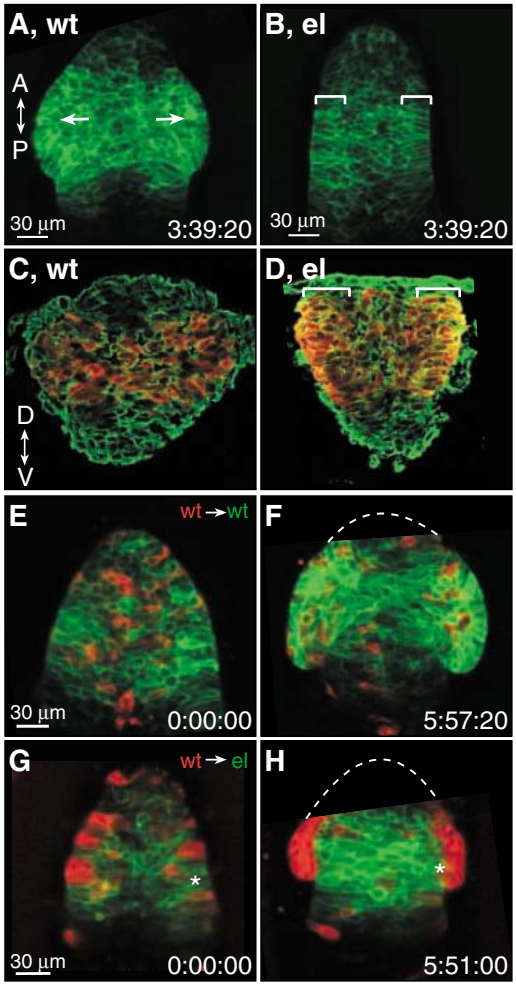

Fig. 2. Cell shape [(A) to (D)] and mosaic analysis [(E) to (H)]. (**A** and **B**) Single confocal planes from *rx3*::mYFP embryos; anterior is at top. (**C** and **D**) α-tubulin (green) and α-GFP (red) stainings on transverse sections of *rx3*::GFP embryos; dorsal is at top. The dynamic morphology of wild-type RPCs during evagination is shown [(A), arrows and (C)]. (B) and (D) Epithelial organization of mutant lateral RPCs is visible (brackets) surrounding the round medial cells. (E to H) Mosaic analysis. Confocal sections of the 4D sequence (neurula to somitogenesis stages) are shown; anterior is at top. (**E**) to (**F**) Normal participation of wild-type cells (membrane-mRFP, red regions) transplanted into the wild-type eye field (*rx3*::mYFP, green regions). (**G**) Wild-type cells (red) in the *eyeless* host (green) at the lateral border of the eye field and at medial positions. (**H**) Cell-autonomous rescue of optic vesicle formation by wild-type cells. Asterisk, mutant tissue remaining in the forebrain; dashed white line, anterior border of the forebrain. Time is reported in hh:mm:ss (h, hours; m, minutes; s, seconds).

the convergence and extension (CE) of the neural plate in *Xenopus* (*23*, *24*). In that model, an unidentified signal polarizes and orients cells toward the midline and defines distinct morphogenetic areas within the posterior neural plate (*23*, *24*). We hypothesize that, during optic vesicle morphogenesis, a neuroectodermal midline signal first promotes convergence movements that are modulated in a cell-autonomous fashion in *rx3*-positive cells. Second, the same or a second signal directs the RPCs during subsequent optic vesicle evagination. Examples of such signals acting on axon growth are known (*25*, *26*). Alternatively, pioneering cells in the optic vesicle could provide attractive cues for the migratory RPCs. It will be interesting to examine whether the signaling mechanisms involved in CE and optic vesicle evagination build on the same molecular players.

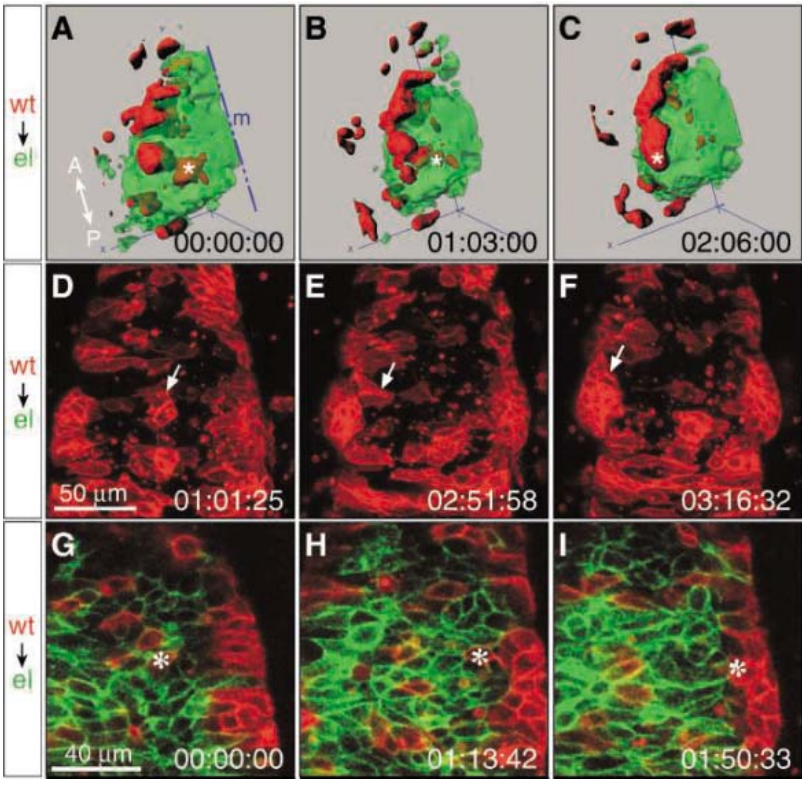

Fig. 3. Individual cell movement. (**A** to **C**) 3D reconstruction of rescued evagination by wild-type cells (red) in the mutant host (green). One half is shown. Dashed blue line, midline (m). Anterior is at top left. Wild-type cells [(A), asterisk] move through mutant tissue (B), forming a small optic vesicle (C). (**D** to **F**) Maximum-intensity projection (MIP) showing wild-type cells (red) in the *eyeless* host (mutant cells not shown). A cluster of four medial wild-type cells [(D), arrow] migrates to the optic vesicle [(E) to (F)]. (**G** to **I**) Single cell (red, asterisk) migrating through *eyeless* mutant tissue (green).

References and Notes

1. H. Spemann, *Verh. Anat. Ges.* **15**, 61 (1901).
2. Y. Hirose, Z. M. Varga, H. Kondoh, M. Furutani-Seiki, *Development* **131**, 2553 (2004).
3. Z. M. Varga, J. Wegner, M. Westerfield, *Development* **126**, 5533 (1999).
4. K. Woo, S. Fraser, *Development* **121**, 2595 (1995).
5. R. L. Chow, R. A. Lang, *Annu. Rev. Cell Dev. Biol.* **17**, 255 (2001).
6. T. Iwamatsu, *Zool. Sci.* **11**, 825 (1994).
7. K. Deschet, F. Bourrat, F. Ristoratore, D. Chourrout, J.-S. Joly, *Mech. Dev.* **83**, 179 (1999).
8. R. E. Campbell *et al.*, *Proc. Natl. Acad. Sci. U.S.A.* **99**, 7877 (2002).
9. S. G. Megason, S. E. Fraser, *Mech. Dev.* **120**, 1407 (2003).
10. Materials and methods are available as supporting material on *Science* Online.
11. K. K. Svoboda, K. S. O'Shea, *Development* **100**, 185 (1987).
12. D. E. Morse, P. S. McCann, *Invest. Ophthalmol. Vis. Sci.* **25**, 899 (1984).
13. E. A. Schmitt, J. E. Dowling, *J. Comp. Neurol.* **344**, 532 (1994).
14. S. S. Easter Jr., J. J. Malicki, *Results Probl. Cell Differ.* **40**, 346 (2002).
15. F. Loosli *et al.*, *Development* **128**, 4035 (2001).
16. M. Andreazzoli, G. Gestri, D. Angeloni, E. Menna, G. Barsacchi, *Development* **126**, 2451 (1999).
17. P. H. Mathers, A. Grinberg, K. A. Mahon, M. Jamrich, *Nature* **387**, 603 (1997).
18. F. Loosli *et al.*, *EMBO Rep.* **4**, 894 (2003).
19. B. N. Kennedy *et al.*, *Dev. Biol.* **270**, 336 (2004).
20. A. Rojas-Munoz, R. Dahm, C. Nusslein-Volhard, *Dev. Biol.* **288**, 348 (2005).

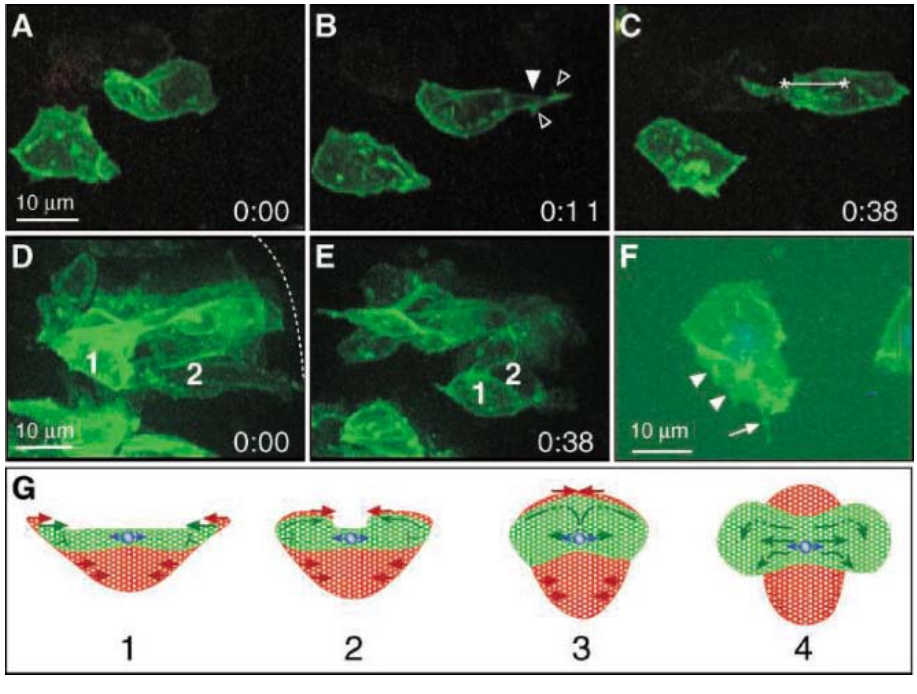

Fig. 4. Cell morphology during migration. Morphology of cells is shown during evagination [(A) to (E)] and convergence (F). An MIP of wild-type cells (*rx3*::mYFP, green) in unlabeled wild-type background is shown. (**A** to **C**) Cell extending a lamellipodium (solid arrowhead) and filopodia (open arrowheads). The line in (C) indicates the distance moved by the cell. (**D** and **E**) Cell (1) moving over a neighboring cell (2). Dashed line, lateral border of eye field. (**F**) Cell in the eye field extending lamellipodia (arrowheads) and filopodia (arrow). (**G**) Model of optic vesicle morphogenesis. RPCs, green; forebrain, red. Panels 1 to 3 show that modulated convergence of ventromedial RPCs (blocked green arrow), as opposed to forebrain cells (red arrows), results in the formation of a wide eye domain. RPCs of the lateral eye field move toward the midline (green arrows in panels 1 and 2) and subsequently toward the forming vesicles (green arrows in panel 3). Evagination is driven by single-cell migration (green arrows in panel 4) at all stages. Hypothetical midline signal (blue circle) or two different signals could direct both processes: the block of convergence and subsequent evagination.

21. S. Winkler, F. Loosli, T. Henrich, Y. Wakamatsu, J. Wittbrodt, *Development* **127**, 1911 (2000).
22. Z. Li, N. M. Joseph, S. S. J. Easter, *Dev. Dyn.* **218**, 175 (2000).
23. T. Elul, R. Keller, *Dev. Biol.* **224**, 3 (2000).
24. A. M. Ezin, P. Skoglund, R. Keller, *Dev. Biol.* **256**, 100 (2003).
25. K. Brose, M. Tessier-Lavigne, *Curr. Opin. Neurobiol.* **10**, 95 (2000).
26. B. J. Dickson, *Science* **298**, 1959 (2002).

27. We thank the Fraser lab for the mRFP-histone construct; the Ellenberg lab for the multilocation imaging macro and their help in establishing functional imaging conditions; D. Gilmour and K. Brown for critical discussion of the manuscript; A. Nowicka, D. Hofmann, and E. Grzebisz for expert fish husbandry; and all members of the Wittbrodt lab for their constructive input. This work was supported by the Human Frontier Science Program and the Deutsche Forschungsgemeinschaft, Collaborative Research Centre 488.

Supporting Online Material
www.sciencemag.org/cgi/content/full/313/5790/1130/DC1
Materials and Methods
Fig. S1
References
Movies S1 to S14

8 March 2006; accepted 6 July 2006
10.1126/science.1127144

Argonaute Slicing Is Required for Heterochromatic Silencing and Spreading

Danielle V. Irvine,[1*] Mikel Zaratiegui,[1*] Niraj H. Tolia,[1*] Derek B. Goto,[1†] Daniel H. Chitwood,[1,2] Matthew W. Vaughn,[1] Leemor Joshua-Tor,[1,2] Robert A. Martienssen[1,2‡]

Small interfering RNA (siRNA) guides dimethylation of histone H3 lysine-9 (H3K9me2) via the Argonaute and RNA-dependent RNA polymerase complexes, as well as base-pairing with either RNA or DNA. We show that Argonaute requires the conserved aspartate-aspartate-histidine motif for heterochromatic silencing and for ribonuclease H–like cleavage (slicing) of target messages complementary to siRNA. In the fission yeast *Schizosaccharomyces pombe*, heterochromatic repeats are transcribed by polymerase II. We show that H3K9me2 spreads into silent reporter genes when they are embedded within these transcripts and that spreading requires read-through transcription, as well as slicing by Argonaute. Thus, siRNA guides histone modification by base-pairing interactions with RNA.

RNA interference (RNAi) results when double-stranded RNA (dsRNA) is processed into siRNA by the ribonuclease (RNase) III–type enzyme known as Dicer. These siRNAs then base-pair with complementary mRNA to target cleavage (and, in some cases, to repress translation). Argonaute proteins facilitate this process by binding the 3′ end of one siRNA strand via the conserved PAZ domain. Target messages complementary to the siRNA are then cleaved by the Argonaute PIWI domain, which is related to RNaseH and contains the highly conserved motif Asp-Asp-His (D-D-H), which is required for endonucleolytic cleavage (or slicing) (*1*). Argonaute proteins are required for transcriptional as well as posttranscriptional silencing in *Drosophila*, *Arabidopsis*, and *Schizosaccharomyces pombe*, which has only one Argonaute protein (Ago1) (*2*–*4*). Heterochromatic repeats, transposable elements (TEs), and some transgenes are associated with modified chromatin when they are transcriptionally silenced. Histone modification in *S. pombe* depends on Argonaute and RNAi (*5*) as well as on the Rik1 complex, which contains the histone methyltransferase Clr4 (*6*). Two models have been proposed for the role of siRNA in histone modification (*7*). First, siRNA might interact with DNA, recruiting modified histones via the RNA-induced initiation of transcriptional silencing (RITS) complex, which includes the chromodomain protein Chp1 as well as Ago1 (*8*). Alternatively, Argonaute might slice heterochromatic transcripts, recruiting RNA-dependent RNA polymerase (RdRP) via free 3′ OH ends, which promote polymerase activity (*9*). Association with nascent transcripts might then recruit the histone modification apparatus to the chromosome (*10*).

We tested the ability of fission yeast Ago1 to cleave target messages in a siRNA-dependent fashion. Recombinant glutathione *S*-transferase (GST)–SpAgo1 fusion proteins were purified from *Escherichia coli* (Fig. 1A) and incubated with two different 23-nucleotide (nt) RNA oligonucleotides complementary to a target message. When labeled message was added to the reaction, RNA fragments were detected, corresponding in size to products cleaved at each siRNA complementary site (Fig. 1B). These fragments were not observed in control reactions supplemented with EDTA, which chelates Mg^{2+} and thereby inhibits cleavage. Thus, Ago1 from fission yeast has "slicing" activity and can direct site-specific cleavage of RNA substrates via siRNA.

In order to assess the role of slicing in heterochromatic silencing, we constructed *ago1*$^{-}$ mutants in the D-D-H motif (*11*–*13*). Alanine substitutions were introduced at each of the three conserved residues (fig. S1), resulting in much lower catalytic activity in vitro (Fig. 1C). The corresponding mutants in yeast were viable and grew normally but accumulated transcripts from both forward and reverse strands of heterochromatic repeats (Fig. 1D). Run-on transcription assays have previously revealed that the reverse strand is transcribed in wild-type cells, although RNA fails to accumulate, whereas the forward strand is not transcribed in detectable quantities and is silenced at the transcriptional level (*3*). The reverse-strand transcript [or pre-siRNA (*14*)] fails to accumulate because it is rapidly converted into siRNA. Thus, our results indicate that both posttranscriptional silencing (of the reverse strand) and transcriptional silencing (of the forward strand) require slicing via the D-D-H motif. In agreement with these results, siRNA from centromeric repeats was undetectable in the slicer mutants (Fig. 1E), as in strains in which the *ago1* gene has been deleted (*15*).

siRNA is derived from dsRNA. Only one strand of the repeats is transcribed in wild-type cells (*3*), so that generation of dsRNA depends on RdRP activity (*9*). DsRNA is then cleaved into 23-nt duplexes by Dicer. Ago1 promotes RdRP activity via interactions between the RITS and the RDRC complexes as well as template RNA (*9*). dsRNA synthesis begins at the 3′ OH end of single-stranded RNA (ssRNA) fragments (*9*), and such ends are generated by slicing (*1*). In slicer mutants, reduction in RdRP activity is expected to lead to loss of dsRNA and therefore loss of siRNA (*1*). Also, sliced transcripts are uncapped, which promotes RdRP activity (*16*). We therefore tested the association of both RdRP and Ago1 itself with centromeric heterochromatin in slicer mutant strains. We found that association of RdRP with the repeats was reduced (although not abolished) in *ago1*$^{-}$ slicer mutants (Fig. 2A). In contrast, association of slicer-defective Ago1 was slightly enriched (Fig. 2B), indicating that Ago1 catalytic activity, and not just localization to the repeats, is important for silencing. Histone H3 lysine-9 (H3K9me2) quantities were only partially reduced at the centromeric repeats

[1]Cold Spring Harbor Laboratory, 1 Bungtown Road, Cold Spring Harbor, NY 11724, USA. [2]Watson School of Biological Sciences, Cold Spring Harbor Laboratory, Cold Spring Harbor, NY 11724, USA.

*These authors contributed equally to this work.
†Present address: Laboratory for Nanosystems Physiology, Research Institute for Electronic Science, Hokkaido University, Sapporo, 060-0812, Japan.
‡To whom correspondence should be addressed. E-mail: martiens@cshl.edu

themselves, as in *ago1*⁻ deletions (*3*) (Fig. 2C). This probably accounts for the retention of slicer-defective Ago1 at the repeats (Fig. 2B), because the RITS complex still binds to H3K9me2, even in the absence of siRNA (*6*, *8*).

The *ura4*⁺ reporter genes integrated into the pericentromeric outer repeats of centromere 1 are transcriptionally silenced in wild-type strains via H3K9me2 and Swi6 (*17*, *18*). Pericentromeric *ura4*⁺ was strongly derepressed in each of the three slicer mutants: H3K9me2 from the reporter gene was reduced to below the limit of detection, and H3K4me2 was increased fourfold (Fig. 2C). Slicer-defective Ago1 was also substantially lost from *ura4*⁺ (Fig. 2B), consistent with the loss of H3K9me2, but most Rdp1 was retained (Fig. 2A). Unlike RITS, whose association with the chromosome depends on H3K9me2, chromatin association of Rdp1 is thought to be dependent on nascent RNA, perhaps accounting for this distinction, although Rdp1 association with *ura4*⁺ is variable in replicate experiments (*9*). In the absence of RNAi, H3K9me2 is retained at pericentromeric repeats by the histone deacetylase Clr3, as previously reported (*19*). But H3K9me2 is lost from *ura4*⁺ reporter genes integrated into transcribed repeats in *ago1*⁻ slicer mutants (Fig. 2C), which resemble the RITS mutant *chp1*⁻ in this respect (*6*). Thus, spreading of H3K9me2 into neighboring reporter genes depends on slicing.

Several *ura4*⁺ reporter genes have been integrated into centromere 1 and differ in the extent to which they are silenced (*17*, *18*). We wondered whether this position effect depended on transcripts from the repeats, and so

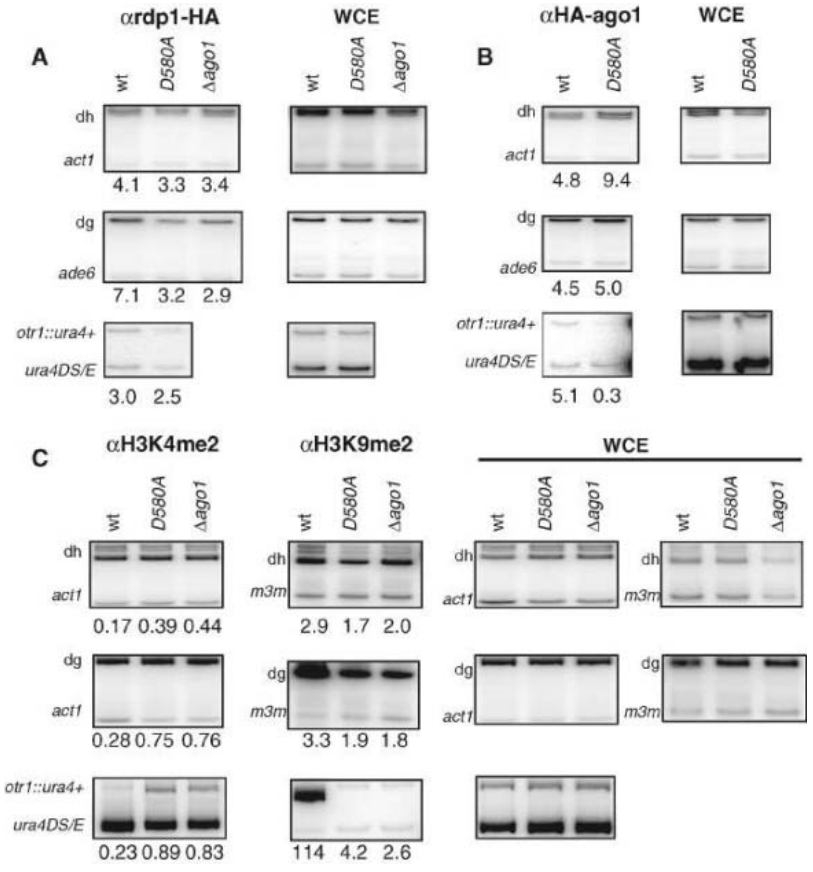

Fig. 2. Histone H3 methylation and localization of RITS and RDRC depend on slicer. Chromatin immunoprecipitation (ChIP) analysis of WT, *ago1D580A* mutant (*D580A*), and *ago1* knockout (Δ*ago1*) strains. In each sample, enrichment for each primer pair was measured relative to control primer pairs in whole cell extract (WCE) and is depicted under each lane. The regions assayed were the *dg* and *dh* repeats, together with regions unaffected by RNAi (*act1*, *ade6*, and *mat3M*), and a *ura4*⁺ insertion in the outer repeat of centromere 1 [*otr1R(SphI)::ura4*⁺], together with a *ura4* minigene (*ura4DS/E*) at the endogenous locus. (**A**) Hemagglutinin (HA)-tagged Rdp1. (**B**) WT and *ago1D580A* slicer-defective HA-tagged Ago1. (**C**) H3K9me2 and H3K4me2.

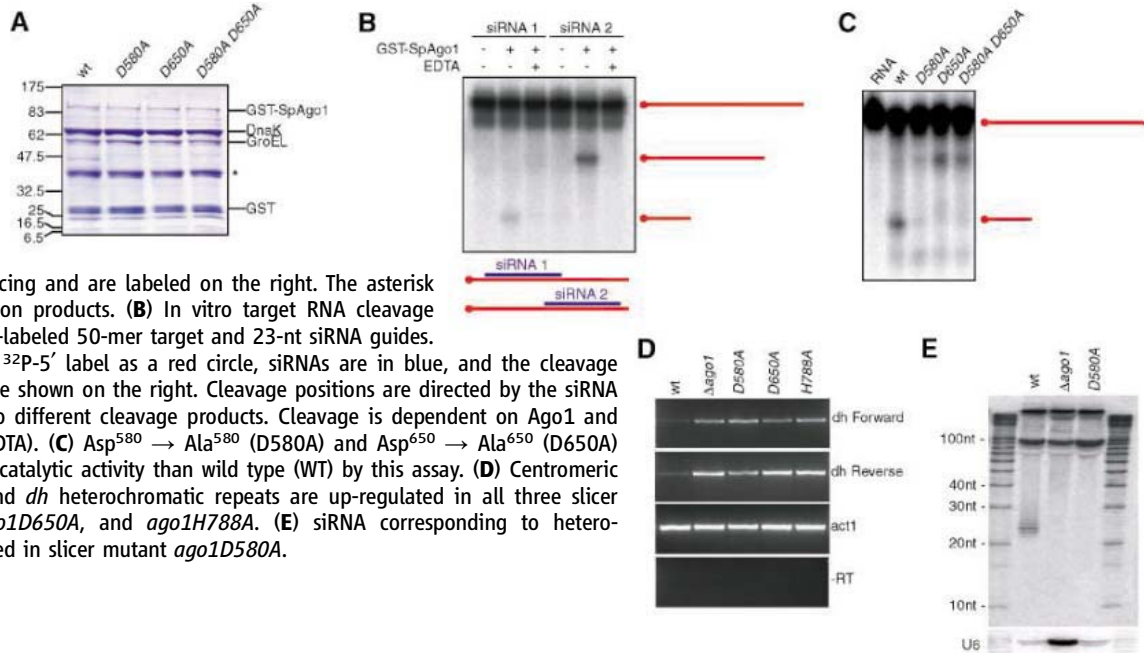

Fig. 1. Slicer mutants in *S. pombe*. (**A**) SDS–polyacrylamide gel electrophoresis (PAGE) after size exclusion chromatography of GST-SpAgo1. Positions for the molecular weight markers (ink D) are labeled on the left. Bands were identified by mass spectrometric sequencing and are labeled on the right. The asterisk denotes SpAgo1 degradation products. (**B**) In vitro target RNA cleavage (slicing) assay using ^{32}P-5′-labeled 50-mer target and 23-nt siRNA guides. Target RNA is in red with ^{32}P-5′ label as a red circle, siRNAs are in blue, and the cleavage products for each siRNA are shown on the right. Cleavage positions are directed by the siRNA sequences, resulting in two different cleavage products. Cleavage is dependent on Ago1 and magnesium (absence of EDTA). (**C**) Asp^{580} → Ala^{580} (D580A) and Asp^{650} → Ala^{650} (D650A) mutants have much lower catalytic activity than wild type (WT) by this assay. (**D**) Centromeric transcripts from the *dg* and *dh* heterochromatic repeats are up-regulated in all three slicer mutants, *ago1D580A*, *ago1D650A*, and *ago1H788A*. (**E**) siRNA corresponding to heterochromatic repeats is reduced in slicer mutant *ago1D580A*.

we sequenced the ends of cDNA clones isolated from *dcr1*⁻ strains by using the *dg* centromeric repeat as a probe. Most of these cDNA clones mapped to the 16 *dg* repeats from centromeres 2 and 3, but one clone matched the *dg* repeat from centromere 1 (fig. S2). Although it was truncated at the 3′ end, the 5′ end of the clone mapped precisely to the promoter of the reverse transcript identified previously (*14*). By comparing these sequences with the *ura4*⁺ insertion sites, we found that reporter genes inserted downstream of the promoter, within the transcription unit of the *dg* repeat, were silenced at least fourfold more efficiently than those inserted upstream of the transcription unit (fig. S2), indicating that transcription itself might play a role in spreading.

Read-through transcripts from *ura4*⁺ insertions in the *dg* repeat downstream of the reverse-strand promoter were present in low quantities in wild-type cells but in high quantities in *ago1*⁻ slicer mutants, indicating they were the targets of slicer activity (Fig. 3, A and B). By using rapid amplification of cDNA ends (RACE) polymerase chain reaction (PCR), we could detect full-length cotranscripts in mutant cells ($^{17}/_{17}$ cloned products), but we could not detect either full-length or cleaved transcripts in wild-type cells (Fig. 3C). Cleavage products could be recovered, however, from the exosome mutant *rrp6*⁻ (Fig. 3C), in which an exonuclease gene had been disrupted. The exosome degrades uncapped and nonpolyadenylated (or cleaved) transcripts (*20*, *21*), such as those cleaved by Ago1 slicer activity on either side of the *ura4*⁺ insertion. In *rrp6*⁻ cells, different cleavage sites were sequenced in the region that matched siRNA ($^{20}/_{27}$ cloned products), but none were detected in the *ura4*⁺ gene itself (Fig. 3D). *ura4*⁺ insertions located within the transcribed *dh* repeat (FY988 and FY939) also gave rise to read-through transcripts in *ago1*⁻ slicer mutants (fig. S2) and were strongly silenced (*17*, *18*). But read-through transcripts corresponding to *ura4*⁺ genes located upstream of the reverse strand promoter (FY496 and FY501) could only just be detected, consistent with reduced silencing in these strains (fig. S2). This reduced silencing is still sensitive to RNAi (*3*) but, unlike downstream *ura4*⁺ insertions silencing, also depends on the histone deacetylase Clr3 (*17*, *18*), which is independent of RNAi (*19*). Similar read-through transcripts were observed when repeats were fused to reporter genes elsewhere in the genome and were also targets of RNAi (*22*). Thus, reporter gene silencing depends, at least in part, on slicing of heterochromatic cotranscripts by Ago1 (Fig. 3C).

The siRNA from the *ura4*⁺ reporter gene was undetectable (fig. S3), suggesting that interactions between siRNA and DNA are unlikely to account for *ura4*⁺ silencing. Instead, recruitment of H3K9me2 and RITS to *ura4*⁺ depends on siRNA from the pericentromeric repeats (*6*, *8*), which are required for slicing of read-through transcripts. Sliced nascent transcripts might recruit the silencing apparatus to reporter genes by virtue of cotranscription (Fig. 3E). A heterochromatic role for polymerase (Pol) II in spreading H3K9me2 is reminiscent of its euchromatic role in spreading H3K4me2 (*23*). In plants, TE insertions bring genes under their control when they integrate within the transcription unit but not when they integrate further away (*5*, *24*). In animals, cotranscription of heterochromatic repeats may also play a role in some forms of position effect variegation, but genes are silenced at much greater distances from heterochromatin and intervening genes can retain activity (*25*), so that other spreading or antispreading mechanisms are likely to be involved (*26*), such as those involving Swi6 (*27*).

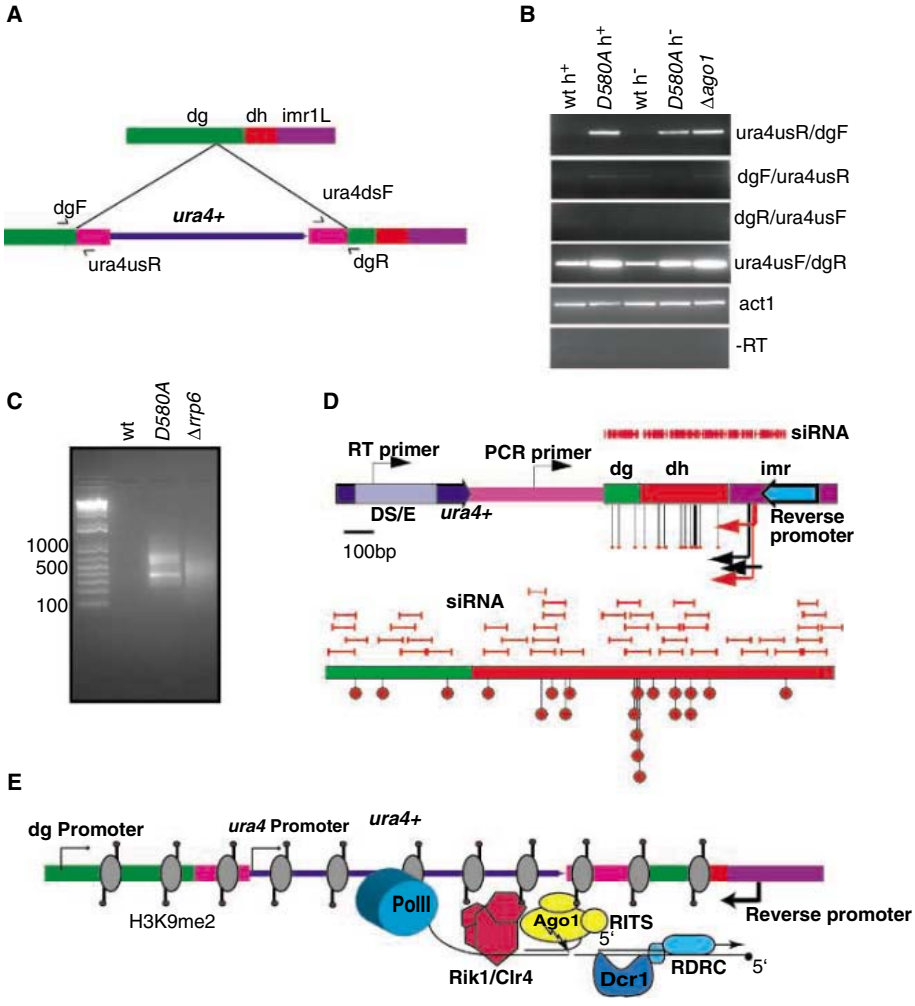

Fig. 3. Spreading of transcriptional silencing requires slicing. (**A**) The FY648 *otr1R(SphI)::ura4*⁺ insertion and the primers used for cotranscript detection are shown. (**B**) *dg*::*ura4*⁺ read-through transcripts were detected by strand-specific reverse transcription (RT) PCR. The first primer listed was used in RT to determine strand specificity. Forward strand transcripts are up-regulated in *ago1D580A* slicer mutants. Reverse strand transcripts are also up-regulated in *ago1D580A* slicer mutants but detectable in WT cells. (**C**) 5′ RACE PCR products were detected from slicer mutant *ago1D580A* and exosome mutant *rrp6*⁻. (**D**) 5′ RACE PCR products from slicer mutant *ago1D580A* (black) and exosome mutant *rrp6*⁻ (red) are shown. Putative transcript start sites [within 20 base pairs of the promoter (*14*)] are shown as arrows, whereas cleavage products are shown as lollipops. (**E**) Pol II reads through the *ura4*⁺ reporter gene from the centromeric repeat promoter. RITS is bound to the repeat via H3K9me2, and Ago1 slices transcripts guided by repeat siRNA. Slicing recruits the Rik1-Clr4 histone modification apparatus and provides templates for RdRP. Dcr1 processes RdRP products into siRNA after they are cleaved and released from the chromosome and is not necessarily associated with nascent transcripts.

References and Notes

1. Y. Tomari, P. D. Zamore, *Genes Dev.* **19**, 517 (2005).
2. D. Zilberman, X. Cao, S. E. Jacobsen, *Science* **299**, 716 (2003); published online 9 January 2003 (10.1126/science.1079695).

3. T. A. Volpe *et al.*, *Science* **297**, 1833 (2002); published online 22 August 2002 (10.1126/science.1074973).
4. M. Pal-Bhadra *et al.*, *Science* **303**, 669 (2004).
5. Z. Lippman, R. Martienssen, *Nature* **431**, 364 (2004).
6. M. Sadaie, T. Iida, T. Urano, J. Nakayama, *EMBO J.* **23**, 3825 (2004).
7. S. I. S. Grewal, D. Moazed, *Science* **301**, 798 (2003).
8. A. Verdel *et al.*, *Science* **303**, 672 (2004); published online 2 January 2004 (10.1126/science.1093686).
9. M. R. Motamedi *et al.*, *Cell* **119**, 789 (2004).
10. R. Martienssen *et al.*, in *RNAi: A Guide to Gene Silencing*, G. Hannon, Ed. (Cold Spring Harbor Laboratory Press, Cold Spring Harbor, NY, 2003).
11. J. Liu *et al.*, *Science* **305**, 1437 (2004); published online 29 July 2004 (10.1126/science.1102513).
12. J. J. Song, S. K. Smith, G. J. Hannon, L. Joshua-Tor, *Science* **305**, 1434 (2004); published online 29 July 2004 (10.1126/science.1102514).
13. F. V. Rivas *et al.*, *Nat. Struct. Mol. Biol.* **12**, 340 (2005).
14. I. Djupedal *et al.*, *Genes Dev.* **19**, 2301 (2005).
15. F. Li *et al.*, *Curr. Biol.* (2005).
16. S. Gazzani, T. Lawrenson, C. Woodward, D. Headon, R. Sablowski, *Science* **306**, 1046 (2004).
17. R. C. Allshire, E. R. Nimmo, K. Ekwall, J. P. Javerzat, G. Cranston, *Genes Dev.* **9**, 218 (1995).
18. J. F. Partridge, K. S. C. Scott, A. J. Bannister, T. Kouzarides, R. C. Allshire, *Curr. Biol.* **12**, 1652 (2002).
19. T. Yamada, W. Fischle, T. Sugiyama, C. D. Allis, S. I. Grewal, *Mol. Cell* **20**, 173 (2005).
20. T. I. Orban, E. Izaurralde, *RNA* **11**, 459 (2005).
21. H. Hieronymus, M. C. Yu, P. A. Silver, *Genes Dev.* **18**, 2652 (2004).
22. T. Volpe *et al.*, *Chromosome Res.* **11**, 137 (2003).
23. M. Hampsey, D. Reinberg, *Cell* **113**, 429 (2003).
24. A. Barkan, R. A. Martienssen, *Proc. Natl. Acad. Sci. U.S.A.* **88**, 3502 (1991).
25. P. B. Talbert, S. Henikoff, *Genetics* **154**, 259 (2000).
26. K. Ahmad, S. Henikoff, *Cell* **104**, 839 (2001).
27. A. J. Bannister *et al.*, *Nature* **410**, 120 (2001).

28. We thank A. Denli, G. Hannon, and R. Allshire for strains and T. Volpe and D. Roh for help with cDNA sequencing. D.V.I. is a C. J. Martin postdoctoral fellow, D.B.G. was a U.S. Department of Energy–Energy Biosciences postdoctoral fellow of the Life Sciences Research Foundation, and M.Z. is supported by a fellowship from the Spanish Ministry of Education. D.H.C is an NSF graduate research fellow and a George A. and Marjorie H. Matheson fellow. Research in the authors' laboratory is supported by grants from NIH to L.J. (R01-GM072659) and to R.M. (R01-GM067014).

Supporting Online Material

www.sciencemag.org/cgi/content/full/313/5790/1134/DC1
Materials and Methods
Figs. S1 to S3
Tables S1 and S2
References

17 April 2006; accepted 29 June 2006
10.1126/science.1128813

Chemical Chaperones Reduce ER Stress and Restore Glucose Homeostasis in a Mouse Model of Type 2 Diabetes

Umut Özcan, Erkan Yilmaz, Lale Özcan, Masato Furuhashi, Eric Vaillancourt, Ross O. Smith, Cem Z. Görgün, Gökhan S. Hotamisligil*

Endoplasmic reticulum (ER) stress is a key link between obesity, insulin resistance, and type 2 diabetes. Here, we provide evidence that this mechanistic link can be exploited for therapeutic purposes with orally active chemical chaperones. 4-Phenyl butyric acid and taurine-conjugated ursodeoxycholic acid alleviated ER stress in cells and whole animals. Treatment of obese and diabetic mice with these compounds resulted in normalization of hyperglycemia, restoration of systemic insulin sensitivity, resolution of fatty liver disease, and enhancement of insulin action in liver, muscle, and adipose tissues. Our results demonstrate that chemical chaperones enhance the adaptive capacity of the ER and act as potent antidiabetic modalities with potential application in the treatment of type 2 diabetes.

Insulin resistance is a common feature of obesity and predisposes the affected individuals to a variety of pathologies, including hypertension, dyslipidemias, cardiovascular disease, and type 2 diabetes mellitus (*1*). Although considerable progress has been made in understanding the molecular mechanisms underlying the insulin resistance and type 2 diabetes, satisfactory treatment modalities remain limited.

Studies in the past decade have demonstrated that obesity is associated with inflammation and established a link between inflammatory responses, particularly through the c-Jun N-terminal kinase (JNK) and inhibitory kappa B kinase (IKK) signaling pathways, and abnormal insulin action (*2*). We have recently shown that obesity also induces ER stress, and this, in turn, plays a central role in the development of insulin resistance and diabetes by triggering JNK activity via inositol-requiring enzyme–1 (IRE-1) and inhibition of insulin receptor signaling (*3*). Subsequent independent studies have also verified the role of ER stress in insulin resistance in several experimental systems (*4*, *5*). Taken together, in vitro and in vivo genetic evidence demonstrate a strong and causal relation between the functional capacity of the ER and insulin action, suggesting the possibility of exploiting this mechanism for therapeutic application.

Chemical or pharmaceutical chaperones, such as 4-phenyl butyric acid (PBA), trimethylamine *N*-oxide dihydrate (TMAO), and dimethyl sulfoxide, are a group of low molecular weight compounds known to stabilize protein conformation, improve ER folding capacity, and facilitate the trafficking of mutant proteins (*6*). Likewise, endogenous bile acids and derivatives such as ursodeoxycholic acid and its taurine-conjugated derivative (TUDCA) can also modulate ER function (*7*). In this study, we investigated whether pharmacologically active, small-molecule chemical chaperones could alleviate the increased ER stress seen in obesity and reverse insulin resistance and type 2 diabetes in experimental models.

To investigate the action of putative chemical chaperones, we first tested whether PBA and TUDCA protected against experimental ER stress in cultured cells. Pretreatment of Fao rat hepatoma cells with PBA suppressed tunicamycin-induced phosphorylation of double-stranded RNA-activated protein kinase–like endoplasmic reticulum kinase (PERK) (Thr-980) and eukaryotic initiation factor 2 alpha (eIF2α) (Ser-51) and JNK activation (fig. S1A). TUDCA pretreatment showed similar effects on tunicamycin-induced ER stress (fig. S1B). Pretreatment of liver cells with TUDCA reduced PERK and eIF2α phosphorylation and JNK activation upon exposure to tunicamycin (fig. S1B). Under these conditions, ER stress–induced splicing of X-box binding protein 1 (XBP-1) mRNA was also markedly reduced by both PBA and TUDCA (fig. S1, C and D). To exclude the possibility that PBA and TUDCA block general stress signaling without specificity for ER stress, we treated Fao cells with anisomycin, which activates JNK independent of ER stress. Neither PBA nor TUDCA prevented anisomycin-induced JNK activation (fig. S1, E and F).

XBP-$1^{-/-}$ mouse embryonic fibroblasts (MEFs) are hypersensitive to ER stress (*3*) because of the decreased ER folding capacity (*8*). Treatment of XBP-$1^{-/-}$ MEFs with PBA (fig. S2) also suppressed low-dose tunicamycin-induced phosphorylation of PERK and eIF2α, and activation of JNK, indicating that chemical chaperone treatment can reduce ER stress in multiple cell types and in a XBP-1–independent manner.

To investigate the in vivo effects of the chemical chaperones, we studied leptin-deficient (ob/ob) mice, a model of severe obesity and insulin resistance. Oral administration of PBA to *ob/ob* mice reduced ambient blood glucose to normoglycemic levels seen in the lean wild-type (WT) controls (434.2 ± 34.7 mg/dl versus 125.8 ± 12.6 mg/dl in vehicle versus PBA-treated *ob/ob* mice at 20 days, $P < 0.001$) (Fig. 1A). Normoglycemia in *ob/ob* mice was established within 4 days of PBA treatment, was maintained for up to 3 weeks, and was not associated with changes in body weight (Fig. 1B). PBA-treated *ob/ob* mice showed a more than twofold reduction ($P < 0.001$) in hyperinsulinemia (Fig. 1C), suggesting that the blood glucose–lowering effect of PBA is due to

Department of Genetics and Complex Diseases, Harvard School of Public Health, Harvard University, Boston, MA 02115, USA.

*To whom correspondence should be addressed. E-mail: ghotamis@hsph.harvard.edu

increased systemic insulin sensitivity. Neither of these parameters—blood glucose and insulin levels—were different between PBA- and vehicle-treated lean WT mice (Fig. 1, A to C).

We next examined whole-body insulin sensitivity by performing glucose tolerance tests (GTTs) and insulin tolerance tests (ITTs) in PBA- and vehicle-treated animals. Vehicle-treated *ob/ob* mice exhibited severe hyperglycemia upon administration of glucose (0.5 g/kg) and exhibited impaired glucose tolerance. PBA treatment significantly improved glucose tolerance in *ob/ob* mice with glucose disposal curves comparable to those of lean animals (Fig. 1D). Similarly, the insulin-stimulated glucose disposal curves in PBA-treated *ob/ob* mice were markedly enhanced compared to those receiving vehicle (Fig. 1E).

If the reversal of hyperglycemia, increased glucose tolerance, and insulin sensitivity are related to decreased ER stress, PBA-treated *ob/ob* mice should display a reduction in indicators of ER stress (*3*). Indeed, in PBA-treated *ob/ob* mice, PERK and IRE-1α phosphorylation in liver was markedly reduced in comparison with vehicle-treated *ob/ob* controls (Fig. 2A). Consistent with these results, JNK activation and insulin receptor substrate 1 (IRS-1) phosphorylation at Ser-307 was significantly suppressed in the liver of PBA-treated *ob/ob* mice (Fig. 2B). Similar results were also observed in adipose tissue of PBA-treated *ob/ob* mice (fig. S3, A and B). We next examined whether these biochemical alterations enhanced the signaling capacity of the insulin receptor (IR) in liver and adipose tissues of obese mice. Treatment with PBA led to improvements in insulin-induced IR (2.3-fold), IRS-1 (1.5-fold), and IRS-2 (19-fold) tyrosine phosphorylation and more distally Akt Ser-473 phosphorylation (3.2-fold) in liver tissue (Fig. 2, C and D). Similarly, insulin receptor signaling in obese mice was improved in adipose tissue after PBA treatment (fig. S3, C and D). Thus, PBA enhances insulin action at peripheral tissues in vivo.

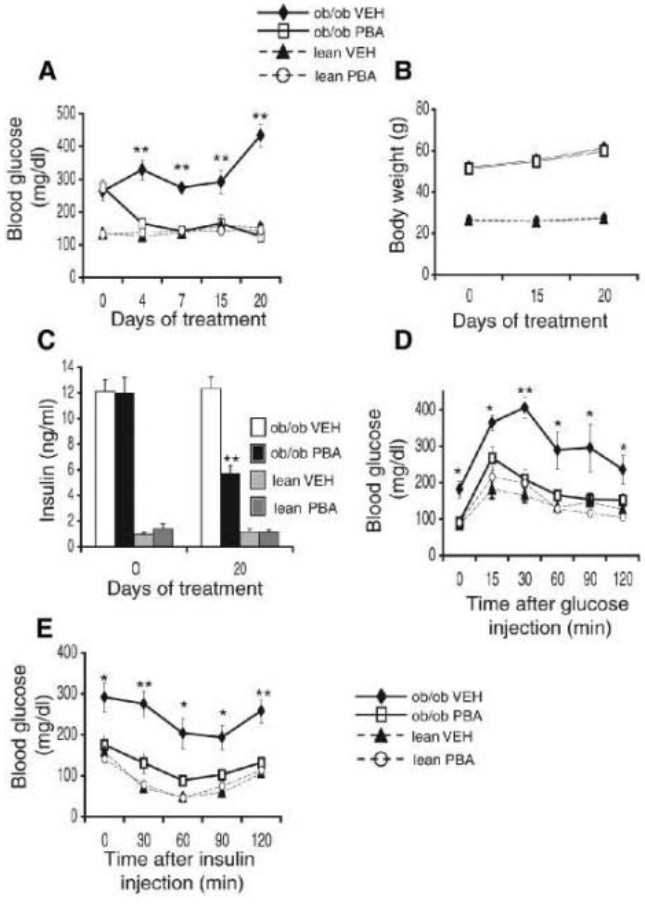

Fig. 1. Effect of PBA treatment on glucose metabolism and insulin sensitivity in *ob/ob* mice. PBA (1 g per kg of body weight) was orally administered to 7- to 8-week-old male *ob/ob* mice and age- and sex-matched WT controls ($n \geq 10$ mice in each group) for 20 days. (**A**) Blood glucose concentrations (mg/dl) in vehicle- or PBA-treated *ob/ob* and WT mice at the fed state. (**B**) Body weights of *ob/ob* and WT mice treated with vehicle or PBA. (**C**) Plasma insulin concentrations (ng/ml) measured after a 6-hour fast at the onset of experiments and after 20 days of treatment with PBA or vehicle. (**D**) Glucose (0.5 g/kg) and (**E**) insulin (2 IU/kg) tolerance tests, performed after 15 and 28 days of vehicle or PBA treatment, respectively. Data are presented as the means ± SEM, and asterisks indicate statistical significance determined by student's *t* test (*$P < 0.05$, **$P < 0.001$).

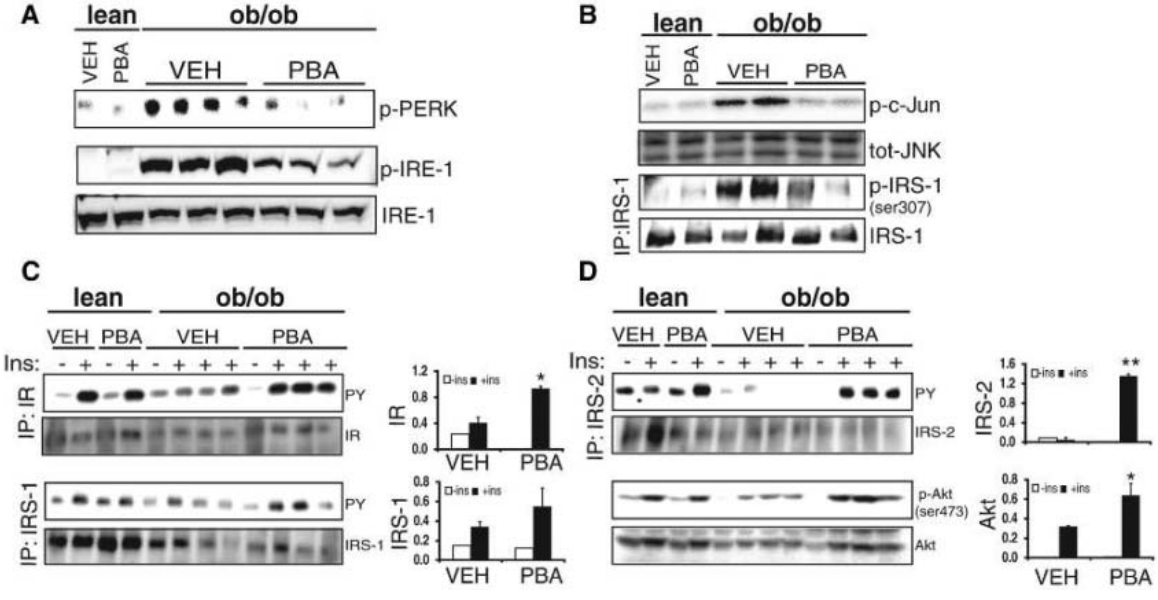

Fig. 2. Effect of PBA treatment on markers of ER stress in the liver tissue of *ob/ob* mice. (**A**) Phosphorylation of PERK (Thr980) and IRE-1α in liver tissues of PBA- or vehicle-treated *ob/ob* mice and lean controls. (**B**) Liver tissue total JNK activity, JNK protein levels, serine phosphorylation of IRS-1 (Ser-307), and total JNK and IRS-1 protein levels in the same group of mice. (**C**) Insulin-stimulated insulin receptor (IR), insulin receptor substrate 1 (IRS-1), insulin receptor substrate 2 (IRS-2), and (**D**) Akt (Ser-473) phosphorylation in liver tissues of PBA- and vehicle-treated lean and *ob/ob* mice upon insulin (2 IU/kg) infusion through the portal vein. The graphs on the right of each blot show the quantitation of phosphorylation for each protein. Data are presented as the means ± SEM, and asterisks indicate statistical significance determined by student's *t* test (*$P < 0.05$, **$P < 0.001$).

TUDCA is a hydrophilic bile acid derivative that, like PBA, diminishes ER stress responses in cultured liver cells (fig. S1B). When administered to ob/ob mice, TUDCA exhibited a potent antidiabetic activity with essentially complete normalization of blood glucose levels within 1 week of treatment (Fig. 3A). In the TUDCA-treated groups, there was a small but statistically significant decrease in body weight (1.3 g in the lean and 4.7 g in the *ob/ob* mice) (Fig. 3B). Normoglycemia in TUDCA-treated mice was maintained at significantly lower levels of blood insulin compared with vehicle-treated *ob/ob* mice (twofold reduction in TUDCA-treated mice, $P < 0.001$) (Fig. 3C). TUDCA treatment had no apparent effect on blood glucose or insulin levels in lean WT controls (Fig. 3, A to E). We next performed ITT and GTT experiments to examine systemic insulin sensitivity. The ability of insulin to decrease blood glucose concentration was markedly reduced in vehicle-treated *ob/ob* mice compared with lean controls (Fig. 3D). TUDCA administration significantly improved the in vivo responses to insulin in the *ob/ob* mice (Fig. 3D). The impaired glucose tolerance seen in vehicle-treated *ob/ob* mice was also corrected upon treatment with TUDCA (Fig. 3E).

Biochemical indicators of ER stress and major elements of IR signal transduction pathway were examined in liver and adipose tissues of TUDCA-treated mice and controls. TUDCA-treated *ob/ob* mice showed suppression of obesity-induced PERK and IRE-1α phosphorylation and JNK activation in the liver (Fig. 4, A and B) and adipose (fig. S4A) tissues. Serine phosphorylation of IRS-1, which negatively regulates insulin receptor signaling, was also suppressed in liver tissues of TUDCA-treated *ob/ob* mice compared to vehicle-treated controls (Fig. 4B). Consistent with these changes, there was a marked recovery of insulin receptor signaling capacity in TUDCA-treated *ob/ob* mice. In liver and adipose tissues, acute insulin stimulation failed to induce IR, IRS-1, IRS-2, and Akt phosphorylations in vehicle-treated *ob/ob* mice compared to their lean controls, and TUDCA treatment restored the insulin signaling capacity in both tissues (Fig. 4, C and D; fig. S4B).

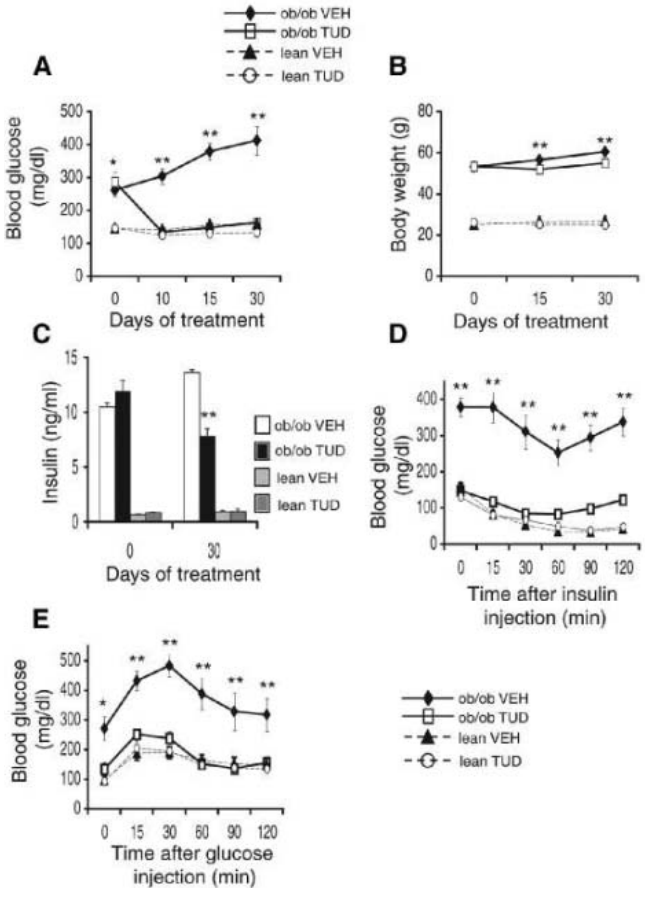

Fig. 3. Effect of TUDCA treatment on systemic glucose metabolism and insulin sensitivity in *ob/ob* mice. (**A**) Blood glucose concentrations (mg/dl) in the fed state in *ob/ob* and WT mice, treated with TUDCA or vehicle. (**B**) Body weights of *ob/ob* and WT mice treated with TUDCA or vehicle. (**C**) Plasma insulin concentrations (ng/ml) measured after a 6-hour fast at the onset of experiments and after 30 days of treatment with TUDCA or vehicle. (**D**) Insulin (2 IU/kg) tolerance and (**E**) glucose (0.5 g/kg) tolerance tests performed after 15 days of treatment with TUDCA or vehicle. The insulin and glucose tolerance tests were performed on different groups of mice. Data are presented as the means ± SEM, and asterisks indicate statistical significance determined by Student's *t* test (*$P < 0.05$, **$P < 0.001$).

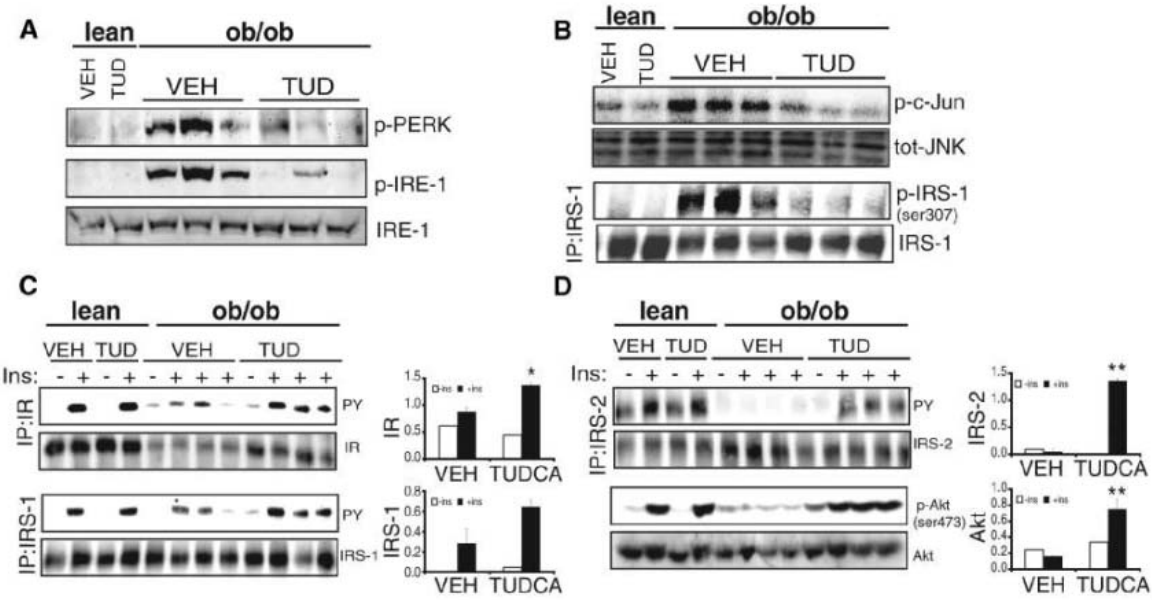

Fig. 4. Effect of TUDCA treatment on ER stress parameters, JNK activation, and insulin receptor signal transduction pathway in the liver of *ob/ob* mice. (**A**) PERK (Thr-980) and IRE-1α phosphorylation, and total IRE-1α levels in liver tissues of TUDCA- or vehicle-treated *ob/ob* mice and lean controls. (**B**) JNK activity and IRS-1 (Ser-307) phosphorylation in liver tissues of *ob/ob* mice after TUDCA administration. (**C**) Insulin-stimulated tyrosine phosphorylation of insulin receptor and IRS-1. (**D**) Insulin-stimulated IRS-2 tyrosine, and Akt serine (Ser-473) phosphorylation in the liver tissues of TUDCA- and vehicle-treated *ob/ob* mice and lean WT controls. The graphs on the right of each blot demonstrate the quantitation of phosphorylation of each molecule. Data are presented as the means ± SEM, and asterisks indicate statistical significance determined by student's *t* test (*$P < 0.05$, **$P < 0.001$).

To analyze the action of the chemical chaperones on systemic glucose metabolism and insulin action in more detail, we performed hyperinsulinemic-euglycemic clamps in *ob/ob* mice that had been treated for 20 days with these drugs (Fig. 5). We found that administration of both PBA and TUDCA significantly suppressed hepatic glucose production (HGP) at baseline and during the clamp studies (Fig. 5, A and B). Glucose infusion rates (GIRs) to maintain euglycemia were also higher in PBA- and TUDCA-treated *ob/ob* mice compared to vehicle-treated controls (Fig. 5C). Consistent with this result, whole-body glucose disposal rates (Rd) during the clamp were significantly increased after PBA and TUDCA treatments (Fig. 5D). We also performed hyperinsulinemic-euglycemic clamps in lean mice, in order to compare the improvement in glucose homeostasis in PBA- and TUDCA-treated ob/ob mice with lean mice. The HGP during clamps in lean mice was 3.9 ± 2.6 mg kg^{-1} min^{-1}, indicating that the HGP is totally normalized in drug-treated *ob/ob* mice. However, Rd and GIR were partially normalized in this protocol because the Rd in lean mice was 52.2 ± 9.5 mg kg^{-1} min^{-1}, and the GIR was 48.3 ± 8.1.

These data indicate that, in addition to suppression of hepatic glucose output, PBA and TUDCA treatment also enhances insulin-stimulated glucose disposal in peripheral tissues, which principally include muscle and adipose tissues. To explore this further, we also determined the rate of glucose uptake in muscle and epididymal adipose tissue during the clamp procedure. In both PBA- and TUDCA-treated mice, glucose uptake in muscle and adipose tissue was increased compared to that in tissues from vehicle-treated control animals (Fig. 5, E and F). These results demonstrate that PBA and TUDCA improve systemic insulin resistance by influencing both hepatic glucose output and glucose disposal in muscle and adipose tissues. Consistent with this conclusion, we found no evidence for glucose storage in liver in the form of glycogen (fig. S5, A and B) or triglyceride (fig. S6, A and B; also see below) in PBA- or TUDCA-treated *ob/ob* mice.

Obesity in mice and humans is associated with alterations in liver lipid metabolism and fatty liver disease. As shown in fig. S6, TUDCA and PBA treatment in *ob/ob* mice resulted in resolution of the obesity-induced lipid accumulation in liver. Analysis of liver triglyceride content showed a significant reduction in both PBA- and TUDCA-treated *ob/ob* mice compared to control animals (fig. S6, A and B). Consistent with the resolution of fatty liver infiltration, liver functional enzymes alanine aminotransferase and aspartate aminotransferase were normalized in both PBA- and TUDCA-treated *ob/ob* mice (fig. S7, A and B).

In summary, we have shown that small-molecule agents that modulate ER and increase folding capacity improve systemic insulin action and may have therapeutic potential for the treatment of insulin resistance and type 2 diabetes. The exact mechanisms triggering ER stress in obesity and type 2 diabetes are unclear but likely involve multiple signals, including chronically increased demand on synthetic machinery along with profound alterations in energy fluxes in metabolically active tissues. Chemical enhancement of ER function to cope with these alterations therefore provides a unique approach to manage metabolic abnormalities associated with obesity and diabetes.

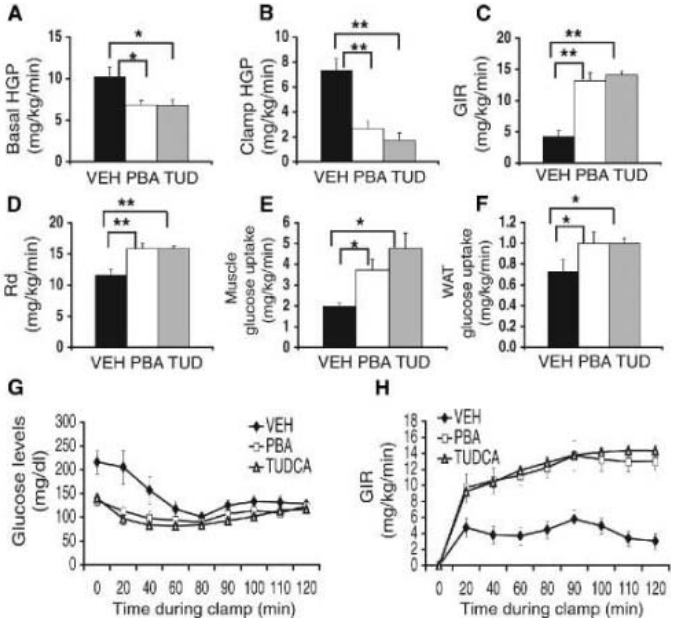

Fig. 5. Hyperinsulinemic-euglycemic clamp studies in *ob/ob* mice treated with PBA or TUDCA. Hyperinsulinemic-euglycemic clamp studies were performed after 20 days of treatment with vehicle, PBA, or TUDCA. (**A**) Basal hepatic glucose production (HGP). (**B**) HGP during the clamp. (**C**) Glucose infusion rates (GIR). (**D**) Glucose disposal rates (Rd). (**E**) Glucose uptake into muscle tissue during the clamp. (**F**) Glucose uptake into white adipose tissue (WAT). (**G**) Glucose levels during clamp procedure. (**H**) Glucose infusion rates during the clamp procedure. Data are presented as the means ± SEM, and asterisks indicate statistical significance determined by analysis of variance, post hoc test–Fisher's Protected Least Significant Difference (*$P < 0.05$, **$P < 0.001$).

Several lines of evidence suggest that chemical chaperones enhance ER functional capacity. For example, PBA increases the trafficking of the cystic fibrosis transmembrane regulator with Δ508 mutation (CFTRΔ508) and enhances the secretion of the mutant α1-ATZ protein in α1-antitrypsin deficiency (*9*). Although data on the chaperone activity of TUDCA are sparse, recent studies demonstrated this compound's ability to prevent ER stress–induced apoptosis (*7*). Our data indicate that both PBA and TUDCA can alleviate ER stress in vitro and in vivo.

The chemical chaperones we studied, PBA and TUDCA, have outstanding in vivo safety profiles. PBA, for example, has been approved by the U.S. Food and Drug Administration for clinical use in urea-cycle disorders as an ammonia scavenger and has been in clinical trials for the treatment of other diseases such as thalassemia and cystic fibrosis (*10*–*12*). TUDCA is a derivative of an endogenous bile acid, and it has been safely used as a hepatoprotective agent in humans with cholestatic liver diseases (*13*, *14*). The ability of these chemical chaperones to alleviate ER stress, establish normoglycemia, and rescue insulin action in mice provides strong support to the recently proposed ER stress–based mechanistic model of type 2 diabetes (*3*) and demonstrates the feasibility of targeting ER function for therapeutic gain. We suggest that chemical chaperones in general, and PBA and TUDCA in particular, may warrant clinical investigation as treatments for type 2 diabetes.

References and Notes

1. M. A. Permutt, J. Wasson, N. Cox, *J. Clin. Invest.* **115**, 1431 (2005).
2. K. E. Wellen, G. S. Hotamisligil, *J. Clin. Invest.* **115**, 1111 (2005).
3. U. Ozcan *et al.*, *Science* **306**, 457 (2004).
4. K. Ozawa *et al.*, *Diabetes* **54**, 657 (2005).
5. Y. Nakatani *et al.*, *J. Biol. Chem.* **280**, 847 (2005).
6. W. J. Welch, C. R. Brown, *Cell Stress Chaperones* **1**, 109 (1996).
7. Q. Xie *et al.*, *Hepatology* **36**, 592 (2002).
8. A. L. Shaffer *et al.*, *Immunity* **21**, 81 (2004).
9. J. A. Burrows, L. K. Willis, D. H. Perlmutter, *Proc. Natl. Acad. Sci. U.S.A.* **97**, 1796 (2000).
10. N. E. Maestri, S. W. Brusilow, D. B. Clissold, S. S. Bassett, *N. Engl. J. Med.* **335**, 855 (1996).
11. A. F. Collins *et al.*, *Blood* **85**, 43 (1995).
12. W. Y. Chen, E. C. Bailey, S. L. McCune, J. Y. Dong, T. M. Townes, *Proc. Natl. Acad. Sci. U.S.A.* **94**, 5798 (1997).
13. R. E. Poupon, A. M. Bonnand, Y. Chretien, R. Poupon, *Hepatology* **29**, 1668 (1999).
14. M. M. Kaplan, M. E. Gershwin, *N. Engl. J. Med.* **353**, 1261 (2005).
15. We thank J. Kim and G. I. Shulman for training and advice on the hyperinsulinemic-euglycemic clamp experiments and R. J. Foote for administrative assistance. Supported by NIH grant DK52539 to G.S.H. M.F is supported by a postdoctoral fellowship from the Japan Society for the Promotion of Science. L.O. is supported by the American Diabetes Association mentor-based postdoctoral fellowship.

Supporting Online Material

www.sciencemag.org/cgi/content/full/313/5790/1137/DC1
Materials and Methods
Figs. S1 to S7
References

4 April 2006; accepted 27 June 2006
10.1126/science.1128294

Storage of Spatial Information by the Maintenance Mechanism of LTP

Eva Pastalkova,* Peter Serrano,* Deana Pinkhasova, Emma Wallace, André Antonio Fenton,† Todd Charlton Sacktor†

Analogous to learning and memory storage, long-term potentiation (LTP) is divided into induction and maintenance phases. Testing the hypothesis that the mechanism of LTP maintenance stores information requires reversing this mechanism in vivo and finding out whether long-term stored information is lost. This was not previously possible. Recently however, persistent phosphorylation by the atypical protein kinase C isoform, protein kinase Mzeta (PKMζ), has been found to maintain late LTP in hippocampal slices. Here we show that a cell-permeable PKMζ inhibitor, injected in the rat hippocampus, both reverses LTP maintenance in vivo and produces persistent loss of 1-day-old spatial information. Thus, the mechanism maintaining LTP sustains spatial memory.

The hippocampus encodes and initially stores experience-dependent spatial information (*1*, *2*). The physiological substrate of information storage in the hippocampus has been proposed to involve LTP, an activity-dependent, persistent increase in synaptic transmission (*3*–*8*). One approach to testing the role of LTP in behavior has been to inhibit the molecular mechanisms mediating plasticity. These mechanisms can be divided into two phases: induction, triggering the synaptic potentiation, and maintenance, sustaining the potentiation over time. The formation of long-term spatial memory can be prevented by inhibitors of molecules critical for inducing LTP, such as the *N*-methyl-D-aspartate receptor (NMDAR), protein kinases including Ca^{2+}/calmodulin–dependent protein kinase II (CaMKII), adenosine 3′,5′-monophosphate (cAMP)–dependent protein kinase (PKA), and conventional/novel isoforms of protein kinase C (c/nPKCs), as well as many other signaling molecules (*4*, *8*). These findings, however, do not distinguish between learning, the initial consolidation into long-term memory, and the persistence of memory storage; thus, they do not directly address the fundamental question of the role of LTP maintenance in the perpetuation of spatial information in the hippocampus. Addressing this question requires testing the hypothesis that inhibition of molecules maintaining LTP causes retrograde loss of information (*4*). This "maintenance hypothesis" has not been testable because inhibitors of NMDARs, CaMKII, PKA, or c/nPKC do not reverse late LTP maintenance (*9*). Indeed, NMDAR antagonists have been found to block the initial encoding, but not the maintenance, of memory (*10*). Thus, no agent specifically reversing established late LTP, critical for testing the maintenance hypothesis, has previously been available (*11*).

However, an unusual, persistently active kinase—the brain-specific, atypical PKC isoform, protein kinase Mzeta (PKMζ), is both necessary and sufficient for LTP maintenance (*9*, *11*–*14*). PKMζ introduced into CA1 pyramidal cells in hippocampal slices strongly potentiates postsynaptic α-amino-3-hydroxy-5-methylisoxazole-4-propionate receptor (AMPAR) responses (*9*, *14*), whereas inhibition of PKMζ reverses established LTP (*9*, *11*, *13*). PKMζ can be inactivated by applications of a cell-permeable synthetic peptide derived from the structure of the full-length PKCζ isoform (Fig. 1A, left) (*9*, *11*, *13*). This myristoylated ζ-pseudosubstrate inhibitory peptide (ZIP) potently and selectively inhibits PKMζ by reconstituting the autoinhibition of the absent PKCζ regulatory domain (Fig. 1A, left) (*9*, *11*, *13*). Bath application of ZIP to hippocampal slices both inhibits the synaptic potentiation produced by intracellular perfusion of PKMζ (*11*) and reverses established late LTP, without reversing early LTP or affecting baseline, nontetanized synaptic transmission (*9*, *11*, *13*). Thus, ZIP is the first tool available to test the maintenance hypothesis. Therefore, we addressed two related questions: Can PKMζ inhibition by ZIP reverse the late phase of LTP in vivo? And if so, does ZIP cause retrograde loss of spatial memory?

We stimulated the perforant path in the angular bundle and recorded stable responses of the field excitatory postsynaptic potential (fEPSP) slope (Fig. 1, A to D) and population spike (PS) amplitude (Fig. 1, E and F, and fig. S1) in the subgranular layer of the dentate gyrus (*15*). We then tetanized with high-frequency stimulation (HFS), using a protocol optimized for inducing strong 24-hour LTP (*16*, *17*). Twenty-two hours after the tetanization, intrahippocampal injection of ZIP (10 nmol in 1 μl saline) rapidly reversed the persistent potentiation of fEPSP slope (Fig. 1, A, right; and C; $P < 0.01$ between baseline and preinjection responses; $P < 0.01$ between preinjection and 2 hours postinjection; and $P = 0.55$ between baseline and postinjection) and PS amplitude (Fig. 1E and fig. S1). In interleaved experiments, saline injections had no effect on potentiation (Fig. 1B; $P = 0.71$ between responses preinjection and 2 hours postinjection). Two-way ANOVA confirmed that the effect of ZIP on potentiated responses was different from the effect of saline [interaction $F(2,18) = 10.3$; $P < 0.001$]. Confirming prior work in hippocampal slices (*9*, *11*, *13*), ZIP had minimal effects on baseline evoked responses (Fig. 1D; $P = 0.91$ between responses preinjection and 2 hours postinjection), which indicated that the circuitry of the hippocampus remains intact after ZIP injections. ZIP also had no effect on baseline synaptic responses when applied after 22 hours of recording, the same time as in our LTP experiments (fig. S2).

For LTP saturation to block hippocampus-dependent learning and memory retrieval, the proportion of stimulated synapses must be optimized (*6*, *7*), which indicates that the synaptic changes that might encode spatial information are widely distributed in the hippocampus (*18*, *19*). To determine the spatial extent of LTP reversal by ZIP within the hippocampus, we recorded LTP at multiple populations of neurons with an array of four recording electrodes, spaced at 0.5-mm intervals from the injection site in CA3 (Fig. 1F, top left). ZIP injection reversed LTP recorded at all four electrodes (Fig. 1E). Immunocytochemistry after injections of 10 nmol biotin-labeled ZIP showed the agent extended both transversely (Fig. 1F, bottom) and 3 to 4 mm longitudinally within the hippocampus, without diffusing substantially into other brain regions except along the cannula track (Fig. 1F, top right).

We next examined active place avoidance, a spatial behavior with the experimental advantages of rapid hippocampus-dependent acquisition and persistent hippocampus-dependent recall (*20*, *21*), which parallels the time course of LTP. The apparatus for the task consists of a slowly rotating platform, open to the room environment, within which a nonrotating 60° sector is a shock zone (Fig. 2A, top; and Supporting Online Material, movie S1). The rotation brings the animal into the shock zone, and the animal rapidly learns to avoid the shock by actively moving to the nonshock areas of the environment. After an initial 10-min exposure to the apparatus without shock (pretraining, Fig. 2A, bottom; 2B, left; C; and D; and movie S1, scene 1), rats were trained in eight 10-min sessions with the shock on, separated by 10-min rest intervals in their home cages (Fig. 2B, middle; and C; and movie S1, scene 2). The animals were tested 24 hours later. Retention of long-term stored spatial information can be measured by the increase in time between the

Departments of Physiology, Pharmacology, and Neurology, The Robert F. Furchgott Center for Neural and Behavioral Science, SUNY Downstate Medical Center, 450 Clarkson Avenue, Brooklyn, NY 11203, USA.

*These authors contributed equally to this work.
†To whom correspondence should be addressed. E-mail: afenton@downstate.edu (A.A.F.); tsacktor@downstate.edu (T.C.S.)

placement of the animal into the apparatus and the initial entry into the shock zone (which slowly accrues during training). In addition, the retention of both short-term and long-term stored information can be tested by the decrease in time spent in the shock zone (which is expressed rapidly after a single training session).

If persistent PKMζ activity is necessary for spatial long-term memory storage, then inhibiting the kinase's activity a day after learning will cause retrograde amnesia. Twenty-two hours after the last training session, we injected either ZIP or saline into both hippocampi. Two hours later, long-term retention was tested on the apparatus without shock (i.e., extinction testing). The saline-injected animals demonstrated long-term spatial information storage by avoiding initial entry into the shock zone (Fig. 2B, above right; C, open circles; and movie S1, scene 3) and spending less time in the shock zone (Fig. 2D). In contrast, the ZIP-injected animals failed to demonstrate spatial information storage by not avoiding entry into the shock zone, actively exploring the entire apparatus as if naïve (Fig. 2B, below right; C, solid circles; and movie S1, scene 4; $P < 0.02$, ZIP compared with saline; $P = 0.13$, pretraining compared with retention after ZIP), and by spending time in the shock zone close to the level of chance (Fig. 2D).

We examined whether PKMζ inhibition disrupted recently acquired, as well as persistently stored, spatial information by taking advantage of the rapid learning measured by time spent in the shock zone. Immediately after testing long-term memory (LTM) retention, we reconditioned the animals with a single training trial and then retested without the shock (Fig. 2A, bottom, and D), to determine short-term memory (STM) retention by the decrease in time in the shock zone. Although the ZIP-injected animals showed near complete loss of LTM, the same animals could nonetheless recall the STM of the conditioned response (Fig. 2D; for ZIP, $P = 0.72$ between pretraining and LTM, and $P < 0.05$ between LTM and STM; for saline, $P < 0.01$ between pretraining and LTM, and between LTM and STM; $P < 0.05$ between ZIP and saline for LTM). ZIP also had no effect on STM without prior LTM training (fig. S3).

We determined the specificity of the effect of PKMζ inactivation on long-term memory retention. We first tested whether the loss of long-

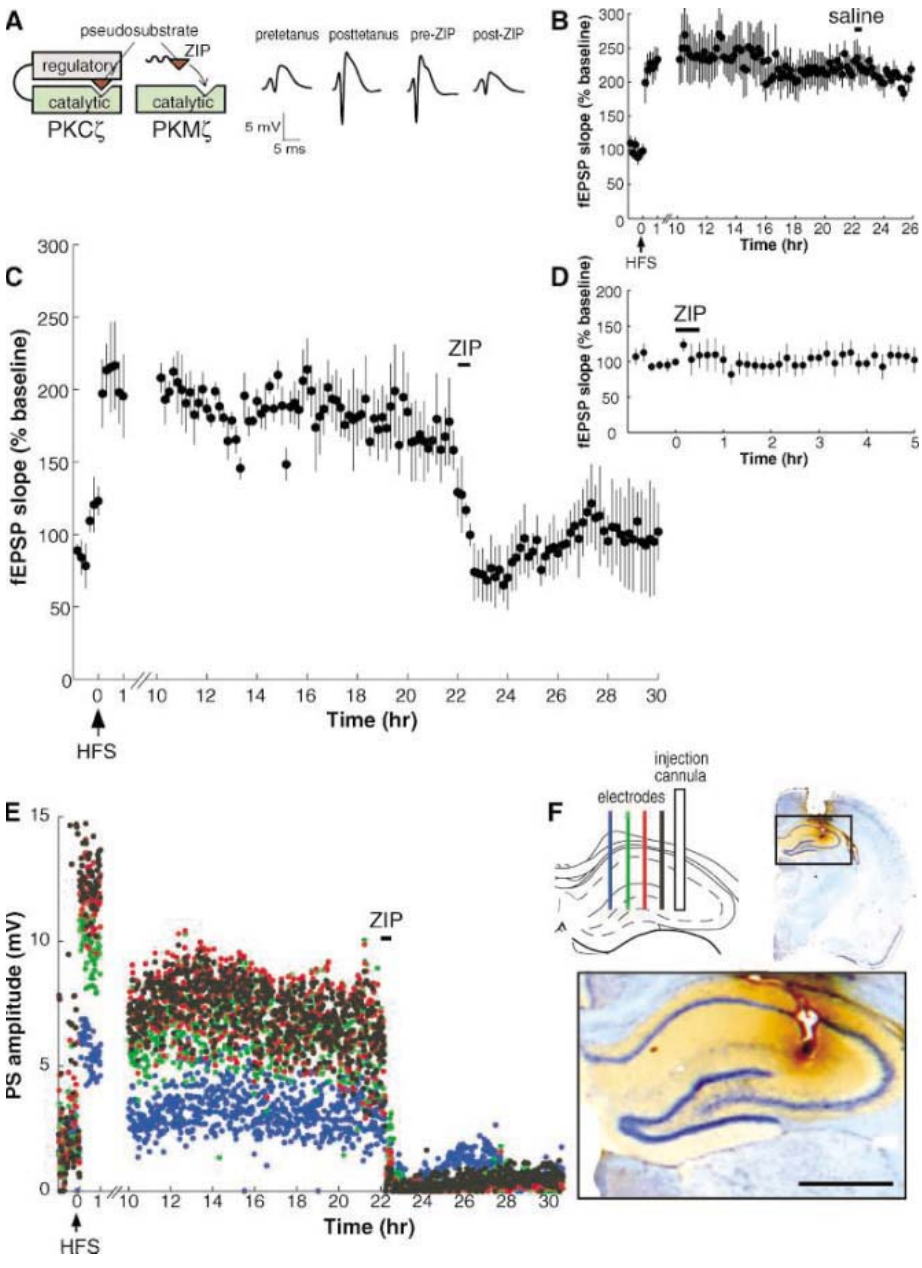

Fig. 1. PKMζ inhibition reverses the maintenance of late-phase LTP in vivo. (**A** to **D**) After recording stable baseline fEPSP responses for at least 1 hour, HFS inducing LTP was delivered. ZIP injection (10 nmol in 1 μl saline) 22 hours posttetanization reverses the persistent potentiation of fEPSP responses. (A, left) Schematic representation of PKCζ in its basal inactive state (left) and PKMζ (right), inhibited by ZIP. PKCζ consists of a catalytic domain (green) and a regulatory domain (gray). The regulatory domain contains a pseudosubstrate sequence (red triangle), which maintains the catalytic domain in an inactive state, until stimulated by second messengers. PKMζ, in contrast, is the independent catalytic domain of PKCζ, produced from a PKMζ mRNA (*27*, *28*), and, lacking a regulatory domain, is autonomously active. ZIP, consisting of the ζ pseudosubstrate sequence with a myristoyl moiety (wavy line) allowing for cell permeability, blocks the constitutive activity of PKMζ by reconstituting the inhibition of the missing regulatory domain. (A, right) Representative traces recorded 30 min pretetanus, 30 min posttetanus, ~2 hours pre-ZIP, and ~2 hours post-ZIP injection. (B) Saline injections 22 hours posttetanization have no effect on potentiation. (C) ZIP injections reverse potentiated responses to pretetanus levels. (D) ZIP injections have minimal effect on baseline responses. Means ± SEM; four rats were used in each experiment. (**E** and **F**) Representative PS amplitudes from four electrodes placed at 0.5-mm intervals from the cannula show ZIP reverses LTP up to 2 mm away from the injection site. (F, top left) Color-coded placement of electrodes and cannula. (F, top right) Immunocytochemistry 2 hours after injection of 10 nmol biotin-labeled ZIP shows the diffusion of the drug (brown) is largely restricted to the hippocampus. (F, bottom) The extent of drug diffusion within the hippocampus. Counterstain is cresyl violet; scale bar represents 4.7 mm (above right) and 1 mm (bottom).

term memory by ZIP was due to the agent's inhibitory effect on PKMζ activity by comparing ZIP with an inactive scrambled version of the myristoylated ZIP peptide (*11*, *13*). Whereas ZIP again disrupted long-term memory retention, the scrambled peptide did not (Fig. 3A; $P = 0.74$ between scrambled ZIP and saline; $P < 0.05$ between scrambled ZIP/saline and ZIP). We then examined the effect of staurosporine, a potent inhibitor of c/nPKC isoforms as well as other kinases, but an ineffective inhibitor of PKMζ (*9*). [Staurosporine blocks LTP induction but does not reverse LTP maintenance (*9*).] Although staurosporine is 10 times as potent in inhibition of the other PKC isoforms, CaMKII, and PKA than ZIP is on PKMζ (*9*), the general kinase inhibitor, injected at the same dose as we had injected ZIP, did not cause retrograde amnesia (Fig. 3B; $P = 0.56$ between staurosporine and vehicle). When injected before training, however, this staurosporine dose abolished place-avoidance learning [Fig. 3B, inset; $P < 0.01$, $F(1,7) = 15.2$ between staurosporine and vehicle; $P < 0.02$ for 24-hour retention].

PKMζ inactivation may disrupt information storage, in which case the effect of ZIP would be persistent, or information retrieval, in which case the effect would be transient. Because the delayed entrance into the shock zone is weakly expressed 1 week after the eight-trial training, we tested the decrease in number of entrances with the shock on, which is strongly retained for 1 week. Twenty-two hours after initial training, animals were injected with ZIP or saline and then returned to their home cages without testing (Fig. 3C, left). One week later, the saline-injected animals demonstrated spatial information storage by avoiding the shock zone (Fig. 3C, right; $P < 0.05$ between training trial 1 and retention at 1 week). In contrast, the animals that had been injected with ZIP showed no evidence of spatial information storage ($P = 0.26$ between training trial 1 and retention at 1 week; $P < 0.01$ between ZIP and saline at 1 week retention). In parallel experiments, no staining of biotin-labeled ZIP was detected in the hippocampus 1 week after its injection, which indicated elimination of the drug.

Immediately after testing the persistent loss of information, we examined whether ZIP persistently disrupted the ability to encode and store new long-term spatial information (Fig. 3C, right). The animals injected with ZIP or saline 1 week earlier showed equivalent performance during retraining from trial 3 onward and equivalent retention 24 hours later [$P = 0.92$ measured by time to first entry on extinction testing (Fig. 3C, inset), and $P = 0.86$ for number of entrances when the shock was turned back on]. Thus, although ZIP caused a persistent loss of previously stored information, once the agent was eliminated, it did not persistently impair relearning or long-term storage of newly acquired information. After the rats were killed, cellular staining with cresyl violet showed the structure of the hippocampi in the ZIP-injected animals was normal (fig. S4).

Finally, we tested whether PKMζ inhibition affected spatial memory that was more than 1 day old. Rats trained with two eight-trial sessions separated by 1 week retained spatial information for 30 days. Injections of ZIP 2 hours before testing abolished the retention of 1-month-old spatial memory (fig. S5).

PKMζ inactivation tested the maintenance hypothesis of LTP and showed that the persistence of synaptic potentiation and the persistence of spatial memory share a common molecular mechanism. PKMζ inhibition specifically disrupted the long-term retention of information because the ability to relearn, recall, and express the conditioned avoidance as a short-term memory was spared. This confirms and extends previous work on associative odor conditioning in *Drosophila*, in which inhibition of the fly PKMζ homolog prevented the formation of persistent, but not short-term, memory (*22*). Furthermore, we showed that the disruption of long-term retention was an effect on information storage, rather than retrieval, because the loss

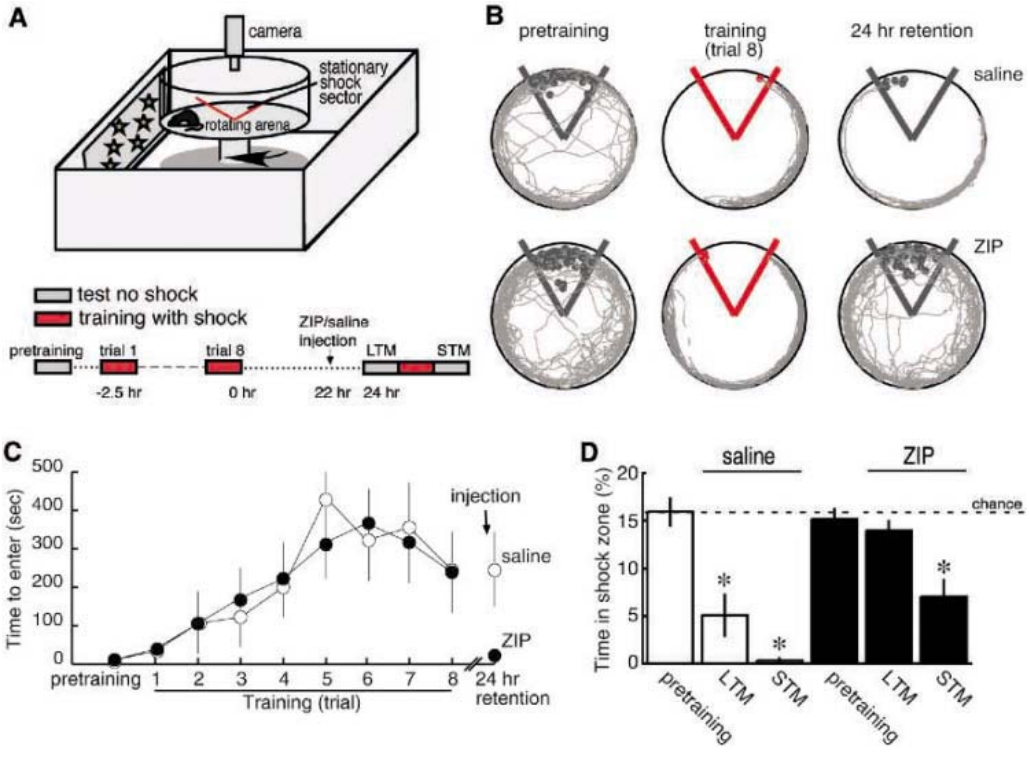

Fig. 2. PKMζ inhibition abolishes long-term retention of spatial information. (**A**) Above, the place avoidance training apparatus consists of a slowly rotating arena, within which a nonrotating 60° sector (delineated in red) is a shock zone. Visual cues are located on the walls of the room. Below, schematic of protocol for measuring effect of ZIP or saline on retention of place avoidance long-term memory (LTM) and short-term memory (STM). (**B**) Paths of individual animals in the apparatus during 10-min sessions. (Left) On first exposure during pretraining, the naïve animals explore the apparatus. Gray circles show locations where animals would have received shocks (delivered every 1.5 s) if the shock had been on. (Middle) By training trial 8, both animals show active place avoidance. Red circles show location of shocks. (Right) Retention testing 24 hours after training trial 8 (2 hours after bilateral intrahippocampal injections of saline or 10 nmol ZIP). The saline-injected animal (above) shows long-term memory retention; the ZIP-injected animal (below) explores the apparatus as if naïve. Gray circles show locations where animals would have received shocks if the shock had been on. (**C**) The time to the initial entrance into the shock zone during pretraining, training, and 24-hour retention testing sessions shows saline-injected animals (open circles) with place avoidance memory, and ZIP-injected animals with near complete loss of long-term stored information (solid circles) (means ± SEM of eight experiments). (**D**) The decrease of time spent in the shock zone demonstrates both long-term memory retention and further short-term memory retention in saline-injected animals. ZIP-injected animals show loss of long-term memory retention, but sparing of short-term memory retention. Dashed line represents time spent in shock zone if exploring the apparatus randomly. Six rats were used for each group.

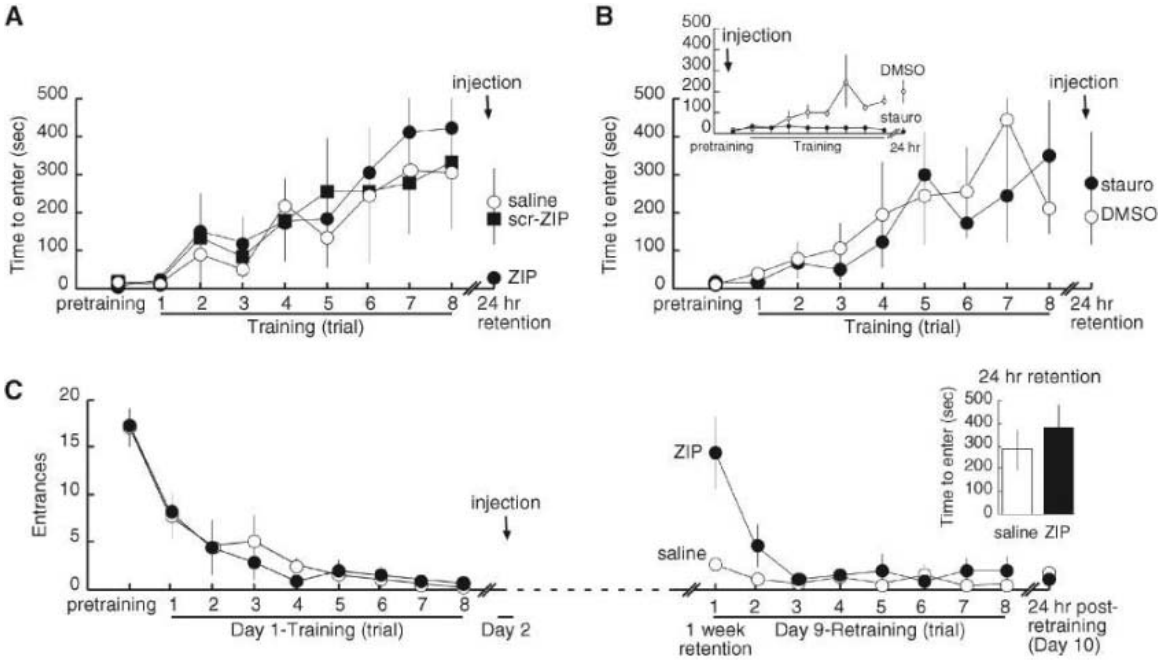

Fig. 3. Inhibition of PKMζ, but not other protein kinases, disrupts memory storage. (**A**) Animals show normal memory retention after injection of 10 nmol inactive scrambled ZIP (scr-ZIP). Five rats were used for each group. (**B**) Injections of 10 nmol staurosporine in 50% dimethylsulfoxide (DMSO) (stauro) does not affect long-term memory storage, compared with 50% DMSO alone. (Inset) Staurosporine (10 nmol) injected 20 min before training blocks place avoidance learning. Four rats were used for each group. (**C**) PKMζ inhibition disrupts memory storage. (Left) Twenty-two hours after training, ZIP or saline is injected without testing. (Right) One week later, ZIP-injected animals show no spatial information retention as measured by number of entrances into the shock zone, whereas saline-injected animals show place avoidance. Immediate retraining of ZIP-injected animals leads to normal acquisition and 24-hour recall of place avoidance, as measured first by time to initial entry into the shock zone, determined during 10 min with the shock off (inset), and then by the number of entrances during 10 min with the shock on. Six rats were used for each group.

persisted even after the elimination of the PKMζ inhibitor. Newly acquired long-term stored information could then be retained, which demonstrated that prior application of ZIP long before any new encoding did not permanently disrupt memory function. Information storage was specifically affected by PKMζ inhibition because staurosporine, a potent, broad-spectrum kinase inhibitor of CaMKII, PKA, and c/nPKCs, but not PKMζ, did not disrupt the long-term retention of stored information, whereas it strongly prevented the acquisition of new information.

The ability of ZIP to eliminate long-term stored information, while leaving recently acquired information intact, correlates well with the agent's ability to reverse late LTP, without disrupting the functional integrity of the hippocampal circuitry (Fig. 1D and fig. S2) or early LTP (*11*, *13*). PKMζ inhibition by ZIP thus contrasts with inactivation of the hippocampal circuit by tetrodotoxin, which disrupts learning and both short-term and long-term recall of place avoidance (*20*, *21*). In addition, the effect of hippocampal inactivation by tetrodotoxin is only transient and, thus, is on information retrieval (*21*, *23*), whereas the loss of long-term retention by ZIP is persistent and, thus, is on information storage. The minimal effect of ZIP on baseline synaptic transmission in the hippocampus suggests that information stored by PKMζ-mediated potentiation may have been sparsely encoded by a few synapses (*6*, *7*).

The ability of PKMζ inhibition to erase memory storage is distinct from an effect on memory reconsolidation. In reconsolidation studies, the combination of the injection of agents such as protein synthesis inhibitors and the reactivation of a memory from long-term stores results in a delayed loss of the memory observable on the following day (*24*, *25*). Here, ZIP produces rapid long-term memory loss detectable shortly after the agent's injection and within seconds of placing the animals into the test apparatus (Fig. 2C). Indeed, ZIP disrupts long-term memory retention without any retrieval close in time to the agent's injection (Fig. 3C). Thus, the persistent activity of PKMζ maintains the spatial memory trace. These findings may be pertinent to disorders of memory storage (*26*).

References and Notes

1. W. B. Scoville, B. Milner, *J. Neurol. Neurosurg. Psychiatry* **20**, 11 (1957).
2. J. O'Keefe, L. Nadel, *The Hippocampus as a Cognitive Map* (Clarendon Press, Oxford, 1978).
3. T. V. P. Bliss, T. Lomo, *J. Physiol.* **232**, 331 (1973).
4. S. J. Martin, P. D. Grimwood, R. G. Morris, *Annu. Rev. Neurosci.* **23**, 649 (2000).
5. O. Paulsen, R. G. Morris, *Nat. Neurosci.* **5**, 289 (2002).
6. V. H. Brun, K. Ytterbo, R. G. Morris, M. B. Moser, E. I. Moser, *J. Neurosci.* **21**, 356 (2001).
7. E. I. Moser, K. A. Krobert, M. B. Moser, R. G. Morris, *Science* **281**, 2038 (1998).
8. J. R. Sanes, J. W. Lichtman, *Nat. Neurosci.* **2**, 597 (1999).
9. D. S. Ling *et al.*, *Nat. Neurosci.* **5**, 295 (2002).
10. M. Day, R. Langston, R. G. Morris, *Nature* **424**, 205 (2003).
11. P. Serrano, Y. Yao, T. C. Sacktor, *J. Neurosci.* **25**, 1979 (2005).
12. T. C. Sacktor *et al.*, *Proc. Natl. Acad. Sci. U.S.A.* **90**, 8342 (1993).
13. S. Sajikumar, S. Navakkode, T. C. Sacktor, J. U. Frey, *J. Neurosci.* **25**, 5750 (2005).
14. D. S. Ling, L. S. Benardo, T. C. Sacktor, *Hippocampus* **16**, 443 (2006).
15. Materials and methods are available as supporting material on *Science* Online.
16. S. Frey, J. Bergado-Rosado, T. Seidenbecher, H. C. Pape, J. U. Frey, *J. Neurosci.* **21**, 3697 (2001).
17. T. Ahmed, S. Frey, J. U. Frey, *Neuroscience* **124**, 857 (2004).
18. M. B. Moser, E. I. Moser, *J. Neurosci.* **18**, 7535 (1998).
19. S. Kubik, A. A. Fenton, *J. Neurosci.* **25**, 9205 (2005).
20. J. M. Cimadevilla, A. A. Fenton, J. Bures, *Neurosci. Lett.* **285**, 53 (2000).
21. J. M. Cimadevilla, M. Wesierska, A. A. Fenton, J. Bures, *Proc. Natl. Acad. Sci. U.S.A.* **98**, 3531 (2001).
22. E. A. Drier *et al.*, *Nat. Neurosci.* **5**, 316 (2002).
23. K. Jezek, M. Wesierska, A. A. Fenton, *Physiol. Res.* **51**, (Suppl 1), S35 (2002).
24. K. Nader, G. E. Schafe, J. E. Le Doux, *Nature* **406**, 722 (2000).
25. C. M. Alberini, *Trends Neurosci.* **28**, 51 (2005).
26. J. F. Crary, C. Y. Shao, S. S. Mirra, A. I. Hernandez, T. C. Sacktor, *J. Neuropathol. Exp. Neurol.* **65**, 319 (2006).
27. A. I. Hernandez *et al.*, *J. Biol. Chem.* **278**, 40305 (2003).
28. I. A. Muslimov *et al.*, *J. Biol. Chem.* **279**, 52613 (2004).

29. Supported by NIH R01 MH53576 and MH57068 (T.C.S.) and Dean's Research Investment Initiative (A.A.F.). We thank the late James H. Schwartz for helpful comments on the manuscript and advice.

Supporting Online Material

www.sciencemag.org/cgi/content/full/313/5790/1141/DC1
Materials and Methods
Figs. S1 to S5
References
Movie S1

12 April 2006; accepted 30 June 2006
10.1126/science.1128657

Human Validated Kinase siRNA Set

The small-interfering RNAs (siRNAs) in the Human Validated Kinase siRNA Set V1.0 have been experimentally verified by stringent real-time reverse transcription–polymerase chain reaction analysis to provide at least 70% target knockdown. RNA interference screening with this set eliminates the possibility of false-negative results and gives the researcher the confidence that the maximum number of positive hits has been achieved. The set is available in a range of formats. It is available in scales of 100 pmol, 0.25 nmol, and 1 nmol, and subsets for tyrosine kinases and serine/threonine kinases are available.
Qiagen For information 800-426-8157 www.qiagen.com

Disposable Shaker Flasks

The Nalgene 2.8L Sterile Disposable Shaker Flask provides the lightweight and economical features of the Nalgene Erlenmeyer flasks in a larger volume. Designed to reduce the risk of cross-contamination, the flasks are suitable for shaker and suspension cell culture, media preparation, and media storage. Made of optically clear, polyethylene terephthalate copolyester (PETG), the flasks molded-in graduations enable quick volume assessment. Users can specify a plain flask bottom for benchtop use or a baffled bottom for use on a shaker table. The flasks are available with leak-proof standard or vented closures.
Nalge Nunc International Corp
For information 800-899-7261
www.nalgenelabware.com

Mammalian Protease Inhibitor

Mammalian ProteaseArrest is a mammalian specific protease inhibitor cocktail, comprised of agents to inhibit serine, cysteine, and mammalian specific proteases, including aminopeptidases, aspartic, cysteine, and trypsin-like proteases. Mammalian ProteaseArrest contains both irreversible and reversible protease inhibitors. An optional EDTA solution is available for enhanced inhibition of metalloproteases.
G-Biosciences/Genotech For information 800-628-7730 www.GBiosciences.com

Automated ImmunoGold Labeling

The automated Leica EM ImmunoGold Labeling (IGL) system is designed to address the needs of researchers who want to localize a wide range of cellular molecules. Preparing tissue and cell samples accurately is essential for optimum transmission electron microscopy (TEM) image quality. The current immunogold labeling methods involve many time-consuming steps that employ complicated manual procedures. The automated IGL system eliminates the need for tedious manual labeling of grids and greatly improves reproducibility of results. The innovative system automatically applies reagents to ultra-thin sections, held on grids in a humidity-controlled environment. Twenty-four grids and 24 antibodies can be processed using one of 99 preset programs.
Leica Microsystems For information 800-248-0123 www.leica-microsystems.us

Electrochemical Array Detector

Version 3.0 application software is designed to increase the effectiveness of the sensitive and selective CoulArray high performance liquid chromatography (HPLC) electrochemical array detector. The new software features single window interface operating controls and enables the detector to effectively handle (<5 min) gradient conditions when higher throughput LC assays require many samples to be processed in a short period of time. The software comes with complete security features, audit trails, electronic signatures, and data traceability. The CoulArray is a state-of-the-art electrochemical detection system for demanding clinical, life science, and pharmaceutical applications. The new software enables the CoulArray to be used more effectively and efficiently in a wide range of fields, especially in pharmaceutical discovery and development.
ESA Biosciences For information +44 1844-239381 www.esainc.com

High-Speed Genotyping Service

A rapid-turnaround mouse genotyping service provides online reporting of genotyping results in as little as 24 hours, giving researchers timely test results and freeing lab staff to perform more productive duties. The service can help biotech and medical researchers working with transgenic, knockout/knockin, transgenic with knockout, or targeted mutagenesis mouse lines. In addition to in-depth sequence identification, the system can also provide positive/negative information on the zygosity of submitted samples. The process is simple. The customer preps and sends a tail-sample using special materials and a pre-printed shipping label supplied by TransnetYX. TransnetYX isolates the DNA and measures it for purity and quality, then screens the sample for the presence of the gene sequence of interest. The customer can then view the results at a secure website. The secret behind the rapid turnaround is a fully automated genotyping system that separates DNA using a unique process that avoids noxious chemicals while providing consistent and pure DNA yields.
TransnetYX For information 888-321-2113
www.transnetyx.com

Newly offered instrumentation, apparatus, and laboratory materials of interest to researchers in all disciplines in academic, industrial, and government organizations are featured in this space. Emphasis is given to purpose, chief characteristics, and availability of products and materials. Endorsement by *Science* or AAAS of any products or materials mentioned is not implied. Additional information may be obtained from the manufacturer or supplier by visiting www.science.labvelocity.com on the Web, where you can request that the information be sent to you by e-mail, fax, mail, or telephone.

POSITIONS OPEN

DEVELOPMENTAL BIOLOGISTS ASSOCIATE PROFESSOR and ASSISTANT PROFESSOR
University of Nevada, Reno

The Biology Department at the University of Nevada, Reno (UNR), seeks two **DEVELOPMENTAL BIOLOGISTS** (one Associate Professor and one Assistant Professor) for tenure-track positions to start July 2007. The Biology Department has targeted developmental biology as a strategic area for growth. We seek one highly successful mid-career scientist whose research complements our current group of four Developmental Biologists, who has a strong track record of securing competitive extramural funding, and who is interested in helping provide leadership to our growing developmental biology group. We also seek an outstanding Assistant Professor with research interests that are either in developmental biology or that complement the Department's existing strengths in developmental biology. The successful candidates will be provided with competitive startup packages and will be expected to maintain nationally recognized, extramurally funded research programs. The Department **(website: http://www.unr.edu/biology/)** has about 640 majors, 23 state-funded faculty, and averaged $4.7 million of extramural awards annually over the last two years. UNR has outstanding core facilities for genomic, proteomic, and bioinformatics research. Reno, Nevada sits on the eastern flank of the Sierra Nevada range and was recently rated one of the best small cities in the United States for overall quality of life. For complete position announcement and requirements, visit **website: http://jobs.unr.edu.** Applicants should submit curriculum vitae, statement of research plans, and a statement of teaching philosophy electronically at **website: http://www.unrsearch.com** and three letters of recommendation to: **Lucy Morris, Search Coordinator, Developmental Biologist Search, Department of Biology/314, University of Nevada, Reno, NV 89557.** Please specify the position for which you are applying. Applications received by October 15, 2006, will receive full consideration.

Equal Employment Opportunity/Affirmative Action. Women and underrepresented groups are encouraged to apply.

TWO TENURE-TRACK VIROLOGY POSITIONS

The Biomedical Sciences and Pathobiology Department of the Virginia-Maryland Regional College of Veterinary Medicine **(website: http://www.vetmed.vt.edu/Organization/Departments/DBSP/index.asp)** invites applications for two tenure-track faculty positions (rank open) in the area of viral pathogenesis and replication as part of an interdisciplinary program focused on emerging and re-emerging infectious diseases. See further information and submit applications via the Virginia Tech **website: http://https://jobs.vt.edu,** using posting number 183918. Fill out the application form and upload: cover letter, curriculum vitae, contact information for three references, and statement of research goals. Review begins August 1, 2006, but positions are open until filled. *Virginia Tech is an Equal Opportunity/Affirmative Action Employer.*

FACULTY POSITION
Institute of Molecular and Cellular Biology
National Taiwan University

The Institute is seeking an outstanding individual to fill a full-time faculty position available on August 1, 2007. The level of appointment is open. The specific research area should be related to molecular and/or cellular biology. Candidates must have a Ph.D. degree and have a postdoctoral experience. Preference will be given to individuals who submit curriculum vitae, a brief statement of research and teaching course(s), and three recommendation letters prior to December 31, 2006, to: **Chair, Faculty Search Committee, Institute of Molecular and Cellular Biology, National Taiwan University, Number 1, Section 4, Roosevelt Road, Taipei, Taiwan 10617. Website: http://cell.lifescience.ntu.edu.tw/english/index.htm.**

POSITIONS OPEN

FACULTY POSITIONS, BIOLOGY PROGRAM
Bard College

The Biology Program at Bard College is seeking applicants for two tenure-track faculty positions beginning September 2007 (rank commensurate with experience). These positions are part of an expansion of the faculty coinciding with the completion of the Gabrielle H. Reem and Herbert J. Kayden Center for Science and Computation in the spring of 2007. The successful candidates will possess a Ph.D., be committed to excellence in undergraduate education, and maintain an active research program involving undergraduates. Although the fields of interest are open, special consideration for one of the positions will be given to candidates who have a significant quantitative or computational component to their research and who will teach our required biostatistics course. Preference for the second position will be given to candidates interested in participating in the teaching of microbiology, molecular biology, or physiology. Successful candidates will be those who share the Program's commitment to increasing opportunities for student research and with research interests that complement those of the current faculty. More information about the curriculum and current faculty research can be found at **website: http://biology.bard.edu.** It is also expected that the successful candidates will participate in the introductory offerings within the Department.

Bard is a private liberal arts college with approximately 1,500 students, located 90 miles north of New York City on the Hudson River. Applicants should submit curriculum vitae, research and teaching statements, and three letters of reference to: **Michael Tibbetts, c/o Human Resources-5806, Bard College, 30 Campus Road, Annandale-on-Hudson, NY 12504-5000.** Review of applications will begin September 15, 2006, and will continue until the positions are filled. *We seek to attract and retain a highly qualified and diverse faculty. Affirmative Action/Equal Opportunity Employer.*

LUTHER COLLEGE. Applicants are invited for a tenure-track position in quantitative biology at the **ASSISTANT PROFESSOR** level. Ph.D. is required; postdoctoral experience preferred. Teaching responsibilities include participation in a team-taught principles of biology course, and courses in at least two of the following areas: biostatistics, computational biology, evolutionary biology, or a field area (such as aquatics or plant biology) using a quantitative approach. The successful candidate will be expected to involve undergraduate students in research and to seek external research funding. Additional information is at **website: http://biology.luther.edu.**

All correspondence, including letter of application, curriculum vitae, three letters of recommendation, statements of teaching and research interests, and official transcripts of undergraduate and graduate work should be sent to: **Dr. Marian Kaehler, Head, Department of Biology, Luther College, 700 College Drive, Decorah, IA 52101-1045, fax: 563-387-1080, e-mail: kaehlerm@luther.edu.** Review of applications will begin on 1 October 2006.

YALE UNIVERSITY
Department of Chemistry

The Department of Chemistry, Yale University, invites applications for positions at the **ASSISTANT PROFESSOR** level to commence July 1, 2007. We seek creative teacher-scholars who show promise for developing outstanding research programs in each of the following areas: biophysical chemistry, chemical biology, and inorganic chemistry. Applicants should send their curriculum vitae and a statement of research plans and arrange for the submission of three letters of recommendation. All materials should be received by October 15, 2006. Send applications to: **Chair, Junior Faculty Search Committee, P.O. Box 208107, Yale University, New Haven, CT 06520-8107.** *Yale University is an Equal Opportunity/Affirmative Action Employer and applications from women and underrepresented minority group members are especially encouraged.*

Careers & Graduate Programs for B.S. & M.S. Scientists

Getting the Most from a Degree

By doing some homework ahead of time, it's possible to select a career-oriented Bachelor's or Master's degree. In fact, some of today's professional Master's programs aim specifically at giving students experience in research labs or companies. In this article, experts from academia, industry, and government give advice for training and grabbing the best position. BY MIKE MAY

In a world of specialization, scientists can benefit from aiming at a specific expertise. Now more than ever, that targeting applies to Bachelor's and Master's programs. Scientists can find specialized degrees in many fields that open doors to exciting career paths. According to Ginger L. Gregory, head of human resources at Novartis Institutes for BioMedical Research, "We have B.S.- and M.S.-level positions across all of the disease areas we research, especially for scientists working at the bench." She adds, "Within both biology and chemistry, we are employing scientists in many exciting positions." That access to jobs exists in many fields, as the following report reveals.

In terms of degrees, some of the experts interviewed here focus on the new family of professional Master's degrees. For example, Suzanne Ortega, vice provost and dean of the graduate school at the University of Washington, says, "First of all, I'd do homework on professional science Master's programs." According the professional science Master's website (http://www.sciencemasters.com), the Alfred P. Sloan Foundation participated in launching such degrees at 45 institutions, and each program works with industry. "These programs are pretty exciting," Ortega says, "and they are closely linked to careers through internship experience and projects with corporate and CONTINUED »

CV Therapeutics
http://www.cvt.com

Millennium Pharmaceuticals
http://mlnm.com

Novartis Institutes for BioMedical Research
http://www.nibr.novartis.com

University of British Columbia
http://www.ubc.ca

University of Illinois at Chicago
http://www.uic.edu

University of Massachusetts, Boston
http://www.umb.edu

University of Washington
http://www.washington.edu

U.S. Centers for Disease Control and Prevention
http://www.cdc.gov

Graduate Programs in the Life Sciences at Northeastern

If you are interested in a university with strong graduate programs in the sciences, a commitment to research excellence, outstanding laboratory and classroom facilities, a vibrant campus in Boston, and a reputation for being one of the fastest-rising universities in the nation, then consider Northeastern University. We offer Ph.D. and M.S. programs in biology, pharmaceutical sciences, and chemistry & chemical biology, as well as professional M.S. programs in bioinformatics, biotechnology, and marine biology.

Professional M.S. Programs

Bioinformatics

www.bioinformatics.neu.edu

We are experiencing an unprecedented boom in the biotechnology and pharmaceutical industries as well as an explosion of genomic information that will transform the biomedical sciences and clinical medicine. Our Professional M.S. Program in Bioinformatics and Computational Molecular Biology features an integrated, interdisciplinary curriculum that is designed to prepare students for exciting and challenging careers at the interface of biology, pharmaceutical sciences, and information technology. The program requires 32 semester hours of study and two years to complete on a full-time basis. A six-month internship in a commercial, academic or government laboratory is required. We tailor curricula to each student's strengths.

Contact: Janeen Greene, gradbio@neu.edu.

Biotechnology

www.biotechms.neu.edu

Our Professional M.S. Program in Biotechnology addresses the needs of students seeking industry employment through rigorous interdisciplinary training in biotechnology coupled with an on site corporate, academic, or governmental internship. Courses are offered in the evenings and the program can be taken full time (in two years) or part time. The first year of study consists of core science courses and biotechnology-specific courses with laboratory training in state-of-the-art proteomics and biotechnology techniques including mass spectrometry. In the second year, students select a track in molecular biotechnology, pharmaceutical biotechnology, or engineering biotechnology.

Contact: Cynthia Bainton, gradbiotech@neu.edu.

Marine Biology

www.marinebioms.neu.edu

The Professional Masters Program in Marine Biology provides the advanced skill set needed to pursue an entry- to mid-level career in marine research, or can serve as a springboard into the nation's top Ph.D. programs in marine biology. This 15-month full-time program is offered in conjunction with Northeastern University's Three Seas Program (see www.threeseas.neu.edu for more information about this unique academic experience in marine biology). In addition to completing the Three Seas Program curriculum for graduate credit, students conduct additional coursework, a research project (but not a formal thesis), and a 6-month internship with academic research scientists, state and federal agencies, or private consulting firms. Now in its 23rd year, the Three Seas program has an impressive record: Our alumni routinely gain admission to the top Ph.D. programs in the country, publish quality research, and are leaders in their fields.

Contact: Salvatore Genovese, s.genovese@neu.edu

www.grad.neu.edu

Northeastern University

Higher Learning. Richer Experience.



Ph.D. and M.S. Programs

Biology

www.biology.neu.edu/graduate_programs.html

We invite outstanding candidates to apply to our M.S. and Ph.D. programs. Our faculty's research addresses questions at all levels of biological organization, from the molecular to the community, with four areas of specialty: Cellular & Molecular Biology and Biochemistry; Marine Biotechnology and Ecology; Microbiology and Immunology; and Neurobiology and Behavior. In addition, three or more faculty work together in each of the following focal areas of expertise: Developmental Initiators and Regulators; Drug Discovery; Bioinformatics; Imaging; Neurobiology and Biomechanics of Locomotion; Biology of Extremophiles; and Evolutionary and Community Ecology.

The department consists of 27 full-time faculty, 20 professional research associates and postdoctoral fellows, and approximately 80 graduate students. Internships with local biotechnology companies are available.

Contact: Janeen Greene, gradbio@neu.edu

Chemistry and Chemical Biology

www.chem.neu.edu

Well-qualified candidates are encouraged to apply to the PhD program in the Department of Chemistry and Chemical Biology. Among the 25 faculty members are winners of numerous awards including NSF (CAREER), NIH (MERIT), ACS National awards, and from the Carnegie, Sloan, and Dreyfus research foundations. Specializations include bioanalytical chemistry, bioorganic and medicinal chemistry, biophysical chemistry, biotechnology, proteomics, computational biology, chemical biology, nanomaterials, and electrochemical energy conversion. The department has strong ties within the Boston-area pharmaceutical and biotechnology industries, including the opportunity to participate in a unique Co-op PhD program. We are allied with key research institutes including the Barnett Institute of Chemical and Biological Analysis, the Center for Drug Discovery, and the NSF engineering centers.

Contact: Nancy Weston, chemistry-grad-info@neu.edu

Pharmaceutical Sciences

www.pharmsci.neu.edu

Pharmaceutical science is concerned with the discovery, design, evaluation and use of drugs. Our specializations include pharmacology, pharmaceutics and drug delivery, toxicology (M.S. only), medicinal chemistry (Ph.D. only), and an interdisciplinary option. Students conduct cutting-edge research with faculty in neuropharmacology, tissue engineering, bioanalytical chemistry, cardiovascular targeting, medicinal chemistry and drug discovery, inflammation and immunology, mitochondrial pharmaceutics, nanomedicine/drug delivery, and toxicology. The department houses or shares faculty with outstanding research centers: The Center for Cardiovascular Targeting, Center for Pharmaceutical Biotechnology and Nanomedicine, Environmental Cancer Research Program, Center for Drug Discovery, and the New England Inflammation and Tissue Protection Institute. The Center for Drug Discovery has been recognized by a grant from the National Institute on Drug Abuse for predoctoral and postdoctoral training.

Contact: Robert Schatz, Graduate Program Director, r.schatz@neu.edu.

The Center for Drug Development training grant: Alexandros Makriyannis or John Gatley, a.makriyannis@neu.edu or s.gatley@neu.edu

General Application Information: Visit program websites for detailed application information. The GRE exam is required, and for those applicants whose first language is not English, the TOEFL exam is also required. Graduate teaching or research assistantships for Ph.D. students provide tuition remission and a competitive annual stipend ($24,000-$30,000, depending on the program). Exceptionally qualified MS students may be invited to receive a partial tuition remission.

Careers & Graduate Programs for B.S. & M.S. Scientists


LON KAUFMAN

government employers." She believes that this kind of experience makes a smooth transition from school to a job. "You've already done many of the things that employers expect," Ortega says. That specialization during a degree appeals to several of the experts interviewed for this article. For instance, Curtis Suttle, professor of earth and ocean sciences, microbiology and immunology, and botany, plus associate dean of science at The University of British Columbia, says, "Find an M.S. program that is really geared toward a profession."

Other scientists in academia also mentioned the value of hands-on experience. "All lab skills are very important," says Manickam Sugumaran, professor and chair of the Biology Department at the University of Massachusetts, Boston. Just any laboratory experience, though, will not do. "People with skills in and knowledge of up-to-date techniques have an edge over other candidates," he says. Some industry experts confirm the value of experience when it comes to getting hired. Michelle Salas, senior staffing specialist at Millennium Pharmaceuticals, says, "A prospective employee really stands out with an internship related to industry."

Other skills also make a difference. "At the M.S. level," Sugumaran says, "you should have some leadership qualities or at least be able to work in a group." Working together, though, is not enough. "You should also be able to work independently and take a project to completion," he says.

Careful Selecting

Some in academia, however, do not see the Master's degree as growing. "In some ways," says Lon Kaufman, professor of biological sciences and vice provost for undergraduate affairs at the University of Illinois at Chicago, "the M.S. degree is dying. It takes a lot of academic input and there is not much payoff to an institution." For anyone set on a Master's program, though, Kaufman offers strong advice: "Find a very active one." In particular, he means finding a program with close ties to industry. He says, "Get in a program that integrates with local business and runs internships with organizations. Then, a student gets a practical degree."

The value of an M.S. degree, however, varies from place to place. "In Canada, there is more inherent value perceived in a Master's degree," says Suttle. "Here the Master's degree is a really valuable one in a student's career path in academic or industrial research. It provides an opportunity to move in many different directions."

Before really getting started in a Master's program, a student should spend some time deciding what kind of degree to pursue. Some degrees focus primarily on course work; the more traditional Master's includes research and a thesis; and the newer approach mentioned by Ortega—the professional Master's degree—aims at preparing students for more specific careers, such as bioinformatics, biotechnology, environmental geoscience, forensic chemistry, industrial mathematics, and many other options. "Your educational experience will be completely different depending on which approach you select," says Ortega. "I don't have a huge preference for one over the other," she says, "but people need to be clear about where their greatest interests are and find a program that's a good fit."

Also, Ortega suggests that potential students check out some statistics of a program before entering it. "What proportion of the students who start complete the program with a degree in hand?" She asks. "How long does it usually take to complete the degree?" Those figures give prospective students some feel for how a program works. Also, a student should want to know how well graduates do. Ortega says, "Make sure that you know what proportion of the graduates have jobs within three to six months of completing the program." Then she adds, "If the people running the program can't tell you that, then they're not doing their job."


DENISE KOO

Industrial Opportunities

At Millennium, B.S.- and M.S.-level scientists can earn positions across all areas. Salas says, "We especially hire these types of scientists in R&D." This includes scientists working in analytical development, biology, formulations, medicinal chemistry, and so on. In some cases, a scientist with a Bachelor's or Master's can even advance to a doctoral-level position at Millennium. "It will depend on each person," says Salas, "but over the years—if they put in their equivalent of industry experience—they can get in those positions." She adds, "Our scientists like the lack of a glass ceiling here."

Other companies also use B.S.- and M.S.-level scientists in a wide range of areas. For example, Matt Krause, director of human resources at CV Therapeutics, says, "Our research programs include multiple, cutting-edge cardiovascular product candidates in various stages of clinical trials and preclinical programs, all of which rely heavily on the contributions from our many B.S.- and M.S.-level scientists." He adds, "We have professionals who hold B.S. and M.S. degrees throughout the entire company—from basic science to business development and sales." Currently, CV Therapeutics really wants scientists who have experience with small molecules, especially if it includes expertise with models CONTINUED »

Looking to the Future?

The future is now at UVA

Biomedical Sciences

Graduate Programs

Cell & Developmental Biology
Biomedical Engineering
Molecular Medicine
Microbiology, Immunology & Infectious Diseases
Biochemistry, Molecular Biology & Genetics
Neuroscience
Structural, Computational Biology & Biophysics

www.med.virginia.edu/bims
bims@virginia.edu

Many Training Programs Peer-Reviewed and Funded by NIH

UNIVERSITY of VIRGINIA

University of Virginia is an equal opportunity, affirmative action employer.

Winning 7 out of 12 Life Science Industry Awards in 2006 was a resounding confirmation of our achievements from the scientific community. Forbes named us to their list of America's best biggest companies and Business 2.0 ranked us in the 100 Fastest Growing Tech Companies. And the list of achievements and accolades goes on.

Proud? You bet! Because behind it all you will find our passionate people collaborating closely to devise the next product or service innovation that will generate scientific breakthroughs around the world. The work is challenging, the rewards are exhilarating and the people are inspiring.

At Invitrogen you will find exceptional career opportunities worldwide in a fast-paced collegial environment, where the potential to learn and grow is virtually unlimited. Our labs and offices are infused with entrepreneurial energy. Yet amidst this dynamic atmosphere all Invitrogen employees share a commitment to integrity and hold fast to the belief that in everything they do, they are making a contribution to a better world. We invite you to join our dedicated team as we continue our quest to improve the human condition.

We are proud to be an equal opportunity employer dedicated to hiring a diverse work team.

Opportunities are available in our **Madison, Wisconsin** facility for scientists with a BS or MS degree.

Sr. Associate Scientist

Protein Biochemist with six years of experience and a solid background in enzymes, chromatography and protein purification.
Req. # 06-0588

Associate Scientist III

Scientists with demonstrated competence in protein purification, preferably with expertise in one or more protein classes.
Req. #s 06-0792, 06-0684, 06-0611

Associate Scientist II

Professionals with 2 years of laboratory experience and strong understanding of biochemistry and a background in cell-based assay development. Working knowledge of florescence technologies desired.
Req. #s 06-0582, 06-0610, 06-0650

Apply online at **www.invitrogen.com/careers**.

The Life Science LSIA 2006 Industry Awards
B2 100 Fastest-Growing Tech Companies
Forbes 2006 THE PLATINUM LIST

invitrogen™

Cincinnati Children's Hospital Medical Center

UNIVERSITY OF Cincinnati

www.cincinnatichildrens.org

A Proven Leader in Molecular Medicine

Molecular and Developmental Biology Graduate Program

University of Cincinnati and Cincinnati Children's Research Foundation

- PhD-granting graduate program
- Broad range of research integrating basic research with translational research into disorders and diseases in children, including:
  - Fundamental mechanisms of development
  - Organogenesis
  - Cell signaling and cancer biology
  - Stem cell biology
  - Reproductive biology
  - Gene therapy and human genetics
  - Model organisms including Xenopus, mouse, fly, chicken, and zebrafish
- Outstanding training in one of the world's top children's research hospitals, with state-of-the-art research labs, and more than 60 faculty
- 10-20 new students per year; 50 students total in the program
- Students publish in top journals, including *Nature*, *Cell*, *PNAS*
- Stipend, tuition and health insurance paid by the program
- Competitive fellowship awards, including two special prize fellowships
- Applications and information at www.cincinnatichildrens.org/dbprog or email mdbprog@cchmc.org

Contact

Tim Le Cras, PhD
Associate Professor, Co-Director of Graduate Recruiting, Molecular and Developmental Biology
mdbprog@cchmc.org

Leslie Mills
MDB Program
Administrative Assistant
mdbprog@cchmc.org

www.cincinnatichildrens.org/dbprog

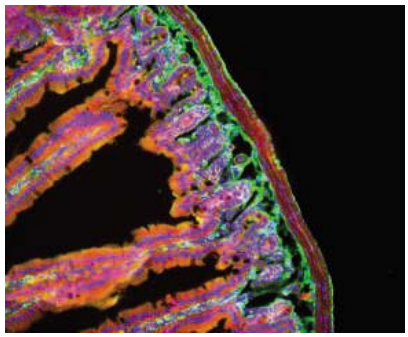

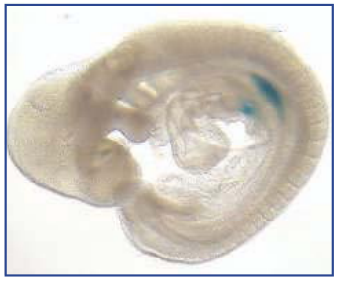

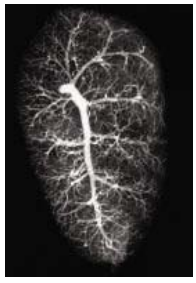

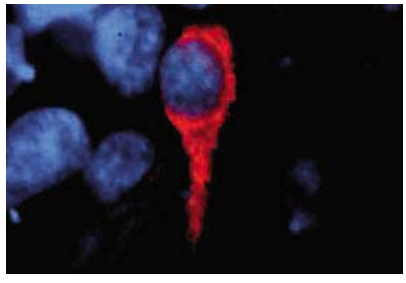

change the outcome®

"Champions of Innovation." That's Pfizer Global Research and Development (PGRD). We're known around the world as the company that improves the lives of millions by bringing to market such outstanding medicines such as Lipitor, Zithromax, Viracept, Zoloft, and Viagra to name a few. And while we're proud of our achievements, we're eager to continue making the world healthier – and that's why we're eager to meet you. Your enthusiasm, drive and willingness to take risks will not only shape our future but it will also shape yours. Here, you'll work collaboratively with some of the most esteemed scientists in the industry and, in turn, you'll become the esteemed scientist you always dreamed of being.

Join us and you'll do more than turn your diploma into live-saving drug discoveries—you'll actually do more than you ever imagined. PGRD will show you how to put your area of specialization to optimum use so that you'll achieve more in a few short years than you would during a lifetime at some other companies. Your knowledge will be continuously challenged and rewarded—and there will never be any limitations put on your ambitions. As you learn and grow and accomplish, you will simultaneously define our future and positively influence an entire industry.

In addition to making the world a better place to live, at PGRD we are also committed to making the lives of our people better.
To learn more about your future, visit our website at: **www.pfizer.com/careers**

Pfizer is proud to be an Equal Opportunity Employer and welcomes applications from people with different experiences, backgrounds and ethnicities.

Pfizer

Working for a healthier world™

www.pfizer.com/careers

of cardiology. Krause says that those people "often stand out as individuals who can jump right in and do the work." CV Therapeutics also offers opportunities for Bachelor's and Master's scientists to advance. Krause says, "We have had people go from the bench into sales, and some who have gone from the bench to project management."

At some companies, getting hired depends on showing experience and skill in teamwork. "We are looking to hire the best of the best," says Gregory of Novartis, "and we want scientists who have worked on projects in team environments." She adds that it helps to have come from a lab with strong scientists doing cutting-edge research. "That is very attractive to us," she says. Once a scientist gets hired at Novartis, the company even offers a career ladder dedicated to scientists with a B.S. or M.S., which is called the technical career ladder. Gregory says, "You can advance if you perform well, and we support movement up the ladder with training and mentoring."

Even with the right training and experience, a prospective employee must perform well during a job interview. To do that, Salas says, "Showing experience is important, but interpersonal skills are almost as important. So be prepared to talk about experiences with collaborations or team situations." She adds, "Give examples of your decision-making abilities and show how you can juggle priorities."

MATT KRAUSE

Pursuing Public Health

Scientists can also choose a career in public service. In particular, public health offers lots of opportunities. At the U.S. Centers for Disease Control and Prevention, Denise Koo, director of the career development division in the office of work force and career development, says, "We definitely can employ people at the M.S. level in biology, chemistry, informatics, and computer science." She adds, "We have fewer opportunities at the B.S. level, but you can get in at the entry level in a range of positions, including bench research and informatics."

Public health jobs also exist at state and local levels. For example, state and local health departments hire many scientists with a Master's degree in epidemiology. And for those with a Master's degree in a laboratory science, Koo says, "State and local public health labs need staff for diagnostics." She adds that public health laboratories serve as a resource for clinical labs or hospitals. "These cutting-edge operations do specialized testing, especially for diseases of public health importance," Koo says.

Visit **www.sciencecareers.org** and plan to attend upcoming meetings and job fairs that will help further your career.

SUZANNE ORTEGA

Scientists at the CDC also do lots of testing and research. Koo says, "We use molecular techniques quite a bit." For example, scientists at the CDC use molecular techniques to genotype strains of disease. "There is so much *Salmonella* in this country," says Koo. "If two people with *Salmonella* have the same, rare molecular fingerprint, you might wonder if something out there is causing problems."

Anyone considering a career in public health, though, should focus on the word public. "We have a responsibility to the public," says Koo, "and the importance and the excitement of this work more than balances out what can be less competitive salaries." Public health scientists often aspire to socially relevant work, such as identifying the cause of an outbreak or developing a new diagnostic tool for monitoring the health of the population. Koo started in college as a biochemist and spent several summers working in a lab. Then she decided to pursue epidemiology and an M.D. "I wanted to see things from a public health perspective," she says.

Although Koo earned an advanced degree, it is possible to move up in the ranks at the CDC without one. "Often," she says, "the folks in charge are at the Ph.D.-level, but M.S.-level folks can get to a pretty high level, especially in the management side of the house." Making that sort of climb, though, requires good people skills and management skills. Koo adds, "With the right skill set, someone with a B.S. can go somewhat far too, but for senior leadership positions more often at least an M.S. is required."

As in industry, part of the right skill set for success in government involves being a good team player. "Public health is so multidisciplinary," says Koo. "We need people who strongly value the contributions of others." To prosper in such an environment, a scientist must recognize that science alone does not influence policy, such as availability of a vaccine. "Scientific methods and results must be extremely rigorous and clearly communicated," says Koo, "and it is especially important when the health of a community is at stake."

In some ways, considering a career in public health might require a new perspective for some scientists. "Some folks think of science as only about research," says Koo. "My point is that science research just for research's sake is not really enough." She knows that science can also contribute to social well-being. "We do exciting, real life science that impacts the health of the people," she says. "This is particularly important in the setting of outbreaks and other public health emergencies, where we might work round the clock to determine the cause." In addition, Koo believes that her colleagues see the value in their work. "We all love what we do and consider it a privilege to provide service to the public and their health needs," she says. CONTINUED »

The Gerstner Sloan-Kettering Graduate School of Biomedical Sciences offers the next generation of basic scientists a program to study the biological sciences through the lens of cancer — while giving students the tools they will need to put them in the vanguard of research that can be applied in any area of human disease.

PhD Program

An Internationally Recognized Research Faculty in:

- Cancer genetics
- Genomic integrity
- Cell signaling and regulation
- Structural biology
- Immunology
- Chemical biology
- Developmental biology
- Computational biology
- Experimental therapeutics
- Experimental pathology
- Imaging and radiation sciences
- Oncology
- Genomics
- Animal models of disease

An Innovative, Integrated Curriculum Provides a Fundamental Understanding of:

- The nature of genes and gene expression
- Cellular organization
- Tissue and organ formation
- Cell-cell interactions
- Cellular response to the environment
- Enzyme activity

Student Support and Services:

Students receive a fellowship package that includes a stipend, tuition, textbook allowance, and health insurance. Students also have access to affordable housing within easy reach of the school.

Please visit our Web site to learn how to apply, for application deadlines, and for more information about our PhD program.

www.sloankettering.edu

gradstudies@sloankettering.edu | 646.888.6639

Gerstner Sloan-Kettering
Graduate School of Biomedical Sciences

New York City

Careers & Graduate Programs for B.S. & M.S. Scientists

More Than a Degree

Lots of scientists come to companies and the government with degrees from prestigious schools. The question is: How can a prospective employee look the best? That can come from not just the degree but what a student did while earning it. For example, Ortega of the University of Washington says, "The more experience you get in managing people—working in teams and building teams—the more desirable you will be to industry."

Just having the diploma—no matter where it's from—is not enough to look like the best candidate for most jobs. At The University of British Columbia, Suttle says, "I always stress getting a paper published or presenting results at a meeting. It shows that you can reach a professional level in your research, be organized, and carry work through to the end."

Others in academia also see the value of publishing your work. "When you go for an interview," says Sugumaran of the University of Massachusetts, Boston, "people look for publications in prominent journals, and that speaks for itself." He adds, "I expect my Master's students to publish." To Sugumaran, publishing is not just a good idea; instead, he sees it as crucial. "Until your work is published in a peer reviewed journal, it is almost like it has not been done," he says.

CURTIS SUTTLE

Top Degrees

To get the benefit of the experts' experience, some of them were asked what degree they would pursue today. Kaufman of the University of Illinois at Chicago sees a couple ways that he might go if he was looking at an M.S. program today. He says that he would consider several fields: biotechnology, chemistry, chemical engineering, or microbiology. "These degrees would prepare you for jobs that are pretty well available in biotechnology and pharmaceutical companies," he says.

To Kaufman, though, the key is learning about technology. He mentions that biotechnology could be applied to forensics and that electronics and computer science can be used in many fields. "The message is technology," Kaufman says. "That is where you want to go, because equipment is the answer in the future."

Thinking about a chance to do it all over, Sugumaran says, "I would pursue biotechnology, mainly because I love it." He started his career as an organic chemistry major, and then he switched to biochemistry. He says, "Genomic and proteomic work makes tremendous opportunities for people to advance themselves in biotechnology or any kind of biomedical science." He adds, "The field is wide open.

Others see integration as more interesting than equipment. Ortega says, "I'm a social scientist and given a chance to do it all again, I'd still be a social scientist." Going back though, she would take a closer look at the business side. She says, "I'd really want to know a lot about the labor force, employment, recruiting, and professional development for employees."

MANICKAM SUGUMARAN

Some of the most exciting opportunities, according to Suttle, lie at the interfaces of technologies. He points out opportunities where biology meets computer science or statistics. "These combinations of knowledge," he says, "let you deal with bioinformatics or biocomputing—very exciting areas." He adds that people with these skills can be very difficult to find.

Suttle also sees other areas that could be valuable for investigating these days. "A B.S. or M.S. that is very hot," he says, "is in mineral exploration. There is an expected shortage of thousands of people in this area over the next decade." Suttle says that even with just a B.S. in geosciences, he sees students "get snatched up immediately."

Speaking of the B.S., Suttle adds, "People don't think there are lots of opportunities with a B.S. alone, but there are." The number of opportunities, though, depend on experience. At The University of British Columbia, Bachelor's students can participate in cooperative programs in which they spend an extra year earning a B.S. because they do work terms in industry. "We have several hundred students in this program," Suttle says. "It has been incredibly successful in microbiology, computer science, physics, and really most of our scientific disciplines." These students work in industry around the world as well as gaining hands-on experience in university research labs. "I'd advise people to look very seriously at such programs," he says. "These opportunities let a student get a degree and perform some work in that field—all at the same time."

In preparing for this interview, Suttle looked over the data for employment of students from his university. For students who earned a Bachelor's degree, many—about 55 percent in the life sciences and around 90 percent in computer science—were working in jobs related to that field.

Just Be Sure

For anyone who wants to go to academics, get a doctoral degree. "You would be terminally frustrated with an M.S. and trying to work in an academic setting," says Kaufman. He also adds that students should not get an M.S. as a test run toward getting a Ph.D. "You can't ride a bike to learn to drive a car," he says, "and an M.S. and Ph.D. are just as different." Instead select a B.S. or M.S. as the final degree only if it can take you where you want to go.

Mike May (mikemay@mindspring.com) is a publishing consultant for science and technology based in the state of Minnesota, U.S.A.

DEPARTMENT OF HEALTH AND HUMAN SERVICES
NATIONAL INSTITUTES OF HEALTH
NATIONAL CANCER INSTITUTE
DIVISION OF CANCER TREATMENT AND DIAGNOSIS
DEVELOPMENTAL THERAPEUTICS PROGRAM
NATURAL PRODUCTS BRANCH

Opening Date: August 17, 2006
Closing Date: October 23, 2006

Announcement Numbers: NCI-06-141960-DE
NCI-06-141960-MP

Chief, Natural Products Branch
GS-1320-15

The Natural Products Branch of the Developmental Therapeutics Program, National Cancer Institute has an opening for a Branch Chief/Chemist to support the acquisition of materials of natural origin, the coordination of the screening and chemical investigation of these materials, and the large-scale procurement of active natural product agents for preclinical and clinical development.

The responsibilities of the position entail: (1) Worldwide procurement of plants, marine organisms and unusual microbes for preparation of extracts, and screening for anticancer activity; (2) coordination of research directed toward the isolation of new agents from active extracts of plant, animal (including marine organism) and microbial sources; (3) large-scale procurement of biomass and isolation of active agents for preclinical and clinical development. The candidate must have the ability to organize, plan and accomplish project tasks in a timely and cost-effective manner. The candidate would serve as the Branch Chief and contacts consists of NCI Senior staff, officials in NIH, DHHS, representatives of Congress and outside organizations to present data and information on NCI programs and activities. Supervision and resource management involves making major decisions and taking actions which have a direct and substantial effect on the organization.

A Ph.D. in natural products chemistry or organic chemistry is highly desirable as well as post-doctoral training and extensive experience and knowledge of medicinal or pharmaceutical chemistry and biochemistry are needed. Training and experience in other aspects of drug development such as pharmaceutics, pharmacology, anti-tumor biology, microbiology and screening methodology is highly desirable. Communication skills and project-management experience are also necessary.

Salary - ranges from $107,521 to $139,774 per annum. Benefits include health and life insurance options, retirement, paid holidays, vacation and sick leave.

U.S. citizenship is required. To apply for this position, please visit: **http://jobsearch.usajobs.opm.gov/a9nih.asp** and keyword search for Vacancy Announcements **(VA), NCI-06-141960-DE and NCI-06-141960-MP** for the mandatory application requirements. For questions about applying to the VA, please contact **Mary Lou Weathers, on (301) 402-5059 or weatherm@mail.nih.gov.**

Individuals interested to learn more about this position are encouraged to contact:

Dr. Jerry Collins, Associate Director, DTP, DCTD, NCI
6130 Executive Boulevard, EPN, Room 8019
Rockville, MD 20852
Tel: (301)496-8720; Fax: (301)402-0831; Email: collinsje@mail.nih.gov

APPLICATIONS MUST BE RECEIVED BY OCTOBER 23, 2006

WWW.NIH.GOV

Associate Director, National Toxicology Program

National Institute of Environmental Health Sciences
Research Triangle Park, North Carolina

The National Institute of Environmental Health sciences (NIEHS) of the National Institutes of Health (NIH) is seeking exceptional candidates to fill the position of tenured investigator to serve as Associate Director, National Toxicology Program (NTP). The NTP is an interagency program whose mission is to evaluate agents of public health concern by developing and applying the tools of modern toxicology and molecular biology. This involves conducting toxicological evaluations of substances of public health concern, developing and validating improved (sensitive, specific, rapid) testing methods, developing approaches and generating data to strengthen the science base for risk assessment, and communicating with all stakeholders.

The NTP maintains a balanced research and testing program that provides data addressing a wide variety of issues important to public health. The NTP actively seeks to identify and select for study chemicals and other substances for which sufficient information is not available to adequately evaluate potential human health hazards.

The NTP relies upon voluntary allocations from the program's core agencies (NIEHS, FDA's National Center for Toxicological Research (NCTR) and CDC's National Institute for Occupational Safety and Health) to support its research, testing, centers and outreach. The program focuses its resources upon three major program activities: toxicology studies, methods development and validation. Within each of these program activities, the NTP targets multiple areas broadly including genetics toxicology, toxicological characterizations (includes immunotoxicology, epidemiology, exposure assessment and general toxicology), reproduction and development and carcinogenesis.

Candidates must have a Ph.D. or equivalent degree in an environmental health science discipline. Candidates should have extensive experience in toxicology with research contributions which advanced the field and administrative experience sufficient to lead a major applied research program. Additionally, the incumbent will have the option of leading an active research group within the Division of Intramural Research. Salary is commensurate with experience and level of accomplishments. An outstanding benefits package will be provided. A recruitment or a relocation bonus may also be available.

Interested persons should send their curriculum vita with a statement of research/administrative accomplishments and plans, and arrange for three letters of recommendation to be submitted to the address below by September 30, 2006. Letters should be from leaders in the field who specifically address recommendation for a tenured investigator position at NIH. For more information concerning the National Toxicology Program, access website **http://ntp.niehs.nih.gov/ Ms. Stephanie Jones (DIR-06-05), National Institute of Environmental Health Sciences, P.O. Box 12233, Maildrop NH-01, Research Triangle Park, NC 27709, 919-541-7913 e-mail: jones17@niehs.nih.gov**

Accelerating and Enhancing Research
From Basic Discovery to Improved Patient Care

The National Center for Research Resources (NCRR)—a part of the National Institutes of Health (NIH)—provides laboratory scientists and clinical researchers with the environments and tools they need to understand, detect, treat, and prevent a wide range of diseases. With this support, scientists make biomedical discoveries, translate these findings to animal-based studies, and then apply them to patient-oriented research. Ultimately, these advances result in cures and treatments for both common and rare diseases. Through collaborations and networks, NCRR connects researchers with one another and with patients and communities across the nation. Together NCRR's four integrated and complementary divisions accelerate and enhance research along the entire continuum of biomedical science.

NCRR has immediate openings for Health Scientist Administrators, with salaries ranging from $77,353 to $118,828 depending on experience. These positions also include the full range of Federal benefits.

Health Scientist Administrators have broad responsibilities in the planning, evaluation, and scientific management of specific national programs with continuing responsibility for adjusting the scope and content of specific programs to meet the emerging needs of biomedical researchers. NCRR is looking for several scientists to help in one of the following areas: developing programs to enhance the competitiveness of biomedical investigators in underserved states and institutions; stimulating basic research that develops new technologies and methods that help researchers who are studying virtually every human disease; enhancing bioinformatics in a basic/clinical and/or translational research setting; and developing informatics infrastructure for biomedical and clinical research. For more information regarding responsibilities of these positions and application details, please look under Announcements on our website at **www.ncrr.nih.gov**. The National Center for Research Resources has a strong commitment to the diversity of its workforce and a biomedical research environment that reflects the diversity of the American population.

The National Institute of Allergy and Infectious Diseases, a major research component of the NIH and the Department of Health and Human Services, is recruiting for a Staff Scientist. The position will be available in the Respiratory Viruses Section of the Laboratory of Infectious Diseases, and scientists with a M.D. or Ph.D. are eligible. The research activity involves (1) the development of live attenuated flavivirus vaccine candidates and their evaluation in rodents and non-human primates as well as in the clinical trials in humans; (2) the use of novel approaches for construction of chimeric viruses to examine basic questions of viral pathogenesis and the molecular basis of attenuation of highly neurovirulent flaviviruses; (3) the evaluation of the immunologic determinants of resistance to infection and illness caused by these flaviviruses. This full-time research position offers a unique opportunity to work on investigations that range from basic molecular biology to applied vaccinology. Staff Scientist applicants should have at least six years of laboratory work experience in molecular virology and immunology; the salary range is $73,178 - $165,195. Preference will be given to candidates who have experience working with neurotropic viruses. Applicants should submit their curriculum vitae, a letter of research interests, and names and addresses of three references to:

Alexander Pletnev, NIAID, NIH, 12735 Twinbrook Parkway, Twinbrook 3, Room 3W13, MSC 8133, Bethesda, MD 20892-8133, FAX: (301) 480-4873, email: apletnev@niaid.nih.gov. Review of applicants will begin **October 1, 2006** and continue until a successful candidate is identified.

Chief, Laboratory of Bacterial Diseases
National Institute of Allergy and Infectious Diseases
National Institutes of Health

The National Institute of Allergy & Infectious Diseases (NIAID), Division of Intramural Research (DIR) is seeking an outstanding individual to head the newly established Laboratory of Bacterial Diseases (LBD) in Bethesda, Maryland. The laboratory is to be located in the new C.W. Bill Young Center for Biodefense and Emerging Pathogens located on the NIH campus in Bethesda, Maryland.

The mission of the LBD will be to study basic and applied aspects of bacterial diseases related to biodefense or emerging and re-emerging pathogens, focusing on pathogenic bacteria. Exceptional scientists with research interests in basic, translational or clinical aspects of bacterial pathogenesis are encouraged to apply. The long-term goals of the Institute include supporting research that enables the development of new diagnostics, vaccines, and therapeutics.

This position requires an M.D., Ph.D. or equivalent with proven leadership abilities and a strong independent research program. Preference will be given to candidates with a documented record of accomplishment in bacterial disease research, and those whose program(s) are consistent with the mission of the NIAID.

The Laboratory Chief will have independent resources to conduct basic and clinical research and will supervise other Principal Investigators with independent research programs. The successful candidate is expected to lead a strong research program in laboratory and/or clinical research. Committed resources include space, support personnel and an allocated annual budget to cover service, supplies, animals and related resources and salaries. A Laboratory Chief in the DIR is equivalent to a Department Chair in a University or Medical School. Applicants must be U.S. citizens or permanent residents and be eligible for the appropriate security clearance under the CDC Select Agent Program. Salary will be commensurate with experience and qualifications.

Interested candidates may contact **Dr. Karyl Barron, Deputy Director, DIR, NIAID at 301/402-2208 or email (kbarron@niaid.nih.gov)** for additional information about the position and/or infectious diseases research at the NIH.

To apply for the position, candidates must submit curriculum vitae, bibliography, a detailed statement of research interests, and reprints of up to three selected publications, preferably via Email to: Lynn Novelli at novelly@niaid.nih.gov. In addition, the names of three potential references must be sent to **Dr. Steven M. Holland, Chair, NIAID Search Committee, c/o Ms. Lynn Novelli, DIR Committee Manager, 10 Center Drive, MSC 1356, Building 10, Room 4A26, Bethesda, Maryland 20892-1356.** Completed applications **MUST** be received by **Monday, September 25, 2006**. Please refer to **AD#004** on all correspondence. Further information on this position and guidance on submitting your application is available on our website at: **http://healthresearch.niaid.nih.gov**

Chief, Laboratory of Virology
National Institute of Allergy and Infectious Diseases
National Institutes of Health

The National Institute of Allergy & Infectious Diseases (NIAID), Division of Intramural Research (DIR) is seeking an outstanding individual to head the newly established Laboratory of Virology (LV) located at the Rocky Mountain Laboratories in Hamilton, Montana. LV will interact with four other Intramural Research Laboratories at this location presently studying infectious diseases involving viruses, bacteria, rickettsia, chlamydia and prions.

The mission of the LV is to study high containment BSL-3 and BSL-4 viral pathogens with the goal of developing diagnostics, vaccines, and therapeutics. The research to be conducted in the LV is to include studies of vector/reservoir transmission, pathogenesis, pathophysiology and host immune response of high containment viral pathogens. In addition, the LV must maintain a flexible infrastructure to permit rapid analysis of newly emerging high containment viral pathogens of special interest.

The selected candidate will supervise research in a newly constructed Integrated Research Facility which houses three BSL-4 lab suites, three BSL-3 lab suites and multiple BSL-2 lab suites, as well as extensive associated BSL-2, 3, and 4 animal facilities.

This position requires a Ph.D., M.D., D.V.M. or equivalent with proven ability to carry out a strong independent research program. Preference will be given to candidates with a record of leadership and accomplishment in BSL-4 or Select Agent BSL-3 viral pathogen research, with program(s) consistent with the mission of the NIAID. The selected person will also be expected to recruit and supervise other Principal Investigators with independent research programs.

The Laboratory Chief will have independent resources to conduct laboratory research and translational/clinical research, as appropriate. Committed resources include space, support personnel and an allocated annual budget to cover service, supplies and salaries. A Laboratory Chief in the DIR is equivalent to a Department Chair in a University or Medical School. Applicants must be eligible for the appropriate security clearance under the CDC Select Agent Program. Salary is dependent on experience and qualifications. Interested candidates may contact **Dr. Karyl Barron, Deputy Director, DIR, NIAID at 301/402-2208 or email (kbarron@niaid.nih.gov)** for additional information about the position.

To apply for the position, candidates must submit a curriculum vitae, bibliography, a detailed statement of research interests, the names of three references, and reprints of three selected publications, preferably via email to: **Felicia Braunstein at braunsteinf@niaid.nih.gov or by US Mail to: Ms. Felicia Braunstein, DIR Committee Manager, 10 Center Drive MSC 1349, Building 10, Rm. 4A-30, Bethesda, Maryland 20892-1349**. Please note search **#006** when sending materials. Completed applications **MUST** be received by **Friday, November 3, 2006**. Further information on working at NIAID is available on our website at: **http://healthresearch.niaid.nih.gov**

WWW.NIH.GOV

Chief, Laboratory of Human Bacterial Pathogenesis
National Institute of Allergy and Infectious Diseases
National Institutes of Health

The National Institute of Allergy & Infectious Diseases (NIAID), Division of Intramural Research (DIR) is seeking an outstanding individual to head the Laboratory of Human Bacterial Pathogenesis (LHBP) in Hamilton, Montana.

The mission of the LHBP is to study human bacterial diseases related to emerging and re-emerging pathogens. The research to be conducted in the LHBP is to include; 1) the molecular basis of host-pathogen interactions, 2) the genetic basis of bacterial virulence and pathogenesis, 3) the use of animal modeling to define host defense mechanisms and biology and immunology of host-pathogen interactions, and 4) development of novel and improved intervention strategies to control bacterial infectious diseases. The ultimate goal is to develop diagnostics, vaccines, and therapeutics for emerging and re-emerging infectious diseases.

This position requires a Ph.D. and/or M.D. or equivalent with proven leadership abilities and a strong independent research program. Preference will be given to candidates with a documented record of accomplishment in bacterial disease research, and especially to those whose program(s) are consistent with the mission of the NIAID to study emerging and re-emerging bacterial pathogens.

The Laboratory Chief will have independent resources to lead and conduct laboratory research and translational/clinical research, as appropriate. Mechanisms are available to conduct clinical studies at the Bethesda campus and/or to obtain clinical samples through contract mechanisms at non-NIH institutions. The individual will supervise other Principal Investigators with independent research programs investigating the pathogenicity of Staphylococcus and Streptococcus species. Committed resources include space, support personnel, animal resources and an allocated annual budget to cover service, supplies and salaries. A Laboratory Chief in the DIR is equivalent to a Department Chair in a University or Medical School. Salary is dependent on experience and qualifications.

Interested candidates may contact **Dr. Karyl Barron, Deputy Director, DIR, NIAID at (301) 402-2208 or email (kbarron@niaid.nih.gov)** for additional information about the position. To apply for the position, candidates must submit a curriculum vitae, bibliography, a detailed statement of research interests, and reprints of up to three selected publications preferably via email to: **Felicia Braunstein at braunsteinf@niaid.nih.gov or by US Mail to: Ms. Felicia Braunstein, DIR Committee Manager, 10 Center Drive MSC 1349, Building 10, Rm. 4A-30, Bethesda, Maryland 20892-1349**. In addition, the names of three referees must be sent to **Dr. Tom Schwan, Chairperson, NIAID Search Committee, c/o Ms. Felicia Braunstein, DIR Committee Manager, 10 Center Drive MSC 1349, Building 10, Rm. 4A-30, Bethesda, Maryland 20892-1349**. Please note search **#005** when sending materials. Completed applications **MUST** be received by **October 6, 2006**. Further guidance on submitting your application is available on our website at: **http://healthresearch.niaid.nih.gov**.

Tenure Track Position in the Laboratory of Immunology

National Institute of Allergy and Infectious Diseases
National Institutes of Health

The Laboratory of Immunology (LI), Division of Intramural Research, National Institute of Allergy and Infectious Diseases, National Institutes of Health invites applications for a tenure track position in immunology.

LI strongly encourages scientists with an interest in any area of biomedical research related to immunology to apply. Candidates should have a Ph.D., M.D. or equivalent degree and an outstanding record of post-doctoral accomplishment. LI wishes to recruit a highly creative individual who will establish an independent research program that takes full advantage of the special opportunity afforded by the stable long-term funding of the Intramural Research Program at NIH. She/he should be interested in developing and applying novel approaches to the study of problems of major biological and /or medical importance, efforts that may be enhanced through participation in emerging trans-NIH initiatives involving technology development, translational investigation, and multidisciplinary science. Generous ongoing support for salary, technical personnel, post-doctoral fellows, equipment, and research supplies will be provided, as well as access to existing or planned core facilities / collaborative centers for projects involving RNAi screening, microarrays, production of transgenic and gene manipulated mice, advanced imaging, and computational biology. In addition to an outstanding international post-doctoral community, a superior pool of graduate and undergraduate students is also available to the successful applicant.

LI has a distinguished history of accomplishment in immunology and is seeking to appoint an outstanding early career investigator who can continue and enhance this record of achievement. Current LI Principal Investigators are Ronald Germain, Michael Lenardo, Rose Mage, David Margulies, William Paul, Ethan Shevach and Tsan Xiao.

Applicants should send a CV and bibliography and an outline of a proposed research program (no more than two pages) electronically to **Mrs. Lynn Novelli (novelly@niaid.nih.gov)**. Three letters of reference should also be sent either electronically or by mail to **Mrs. Lynn Novelli, Committee Manager, 10 Center Drive, MSC 1356, Building 10, Room 4A26, Bethesda, Maryland 20892-1356**. Please refer to **Ad #011** on all communications. Further information about this position may be obtained by contacting **Dr. William Paul (301 496-5046; wpaul@niaid.nih.gov). Applications must be received by October 14, 2006**.

A full package of benefits (including retirement, health, life and long term care insurance, Thrift Savings Plan participation, etc.) is available. Women and minorities are especially encouraged to apply. U.S. citizenship is not required.

Endowed Professorship Bioinformatics

Applications and/or nominations are invited for the **Endowed Professorship in Bioinformatics** at the College of Charleston. This is the first of two appointments to be made within the Center for Economic Excellence in Marine Genomics, a partnership between the College and the Medical University of South Carolina. It is anticipated that the appointment will be made at the level of Associate Professor or Professor in the Department of Biology at the College with a joint appointment at the Medical University. For information about the department, see **www.cofc.edu/~biology**.

The successful applicant will have a demonstrated track record as a collaborative scholar, a strong commitment to teaching and mentoring graduate and undergraduate students, and, ideally, will also have significant experience with the mechanisms for enhancing research value through economic development. Experience as a research team leader/program director is highly desirable. The successful candidate will provide academic and program leadership to the Bioinformatics Group within the Marine Genomics program in Charleston. This program focuses on applying genomic approaches to increasing understanding of the interactions of marine organisms with their environment, including infectious diseases, and the relationship between the oceans and human health. The Chairholder will lead an existing team of programmers and computational biologists and will drive the conceptual and theoretical interpretation of experimental results.

Historic Charleston SC, on the biologically diverse southeast Atlantic marsh, is a natural laboratory for an integrated effort to monitor, understand, protect and manage the marine environment. The Marine Genomics program currently comprises over 40 faculty, students and staff from the College, Medical University, SC Department of Natural Resources, National Oceanic and Atmospheric Administration and National Institute of Standards and Technology, as well as the Hollings Marine Laboratory (a partnership of the five Ft. Johnson organizations) on the Ft. Johnson marine campus, five miles from downtown Charleston. Information about the current Marine Genomics bioinformatics infrastructure can be found at: **http://marinegenomics.org** (see also BMC Genomics 2005,6:34).

More information about this position can be obtained at the School of Sciences and Mathematics website: **www.cofc.edu/~ssm** or from **Dr. Norine Noonan**, Dean, School of Sciences and Mathematics, at **NoonanN@cofc.edu** or the chair of the search committee, **Dr. Louis Burnett**, at **BurnettL@cofc.edu**. Applicants should send a statement of research interests and accomplishments, a *Curriculum vitae*, and the names and contact information for at least three references to: **Bioinformatics Chair, Office of the Dean, School of Sciences and Mathematics, College of Charleston, 66 George St., Charleston, SC 29424**. Nominations should be sent directly to the Dean. Applications and nominations will be held in confidence to the extent possible. Review of applications will begin on **August 28, 2006** and will continue until the position is filled.

STANFORD
SCHOOL OF MEDICINE

Stanford University Medical Center

Associate/Co-Director of Histocompatibility, Immunogenetics and Disease Profiling Laboratory at Stanford University School of Medicine Blood Center

Open Rank (Medical Center Line)

The Department of Pathology is seeking an Associate Director or Co-Director of the Histocompatibility, Immunogenetics, and Disease Profiling Laboratory at Stanford University Medical School Blood Center. The individual will share responsibility with the Director of the Laboratory for oversight of the clinical laboratory including clinical reporting, clinical consultation, research and development, administrative duties related to the laboratory, and teaching, including training of clinical residents and fellows. Service responsibilities include reviewing and reporting clinical cases; clinical consultation; methods development; all aspects of safety, quality assurance, quality control, personnel and budget management; compliance with applicable accrediting agency, state and federal regulations; and for ensuring that delegated duties are properly performed. Depending on the experience and interests of the successful candidate, and the results of discussions with the Director of the Laboratory and the Department Chair, the position could be either as Associate Director of the Laboratory or Co-Director (along with the current Director, Dr. Dolly Tyan). The Co-Director would share responsibility for the laboratory equally with the current Director.

The successful candidate will be expected to develop a research program related to the mission of the laboratory. A key selection criterion will be the outstanding potential to develop a high quality research program related to novel approaches for disease profiling and/or therapeutic testing at the molecular, genetic and/or cellular levels and for using such approaches to guide diagnosis, prognosis, disease monitoring, and/or therapeutic decisions in fields such as immunology, genetics, cancer, infectious diseases and/or transplantation. A wide range of opportunities for research is available, and there is departmental support for research related to the goals of the Laboratory. The department supports high quality basic science, translational and clinical research programs, and directors of service laboratories maintain strong associations with investigators in other basic science and clinical departments on campus. Areas of investigation in the department include genomics, proteomics, cell and developmental biology, biochemistry, cancer biology, cell signaling, immunology and studies of human disease in animal models.

Requirements for the position include an MD or PhD with experience in human clinical histocompatibility testing and demonstrated expertise in novel test development. Licensure, or eligibility for such licensure, by the State of California as a Histocompatibility Laboratory Director and Board certification at the Diplomate level, or eligibility for such certification, by the American Board of Histocompatibility and Immunogenetics (ABHI) are required. Academic rank in the Medical Center Line will be commensurate with experience and accomplishments. The major criteria for appointment for faculty in the Medical Center Line shall be excellence in the overall mix of clinical care, clinical teaching, and scholarly activity that advances clinical medicine, and institutional service—appropriate to the programmatic need the individual is expected to fulfill.

Applicants should submit a curriculum vitae and bibliography, together with a brief description of past and present scholarly interests and accomplishments, and a concise statement of plans for future research, ideally by **December 15, 2006**. These and the names of three references should be sent to:

Stephen J. Galli, M.D., Chair
c/o Ms. Cynthia Llanes
Department of Pathology
Stanford University School of Medicine
Stanford, CA 94305
cllanes@stanford.edu

Stanford University is an Equal Opportunity Employer and is committed to increasing the diversity of its faculty. It welcomes nominations of and applications from women and members of minority groups, as well as others who would bring additional dimensions to the university's research, teaching and clinical missions.

POSITIONS OPEN

ASSISTANT/ASSOCIATE PROFESSOR
Bioinformatics
Clemson University

The Department of Genetics and Biochemistry **(website: http://www.clemson.edu/genbiochem/)** invites applications for an Assistant or Associate Professor position in bioinformatics. This position is a tenure-track, 75 percent research/25 percent teaching appointment at Clemson University. Successful candidates will be expected to develop extramurally funded research programs and mentor undergraduate and graduate students from the Department of Genetics and Biochemistry. Teaching responsibilities include an upper-level undergraduate course and a graduate level course in bioinformatics. The position includes office and informatics suite space located in the new Biosystems Research Complex.

Applicants must have a Ph.D. degree, a strong publication record, and at least two years of postdoctoral experience in bioinformatics or a related discipline. Special consideration will be given to candidates with research programs in DNA sequence analysis, bioinformatics tool development, biological database management, data mining, computational analysis of functional and proteomic data, computational modeling of regulatory and metabolic networks, or comparative genomics. Future or current collaborative efforts with researchers at the Clemson University Genomics Institute are desirable. To apply, submit a cover letter, curriculum vitae, future research plan, and the names of three references as a PDF file to **e-mail: bioinfo@clemson.edu** with bioinformatics position in the subject heading. Please submit electronic copies of letters from the three references to **e-mail: bioinfo@clemson.edu.** Applications received by September 29, 2006, will receive full consideration. *Clemson University is an Equal Employment Opportunity/Affirmative Action Employer and does not discriminate against any individual on the basis of age, color, disability, gender, national origin, religion, sexual orientation, or veteran status.*

UNIVERSITY OF ROCHESTER. The Department of Chemistry invites applications for positions in all areas of experimental chemistry at the **ASSISTANT, ASSOCIATE**, and **FULL PROFESSOR** levels. Candidates with research interests in organic chemistry, broadly defined, are especially encouraged to apply. Candidates are expected to establish an outstanding program of original research and be effective teachers at the graduate and undergraduate levels. Applicants should send curriculum vitae, a statement of research plans, teaching interests, and arrange for three letters of recommendation to be sent, preferably in electronic form, to **Ms. Karen Dean, e-mail: dean@chem.rochester.edu**, or mail to: **Chemistry Faculty Search Committee, c/o Ms. Karen Dean, Department of Chemistry, University of Rochester, RC Box 270216, Rochester, N.Y. 14627-0216.** Review of applications will begin on October 16, 2006. *The University of Rochester is an Equal Opportunity Employer. Women and minority candidates are strongly encouraged to apply.*

PROTEIN BIOCHEMIST. The Carlson School of Chemistry and Biochemistry at Clark University invites applications for a tenure-track appointment as **ASSISTANT PROFESSOR** to begin fall 2007. Candidates are expected to show promise of excellent teaching in biochemistry at both undergraduate and graduate levels, and to develop an active, externally funded research program in protein (bio)chemistry involving graduate and undergraduate students. Additional information on the Department is available at **website: http://www.clarku.edu/~chem.** Send curriculum vitae, summary of teaching experience and interests, statement of research plans, and arrange for three letters of reference to be sent to: **Chair, Search Committee, Gustaf H. Carlson School of Chemistry and Biochemistry, Clark University, 950 Main Street, Worcester, MA 01610-1477.** E-mail enquiries may be directed to **e-mail: fgreenaway@clarku.edu.** Review of applications begins October 15, 2006. *Affirmative Action/Equal Opportunity Employer. Minorities and women are especially encouraged to apply.*

The Physics Department, the James Franck Institute, and the Enrico Fermi Institutes at the University of Chicago invite applications for a **TENURE-TRACK FACULTY APPOINTMENT** in the general area of experimental atomic, molecular, and optical physics (AMO). The appointment will start in the fall of 2007. We encourage applications from candidates with an outstanding record of research in areas such as ultracold atoms and molecules, precision measurements, quantum optics, quantum information, as well as ultrafast laser physics. The successful candidate must have a doctoral degree in physics or related fields, and is expected to establish an independent research program while effectively contributing to the Department's undergraduate and graduate teaching programs. The appointment is expected to be at the **ASSISTANT PROFESSOR** level. Appointment at the level of **ASSOCIATE PROFESSOR** or **FULL PROFESSOR** is possible for exceptionally well-qualified candidates. Applicants should send curriculum vitae, a list of publications, a brief research statement, and arrange to have at least three reference letters sent to: **Professor Steven Sibener, Director, James Franck Institute, The University of Chicago, CIS E 145, 929 E. 57th Street, Chicago, IL 60637-1434.** E-mail should be sent to **Ms. Rosemary Garrison** at **e-mail: rg-garrison@uchicago.edu.** Review of applications will start in the fall of 2006, and will continue until the position is filled. To ensure full consideration, applications should be received no later than November 1, 2006. *The University of Chicago is an Equal Opportunity, Affirmative Action Employer.*

ECOLOGY AND EVOLUTION OF ORGANISMS

The Department of Ecology, Evolution, and Organismal Biology at Iowa State University seeks a tenure-track **ASSISTANT PROFESSOR** who excels in any area compatible with our Department's interests in the ecology and evolution of organisms. Potential research areas include form, function, and adaptation; plasticity, perceptory systems and behavior; population dynamics, species interactions, and ecological organization; and diversification and systematics. The successful candidate will join a dynamic Department of 34 faculty who use integrative approaches that bridge disciplines and span multiple levels of biological organization. Applicants must have a Ph.D. in a biological science and are expected to develop a nationally recognized research program and contribute to undergraduate and graduate teaching. Submit curriculum vitae, three reprints, research and teaching statements, and three letters electronically to **e-mail: eeobsearch@iastate.edu** by 15 October 2006 (see **website: http://www.eeob.iastate.edu/search** for instructions). Direct questions to **Dr. Carol Vleck, Search Committee Chair, e-mail: cvleck@iastate.edu.** *The Department is committed to fostering a culturally diverse educational environment. Iowa State University is an Equal Opportunity/Affirmative Action Employer.*

RESEARCH ASSOCIATE
Molecular/Cellular Biology and MRI

A Research Associate position is available for a Cellular/Molecular Biologist in the Department of Biological Sciences at Carnegie Mellon University. Candidates will participate in the development of novel agents for in vivo cellular/molecular imaging utilizing magnetic resonance imaging (MRI). Previous experience with MRI is nonessential. A Ph.D. is required, with a background in a broad range of recombinant DNA techniques; construction of viral vectors and/or transgenic technologies; gene expression detection methods; mammalian tissue culture; strong scientific problem solving skills; ability to communicate results in a clear manner verbally and in writing; record of scientific achievement as documented by peer-reviewed journal publications.

Interested candidates should send curriculum vitae and names of three references to: **Dr. Eric T. Ahrens, Department of Biological Sciences, Carnegie Mellon University, 4400 Fifth Avenue, Pittsburgh, PA 15213 U.S.A., fax: 412-268-7083, e-mail: eta@andrew.cmu.edu.** *Carnegie Mellon is an Equal Opportunity/Affirmative Action Employer.*

The University of Montreal and Sainte-Justine Hospital Research Center seek applications for a **CANADA RESEARCH CHAIR** in statistical genetics and epidemiology (Tier II, University appointment at the **ASSISTANT PROFESSOR** level). Candidates must have strong academic background in statistics and/or computer science, a Ph.D. degree plus two to four years of postdoctoral experience in the field, an interest in medical and human population genetics, as well as knowledge of contemporary genomic research tools. The successful applicant will develop his/her own competitive research program and also collaborate with existing research groups utilizing genetic methodologies. Postgraduate teaching will be encouraged.

French language skills are not required upon hiring, but should be developed during the first three years. International applicants are welcome. Applications will be considered beginning September 1, 2006, until the position is filled. Applicants should send current curriculum vitae plus a statement of research interests, either by e-mail or mail, and arrange to have three letters of recommendation sent to:

Dr. Damian Labuda
Selection Committee
Sainte-Justine Hospital Research Center
3175 Cote Sainte-Catherine
Montreal, QC H3T 1C5
Canada
E-mail: damian.labuda@umontreal.ca.

Copy to **e-mail: dominika.kozubska@recherche-ste-justine.qc.ca.**

ASSISTANT PROFESSOR. The Department of Biochemistry, Biophysics, and Molecular Biology at Iowa State University seeks a tenure-track Assistant Professor interested in studying molecular mechanisms underlying biological processes. Possible research areas include but are not limited to: cellular signaling and architecture, metabolism, macromolecular structure, and dynamics. Individuals whose research includes the use of nuclear magnetic resonance (NMR) spectroscopy are especially encouraged to apply. The successful applicant will have access to two recently installed high field NMR spectrometers equipped with a cryogenically cooled probe and an established, state-of-the-art NMR research service facility **(website: http://www.bb.iastate.edu/).** Applicants should have a Ph.D. with research experience. The successful candidate will be expected to establish a vibrant research program and to actively participate in graduate and undergraduate teaching. To apply, please provide curriculum vitae, a two-page summary of prior research, a concise description of future research plans, a statement regarding teaching philosophy and interest, and arrange to have three letters of recommendation sent to: **Biochemistry, Biophysics, and Molecular Biology Faculty Search, 1210 Molecular Biology Building, Iowa State University, Ames, IA 50011.** Applications received by November 1, 2006, are guaranteed consideration. *Iowa State University is an Equal Opportunity/Affirmative Action Employer.*

ASSISTANT PROFESSOR
The University of Chicago, Department of Chemistry

The Department of Chemistry of the University of Chicago invites applications from outstanding individuals for the position of Assistant Professor of chemistry. This search is in the areas broadly defined as inorganic, organic, and physical chemistry. Applicants must mail hardcopies of curriculum vitae, a list of publications, and a succinct outline of their research plans, and arrange for three letters of recommendation to be sent by mail to: **Michael D. Hopkins, Chairman, Department of Chemistry, The University of Chicago, 5735 S. Ellis Avenue, Chicago, IL 60637.** Review of completed applications will begin October 1, 2006; to ensure full consideration, all material should be submitted by that date.

An Equal Opportunity/Affirmative Action Employer.

POSITIONS OPEN

TENURE-TRACK ASSISTANT PROFESSOR
Terrestrial Plant Ecology

The Department of Botany, University of British Columbia (UBC), **website: http://www.botany.ubc.ca,** seeks applications for a tenure-track position in terrestrial plant ecology. All areas of plant ecology will be considered, and preference will be given to candidates with a field-based component to their research. The successful applicant will develop a strong research program, teach courses in ecology or organismal biology in the UBC Biology Program, and interact with the UBC Biodiversity Research Centre **(website: http://www.biodiversity.ubc.ca).** Salary will be commensurate with experience. Appointment will be at the **ASSISTANT PROFESSOR** level and is subject to final budgetary approval.

Applicants should send curriculum vitae, a summary of research interests, a statement of teaching philosophy, reprints of key publications, and should arrange to have three letters of reference sent directly to the Department. Applications should be addressed to the: **Chair, Ecology Search, Department of Botany, University of British Columbia, 6270 University Boulevard, Vancouver, BC, Canada, V6T 1Z4.** Electronic applications to **e-mail: ecology@interchange.ubc.ca** are preferred, but paper applications will be accepted. Application deadline is November 1, 2006.

The University of British Columbia hires on the basis of merit and is committed to employment equity. All qualified applicants are encouraged to apply; however, Canadian citizens and permanent residents of Canada will be given priority.

The Department of Biomedical Sciences at the University of South Alabama (USA) seeks candidates for a tenure-track faculty position at the **ASSISTANT** or **ASSOCIATE PROFESSOR** level. The USA Biomedical Sciences Department offers a B.S. degree and is responsible for the undergraduate education of students interested in pursuing postbaccalaureate study in medicine, health professions, or basic sciences. Candidates must have a Ph.D., or equivalent, in one of the biomedical sciences, two years of postdoctoral experience, and expertise to teach human anatomy. The successful candidate will also be expected to develop an active research program and mentor undergraduate research projects. Review of applications will begin on October 15, 2006, and will continue until the position is filled, with an estimated start date of June 1, 2007. Applications should include a cover letter of interest, curriculum vitae, and three letters of reference. The application material should be sent via regular mail or e-mail to: **Dr. Michael P. Spector, Professor, Department of Biomedical Sciences, UCOM 6000, University of South Alabama, Mobile, AL 36688-0002** or **e-mail: mspector@usouthal.edu. Website: http://www.southalabama.edu/alliedhealth/biomedical.** *Affirmative Action/Equal Employment Opportunity/Minorities/Females/Persons with Disabilities.*

QUATERNARY VERTEBRATE PALEONTOLOGIST, CURATOR OF GEOLOGY
Illinois State Museum

Illinois State Museum seeks Quaternary Vertebrate Paleontologist to serve as Curator of geology to oversee and upgrade collections and databases; research and publish; participate in interdisciplinary landscape history and educational programs. Required: Ph.D. in geology or related discipline; education background and research experience in quaternary vertebrate paleontology and relevant midwestern geology; prior experience in museum or university; collections experience; strong publication and grant-supported research record. Preferred: experience with public programming. Starting date November 2006; open until filled. Salary and rank commensurate with experience. Send cover letter, curriculum vitae, and names of three references by September 15, 2006, to: **Human Resource Manager, Illinois State Museum, 502 South Spring Street, Springfield, IL 62706-5000, e-mail: cmontgom@museum.state.il.us.** Technical queries to **Dr. Jeffrey Saunders, e-mail: saunders@museum.state.il.us.** *Affirmative Action/Equal Employment Opportunity.*

PRINCIPAL INVESTIGATOR
Hebei Normal University
Hebei Province, China

The College of Life Science at Hebei Normal University, China, invites applications for full-time faculty positions at the Principal Investigator level. Hebei Normal University is located in north China, close to Beijing. The College of Life Science is one of the most active groups in Hebei Normal University. Under the leadership of **Academician Sun Daye,** the College possesses excellent plant biology and zoology researches, with substantial support for the establishment of new research groups and new facilities for relative studies, in an atmosphere that encourages innovation and provides a highly supportive learning environment for young scientists. Outstanding scientists expert in the following areas are encouraged to apply: (1) Plant development and hardiness biology; (2) Animal physiology or cell biology; (3) Ecology; (4); Animal development biology (5) Molecular immunology; (6) Bryology et cetera. The positions offer startup funds (US$120,000 to $300,000) and excellent laboratory space. Successful candidates will be provided a competitive salary (US$10,000 to $30,000 per annum) and housing benefits. Candidates should have a Ph.D., with significant postdoctoral research accomplishments or similar experience and an ability to develop innovative research programs. Excellent writing skills, communication, and interpersonal skills are required. Please submit a cover letter outlining research plans, curriculum vitae, and the contact details of three references to: **Professor Liu Jingze, Dean of the College.** E-mail contact **(e-mail: liujingze@mail.hebtu.edu.cn)** is preferred at the beginning. Applications will be reviewed upon receipt and accepted until the positions are filled. For further information visit **website: http://202.206.100.3/xi/smxy/index.htm.**

The Department of Biology at the University of Louisville, **website: http://www.louisville.edu/a-s/biology,** invites applications for a tenure-track **ASSISTANT PROFESSOR** position in conservation biology. Ph.D. required. The ideal applicant would complement existing strengths of the Department in ecosystem, restoration, and organismal ecology, provide new perspectives and tools from their own research area, and be able to work on interdisciplinary projects with colleagues across campus and the state. The successful candidate is expected to contribute to undergraduate and graduate programs and to maintain an excellent record of research productivity and external funding. Applicants must apply online at **website: http://www.louisville.edu/job** and attach the following documents: curriculum vitae, statements of research and teaching interests, and contact information for three references. Please select job identification number 20503. Send representative reprints directly to: **Conservation Biology Search, Department of Biology, University of Louisville, Louisville, KY 40292.** Review of applications will begin on October 1, 2006, and will continue until the position is filled. *The University of Louisville is an Affirmative Action, Equal Opportunity, Americans with Disabilities Employer, committed to diversity and in that spirit, seeks applications from a broad variety of candidates.*

POSTDOCTORAL POSITIONS
Duke University
Durham, North Carolina

Postdoctoral positions are available immediately to investigate focused ultrasound-modulated anti-tumor immune response and to develop novel technologies to combine synergistically high-intensity focused ultrasound and gene/immunotherapy for cancer therapy. The successful candidate will join a multidisciplinary team of investigators from the Pratt School of Engineering and Duke Comprehensive Cancer Center. Candidates with a strong background in molecular biology, cancer immunology, and working experience with mouse tumor models are desirable. Please send curriculum vitae and three letters of references to **Pei Zhong, Ph.D., e-mail: pzhong@duke.edu.**

PROFESSOR AND HEAD
Department of Physiology and Pharmacology

Applications are requested for the position of Professor and Head of the Department of Physiology and Pharmacology, College of Veterinary Medicine at the University of Georgia. The Department, which has a strong record of outstanding research and teaching, is seeking a recognized scientist to provide scholarly leadership. The Departmental mission emphasizes excellence in the basic sciences, and is strongly committed to both research and professional/graduate education in the fields of physiology, pharmacology, endocrinology, toxicology, and nutrition. Departmental faculty also participate in campuswide interdisciplinary graduate programs in toxicology and neuroscience, as well as in the D.V.M./Ph.D. dual degree program. The successful candidate will be a respected scholar with an established, externally funded research program in any of the above areas, and should also possess strong leadership and interpersonal skills. In addition, the ability to promote interdisciplinary collaborative programs is desirable. Qualifications for the position include the Ph.D. degree; a D.V.M. degree, while desirable, is not required. For more information, log onto **website: http://www.vet.uga.edu/vph/positions.html.** Interested applicants should submit a letter of application including a statement of research plans, career goals, and teaching interests, along with curriculum vitae and the names and contact information for three references to: **Dr. Fred Quinn, Chair of the Search Committee, College of Veterinary Medicine, University of Georgia, 501 DW Brooks Drive, Athens, GA 30602,** or electronically to **e-mail: teidson@vet.uga.edu.** Applications received before October 1, 2006, are assured full consideration. *The University of Georgia is an Equal Opportunity/Affirmative Action employer.*

NATIONAL TSING HUA UNIVERSITY
College of Life Science
Hsinchu 30013, Taiwan, ROC

The College of Life Science of the National Tsing Hua University (NTHU) in Hsinchu, Taiwan has faculty openings at all levels beginning February 1, 2007, or August 1, 2007 **(website: http://life.nthu.edu.tw/).** The College of Life Science consists of four Institutes; we are seeking outstanding candidates in all fields of life sciences. Our special emphases are on medicinal microbiology, neurosciences, neuroengineering, human genetics and molecular mechanisms of disease for the institute of molecular medicine; development and evolution and cancer biology for the institute of molecular and cellular biology; transgenic animal models, drug design and pharmaceutics, brain sciences, immunology and nanobiotechnology for the Institute of Biotechnology; and structural biology, bioinformatics and plant functional genomics for the Institute of Bioinformatics and Structural Biology. Cross-disciplinary appointments with other colleges in the University are possible and encouraged. NTHU ranks academically among the top universities in Taiwan. Excellence in research and teaching are the main qualifications for consideration to an appointment. Proficiency in Chinese or English is a requirement as NTHU intends to become a fully bilingual institution within ten years. Applicants should submit their curriculum vitae plus a statement of their current research interests, a copy of Ph.D. diploma, future plans, and the Institutes of relevance (two or more) to the candidate. Please arrange for three letters of references to be sent by September 30, 2006, to **Dr. Tsai-Yun Lin.** Inquiries can be made by e-mail at **e-mail: tylin@life.nthu.edu.tw.**

POSTDOCTORAL/RESEARCH SCIENTIST POSITIONS available to study the role of membrane-anchored metalloproteinases in angiogenesis and metastasis (*Cell* **114:** 33, 2003; *J. Cell Biol.* **167:** 769, 2004; *Genes Dev.* **19:** 979, 2005). Strong background in cell or molecular biology required. *U.S. citizens and resident aliens only.* Send curriculum vitae and letters of reference to: **Stephen J. Weiss, M.D., Upjohn Professor of Medicine, Chief, Molecular Medicine and Genetics, University of Michigan, 5000 LSI, 210 Washtenaw, Ann Arbor, MI 48109-0640.**

POSITIONS OPEN

ASSISTANT/ASSOCIATE PROFESSOR
Department of Biochemistry and Molecular Biology
State University of New York
Upstate Medical University

We seek applications to fill two tenure-track positions at either the **ASSISTANT** or **ASSOCIATE PROFESSOR** levels from individuals studying fundamental molecular processes in eukaryotic organisms. We encourage applications that expand existing programs, including structural biology, genomics, proteomics, and computational biology. The successful applicants will be expected to develop well-funded research programs and to contribute to medical and graduate teaching. We offer a highly competitive start-up package and salary. Further information about the Department can be found at **website: http://www.upstate.edu/biochem.**

Candidates should have a Ph.D. or equivalent, postdoctoral experience, and a strong publication record. Applicants should e-mail a PDF file containing curriculum vitae, a summary of research accomplishments and future research plans to **e-mail: biochem@upstate.edu.** In addition, three letters of reference should be mailed directly to: **Dr. Barry E. Knox, Search Committee Chair, Department of Biochemistry and Molecular Biology, 750 East Adams Street, Syracuse, NY 13210.**

Review of applications will begin on November 1, 2006, and continue until the positions are filled. *Women and minorities are highly encouraged to apply. Upstate Medical University is an Equal Opportunity/Affirmative Action Employer.*

FACULTY POSITION IN MOLECULAR BIOPHYSICS
Johns Hopkins University School of Medicine

The Department of Biophysics and Biophysical Chemistry **(website: http://biophysics.med.jhmi.edu)** seeks outstanding candidates for the position of **ASSISTANT PROFESSOR.** Applications are sought in all areas of molecular biophysics and biophysical chemistry, including, but not limited to, enzymology, structural biology, single molecule studies, computational biophysics, biological spectroscopy, and mechanistic chemical biology. Priority will be given to applications received by November 1, 2006. Please submit paper copies of curriculum vitae, a summary of current and proposed research, and arrange to have three letters of recommendation sent to:

Search Committee
Department of Biophysics and Biophysical Chemistry
Johns Hopkins University School of Medicine, WBSB 713
725 North Wolfe Street
Baltimore, MD 21205-2185
Fax: 410-502-6910

The Johns Hopkins University is an Equal Opportunity Employer.

ASSISTANT PROFESSOR
Biomolecular Chemistry
University of Wisconsin, Madison
School of Medicine and Public Health

We invite applications for a tenure-track position, beginning fall 2007. We seek colleagues eager to establish a vigorous biochemical or molecular biological research program of medical significance, and to teach at several levels. A doctorate and significant postdoctoral experience is required. Physician scientists addressing problems at the molecular level are encouraged to apply. The University of Wisconsin, Madison has a long storied tradition of research excellence, and is located in the heart of one of the country's most livable cities.

Deadline to ensure consideration is October 16, 2006. Send curriculum vitae, a two-page research plan, and three letters of reference to: **Search Committee, Biomolecular Chemistry, 587 MSC, Univeristy of Wisconsin School of Medicine and Public Health, 1300 University Avenue, Madison, WI 53706-1532. E-mail: cayers@wisc.edu. Website: http://www.bmolchem.wisc.edu.** *Equal Opportunity/Affirmative Action Employer. Minorities and women are encouraged to apply.*

INSTITUT PASTEUR

POSTDOCTORAL FELLOWSHIPS
Institut Pasteur, Paris, France

Founded in 1887 by Louis Pasteur and located in the heart of Paris, the Institut Pasteur is a world-renowned private research organization. The Pasteur Foundation is seeking outstanding Fellowship Applicants. Candidates may apply to any laboratory within 10 departments: cell biology and infection; developmental biology; genomes and genetics; immunology; infection and epidemiology; microbiology; neuroscience; parasitology and mycology; structural biology and chemistry; and virology. See website for details.

Fellowships are $60,000 per year for three years ($45,000 stipend plus $15,000). *U.S. citizenship required.* Deadline: February 2, 2007.

E-mail: pasteurus@aol.com.

Website: http://www.pasteurfoundation.org.

Swarthmore College invites applications for two tenure-track positions in the Department of Chemistry and Biochemistry at the **ASSISTANT PROFESSOR** level. The first position is in inorganic or bioinorganic chemistry. Primary teaching responsibilities will center around intermediate and advanced inorganic chemistry as well as general chemistry. The field for the second position is open, but with the expectation that the appointee will assume a leadership role in developing and implementing a junior-level course in the theory and practice of laboratory instrumentation and/or analytical methods. Primary teaching responsibilities will be in this course, which the Department plans to offer beginning in the fall of 2007, as well as in other areas of the curriculum matching the appointee's expertise. Research interests with a biochemical dimension will be regarded as a plus. It is expected that both appointees will conduct active research programs involving undergraduates. The College offers a generous sabbatical policy, and also provides competitive startup funds and internal support for student summer stipends and supplies. Both appointments will begin on September 1, 2007. Ph.D. required; postdoctoral experience is preferred. Candidates are requested to submit curriculum vitae, copies of graduate and undergraduate transcripts, a statement of research goals, and a cover letter describing their interest in a faculty career at Swarthmore. Applicants are also requested to arrange for a minimum of three letters of recommendation to be sent to: **Professor Paul R. Rablen, Chair, Department of Chemistry and Biochemistry, Swarthmore College, 500 College Avenue, Swarthmore, PA 19081-1397.** Applications must be completed by October 2, 2006, to assure full consideration. *Swarthmore is an Equal Opportunity Employer; women and members of underrepresented minorities are encouraged to apply.*

RESEARCH TECHNICIAN

The Department of Anatomy and Physiology invites applications for the position of Research Technician. Duties include: plasmid DNA preparation and analysis, isolation and analysis of DNA and RNA, electrophoresis of protein samples, immunoblotting and mammalian cell culture, as well as general laboratory organization. A minimum of an M.S. degree in natural or physical science with previous laboratory experience is required. Screening of applications will begin on September 18, 2006. Materials to be submitted: letter of interest, current resume, and contact information for three references. Submit to **Dr. Peying Fong** via **e-mail: pfong@vet.k-state.edu** or send to: **Anatomy and Physiology Department, 228 Coles Hall, Manhattan, KS 66506-5802.** *Kansas State University (KSU) is an Equal Opportunity-Affirmative Action Employer. KSU actively seeks diversity among its employees.*

SUPERVISORY MANAGEMENT AND PROGRAM ANALYST, GS-0343-15, salary range: $107,521 to $139,774. The Climate Program Office of the National Oceanic and Atmospheric Association (NOAA) is seeking an energetic individual with considerable experience in management, scientific program planning, and administration to serve as **DEPUTY DIRECTOR.** The Climate Program Office leads NOAA's Climate Mission Goal and Climate Competitive Research Program. The Deputy Director is responsible for the management role for all divisions, programs, and activities within the Office. The incumbent is responsible for managing the execution and integration of a network of activities that maintain well-structured paths from observations, modeling, and research to decision support. This is accomplished through a process of: soliciting competitively sponsored research and development activities; transitioning successful sustained products to operations or applications; developing and evaluating a suite of both research and operational climate products and services; and providing educational, outreach, and training activities to enhance the reach and relevance of climate services. The ideal candidate will have demonstrated experience in line management and supervision, scientific program planning, direction and administration, including management of programs, funds, resources, and staff. Excellent verbal and written communication skills are essential as is the ability to work with a team of Senior Managers in support of agency goals and mission requirements. Detailed job information and applicant instructions can be found at **website: http://www.usajobs.opm.gov** on or near August 28, 2006, under vacancy numbers OAR-HQ-2006-0136 and 0137. *Open to all U.S. citizens. The United States Department of Commerce is an Equal Opportunity Employer.*

FACULTY POSITION IN ORGANIC CHEMISTRY
University of California, Davis

The Chemistry Department **(website: http://www.chem.ucdavis.edu/)** at the University of California, Davis, invites applications for one faculty position at the **ASSISTANT PROFESSOR** level in organic chemistry. The preferred candidate will develop a strong research program in organic chemistry at the biological interface. A Ph.D. or equivalent in chemistry, medicinal chemistry, or pharmaceutical sciences is required. The candidate must also demonstrate a strong commitment to undergraduate and graduate teaching. This position is open until filled; but to assure full consideration, applications should be received no later than September 22, 2006. The targeted start date is July 1, 2007. Interested candidates should arrange for three letters of recommendation and both paper and electronic (PDF format) copies of curriculum vitae, publication list, teaching statement, and research plans to be sent to:

Organic Search Committee
Department of Chemistry
University of California at Davis
One Shields Avenue
Davis, CA 95616

The University of California is an Affirmative Action/Equal Opportunity Employer.

MEDICAL WRITER

Physicians' Education Resource (PER) is seeking a Medical Writer/Editor to join its team. PER is a medical education company, located in Dallas, Texas, specializing in the field of oncology. Successful candidates will be responsible for writing manuscripts from original data, reporting highlights from cancer meetings, creating slide sets for pharmaceutical companies, and editing and rewriting author-submitted manuscripts. This full-time position requires a Ph.D. in a biomedical science. Send resume and salary requirements to: **Barb Schmaedeke, Human Resources Director, 3535 Worth Street #185 Dallas, TX 75246. E-mail: hr@pergrouplp.com.**

POSITIONS OPEN

FACULTY POSITION
Section of Neurobiology
The University of Texas at Austin

The Section of Neurobiology of the School of Biological Sciences at the University of Texas at Austin is seeking applicants for a tenure-track **ASSISTANT PROFESSOR** position in neurobiology. In special cases, appointments at more senior levels will be considered. Qualifications must be commensurate with rank and include an outstanding academic record, significant achievement in original research, and a commitment to quality teaching.

The University of Texas at Austin is undergoing a significant expansion in neuroscience, with a number of newly recruited faculty members joining a strong existing faculty base in biological sciences, psychology, pharmacy, computer sciences, engineering, and physical sciences.

Faculty in the Section of Neurobiology use a wide array of technical approaches applied to research interests in cellular, molecular, and systems levels of organization. Applicants working in any area of modern neuroscience are welcome. Successful candidates will be expected to develop and maintain an active research program within an exciting and interactive academic environment.

Interested applicants should send curriculum vitae, summary of research interests, and the names of five references (all as electronic documents) to:

Dr. Richard Aldrich
Chair
Section of Neurobiology
The University of Texas at Austin
E-mail: neurosearch1@uts.cc.utexas.edu.

Background check conducted on applicant selected.

The University of Texas at Austin is an Affirmative Action/Equal Opportunity Employer. Minorities and women are encouraged to apply.

ORGANIC CHEMISTRY
Dartmouth College

Applications are invited for a faculty position at the **ASSISTANT PROFESSOR** level starting July 2007. The Chemistry Department seeks an individual who will establish a nationally recognized research program in organic chemistry at Dartmouth, and who will excel at teaching in our undergraduate and Ph.D. curriculum. Candidates will be expected to be able to teach introductory and advanced courses in organic chemistry, as well as graduate courses in their area of research. Applicants should submit curriculum vitae, a description of their research plans, and a brief statement about their teaching interests. Applicants should also arrange to have three letters of recommendation sent on their behalf. All inquiries and applications will be treated confidentially. Application materials should be sent to: **Chair, Organic Chemist Search Committee, Department of Chemistry, 6128 Burke Laboratory, Dartmouth College, Hanover, NH 03755-3564.** The Committee will begin to consider completed applications on October 15, 2006. *With an even distribution of male and female students and over a quarter of the undergraduate student population members of minority groups, Dartmouth is committed to diversity and encourages applications from women and minorities. Dartmouth College is an Equal Opportunity and Affirmative Action Employer.*

YALE UNIVERSITY
Department of Chemistry

The Department of Chemistry, Yale University, invites applications for two tenured positions at the **FULL PROFESSOR** level to commence July 1, 2007. We seek creative teacher-scholars with an international reputation for outstanding research in the fields of mechanistic and synthetic inorganic chemistry and synthetic organic chemistry. Applicants should send curriculum vitae and a statement of research plans. All materials should be received by October 15, 2006. Send applications to: **Chair, Senior Search Committee, P.O. Box 208107, Yale University, New Haven, CT 06520-8107.** *Yale University is an Equal Opportunity/Affirmative Action Employer; applications from women and underrepresented minority group members are especially encouraged.*

POSITIONS OPEN

USDA ARS Agricultural Research Service
www.ars.usda.gov

RESEARCH ENTOMOLOGIST
GS-0414-12/13/14
Salary Range of $62,291 to $113,791

The United States Department of Agriculture, Agricultural Research Service (USDA/ARS), Arthropod-Borne Animal Diseases Research Laboratory in Laramie, Wyoming, is seeking a permanent, full-time Research Entomologist to conduct research in collaboration with other scientists in ARS, universities, and industry. The goal of the research is to protect U.S. livestock from vector-borne pathogens, ultimately contributing to integrated disease management programs. The emphasis of the research is protection of livestock, but extends to protection of wildlife and humans from arthropod vectored pathogens. To have a printed copy of the vacancy announcement mailed to you, call **Bobbie Bobango** at **telephone: 307-766-3606,** or access information online at **website: http://www.afm.ars.usda.gov/divisions/hrd/index.html.** Send applications for announcement ARS-X6W-0321 to: **USDA, Agricultural Research Service, Human Resources Division, Attn: Keli A. Martin, 5601 Sunnyside Avenue, Stop 5106, Beltsville, MD20705-5106, fax: 301-504-1535; e-mail: scirecruit@ars.usda.gov.** Applications must be marked ARS-X6W-0321 and postmarked by September 20, 2006. *Citizenship is required.*

USDA/ARS is an Equal Opportunity Employer and Provider.

RESEARCH SCIENTIST

Applications are invited for a Research Scientist position in the Nutrition and Metabolic Disease Research Institute (NAMDRI) at Sioux Falls, South Dakota. NAMDRI is part of the South Dakota Health Research Foundation (SDHRF), which is a partnership between the Sanford School of Medicine at the University of South Dakota and the Sioux Valley Hospitals and Health System. This position is in the Center for Omega-3 Research (COR) which focuses on understanding the mechanisms by which omega-3 fatty acids alter metabolism and reduce risk for a variety of chronic diseases. An academic appointment with the School of Medicine University of South Dakota is available for this position based on qualifications and experience.

Applicants must have an M.D., Ph.D. or equivalent in biomedical sciences with at least three years of postdoctoral research training. Prior experience in lipoprotein metabolism and kinetics, preferably in humans, is desired. Excellent oral and written communication and personnel skills are essential in addition to being highly self-motivated and disciplined.

Applicants should submit a letter of interest, curriculum vitae, and the contact information of three references to: **Human Resources, South Dakota Health Research Foundation, 1100 East 21st Street, Suite 700, Sioux Falls, SD 57105; fax: 605-328-1355; e-mail: bpoppens@usd.edu.**

Applications will be accepted until the position is filled. Review of applications will begin in September 2006, until a suitable candidate is found.

SDHRF is an Equal Opportunity/Affirmative Action Employer.

POSITIONS OPEN

POSITIONS IN BIOLOGY

Two tenure-track positions in the Biology Department, Eastern Connecticut State University, starting fall 2007. Ph.D. required, with aptitude for teaching undergraduates. Postdoctoral experience an advantage and competency in relevant computer technologies expected. Opportunities to teach in tropical biology field courses. Academic advisement, continued professional development, scholarly activity, and course development for liberal arts core curriculum expected. Send curriculum vitae, transcript of all graduate work, a statement of teaching philosophy and research interests, documentation of teaching ability, and three current letters of recommendation to the appropriate **Search Chair** (below), **Biology Department, Eastern Connecticut State University, Willimantic, CT 06226.** Searches will continue until positions are filled.

ASSISTANT PROFESSOR of conservation biology. Expertise in animal biology and experience in the application of molecular techniques to relevant conservation biology issues required. Will teach upper-level courses in conservation biology/molecular ecology, introductory biology, and participate in a sophomore-level genetics course. **Search Chair: Dr. Phillip Elliott.**

ASSISTANT PROFESSOR of plant ecology. Expertise in plant ecology and field research experience required. Will teach introductory and upper-level courses including field work in plant ecology and introductory ecology. **Search Chair: Dr. Ross Koning.**

Eastern Connecticut State University is an Affirmative Action/Equal Opportunity Employer.

MARKETPLACE